Evaluating the role of CD200 in non-small cell lung carcinoma immune evasion

Charlotte Lovatt

Thesis submitted for the award of PhD

2022

The European Cancer Stem Cell Research Institute

School of Biosciences

Cardiff University

Ysgoloriaethau Sgiliau Economi Gwybodaeth
Knowledge Economy Skills Scholarships

UNDEB EWROPEAIDD
EUROPEAN UNION

Llywodraeth Cymru
Welsh Government

Cronfa Gymdeithasol Ewrop
European Social Fund

Acknowledgments

First and foremost, I would like to thank Kess2 and the Aneurin Bevan Health Board for funding my PhD project, without their support this research would not have been possible. Furthermore, my upmost thanks to the Wales Cancer Bank and the patients who kindly donated samples for this study.

I am incredibly thankful to Dr.Girish Patel for giving me this opportunity and supporting me over the past 3.5+ years and during my PTY project preceding that. I am also grateful to my second supervisor Dr.Richard Clarkson for his advice and support. I owe my ongoing passion for science and resilience to the both of them. To all the members, past and present, of the GKP lab I do not think any of this would have been possible without you. Elisa, Carlotta, and Huw have been excellent mentors and were always there to help troubleshoot, give me advice and lend an ear whenever everything felt like too much. I have been lucky to share this GKP PhD journey with Gemma and Alex, both excellent scientists and two of my most valued friend, I don't know what I would have done without them, and I wish them all the best in finishing their PhDs.

I have been so incredibly lucky to work in ECSCRI over the last few years, the students and staff of which have made this PhD unforgettable. Not only are they incredible scientists and inspirational people, but they are also the kindest and most caring people to have shared this journey with. I have made friendships that I will hold dear for many years to come, and I miss them all every day! A special thank you to Val, Sarah, Manisha, Alice, Adam, Katie and Liam for keeping me sane and reminding me that things will be alright in the end (particularly during the 13-month phase of 9-hour image analysis sessions). Thank you to Mark for always helping me with FACs and not shouting at me when I almost break the Fortessa with my avant-garde data saving methods. My heartfelt gratitude goes to Jolene, not only does she keep ECSCRI going every day, but she has also been an incredible friend and one-woman support network who was always there to give me sound advice and make me smile when the world felt like it was ending.

To my family and friends, thank you for always supporting me and listening to my mad ramblings about my PhD even when you had no idea what I was going on about. I am eternally grateful for you; this thesis would not have been possible without you all. Mum and Dad thank you for always letting me make my own decisions and forge my own path in life…I promise I am finally leaving education! Finally, to my fiancé Luke, thank you for putting up with my nonsense over the past few years, thank you for supporting me in

every way possible and encouraging me to complete this journey…it's almost over I promise!

This thesis is dedicated to Mister. Reggie.

Summary

Lung cancer is the 3rd most common cancer in the UK, accounting for 13% of all new cancer cases and is the most common cause of cancer death in the UK, accounting for 21% of all cancer deaths. Over recent years, the introduction of immunotherapies targeting the PD-1/PD-L1 immune checkpoint pathway has revolutionised the treatment of non-small cell lung carcinoma (NSCLC) patients; as a tumour with a typically highly infiltrated immune reactive tumour microenvironment (TME) rich in neoantigens, NSCLC tumours represent an ideal candidate for immunotherapies, as reflected in the durable clinical efficacy seen in some responder patients. However, most patients treated with PD-1/PD-L1 immunotherapies either demonstrate an initial response followed by disease progression or, in the case of 47-63% of patients, demonstrate no response or benefit. Therefore, identification of predictive markers of immune checkpoint inhibitor (ICI) therapy response or the generation of multi-modality immunological therapies targeting multiple immune checkpoints could greatly improve the success of PD-1/PD-L1 ICI therapies in NSCLC. One of the most promising strategies for overcoming resistance and prolonging therapeutic benefit from ICIs is the use of dual immune checkpoint blockade. Therefore, the aim of this thesis was to determine whether the immune checkpoint CD200 may be a relevant immunotherapeutic target in NSCLC patients.

CD200 is a type I transmembrane glycoprotein structurally related to the B7 family of receptors that signals through its receptor, CD200R, which is expressed on several immune cell populations including those of myeloid lineage, B cells, NK cells and activated T cells. Engagement of CD200R results in a negative immunoregulatory signal to maintain immune homeostasis and prevent over-activation of the immune system. CD200 is also expressed by several solid and haematological malignancies, with its expression correlating with an increase in immunosuppressive Treg cells, a decrease in memory T cells, and dysfunction of cytotoxic effector NK cells. Furthermore, CD200 is a potent regulator and suppressor of myeloid cell function, suggesting that targeting CD200 signalling may decrease immune suppression and increase the anti-tumour immune response. As a critical regulator of immune homeostasis in normal lung, CD200 may also be expressed by tumour cells to evade immune attack and promote tumour growth.

In this thesis, CD200 expression was first characterised in the normal mouse and human lung where it was demonstrated to be strongly expressed throughout the distal lung by both type I and type II alveolar cells. Upon malignant transformation, CD200 expression was demonstrated on both SCC and adenocarcinoma tumours, although to a greater extent in adenocarcinoma tumours. We suggest that type II alveolar cells, the predominant cell of origin

of adenocarcinoma tumours and some SCC tumours, retain CD200 expression upon transformation as a method of immune evasion.

Furthermore, using a combined RNA-seq and IHC labelling technique the relationship between tumour CD200 expression and the absolute and relative frequencies of infiltrating immune cells was established. In SCC and adenocarcinoma tumours, CD200 expression positively correlated with the frequencies of immunosuppressive Tregs and in adenocarcinoma tumours, tumour CD200 expression consistently negatively correlated with the frequencies of cytotoxic NK cells. *In vitro* analysis of CD200R+ NK cell activity demonstrated that CD200+ tumour cells induce NK cell dysfunction as characterised by decreased degranulation, inhibited cytokine production, altered activating receptor expression and a decreased capacity to kill tumour cells. Blocking of CD200 with an antibody was sufficient to restore the NK cell anti-tumour response and increase tumour cell death, suggesting that blocking CD200 signalling in CD200+ tumours could increase NK cell-mediated tumour cell killing. Furthermore, single-cell analysis and IHC labelling demonstrated that CD200R is expressed on almost all of the infiltrating immune cell subtypes studied, suggesting immunoregulatory control of the immune response beyond that which was studied in this thesis. Taken together, this data suggests a mechanism by which NSCLC tumour cells express CD200 as a mechanism of immune evasion and that blocking CD200 signalling alone, or in combination with PD-1 inhibition to synergistically increase immune checkpoint therapy efficacy, may represent a novel therapeutic target in NSCLC.

Word Count: **75 249**

Table of Contents

List of figures

List Of Tables

Abbreviations

ADAM	A distegrin and metalloproteinase
ADCC	Antibody-dependent cellular cytotoxicity
Akt	Protein kinase B
ALK	Anaplastic lymphoma kinase
AML	Acute myeloid leukaemia
APCs	Antigen presenting cells
APM	Antigen presentation machinery
ATCC	American Type Culture Collection
ATP	Adenosine triphosphate
BCA	Bicinchoninic acid
BCC	Basal cell carcinoma
BCL-XL	B cell lymphoma extra-large
BCR	B cell receptor
BEGM	Bronchial epithelial cell growth medium
bp	Base pairs
Bregs	Regulatory B cells
BSA	Bovine serum albumin
C/EBP-β	CCAAT/enhancer-binding protein beta
CAFs	Cancer associated fibroblasts
CCL	Chemokine (C-C motif) ligand
CCSP	Club cell secretory protein
CD200	Cluster of differentiation 200
CGA	Cancer-germline antigen
CIA	Collagen-induced arthritis
CIBERSORT	Cell type identification by estimating relative subset of unknown RNA transcripts
CLL	Chronic lymphocytic leukaemia
CMV	Cytomegalovirus
CNS	Central nervous system
CrkL	Cellular homologue-like
CSCs	Cancer stem cells
CT	Threshold cycle
CTG	CellTiter-Glo
CTLs	Cytotoxic lymphocytes
Ctsk	Collagen cytesine protease cathepsin K
CTLA-4	Cytotoxic T lymphocyte antigen 4
CV	Coefficient of variance
CXCL	C-X-C motif chemokine ligand
CXCR	C-X-C chemokine receptor
DAB	Diaminobenzidine

DAMPs	Damage-associated molecular patterns
DAP12	DNAX activation protein of 120kDa
DCs	Dendritic cells
DDR2	Disocdin domain-containing receptor 2
DMEM	Dulbecco's Modified Eagle Medium
DMSO	Dimethyl sulfoxide
DOK	Downstream of tyrosine kinase
DR5	TRAIL death receptor 5
EAE	Experimental autoimmune encephalomyelitis
EAU	Experimental autoimmune uveoretinitis
ECACC	European Collection of Authenticated Cell Cultures
EGFR	Epidermal growth factor receptor
EOMES	Eomesodermin
ERK	Extracellular signal-related kinase
FAD	Flavin Adenine Dinucleotide
FasL	Fas ligand
FBS	Foetal bovine serum
FDA	Food and Drug Administration
FGFR	Fibroblast growth factor receptor
FOXA1	Forkhead box a1
GDT	γδ T cells
GFP	Green fluorescent protein
GM-CSF	Granulocyte/monocyte colony-stimulating factor
GNLY	Granulysin
GTP	Guanosine-5'-triphosphate
GZMA	Granzyme A
GZMK	Granzyme K
HER	Human epidermal growth factor receptor
HLA	Human leukocyte antigen
HR	Hazard ratio
HRP	Horseradish peroxidase
HS	Horse serum
ICI	Immune checkpoint inhibitors
IDO	Indoleamine 2,3-dioxygenase
IFN-γ	Interferon-γ
Ig	Immunoglobulin
IKK2	Inhibitor kappa B kinase 2
IKKα	Nuclear factor-κB kinase subunit-α
IL	Interleukin
IPEX	Immune dysregulation polyendocrinoptahy Enteropathy X linked
IRF-1	Interferon-regulatory factor
IS	Immunological synapse
ITSM	Immunoreceptor tyrosine-based switch motifs

KEAP1	Kelch like ECH associated protein
KIR	Killer cell immunoglobulin-like receptors
LAG-3	Lymphocyte-activation gene 3 protein
LUAD	Lung adenocarcinoma
LKB1	Joint liver kinase B1
LUSC	Lung squamous cell carcinoma
M1	Type I macrophage
M2	Type 2 macrophage
MA	Memory activated
Mabs	Monoclonal antibodies
MAGE	Melanoma-associated antigen
MAIT	Mucosal associated invariant T cells
MAPK	Mitogen-activated protein kinase
MCA	3'-methylcholantherene
MDSC	Myeloid derived depressor cell
MEM	Minimum Essential Medium
MHC	Major histocompatibility complex
MMP	Matrix metalloproteinases
MR	Memory resting
MZ	Marginal zone
nAbs	Natural antibodies
NADH	Nicotinamide adenine dinucleotide
NCRs	Natural cytotoxicity receptors
NELSON	Nederlands-Leuvens Longkanker Scrrenings Onderzoek
NF-κB	Nuclear factor kappa-light-chain-enhancer of activated B cells
NF1	Neurofibromin 1
NK	Natural killer
NKG2	Natural killer group 2 member
NSCLC	Non-small cell lung carcinoma
OD	Optical density
OS	Overall survival
PAMPs	Pathogen-associated molecular patterns
PBS	Phosphate-buffered saline
PCR	Polymerase chain reaction
PD-1	Programmed cell death protein 1
PDGF	Platelet-derived growth factor
PFS	Progression-free survival
PI3K	Phosphoinositide 3-kinase
PRECOG	Prediction of clinical outcomes from genomic profiles
PTB	Phosphotyrosine-binding domains
PTEN	Phosphatase and tensin homolog
qRTPCR	Real time quantitative reverse transcription PCR
RASGAP	Ras p21 protein activator 1

RB1	RB transcriptional corepressor 1
RNA	Ribonucleic acid
ROS1	Receptor tyrosine kinase
RSEM	Accurate Transcript Quantification from RnA-seq data with or without Reference Genome
RT	Room temperature
SCC	Squamous cell carcinoma
SCD200	Soluble CD200
SCLC	Small cell lung carcinoma
SDS	Sodium dodecyl sulphate
SHP	Src homology region 2 domain-containing phosphatase
SOS-1-vav1-grb2	Son of sevenless homolog 1 – vav guanine nucleotide exchange factor 1-growth factor receptor bound protein 2
SOX2	SRY-box 2
SPC	Surfactant protein C
Stat5	Activator of transcription 5
TAMs	Tumour-associated macrophages
TANs	Tumour-associated neutrophils
TCGA	The Cancer Genome Atlas
TCR	T cell receptor
TDLN	Tumour draining lymph nodes
Tfh	T follicular helper cell
TGF-β	Transforming growth factor beta
Th1	Type 1 T helper cell
Th17	Type 17 T helper cell
Th2	Type 2 T helper cell
TIGIT	T cell immunoreceptor with Ig and ITIM domains
TIM3	T cell immunoglobulin mucin receptor 3
TKIS	Tyrosine kinase inhibitors
TMA	Tissue microarray
TMB	Tumour mutational burden
TME	Tumour microenvironment
TNF-α	Tumour necrosis factor-α
TP53	Tumour suppressors tumour protein 53
TPM	Transcripts per Million
TRAIL	TNF-related apoptosis-inducing ligand
Tregs	Regulatory T cells
TTF1	Thyroid transcription factor 1
VEGF	Vascular endothelial growth factor
WT	Wild type
Zap-70	Zeta-chain-associated protein kinase 70

Chapter 1:
Introduction

1. Introduction

1.1 Cancer and the immune system

The existence of a functional relationship between the immune system and cancer was first proposed by Virchow in the 19th century upon the observation that tumours often arose at sites of chronic inflammation (Balkwill and Mantovani 2001). Although this hypothesis was initially overlooked for many years, in the last few decades our knowledge of the complex relationship between the immune system and tumorigenesis has rapidly evolved and it is now clear that the immune system can impact every stage of tumorigenesis, from initiation to metastasis, with infiltrating immune cells possessing both pro- and anti-tumorigenic properties.

Inflammation mediated by cells of the innate immune system is vital to successfully fight infections and heal wounds; however, unlike during the course of normal wound healing and response to infection where immune cells appear transiently and disappear, the immune response associated with cancer is similar to that seen with chronic inflammation (Mantovani *et al.* 2008). This low-grade inflammatory response can be associated with promotion of an immunosuppressive tumour microenvironment (TME) and production of growth factors and angiogenic factors which stimulate cancer cell survival, progression and metastatic dissemination (Shalapour *et al.* 2015). Many environmental causes and risk factors of cancer are associated with triggering chronic inflammation; 30% of cancers are linked to tobacco smoking or inhaled pollutants known to trigger chronic inflammation of the lung; 35% can be attributed to dietary factors; 12-20% to obesity; and up to 20% are linked to persistent bacterial and viral infections such as *Helicobacter Pylori* and *Human papilloma virus* with gastric cancer and cervical cancer, respectively (Aggarwal *et al.* 2009).The inflammatory state of pre-malignant and malignant lesions is now identified, along with the genomic instability of tumour cells, as one of the two enabling characteristics that drives the acquisition of the six hallmarks of cancer: a set of distinctive and complementary capabilities that enable cancer cells to survive, proliferate and metastasise. Inflammation can contribute to multiple cancer hallmark capabilities through the tumour-promoting effects of infiltrating immune cells, largely of the innate immune system. Immune cells can supply bioactive molecules to the tumour microenvironment including survival factors that limit cell death, growth factors that sustain proliferative signalling, pro-angiogenic factors, inductive signals that lead to the activation of hallmark-facilitating programs such as epithelial-to-mesenchymal transition, and extracellular matrix-modifying enzymes that facilitate invasion, metastasis, and angiogenesis. Furthermore, inflammatory cells can release chemicals, notably reactive oxygen species, which can provide mutagenic signals to cancer cells within the tumour microenvironment to accelerate their genetic evolution. The genomic instability of tumour cells, the second enabling characteristic, depends on the succession of genetic alterations within the genomes of tumour cells, with certain mutations conferring a selective advantage to subclones of cells which enable them to outgrow and dominate the

local tissue environment. Together, these genetic alterations which drive tumour progression in combination with the inadvertent support of multiple hallmark capabilities from infiltrating innate immune cells provide tumour cells with the functional capabilities to survive, proliferate, and metastasise (Hanahan and Weinberg 2011).

By contrast, acute vigorous inflammatory reactions as seen during allograft rejection and pathogen clearance favour the generation of an immune response capable of inducing tumour cell death (Mantovani *et al.* 2008). The idea that malignantly transformed cells are detected and eradicated by the immune system before they clinically manifest was first proposed by Ehrlich in 1909; however, this concept of immune surveillance was not fully accepted until the observation that mice deficient in lymphocytes were significantly more susceptible to the induction of chemically-induced and spontaneous tumours (Shankaran *et al.* 2001). Furthermore, immunosuppression in organ transplant recipients is associated with a heightened risk (3- to 100-fold) of developing a number of cancers, including those of non-viral origin, suggesting that the immune system plays a critical role in suppressing tumour growth (Buell *et al.* 2005). In summary, tumour growth may be initiated by an exuberant immune response, as occurs in chronic inflammation, yet the process of tumour growth itself induces an anti-tumour immune response that must be evaded. Tumour cells have developed a number of strategies to avoid immune cell recognition and elimination, allowing them to evade immune attack and become stablished in the host. This escape from immunity is now recognised as an emerging hallmark of cancer (Hanahan and Weinberg 2011). Therefore, in order to delineate the underlying basis for cancer immune evasion, it is essential to understand how immune cells and the tumour interact.

1.1.1 The immune system

The immune system is a complex interactive network comprised of lymphoid organs, cells, humoral factors, and cytokines that function to protect the host from foreign antigens such as microbes, viruses, mutated cells, and toxins (Turvey and Broide 2010). Composed of cells derived from common myeloid and lymphoid progenitors, the immune system can be broadly divided into two arms: innate and adaptive immunity (Taylor *et al.* 2016)(Figure 1.1). The innate immune system represents the first response to foreign materials and can be activated within hours of encountering an antigen (Marshall *et al.* 2018). Through a limited number of germline-encoded receptors, innate immune cells can detect a broad spectrum of conserved microbial structures and damage-associated molecular patterns (DAMPs) released as a consequence of infection and inflammation. Innate immune cells also detect mutated or infected cells through the detection of “missing self” where molecules expressed by healthy

cells that normally provide an inhibitory signal to the innate immune system are lost, providing the innate immune system with the capacity to attack the damaged host tissue (Turvey and Broide 2010). Cells of innate immunity are comprised largely of cells of myeloid origin: granulocytes (basophils, eosinophils, neutrophils, mast cells), macrophages, dendritic cells (DCs), with lymphoid-derived natural killer (NK) cells and innate lymphoid cells (ILCs) comprising the lymphoid arm of innate immunity.

As well as providing the initial protective inflammatory response, the innate immune system is also responsible for generating an effective adaptive immune response. The adaptive immune system consists of T and B cells which, upon presentation of antigens from cells of the innate immune system, generate clonal populations which are antigen specific (Rosenberg and Huang 2018)(Figure 1.1). Upon resolution of the infection, a small population of clonal cells persist as memory cells which provides the host with the ability to mount a more rapid and effective antigen-targeted response upon subsequent antigen exposure (Shalapour *et al.* 2015).

The innate and adaptive immune effector response can be broadly defined into two categories: type 1 and type 2, which ensure a tailored and maximally protective response against a great variety of antigens. Type 1 immune responses are pro-inflammatory and are effective against intracellular microbes such as bacteria, protozoa and some viruses and are comprised of type 1 CD4+ helper T cells (Th1), type 17 CD4+ helper T cells (Th17), and cytotoxic lymphocytes, namely NK cells and CD8+ cytotoxic T cells. Type 1 immune responses are characterised by the presence the pro-inflammatory cytokines interferon-γ (IFN-γ) and tumour necrosis factor (TNF)(Annunziato et al. 2015). Type 2 immune responses are characterised by type 2 CD4+ helper T cells (Th2), eosinophils, mast cells, basophils and macrophages and the cytokines interleukin-4 (IL-4), IL-5, IL-9, and IL-13. Although responsible for protection against large extracellular parasites, elements of the type 2 immune response are also important in regulating and suppressing type 1-associated inflammation in order to prevent over-activation of the type 1 immune response (Wynn 2015). Th17 cells, a Th subset characterised by production of IL-17A, IL-17F, IL-21, and IL-22, play an important role in host defence against extracellular bacterial and fungal infection, particularly at mucosal surfaces wherein the production of IL-17 and IL-22 upon Th17 cell activation improves mucosal barrier function, recruits neutrophils, and stimulates the release of anti-microbial peptides (Waite and Skokos 2012).

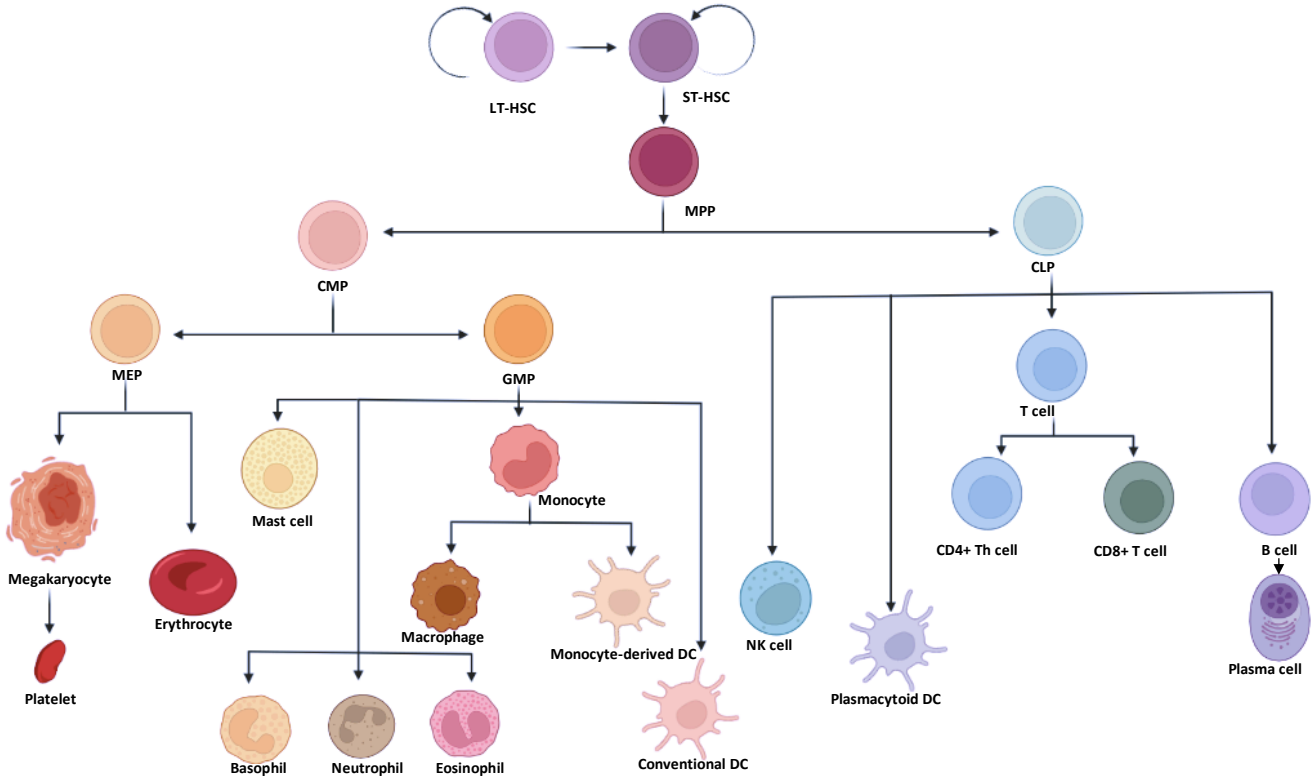

Figure 1.1 Schematic diagram of the adult haematopoietic cell differentiation hierarchy.

In this classical model of adult haematopoiesis, long term haematopoietic stem cells (LT-HSCs) sit at the top of the hierarchy and possess strong self-renewal capacity. LT-HSCs then differentiate into short term HSCs (ST-HSCs), which also possess self-renewal capacity. ST-HSCs subsequently differentiate into multipotent progenitors (MMPs) with reduced self-renewal ability. Downstream of MMPs, a strict separation occurs between the common myeloid progenitor (CMP) and common lymphoid progenitor (CLP) into myeloid and lymphoid branches, respectively. CMPs can generate megakaryocyte-erythrocyte progenitors (MEPs) which can differentiate into megakaryocytes/platelets and erythrocytes, and granulocyte-macrophage progenitors (GMP) which produce granulocytes (mast cells, basophils, neutrophils, eosinophils), macrophages and dendritic cells (DCs). CLPs can differentiate into natural killer (NK) cells, plasmacytoid DCs, T (CD4+ helper T(Th) cells CD8+ cytotoxic T cells) and B cells/plasma cells. The innate immune system is primarily composed of cells of myeloid origin, NK cells and plasmacytoid DCs, with the adaptive immune system comprised of T and B cells. Adapted from (Cheng et al. 2020). Created in Biorender.com.

1.1.2 Innate immune cells

1.1.2.1 Granulocytes

Arising from a common granulocyte-macrophage progenitor (GMP), granulocytes are named due to the dense granule content within their cytoplasm and are comprised of four main cell types: basophils, eosinophils, neutrophils, and tissue-resident mast cells, all of which are relatively short lived and produced in increased numbers during the initial immune response (Marshall *et al.* 2018). Although basophils are the least abundant granulocyte population, comprising less than 1% of peripheral blood leukocytes, they play a critical role in protective immunity against parasitic infection as well as in both allergic and non-allergic disorders. Basophils possess basophilic granules, express the allergen- and parasite-responsive high-affinity Immunoglobulin E (IgE) receptor FcεR and release pro-inflammatory mediators such as histamine upon activation (Cromheecke *et al.* 2014). Furthermore, basophils can be induced to produce cytokines which regulate and promote an adaptive immune response (Siracusa *et al.* 2013). Eosinophils represent ~1% of leukocytes and are characterised by large secretory granules containing proteases, cytokines, enzymes and growth factors which, upon activation, can induce a protective immune response against parasites, viral and microbial pathogens (Jacobsen *et al.* 2012). Eosinophils also express a large number of surface molecules which allow them to regulate both the innate and adaptive immune response (Rosenberg *et al.* 2013). Neutrophils are the most abundant immune cell population, representing 50-70% of leukocytes, and are one of the primary responders during acute inflammation. As part of the first line of defence against pathogens neutrophils are potent phagocytes that, upon recruitment to sites of infection, engulf and eliminate microorganisms using an arsenal of cytokines, chemokines and cytotoxic substances (Liew and Kubes 2019). Unlike the other granulocytes, tissue-resident mast cells are long-lived and act as sentinels of their surrounding environment; these mature cells are distributed throughout nearly all human tissues and are most abundant in tissues at the host-environment interface. Upon activation, mast cells release a wide spectrum of mediators which induce a protective immune response against microbial and viral pathogens (Debruin *et al.* 2014).

1.1.2.2 Monocytes

Monocytes are mononuclear phagocytic cells with the plasticity to develop into macrophages or DCs, representing 5-10% of peripheral immune cells with considerable marginal pools in the lung and spleen that can be mobilised on demand. Monocytes are crucial for an effective immune response to most pathogens and are equipped with adhesion receptors and chemokine receptors that modulate their migration from the blood to sites of infection or injury. During inflammation, monocytes are rapidly recruited to sites of injury where they can

differentiate into mononuclear phagocytes, including macrophages and DCs, in the tissue (Ginhoux *et al.* 2014). Under inflammatory conditions in the skin, monocytes migrate into the epidermis and differentiate into Langerhans cells, whilst in the lung recruited monocytes give rise to pulmonary DCs which help to modulate disease progression. Although neutrophils are the immediate responders to injury and infection, monocytes have been identified as necessary modulators of the inflammatory response through production of cytokines, such as IL-6, IL-1β and TNF (Karlmark et al. 2012).

1.1.2.3 Macrophages

Macrophages are a heterogenous population of terminally differentiated, tissue-resident myeloid cells that originate from circulating monocytic precursors. As sentinels of tissue homeostasis, macrophages assume a number of roles including pathogen destruction, regulation of the adaptive immune response and tissue repair (Gordon and Taylor 2005). Broadly speaking, there are two main differentiation states of macrophages: the classically activated type 1 macrophage (M1) and the alternatively activated type 2 macrophage (M2), the polarisation of which is regulated by cytokines and chemokines in the local environment (Mills *et al.* 2000). M1 macrophages are well adapted to promote a strong immune response. Upon activation by bacterial stimuli and Th1 cytokines such as IFN-γ and TNF these cells phagocytose and destroy microbes, produce high levels of pro-inflammatory cytokines such as IL-12 and IL-23 and present antigens to T lymphocytes to elicit an adaptive immune response. Conversely, exposure to Th2 cytokines such as IL-4, IL-10, IL-13 and transforming growth factor beta (TGF-β) promotes M2 polarisation. In general, these cells suppress Th1 mediated-inflammation through production of IL-10 and IL-1β and promote tissue remodelling and wound healing through the production of matrix metalloproteinases and pro-angiogenic factors (Jayasingam *et al.* 2020).

1.1.2.4 Dendritic cells

DCs are a heterogenous group of cells arising from both myeloid progenitors (monocyte-derived DCs; conventional DCs) and lymphoid progenitors (plasmacytoid DCs (pDCs)) which exist within the blood and peripheral lymphoid and non-lymphoid tissues (Lipscomb and Masten 2002). In response to danger signals i.e., microbes, tissue damage, and inflammatory cytokines, immature DCs migrate towards sites of infection where they take up antigens by phagocytosis and process them into peptide fragments (Kaiko *et al.* 2008). Antigen-loaded DCs then begin a maturation process which transforms them into professional antigen presenting cells (APCs) which migrate to T cell regions of draining lymph nodes to present

these antigenic peptides to T cells and efficiently initiate an adaptive antigen-specific immune response (discussed further in Section 1.1.2.2.2a)(Benencia *et al.* 2012).

1.1.2.5 Natural killer cells

NK cells are large granular innate lymphoid cells that constitute around 5-15% of circulating lymphocytes in healthy individuals. In contrast to cytotoxic T cells which require prior antigen exposure to mount an immune response, NK cells are naturally cytotoxic and possess the ability to recognise and kill infected cells and provide a rapid early source of immunoregulatory cytokines to modulate other aspects of the immune system (Freud *et al.* 2017). NK cells arise from a common lymphoid progenitor and have been shown to mature in the bone marrow and in secondary lymphoid organs such as the lymph nodes and tonsils (Abel *et al.* 2018).

Based on the relative expression of CD16 (FcγRIII), a low affinity receptor for the Fc portion of IgG, and CD56, an isoform of neural cell adhesion molecule which mediates homotypic adhesion, five NK cell subpopulations can be identified: (1) $CD56^{bright}CD16^{-}$ (~10% circulating NK cells), (2) $CD56^{bright}CD16^{dim}$ (rare), (3) $CD56^{dim}CD16^{-}$ (rare), (4) $CD56^{dim}CD16^{bright}$ (~90% circulating NK cells), (5) $CD56^{dim}CD16^{-}$ (rare) (Poli *et al.* 2009). $CD56^{dim}$ cells comprise the majority of circulating NK cells and possess significantly higher cytolytic capacity against target cells compared to $CD56^{bright}$ cells due to their greater expression of perforin, granzymes, cytolytic granules and CD16. In contrast $CD56^{bright}$ cells, which constitute the majority population in secondary lymphoid organs, rapidly produce large amounts of cytokines such as IFN-γ, TNF-β, IL-10 and IL-13 upon activation (Caligiuri 2008).

1.1.2.5a Regulation of NK cell activity

NK cells are poised and ready to immediately respond to and attack malignant or infected cells. The intrinsic cytotoxic capacity of these cells may present danger to healthy cells in the event of inappropriate NK cell activation; therefore, the process of NK cell activation is tightly regulated based upon the balance of function of numerous specific inhibitory and activating receptors which determine whether an NK cell will exert its effector functions (Pegram *et al.* 2011). There are two main mechanisms by which NK cells can detect and destroy infected or transformed cells: release of cytotoxic granules, and induction of death receptor-mediated apoptosis through expression of cognate ligands, in addition NK cells also possess the capacity to secrete immunoregulatory cytokines. All of these effector functions are dependent on the presence or absence of ligands for multiple NK cell receptors (Figure 1.2). There is sizeable heterogeneity within the different combinations of activating and inhibitory receptors

expressed by NK cells, bestowing them with the ability to respond to a large range of stimuli and to regulate the immune response under a variety of pathological conditions (Mandal and Viswanathan 2015)(Table 1.1).

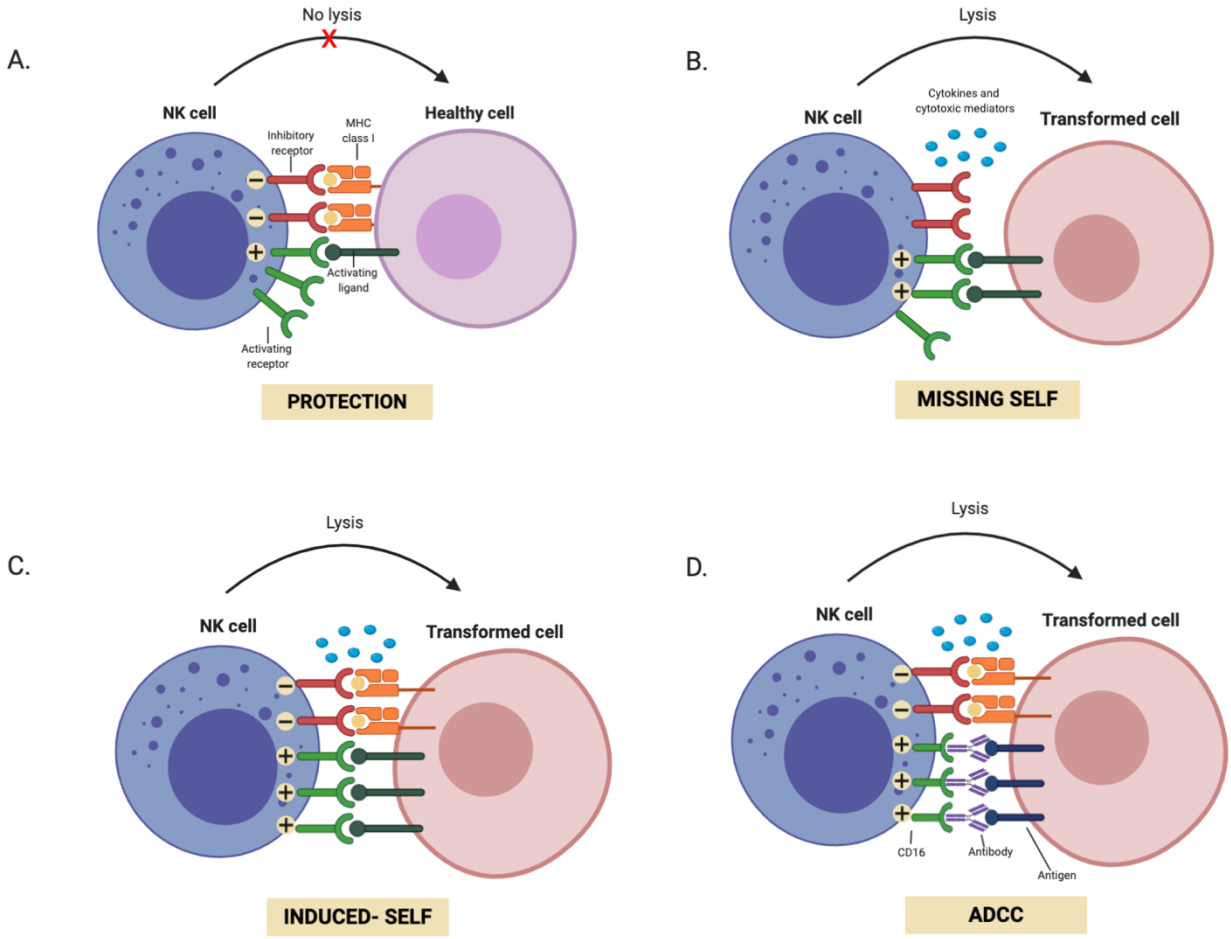

Figure 1.2 Schematic representation of physiological NK cell functions.

A. NK cells are tolerant to healthy cells as the activating signals they receive are dampened by the engagement of MHC class I ligands with inhibitory receptors. B. Cells that lose expression of MHC class I molecules ("missing self") are susceptible to attack by NK cells as they no longer receive inhibitory signals. C. Cells can overexpress stress-induced activating ligands upon infection or malignant transformation, these override the inhibitory signals and result in "induced-self" NK cell activation. D. Antigen-specific antibodies can bind to CD16 and elicit antibody-dependent cytotoxicity (ADCC). MHC, major histocompatibility complex; NK, natural killer. Adapted from Vivier et al. (2012) & Morvan and Lanier (2016). Created in Biorender.com.

Table 1.1 NK cell receptors and their ligands

Inhibitory receptor	Ligand	Activating receptor	Ligand
KIR2DL1	HLA-C2 (MHC class I)	**KIR2DL4**	HLA-G (MHC class I)
KIR2DL2	HLA-C1(MHC class I)	**KIR2DS1**	HLA-C2 (MHC class I)
KIR2DL3	HLA-C1 (MHC class I)	**KIR2DS2**	HLA-C1 (MHC class I)
KIR2DL5	Unknown	**KIR2DS3**	Unknown
KIR3DL1	HLA-Bw4 (MHC class I)	**KIR2DS4**	Unknown
KIR3DL2	HLA-A3/-A11 (MHC class I)	**KIR2DS5**	Unknown
IRp60	Unknown	**CD94 (NKG2C / NKG2E)**	HLA-E (MHC class I)
CD94 (NKG2A)	HLA-E (MHC class I)	**NKG2D**	MIC-A/-B ULBP-1/-2/-3/-4
LILR	MHC class I UL18	**NKp30**	BAT-3 HSPG B7-H6
CD244 (2B4)	CD48	**NKp44**	Viral HA
KLRG1	Cadherins	**NKp46**	Viral HA, HSPG
LAIR1	Collagen	**NKp80**	AICL
NKR-P1A	LLT-1	**CD244 (2B4)**	CD48
AIRM1	Unknown	**DNAM-1**	PVR, CD122
		CD16	Fc portion of IgG

Abbreviations: AICL, activation-induced C-type lectin; AIRM1, adhesion inhibitory receptor 1; BAT-3, HLA-B-associated transcript 3; HA, hemagglutinin; HLA, human leukocyte antigen; HSPG, heparan sulphate proteoglycan; KLRG1, killer cell lectin-like receptor G1; LAIR1, leukocyte-associated immunoglobulin-like receptor 1; LILR, leukocyte immunoglobulin-like receptor; LLT-1, lectin-like transcript 1; MIC, MHC class I polypeptide-related sequence; NKR-P1A, NK receptor P1A; PR, polo virus receptor; ULBP, UL16 binding protein.

1.1.2.5ai Inhibitory receptors

Inhibitory receptors specific for both major histocompatibility complex (MHC) class I molecules (also known as the human leukocyte antigen (HLA) system) and non-MHC molecules are an important regulator of NK cell effector function. These ligands are expressed by most healthy cells in steady-state conditions and provide NK cells with a mechanism to ensure tolerance through inhibition of cytotoxicity (Morvan and Lanier 2016). Cells presenting MHC class I molecules interact with inhibitory receptors on NK cells and prevent activation to maintain tolerance to healthy cells (Figure 1.2a). One mechanisms of NK cell activation is through the 'missing self' hypothesis; virally infected or malignantly transformed cells often downregulate MHC class I expression to escape recognition by cytotoxic T cells however, this results in NK cell detection and attack. NK cells will attack any cell which loses or displays aberrant self-molecule expression due to the loss of inhibitory signals preventing NK cell activation (Kumar 2018) (Figure1.2b).

NK cells express two major classes of inhibitory receptors: killer cell immunoglobulin-like receptors (KIR) and CD94- natural killer group 2 member A (NKG2A) heterodimers. KIRs are type I transmembrane glycoproteins of the Ig superfamily which recognise HLA-A/B/C expression, while NKG2A is a type II transmembrane receptor with a C-type lectin-like scaffold

recognising the non-classical HLA-E (Kumar 2018) (Table 1.1). Both inhibitory receptors contain an immunoreceptor tyrosine-based inhibitory motif (ITIM) within their cytoplasmic domains which, upon receptor-ligand engagement, is phosphorylated by a Src family kinase, resulting in the recruitment and activation of tyrosine phosphatase Src homology region 2 domain-containing phosphatase-1 (SHP-1) and SHP-2. The recruitment of these tyrosine phosphatases to the interface between the NK and target cells leads to the suppression of NK cell activation through the dephosphorylation of factors which are required by nearby activating receptors, resulting in inhibition of degranulation, cytokine production and proliferation of NK cells. This inhibition of NK cell activity is transient and spatially localised so as to allow the same NK cell to become re-activated upon encountering a subsequent target cell lacking ligands for NK inhibitory receptors (Lanier 2008).

1.1.2.5aii Activating receptors

The lack of MHC class I expression on target cells is not sufficient to trigger NK cell activation; full NK cell activation also requires the expression and recognition of ligands for activating receptors whose expression is increased upon viral infection and malignant transformation of cells. This upregulation of stress-induced ligands on transformed or distressed cells overcomes the inhibitory signals delivered by MHC class I molecules, leading to NK cell activation (Paul and Lal 2017) (Figure 1.2c). Much like with inhibitory receptors, NK cells do not possess a single dominant activating receptor, but rather rely on a wide combinatorial array of activating receptors to initiate effector functions (Lanier 2008) (Table 1.1).

A majority of activating NK cell receptors including CD16, KIRs and the natural cytotoxicity receptors (NCRs) NKp30, NKp44 and NKp46 signal through immune-receptor tyrosine-based activation motifs (ITAMs) within their cytoplasmic domains. Tyrosine residues within the ITAMs associate with gamma chains of the high affinity IgE receptor FcεRI (FcεRI-γ), zeta chains of CD3 (CD3-ζ) and DNAX activation protein of 120kDa (DAP12) transmembrane-anchored proteins to form homo- and hetero-dimer signalling subunits. Engagement of these receptors results in the phosphorylation of the ITAM tyrosine, presumably by Src family members and subsequent binding of the tyrosine kinases SYK and zeta-chain-associated protein kinase 70 (ZAP-70), which in turn leads to signalling through a number of pathways including mitogen-activated protein kinase/ extracellular signal-related kinase (MAPK/ERK) and phosphoinositide 3-kinase/ protein kinase B (PI3K/Akt) to regulate actin reorganisation, cytokine and chemokine gene transcription and degranulation (Lanier 2008).

NKG2D is a type II transmembrane receptor that is only distantly related to the NKG2 family. NKG2D does not form a heterodimer with CD94, but instead forms a hexamer receptor complex by associating with two DAP10 homodimer signalling subunits. Ligands for NKG2D include homologues of MHC class I molecules which are regulated by both the heat shock response and DNA damage pathways (Lanier 2008). Upon activation, the p85 subunit of PI3K and the son of sevenless homolog 1 – vav guanine nucleotide exchange factor 1- growth factor receptor bound protein 2 (Sos-1-Vav1-Grb2) complex are recruited to the phosphorylate motif in the DAP10 domain, leading to the downstream activation of Guanosine-5'-triphosphate (GTP)ases, ERK, Akt and signal transducer and activator of transcription 5 (STAT5) which promote NK cell target adhesion and immunological synapse formation (Sutherland *et al.* 2002).

In addition to recognition of stress-related ligands, CD16 expression allows NK cells to recognise the constant Fc portion of IgG antibodies bound to specific antigens displayed on infected or transformed cells. Upon recognition, NK cells are able to kill these cells through a process termed antibody-dependent cell cytotoxicity (ADCC) (Morvan and Lanier 2016) (Figure 1.2d). CD16 is a potent activator of NK cells as demonstrated by studies using *Drosophila* cells reconstituted to express individual NK receptor ligands. Of the receptors NKG2D, DNAM-1 (CD226), CD244 and CD16, all were able to promote adhesion to the target cell upon activation however, CD16 was the only receptor capable of also inducing degranulation upon engagement (Bryceson *et al.* 2005; Bryceson *et al.* 2009).

1.1.2.5b NK cell activity

The interaction of an NK cell and a target cell either lacking in the appropriate inhibitory ligands for NK cell inhibitory receptors or expressing a number of activating ligands indicative of cellular stress results in the generation of an activating NK cell immunological synapse (Figure 1.2b-d). Contact with the target cell and the subsequent tightly controlled complex process of immunological synapse (IS) formation facilitates NK-induced target cell death through two critical effector mechanisms: direct lysis of cells through degranulation of lytic molecules into the cell and target cell death receptor ligation (Abel *et al.* 2018).

NK-mediated cytotoxicity can be divided into four major stages (Paul and Lal 2017): (1) formation of the IS between NK cell and target cell and stimulation of actin polymerisation and accumulation at the synapse; (2) polarisation and translocation of the microtubule organising centre towards the IS; (3) docking of secretory lysosome with the NK cell plasma membrane and (4) fusion of the lysosome with the plasma cell membrane and release of the lytic granules

into the target cell. NK cell lytic granules contain perforin, granzymes, Fas ligand (FasL; CD178), TNF-related apoptosis-inducing ligand (TRAIL), granulysin and small anti-microbial peptides. Following the release of these enzymes from the granules, perforin inserts itself into the membrane of the target cell where it oligomerises and generates pores which allows the subsequent delivery of apoptosis-inducing granzymes into the cytoplasm of the target cells (Abel *et al.* 2018). Granzymes are able to trigger apoptosis by both caspase-dependent and independent mechanisms. Granzyme B has been shown to directly cleave and activate caspase-3, -7, -8 and -10 (Adrain *et al.* 2005); in addition, granzymes B and K have also been shown to induce apoptosis through initiation of the mitochondrial apoptosis pathway (Adrain *et al.* 2005; Zhao *et al.* 2007). NK cells also induce the extrinsic apoptosis pathway through the fusion and expression of FasL and TRAIL on the NK cell membrane. Death receptors for FasL and TRAIL, Fas and TRAIL-R respectively, on target cells are ligated and subsequently activated, leading to the formation of the death-inducing signalling complex, activation of the caspase cascade and induction of target cell death (Guicciardi and Gores 2009).

In addition to their cytolytic function, activated NK cells are also effective producers of a wide range of pro-inflammatory cytokines including IFN-γ, TNF, granulocyte/monocyte colony-stimulating factor (GM-CSF) and IL-10 and chemokines such as chemokine (C-C motif) ligand 3 (CCL3), CCL4 and CCL5 (Paul and Lal 2017). These allow NK cells to mediate protective immunity by facilitating the activation of other innate immune cells such as neutrophils, macrophages and DCs and attracting effector myeloid and lymphoid cells to the sites of inflammation. Of these effector cytokines, IFN-γ, whose production and secretion has been linked to signalling through NKG2D and IL-12 produced by other innate immune cells, is one of the most potent and plays a crucial role in antibacterial, antiviral and anti-tumour immunity (Ortaldo *et al.* 2006).

1.1.3 Adaptive immune cells

The adaptive arm of the immune system is comprised of T and B cells, both of which arise from a common lymphoid progenitor within the bone marrow. Those which are destined to become T cells, cells responsible for cellular immunity, migrate to the thymus where they differentiate into early thymic progenitors which become reprogrammed into fully mature and functional T cells. B cells have the ability to transform into plasma cells responsible for producing antibodies and are therefore responsible for humoral immunity. B cell development occurs in the bone marrow within complex niches which provide the appropriate stimuli and factors to initiate B cell survival and differentiation. In adults new B cells are continually produced in the bone marrow, whilst development of new T cells in the thymus slows down and T cell numbers are maintained through division of mature T cells outside of the lymphoid organs (Cano and Lopera 2013).

1.1.3.1 B lymphocytes

B cells are the centre of the humoral compartment of adaptive immunity through their production of antigen-specific Ig antibodies which are capable of directly neutralising the infectivity of pathogens, activating the complement cascade and mediating ADCC and phagocytosis of infected cells via cells of the innate immune system (Smith and Crowe 2015). Additionally, B cells can act as APCs and secrete cytokines to strengthen innate and adaptive immune responses. B cells develop from a common lymphoid progenitor in the foetal liver and bone marrow and undergo diversification through the rearrangement of the Ig heavy and light chain gene loci to create a complete Ig molecule (Lebien and Tedder 2008). These surface IgM class Ig molecules, in association with Igα and Igβ form a unique B cell receptor (BCR) for antigen; BCRs which bind to self-antigens within the bone marrow are either deleted or edited in order to generate a state of central tolerance. After production in the bone marrow, immature IgM+ B cells migrate to secondary lymphoid organs such as lymph nodes and the spleen where they differentiate into long-lived follicular (FO) B cells or marginal zone (MZ) B cells. Upon binding of an antigen to the BCR by an APC, B cells can undergo either a T cell-independent or T cell-dependent activation process to form antibody-producing plasmablasts and long-lived plasma cells and memory B cells for immediate and more persistent protection, respectively (Yam-Puc *et al.* 2018). A third subtype, B1 cells, predominantly populate the peritoneal and pleural cavities and produce low affinity natural antibodies (nAbs) in the absence of exogenous antigenic stimulation (Hernandez and Holodick 2017).

1.1.3.2 T lymphocytes

T cells arise from committed lymphoid progenitors within the bone marrow and migrate to the thymus where they lose the potential to become B cells and NK cells and undergo differentiation, selection, and proliferation. Once in the thymus, the T cell precursors express a pre-T cell receptor (TCR) which is composed of a non-rearranging pre-Tα chain and a rearranged TCR β-chain. Successful pre-TCR expression leads to proliferation, upregulation of the CD4 and CD8 co-receptors and replacement of the pre-Tα chain with a newly rearranged TCR α-chain yielding a complete αβ TCR (Germain 2002). T cell progenitors can also rearrange TCR-γ and TCR- δ chains to generate γδ T cells, accounting for 0.5-5% of all T lymphocytes (Zhao *et al.* 2018). Upon successful rearrangement of a unique TCR, CD4+CD8+ double-positive cells interact with endogenous peptides presented on MHC class I and II molecules within the thymus to select an appropriate mature T cell repertoire for the host environment. Cells expressing TCRs that recognise self-ligands and generate an intermediate intensity signal upon TCR:MHC interaction undergo positive selection and

differentiate into either CD4+ or CD8+ mature T cells which then migrate into secondary lymphoid organs (Germain 2002).

1.1.3.2a Antigen presentation

T cells are key effector cells in the adaptive immune responses against infected and transformed cells and play crucial roles in autoimmunity, allergy, and transplant rejection; crucial to almost all of these functions is the activation and programming of T cells by APCs of the innate immune system (Pennock *et al.* 2013). Upon encountering a pathogen, mature APCs (DCs, macrophages, B cells) migrate into lymph nodes where they provide naïve T cells with three signals that will stimulate differentiation and proliferation of antigen-specific T cells with a range of functions appropriate for the immunological challenge (Kaiko *et al.* 2008)(Figure 1.3). The first signal is provided through the TCR by antigenic peptides bound to MHC class I and II molecules; the TCR is associated with the γ, δ and ε chains of the CD3 complex which mediates intracellular signalling through its ITAM domains upon TCR ligation. The second signal is mediated by co-stimulatory and co-inhibitory ligands on APCs through their respective receptors on T cells, the expression of which is programmed by pathogen-associated molecular patterns (PAMPs) and tissue factors released at the site of infection (Chen and Flies 2013). These ligands signal through their respective receptors on T cells and provide co-signals that direct T cell function and fine tune the T cell response to fit the inflammatory milieu in which it is stimulated. The release of polarising factors from APCs represents the third signal; inflammatory cytokine mediators are the predominant factor in directing the differentiation of T cells into an effector cell phenotype appropriate for the immunological response required (Kaiko *et al.* 2008). The successful activation and differentiation of antigen-specific T cells leads to clonal expansion of the cell populations as they rapidly begin to migrate to the site of infection. Upon successful elimination of the pathogen the majority of the T cells die, leaving behind a small population of memory T cells which are able to mediate a rapid immune response upon reinfection (Pennock *et al.* 2013).

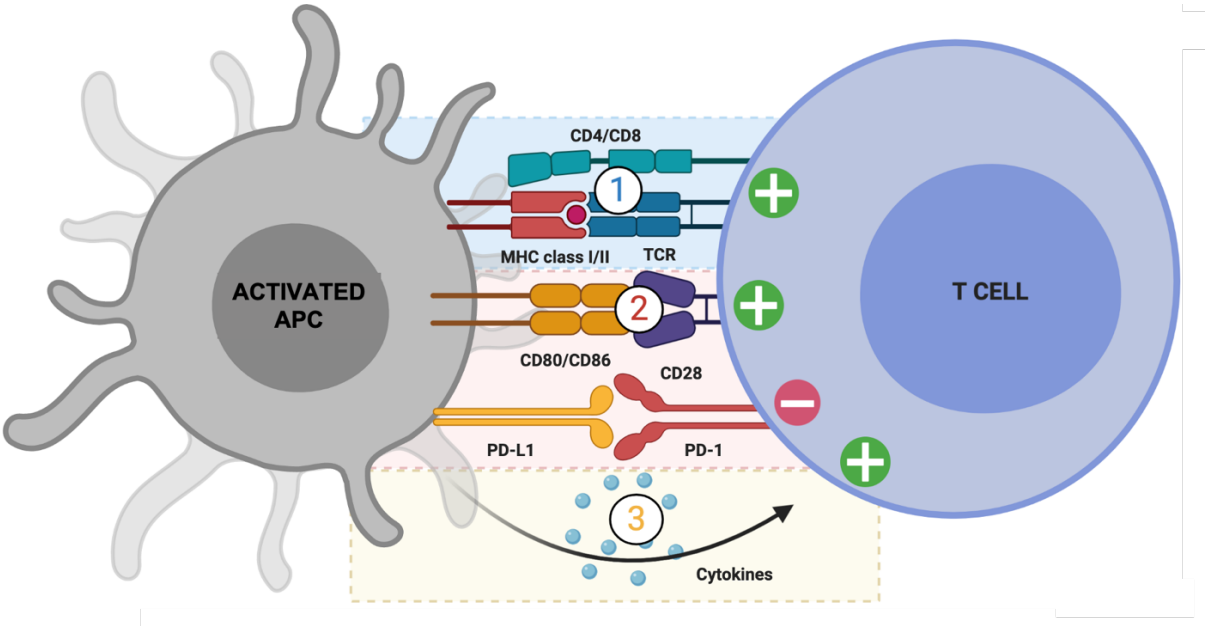

Figure 1.3 Schematic of antigen presentation and T cell activation by an antigen presenting cell.

The generation of an antigen-specific T cell requires 3 signals for effective activation: (1) antigen must be presented on an MHC class I/II molecule to the TCR; (2) co-stimulatory signals such as that of CD80/86 binding to CD28. Co-inhibitory signals such as PD-L1:PD-1 may also be present to fine tune the T cell response; (3) polarising factors such as inflammatory cytokines release by the APC. APC, antigen-presenting cell; MHC, major histocompatibility complex; PD-1, programmed cell death protein 1; PD-L1 programmed death ligand 1. Adapted from Willerslev-Olsen *et al.* (2013). Created in Biorender.com.

1.1.3.2b CD4+ helper T cells

CD4+ T cells, also known as Th cells, play a central role in the adaptive and innate immune responses; they do so through their capacity to assist B cells in making antibodies, by enhancing macrophage microbial activity, recruiting innate immune cells to sites of infection and through their production of chemokines and cytokines which augment both cellular and humoral immune responses (Zhu and Paul 2009). Naïve Th cells are activated through recognition of peptide antigens presented by MHC class II molecules and can differentiate into one of 7 phenotypes, with the nature and concentration of antigen, the type of APC, the cytokine environment and the presence and quantity of co-stimulatory molecules determining this fate decision. The seven lineages of Th cell are Th1, Th2, Th17, Th9, Th22, T follicular helper (Tfh) and induced regulatory T cells (Tregs), all of which are defined by their functions and cytokine profiles (Kennedy and Celis 2008).

Th1 cell differentiation is induced by IL-18, IL-12, and type 1 IFNs secreted by macrophages and DCs upon activation by intracellular pathogens. As critical regulators of type 1 immunity through their production of pro-inflammatory cytokines, Th1 cells can stimulate neighbouring cells like macrophages and DCs to elevate their phagocytic and antigen-presenting properties, further enhancing the immune response (Zhu and Paul 2009). Th2 cells mediate type 2 immunity and are induced by extracellular pathogens and allergens through secretion of IL-4, IL-11, IL-25 and IL-33 by eosinophils and mast cells. Th2 cells can induce immunoglobulin class switching to IgE which in turn activates cells of the innate immune system, such as mast cells and basophils, alongside stimulation of B cell proliferation and antibody production (Kaiko *et al.* 2008). Th17 cells are induced by IL-6, IL-21, IL-23 and TGF-β, they are responsible for mediating responses against extracellular bacteria and fungi through the production of IL-17, IL-22, TNF, and CCL20, and appear to be integral to the recruitment and activation of neutrophils to sites of infection. Th17 cells are primarily located in the digestive and pulmonary mucosa (Guéry and Huges 2015). Th9 cells produce IL-9 and IL-10 and are induced through the production of TGF-β and IL-4, with the secretion of IL-9 promoting the growth of mast cells and the secretion of pro-inflammatory cytokines. During infections by helminths and allergic processes Th9 cells also play an important role in the indirect induction of mucus production and eosinophil infiltration. The combination of IL-6 and TNF, with the participation of plasmacytoid DCs, is responsible for the generation of Th22 cells. Th22 cells are characterised by the production of IL-22 and TNF and are primarily associated with inflammation of the skin, with expression of chemokine receptor 4 (CCR4), CCR6 and CCR10 allowing infiltration into the epidermis wherein they play an important role in anti-microbial peptide production and wound healing (Cano and Lopera 2013). Tfh cells are located in the

germinal centre of secondary lymphoid tissues, with their differentiation dependent on IL-6, IL-12, and IL-21. Tfh cells are important regulators of B cell activity and can induce germinal centre formation, transform B cells into antibody-producing plasma cells, aid in the production of antibodies with different isotypes and in the production of memory B cells. Of all the Th subsets, Tfh cells express the greatest quantity of co-stimulatory molecules and possess the TCR with the highest affinity for antigen (King 2009).

1.1.3.2c CD4+CD25+Foxp3+ regulatory T cells

The existence of a highly immunosuppressive subset of CD4+CD25+ Forkhead box P3 (Foxp3)+ Tregs that serve to maintain immune homeostasis by actively suppressing the function of macrophages, DCs, B and T cells is a key mechanism by which the immune system limits excessive and inappropriate immune responses (Workman *et al.* 2009). Treg cells may develop in the thymus as functionally mature cells (natural Tregs; nTregs) as well as peripherally from conventional CD4+ T cells (induced Tregs; iTregs). nTregs constitutively express Foxp3, a forkhead family transcription factor that is a critical regulator of Treg development, function and homeostasis and possess a TCR that is of relatively high auto-affinity compared to that of conventional T cells. nTregs are predominant in the lymph nodes and bloodstream and are mainly involved in providing tolerance to self-antigens (Togashi *et al.* 2019). Peripherally, under certain conditions, CD4+ effector T cells in the presence of IL-2 and TGF-β begin to express Foxp3 and gain regulatory functions. iTreg TCRs recognise foreign antigens with high affinity and are induced in the absence of optimal co-stimulation and in states of chronic inflammation; such iTregs are most common in barrier tissues and prevent local excessive inflammation in the presence of exogenous antigens (Shevyrev and Tereshchenko 2020). The importance of Tregs in immune regulation first became apparent in humans, when it was found that deleterious mutations affecting Foxp3 resulted in the development of a fatal systemic autoimmune disorder known as Immune dysregulation polyendocrinoptahy Enteropathy X linked (IPEX) syndrome due to impaired development and/or dysfunction of Tregs (Workman *et al.* 2009). Tregs regulate the immune response and help maintain immune homeostasis through four modes of action: metabolic disruption, cytolysis, release of inhibitory cytokines and modulation of APC function (Workman *et al.* 2009; Togashi *et al.* 2019; Shevyrev and Tereshchenko 2020) (Figure 1.4).

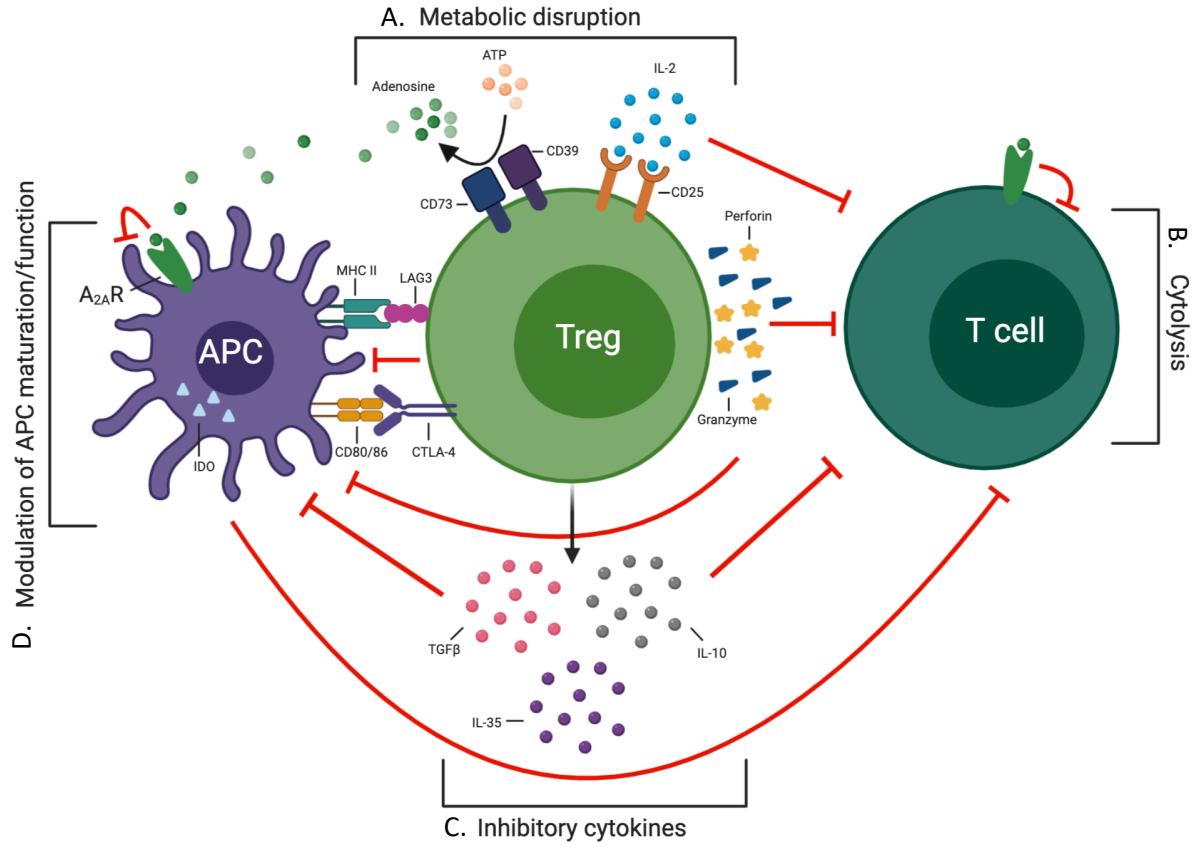

Figure 1.4. Schematic representation of the mechanisms of Treg-mediated immunosuppression.

Tregs possess an arsenal of regulatory mechanisms which can be categorised into 4 groups. (A) Metabolic disruption: ATP is degraded to the immunomodulatory metabolite adenosine by CD39/CD73, adenosine signals through the Adenosine A2A receptor on DCs and activated effector T cells to inhibit antigen presentation and suppress T cell proliferation. Due to high IL-2 receptor (IL-2R; CD25) expression, Tregs can deprive T cells of IL-2, thus inhibiting the CD8+ CTL proliferative response. (B) Cytolysis: Tregs are able to kill T cells and APCs through perforin-granzyme cytolysis. (C) Inhibitory cytokines: Tregs produce the immunosuppressive cytokines TGF-β, IL-10 and IL-35 which can suppress the activation and proliferation of effector T and B cells, directly induce iTregs and inhibit antigen presentation by APCs, which in turn enables iTreg induction. (D) Modulation of APC maturation/function: Tregs suppress effector cell activation by augmenting APC function, primarily though interaction of immune checkpoint molecules such as CTLA-4 and LAG3 which interact with CD80/86 and MHC class II, respectively, to reduce the ability of APCs to activate T cells. Tregs also mediate the production of IDO, which decreases the concentration of tryptophan available to induce effector T cell proliferation. APC, antigen-presenting cell; CTLA-4, cytotoxic T lymphocyte associated antigen 4; IDO, Indoleamine 2,3-dioxygenase; LAG3, lymphocyte-activation gene 3; TGF-β, transforming growth factor β; Treg, regulatory T cell. Adapted from Workman et al. (2009); Togashi et al. (2019); Shevyrev and Tereshchenko (2020). Created in Biorender.com.

1.1.3.2d CD8+ cytotoxic T cells

CD8+ T cells are highly cytotoxic cells which primarily function to kill infected or malignant cells in an antigen-dependent manner. Upon recognition of antigenic peptides presented by target cell MHC class I molecules, CD8+ T cells rapidly proliferate and differentiate into cytotoxic lymphocytes (CTLs) and memory CD8+ T cells (Reiser and Banerjee 2016). Terminally differentiated CTLs are IL-2 dependent and are highly cytotoxic, rapidly expressing IFN-γ, TNF, perforin and granzymes upon antigen recognition (Pipkin *et al.* 2010). CTLs can kill target cells by one of three distinct mechanisms, two of which involve direct cell-to-cell contacts, with the third mediated by cytokines such as IFN-γ and TNF which are produced and secreted for as long as TCR stimulation occurs. FasL expressed on the surface of CTLs can bind to Fas on target cells to trigger the classical caspase cascade, resulting in apoptosis of the target cell. The other mechanism requiring cell-to-cell contact is the synaptic exocytosis of lytic granules containing the pore-forming perforin which results in the degradation of the target cell membrane, and granzyme proteases which induce target cell apoptosis and eventual phagocytosis (Gulzar and Copeland 2005). The production of TNF and IFN-γ mediates further triggering of the caspase cascade and transcriptional activation of the MHC class I and Fas pathways, resulting in enhanced antigen presentation and Fas-mediated apoptosis (Andersen *et al.* 2006).

The generation of long-term immunity against viral and bacterial agents is dependent on the formation of large numbers of long-lived antigen-specific memory CD8+ T cells. These memory T cells exist in greater numbers than naïve CD8+ T cells and demonstrate an increased ability to survey peripheral sites for the presence of infection. Memory CD8+ T cells are poised to rapidly respond to secondary infections as they exist in a “pro-growth” state characterised by the maintenance of mRNA expression of several anti-viral cytokines, cytotoxic proteins, and chemokines, allowing these memory cells to expand and develop effector function faster than naïve CD8+ T cells. In humans, memory CD8+ T cells are maintained through self-renewal driven by IL-15 and IL-17 and can survive for over 50 years in humans in the absence of antigen (Joshi and Kaech 2008).

1.1.4 The cancer-immunity cycle

For a successful anti-tumour immune response to occur a series of self-sustaining stepwise events, collectively known as the cancer-immunity cycle, must be initiated in order for the immune system to obtain efficient control over the growth of the tumour (Chen and Mellman 2013) (Figure 1.5). In the first step, neoantigens generated through the loss of cellular regulatory processes and the accumulation of genetic alterations are released and captured

by DCs for processing. In order for this step to generate an anti-tumour immune response, the capture of antigens must be accompanied by pro-inflammatory immunogenic signals such as those from cell death; in the absence of such signals peripheral tolerance to the tumour may be induced. Next, DCs present the captured tumour antigens on MHC class I and II molecules to T cells (step 2), leading to the priming and activation of effector T cells (step 3) within tumour-draining lymph nodes or tertiary lymphoid structures. It is at this stage that the nature of the immune response is determined, in part, through the critical balance between production of effector T cells and Tregs which then traffic through the blood to the tumour (step 4). These tumour antigen-specific T cells then infiltrate the tumour (step 5) wherein they recognise the tumour cells through interaction between the TCR and its cognate antigen presented on a cancer cell MHC class I molecule (step 6). This interaction results in killing of the cancer cell (step 7) and subsequent release of additional tumour-associated antigens (step 1), thus continuing the revolutions of the cancer-immunity cycle (Chen and Mellman 2013; Chen and Mellman 2017).

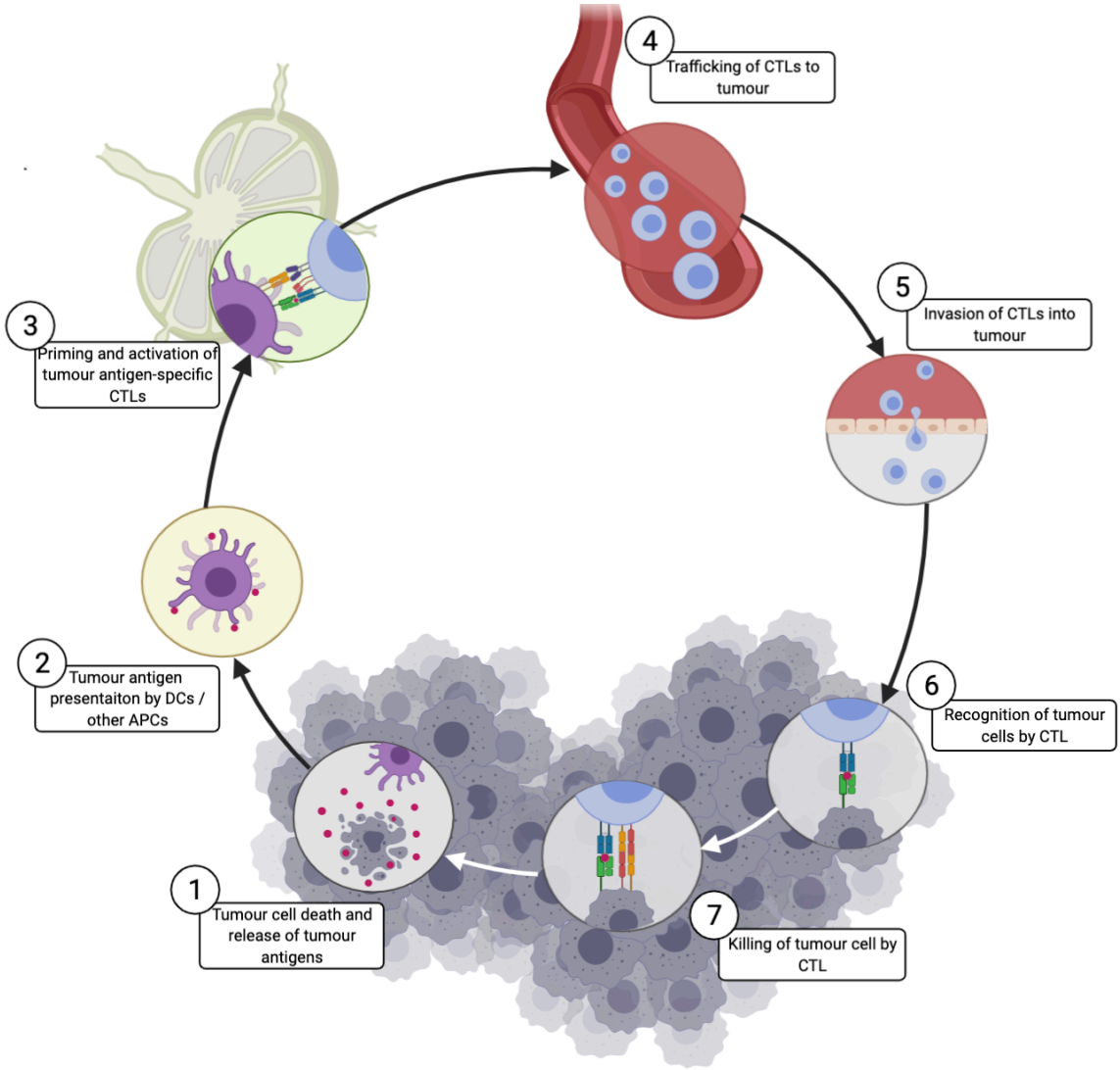

Figure. 1.5. The cancer immunity cycle.

The cancer-immunity cycle is a self-sustaining process which leads to the generation of an anti-tumour immune response. APCs, antigen presenting cells; CTLs, cytotoxic lymphocytes; DCs, dendritic cells. Adapted from Chen and Mellman (2013) & Pio et al. (2019). Created in Biorender.com.

1.1.4.1 Tumour associated antigens

CTLs are considered major drivers of anti-tumour immunity through their ability to directly kill tumour cells by recognition of tumour antigens. The first human tumour antigen recognised by CTLs was identified in melanoma and was designated melanoma-associated antigen (MAGE)-1 (Van Barren *et al.* 1991). Subsequently, several other MAGE family antigens and other cancer-germline antigen (CGA) families were characterised in a large variety of human cancer types, predominantly through isolation of CTL clones that were reactive to tumour cell lines (Durgeau *et al.* 2018). In more recent years, identification of mutations that result in novel protein formation have been identified by deep sequencing of the exome of individual tumours; these sequences are then analysed for potential MHC binding peptides and the resulting set of potential antigens tested for T cell reactivity. This technique has led to the identification of a large repertoire of tumour-specific antigens (neoantigens) across a wide range of cancer types (Schumacher and Schreiber 2015).

1.1.5 Cancer immunoediting

Persistent tumour growth may occur when the cancer-immunity cycle does not perform optimally. Antigens may not be detected, sufficient pro-inflammatory signals may not be present thus resulting in tolerance, T cells may not successfully home to or infiltrate the tumours and factors generated in the TME could suppress or alter the phenotype of the anti-tumour effector cells that are produced (Vinay *et al.* 2015). The subversion of infiltrating immune cell phenotypes combined with the multiple other mechanisms employed by the tumour and TME to prevent effective anti-tumour immunity have made it clear that cancer immunosurveillance and the cancer immunity cycle represent just one dimension of the complex relationship between tumour cells and the immune system.

Developments throughout the last 20 years now clearly demonstrate that the immune system can also promote the emergence of tumours with reduced immunogenicity that possess the ability to evade immune detection and destruction (Dunn *et al.* 2004). A landmark study in 2001 using chemically induced sarcomas grown in RAG2$^{-/-}$ immunodeficient and wild-type (WT) mice demonstrated that tumours grown in the presence of an intact immune system were capable of establishing tumours upon transplantation into naïve immunocompetent mice. In contrast, a majority of the tumours grown in the absence of an intact immune system were rejected upon transplantation, thus demonstrating that tumours formed in the face of immune pressures are less immunogenic than those arising in immunodeficient mice. This suggested that the immune system was responsible for shaping the immunogenicity of the tumours, with the immune response ultimately working to select those cells which were capable to surviving

immune attack (Shankaran *et al.* 2001). These findings prompted the development of the cancer immunoediting hypothesis to more broadly acknowledge the potential tumour-destructive and tumour-sculpting functions of the immune system during tumour development. This dynamic process is composed of three phases: elimination, equilibrium and escape (Schreiber *et al.* 2011) (Figure 1.6).

1.1.5.1 Elimination

The elimination phase represents the original concept of cancer immunosurveillance, in which immune cells work to detect transformed cells that have escaped cell-intrinsic mechanisms of tumour suppression and eliminate them before they become clinically apparent (Schreiber *et al.* 2011)(Figure 1.6a). This process requires a coordinated and balanced activation of innate immune cells, combined with the additional expression of tumour antigens and "danger signals" capable of promoting the maturation and migration of DCs to tumour draining lymph nodes, resulting in the activation and expansion of effector CD4 and CD8 T cells (Kim 2007). If the transformed cells are successfully eliminated this represents the endpoint of the immunoediting process.

1.1.5.2 Equilibrium

In cases where the tumour is not successfully eradicated in the elimination phase the surviving tumour subclones enter a dynamic equilibrium phase with the host immune system, wherein anti-tumour immunity contains but does not fully eradicate the heterogenous tumour cell population (Dunn *et al.* 2004)(Figure 1.6b). Evidence that the host immune system could hold tumour cells in an equilibrium state came from primary tumorigenesis mouse studies in which immunocompetent mice treated with low doses of the chemical carcinogen 3'-methylcholantherene (MCA) harboured tumour cells for extended periods of time without developing apparent tumours. Upon ablation of T cells and IFN-γ using monoclonal antibodies (mABs), sarcomas rapidly grew at the original injection sites in half of the mice; in contrast mABs that depleted NK cells and blocked their recognition and function failed to cause the progression of tumours (Koebel *et al.* 2007). Therefore adaptive, not innate, immunity is responsible for immunologically restraining tumour growth, thus distinguishing the equilibrium phase from the elimination phase in which both innate and adaptive immunity are required. Clinically, the equilibrium phase has been demonstrated by the transmission of tumours from organ donors to organ transplant recipients wherein the pharmacological suppression of the host immune system facilitates the progression and outgrowth of donor tumour cells that were restrained in the intact immune system of the donor (Chapman *et al.* 2013).

Equilibrium can extend through the life of the host and may represent a second endpoint in the process. However, during the equilibrium phase the potent selection pressure exerted onto the heterogenous tumour cell population containing genetically unstable and rapidly mutating cells can lead to the immune selection of tumour subclones with reduced immunogenicity. Those cells which are capable of surviving in an immunocompetent host emerge from the equilibrium phase conditioned and shaped by the host immune system into tumour cells which can now progress into the escape phase and present as clinically apparent disease (Dunn *et al.* 2002).

1.1.5.3 Escape

In the final stage of immunoediting, surviving tumour cell variants that have acquired genetic and epigenetic changes which provide them with the ability to evade detection and elimination by the immune system are able to emerge as clinically apparent disease. This escape from detection and elimination in an immunologically intact environment allows for the unrestrained growth of the tumour, with the tumours likely to be capable of evading both the innate and adaptive immune compartments (Dunn *et al.* 2004) (Figure 1.6c). The mechanisms of tumour cell escape can be classified into three main categories: i) downregulation or loss of strong tumour antigens and antigen-presenting machinery, or a lack of co-stimulatory molecules, resulting in reduced immune recognition and stimulation; ii) upregulation of resistance mechanisms against the cytotoxic effects of immunity and iii) establishment of an immunosuppressive TME through induction of suppressive immune cells, production of anti-inflammatory cytokines and expression of immune inhibitory ligands such as immune checkpoints (Teng *et al.* 2015).

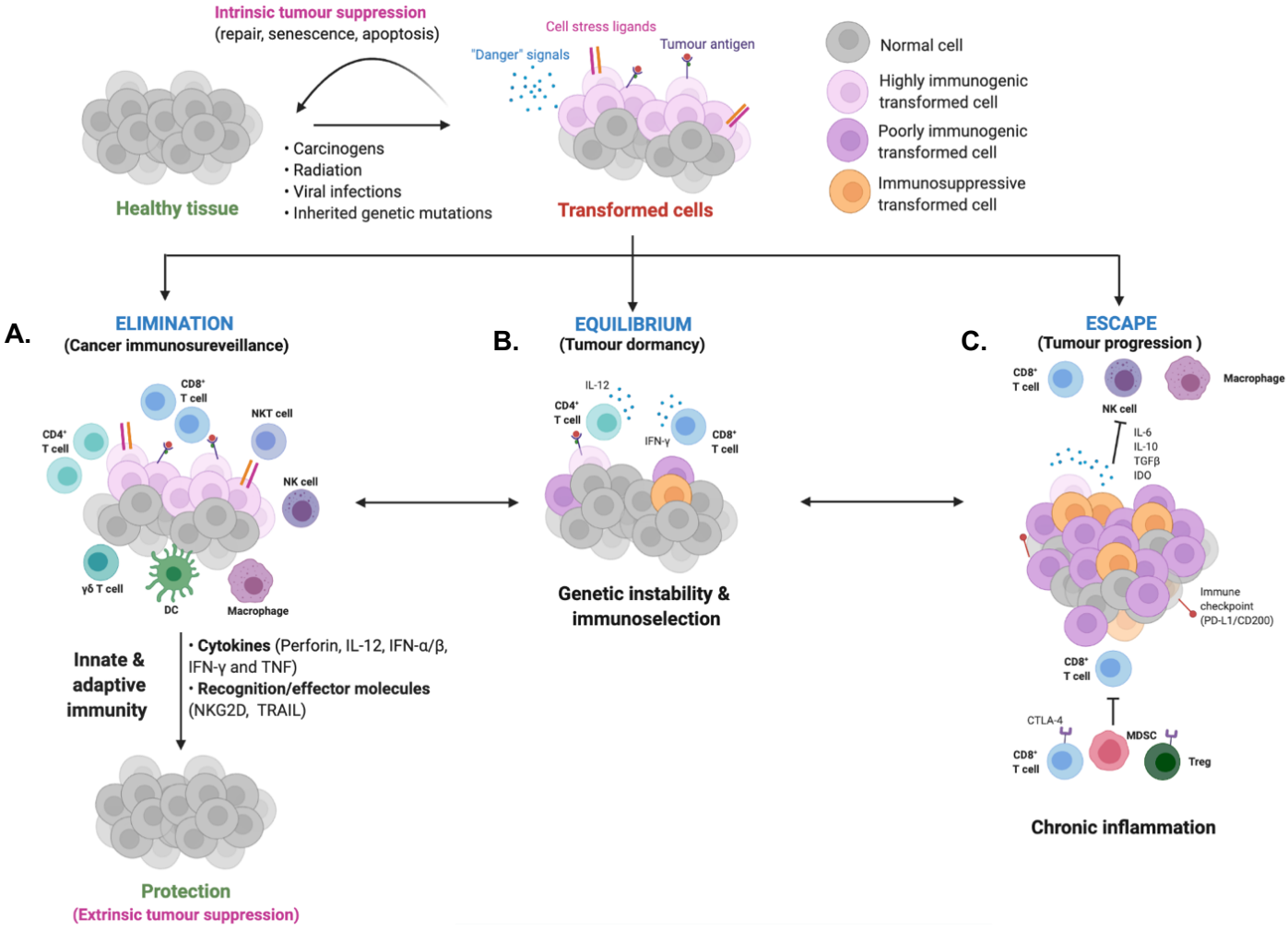

Figure. 1.6 Cancer immune editing.

The three phases of cancer immunoediting. Normal healthy cells which become mutated following a loss of intrinsic tumour suppression mechanism transform into tumour cells. (A) The immune system may act as an extrinsic tumour suppressor to identify and eliminate tumour cells. These highly immunogenic cells express high levels of cell stress ligands and tumour antigens, making them recognisable to both the innate and adaptive immune system. In this elimination phase, cells of the innate and adaptive immune system recognise transformed cells and destroy them. However, if the immune system is unable to completely eliminate the transformed cells, surviving tumour cell variants may enter the equilibrium phase. (B) In the equilibrium phase, tumour cells are either maintained chronically in an equilibrium state upon which cells of the adaptive immune system prevent further growth of the tumour or become immunologically sculpted into a population of cells with reduced immunogenicity. (C) These poorly immunogenic and immunosuppressive cell variants may eventually acquire further mutations which allow them to escape from immune control and become clinically detectable. There are several mechanisms that the tumour cells can utilise to escape immune control including: decreased immune recognition, increased resistant to immune effector responses and the generation of an immunosuppressive TME through the recruitment and subversion of immunosuppressive immune cells, expression of negative co-stimulatory immune checkpoints and immunosuppressive cytokines. CTLA-4, cytotoxic T lymphocyte associated antigen 4; DC, dendritic cell; MDSC, myeloid derived suppressor cell; NK, natural killer; NKT, natural killer T; PD-1, programmed death receptor 1; Treg, regulatory T cell. Adapted from Vesely et al. (2011) & Vinay et al. (2015). Created in Biorender.com.

1.1.6 Mechanisms of immune escape

Tumour cells undergoing continuous remodelling at the genetic, epigenetic, and metabolic levels generate the critical modifications necessary for these cells to escape both innate and adaptive immune control, thus leading to the malignant progression and growth of the tumour in the face of a competent immune system. Tumour cell escape can result from changes at the level of the tumour through inhibition of immune cell recognition and the selection of tumour variants that are resistant to immune effectors or through the induction and recruitment of distinctive immunosuppressive immune cells and cytokines within the TME which prevent an effective anti-tumour immune response, as outlined below. The identification of these escape mechanisms and the elucidation of the functional mechanisms underlying the promotion of an immunosuppressive TME provides the basis for the generation of several different immunotherapeutic strategies (Vesely *et al.* 2011).

1.1.6.1 Decreased immune recognition

The ability of the immune system to discriminate malignant cells from healthy ones relies, at least in part, on the antigenicity of tumour cells; in other words, the ability of tumour cells to express and present antigens in the form of MHC-antigen complexes on their cell surface that are recognised by antigen-specific T cells (Allard *et al.* 2018). Cells which are presenting foreign or other immunogenic antigens are subsequently identified and eliminated by T cells. Although tumours originate initially from a single transformed cell, the genetic instability generally results in a genetically heterogenous tumour with tumour cells expressing a wide variety of antigens which are unevenly distributed and induce different immune responses. Tumours with high mutational burdens, such as melanoma and non-small cell lung carcinoma (NSCLC), are theoretically more antigenic and generate a TME with increased immunogenicity. However, in order to avoid recognition and destruction by the immune system, many tumours evolve towards reduced antigenicity, often in a dynamic process induced by immune attack (Vinay *et al.* 2015). There are several mechanisms by which tumour cell variants can reduce their recognition by immune cells; through depletion or mutation of antigens on their cell surface, reducing the cell surface expression of MHC I or through mutations of components of the antigen presentation machinery (APM) (Jhunjhunwala *et al.* 2021).

One of the main mechanisms to reduce tumour antigenicity and subsequent immune recognition involves downregulation of MHC class I molecules on the cell surface. MHC class I molecules and most of the other components of the APM are not essential for cell survival and growth, therefore tumour cells can down-regulate or mutate various components of the

APM to reduce or completely prevent antigen presentation without impairing the ability of the tumour to grow and metastasise. Downregulation of expression of MHC class I has been observed in 20-60% of patients with melanoma, lung, prostate and breast cancers, with MHC class I expression an independent prognostic factor in many cancers (Campoli and Ferrone 2008; Zhao *et al.* 2017). Furthermore, several tumour antigens are a by-product of dysregulation of expression of their encoding genes and the majority of neoantigens are derived from passenger mutations that are dispensable to the tumour. Therefore, if these immunogenic antigens presented on the cell surface are non-essential for cell survival, the tumour cells can lose or mutate these antigens to decrease their antigenicity and evade immune recognition (Jhunjhunwala *et al.* 2021).

Downregulation of antigen presentation and an enhanced ability to escape from T cell killing is also seen in normal tissue stem cells to protect the rare stem cell pool and ensure that the functionality of the tissue is sustained during times of physiologic need. Regulation of quiescence, differentiation, and self-renewal are all key to ensuring long-lived stem cells can evade immune surveillance. Slow-cycling, non-proliferating stem cells of the hair follicle are devoid of MHC class I expression and β2-microglobulin expression, which is required for proper MHC class I formation and expression at the cell surface, suggesting that these quiescent cells demonstrate decreased antigen presenting capacity (Agudo *et al.* 2018). These molecular programs that control the function and phenotype of stem cells are also present in subsets of tumour cells termed cancer stem cells. Cancer stem cells (CSCs) are cancer-initiating cells responsible for tumour initiation, progression and metastasis through their enhanced self-renewal capacity and pluripotent ability. CSCs can derive from normal stem cells, suggesting that through co-opting of the immune evasion properties of quiescent stem cells, CSCs may be the earliest tumour cells to evade immune surveillance. Indeed, it has been demonstrated that the immune evasion of metastatic tumour cells is directly correlated with a slow-cycling stem-cell-like state, with the immune privileged status of these cells linked to their ability to enter a quiescent state, with MHC class I expression and subsequent immune recognition re-instated upon proliferation of these cells (Malladi *et al.*2016)

In principle, MHC class I loss should result in NK cell mediated-killing of these cells through the missing self-process and yet there is no evidence that MHC I negative tumours are infiltrated with more NK cells than those which are MHC class I sufficient (Lin and Yan 2018). Despite NK cells being a potential second line of defence against these tumours, there are several mechanisms by which tumour cells effective in downregulation of antigen presentation

can also evade NK cells and interfere with the effectiveness of NK cell anti-tumour activity to overcome missing-self surveillance by NK cells (Dhatchinamoorthy *et al.* 2021).

1.1.6.2 Immune resistance

Tumour cells which continue to express tumour antigens and are unable to avoid immune cell detection may develop mechanisms to evade immune-mediated killing. Cell variants can become resistant to the cytotoxic effects of immune effector cells through the expression of anti-apoptotic molecules such as FLIP and B cell lymphoma extra-large (BCL-XL) or through the persistent activation of pro-oncogenic transcription factors such as STAT3. Alternatively, cells can become resistant to lysis by CTLs and NK cells through the downregulation and mutation of death receptors such as the TRAIL death receptor 5 (DR5) (Vesely *et al.* 2011).

1.1.6.3 Immunosuppressive TME

The development of a locally immunosuppressive TME is a primary cause of tumour immune escape. The TME is a highly complex and heterogenous ecosystem in which tumour cells co-exist and interact with the extracellular matrix, fibroblasts, endothelial cells, tumour vasculature, lymphatics and infiltrating immune cells. Interactions between the tumour cells and the surrounding cells of the TME, in particular the immune cell component, are fundamental in determining tumour growth, invasion and metastasis (Giraldo *et al.* 2019). A variety of innate (macrophages, neutrophils, eosinophils, mast cells, NK cells, DCs) and adaptive (T cells, B cells) immune cells can infiltrate tumours, with their composition and organisation within the TME strongly associated with the clinical outcomes of patients. The abundance and activation state of these cells, along with their production of cytokines, chemokines, cytotoxic mediators and immune modulators all affect the balance between anti-tumour immunity and an inflammatory pro-tumour environment (Hui and Chen 2015). Immune cells which have been recruited to the TME can communicate with the tumour via secretion of regulatory cytokines, growth factors and proteases which work together to alter the phenotype of the immune infiltrate and further recruit regulatory cells to prevent an effective anti-tumour immune response (Liu and Cao 2016).

1.1.6.3.1 Innate immune cells in the TME

Despite being the first effectors against malignantly transformed cells, innate immune cells are also one of the major sources of angiogenic factors, growth factors, matrix-remodelling enzymes, and anti-inflammatory mediators within the TME. Therefore, although initially recruited to these sites to destroy malignant cells, due to the plasticity of these cells, tumours

are able to recruit and subvert these cells to promote tumour growth, invasion and metastasis (Berraondo *et al.* 2016).

1.1.6.3.1a Tumour associated neutrophils

Chemotactic factors such as IL-8, C-X-C motif chemokine ligand 8 (CXCL8) and TGF-β are secreted by various cells within the TME to recruit circulating neutrophils which, upon entry into an inflammatory and hypoxic TME, become long-lived tumour-associated neutrophils (TANs) (Coffelt *et al.* 2016). TANs have been demonstrated to play an important role in the initiation of inflammation-induced tumours and through the production of pro-tumour cytokines, reactive oxygen species, and proteinases such as cathepsin G, matrix metalloproteinases (MMP)-8/9, proteinase-3 and neutrophil elastase, are capable of promoting tumour angiogenesis, growth and invasion (Houghton 2010). TANs possess both pro- and anti-tumour functions, with chemical stimuli within the TME determining the TAN response. The presence of the anti-inflammatory cytokine TGF-β has been shown to drive the development of pro-tumour TANs which are capable of suppressing CTL responses; in the absence of TGF-β TANs were able to promote CTL responses through the production of pro-inflammatory factors such as TNF, nitric oxide and CCL3 (Fridlender et al. 2009). Furthermore, TANs harvested from melanoma and fibrosarcoma tumours in IFN-β deficient mice demonstrated increased expression of the pro-angiogenic factors vascular endothelial growth factor (VEGF), MMP9 and the homing receptor C-X-C chemokine receptor type 4 (CXCR4); the expression of which was reduced to control levels upon treatment with IFN- β, suggesting IFN-β inhibits tumour angiogenesis and is an important suppressor of angiogenic and homing factors in TANs (Jablonska et al. 2010). These studies highlight the functional plasticity of TANs and gave rise to the suggestion that unlike T cells and macrophages, which are associated with functional subsets due to transcriptional changes, TANs represent various functional activation states; these TAN states are characterised by their levels of activation and immunogenic factor production in response to stimuli within the TME rather than committed genomic phenotypic changes (Gregory and Houghton 2011). Although the prognostic and predictive power of neutrophil infiltration is variable, meta-analysis of tumour gene expression profiles from 18 000 patients identified TANs as the most significant adverse cancer-wide prognostic immune population (Gentles et al. 2015).

1.1.6.3.1b Tumour associated macrophages

The high phenotypic plasticity of monocytes recruited to the TME through the production of growth factors and chemoattractants results in the generation of classically activated M1 and alternatively activated M2 tumour associated macrophages (TAMs). Exposure of monocytes

to M-CSF and GM-CSF promotes macrophage differentiation, with Th1 and Th2 cytokines present in the TME ultimately resulting in the polarisation of uncommitted M0 macrophages into M1 and M2 states, respectively (Noy and Pollard 2014). A TME rich in anti-inflammatory mediators such as IL-4, IL-10, IL-13 and TGF-β promotes M2 polarisation whilst IFN-γ and TNF are strong stimulators of M1 polarisation (Mantovani *et al.* 2017). M1 macrophages have been observed to produce pro-inflammatory cytokines such as IL-23, IL-2, TNF and IL-2 and can promote anti-tumour CD8+ T cell responses. Conversely, M2-like macrophages produce anti-inflammatory cytokines such as IL-10 and TGF-β which have been shown to suppress CTL activity and facilitate tumour growth, angiogenesis and metastasis (Mantovani *et al.* 2017). Although generally greater densities of TAM are associated with advanced disease stage and worse overall survival in many cancers, it is suggested that identification of the M1:M2 ratio is a more relevant prognostic marker (Jayasingam *et al.* 2020). In NSCLC, patients whose TAMs were predominantly of an M1-like phenotype demonstrated extended survival compared to those enriched with M2-like phenotypes (Ohri *et al.* 2009). Similarly, cervical cancer patients with a greater M1:M2 ratio demonstrated greater response to chemoradiation and increased survival compared to those with a predominantly M2 phenotype (Petrillo *et al.* 2015).

1.1.6.3.1c Myeloid-derived suppressor cells

Myelopoiesis is the process which generates activated neutrophils, macrophages and DCs from a common myeloid progenitor. Classic activation of these cells occurs in response to strong signals from pathogens, primarily in the form of PAMPs and DAMPs, resulting in robust phagocytosis, respiratory bursts, and the production of pro-inflammatory cytokines. This response is relatively short-lived and resolves upon cessation of the stimuli. By contrast, during unresolved inflammation such as that in persistent infection or cancer, the relatively weak and long-lived signals result in the induction of modest but persistent myelopoiesis (Gabrilovich 2017). Myeloid cells generated under these conditions possess an immature morphology and phenotype, weak phagocytic ability, increased background levels of reactive oxygen species and nitric oxide and increased anti-inflammatory cytokine production. These pathologically activated myeloid cells, known as myeloid-derived suppressor cells (MDSC), support tumour growth and inhibit anti-tumour immunity. MDSCs are a heterogenous group of cells consisting of two main types: polymorphonuclear MDSCs (PMN-MDSC) which are morphologically and phenotypically similar to neutrophils, and monocytic MDSCs (M-MDSCs) which are similar to monocytes (Veglia *et al.* 2018).

Although in the early stages of cancer MDSCs are rarely detected, two distinct types of signals from the tumour and surrounding stroma result in the gradual accumulation of MDSCs within the TME as the tumour progresses. The first group of signals is driven by tumour-derived factors such as GM-CSF,G-CSF and VEGF and are responsible for the expansion of immature myeloid cells and the inhibition of their terminal differentiation (Veglia *et al.* 2018). The second group of signals is mediated by inflammatory cytokines such as IFN-γ, IL-1β, IL-4, IL-6, IL-13 and TNF in the TME and are responsible for the pathological activation of MDSCs and subsequent immune suppression and promotion of tumour progression (Gabrilovich 2017). MDSCs negatively regulate the immune response through suppression of T cell proliferation, attenuation of T cell and NK cell cytotoxicity, and polarisation of immunity towards a tumour-promoting type 2 response; furthermore, MDSCs can promote tumour angiogenesis and metastasis (Rodriguez *et al.* 2002; Suzuki *et al.* 2005; Sinha *et al.* 2007; Condamine *et al.* 2015).

1.1.6.3.1d Tumour associated DCs

The primary role of DCs in tumour immunity is to activate an anti-tumour T cell response by endocytosing cellular debris and dead neoplastic cells within the TME to process tumour antigens (Gardner and Ruffell 2016). In addition, immature DCs have demonstrated direct cytotoxic activity against tumour cells *in vitro* (Liu *et al.* 2001; Janjic *et al.* 2002). Despite only constituting a minority of the myeloid cells within the TME, DCs are significantly associated with greater overall survival across multiple cancer types including breast cancer, lung adenocarcinoma and head and neck squamous cell carcinoma (SCC)(Broz *et al.* 2014). However, it is now well established that a majority of tumour associated DCs are defective in their functional activity and are poor stimulators of an immune response due to a number of mechanisms utilised by the tumour and the TME to prevent an anti-tumour immune response (Lee and Radford 2019). DC activity can be subverted at an early stage through inhibition of initial DC priming through tumour cell secretion of sterol metabolites which suppress expression of CCR7 on the surface of DCs, thus disrupting DC migration to the lymph nodes (Villablanca *et al.* 2010). Furthermore, tumour cells can secrete IL-10 which can reduce the capacity of DCs to process antigens and skew the generation of T cell responses towards a type 2 immune response (Aruga *et al.* 1997). Signals within the TME can also subvert the differentiation of monocytes to macrophages, prevent efficient DC maturation and suppress DC function through metabolic dysfunction (Palucka and Banchereau 2012).

1.1.6.3.1e Tumour associated NK cells

Upon neoplastic transformation cells often demonstrate low expression of ligands for NK cell inhibitory receptors in combination with increased expression of ligands for activating receptors, resulting in direct lysis of the tumour cells by NK cells (Pahl and Cerwenka 2017). In addition to spontaneously detecting and killing tumour cells, the release of chemokines such as CCL5, XCL-1 and XCL-2 by NK cells has been demonstrated to recruit DCs and prime their function to mount an antigen-specific adaptive immune response *in vivo* (Böttcher *et al.* 2018). The importance of NK cells in anti-tumour immunity was initially highlighted by a number of mouse models in which mice lacking NK cell function demonstrated increased tumour growth and metastasis of solid and haematological tumours (Talmadge *et al.* 1980; Cerwenka *et al.* 2001; Kelly *et al.* 2002). Clinically, NK cell activity has been inversely correlated with cancer incidence as demonstrated by an 11-year epidemiological study which reported that individuals with low NK cell cytotoxic activity had a significantly higher risk of developing cancer (Imai *et al.* 2000). Furthermore in lung, gastric, colorectal and breast cancers high numbers of tumour-infiltrating NK cells are significantly associated with better patient outcomes, highlighting the fundamental role NK cells play in controlling tumour growth (Stojanovic and Cerwenka 2011; Böttcher *et al.* 2018).

Unlike other tumour associated innate immune cells, NK cells themselves do not appear to subvert into a pro-tumour phenotype but rather factors within the TME cause NK exhaustion resulting in inefficient anti-tumour effector function. Adoptive transfer of NK cells into NK-sensitive tumours *in vivo* failed to suppress tumour growth despite successful homing to the TME and an initial enhancement of anti-tumour activity. Isolated NK cells demonstrated a loss of IFN-γ production early after transfer, with reductions in activating receptor expression and decreased cytotoxic activity progressing with prolonged tumour exposure. These functional changes were associated with an increase in homeostatic NK cell proliferation, suggesting that factors within the TME caused a proliferation-induced exhausted NK phenotype (Gill *et al.* 2012). Furthermore, NK cells isolated from the TMEs of pancreatic, colorectal, liver and NSCLC patients demonstrate reduced cytolytic and cytotoxic activity *in vitro*, as evidenced by a reduction in the cytolytic mediators granzyme, perforin, FasL and TRAIL and an impaired ability to produce IFN-γ upon stimulation when compared with NK cells isolated from peripheral blood or peri-tumoral regions (Platonova *et al.* 2011; Peng *et al.* 2013; Sun *et al.* 2017). Factors such as tumour-associated exosomes and TGF-β, and TME characteristics such as hypoxia have been identified as mediators of NK cell exhaustion, with their presence associated with reductions in activating receptor expression, suppression of IFN-γ and TNF production and decreased degranulation (Bi and Tian 2017).

1.1.6.3.2 Adaptive immune cells in the TME

1.1.6.3.2a B lymphocytes

B cells represent an important proportion of infiltrating immune cells, accounting for up to 25% of immune cells within the TME of breast, ovarian, renal and NSCLC tumours (Largeot *et al.* 2019). In the majority of cases, B cell infiltration is associated with good prognosis; tumour-infiltrating B cells were identified as the second-best predictor of increased survival in a study of metastatic melanoma and tumour-infiltrating B cells correlated with lower relapse rates and increased survival in cervical and lung cancer, respectively (Al-Shibli *et al.* 2008; Nedergaard *et al.* 2008; Erdag *et al.* 2012). B cells play critical roles in anti-tumour immunity through the production of antibodies, secretion of inflammatory cytokines, and by acting as APCs to trigger an active T cell response. Antibodies directed against tumour antigens can lead to tumour cell killing through activation of the complement cascade, phagocytosis by macrophages, and NK cell lysis via ADCC (Yuen *et al.* 2016).

Alongside anti-tumour activity, mainly through the production of antibodies, B cells can also be mediators of tumour growth. Circulating immune complexes, comprised of antibodies bound to a soluble antigen, are detected in the circulation and tumour tissue in many cancers and are known to induce tumour-promoting inflammation through their recognition by Fc receptors on innate immune cells (Andreu *et al.* 2010). Furthermore, tumour-associated B cells can produce VEGF within the TME, leading to increased angiogenesis (Yang *et al.* 2013). In addition, a diverse subset of regulatory B cells (Bregs) can acquire regulatory activity and maintain immune tolerance within the TME, either directly through the secretion of IL-10 or indirectly through the prediction of TGF-β and the inhibition of CD4+ T cell proliferation and conversion of resting CD4+ T cells into Tregs (Largeot *et al.* 2019). The differentiation of B cells into Bregs within the TME can be directly influenced by metabolites and cytokines produced by tumour cells and by tumour-derived extracellular vesicles containing growth factors (Ye *et al.* 2018; Largeot *et al.* 2019). The hypoxic condition of the TME can also generate hypoxia-inducible factors which suppress anti-tumour B cell proliferation and antibody production (Caro-Maldonado *et al.* 2014).

1.1.6.3.2b T lymphocytes

1.1.6.3.2bi CD4+ helper T cells

CD4+ Th cells are highly versatile, polyfunctional cells that can differentiate into one of several functional subtypes in response to context-dependent signals within the TME. Th1 cells are dependent on IL-2 and IFN-γ for their generation; IL-12 recruits NK cells to produce IFN-γ which together leads to the activation of Th1 differentiation by suppressing Th2 and Th17

formation (Basu *et al.* 2021). Th1 cells are primarily responsible for activating and regulating the development of an antigen-specific CTL response (Giuntoli *et al.* 2002). Furthermore, IFN-γ produced by Th1 cells activates APCs to upregulate MHC class I to increase antigen presentation to CTLs and induces the production of opsonising antibodies which further enhance tumour cell uptake by APCs (Knutson and Disis 2005). In addition to these indirect effects, Th1 cells can also directly kill tumour cells through interaction with MHC class II molecules; upon recognition of antigens Th1 cells then use the Fas/FasL and TRAIL apoptosis or granzyme-perforin lysis pathways to directly kill tumour cells (Thomas and Hersey 1998; Echchakir *et al.* 2000). Recent comprehensive mass cytometric analysis of immune subsets in cancer immunity highlighted that peripheral activated effector memory Th1 cells were capable of orchestrating potent anti-tumour immunity, with these cells demonstrating significantly greater protection than CD8+ T cells when transplanted into tumour-bearing mice (Spitzer *et al.* 2017).

Th2 cells are not directly cytotoxic and favour a predominantly humoral immune response. Promoted by IL-4 signals in the absence of IL-12, Th2 cells mediate effector functions through secretion of type 2 cytokines. Whilst IL-4, IL-5 and IL-13 have been demonstrated to contribute to tumour growth and metastasis, IL-10 mediates inhibition of APC antigen processing and presentation and activates immunosuppressive Tregs within the TME. Conversely, Th2 cells can also activate the innate immune system through recruitment of macrophages, granulocytes, eosinophils, and NK cells to tumour sites suggesting a role for Th2 cells in anti-tumour immunity (Chraa *et al.* 2019).

Although abundant in mucosal tissues, Th17 cell comprise a small population in the peripheral blood (~0.1%) (Kagami *et al.* 2010). However, upon malignant transformation, tumours demonstrate a significant increase in Th17 cell infiltration, suggesting that cells within the tumour produce factors which promote Th17 cell trafficking to the TME. Although important in infectious immunity and the pathogenesis of autoimmune disease, the role of Th17 cells in the TME is still ambiguous. Several studies have demonstrated that Th17 cells have dual roles in tumorigenesis, with their presence associated with increases in anti-tumour NK and CTL activity as well as the promotion of tumour development through activation of tumour angiogenesis. Inflammatory cytokines secreted by Th17 cells, such as IL-17A, IL-17F, IL-21 and IL-22 mediate tumour growth by driving angiogenesis and suppressing anti-tumour immunity, whilst secretion of IL-17F, IL-21 and IL-22 has also been associated with anti-angiogenic activity. The ability of Th17 cells to possess either inflammatory or regulatory functions in anti-tumour immunity depends on the stimuli they encounter within the TME.

Indeed, in colon and pancreatic cancer patients, Th17 cell infiltration is associated with poor prognosis, whilst in ovarian cancers Th17 cells are associated with increased survival, thus highlighting the mutable immunological properties Th17 cells possess in tumour immunity (Bailey *et al.* 2014).

Cytokines and factors within the TME are crucial determinants of whether there is an initial shift and subsequent agnostic positive cytokine feedback loop for either Th1 or Th2 cells. A prevalence of Th2 cells and a high Th2:Th1 ratio is a predictor for decreased survival in many cancer types, whilst a high level of Th1 infiltration and decreased Th17 presence was associated with prolonged survival in colorectal cancer (Gabitass *et al.* 2011; Geng *et al.* 2015; Fridman *et al.* 2017). Although the dual role of some Th cell subtypes adds more complexity to their prognostic significance, in general IFN-γ-producing Th1 cells are associated with a favourable prognosis, whilst the prognostic significance of other Th subtypes is cancer type dependent (Guisier *et al.* 2020).

1.1.6.3.2bii Tregs

To maintain peripheral tolerance, Tregs prevent reactivity to self-antigens; however, tumour cells are often seen as self and thus Tregs try to inhibit the development of anti-tumour immunity through the suppression of tumour-specific T cells. The role of Tregs in anti-tumour immunity was first demonstrated in mice treated with an anti-CD25 mAb prior to injection of eight different tumour types. Administration of the anti-CD25 mAb resulted in a reduction in CD4+CD25+ cells and subsequent regression in 6/8 of the tumours, suggesting that CD4+CD25+ cells were involved in suppressing anti-tumour immunity (Onizuka *et al.* 1999).

The TME generally contains an abundance of Tregs, accounting for 10-50% of CD4+ T cells within the tumour compared with 2-5% in the periphery of healthy individuals (Togashi *et al.* 2019). Tregs can be recruited and accumulate with the TME via several mechanisms. Chemokines secreted by tumour cells, innate immune cells and exhausted CD8+ T cells recruit Tregs, whilst tumour intrinsic driver mutations such as epidermal growth factor receptor (*EGFR*) have also been demonstrated to promote Treg infiltration primarily by changing the local chemokine and metabolic environment. Furthermore, once recruited into the TME, TGF-β, IL-10 and adenosine can increase Treg proliferation and convert non-suppressive T cells into Tregs (Ondondo *et al.* 2013). Transcriptional analysis of tumour infiltrating Tregs isolated from colorectal, breast, gastric and NSCLC patients demonstrated that these cells shared a phenotype distinct from that of Tregs in peripheral tissues (De Simone *et al.* 2016). Tumour-infiltrating Tregs overexpress immunosuppressive immune checkpoint molecules such as

cytotoxic T lymphocyte antigen 4 (CTLA-4), programmed death ligand 1 (PD-1) and T cell immunoreceptor with Ig and ITIM domains (TIGIT) and express high levels of Treg activation markers including lymphocyte-activation gene 3 protein (LAG-3), OX40, and T cell immunoglobulin mucin receptor 3 (TIM3) (Kim *et al.* 2020). Tregs isolated from the TME exhibit enhanced suppressive capacity compared to Tregs from peripheral blood or healthy tissue, this may be due in part to the increased activation of these cells within the TME. One possible mechanism for the increased activation of these cells is that dying and proliferating tumour cells produce many self-antigens which are recognised by Tregs with a higher affinity than other T cells, thus enabling preferential activation (Chaudhary and Elkord 2016).

Tregs can exert their immunosuppressive functions in the TME through various cellular and humoral mechanisms which ultimately suppress effective T cell responses (Figure 1.4). By competing for the consumption of IL-2, Tregs can limit its availability to activate T cells, whilst production of the immunosuppressive cytokines IL-10, IL-35 and TGF-β can further inhibit an immune response (Thornton and Shevach 1998; Togashi *et al.* 2019). Tregs have also been shown to convert adenosine triphosphate (ATP) into the metabolite adenosine, which can prevent optimal T cell activation and has even demonstrated direct anti-effector cell activity through the secretion of perforin and granzymes (Grossman *et al.* 2004; Deaglio *et al.* 2007). The increased expression of immune checkpoints and inhibitory receptors such as CTLA-4, PD-1, and LAG-3, which act to dampen immune responses and prevent excessive T cell activation during physiological immune responses, provide Tregs with greater suppressive activity. Indeed, a meta-analysis of 76 articles encompassing 17 different solid cancer types reported a significant association between high Foxp3+ density and lower overall survival rates, further supporting the pro-tumour role of immunosuppressive Tregs in the TME (Shang *et al.* 2015).

1.1.6.3.2biii CD8+ cytotoxic T cells

Naïve CD8+ T cells are primed by APCs into effector CD8+ T cells primarily in tumour-draining lymph nodes but can become primed directly in the TME by cross-presenting APCs and tumour cells themselves. Multiple *in vitro* and *in vivo* studies have demonstrated the ability of CTLs to recognise and lyse tumour cells; indeed, a meta-analysis of 23 studies determined that the presence of CD8+ T cells within the TME of multiple cancers including ovarian, colorectal, lung and renal cell carcinoma was associated with good prognosis for all survival endpoints tested (Gooden *et al.* 2011).

Therefore, to effectively evade immune attack, the tumour and TME must induce CD8+ T cell dysfunction. The TME can influence the fate of CD8+ T cells through the expression of cytokines, cell surface immunomodulatory ligands and inhibition of nutrient and oxygen availability to cause CD8+ T cell dysfunction and phenotypic changes which facilitate the switch from a highly active CTL population to a chronically stimulated dysfunctional states (Maimela *et al.* 2019). The absence of inflammation and/or lack of efficient co-stimulation for CD8+ T cells in the TME leads to the generation of a hyporesponsive subset of anergic T cells which are characterised by low IL-2 production and decreased effector function (Crespo *et al.* 2013). Furthermore, prolonged exposure of CD8+ T cells to their cognate antigen can result in an exhausted phenotype, characterised by low IL-2 and IFN-γ production, reduced proliferative potential and reduced cytotoxic activity; these cells also upregulate several immunosuppressive immune checkpoints on their surface including PD-1, CTLA-4, Lag-3 and CD160 which further attenuate the anti-tumour response (Reiser and Banerjee 2016). Soluble molecules such as IL-10, IFNs, adenosine, VEGF and TGF-β produced by tumour and immune cells within the TME can also mediate T cell dysfunction. Furthermore, the TME represents an environment low in glucose, amino acids, oxygen, and pH all of which further induce T cell dysfunction and impair the anti-tumour immune response (Thommen and Schumacher 2018).

1.1.6.3.3 Immunoregulatory cytokines

As evidenced above, tumour cells can produce several immune regulatory cytokines which cripple anti-tumour immune function and generate a locally immunosuppressive TME through the recruitment and subversion of immunosuppressive immune cells. TGF-β is a chief mediator of this activity and can simultaneously inhibit multiple stages of anti-tumour immunity from the inhibition of DC activation to the direct inhibition of NK and T cell function (Wrzesinski *et al.* 2007). The production of VEGF by tumour and immune cells has also been demonstrated to inhibit the differentiation of progenitors within the TME into DCs and inhibit their maturation, thus further preventing sufficient uptake and antigen presentation (Gabrilovich *et al.* 1996). VEGF is also a critical factor for the establishment of tumour angiogenesis, a hallmark of cancer, with the formation of new abnormal endothelial vessels forming a physical barrier to the trafficking and extravasation of effector immune cells into the tumour (Tang *et al.* 2020).

In addition to the production of cytokines and growth factors which downregulate the anti-tumour immune response, tumour cells can secrete several enzymes such as indoleamine 2,3-deoxygenase (IDO) and arginase which may also contribute significantly to tumour immune evasion through inhibition of T cell activity (Vinay *et al.* 2015). T cell activation and

proliferation can be restricted by the lack of any single essential amino acid, with the depletion of L-tryptophan and L-arginine by IDO and arginase, respectively impacting on T cell activity. IDO serves as the rate-limiting enzyme in the conversion of L-tryptophan to kynurenine along the kynurenine metabolic pathway. Overexpression of IDO in tumours leads to the depletion of L-tryptophan and the expression of kynurenine and downstream catabolites which can cause cell cycle arrest and dysfunction of T cells, promotion of CD4+ T cell apoptosis and the proliferation and activation of MDSCs (Munn *et al.* 2005; Holmgaard *et al.* 2015; Cheong and Sun 2018). In addition to metabolising L-arginine to L-ornithine and urea in the hepatic urea cycle, arginase is also expressed within the TME where its activity is linked to T cell suppression. Depletion of L-arginine by arginase potently inhibits T cell proliferation, decreases cytokine production, and affects the formation of immune synapses between T cells and APCs (Gryzwa *et al.* 2020)

1.1.6.3.4 Negative co-stimulatory pathways

As described above, distinct subsets of adaptive immune cells mediate protective immunity against infection and malignant transformation; however, these effector cells must be tightly regulated to prevent acute and chronic inflammation which can lead to autoimmunity. Immune regulation is mediated by regulatory cells including MDSCs, M2-like macrophages and Tregs, regulatory cytokines such as TGF-β and IL-10 and immune checkpoints such as CTLA-4, PD-1, LAG-3 and TIM-3. Under normal physiological conditions these mechanisms protect the host, yet there is evidence that tumour cells can enhance these regulatory mechanisms as a form of immune subversion to enable immune escape and growth (Dyck and Mills 2017). Immune checkpoints are negative co-stimulatory pathways which interact with their ligands to regulate the activation and function of T cells at multiple stages during the immune response. CTLA-4, LAG-3, TIM-3 and TIGIT all primarily interact with their ligands during the T cell priming stage, thereby limiting T cell activation, whilst PD-1:PD-L1 interactions occur predominantly in the periphery to regulate activated T cells during the effector phase (Dyck and Mills 2017). The ligation of these receptors on immune cells results in signalling through ITIM and immunoreceptor tyrosine-based switch motifs (ITSM) to deliver inhibitory signals, the activity of which can be easily inhibited by blocking antibodies which prevent ligand-receptor interactions. There are now several monoclonal checkpoint inhibitor antibodies licenced to treat a number of cancers including melanoma, NSCLC, renal, bladder and haematological cancers which aim to reduce T cell suppression and induce an immune response (He and Xu 2020).

1.1.6.3.4a CTLA-4

CTLA-4 was the first immune checkpoint to be clinically targeted; it is expressed exclusively on Tregs and activated effector T cells where it regulates the amplitude of T cell activation during priming. In resting naïve T cells, CTLA-4 is located primarily intracellularly but is rapidly induced on the cell surface in a graded fashion upon T cell stimulation, conversely Tregs express CTLA-4 constitutively where it appears to be crucial for their suppressive function (Linsley *et al.* 1996; Takahashi *et al.* 2000). There are several mechanisms by which CTLA-4 can suppress T cell responses. As discussed in Section 1.2.2.2a, two signals are required for T cell activation: TCR recognition of antigen presented by MHC and co-stimulation through CD28 binding to the B7 ligands CD80 (B7.1) or CD86 (B7.2) expressed on APCs. Sufficient co-stimulatory signalling results in proliferation of T cells, increased cell survival and differentiation into effector or memory cells (Chen and Flies 2013)(Figure 1.3). CTLA-4 is a structural CD28 homolog which binds to CD80 and CD86 with a higher affinity and at a lower surface density than CD28, thereby outcompeting it (Alegre *et al.* 2001). Binding of CTLA-4 to CD80/86 does not produce a stimulatory signal and instead prevents T cell activation, with the relative amount of CD28 versus CTLA-4 binding determining whether T cells undergo activation or anergy (Buchbinder and Desai 2016). CTLA-4 binding has also been shown to inhibit IL-2 production, block T cell proliferation and induce cell cycle arrest (Krummel and Allison 1996; Greenwald *et al.* 2002) (Figure 1.7a). Additionally, Tregs have been shown to sequester CD80/86 co-stimulatory ligands on APCs via CTLA-4-mediated binding to prevent binding of effector T cells to APCs (Tekguc *et al.* 2021)(Figure 1.7b). Furthermore, CTLA-4 has been observed to confer T cell inhibition through the active removal of CD80/86 from the surface of APCs through transendocytosis; this results in APCs unable to bind CD28 on conventional T cells to provide appropriate co-stimulation (Qureshi *et al.* 2011)(Figure 1.7c).

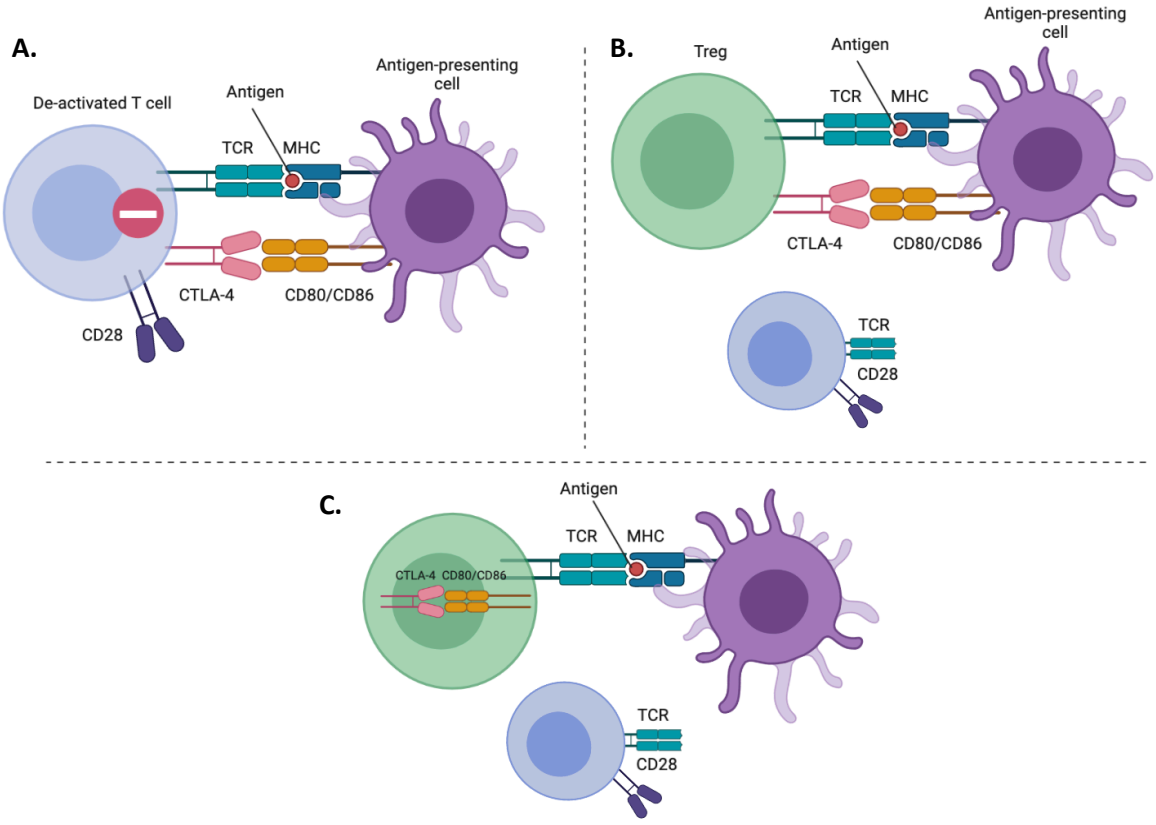

Figure. 1.7 CTLA-4 mechanisms of T cell inhibition.

(A) T cells are activated upon TCR binding of antigens displayed on MHC molecules on APCs in combination with co-stimulatory signals from CD28:CD80/86. CTLA-4 binds with a higher affinity than CD28 to CD80/86 on APCs thus preventing T cell activation and resulting in a net negative signal which limits IL-2 production, T cell proliferation, and limits T cell survival. (B) Tregs express CTLA-4 constitutively and can bind to and sequester CD80/86 on APCs thus preventing T cell antigen presentation by APCs. (C) Tregs can physically remove CD80/86 costimulatory molecules from the surface of APCs via CTLA-4-meiated transendocytosis to further prevent T cell activation. CTLA-4, cytotoxic T lymphocyte associated antigen 4; MHC, major histocompatibility complex; TCR, T cell receptor; Treg, regulatory T cell. Adapted from Jain et al. (2010) & Buchbinder and Desai (2016). Created in Biorender.com.

1.1.6.3.4b PD-1/PD-L1

The inhibitory receptor PD-1 and its ligands PD-L1 and PD-L2 have gained significance in the past few years, with the approval of several checkpoint inhibitors targeting the pathway approved for treatment of many cancers. PD-1 and PD-L1/2 are members of the B7 family of receptors and ligands; a family of structurally related ligands which bind to their associated receptors on T and B cells to initiate downstream co-stimulatory or co-inhibitory signalling (Curran *et al.* 2010). PD-1 is a member of the B7/CD28 family of co-stimulatory receptors and is expressed on T cells, B cells, NK cells and certain myeloid cells; although, its role in best characterised in T cells wherein its expression is induced on the cell surface following antigen stimulation (Dyck and Mills 2017). Similar to CTLA-4 signalling, PD-1 binding with its ligands inhibits T cell function by reducing the intensity of IFN-γ, TNF and IL-2 production, reducing T cell survival through the inhibition of anti-apoptotic gene production and suppressing T cell proliferation (Keir *et al.* 2008; Buchbinder and Desai 2016) (Figure 1.8). If a T cell experiences both PD-1 and TCR signalling, PD-1 signalling will prevent phosphorylation of key TCR signalling components, further reducing T cell activation (Bennett *et al.* 2003). Unlike CTLA-4 which exerts its function during the early priming phase of T cell activation, PD-1 mainly functions during the effector phase in the periphery, where T cells encounter PD-1 ligands. Chronic antigen exposure such as that in chronic infection or cancer can result in high levels of persistent PD-1 expression on T cells, which upon ligation with PD-L1/2 results in T cell anergy and exhaustion (Pardoll 2012). PD-L1 and PD-L2 are expressed on a variety of cell types including DCs, T cells, B cell, myeloid cells and can be induced on parenchymal cells following inflammatory cytokine exposure. PD-L2 is expressed primarily on DCs and monocytes but can also be induced on several other cells depending on the microenvironment (Buchbinder and Desai 2016). Furthermore, tumour cells can express PD-L1 to inhibit anti-tumour T cell responses within the TME where it's expression is associated with poor prognosis in many cancers (Dyck and Mills 2017).

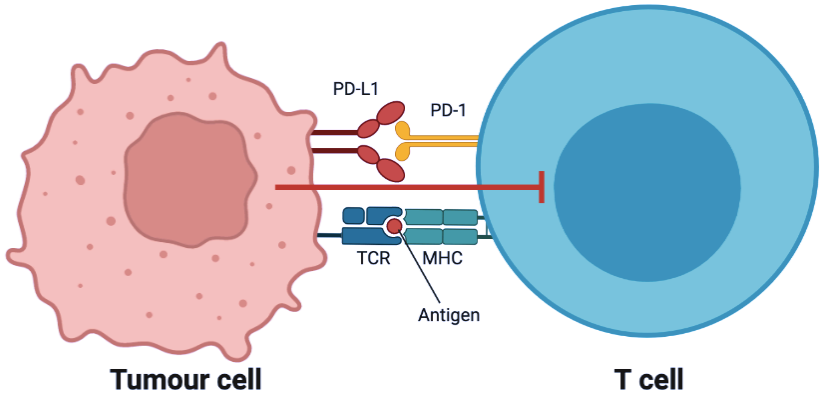

Figure. 1.8 PD-1/PD-L1 mechanisms of T cell inhibition.

PD-1 binding with its ligand PD-L1 inhibits T cell function by reducing the intensity of IFN-γ, TNF and IL-2 production, reducing T cell survival through the inhibition of anti-apoptotic gene production and suppressing T cell proliferation. If a T cell experiences both PD-1 and TCR signalling, PD-1 signalling will prevent phosphorylation of key TCR signalling components, further reducing T cell activation. PD-1 mainly functions during the effector phase in the periphery, where T cells encounter PD-1 ligands.Tumour cells have been demonstrated to express PD-L1 to inhibit anti-tumour T cell responses. MHC, major histocompatibility complex; PD-1, programmed death protein 1; PD-L1. Programmed death ligand 1; TCR, T cell receptor. Created in Biorender.com.

1.1.6.3.4c Immune checkpoint inhibitors

Immune checkpoint inhibitors (ICIs) targeting CTLA-4 and PD-1/PD-L1 have been approved for the first- and second-line treatment for several cancers including melanoma, NSCLC, renal cell carcinoma, head and neck carcinoma and bladder cancer (Table 1.2). These monoclonal antibodies aim to reverse T cell exhaustion, inhibit Treg activity and reinvigorate T cells to promote anti-tumour immunity (Dyck and Mills 2017). PD-1/PD-L1 antibodies primarily reinvigorate tumour reactive T cells, rather than induce their formation, therefore the best responses to these therapies are seen in cancers which have a high somatic tumour mutation burden (TMB). With UV- and carcinogen-induced genomically unstable tumours such as melanoma and NSCLC demonstrating TMEs rich in neoantigens which can be recognised and promote potent anti-tumour T cell responses upon treatment (Vareki 2018). High response rates are also seen in colorectal cancers with microsatellite instability or mismatch repair as these mutations increase the likelihood of neoantigen formation by the tumours (Germano *et al.* 2017). Furthermore, highly infiltrated immune active TMEs, such as those seen in melanoma, NSCLC, head and neck SCC, bladder, renal and hepatocellular carcinomas, are evidence of pre-existing anti-tumour immunity that can be reinvigorated upon ICI treatment, hence why these antibodies have been approved for use in these cancers (Vareki 2018).

Table 1.2 Clinically available ICIs and their use.
Adapted from Robert (2020) & Yang et al. (2020) & Wojtukiewicz et al. (2021)

Drug	Cancer type	Indication
CTLA-4 inhibitors		
Ipilimumab	Melanoma	• Monotherapy for metastatic and unresectable disease. • As adjuvant therapy for resectable high-risk disease.
PD-1 inhibitors		
Nivolumab	Melanoma	• Adjuvant therapy for resectable high-risk disease • As monotherapy for unresectable disease • As therapy for advanced disease that no longer responds to drugs
	NSCLC	• Metastatic disease that has progressed on or after chemotherapy
	Small cell lung carcinoma	• Metastatic disease that has progressed on or after chemotherapy
	Head and neck SCC	• Recurrent or metastatic disease that has progressed on or after chemotherapy
	Bladder cancer	• Adjuvant therapy for patients at high risk after resection
	Renal cell carcinoma	• Metastatic disease
	Hepatocellular carcinoma	• For patients previously treated with kinase inhibitors
	Hodgkin lymphoma	• Classical Hodgkin lymphoma that has relapsed or progressed following

		autologous hematopoietic stem cell transplantation
	Colorectal cancer	• Microsatellite instability-high or mismatch repair deficient metastatic disease that has progressed following previous treatment
Pembrolizumab	Melanoma	• Adjuvant therapy for lymph node involvement following complete resection • Metastatic disease
	NSCLC	• First line therapy for metastatic disease irrespective of PD-L1 expression
	Small cell lung carcinoma	• Metastatic disease
	Head and neck SCC	• Monotherapy for tumours that express PD-L1 • Combination first-line therapy for unresectable or metastatic disease
	Bladder cancer	• Monotherapy for unresponsive high-risk non-muscle invasive in situ disease
	Hodgkin lymphoma	• Relapsed or refractory classical Hodgkin lymphoma
	Stomach and oesophageal cancer	• Recurrent locally advanced or metastatic disease • Adjuvant therapy for non-resectable disease

PD-L1 inhibitors		
Atezolizumab	Urothelial cancer of the bladder	• Locally advanced or metastatic disease that expresses PD-L1 or is not eligible for chemotherapy
	NSCLC	• Adjuvant therapy following resection and chemotherapy whose tumours have >1% PD-L1 tumour expression • First-line treatment for high PD-L1 expressing metastatic disease • First-line therapy for metastatic disease with no *EGFR* or *ALK* mutations • Metastatic disease that has progressed on or after chemotherapy
	Small cell lung carcinoma	• First-line combination therapy for advanced disease
	Hepatocellular carcinoma	• Combination therapy for unresectable or metastatic disease
	Melanoma	• Combination therapy for *BRAF* V600 mutated unresectable or metastatic disease
Durvalumab	NSCLC	• Unresectable advanced disease that has not progressed on chemotherapy or radiation
	Small cell lung carcinoma	• First-line combination therapy for advanced disease
Avelumab	Merkel cell carcinoma	• Metastatic disease
	Urothelial cancer of the bladder	• Locally advanced or metastatic disease that has not progressed with first-line chemotherapy

	Renal cell carcinoma	• First-line treatment for advanced disease
Combined CTLA-4 and PD-1 inhibitors		
Ipilimumab with Nivolumab	Melanoma	• Unresectable or metastatic disease
	Renal cell carcinoma	• First-line treatment for previously untreated patients with intermediate- and poor-risk advanced disease
	Colorectal cancer	• Microsatellite instability high or mismatch repair deficient metastatic disease that has progressed on other treatment
	NSCLC	• First-line treatment for metastatic disease with >1% tumour PD-L1 expression and no *EGFR* or *ALK* mutations

1.1.6.3.4ci Anti-CTLA-4 antibodies

CTLA-4 was the first immune checkpoint to be targeted in cancer, with preclinical mouse models of melanoma, bladder and brain tumours demonstrating that blocking CTLA-4 lead to a regression or delay in tumour growth associated with increased tumour T cell infiltration (Grosso and Jure-Kunkel 2013). Ipilimumab, a fully humanised IgG1α CTLA-4 mAb, was the first ICI approved by the U.S. food and drug administration (FDA) in 2011 for the treatment for metastatic and/or surgically unresectable melanoma following a clinical trial in which treatment with Ipilimumab increased median overall survival by 10 months; pooled analysis from 12 clinical trials has revealed that treatment with Ipilimumab can result in survival of up to 10 years in some patients (Hodi *et al.* 2010; Ribas and Flaherty 2015). Furthermore, Ipilimumab is now also used as an adjuvant therapy for melanoma patients following surgical resection to reduce the risk of disease recurrence (Wojtukiewicz *et al.* 2021).

The exact mechanism by which CTLA-4 ICIs induce an anti-tumour immune response remains unclear, however research to date suggests that blocking CTLA-4 enhances T cell priming by promoting activation and proliferation of effector T cells, regardless of TCR specificity, upon release of CTLA-4-mediated suppression (Dyck and Mills 2017). Furthermore, there is evidence that Treg-mediated suppression is also reduced through the depletion of intra-tumoral Tregs (Jain *et al.* 2010) (Figure 1.9). Melanoma and prostate cancer patients treated with Ipilimumab demonstrated an increase in the diversity of the peripheral T cell pool following CTLA-4 blockade which was continuously evolving throughout treatment, suggesting a dynamic response to the tumour over time. Furthermore, there was preferential expansion and maintenance of pre-existing high-affinity memory TCR clonotypes, suggesting that effective CTLA-4 blockade may be dependent on the ability of a patient to retain pre-existing anti-tumour T cells (Cha *et al.* 2014). However, despite the long-term responses seen in some patients, the broad non-specific activation of the immune system generated by CTLA-4 blockade generates unusual and sometimes severe immune-related adverse events (IrAEs), the incidence of which is positively associated with good clinical outcomes (Petrelli *et al.* 2020). These auto-immune adverse events, such as rashes, endocrinopathies, and gastrointestinal problems are consistent with a disruption in immune homeostasis characterised by the clonal expansion and activation of new self-reactive T cell clones which are normally prevented by CTLA-4-mediated control of CD80/CD86 signalling (De Silva *et al.* 2021).

1.1.6.3.4cii Anti-PD-1/PD-L1 antibodies

Increasing evidence from animal models and clinical data suggests that PD-1 plays a crucial role in inhibiting the anti-tumour response, with pre-clinical mouse models of melanoma,

ovarian, and colon cancer demonstrating that blocking PD-1 or PD-L1 results in a reduction in tumour growth associated with a restoration of T cell function (Dyck and Mills 2017). Treatment with antibodies targeting PD-1 or PD-L1 targets the T cell effector phase to restore the function of exhausted T cells and is associated with an increase in CD8+ T cell activation, an elevation in the CD8+ T cell:Treg ratio and an increase in CD8+ T cell infiltration induced by increased chemokine production (Curran *et al.* 2010; Peng *et al.* 2012; Duraiswamy *et al.* 2013)(Figure 1.9). PD-L1 expression has been noted on many cancers but is particularly abundant in NSCLC, melanoma, and ovarian cancers (Buchbinder and Desai 2016). The first PD-1 ICI, Pembrolizumab, is a humanised IgG4 mAB with 10x higher affinity for PD-1 than other PD-1 ICIs. Pembrolizumab was first approved for the treatment of advance or unresectable melanoma but has since been approved for the treatment of PD-1+ metastatic NSCLC tumours following disease progression on first-line treatments, chemotherapy-resistant head and neck SCC and several more cancers (Deeks 2016; Lim *et al.* 2016; Haque *et al.* 2017) (Table 1.2). Similarly, the PD-1 IgG4 humanised mAb Nivolumab has been approved for the treatment of many cancers including melanoma, NSCLC, and renal carcinoma. The PD-L1 inhibitors Atezolizumab, Durvalumab and Avelumab have been approved for the first-line and adjuvant treatment of several cancers (Table 1.2); by inhibiting PD-L1 specifically rather than PD-1, these ICIs provides a more targeted inhibition as it allows for the preservation of PD-1: PD-L2 interactions, thus preserving an aspect of self-tolerance to limit toxicities related to over-activation of the immune system (Pardoll 2012).

PD-1 blockade works during the effector stage of the T cell response restoring function to anti-tumour T cells in the periphery, as opposed to CTLA-4 which functions in the priming stage of T cell responses. As PD-1/PD-L1 signalling is typically restricted to the TME, the more targeted immune re-activation induced by PD-1 blockade is much less global than that of CTLA-4 blockade and leads to a decreased incidence of IrAEs. Up to 60% of patients receiving Ipilimumab present with IrAEs, with 10-30% of these considered serious, in comparison to 5-20% of patients receiving anti-PD-1 therapies presenting with IrAEs. This increased toxicity has limited the appeal of ati-CTLA-4 therapies as a single agent (Martins *et al.* 2019). Despite this, therapies using Ipilimumab in combination with Nivolumab have now been approved for the use in NSCLC, melanoma, colorectal and renal carcinomas, with the differences in the timing, location, and non-redundant effects CTLA-4 and PD-1/PD-L1 have on the activation of T cells providing additive and potentially synergistic effects in enhancing the anti-tumour immune response (Dyck and Mills 2017)(Table 1.2). The combination of immune checkpoint inhibitors working in both the priming and effector phases does leads to a significant increase in IrAEs, with 54% of patients presenting with severe adverse events such as colitis,

dermatological and hepatic events (Martins *et al.* 2019). However, the improved efficacy seen with this dual treatment in combination with efficient monitoring and treatment of these events is of great clinical benefit to subsets of patients.

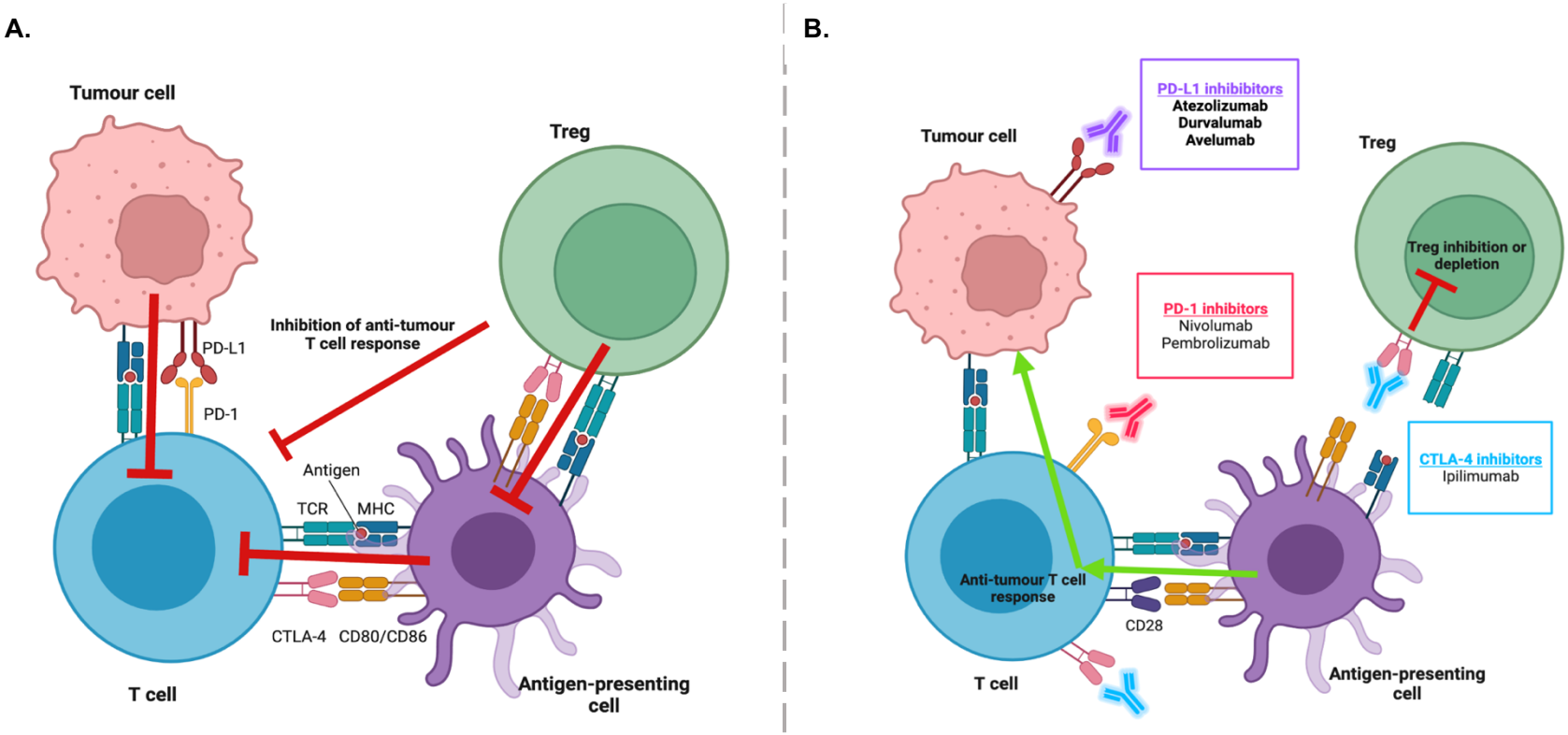

Figure. 1.9 Mechanisms of T cell suppression by immune checkpoints and reactivation following immune checkpoint inhibition.

(A) Binding of CD80/86 co-stimulatory ligands on APCs to CTLA-4 on effector T cells or Tregs results in an inhibition of T cell activation both directly via APCs and indirectly through Treg-mediated suppression. Furthermore, PD-1 engagement by PD-L1 on tumour cells leads to exhaustion and anergy of T cells. Overall, the presence of immune checkpoint signalling results in a dampened anti-tumour T cell response and ultimately tumour cell escape. (B) Immune checkpoint inhibition with monoclonal antibodies against ligands (PD-L1) and receptors (CTLA-4 and PD-1) successfully reinvigorates anti-tumour T cell responses through the activation of T cells and suppression and/or depletion of Tregs. CTLA-4, cytotoxic T lymphocyte associated antigen; MHC, major histocompatibility complex; PD-1, programmed death receptor 1; PD-L1 programmed death receptor ligand 1; TCR, T cell receptor; Treg, regulatory T cell. Adapted from Buchbinder and Desai (2016) & Ayoub *et al.* (2019). Created in Biorender.com.

1.2. The immune checkpoint CD200

1.2.1 CD200

CD200 (cluster of differentiation 200), formerly known as OX-2, is a type I transmembrane glycoprotein structurally related to the B7 family of receptors; it is comprised of two Ig-like domains, a single transmembrane domain and a short 19 amino acid intracellular domain with no known signalling motifs (Clark et al. 1985)(Figure 1.10). CD200 expression was first described in the rat and is seen in a variety of cells and tissues including neurons, endothelium, epithelium, thymocytes, DCs, B cells and activated T cells (McMaster and Williams 1979; Barclay 1981; Barclay and Ward 1982; Webb and Barclay 1984). This distribution was found to be well conserved across species, consistent with CD200 having an important biological function (Wright et al. 2001). Constitutive baseline CD200 expression is regulated at the transcriptional level by CCAAT/enhancer-binding protein beta (C/EBP-β), whilst inducible CD200 expression is regulated through IFN-γ and TNF in an additive manner mediated by nuclear factor kappa-light-chain-enhancer of activated B cells (NF-κB), STAT1 and interferon-regulatory factor (IRF-1) binding (Chen *et al.* 2006; Chen *et al.* 2009). Furthermore, CD200 expression is induced by p53-target genes and activated caspases upon apoptosis of DCs (Rosenblum *et al.* 2006).

1.2.2 CD200R

CD200 receptor (CD200R) was first identified on rat peritoneal macrophages by searching for proteins which demonstrated low-affinity interactions on a soluble recombinant form of CD200 immobilised on fluorescent beads (Preston *et al.* 1997). Purification from rat splenic lysates of a mAb that blocked this interaction and subsequent cloning and sequencing found CD200R to also contain two Ig-like domains, a transmembrane domain and a cytoplasmic region, however this cytoplasmic domain was larger (67 amino acids) and contained three tyrosine residues, suggesting potential signalling capacity (Wright *et al.* 2000)(Figure 1.10). The distribution of CD200R is similar between species, with expression demonstrated on several immune cells including those of myeloid lineage, B cells, NK cells and activated T cells (Wright *et al.* 2003; Shiratori *et al.* 2005; Rijkers *et al.* 2008). The broad tissue distribution of CD200 and the immunologically restricted expression of CD200R is consistent with CD200 possessing an immunoregulatory function.

To date, five isoforms of CD200R (1-5) have been described, of which only 1 (CD200R1) has been identified in humans and is presumed to represent the only functional receptor for CD200, with human CD200R1 demonstrating 53% and 52% amino acid homology with rat and mouse CD200R, respectively (Kotwica-Mojzych *et al.* 2021). CD200R2-5 have been

described in rodents and lack an intracellular signalling domain but are thought to signal through co-opted transmembrane domains that contain consensus docking motifs for DAP10/12 adaptor molecules (Wright *et al.* 2000; Hatherley *et al.* 2005). The role of these alternative CCD200Rs has not been fully characterised but it is suggested that through interactions with as yet uncharacterised low-affinity ligands, these receptors could theoretically function as activating receptors following binding to the DAP adaptor molecules within the transmembrane domains (Voehringer *et al.* 2004; Jiang and Barclay 2009). Currently, there is little evidence that these alternate receptors are present in humans (Wright *et al.* 2003).

1.2.3 CD200:CD200R signalling

Unlike most immunoregulatory receptors CD200R does not contain an ITIM domain within its cytoplasmic region, instead it mediates its immune inhibitory effects through an NxPY domain within its most distal tyrosine residue (Wright *et al.* 2000)(Figure 1.10). The NxPY domain binds to phosphotyrosine-binding domains (PTB) within adaptor proteins, which in turn mediate downstream signalling. Studies in human and mouse myeloid cells have shown that CD200R signalling is dependent on the most distal tyrosine residue and phosphorylation of the proximal tyrosine may function to stabilise interactions with the NxPY domain; the second tyrosine residue appears to have no functional role in CD200R signalling (Zhang and Phillips 2006; Mihrshahi *et al.* 2009). Activation and tyrosine phosphorylation of CD200R by CD200 leads to recruitment of downstream of tyrosine kinase 1 (DOK1) and DOK2 which subsequently bind SHIP and Ras p21 protein activator 1 (RasGAP), this leads to inhibition of the Ras-MAPK pathway (Zhang *et al.* 2004; Mihrshahi *et al.* 2009)(Figure 1.10). DOK1 has a greater affinity for phosphorylated DOK2 than CD200R, therefore it is likely that DOK1 is recruited to the CD200R signalling complex via DOK2. siRNA knockdown of DOK1 and DOK2 in human myeloid cells demonstrated that the interaction between CD200R and DOK2 is essential for initiating CD200R signalling, whereas knockdown of DOK1 or SHIP had no effect (Mihrshahi *et al.* 2009). It is now thought that DOK1 forms a complex with the closely related adaptor protein CT10 sarcoma oncogene cellular homologue-like (CrkL) to initiate a negative feedback loop on DOK2 and RasGAP to regulate CD200R signalling (Mihrshahi and Brown 2010).

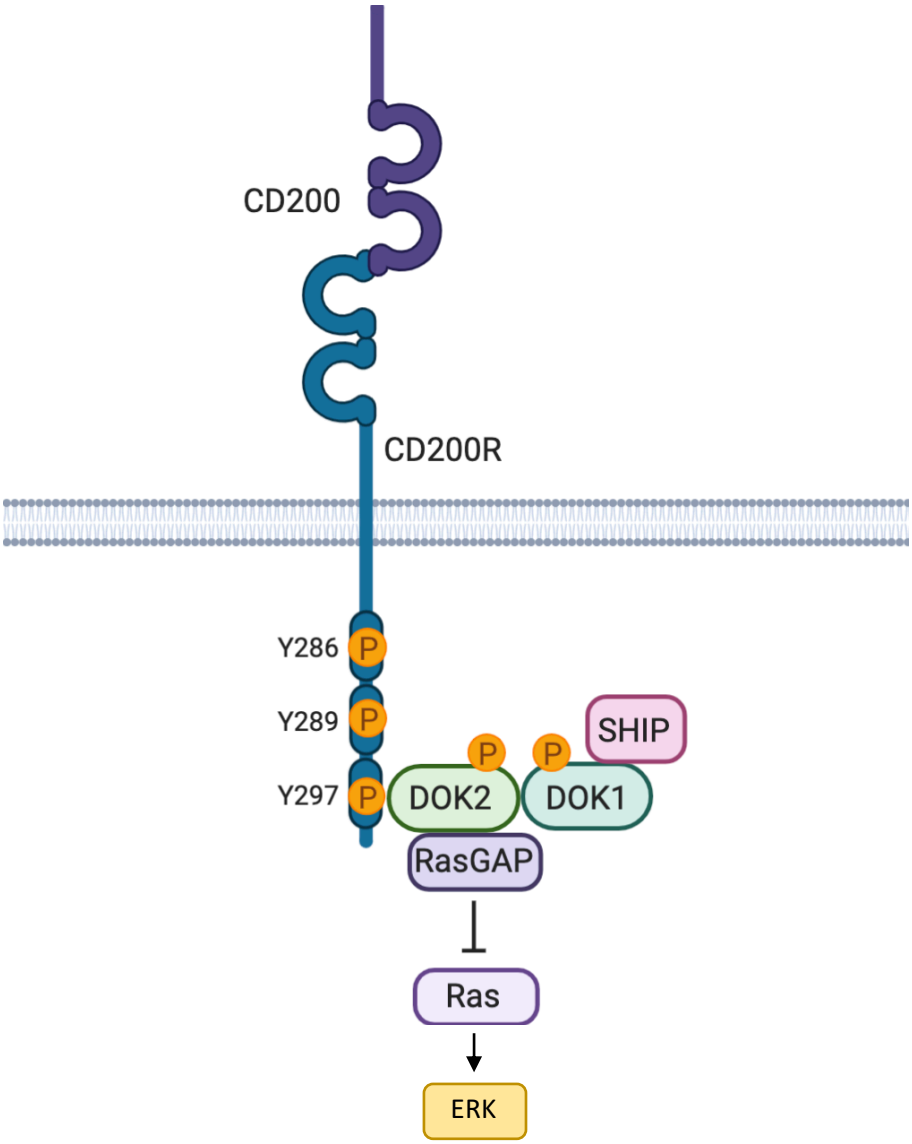

Figure.1.10 Schematic of downstream CD200R signalling following binding with CD200.

Upon ligand binding, CD200R tyrosine residues become phosphorylated and recruit DOK1 and DOK2 which subsequently bind the inhibitory effectors SHIP and RasGAP and reduce downstream signalling through the RAS-MAPK pathway. CD200R, CD200 receptor; DOK, downstream of tyrosine kinase; RasGAP Ras p21 protein activator 1. Created in Biorender.com.

1.2.4 Soluble CD200

Release of membrane-bound immunoregulatory molecules as soluble forms within the extracellular environment plays an important role in the control of immune responses. Soluble forms of cell-surface receptors can be generated by alternative mRNA splicing, by enzymatic cleavage by a distegrin and metalloproteases (ADAMs) and MMPs or by release from the cell surface in exosomes. Much like several other membrane-bound immunoregulatory molecules, CD200 also exists in a functionally active soluble form (sCD200) within the serum where it is believed to play a functional role in a number of disease states, including proliferative diabetic retinopathy, bone loss associated with reduced skeletal loading and chronic lymphocyte leukaemia (Wong *et al.* 2012; Kos *et al.* 2014; Xu *et al.* 2015). In diabetic retinopathy patients, vitreous levels of sCD200 were significantly elevated compared to healthy individuals and correlated with different vitreoretinal conditions, whilst in chronic lymphocyte leukaemia patient serum sCD200 levels correlated with disease aggressiveness and tumour burden (Wong *et al.* 2012; Xu *et al.* 2015).

1.2.5 CD200 and immunosuppression

The generation of C57B/6 mice lacking functional CD200 (CD200-/-) first demonstrated the immunomodulatory functions of CD200 *in vivo* (Hoek et al. 2000). The mice were normal in appearance and exhibited normal life span and breeding behaviour. Leukocyte populations were phenotypically comparable between CD200-/- and WT mice with the exception of the CD11b+ myeloid population. In the spleen there was a doubling of CD11b+ cells with significant expansion of both the granulocyte and activated macrophage populations within the splenic red pulp region and an increase in activated DCs residing in the white pulp. Enlarged lymph nodes containing significantly expanded activated macrophages and aggregates of microglia (resident central nervous system (CNS) macrophages) were also observed. On the basis that an absence of CD200 resulted in an increase in myeloid cells, a population demonstrated to express CD200R, it was hypothesised that CD200-/- mice represent a state of persistent myeloid cell activation due to a loss of CD200-mediated control of myeloid cell function (Hoek *et al.* 2000; Rijkers *et al.* 2008).

1.2.5.1 Autoimmunity

The importance of CD200-mediated control over myeloid cell activity was further highlighted by an increased susceptibility to autoimmune diseases such as collagen-induced arthritis (CIA) and experimental autoimmune encephalomyelitis (EAE) in mice lacking functional CD200. CIA is an autoimmune model of rheumatoid arthritis, a disease characterised by persistent inflammation of synovial joints due to an influx of innate and adaptive immune cells.

C57BL/6 mice are normally resistant to CIA however, both $CD200^{-/-}$ mice and CD200R-Ig-treated mice developed moderate to severe arthritis with a majority of the activated inflammatory cells characterised as $CD68^{+}$ macrophages, cells which are central to the disease process (Hoek *et al.* 2000; Kinne *et al.* 2007). Advanced disease mediated by the presence of inflammatory macrophages was also demonstrated in the EAE model of multiple sclerosis. Disease in both these autoimmune models is dependent upon self-antigen-specific T cells, but there was no evidence for T cell dysregulation in either model, suggesting that these effects appear to be a result of direct deregulation of CD200-mediated control of myeloid/macrophage cells, thus highlighting the importance of CD200 signalling in the prevention of autoimmune reactions (Hoek *et al.* 2000).

1.2.5.2 Transplant tolerance

Mice overexpressing CD200 due to infusion of CD200-Fc or systemic overexpression of a CD200 transgene demonstrated tolerance and long-term survival of skin, renal and cardiac allografts, associated with an increase in infiltrating Tregs (Gorczynski et al. 1999; 2009; 2011). Engagement of CD200R on DCs *in vitro* altered the phenotype of these cells into cells which preferentially induced Treg cells and were capable of inhibiting CTL induction in mixed lymphocyte cultures (Gorczynski et al. 2008). Furthermore, CD200-stimulated DCs added to mixed lymphocyte cultures stimulated the shift of CD4+ Th cell cytokine production from type 1 (IL-2, IFN-γ, TNF) to type 2 (IL-4, IL-10, TGF-β), resulting in inhibition of CTL induction and T cell proliferation (Gorczynski et al. 2004). A further synergistic effect was seen upon addition of CD200R+ macrophages to these cultures (Gorczynski 2001). These studies identified a role for CD200 signallinng in the generation of tolerogenic T cell responses. This role for CD200 signalling in altering T cell phenotype and function may be direct or may occur indirectly through other CD200R+ cells such as DCs and macrophages, which are implicated in shaping T cell responses.

1.2.6 CD200 and immune homeostasis

Maintenance of immune homeostasis is critical for host survival and as an immune checkpoint CD200 is crucial in regulating and maintaining self-tolerance and preventing over activation of the immune system. In the CNS, CD200 expression on neurons interacts with CD200R on microglia to deliver immune inhibitory signals to prevent pro-inflammatory microglial activation under homeostatic conditions. Loss of CD200 in mouse models results in an accumulation of activated microglia which enhance the progression of neuroinflammatory disease models such as EAE and experimental autoimmune uveoretinitis (EAU) (Wright *et al.* 2000; Copland *et al.* 2007). On the contrary, mice with a spontaneous mutation which increases neuronal CD200

expression possess protection against axonal injury, less severe EAE symptoms and decreased microglial activation (Chitnis *et al.* 2007). Furthermore, during pregnancy CD200 expression by trophoblast cells at the foetal-maternal interface alters the maternal immune response to ensure successful pregnancy, in part through the production of local Th2 cytokines (Gorczynski *et al.* 2002; Clark *et al.* 2003).

1.2.7 CD200 and myeloid cells

The CD200:CD200R interaction is now considered a direct mechanism by which myeloid cell function is controlled. Further studies have demonstrated that ligation of myeloid cell CD200R resulted in inhibition of degranulation and inflammatory cytokine release by mast cells, monocytes and macrophages as well as decreased histamine release by basophils (Gorczynski 2001; Cherwinski *et al.* 2005; Shiratori *et al.* 2005). Additionally, engagement of CD200R on plasmacytoid, tolerogenic (CD8+) and immunogenic (CD8-) DCs imparted suppressive properties to these cells which either reinforced or induced tolerogenic functions to these cells (Fallarino *et al.* 2004). A summary of the immune regulatory effects of CD200:CD200R can be found in Figure 1.11.

1.2.8 CD200 and lymphoid cells

CD200R expression has also been demonstrated on mouse and human T, B and NK cells. In humans, CD200R is differentially expressed on T and B cell subsets, with CD4+ T cells demonstrating greater expression than CD8+ T cells and CD200R expression increasing as B cells mature from naive to memory cells. The differentially regulated expression of CD200R on these cells suggests that CD200:CD200R signalling may also be a direct regulator of lymphoid cell function (Rijkers *et al.* 2008).

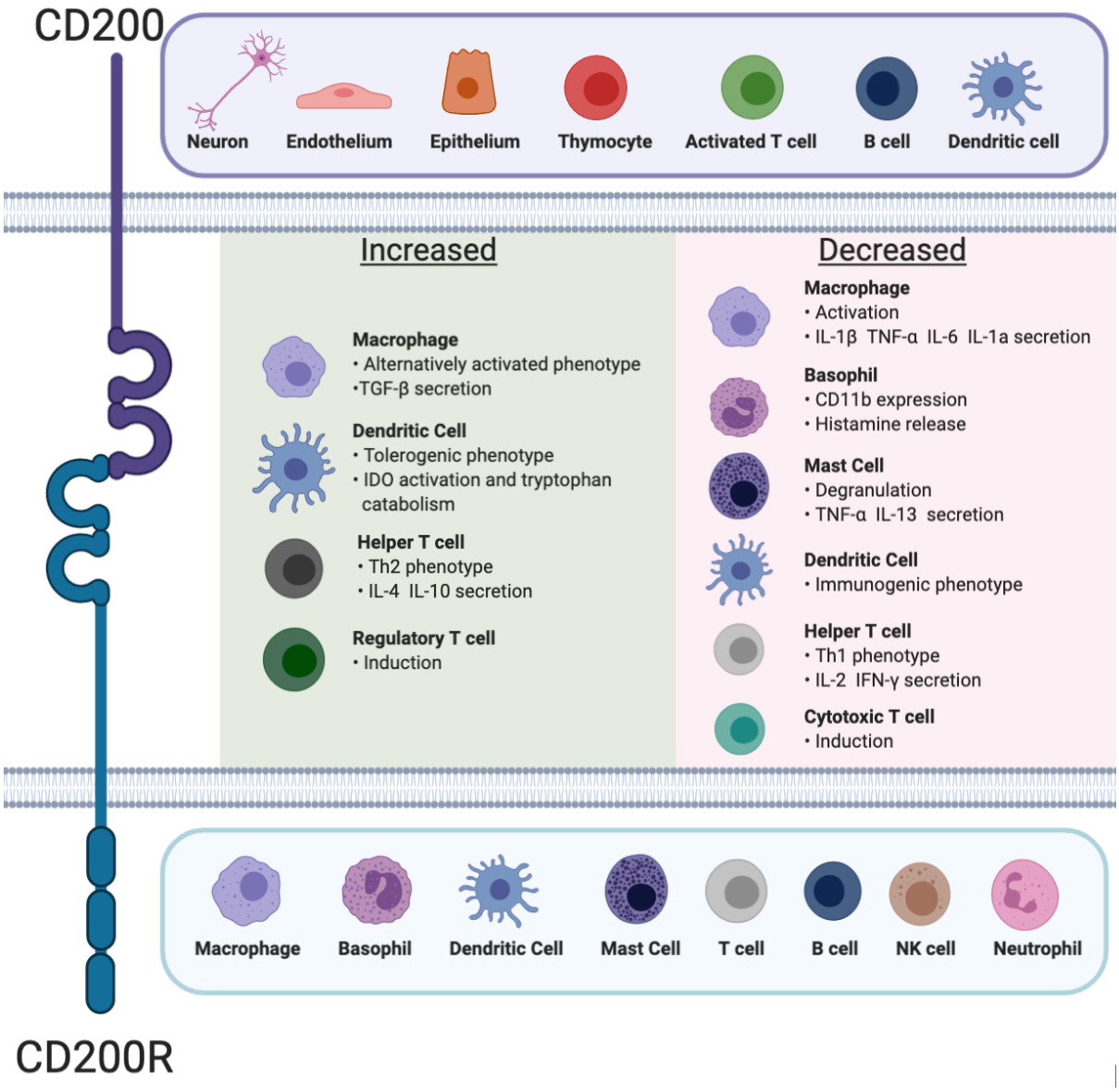

Figure.1.11 Summary of the immunomodulatory effects of CD200 signalling on immune cell function.

Binding of CD200 to CD200R expressed on immune cells results in downstream inhibition of RAS/MAPK signalling and changes in immune cell function. Changes in immune cell function through CD200 signalling are vital in maintaining immune homeostasis and preventing over-activation of the immune system. CD200R, CD200 receptor; IDO, Indoleamine 2,3-dioxygenase; TGF-β, transforming growth factor β; Th, T helper cell; NK, natural killer. Created in Biorender.com.

1.2.9 CD200 viral homologs

The identification of CD200-like sequences in the genomes of several evolutionary diverse viruses suggests that expression of this immunosuppressive molecule provides a strong selective advantage to these viruses that has led to an increase in their evolutionary fitness. CD200-like sequences have been identified in human herpesvirus, myxoma virus and adenovirus and it has been suggested that these decoy ligands for CD200R play a vital role in allowing viruses to evade the immune system (Foster-Cuevas *et al.* 2004; Cameron *et al.* 2005; Shiratori *et al.* 2005). Despite amino acid homologies of less than 40%, viral CD200 homologues bind human CD200R with identical kinetics to human CD200 and are able to directly mimic CD200 function. The human herpesvirus-8 CD200 homologue downregulates macrophage activation, inhibits basophil degranulation and diminishes the cytolytic activity of NK cells *in vitro* (Foster-Cuevas *et al.* 2004; Shiratori *et al.* 2005). Moreover, *in vivo* studies have shown that rabbits infected with a myxoma virus harbouring a deletion for the CD200 homologue made a full recovery due to the increased presence of T cells and activated macrophages at the sites of infection. Thus further demonstrating that several viral families have evolved to exploit the CD200:CD200R axis to suppress anti-viral innate and adaptive immune responses and control the host immune response to infection (Cameron *et al.* 2005).

1.2.10 CD200 and cancer

Evidence for a regulatory function for CD200:CD200R interactions in cancer first came from studies using EL4 thymoma-bearing mice receiving allogeneic bone marrow transplants. Two thirds of the mice generated a graft versus leukaemia response and rejected tumours; however, upon infusion of a soluble form of CD200 there was increased mortality due to inhibition of tumour immunity and loss of tumour growth suppression (Gorczynski *et al.* 2001). Subsequent analysis of cancer patients has confirmed CD200 expression in a number of haematological malignancies including multiple myeloma (MM), acute myeloid leukaemia (AML) and chronic lymphocytic leukaemia (CLL) as well as in solid cancers such as ovarian, breast, testicular, renal, melanoma, bladder, prostate and lung (Moreaux *et al.* 2006; Tonks *et al.* 2007; Moreaux *et al.* 2008; Wong *et al.* 2010).

1.2.10.1 CD200 and cancer stem cells

It has been suggested that the enhanced tumour forming capabilities of cancer stem cells (CSCs) are due in part to the ability of these cells to evade immune detection and elimination. CD200 has been demonstrated to be co-expressed with a number of CSC surface markers found on glioblastoma ($CD133^+$), colon ($CD133^+$), breast ($CD44^+CD24^-$) and prostate cancer cells ($CD44^+$) suggesting that CD200 may serve as a putative marker of CSC populations

(Kawasaki *et al.* 2007). In addition, a rare subpopulation of basal cell carcinoma (BCC) cells identified by CD200 expression possessed increased tumour initiating capacity *in vivo* (Colmont *et al.* 2013). $CD200^{+}CD45^{-}$ cells isolated from patient tumours represented 1.63% ±1.11 of the tumour cell population but were capable of initiating tumours in a xenograft model with as few as 1 x 10^{4} cells, a tumour-initiating capacity 1500-fold greater than that of $CD200^{-}$ BCC cells. CD200 is also a marker of human hair follicle bulge stem cells, a population of mesenchymal stem cells which reside within an "immune privileged" site which protects the cells from immune attack (Ohyama *et al.* 2006). Given the role of CD200 in immune tolerance and tumour immunity and its association with stem cells, it is hypothesised that CD200 defines a population of CSCs equipped with the capacity to evade immune detection (Kawasaki and Farrar 2008).

1.2.10.2 CD200 and haematological cancers

1.2.10.2a CD200 and acute myeloid leukaemia

CD200 is frequently overexpressed in AML tumour cells where it is associated with poor prognosis; patients with high CD200 expression demonstrated significantly worse overall survival and an increased risk of relapse (Tonks et al. 2007). CD200-mediated immunosuppression in AML is associated with changes in the adaptive immune compartment, such changes include the suppression of memory T cell function and an increase in Treg frequencies (Coles *et al.* 2012a; Coles *et al.* 2012b). When patients were stratified into $CD200^{high}$ and $CD200^{low}$ cohorts, CD200 expression significantly correlated with the frequency of $CD4^{+}CD25^{++}Foxp3^{+}$ Treg cells; analysis of Treg cells from $CD200^{high}$ patients demonstrated that these cells were capable of suppressing T cell proliferation *in vitro* (Coles et al. 2012a). $CD200^{high}$ patients also demonstrated a significant reduction in the frequency of cytotoxic $CD8^{+}$ memory T cells and type 1 (TNF, IL-2 and IFN-γ producing) $CD4^{+}$ memory T cells. The suppression of memory T cell cytotoxic responses was demonstrated to be due to a direct interaction between tumour CD200 and CD200R on patient T cells (Coles *et al.* 2012c). CD200 expression in AML is also associated with changes in the innate immune compartment, with $CD200^{high}$ patients demonstrating a significant reduction in overall NK cell frequency associated with a two-fold reduction in the frequency of $CD56^{+}CD16^{+}$ cytolytic NK cells. In addition, there was a reduction in NCR expression (NKp30, NKp44 and NKp46) on all cytolytic NK cell subpopulations and both degranulation and IFN-γ responses to autologous tumour cells were significantly reduced in NK cells from $CD200^{high}$ patients (Coles et al. 2011). Blockade of CD200:CD200R signalling in AML was sufficient to restore both memory T cell and NK cell function, demonstrating a direct role for CD200-mediated immunosuppression in AML (Coles *et al.* 2011; Coles *et al.* 2012b).

1.2.10.2b CD200 and chronic lymphocyte leukaemia

CD200 expression is found on the surface of all CLL cells but, unlike in AML, conflicting results have been reported on its prognostic significance. CD200 expression does not correlate with any other clinical parameter and is observed at all disease stages, suggesting that CD200 is upregulated early in the disease process and has an important function in CLL (Mcwhirter *et al.* 2006). Direct suppression of patient's T cell activity by tumour cells is a key event in CLL pathogenesis and *in vitro* studies have shown that tumour CD200 expression is responsible for suppression of T cell proliferation, suppression of tumour-antigen specific T cell reactivity, Th2 cytokine polarisation and enhancement of Treg populations (Kretz-Rommel *et al.* 2007; Pallasch *et al.* 2009; Wong *et al.* 2010). Further evidence for the important role of the CD200:CD200R axis in CLL came from the simultaneous injection of $CD200^+$/$CD200^-$ CLL cells and human PBMCs into immune-deficient mice. CD200 tumour expression resulted in significantly less tumour growth inhibition, with treatment of $CD200^+$ tumours with anti-CD200 antibody significantly inhibiting tumour growth associated with an increase in cytotoxic $CD8^+$ T cells and IFN-γ production, suggesting cytotoxic T cell activation (Kretz-Rommel *et al.* 2007).

1.2.10.3 CD200 and solid cancers

Unlike in haematological cancers where CD200 expression is associated with poor prognosis and increased tumour growth, its role in solid cancers appears to be more complex. CD200 expression has been demonstrated in breast, skin, pancreatic, ovarian, colorectal, CNS and renal cancers where its interaction with CD200R-expressing immune cells promotes suppression of the immune response within the TME (Siva *et al.* 2008; Moertel *et al.* 2014; Zgodziński *et al.* 2018; Bisgin *et al.* 2019; Choueiry *et al.* 2020; Tronik-Le Roux *et al.* 2020). In general, these studies correlate increasing CD200 expression with tumour progression and reduced patient survival; however, the effects of this immune modulation are dependent on several factors and vary amongst tumour types, with CD200 demonstrating anti-tumour effects in some tumour models.

1.2.10.3a CD200 and breast cancer

In breast cancer, CD200 signalling appears to have a bidirectional role in tumour development and metastasis; the dichotomous role of CD200 in breast cancer immune responses is highlighted in mouse models in which the role of CD200 expression appears to be determined by the aggressiveness of the tumour and the tumour-induced inflammatory response (Erin *et al.* 2015). The pro-tumour role of CD200 in breast cancer progression was first established in several mouse models using the murine EMT6 breast cancer cell line. It was shown that tumour CD200 expression significantly increased upon immune challenge *in vivo* with CD200

levels in immunocompetent mice significantly greater than those from immunocompromised mice, suggesting active immune editing. This immune selection for CD200 expression due to immune pressure resulted in increased tumour growth and metastasis to tumour-draining lymph nodes (TDLN) with the addition of CD200 mAbs negating this effect and leading to decreased tumour growth (Gorczynski *et al.* 2010; Podnos *et al.* 2012). In a further study using CD200-silenced EMT6 cells it was shown that the smaller tumour size and decreased metastasis in these mice was due to the increased presence of cytotoxic infiltrating $CD8^+$ T cells and myeloid cells (Curry *et al.* 2017).

Conversely, the pro-tumour role of CD200 in EMT6 breast cancer growth was reversed in models of 4THM breast cancer growth, with CD200 expression associated with decreased tumour growth and metastasis. 4THM is an aggressive and inflammatory breast cancer cell line known to induce a systemic inflammatory response and is suggested to be less immunogenic and possess greater metastatic potential than EMT6 cells (Erin *et al.* 2006). Primary 4THM tumour growth and lung and liver metastasis were significantly greater in $CD200R^{-/-}$ compared to $CD200^{tg}$ mice, with tumours in $CD200R^{-/-}$ mice demonstrating decreased numbers of tumour-infiltrating cytotoxic T cells and increased neutrophil infiltration and production of inflammatory cytokines (TNF and IL-6) (Erin *et al.* 2015). In this highly inflammatory breast cancer model, tumour-induced chronic inflammation is a tumour promoter; therefore, CD200 exerts a potent anti-tumoral effect through suppression of the immune response.

1.2.10.3b CD200 and skin cancer

CD200 expression in SCC is rarely observed in well-differentiated tumours but rather is associated with metastatic lesions and poorly differentiated tumours, especially at the invasive front, suggesting a role for CD200 in SCC metastasis (Stumpfova *et al.* 2010). Injection of $CD200^+$ and $CD200^-$ metastatic SCC cells into WT mice demonstrated that CD200 expression did not affect the growth of primary tumours, yet $CD200^+$ metastatic SCC cells injected into tail veins possessed significantly increased metastatic capacity. Within the stroma of these metastatic lesions were dense populations of infiltrating CD200R+CD11b+ MDSC-like and TAM cells, the activity of which were dependent on engagement of CD200R. Furthermore, engagement of CD200R induced these cells to produce the collagen cytesine protease cathepsin K (Ctsk), a remodelling enzyme responsible for bulk collagen degradation during bone remodelling. Inhibition of Ctsk significantly inhibited cell migration and metastasis, suggesting that CD200 signalling stimulates SCC invasion and metastasis via induction of Ctsk in infiltrating CD200R+ myeloid cells (Khan *et al.* 2021).

In melanoma, CD200 is expressed in melanocytic lesions and correlates with progression from nevi to melanoma, with a marked increase in expression compared to quiescent melanocytes (Siva *et al.* 2008). Furthermore, expression of CD200 on melanoma cells is associated with significant inhibition of type 1 cytokine production (IFN-γ, IL-2) and T cell proliferation, with blockade of CD200 signalling attenuating this suppression of T cell activation and a shift towards type 1 cytokine production (Petermann *et al.* 2007; Siva *et al.* 2008). Yet other models exploring the role of CD200 in melanoma have, much like in the case of breast cancer, highlighted the complexity of the role of CD200 in tumour growth. CD200 expression on B16 melanoma cells significantly inhibited the growth of tumours, formation of lung metastasis and promoted survival of tumour-bearing mice, with $CD200^+$ tumours infiltrated with significantly greater numbers of $CD4^+$ and cytotoxic IFN-γ producing $CD8^+$ T cells (Talebian *et al.* 2012; Liu *et al.* 2016). $CD200^+$ tumours grown in $CD200R^{-/-}$ mice were larger and contained a greater number of tumour-associated myeloid cells and increased expression of the pro-angiogenic factors VEGF and HIF-1α. This suggests a model in which CD200 expression on melanoma cells interacts with CD200R on myeloid cells to prevent their accumulation and activation within the TME (Talebian *et al.* 2012). It is hypothesised that in these tumours the suppression of CD200R-expressing myeloid cells by tumour CD200 prevents expansion of pro-tumour myeloid cells which can promote tumour angiogenesis and inflammation, leading to increased tumour growth and metastasis (Liu *et al.* 2020). Indeed, in another *in vivo* melanoma model, anti-CD200 treatment led to a reduction in T cell responses and failed to show benefits either alone or in combination with PD-1 and CTLA-4 inhibitors, suggesting that although melanoma has shown good clinical responses to these ICIs, blocking CD200 may not be of clinical benefit (Talebian *et al.* 2021).

Currently it is not known why CD200 appears to have a dual role in some solid tumours but appears to only be pro-tumorigenic in haematological malignancies, where its expression is often positively associated with worse clinical outcomes. CD200 can possess an anti-tumour role in aggressive and inflammatory solid tumours where it can suppress the activity of myeloid cells thus suppressing tumour-induced chronic inflammation, a known tumour-promoting phenomena. However, studies on the role of tumour CD200 expression on interacting myeloid cells in haematological malignancies have been limited. Further investigations into these complex interactions may give insights into the potential dual role CD200 may also play in the haematological cancers.

1.2.10.4 Immune checkpoint inhibition of CD200

The accumulated evidence for the role of CD200 in the growth and immune evasion of several cancers led to the generation of a novel humanised monoclonal antibody that specifically blinds to CD200: Samalizumab. Samalizumab is engineered with an Ig constant G2/G4 region to minimise effector function and prevent ADCC of CD200-expressing immune cells; instead it functions by blocking the interaction between CD200 and CD200R (Kretz-Rommel et al. 2008; Mahadevan et al. 2019). The first in human clinical trial looked at the therapeutic benefit of CD200 immune checkpoint inhibition in 23 CLL and 3 multiple myeloma patients. After multiple dosing cycles there was a dose-dependent decrease in CLL CD200 expression and a sustained reduction in CD200+CD4+ T cells at higher doses; 64% of patients demonstrated a reduction in tumour burden, with 70% of CLL patients achieving stable disease. One chemotherapy naïve CLL patient presented with a durable partial response demonstrated by >50% reduction in overall tumour burden with a concomitant increase in CD8+ T cells and a reduction in Tregs. All MM patients had disease progression with little change in T cell subsets. These positive preliminary results combined with a good safety profile with generally mild to moderate adverse events support further development of samalizumab as a CD200 immune checkpoint inhibitor (Mahadevan et al. 2019).

1.3 Lung cancer

Lung cancer is the 3rd most common cancer in the UK, accounting for 13% of all new cancer cases, with an average of 48 459 patients diagnosed each year (Cancer Research UK). Lung cancer incidence rates remained stable in the UK over the past decade due to a decrease in male cases (12%) combined with a slight increase in female cases (13%) and are projected to fall by 7% between 2014 – 2035 from 94 in 100 000 cases to 88 cases per 100 000 by 2035 (Cancer Research UK). Across the UK and particularly in Wales, lung cancer incidence rises steeply with increasing socioeconomic deprivation, with cases 202% higher in the most deprived quintile compared to the least deprived quintile (Public Health Wales). Due to the high incidence rates and poor long-term survival, lung cancer is the most common cause of cancer death in the UK, accounting for 21% of all cancer deaths, with an average of 35 349 lung cancer deaths per year (Cancer Research UK). This is attributed, in part, to the late stage at which most lung cancer cases are diagnosed; with increasing stage, the possibility of curative treatment, such as surgery, decreases with over half of patients diagnosed at stages I-III receiving palliative or no active treatment (Royal College of Physicians 2021). Lung cancer mortality rates are also greater in more deprived groups, with age-standardised deaths per 100 000 people 290% greater in the most deprived quintile compared to the least deprived in Wales (Public Health Wales). This increased incidence and mortality in lower socioeconomic

groups has been associated with poorer health-seeking behaviours, increased smoking rates and less effective primary healthcare services (Baldwin 2017).

1.3.1 Lung cancer subtypes

Lung cancers are categorised into two main histological subtypes based on their cellular morphology: small cell lung carcinoma (SCLC) and NSCLC which constitute 15% and 85% of cases, respectively (Herbst *et al.* 2018). SCLC is an aggressive high-grade pulmonary neuroendocrine tumour arising from the bronchial epithelium of larger airways, tending to arise more proximally in the lung (Sabari *et al.* 2017) (Figure 1.12). The rapid doubling time, high growth fraction and propensity to metastasise early in the disease course contributes to the poor prognosis of SCLC, with ~90% of patients presenting with metastatic disease to at least the regional lymph nodes (Johnson *et al.* 2014). Among the major lung cancer subtypes SCLC has the strongest association with smoking, with just 2% of patients never-smokers. This is reflected in the mutational profile of SCLC which demonstrates a strong smoking signature associated with the inactivation of the tumour suppressors tumour protein 53 (TP53) and RB transcriptional corepressor 1 (RB1) and a high mutational burden (Rudin *et al.* 2021). This is distinct from NSCLC in which oncogenic driver mutations seem to be essential for tumorigenesis. The highly aggressive nature of this disease is highlighted by a median overall survival rate of less than 10 months, with 5-year survival rates between 1-5% (Nicholson *et al.* 2016).

The remaining 85% of cases are comprised of NSCLC of which SCC and adenocarcinoma are the most common subtypes, accounting for ~40% and ~50% of cases, respectively (Osmani *et al.* 2018). In general, SCCs arise in the more proximal airways and are more strongly associated with chronic inflammation and smoking than adenocarcinomas which arise in the more distal airways. A third NSCLC subtype, large cell carcinoma, is diagnosed upon the exclusion of adenocarcinoma and SCC based on cell morphology and tumour specific biomarkers; however, it is unclear whether large cell carcinomas are genetically distinct from SCC and adenocarcinoma (Chen *et al.* 2014).

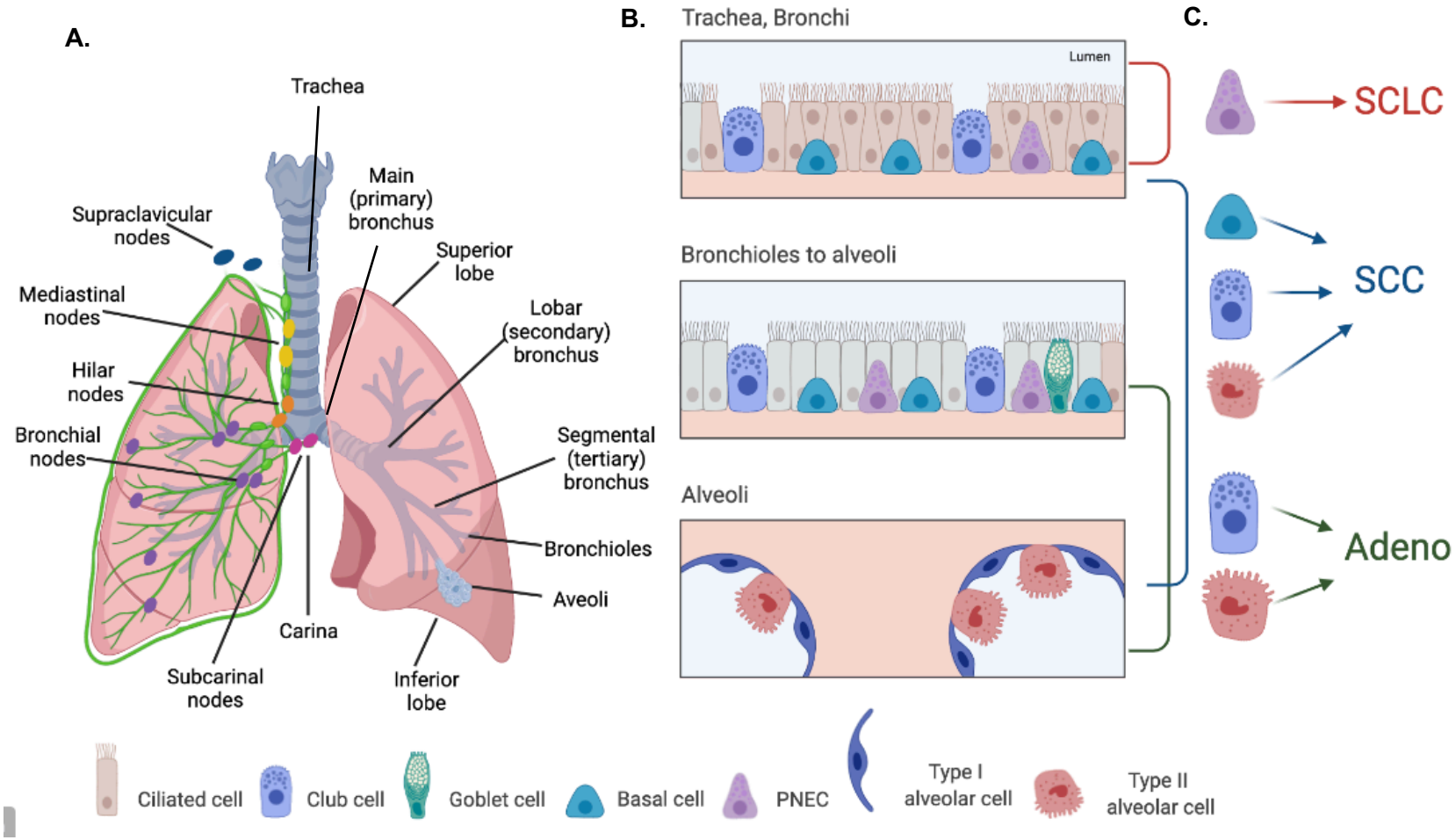

Figure.1.12 Schematic of the structure of the lung and its associated lymph nodes, the epithelial composition at each level of the lung and the cells of origin of the different lung cancer subtypes.

(A) Structure of the lung and the most common sites of lymph node metastasis. (B) The epithelial structure and composition at each stage of the respiratory tree is comprised of specialised cells that carry out essential functions for respiration. (C) Cells of origin of each lung cancer subtype as determined through genetic mouse models. PNEC, pulmonary neuroendocrine cell; SCC, squamous cell carcinoma; SCLC, small cell lung carcinoma. Created in Biorender.com.

1.3.1.1 Squamous cell carcinoma

SCC tumours are characterised by squamous differentiation reminiscent of the pseudostratified columnar epithelium that lines the trachea and larger upper airways and positivity for cytokeratins5/6, p40 and desmoglein-3 (Takamochi *et al.* 2016)(Figure 1.12). It has long been hypothesised that SCC tumours arise from basal cells within the trachea and bronchi as the tumours predominantly arise in the proximal lung and are positive for the basal cell markers p63, SRY-box 2 (SOX2) and keratins 14 and 5 (Chen *et al.* 2014). Squamous tumours arising from lung epithelium have been modelled in mice through germline inhibition of nuclear factor-κB kinase subunit-α (*IKKα*) and through joint liver kinase B1 (*Lkb1*) and phosphatase and tensin homolog (*Pten)* inhibition (Xiao *et al.* 2013; Xu *et al.* 2014). However, SCC tumours can also occur in the peripheral lung, with more targeted genetic approaches suggesting that club cells and alveolar type II cells can also be induced to form SCCs, although it should be noted that the driver mutation combinations and the order in which they accumulate plays an important role in tumour initiation (Ferone *et al.* 2020). Models of biallelic deletion of *Pten* and *Cdkn2ab* combined with overexpression of *Sox2* generated SCC tumours from club cells and alveolar type II cells, with models of *Kras* activation combined with thyroid transcription factor 1 (*TTF-1)* deletion and disruption of Forkhead box a1 (*Foxa1)* or *Foxa2* also generating alveolar type II derived SCC tumours (Ferone *et al.* 2016; Camolotto *et al.* 2018).

SCC tumours are characterised by their discernible genomic complexity and high overall mutation rate of 8.1 mutations per megabase. Almost all tumours demonstrate somatic mutations of the tumour suppressors *TP53* (~90%) and *CDKN2A* (>70%) with frequent mutations identified in the *CDKN2A/RB1*, *PI3K/AKT* and *SOX2/TP63/*Notch receptor 1 (*NOTCH1)* pathways, suggesting common dysfunction in cell cycle control, apoptotic signalling and squamous cell differentiation (Hammerman *et al.* 2012). Furthermore, recurrent mutations have also been identified in disocdin domain-containing receptor 2 (*DDR2*), fibroblast growth factor receptor 1 (*FGFR1), FGFR2, FGFR3, Pten,* and genes in the PI3K pathway (Hammerman *et al.* 2012; Chen *et al.* 2014). Loss of function mutations in the *HLA-A* MHC class I gene, suggesting active immune evasion through mutations in antigen presentation machinery, have also been identified (Hammerman *et al.* 2012). However, unlike adenocarcinomas which harbour mutations in receptor tyrosine kinases that can be successfully targeted with molecular therapies, these mutations are very rarely seen in SCCs (Roy S. Herbst *et al.* 2018).

1.3.1.2 Adenocarcinoma

Adenocarcinomas often demonstrate a glandular histology and express markers consistent with an origin in the distal lung such as TTF-1 and keratin 7 (Davidson *et al.* 2013). Due to

their location predominantly in the peripheral lung, adenocarcinomas have historically been proposed to arise from bronchial club cells and alveolar type II cells (Chen *et al.* 2014)(Figure 1.12). Adenocarcinoma tumours have been generated in models of Kirsten rat sarcoma (*Kras)* activation with and without concomitant *Trp53* or *Lkb1* tumour suppressor loss and *EGFR* activation with or without *TP53* loss (Meuwissen *et al.* 2001; Kim *et al.* 2005; Lin *et al.* 2012; Mainardi *et al.* 2014). For a period, based on the observation that cells at the bronchioalveolar junction were the first to hyperprolfierate upon the induction of oncogenic changes, it was proposed that a population of multipotent stem cells double positive for markers of club cells (club cell secretory protein (CCSP)) and alveolar type II cells (surfactant protein C (SPC)) were the cells of adenocarcinoma origin (Kim *et al.* 2005). However, in more recent studies using targeted expression of oncogenic *Kras* in either CCSP or SPC expressing cells, alveolar type II cells were the only cells capable of giving rise to adenocarcinoma tumours, with club cells and bronchioalveolar stem cells driving bronchiolar hyperplasia (Xu *et al.* 2012). Furthermore, in models of inflammation and injury such as adenovirus infection or naphthalene-induced injury, which more closely mimic human tumour initiation, only alveolar type II cells and club cells could produce peripheral adenocarcinoma tumours in the alveolar space (Kim *et al.* 2005; Xu *et al.* 2012; Sutherland *et al.* 2014).

The most commonly mutated genes in adenocarcinoma include *EGFR* (14%), *BRAF* (7%) and *KRAS* (33%) and the tumour suppressors *TP53* (46%)*,* kelch like ECH associated protein (*KEAP1) (*17%)*, Lkb1* (17%) and neurofibromin 1 (*NF1)* (11%)(Collisson *et al.* 2014). Furthermore, mutations and amplifications have been identified in human epidermal growth factor receptor 2 (*HER2), FGFR1, FGFR2,* receptor tyrosine kinase (*ROS1*) and anaplastic lymphoma kinase (*ALK*) (Chen *et al.* 2014). A majority of adenocarcinoma tumours (~64%) possess mutations in one or more receptor tyrosine kinases such as *EGFR, ALK* and *ROS1*; these oncogenic drivers are targetable and predict sensitivity to tyrosine kinase inhibitors, with adenocarcinoma patients greatly benefiting from these targeted therapies in the clinic (Collisson *et al.* 2014; Kris *et al.* 2014; Roy S. Herbst *et al.* 2018).

1.3.2 Aetiology

The most common aetiology for lung cancer is tobacco smoking; 71% of lung cancers are caused by smoking in the UK, with a further 1% caused by second-hand smoke (Cancer Research UK). Tobacco smoke contains over 50 known carcinogens and demonstrates a dose-response relationship between smoking and the risk of developing lung cancer, with individuals who smoke 30-times more likely to develop cancer than non-smokers (Walser *et al.* 2008). Although smoking is associated with all subtypes, the association is stronger with SCC and SCLC, with adenocarcinoma being the predominant subtype in never-smokers. Lung

cancer in never-smokers is more common in women and is associated with pollution, occupational carcinogens, inherited genetic susceptibility and second-hand smoke (Sun *et al.* 2007). Never-smoker tumours possess 5-6 times fewer mutations than smokers, demonstrate a predominant transition of cytosine to thymine (C>T) nucleotide transversions and an increased prevalence of actionable mutations in the receptor tyrosine kinases *EGFR, ROS1* and *ALK*. Conversely, smoker tumours demonstrate a predominant cytosine to adenine (C>A) transversion and an increased frequency of non-actionable mutations such as *Kras* and *TP53* (Roy S. Herbst *et al.* 2018). Additional environmental risk factors for lung cancer include environmental pollution, exposure to workplace carcinogenic materials such as asbestos, silica, mineral oils and arsenic, and indoor ionising radiation exposure to radon (Osmani *et al.* 2018). Radon is a natural air pollutant, the concertation of which is greater indoors, arising from decay of uranium-238 present in the earth's crust. Radon levels vary across the country but each year around 3.3% of cancer deaths in the UK are related to radon levels in the home (Cancer Research UK). In addition to environmental risk factors, lung cancer incidence is also increased, independently of smoking status, in those whose sibling or parent has had lung cancer, with an increased risk of 82% and 25-37%, respectively (Cancer Research UK). Chronic inflammation of the lung, usually associated with smoking, has also been demonstrated to increase lung cancer risk, with individuals with a history of emphysema 104-144% more likely to develop lung cancer whilst chronic bronchitis increases the risk by 47-52% (Cancer Research UK). In total, around 20% of cancer-related deaths worldwide could be prevented through smoking cessation (Cancer Research UK).

1.3.3 Staging

Lung cancer cases in the UK are staged using the TNM lung cancer staging system; this classification categorises lung cancer tumours based on the size and invasiveness of the tumour (T), it's lymph node involvement (N) and the presence and location of distant metastases (M) (Birerley *et al.* 2017)(Table 1.3). The TNM stage then relates to an overall disease stage from I – IV (Table 1.4). This precise staging system allows for a more accurate diagnosis and plays a key role in optimal disease management when it comes to treatment options and prognosis (Alexander *et al.* 2020). Diagnosis of lung cancer at the earliest stage is strongly associated with improved survival, with 1-year survival 87.7% for those diagnosed with stage I disease. On the contrary, 1-year survival at stage IV, for which 49% of patients present with at diagnosis, is only 19.3% (Cancer Research UK) (Table 1.4). This is further highlighted by 5-year survival rates, with 56.6% and 2.9% survival for stages I and stage IV, respectively (Table 1.4). Clinically most patients present with locally advanced or metastatic disease, with 63% of patients in England diagnosed at stages III or IV in 2020, at which point surgical resection may not be an option (Royal College of Physicians 2022). Where possible,

patients with early stage (I or II) or locally advanced (IIIa) disease are treated with surgical resection with curative intent (15% of patients) followed by systemic and more targeted therapies, with the treatment of more advanced disease reliant on systemic and multi-modality treatments (Evison 2020). However, due to the late stage of presentation in most patients, only 73% of patients receive some form of active treatment with curative intent, with the remaining 17% receiving no or palliative treatment (Royal College of Physicians 2022).

Table 1.3 Lung cancer TNM staging classification.
Adapted from Birerley et al. (2017)

TMN Descriptors	
T Primary tumour	
Tx	Primary tumour cannot be assessed, *or* the tumour has been proven by the presence of malignant cells in sputum/bronchial washing but has not been visualised
T0	No evidence of primary tumour
Tis	Carcinoma in situ
T1	Tumour ≤3 cm in greatest dimension and is surrounded by lung or visceral pleura without evidence of invasion more proximal than the lobar bronchus (i.e., not in the main bronchus)
T1a	Tumour ≤1 cm in greatest dimension
T1b	Tumour ≥1 cm but ≤2 cm in greatest dimension
T1c	Tumour ≥2 cm but ≤3 cm in greatest dimension
T2	Tumour ≥3 cm but ≤5 cm in greatest dimension *or* tumour with any of the following features: • Involves main bronchus regardless of distance to the carina, but without carina involvement • Invades visceral pleura • Associated with obstructive pneumonitis or atelectasis that extends to the hilar region either involving part or the entire lung
T2a	Tumour ≥3 cm but ≤4 cm in greatest dimension
T2b	Tumour ≥4 cm but ≤5 cm in greatest dimension
T3	Tumour ≥5 cm but ≤7 cm in greatest dimension *or* directly invades parietal pleura, chest wall, phrenic nerve, parietal pericardium; *or* separate nodule(s) in the same lobe as the primary tumour
T4	Tumour ≥7 cm *or* of any size that invades diaphragm, mediastinum, heart, great vessels, trachea, recurrent laryngeal nerve, oesophagus, vertebral body, carina; *or* separate tumour nodule(s) in a different ipsilateral lobe to the primary

N Regional lymph nodes	
Nx	Regional lymph nodes cannot be assessed
N0	No regional lymph node metastasis
N1	Metastasis in ipsilateral peribronchial *and/or* ipsilateral hilar lymph nodes and intrapulmonary nodes, including involvement by direct extension
N2	Metastasis in ipsilateral mediastinal *and/or* subcarinal lymph node(s)
N3	Metastasis in contralateral mediastinal, contralateral hilar, ipsilateral or contralateral scalene, or supraclavicular lymph node(s)
M Distant metastasis	
M0	No distant metastasis
M1	Distant metastasis
M1a	Separate tumour nodule(s) in a contralateral lobe; tumour with pleural or pericardial nodules or malignant pleural or pericardial effusion
M1b	Single extrathoracic metastasis in a single organ
M1c	Multiple extrathoracic metastasis in a single or multiple organs

Table 1.4 Lung cancer stages based on TNM classification, the % of patients diagnosed at each stage and the 1-year and 5-year survival rates.
Adapted from Birerley *et al.* (2017) & Cancer Research UK (2021) & Royal College of Physicians (2022)

Stage	Grouping			Stage at diagnosis (England 2020)	1-year survival	5-year survival
Stage IA	T1a	N0	M0	20%	87.7%	56.6%
	T1b	N0	M0			
Stage IB	T2a	N0	M0			
Stage IIA	T1a	N1	M0	7%	73%	34.1%
	T1b	N1	M0			
	T2a	N1	M0			
	T2b	N0	M0			
Stage IIB	T2b	N1	M0			
	T3	N0	M0			
Stage IIIA	T1	N2	M0	19%	48.7%	12.6%
	T2	N2	M0			
	T3	N1	M0			
	T4	N2	M0			
	T4	N0	M0			
	T4	N1	M0			
Stage IIIB	T4	N2	M0			
	Any T	N3	M0			
Stage IV	Any T	Any N	M0	44%	19.3%	2.9%

1.3.3.1 Improving early detection

A significant shift in the outcomes of lung cancer could be achieved upon improved early detection. Broadly, this can be achieved through improving awareness of lung cancer symptoms, clearer referral pathways and an introduction of screening initiatives in patients who are deemed high-risk for developing lung cancer (Jones and Baldwin 2018). National lung cancer screening using low dose computerised tomography (CT) scanning have been suggested by the NHS as a means of reaching their target of diagnosing at least 75% of all cancer at stage I/II by 2028 (Royal College of Physicians). The largest trial to date using this technique was the National Lung Cancer Screening Trial in America; this randomised trial scanned, with either X-ray or CT, 53 454 patients who were 55-74 years old and were current or ex-smokers within the last 15 years. A 20% reduction in lung cancer specific mortality was demonstrated in the CT group, suggesting that CT scanning of high-risk individuals could increase the early detection of lung cancers (National Lung Cancer Screening Team 2011). Furthermore, the NELSON (Nederlands-Leuvens Longkanker Scrrenings Onderzoek) trial demonstrated a 24% and 33% decrease in 10-year lung cancer mortality for high-risk men and women, respectively (de Koning *et al.* 2020). A similar pilot trail conducted in the UK randomised patients to CT or no scanning and, although they saw no statistically significant changes in mortality rates, 86% of lung cancer cases diagnosed were of stage I or II, with 83% of patients receiving surgical resection (Field *et al.* 2021). Taken together, these trials suggest that low-dose CT screening of high-risk patients significantly increases the number of lung cancer cases diagnosed at an early stage and decreases the mortality rate. However, these findings have not been echoed in real world practice, with early detection of lung cancer instead still reliant on prompt patient presentation and GP referrals upon symptoms indicative of lung cancer (McCutchan *et al.* 2020).

1.3.4 Lung cancer treatment

Over the past 20 years treatment options for advanced and non-resectable lung cancer have evolved from the use of systemic cytotoxic therapies to multi-modality therapies that target specific molecular subtypes or immune checkpoints in combination with chemotherapy and radiotherapy (Roy S. Herbst *et al.* 2018). Lung cancer treatment is dependent on stage at diagnosis and in the case of adenocarcinomas, on the presence of genetic mutations in receptor tyrosine kinases. In patients where surgical resection is not an option or following resection of the primary tumour, the first-line treatment options for SCC tumours are either systemic chemotherapy or chemotherapy plus immune checkpoint inhibition, dependent on the presence of the immune checkpoint PD-L1 (NICE 2021)(Figure 1.13). PD-1/PD-L1 immunotherapies are used as single agent first-line therapies for patients with high tumour PD-L1 expression or as first-line chemoimmunotherapy for patients with low tumour PD-L1

expression. In patients who receive chemotherapy as a first-line treatment, PD-1/PD-L1 immunotherapies can be used as second-line therapies upon disease progression (NICE 2021)(Figure 1.13). Conversely, adenocarcinoma treatments are dependent on the presence of mutations in *EGFR, ALK,* and *ROS1,* with those that are negative for all targetable receptor tyrosine kinase mutations then dependent on PD-L1 expression (NICE 2021)(Figures 1.14 & 1.15). Patients with actionable mutations in the receptor tyrosine kinases are initially treated with tyrosine kinase inhibitors (TKIs). Upon disease progression, typically down to acquired TKI resistance, patients are treated with a selection of other second- and third-line TKIs; further progression is then treated with either chemotherapy combinations, immunotherapeutic and targeted therapies in combination with chemotherapy or immunotherapies alone (NICE 2021)(Figure 1.14). In tumours harbouring no actionable mutations, PD-1/PD-L1 ICIs are offered alone or in combination with chemotherapy and targeted therapies, with second- and third-line single agent immunotherapies offered for patients who received chemotherapy as a first-line treatment (NICE 2021)(Figure 1.15).

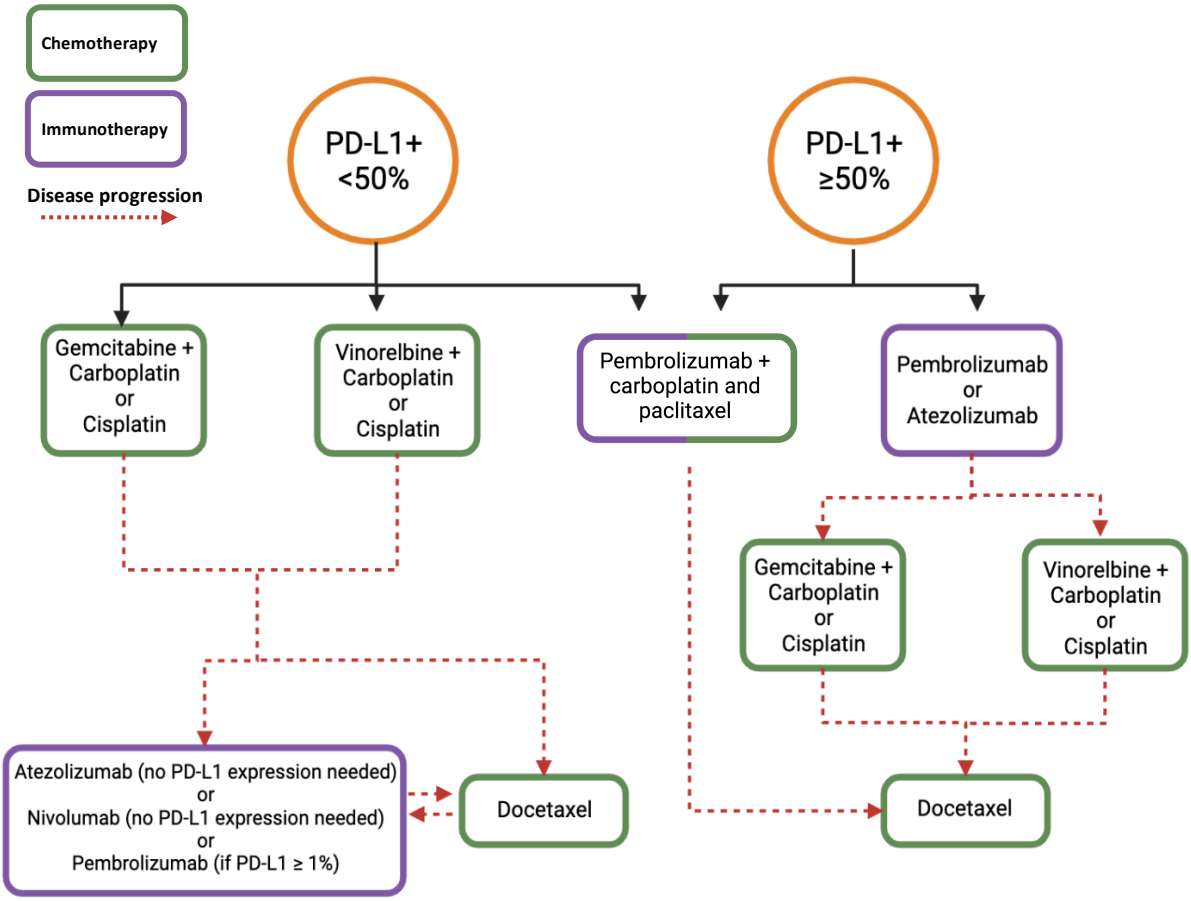

Figure 1.13 Treatment options for SCC patients.

Patient first-line treatment options are dependent on the level of tumour PD-L1 expression and will determine whether a patient receives first-line chemotherapy, chemoimmunotherapy or single agent immunotherapy. Upon disease progression, patients are either treated with platinum doublet and single chemotherapeutic agents or single agent PD-1/PD-L1 ICIs. PD-L1, programmed death-ligand 1. Created in Biorender.com.

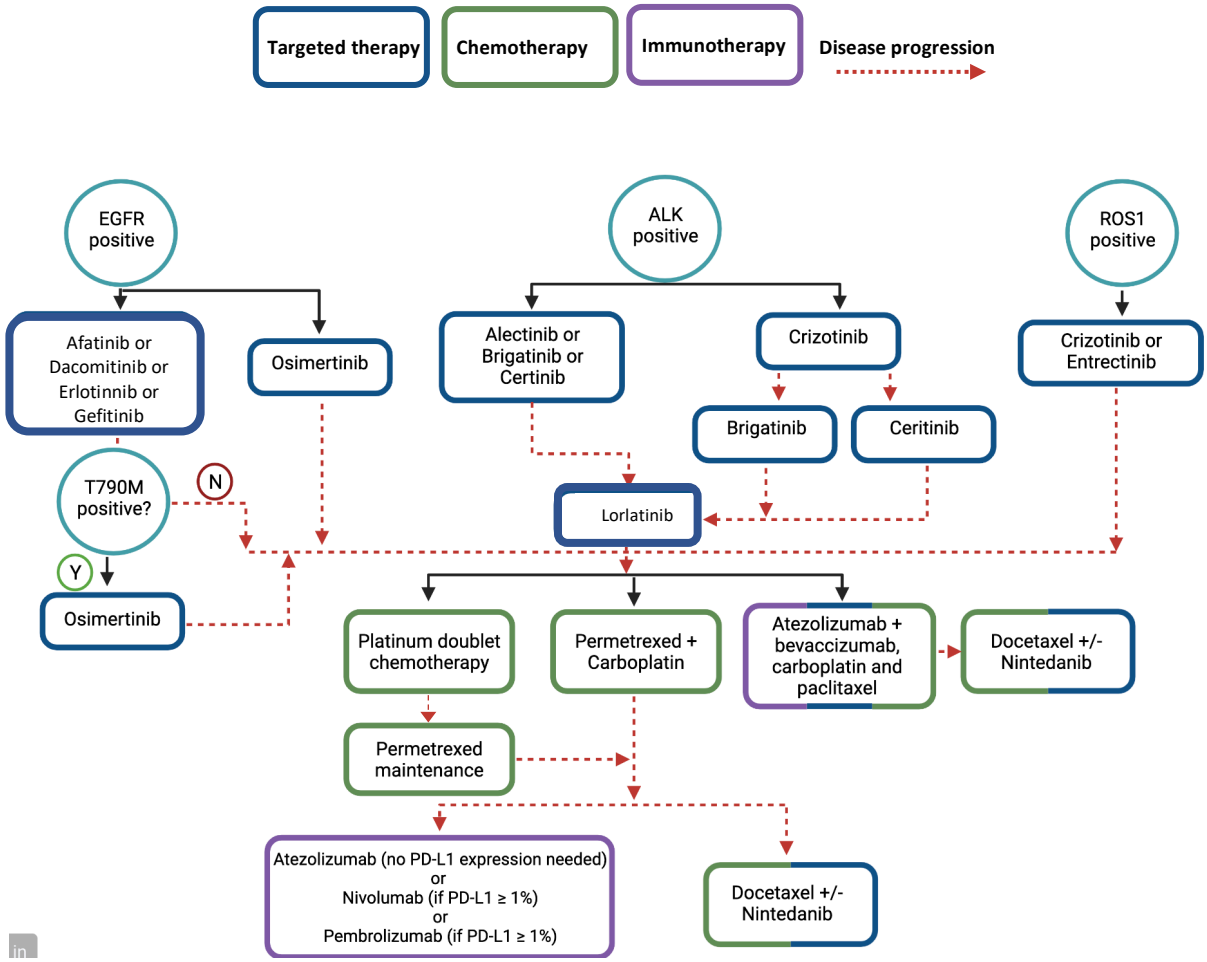

Figure 1.14 Treatment options for adenocarcinoma patients harbouring an actionable mutation in a receptor tyrosine kinase.

First-line targeted treatment options are dependent on the presence of mutations in the targetable receptor tyrosine kinases. Following disease progression due to acquired resistance, patients can be treated with second- and third- generation tyrosine kinase inhibitors before treatment with chemotherapy, chemoimmunotherapy with VEGF targeted therapy, chemotherapy with VEGF targeted therapy or single agent immunotherapy. PD-L1, programmed death-ligand 1. Created in Biorender.com.

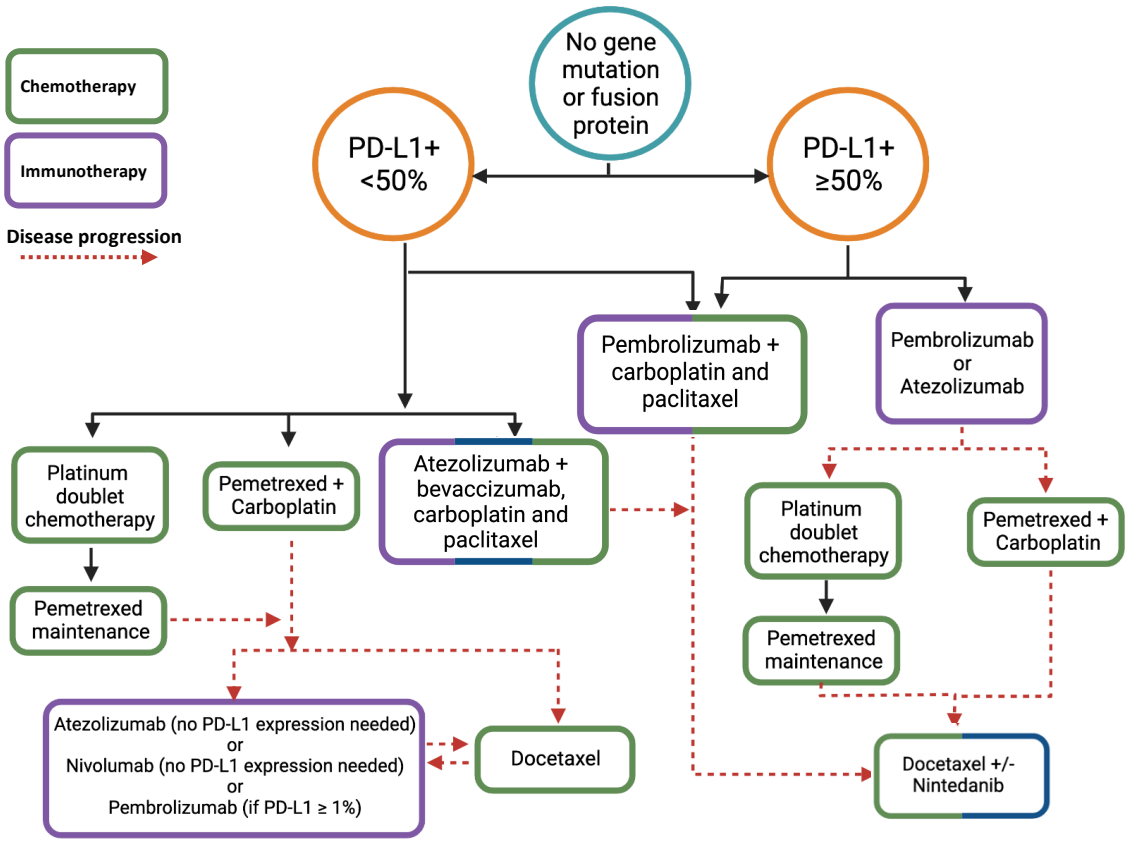

Figure 1.15 Treatment options for adenocarcinoma patients harbouring no targetable receptor tyrosine kinase mutations.

Patient first-line treatment options are dependent on the level of tumour PD-L1 expression and will determine whether a patient receives first-line chemotherapy, chemoimmunotherapy, chemoimmunotherapy with VEGF targeted therapies or single agent immunotherapy. Upon disease progression, patients are either treated with chemotherapy or chemotherapy with VEGF targeted therapies or single agent PD-1/PD-L1 ICIs. PD-L1, programmed death-ligand 1. Created in Biorender.com.

1.3.4.1 Surgery

In medically fit patients with early-stage disease (I-IIIa) surgical resection is the most effective therapy in terms of overall survival and cure rates, with lobectomy with systematic nodal

dissection the definitive treatment option (Herbst *et al.* 2018). In the UK resection rates have continued to rise slowly, with 59% of patients with stage I/II disease and a good performance status i.e., the ability of an individual to undertake everyday tasks, receiving surgery in 2019 (Royal College of Physicians 2022). However, despite most patients remaining disease-free following surgery, 30-55% of tumours will recur due to the presence or development of micrometastases; therefore, following surgery patients also receive adjuvant combination chemotherapies (Uramoto and Tanaka 2014; Duma *et al.* 2019). Neoadjuvant chemotherapy can also be used as a first-line treatment prior to surgery where it demonstrates more tolerant toxicities than adjuvant therapies and has been associated with tumour shrinkage and a decrease in micrometastases (Duma *et al.* 2019).

1.3.4.2 Radiotherapy and chemotherapy

The standard therapy for patients with unresectable locally advanced tumours is a combination of systemic cytotoxic therapies and thoracic radiation, with a survival advantage demonstrated for concurrent regimes over sequential approaches (Herbst *et al.* 2018). Whilst systemic therapies have become increasingly personalised over the past few decades, curative radiotherapy is still prescribed according to the TNM stage and performance stage of the patient, taking no account for tumour biology (Brown *et al.* 2019). Stereotactic ablative radiotherapy delivers an ablative dose of radiation with high precision to small tumour lesions and is primarily used for patients with early-stage disease who are unable/unwilling to undergo surgical resection, with 62% of stage Ia-IIb patients who did not undergo surgery receiving some form of radiotherapy (Jones and Baldwin 2018; Royal College of Physicians 2022). Furthermore, patients with locally advanced disease can receive concurrent chemoradiotherapy with curative intent, with palliative radiotherapy offered for late-stage patients to relieve patients of symptoms such as pain and cough (Brown *et al.* 2019).

As mentioned previously, early-stage patients who undergo surgical resection may receive neoadjuvant or adjuvant chemotherapy to decrease the likelihood of distant metastases and disease recurrence (Duma *et al.* 2019). In patients presenting with metastatic disease systemic treatment with chemotherapy, alone or in combination with radiotherapy, immunotherapies or targeted therapies, is required for disease control (NICE 2021). Platinum-based doublet therapy using a platinum-based anti-neoplastic agent in combination with a second agent targeting the cell cytoskeleton has been the standard chemotherapy regimen for patients with advanced stage NSCLC (Evans 2013). Gemcitabine, Carboplatin and Cisplatin are all platinum-based chemotherapeutic agents which inhibit DNA synthesis and replication in fast dividing cells, whilst Vinorelbine (microtubule-destabilising), Paclitaxel and Docetaxel (microtubule-stabilising) target the cytoskeleton of fast-dividing cells to inhibit

mitosis (Jordan and Wilson 2004; Horita *et al.* 2017). These chemotherapy agents can be used alone or in combination with one another or with targeted or immunotherapeutic targets at various stages of disease progression (NICE 2021)(Figures 1.12 & 1.13 &1.14).

1.3.4.3 Targeted therapies

Targeted TKI therapies against clonal genetic alterations in the tyrosine kinases *EGFR, ALK* and *ROS1* have demonstrated improved clinical outcomes in a significant proportion of adenocarcinoma patients presenting with advanced disease. Molecularly targeted inhibitors were first introduced in the 1990s with the use of the *EGFR* TKI Gefitinib, with the introduction of molecular therapies targeting *ALK, MET* and *ROS1* demonstrating favourable and durable response rates in many adenocarcinoma subtypes (Alexander *et al.* 2020). However, these high response rates are often short-lived, with acquired resistance to chronic TKI treatment often developing within 9-12 months in most patients, hence the need for the use of multimodality treatments in advanced NSCLC patients (Chen *et al.* 2014).

1.3.4.3a EGFR inhibitors

EGFR is a receptor tyrosine kinase that, upon activation, leads to downstream signalling involved in increased cell survival, proliferation, invasion, and angiogenesis (Wheeler *et al.* 2010). Heterozygous sensitising mutations clustering around the ATP-binding pocket of the tyrosine kinase domain of EGFR are seen in 14% of adenocarcinoma patients and lead to constitutive EGFR activation and ligand independence (Collisson *et al.* 2014). The first-generation TKIs Erlotinib and Gefitinib are reversible competitive ATP inhibitors that only target EGFR, whilst the second-generation TKIs Afatinib and Dacomitinib function through irreversibly inhibiting ATP in EGFR, HER2 and HER4 (Roy S. Herbst *et al.* 2018) (Figure 1.13). *EGFR* mutation-positive adenocarcinoma patients demonstrate an 80% response rate to EGFR TKIs, with 10-14 months of progression-free survival (PFS), yet most patients will eventually develop disease progression due to acquired resistance (Mok *et al.* 2009; Wu *et al.* 2014). The most common cause of acquired resistance to these TKIs is a further *EGFR* mutation on the codon 790 (T790M), with further mutations and amplifications in *HER2*, *BRAF* and *P13KCA* further limiting the long-term efficacy of these TKIs (Sequist *et al.* 2011; Camidge *et al.* 2014). Treatment with the third-generation EGFR TKI Osimertinib, a selective inhibitor of both the original sensitising mutation and TP790M mutation, binds covalently to codon 797 thus overcoming the enhanced ATP affinity from the T790M mutation (Roy S. Herbst *et al.* 2018). Second-line Osimertinib is effective in patients harbouring the T790M mutation following progression after first-line EGFR TKI therapy, with PFS and overall response rate significantly greater than second-line platinum chemotherapy alone (Mok *et al.* 2016) (Figure 1.13). Yet despite these good clinical responses, just 14% of stage IIIb-IV non-squamous

NSCLC patients in England had their *EGFR* mutation status recorded in 2018 (Royal College of Physicians 2021) . Furthermore, mutations at codon 797 (C797S) confer further resistance to third-generation TKIs, with tumours harbouring an initial sensitising *EGFR* mutation, TP790M and C797S resistant to all EGFR TKIs (Roy S. Herbst *et al.* 2018).

Interestingly, CD200 expression by cancer-associated fibroblasts (CAFs) appears to augment the sensitivity of *EGFR* mutated lung adenocarcinomas to *EGFR* TKIs. Using patient-derived CAF clones, Ishibashi *et al.* (2017) demonstrated that clones which highly expressed CD200 were able to enhance the anti-tumour effect of Gefitinib treatment on PC9 adenocarcinoma cells *in vitro.* Moreover, the PFS after Gefitinib treatment for patients with CD200-positive CAFs tended to be longer than in those with CD200-negative CAFs (p=0.057). PC9 cells do not express CD200R, therefore CD200 exerts its effects through an as yet unknown receptor, or it may induce conformational changes in other associated molecules thus triggering the pro-apoptotic signalling cascade upon *EGFR* TKI treatment. Although this effect requires further investigation, it is interesting to consider the effect potentially blocking CD200 as an immunotherapy may have on the other treatment modalities. Currently in adenocarcinoma, immunotherapies are used once disease progression has been made on all available *EGFR* TKIs, therefore blocking this interaction further down the treatment pipeline may not affect TKI sensitivity.

1.3.4.3b ALK and ROS1 inhibitors

Gene rearrangements of the transmembrane receptor tyrosine kinase ALK occur in ~5% of adenocarcinoma patients (Alexander *et al.* 2020). The first-generation TKI Crizotinib is an oral competitive ATP inhibitor of ALK, MET and ROS1 that is associated with improved objective response rates and PFS compared to cytotoxic therapies. Patients who demonstrate acquired resistance to Crizotinib benefit from treatment with the second-generation ALK TKIs Certinib, Alectinib and Brigatinib (Kwak *et al.* 2010). Acquired resistance to ALK inhibitors is predominantly caused by secondary *ALK* mutations, or through upregulation of bypass signalling pathways such as EGFR and MAPK. The most common secondary *ALK* mutation (G1202R) confers resistance to all ALK inhibitors except Lorlatinib, a potent third-generation ALK TKI with activity against most known *ALK* resistance mutations (Shaw *et al.* 2017)(Figure 1.13). *ROS1* encodes a receptor tyrosine kinase with a high degree of homology to ALK that becomes constitutively activated when rearrangement leads to fusion of its tyrosine kinase domain with a partner gene such as CD74 (Facchinetti *et al.* 2017). Due to the high homology in kinase domains between ROS1 and ALK, patients with *ROS1* rearrangement (1-2%) can be treated with Crizotinib, Entecinib and Lorlatinib (Herbst *et al.* 2018; Alexander *et al.* 2020; NICE 2021)(Figure 1.13).

1.3.4.3c Other targeted therapies

The identification of oncogenic driver mutations in adenocarcinoma has transformed how patients are treated, with chemotherapy no longer a standard of care but a default if patients do not present with an actionable driver mutation. In a multicentre Lung Cancer Mutation Consortium, targetable oncogenic mutations were observed in 64% of adenocarcinoma patients, with those who could be treated with targeted therapies associated with improved overall survival over those without targeted treatments (Kris *et al.* 2014). Of the 7% of adenocarcinoma patients that harbour a BRAF mutation, around half present with a single transversion at residue 600 of exon 15 (V600E) that can be targeted with the BRAF inhibitors Dadrafenib and Vemurafenib as single agents or in combination with the MEK inhibitor Trametinib (Collisson *et al.* 2014; Planchard *et al.* 2016). Furthermore, somatic mutations in MET have been identified, suggesting patients may respond to the MET inhibitors Crizotinib and Cabozantinib (Paik *et al.* 2015).

Adenocarcinoma patients have also shown good responses to the VEGF inhibitor Bevaccizumab and the VEGF receptors 1-3, platelet-derived growth factor (PDGF) receptors α/β and FGF receptors 1–3 angiokinase inhibitor Nintedanib in combination with chemotherapy either following immunotherapy or in combination with the PD-L1 inhibitor Atezolizumab (Grohé *et al.* 2022) (Figures 1.13 & 1.14). These inhibitors of angiogenic factors have been demonstrated to be effective in patients who have acquired resistance to ICIs by supporting vessel normalisation and improving infiltration of immune cells into the TME, thus tipping the balance towards an immune-supportive TME through an angio-immunogenic switch (Fukumura *et al.* 2018). There is clear evidence that angiogenesis is associated with the development of an immunosuppressive TME which can promote resistance to ICI therapies; moreover, VEGF within the TME can promote immunosuppression by modulating immune cell functions and preventing successful immune cell infiltration. The angio-immunogenic switch theory suggests that adjuvant or combination anti-angiogenic treatment could reverse the immunosuppressive angiogenic signals which contribute to the initial failure of ICI treatment (Fukumura *et al.* 2018; Grohé *et al.* 2022). Indeed, Nintedanib plus docetaxel in the third-line setting demonstrated a high response rate and disease stabilisation in patients whose disease had progressed on prior chemotherapy and ICI treatment (Grohé *et al.* 2022). Furthermore, patients treated with Atezolizumab combined with Carboplatin + Paclitaxel + Bevacizumab demonstrated significantly prolonged PFS and OS than those treated without Bevacizumab, suggesting that blocking angiogenesis can benefit NSCLC patients receiving ICIs (Reck *et al.* 2019).

1.3.4.4 Immunotherapies

Despite the success of molecularly targeted therapies in NSCLC treatment, most tumours do not harbour an actionable driver mutation; in these patients anti-PD-1/PD-L1 ICI immunotherapy either alone or in combination with chemotherapy have become the first-line standard of care for advanced SCC and adenocarcinoma tumours (Grant *et al.* 2021). The anti-PD-1 antibodies Pembrolizumab and Nivolumab and the anti-PD-L1 antibody Atezolizumab have now been approved for the first- second- and third-line treatment of driver-negative NSCLC, with these ICIs also approved for the second- and third-line treatment of driver-positive NSCLC tumours (Grant *et al.* 2021; NICE 2021)(Figures 1.13 & 1.14 & 1.15). ICIs treatment has had a profound effect on the survival of patients with advanced NSCLC. In metastatic patients, first-line ICIs either alone or in combination with platinum doublet chemotherapy offered a 15-20% OS benefit at 1 year compared with chemotherapy alone (Conforti *et al.* 2018; Brueckl *et al.* 2020). Furthermore, second-line ICI therapy increased 1 year survival by 10% and maintenance PD-L1 ICI with concurrent chemoradiation demonstrated a 10% OS benefit at 2 years compared to placebo (Naqash *et al.* 2020). The high somatic TMB, particularly in smokers, of NSCLC tumours makes NSCLC a prime candidate for ICI therapy, as reflected in the durable clinical efficacy seen in responder patients (Grant *et al.* 2021). However, despite subsets of patients deriving durable benefits with PD-1/PD-L1 ICI therapy overall response rates are 47-63%, with non-responder patients demonstrating both cell intrinsic and extrinsic primary resistance mechanisms as described in Section 1.1.6 (Doroshow *et al.* 2019). Furthermore, of those that do show an initial or sustained response, disease relapse and progression occurs in most cases due to acquired secondary resistance mechanisms within the TME (Popat *et al.* 2020). Therefore, identification of predictive markers of ICI therapy response or the generation of multi-modality immunological therapies could greatly improve the success of PD-1/PD-L1 ICI therapies in NSCLC.

1.3.4.4a PD-1/PD-L1 ICIs

PD-1/PD-L1 antibodies were approved for the second- and third-line treatment of metastatic NSCLC without targetable driver mutations in 2015. Since then, PD-1/PD-L1 ICIs have been approved for the first-line monotherapy treatment of tumours with PD-L1 ≥ 50% expression or in combination with chemotherapy independent of PD-L1 expression (Brueckl *et al.* 2020; NICE 2021). Subsets of patients who respond to these therapies demonstrate exceptionally long-lasting responses and survival, with 31.9% of stage IV patients treated with Pembrolizumab in the first-line and 16% of stage IV patients treated with Nivolumab in the second-line still alive at 5 years following treatment (Reck *et al.* 2016; Gettinger *et al.* 2018; Shiono *et al.* 2019). However, although PD-1/PD-L1 ICIs have been approved for the treatment of NSCLC patients who harbour targetable driver mutations, these immunotherapies

appear to have limited responses in these patients. In a retrospective analysis, only 3.7% of patients with *EGFR* or *ALK* mutations demonstrated response to PD-1/PD-L1 ICIs compared to 23.3% of driver negative tumours (Gainor *et al.* 2016). Moreover, a meta-analysis of 5 trials looking at PD-1/PD-L1 ICIs in advanced NSCLC saw that among patients with *EGFR* mutations, OS was not improved when compared to Docetaxel alone suggesting that currently ICIs are minimally effective in driver mutation positive NSCLC patients (Lisberg *et al.* 2018).

The observation that tumour PD-L1 expression was a predictor of response to PD-1/PD-L1 ICI in patients with advanced stage NSCLC led to the implementation of PD-L1 tumour expression, as determined by IHC, as a biomarker for determining the optimal immunotherapy treatment strategy for patients (Taube *et al.* 2014; Grant *et al.* 2021). Monotherapy with Pembrolizumab and Atezolizumab is only approved in the first-line setting for patients with a PD-L1 tumour expression of ≥ 50%, with tumours demonstrating lower PD-L1 expression approved for first-line Pembrolizumab in combination with platinum doublet chemotherapy (NICE 2021). However, despite consideration and validation of the 50% tumour cell PD-L1 expression cut-off, not all patients with high PD-L1 expression respond to PD-1/PD-L1 antibodies. Similarly, a subset of patients with low PD-L1 expression have demonstrated good clinical responses and long-term disease control (Herbst *et al.* 2018; Garon *et al.* 2019; Herbst *et al.* 2020).

The PD-1 IgG4 humanised mAb Nivolumab was the first PD-1 ICI to demonstrate significant anti-tumour activity in pre-treated metastatic SCC and adenocarcinoma patients, demonstrating extended OS when compared with standard second-line Docetaxel alone. An updated survival analysis demonstrated a median OS of 9.2 months versus 6 months for patients with SCC and a median OS of 12.2 months versus 9.5 months for adenocarcinoma patients when treated with Nivolumab versus Docetaxel only (Borghaei *et al.* 2015; Brahmer *et al.* 2015). Furthermore, Nivolumab patients revealed an unprecedented 4-year survival of 14% compared with 5% for Docetaxel, thus highlighting a durable anti-tumour response for a subset of patients (Horn *et al.* 2017). Subsequently the PD-1 inhibitor Pembrolizumab and the PD-L1 inhibitor Atezolizumab were approved for NSCLC treatment and have demonstrated durable clinical responses (Grant *et al.* 2021). Pembrolizumab, when used as a first-line treatment in patients with advanced disease and a tumour PD-L1 expression of ≥50% demonstrated significant response rates when compared to chemotherapy alone, with a median OS of 30 months compared to 14.2 months and a 5-year OS of 32% compared to 16% in the chemotherapy arm (Reck *et al.* 2016; Reck *et al.* 2019). Pembrolizumab has also shown an OS benefit in patients with a tumour PD-L1 expression of ≥ 1%, with patients receiving ICIs demonstrating extended median OS compared to chemotherapy alone (Lopes

et al. 2018). The PD-L1 inhibitor Atezolizumab also demonstrated improved OS when compared to chemotherapy alone, with a median OS of 13.8 months compared to 9.6 months (Rittmeyer *et al.* 2017). Moreover, the clinical success of this ICI appears to be associated with tumour PD-L1 expression, with patients with the highest PD-L1 tumour expression deriving the greatest overall response rates and increases in OS duration (Herbst *et al.* 2014). Pembrolizumab and Atezolizumab have also been approved in combination with platinum doublet chemotherapy where they have demonstrated significant improvements in OS (Grant *et al.* 2021).

1.3.4.4b Improving PD-1/PD-L1 ICIs response rates

Patients treated with PD-1/PD-L1 immunotherapies either demonstrate durable responses, an initial response followed by disease progression or, in the case of approximately half of patients, demonstrate no response or benefit (Popat *et al.* 2020). ICIs work by reactivating an exhausted and suppressed anti-tumour immune responses through inhibition of negative immunoregulatory immune checkpoint pathways (Johnston *et al.* 2014). Therefore, tumour infiltrating immune cells are the most important component for an active response to ICIs, with the presence of a prominent T cell infiltration prior to treatment associated with increased sensitivity and survival (Schalper *et al.* 2015; Doroshow *et al.* 2019). In general, TMEs can be classified into three types based on the presence of infiltrating immune cells and the level of immunosuppression or immune evasion within the TME (Jenkins *et al.* 2018). The first is an immune inflamed TME characterised by a dense functional CD8+ T cell infiltration; these TMEs are most associated with responders (Brueckl *et al.* 2020). Patients presenting with either acquired or primary resistance tend to have TMEs that either have an excluded immune infiltrate, characterised by abnormal angiogenesis and an immunosuppressive stroma that prevents immune cell infiltration, or an immune ignorant TME that has a low tumour mutational burden and decreased antigen presentation (Hegde *et al.* 2016; Yi *et al.* 2019). To overcome these mechanisms of immunotherapy resistance, several additional therapies can be used in combination with PD-1/PD-L1 ICIs to overcome the boundaries that the reactivated anti-tumour immune response is faced with. The use of anti-angiogenic drugs to support vessel normalisation and increase immune cell infiltration and/or systemic chemotherapy to induce immunogenic cell death and thus increase the antigenicity, immunogenicity, and susceptibility of tumour cells have been approved for use in combination with PD-1/PD-L1 ICIs (Zitvogel *et al.* 2013; Yi *et al.* 2019). However, these combination regimes have only demonstrated minimal improvements in increasing response rates and survival.

1.3.4.4c Combination ICIs

One of the most promising strategies for overcoming resistance and prolonging therapeutic benefit from ICIs is the use of dual immune checkpoint blockade (Jenkins *et al.* 2018). By

targeting two immunoregulatory pathways at distinct yet synergistic stages in the immune response, namely the priming and effector phases of the adaptive immune response for CTLA-4 and PD-1 respectively, the likelihood of a successful anti-tumour immune response is increased (Das *et al.* 2015). Data from several early phase trials suggests that first-line doublet Nivolumab and Ipilimumab increases overall survival for advanced stage NSCLC patients, with similar increases in overall survival seen in patients with both PD-L1 positive and negative tumours (Hellmann *et al.* 2019; Ramalingam *et al.* 2020). The median overall survival of 17.2 months with combination immunotherapy compared to 12.2 months for Nivolumab and chemotherapy is particularly promising, as this subgroup of low PD-L1 patients have consistently demonstrated less benefit from PD-1/PD-L1 ICIs (Mariniello *et al.* 2020). Preliminary data also shows that Atezolizumab in combination with the anti-T cell immunoreceptor with Ig and ITIM domains (TIGIT) ICI Tiragolumab enhances anti-tumour activity when compared with Atezolizumab alone in advanced NSCLC patients (Rodriguez-Abreu *et al.* 2020). TIGIT is a coinhibitory receptor that works in the effector phase of the adaptive immune response to synergise with PD-1/PD-L1 to potently inhibit effector T cell function, suggesting that dual blockade of immune checkpoints that function in the same stages of the immune response can also synergise to increase the anti-tumour immune response (Johnston *et al.* 2014). These promising findings from dual checkpoint inhibition trials have led to several more novel combination immunotherapy strategies, with trials looking at the effects of inhibition of TIM-3 and LAG-3, both immune checkpoints which function during the effector phase of the immune response, in combination with PD-1/PD-L1 ICI currently underway (Lipson *et al.* 2021; ClinicalTrials.gov NCT02817633).

1.4 Aims of this thesis

PD-1/PD-L1 ICIs have increased overall survival in NSCLC patients, however only a subset of patients show durable clinical responses due to primary and acquired resistance mechanisms, such as the expression of other immune checkpoint molecules. Therefore, the identification of new immune checkpoints to be inhibited in combination with current ICIs may benefit these patients by further alleviating the immunosuppressive signals which allow the tumour cells to escape anti-tumour immunity. As a critical regulator of immune homeostasis in normal lung, the immune checkpoint CD200 may also be expressed by tumour cells upon malignant transformation to evade immune attack and promote tumour growth. CD200 is expressed by several solid and haematological malignancies, with its expression correlating with an increase in immunosuppressive Treg cells, a decrease in memory T cells and dysfunction of cytotoxic effector NK cells. CD200 functions in the effector phase of T cell responses and therefore blocking CD200 signalling has the potential to synergise with PD-1 blockade to re-activate an anti-tumour T cell response. Furthermore, CD200 is a potent

regulator and suppressor of myeloid cell function, suggesting that targeting CD200 signalling may further decrease immune suppression and increase the innate anti-tumour immune response.

Aims:

1. Define CD200 expression in the normal human lung and NSCLC tumours
    a. Determine whether the cells of origin of adenocarcinoma and SCC tumours express CD200 in healthy tissue
    b. Define the expression pattern of CD200 in adenocarcinoma and SCC tumours and determine whether this has any correlation with patient clinical characteristics and survival
2. Investigate the relationship between CD200 expression and the composition of the immune infiltrate in NSCLC tumour tissue using a combined bioinformatics and immunohistochemical approach
    a. Explore the relationship between immune cell infiltration and patient clinical characteristics and survival
    b. Determine the relationships between tumour CD200 expression and the absolute and relative infiltration of cytotoxic and regulatory immune cells
3. Determine the effects of tumour CD200 expression on NK cell cytotoxic and cytolytic activity and investigate whether blockade of CD200 signalling using an anti-CD200 antibody is sufficient to restore anti-tumour immunity *in vitro*.

Chapter 2:
Materials and Methods

2.Materials and Methods

2.1 Tissue samples

2.1.1 Mouse tissue samples

Normal mouse back skin and lung tissue were obtained from wild type (WT) FVB/N mice. All animals were maintained on an outbred background and housed in a standard facility in accordance with institutional animal care guidelines and UK Home Office regulations (project licence P4EF9C98F). All animals were given access to RM3(E) standard diet (Special Diets Service UK) and fresh water ad libitum.

2.1.2 Human tissue samples

Normal human lung, human tonsil, and lung cancer tissue microarrays (TMAs) were obtained from US Biomax, Zyagen. Lung cancer tumour sections were obtained from the Wales Cancer Bank (WCB project numbers 18/022 & 20/066). Normal human skin sections were obtained with a protocol approved by the local independent research ethics committee (09/WSE/02/01).

2.2 Patient data

Ethical approval for the collection and use of NSCLC tissue was gained by the Wales Cancer Bank (project 20/066). Informed consent for the sampling of tumour sections was obtained from NSCLC patients undergoing surgical resection, with consent and sample collection performed by WCB staff. Histological assessment and diagnosis were performed by a certified NHS histopathologist. Relevant patient data for 238 of the 240 patients was obtained from the Wales Cancer Bank and is shown in Table 2.1. Overall survival was determined from the date of procedure to the date of death (range 0.5 - 126 months); where stated, deaths unrelated to cancer were censored. At the time of record collection, all patients still alive were censored at 126 months.

Table 2.1 Primary demographics for samples used in this project

Demographics	**All patients with data available = 238 (%)**	
Sex	Male	94 (39.5)
	Female	144 (60.5)
Age at diagnosis, years	Median	71
	Range	45 - 91
Tumour stage	T1	71 (29.8)
	T2	122 (51.3)
	T3	37 (15.5)
	T4	8 (3.4)
Node stage	N0	139 (58.4)
	N1	54 (22.7)
	N2	25 (10.5)
	Nx	20 (8.4)
Disease Stage	I	92 (38.7)
	II	104 (43.7)
	III	42 (17.6)
Smoking status	Ever	189 (79.4)
	Never	12 (5.1)
	Unknown	37 (15.5)
Overall survival, months	Median	71
	Range	0.5 - 126

2.3 Immunohistochemistry & Immunofluorescence

2.3.1 Immunofluorescence (IF)

Paraffin embedded tissue sections were baked for 30 min at 60˚C and dewaxed and rehydrated using the following method: Xylene (10 min x 2), 100% ethanol (5 min x 2), 95% ethanol (5 min x 1), 70% ethanol (5 min x 1) then PBS (5 min x 1). For antigen retrieval, sections were incubated in citrate buffer (8 mM sodium citrate, pH 6.0) in a pressure cooker and heated in a microwave at full power (750 W, 10 min). Tissue sections were surrounded with a hydrophobic barrier using an ImmEdge PAP pen (Vector Laboratories). Non-specific binding was blocked with 10% donkey serum in PBS for 1 hour at room temperature (RT). Specimens were washed in PBS (5 min x4) and then incubated overnight at 4˚C with primary antibodies in 5% serum in PBS. A summary of primary and secondary antibodies used can be found in Table 2.2. Sections were washed in PBS-Tween20 (0.05%) (5 min x4) and incubated at RT for 1 hour with fluorescence-conjugated secondary antibodies diluted in 1:1 volume PBS and BlockAid (Thermo Fisher Scientific) with 1 µl of 20 µg/ml DAPI for nuclear staining. Specimens were then washed in PBS-Tween20 (0.05%) (5 min x4) and a coverslip mounted using Vectashield mounting medium (Vector Laboratories). Images were acquired using a DM6000B upright fluorescence microscope (Leica Microsystems) and a Zeiss Axioscan.Z1 slide scanner (Carl Zeiss Microscopy). Image analysis was performed using ImageJ (National Institutes of Health) and QuPath software (Bankhead *et al.* 2017). Hair follicle bulge cells from mouse and human skin sections were used as CD200 positive tissue controls and for primary antibody titration. Secondary antibody specificity was confirmed by performing the entire procedure in the absence of primary antibody.

Table 2.2 Primary antibodies used for IF

Primary antibody	**Dilution**	**Species**	**Isotype**	**Clone**	**Serum**	**Source**
CD200	1:100	Goat	IgG	Polyclonal	Donkey	R&D Systems
Secondary antibody	**Dilution**	**Species**	**Isotype**	**Clone**	**Fluorochrome**	**Source**
Donkey anti-goat	1:500	Donkey	IgG	Polyclonal	Alexa Fluor 488	Invitrogen

2.3.2 Immunohistochemistry (IHC)

Baking, dewaxing, and rehydration were performed as described above (Section 2.2.1). Sections were incubated in Tris-EDTA buffer (10 mM Tris, 1 mM EDTA, 0.05% Tween-20, pH 9.0) in a pressure cooker and heated in a microwave at full power (750 W, 20 min) for antigen retrieval. After cooling, specimens were washed in PBS (5 min x 1) and a hydrophobic barrier was drawn around the tissue. Endogenous peroxidase activity was blocked with DAKO Dual Endogenous Enzyme-Block (Agilent Technologies) for 10 min at RT followed by blocking for 1 hour at RT in 10% serum in PBS. Tissue sections were washed (PBS; 5min x 4) and

incubated overnight with primary antibodies diluted in 5% serum (list of antibodies and serum used is summarised in Tables 2.3a). The next day, sections were washed in PBS-Tween20 (0.05%) (5 min x 4) and incubated for 1 hour at RT with biotinylated secondary antibodies diluted in 5% serum (Table 2.3b). Expression was detected using Vectastain avidin-biotin enzyme complex-horseradish peroxidase (ABC-HRP; Vector Laboratories) with 3,3-Diaminobenzidine (DAB) as the chromogen (DAKO). After washing, sections were incubated with ABC-HRP for 30 min at RT and washed again before addition of DAB under the microscope until optimal staining was observed (development times for each antibody can be found in Table 2.3a). Sections were then washed in PBS-tween, counterstained with haematoxylin (Atom Scientific) for 1 minute and then dehydrated using the following method: 70% ethanol (20 sec x 1), 95% Ethanol (20 sec x 1), 100% ethanol (2 min x 2), Xylene (2 min x 2). Slides were mounted with DPX mountant (Merck) and images acquired using either a Zeiss Axioscan.Z1 (Carl Zeiss Microscopy) or an Olympus Slideview VS2000 slide scanner. Controls for CD200 were as described above (Section 2.2.1). Human tonsil was used as control tissue for all immune cell markers with their respective cells as positive controls and the remaining cells within the tonsil used as negative controls. Secondary antibody specificity was confirmed through no primary antibody controls.

2.3.2a Multi-label IHC

For multi-label IHC, staining was performed as above with ABC-alkaline phosphatase (ABC-AP; Vector Laboratories) and Immpact Vector Red (Vector Laboratories) in place of DAB. Following staining visualisation, sections were then washed before a 15 min incubation with Avidin block, followed by a PBS-Tween20 rinse and then a 15 min incubation with Biotin block (Vector Laboratories). Tissue was then blocked in 10% serum for 1 hour before overnight incubation at 4˚C with primary antibodies diluted in 5% serum (Table 2.3a). The next day, samples were washed and incubated for 1 hour at RT with secondary antibodies diluted in 5% serum (Table 2.3b) before washing and addition of ABC-HRP for 30 minutes. Optimal staining with DAB was achieved under the microscope before counterstaining, dehydrating and mounting as above (Section 2.2.2). Additional controls for multi-label IHC include performing the entire first stain to completion, with each control section removing successive steps of the second staining process i.e., no primary antibody, no secondary antibody, no ABC etc. to confirm there is no cross-reactions between the two visualisation methods.

Table 2.3a. Primary antibodies used for IHC

Antibody	Dilution	Species	Isotype	Clone	Serum	Source	Chromogen incubation time
CD200	1:100	Goat	IgG	Polyclonal	Donkey	R&D Systems	10 mins (Vector Red)
TTF-1	1:250	Rabbit	IgG	EP1584Y	Goat	Abcam	1 min (DAB)
CD4	1:100	Rabbit	IgG	EPR6855	Goat	Abcam	30 seconds (DAB)
CD8	1:100	Mouse	IgG1, κ	C8/144B	Sheep	Dako	30 seconds (DAB)
CD45	1:100	Rabbit	IgG1	2D1	Goat	R&D Systems	20 seconds (DAB)
CD200R	1:100	Rabbit	IgG	BC069661	Goat	Abcam	30 seconds (DAB)
Foxp3	1:100	Rabbit	IgG	D2W8E	Goat	CST	45 seconds (DAB)

Table 2.3b. Secondary antibodies used for IHC

Antibody	Dilution	Isotype	Clone	Serum	Source
Donkey anti sheep/goat	1:200	IgG	Polyclonal	Donkey	GE Healthcare
Sheep anti mouse	1:200	IgG	Polyclonal	Sheep	GE Healthcare
Goat anti rabbit	Ready-to-use	IgG	Polyclonal		Vector Laboratories

2.3.3 Defining TMA CD200 expression

To determine tumoral CD200 expression, images were opened in Qupath (Bankhead *et al.* 2017) and annotations drawn around the tumour sections to exclude any stromal or immune cells from the analysis (Figure 2.1a). The number of cells was then determined using the automated cell detection tool: nuclei with either a haematoxylin or DAB optical density over the defined intensity threshold were counted (Figure 2.1b). CD200 positivity was then defined based on the mean optical density value of the residual (red) stain within the cells; representative sections of low (1+), medium (2+) and high (3+) staining were used to determine these threshold values (Figure 2.1c). These values were then used to dynamically calculate a tumour H-score to semi-quantitively measure tumoral CD200 expression; the H-score comprises values between 0-300 and captures both the intensity (0-3) and proportion (0-100) of CD200 expression, thereby offering a semi-quantitative method of determining the dynamic range of CD200 expression (Figure 2.1d). The script for this workflow can be seen in Figure 2.1e.

A.

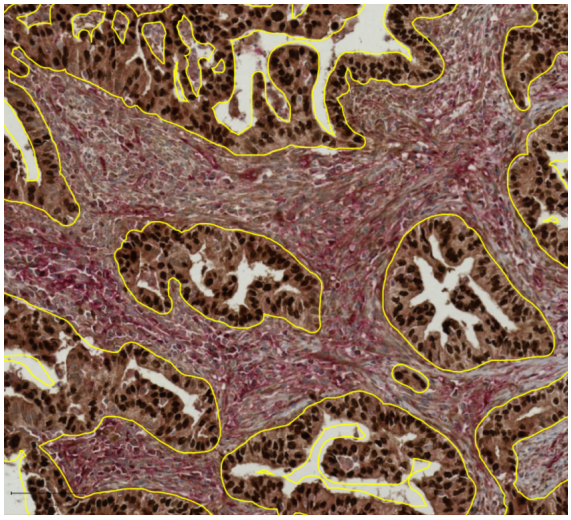

B

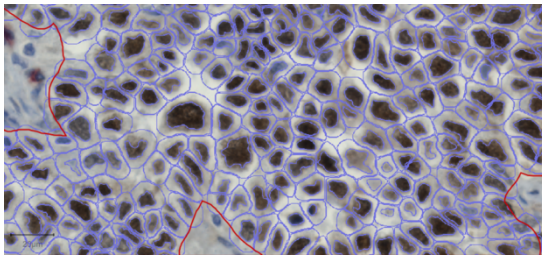

C.

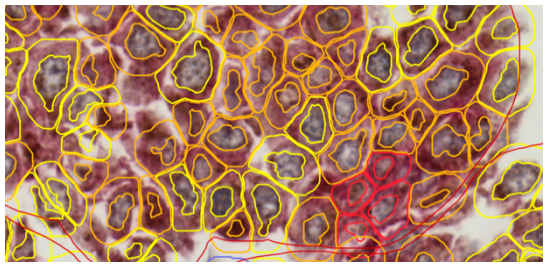

D.

$$H - Score = [1 \times (\%\ of\ 1 + cells) + 2 \times (\%\ of\ 2 + cells) + 3 \times (\%\ of\ 3 + cells)]$$

E.

```
setImageType('BRIGHTFIELD_OTHER');
setColorDeconvolutionStains('{"Name" : "H-RED", "Stain 1" : "Hematoxylin", "Values 1" : "0.65111 0.70119
0.29049 ", "Stain 2" : "DAB", "Values 2" : "0.26917 0.56824 0.77759 ", "Stain 3" : "vector red", "Values 3" : "0.40691
0.68185 0.60787 ", "Background" : " 255 255 255 "}');
runPlugin('qupath.imagej.detect.cells.PositiveCellDetection', '{"detectionImageBrightfield": "Hematoxylin OD",
"requestedPixelSizeMicrons": 0.5,  "backgroundRadiusMicrons": 8.0,  "medianRadiusMicrons": 0.0,  "sigmaMicrons":
1.5,  "minAreaMicrons": 15.0,  "maxAreaMicrons": 500.0,  "threshold": 0.1,  "maxBackground": 2.0,
"watershedPostProcess": true,  "excludeDAB": false,  "cellExpansionMicrons": 5.0,  "includeNuclei": true,
"smoothBoundaries": true,  "makeMeasurements": true,  "thresholdCompartment": "Cell: vector red OD mean",
"thresholdPositive1": -0.7,  "thresholdPositive2": 0.1,  "thresholdPositive3": 0.8,  "singleThreshold": false}');
```

Figure 2.1 Semi-quantitative scoring of CD200 expression.

Representative images demonstrating the automated method used to define CD200 tumour H-scores. (A) Annotations were drawn around tumour sections within each core. (B) An automated cell detection tool was then run to determine the number of cells within each annotation. (C) CD200 positivity was then classified as either 0, 1+ (yellow), 2+ (orange) or 3+ (red) based on pre-determined residual (red) values. (D) These values then generated a H-score for tumour CD200 expression (E) The workflow script used for automated analysis of the TMA cores.

2.3.4 Defining whole section CD200 expression

Due to the volume of slides being analysed several scripts were written within Qupath (Bankhead *et al.* 2017) in order to enable automated batch analysis. Script 1 (Figure 2.2a) first set the image type to brightfield (other) and defined the staining vectors for each of the 3 stains. In order to separate the haematoxylin, DAB and residual (red) stains within the image, annotations were drawn around representative areas of each stain enabling them to be digitally separated using the colour deconvolution method (Ruifrok and Johnston 2001).

Next, the script ran a tissue detection tool to draw an annotation around the entire sample, seen in red in Figure 2.2aii. Annotations were defined using a pixel value between that of the tissue and background. Prior to running of the second script, any artefacts such as tissue folds and areas of necrosis were manually removed using the wand tool.

In order to distinguish between tumoral and stromal CD200 expression the Qupath (Bankhead *et al.* 2017) object classification tool was used to classify all detected cells as either tumour (green) or stroma (purple). Based on annotations drawn around 5-30 representative tumour and stromal areas on each image, the tool used a random trees approach to classify each detected cell based on over 140 measurements (Figure 2aii). Once areas had been defined, a cell detection command was run to detect each cell in the image (seen in red in Figure 2bi) before running cell classification to define each cell as either tumour (green) or stroma (purple) (Fig 2.2bii). A CD200 positivity H-score for tumour and stroma was determined as above (section 2.2.3), with CD200 staining intensity visualised using a graded colour map; dark blue represents the lowest staining intensities and yellow represents the highest (Fig 2.2c).

A. **setImageType**('BRIGHTFIELD_OTHER');
setColorDeconvolutionStains('{"Name" : "H-DAB modified", "Stain 1" : "Hematoxylin", "Values 1" : "0.50897 0.67196 0.53797 ", "Stain 2" : "DAB", "Values 2" : "0.26092 0.59682 0.75877 ", "Stain 3" : "Residual", "Values 3" : "0.13591 0.79246 0.59459 ", "Background" : " 255 255 255 "}');
runPlugin('qupath.imagej.detect.tissue.SimpleTissueDetection2', '{"threshold": 222, "requestedPixelSizeMicrons": 20.0, "minAreaMicrons": 10000.0, "maxHoleAreaMicrons": 1000000.0, "darkBackground": false, "smoothImage": true, "medianCleanup": true, "dilateBoundaries": false, "smoothCoordinates": true, "excludeOnBoundary": false, "singleAnnotation": true}');

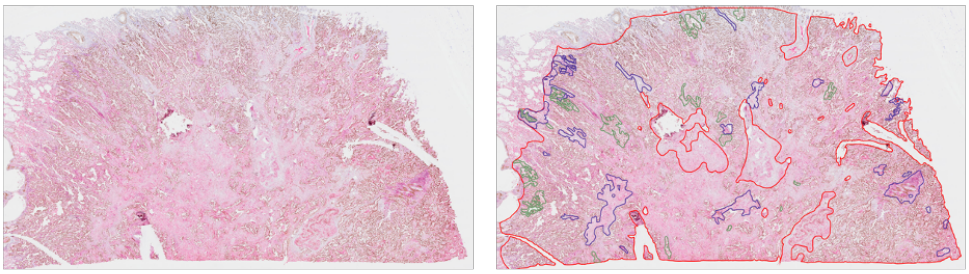

B. **selectAnnotations**();
runPlugin('qupath.imagej.detect.cells.WatershedCellDetection', '{"detectionImageBrightfield": "Hematoxylin OD", "requestedPixelSizeMicrons": 0.5, "backgroundRadiusMicrons": 8.0, "medianRadiusMicrons": 0.0, "sigmaMicrons": 1.5, "minAreaMicrons": 10.0, "maxAreaMicrons": 400.0, "threshold": 0.0, "maxBackground": 1.0, "watershedPostProcess": true, "excludeDAB": false, "cellExpansionMicrons": 5.0, "includeNuclei": true, "smoothBoundaries": true, "makeMeasurements": true}');

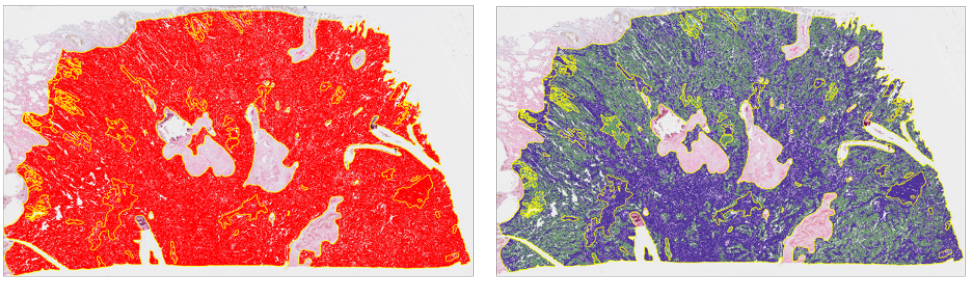

C. **selectAnnotations**();
setCellIntensityClassifications("Cell: Residual OD mean", 0.01, 0.1, 0.5

H-score = [1 x (% of cells 1+) + 2 x (% of cells 2+) + 3 x (% of cells 3+)]

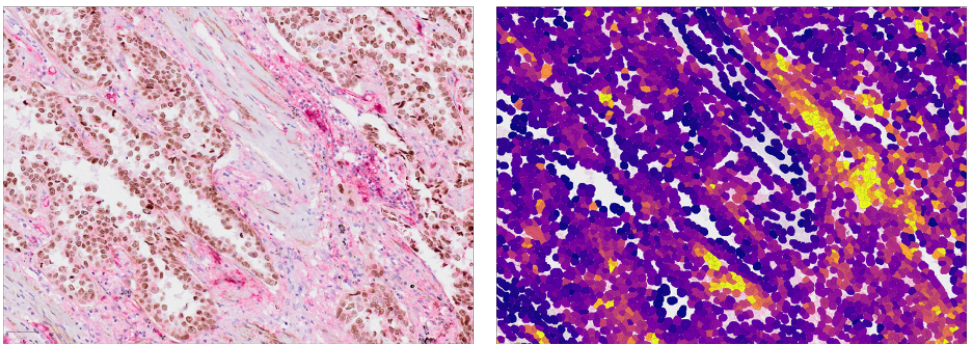

Figure 2.2. Scripted batch analysis of CD200 expression in NSCLC samples.

Scripts and representative images of each stage of the scripted batch analysis to semi-quantitively determine tumoral CD200 expression in NSCLC samples. (A) Script to define and separate the stains within the image and draw an annotation around the tissue sample. (B) Annotations were drawn around representative tumoral and stromal areas before running the script for cell detection. Once cells were detected, the cell classification tool was run (tumour and stroma represented by green and purple, respectively). (C) Negative (0), low (1+), medium (2+) and high (3+) CD200 staining intensity was determined using pre-determined threshold cell residual OD mean values, with tumoral CD200 expression presented as a H score (minimum value = 0, maximum value = 300). CD200 staining intensity is represented by a heat-map gradient, with dark blue being the weakest and yellow the strongest staining intensities.

2.3.5 Quantifying immune cell infiltration

To determine the quantity of specific immune cell populations within each patient sample, images were uploaded into Qupath (Bankhead *et al.* 2017) before separating the staining vectors and generating annotations around the tissue as previously described (section 2.24). Areas of necrosis, tissue folds and artefacts within the tissue were then manually removed from the annotations using the wand tool, prior to running of the positive cell detection script. Unlike the CD200 scripts, positivity was based on a single intensity parameter; parameters for each immune cell script are presented in Table 2.4a and Table 2.4b. For each stain, a minimum of 15 sections were both manually and automatically counted to validate the accuracy of the program (Figures 2.3 & 2.4). All manual vs automatic count linear regressions had an R^2=0.99, suggesting strong correlation in the numbers counted manually and with the automatic scripts. Immune cell numbers were presented as either absolute or relative. Absolute immune cell positivity was presented as the number of positive cells per mm^2. Relative immune cell positivity was defined by:

$$\frac{Number\ of\ positive\ immune\ cells\ per\ mm\text{^}2}{Number\ of\ CD45\ positive\ cells\ per\ mm\text{^}2} \text{ x } 100$$

Table 2.4a Workflow parameters for batch analysis of immune cell positivity in SCC samples.

			CD45	CD56	CD8	Foxp3	CD200R
Script 1		Colour deconvolution stains	Haematoxylin: 0.55215, 0.6842, 0.50915 DAB: 0.35911, 0.61818, 0.69921 Background: 255, 255, 255	H: 0.64715, 0.63815, 0.4171 D: 0.50982, 0.60279, 0.61378 B: 255, 255, 255	H: 0.5892, 0.68723, 0.41214 D:0 .35721, 0.58835, 0.72543 B: 255, 255, 255	H: 0.65732, 0.63731, 0.4022 D: 0.33184, 0.56472, 0.75563 B: 255, 255, 255	H: 0.57642, 0.6854, 0.4325 D: 0.34569, 0.56765, 0.7609 B: 255, 255, 255
		Tissue detection threshold	220		215	216	218
Script 2	*SETUP PARAMETERS*	Detection image	Haematoxylin OD sum		Optical density (OD) sum		
	NUCLEUS PARAMETERS	Background radius (µm)	8				
		Median filter radius (µm)	0				
		Sigma (µm)	1.5				
		Minimum area (µm^2)	5	10			
		Maximum area (µm^2)	400				
	INTENSITY PARAMETERS	Threshold	0.05				
		Maximum background intensity	1				
	INTENSITY THRESHOLD PARAMETERS	Score compartment	Nucleus DAB OD mean	Cytoplasm DAB OD mean	Nucleus DAB OD mean	Nucleus DAB OD sum	Cell DAB OD mean
		Threshold	0.2	0.12	0.3	0.2	0.2

Table 2.4b Workflow parameters for batch analysis of immune cell positivity in adenocarcinoma samples.

			CD45	CD56	CD8	Foxp3	CD200R
Script 1		Colour deconvolution stains	H: 0.53594, 0.66593, 0.51894 D: 0.32798, 0.66096, 0.67496 B: 255, 255, 255	H: 0.75384, 0.60388, 0.25895 D: 0.3999, 0.61585, 0.67883 B: 255, 255, 255	H: 0.68864, 0.64214, 0.3368 D: 0.21655, 0.65108, 0.72741 B: 255, 255, 255	H: 0.68764, 0.62644, 0.31876 D: 0.37657, 0.64360, 0.68763 B: 255, 255, 255	H: 0.64695, 0.67439, 0.43198 D: 0.38750, 0.64076, 0.72488 B: 255, 255, 255
		Tissue detection threshold	216	220	230		218
Script 2	*SETUP PARAMETERS*	Detection image	Haematoxylin OD sum				
	NUCLEUS PARAMETERS	Background radius (µm)	8				
		Median filter radius (µm)	0				
		Sigma (µm)	1.5				
		Minimum area (µm^2)	5				
		Maximum area (µm^2)	400				
	INTENSITY PARAMETERS	Threshold	0		0.05	0	0.05
		Maximum background intensity	1		2.5	2	1
	INTENSITY THRESHOLD PARAMETERS	Score compartment	Cell DAB OD mean	Nucleus DAB OD mean		Nucleus DAB OD max	Cell DAB OD mean
		Threshold	0.13	0.1	0.21	0.2	0.2

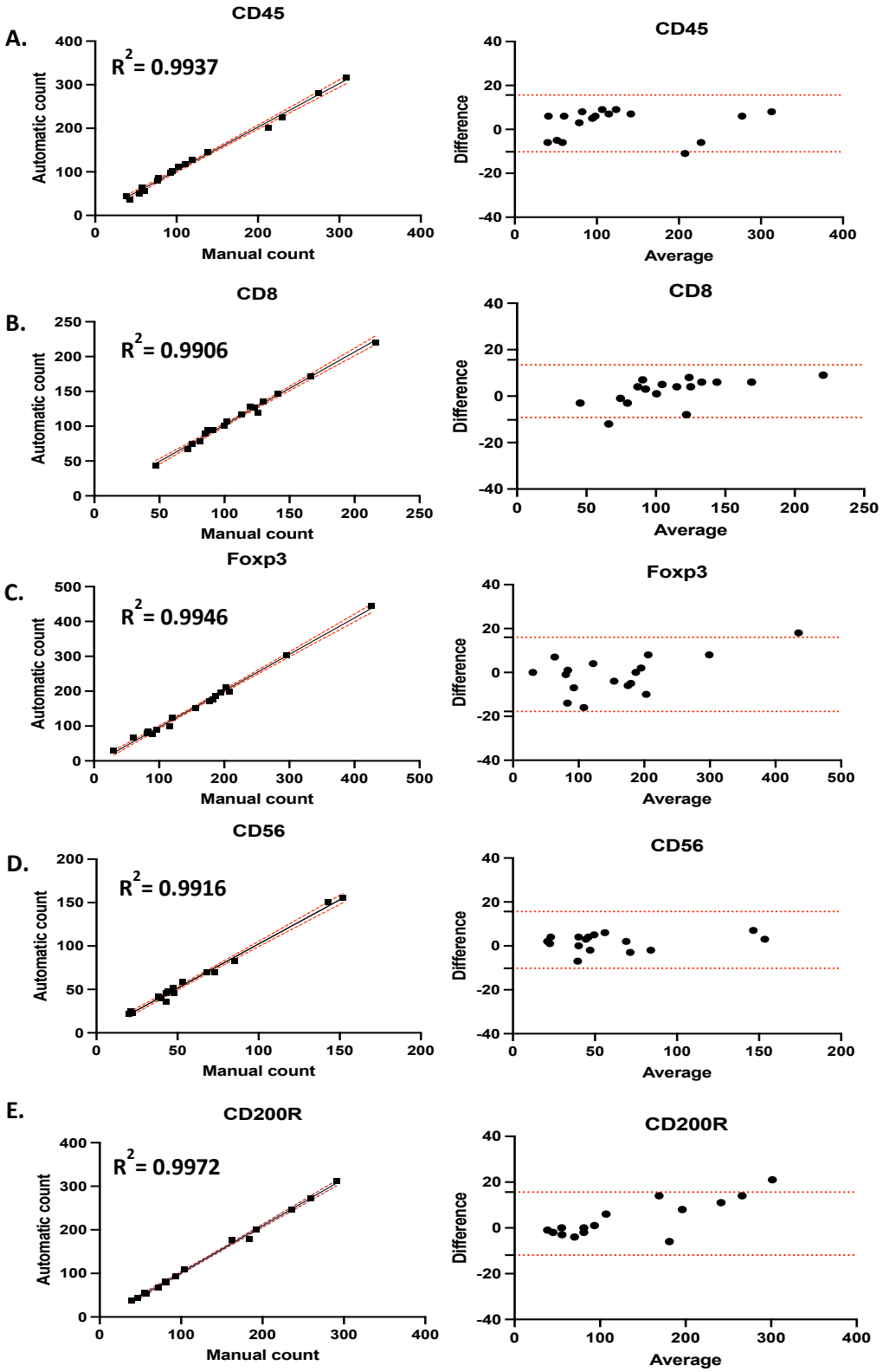

Figure 2.3 Validation graphs for automatic immune cell counting in SCC in Quapth.

Simple linear regression with 95% confidence intervals (red dotted lines) and Bland-Altman graphs with 95% confidence intervals (red dotted lines) of manual vs automatic cell counts of selected areas. All R^2= 0.99 suggesting strong correlation between manual and automatic counting. (A) CD45 (B) CD8 (C) Foxp3 (D) CD56 (E) CD200R.

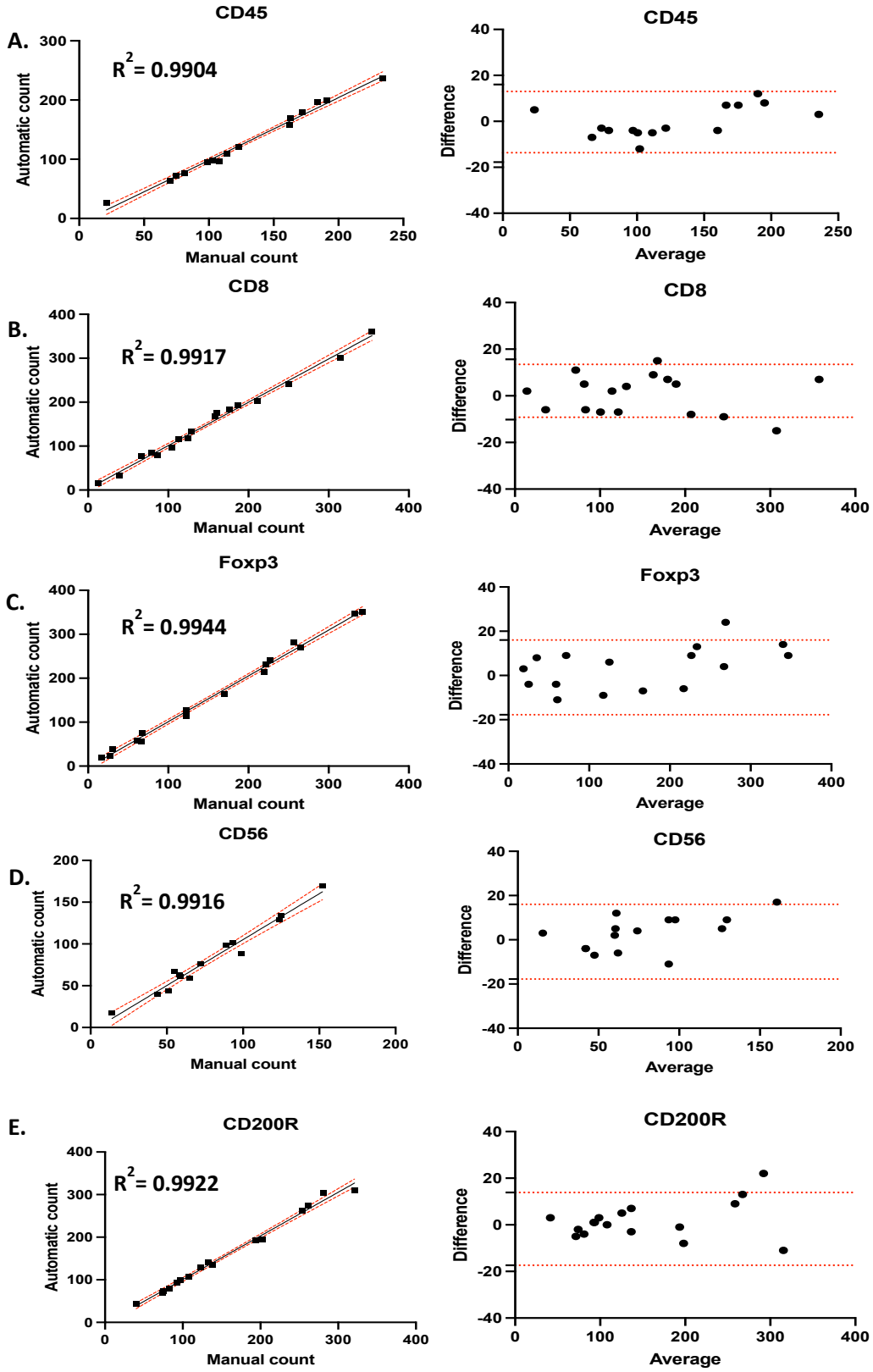

Figure 2.4 Validation graphs for automatic immune cell counting in adenocarcinoma in Quapth.

Simple linear regression with 95% confidence intervals (red dotted lines) and Bland-Altman graphs with 95% confidence intervals (red dotted lines) of manual vs automatic cell counts of selected areas. All R^2= 0.99 suggesting strong correlation between manual and automatic counting. (A) CD45 (B) CD8 (C) Foxp3 (D) CD56 (E) CD200R.

2.4 Online bioinformatic analysis

2.4.1 The Cancer Genome Atlas (TCGA) cohort

The gene expression data of lung adenocarcinoma and squamous cell carcinoma was downloaded from The Broad Institute up to April 3rd 2020 (https://gdac.broadinstitute.org/) using the FireBrowse tool (http://firebrowse.org/). Illimminahiseq-rnaseqv2-RSEM_genes_normalised data was downloaded for adenocarcinoma (LUAD) and SCC (LUSC) consisting of RNA-seq by expectation-maximisation (RSEM) gene-normalised RNA-seq data for 515 and 501 patients, respectively. Corresponding demographic and clinical pathologic data for the patients including age, gender, race, histological classification, tumour location and stage, T/N/M stage, overall survival (OS) time, OS status, progression-free survival (PFS) time and PFS survival status was retrieved from cBioPortal (TCGA, FireHose Legacy) (http://www.cbioportal.org/).

2.4.2 CIBERSORT: Estimating infiltrating immune cell fractions

CIBERSORT (Cell type identification by estimating relative subset of unknown RNA transcripts) is a deconvolution algorithm that analyses the relative expression of 547 genes to predict the proportion of 22 types of infiltrating immune cells (Newman *et al.* 2015). LM22 provides the annotated gene expression signatures for 22 immune cell subtypes, namely: naïve and memory B cells, plasma cells, CD8+ T cells, naïve, memory resting, and memory activated CD4+ T cells, Tregs, T follicular helper cells, gamma-delta T cells, resting and activated NK cells, M0, M1 and M2 macrophages, resting and activated DCs, resting and activated mast cells, eosinophils, and neutrophils. Normalised TCGA data was uploaded to the CIBERSORT website (https://cibersortx.stanford.edu/) and the algorithm run based on the LM22 signatures with significant results ($p < 0.05$) selected for subsequent analysis. As the LM22 matrix was generated from microarray and the input data sets were from RNA-seq, bulk-mode batch correction was enabled to minimise the impact of cross-platform variation. Quantile normalisation was disabled. The permutations for significance analysis were set to 500. The fractions of tumour infiltrating immune cells were evaluated as a whole for each subtype and as individual samples. The Mann-Whitney test was performed to determine the differences in infiltrating immune cell fractions between the upper and lower quartiles of CD200 expression in each subtype. Correlation between CD200 expression levels and infiltrating immune cell fractions was calculated using the spearman correlation.

2.4.3 iPRECOG: Prediction of clinical outcomes from inferred immune fractions

iPRECOG (immune prediction of clinical outcomes from genomic profiles) applies the CIBERSORT algorithm to PRECOG datasets to deconvolute the contribution of each immune

cell expression profile to patient outcomes (https://precog.stanford.edu/iPRECOG.php) (Gentles *et al.* 2015). The inferred immune fractions can then be associated with survival outcomes with a meta z-score. The z-score is directly related to a p value but encodes both the robustness and directionality of statistical associations; to facilitate cross-cancer analysis these z-scores were combined to yield a 'meta z-score'. Z-scores represent the number of standard deviations from the mean of normal distribution e.g., $z > 1.96 = p < 0.05$. Meta-z scores for each infiltrating immune fraction were generated for 902 and 408 cases of adenocarcinoma and SCC, respectively.

2.5 Cell lines

The cell lines used in this project can be found in Table 2.4. The cell lines A549, COR-L32, IMR-90, MRC-5 and SKMES-1 were kindly provided by Dr. A Sanders, Cardiff University School of Medicine. All other cells were obtained from the American Type Tissue Collection (ATCC) or the European Collection of Authenticated Cell Cultures (ECACC). Cultures were regularly tested for the presence of mycoplasma. All cell culture products are from Gibco unless stated.

2.5.1 Maintenance of cell lines

2.5.1a Adherent cells

A summary of the growth media used for each culture can be found in Table 2.5; all culture reagents were from Gibco unless specified. Adherent cell lines were maintained in T75 flasks in 15 ml of media in a New Brunswick Galaxy 170s CO_2 incubator (Eppendorf) at 37˚C in an atmosphere containing 5% CO_2. Cells were subcultured once they reached 80-90% confluency (3-5 days). To subculture adherent cells media was aspirated, and cells washed once with phosphate-buffered saline (PBS) before the addition of 5 ml of either Trypsin (0.05%) or Versene. Cells were incubated at 37˚C for 5 mins, or until cells became detached; cell detachment was confirmed with microscopy. 8 ml of media was then added to the suspension to inactivate the dissociation reagents, transferred to a 15 ml falcon tube and centrifuged at 200 x g for 5 mins at room temperature to pellet the cells. Supernatant was then removed, and cell pellets resuspended and seeded into flasks/culture plates at the desired densities.

2.5.1b Non-adherent cells

The NK-92MI cell line was maintained in a T175 flask with 25-35 ml of media. Cultures were maintained by the addition of fresh medium every 2-3 days with cells maintained at a cell density between $2x10^5$ – $1x10^6$ cells/ml. Centrifugation and replacement with fresh medium

was avoided where possible as the cells prefer to grow in aggregates within conditioned medium. When necessary, cells were centrifuged at 120 x g for 5 mins.

Table 2.5 Summary of cell lines used and their culture conditions

Cell line name	Cell type	Growth medium	Subcultivation ratios
A549 (ATCC, CCL-185)	Human lung adenocarcinoma	*Dulbecco's Modified Eagle Medium (DMEM)* • 10% foetal bovine serum (FBS) • 1% L-Glutamine • 1% Penicillin and Streptomycin	1:10
BEAS-2B (ATCC, CRL-9609)	Human bronchial epithelium	*Bronchial epithelial cell growth medium (BEGM; Lonza)* • BEGM Singlequots supplements and growth factors (Lonza) • 1% Penicillin and Streptomycin	1:10
COR-L23 (ECACC, 92031919)	Human large cell lung carcinoma	*RPMI 1640* • 10% FBS • 1% L-Glutamine • 1% Penicillin and Streptomycin	1:10
H226 (ATCC, CRL-5826)	Human squamous cell lung carcinoma		1:20
H596 (ATCC, HTB-178)	Human adenosquamous lung carcinoma		1:10
H838 (ATCC, CRL-5844)	Human lung adenocarcinoma		1:10
HeLa (ATCC, CCL-2)	Human cervical adenocarcinoma		1:10
IMR-90 (ATCC, CCL0186)	Human lung fibroblasts	*Minimum Essential Medium (MEM)* • 10% FBS • 1% MEM Non-Essential Amino Acids Solution (100X) • 1% L-Glutamine • 1% Penicillin and Streptomycin	1:10
MRC-5 (ATCC, CCL-171)	Human lung fibroblasts		1:10
SK-MES-1 (ATCC, HTB-58)	Human lung squamous cell lung carcinoma		1:20
NK-92MI (ATCC, CRL-2408)	Human natural killer cells	*RPMI 1640* • 10% heat-inactivated FBS • 10% heat-inactivated horse serum (HS) • 1% L-Glutamine • 1% Penicillin and Streptomycin	

2.5.2 Cryopreservation of cell lines

To cryopreserve cells all cell lines were prepared as above for subculturing; once resuspended in fresh media 100 µl of cell suspension was taken and cells counted using a Via1-Cassette in a NuceloCounter (Chemometec). All adherent cells were frozen at a concentration of 1-2 x 10^6 cells/ml in freezing media, NK92MI vials contained 5-10x10^6 cells/ml. Freezing media for adherent cells contained 90% media and 10% of the cryoprotectant dimethyl sulfoxide (DMSO); freezing media for NK-92MI was CyroStor CS10 (StemCell Technologies) a serum-free, animal component-free cryopreservation media containing 10% DMSO designed for sensitive cultures. Cells were transferred to 2 ml cryovials and placed in a CoolCell cell freezing container (BioCision) at -80˚C to be gradually frozen for 24 hours before being transferred to liquid nitrogen for long-term storage.

2.5.3 Thawing of cell lines

Cells stored in liquid nitrogen were removed and placed on dry ice before being rapidly thawed in a bead bath at 37˚C. Thawed cells were then placed in a 15 ml tube with 9 ml of fresh media and centrifuged at 200 x g for 7 mins (120 x g for NK92MI). The supernatant was then removed, and the cells resuspended and plated at the desired ratios in flasks.

2.5.4 Mycoplasma testing and treatment

Mycoplasma is the most prevalent microbial contaminant of cell culture systems owing to the absence of symptoms or morphological changes within infected cultures. Therefore, it is essential that routine mycoplasma testing was undertaken to ensure the validity of cell culture results. Cell cultures were routinely tested for the presence of mycoplasma using the PromoKine polymerase chain reaction (PCR) mycoplasma test kit. 1 ml of supernatant was removed from 90-100% confluent cultures after 48 hours and spun at 500 x g for 5 mins to pellet any cellular debris, the supernatant was then transferred to a fresh tube and centrifuged at a minimum of 14000 x g for 15 mins before resuspension of the resultant Mycoplasma pellet in 100 µl of fresh culture medium. Test reaction tubes containing nucleotides, Hot-Start Taq DNA Polymerase, an inert gel loading dye, internal control DNA and a primer set against a DNA sequence within the highly conserved region of the Mycoplasma genome were rehydrated with 23 µl Rehydration Buffer and either 2 µl of sample or fresh medium (negative control) were added to each tube. A pre-prepared positive control tube containing positive DNA to assure reproducibility was rehydrated and 2 µl DNAse-free water added. Tubes were mixed by flicking and allowed to dissolve by incubating at RT for 5 mins before thermal cycling under the following conditions for 40 cycles: 95˚C for 2 minutes, 94˚C for 30 seconds, 55˚C for 30 seconds then 72˚C for 40 seconds and cooling to 4˚C. The initial 2 minute high

temperature step is required to melt all nucleic acids and to activated the Taq DNA Polymerase. A 200 ml 1.5% standard agarose gel containing 10 µl Safeview nucleic acid stain (NBS Biologicals) was loaded with 8 µl of each PCR reaction and run until a 2-3cm run distance was achieved. An internal control DNA band at 479 base pairs (bp) indicated a successful PCR; mycoplasma-positive samples showed a distinct band at 265-278 bp and negative samples showed the internal control band only. All positive cultures were treated for 14 days with Plasmocin (Invivogen); successful treatment was confirmed with a negative PCR reaction after 1 passage post-treatment.

2.5.5 Transduction of GFP+ CD200+ and CD200- cells

Complementary DNA for CD200 was provided by IMAGE consortium (clone ID 5299899) and subsequently subcloned into the PINCO retroviral expression vector which co-expresses green fluorescent protein (GFP) from an internal cytomegalovirus (CMV) promoter (both kindly gifted from Alex Tonks, Department of Haematology, Cardiff University). Phoneix packaging cells were transfected with either PINCO-CD200-GFP (CD200+) or PINCO-GFP (CD200-) using calcium phosphatase precipitation and cultured in DMEM +10% FBS +2% 200mM L-glutamine and 20U/ml Gentamicin. 8 ml of media was added onto sub-confluent cultures and the viral media harvested through centrifugation at 450 x g for 10 mins after 48 hours incubation at 37˚C. $1.8x10^6$ cells were plated in a 24 well plate and retrovirally transduced by incubation with 500 µl of retroviral supernatant for 24 hours. Cells were then washed twice with PBS to remove any trace of the virus before being left to grow for 2 weeks in their respective media prior to flow cytometric sorting for GFP+ cells. GFP+ cells were then expanded. CD200 expression was confirmed in the cell lines by flow cytometry and western blot.

2.5.5a Fluorescent-activated cell sorting

Cells were dissociated with Versene, centrifuged for 5 min at 200 x g and resuspended in cell media for counting. A total of $10x10^6$ cells were placed in a FACS tube, centrifuged, and washed with 1 ml FACS buffer (PBS containing 10% FBS and 0.1% sodium azide) before re-pelleting and resuspension in 500 µl of buffer. Cells were then passed through a 70 µm cell strainer prior to sorting. A control sample of un-transduced GFP negative cells were used for gating. GFP+ cells were sorted into 96 well plates at a concentration of $1x10^4$ cells/well and expanded into T75 flasks.

2.6 RNA analysis

2.6.1 RNA extraction

Cultured cells were washed, dissociated with Versene and pelleted by centrifugation at 200 x g for 5 mins. Cells were counted and $1x10^6$ cells were removed and re-pelleted before being placed on ice. RNA was extracted using the RNeasy Mini Kit (Qiagen) as per manufacturer's instructions and quantified using a Nanodrop 2000 spectrophotometer (ThermoFisher).

2.6.2 Preparation of cDNA

cDNA was synthesised from 1 µg RNA using the QuantiTect Reverse Transcription Kit (Qiagen) in a BioRad T100 Thermocycler using the cycling conditions outlined in Table 2.6 for 1 cycle.

Table 2.6 cDNA synthesis thermocycler conditions

Stage	Temperature	Time
Annealing	25˚C	5 minutes
Synthesis	42˚C	30 minutes
Reverse transcriptase inactivation	85˚C	5 minutes

2.6.3 Quantitative real-time polymerase chain reaction (qRT-PCR)

All qRT-PCR reactions were performed using TaqMan pre-designed probes from ThermoFisher (summarised in Table 2.7)(ThermoFisher). All reactions were prepared in either 96- or 384-well MicroAmp optical plates in technical triplicates using Taqman Universal Mastermix (Applied Biosystems) for a final volume of 15 µl and 10 µl respectively. For each gene a non-template control reaction with sterile water was run to ensure product specificity and lack of contamination. Where possible, two housekeeping genes (GAPDH, β-actin) were used as reference genes for each plate. Plates were read using the QuantStudio 7 Flex Real-Time PCR System (Thermo Fisher Scientific). Cycling conditions can be found in Table 2.8. Relative gene expression levels were determined using the ΔCT method with GAPDH and β-actin as controls for normalisation; values are expressed as arbitrary units.

Table 2.7 Probes used for qPCR

Gene Symbol	Exon Boundary	Product Length	Assay ID
ACTB	1-2	77 base pairs	Hs00357333_g1
B2M	3-4	81 base pairs	Hs00984230_m1
CD200	5-6 / 6-7	64 base pairs	Hs01033303_m1
GAPDH	6-7 / 7-8	93 base pairs	Hs02758991_g1

Table 2.8 Fast qRT-PCR cycling conditions

Stage	Temperature	Time	Cycles
Hold	50˚C	2 minutes	1
Hold	95˚C	10 minutes	
Melt	95˚C	15 seconds	40
Annealing and extension	60 ˚C	1 minute	

2.6.3a Identification of stable reference genes for qRT-PCR

The accuracy of RT-qPCR results strongly depends on a careful selection of appropriately stable reference genes for normalisation of gene expression. Many studies have demonstrated that the expression of common reference genes varies among different cell types and experimental conditions. Since there are no universal reference genes for accurate normalisation, it is crucial to specifically select the most suitable reference gene for each experimental design. The MIQE guidelines advise that no fewer than three reference genes should be used for data normalisation (Bustin *et al.* 2009).To identify the most appropriately stable genes for qRT-PCR analysis, the stability of the mRNA of three reference genes in all cell lines was analysed using four different software's (BestKeeper, Delta-Ct method, geNorm and Normfinder) on the web-based tool RefFinder (https://www.heartcure.com.au/reffinder/). BestKeeper evaluates the tested reference genes' inter-gene relationship; the most stable genes are the ones which exhibit low coefficient of variance (CV) and standard deviation (SD)(Pfaffl *et al.* 2004) (Figure 2.5a). The comparative delta-Ct method compares the SD of the threshold cycle (Ct) values for each sample; a low SD means the gene is more stable (Silver *et al.* 2006)(Figure 2.5b). The GeNorm programme calculates reference gene stability by calculating the average pair-wise variation between the single reference gene and all other reference genes; a low M-value defines stable expression of an individual reference gene (Vandesompele *et al.* 2002)(Figure 2.5c). NormFinder uses an ANOVA-based model to estimate and take into consideration inter- and intra-group variability to rank the reference genes according to their stability (Anderson *et al.* 2004)(Figure 2.5d). RefFinder then integrates the results from each analysis performed by assigning an appropriate weight to an individual gene and calculating the geometric mean of their weight; this overall final ranking is

used to rank the reference genes from most to least stable (Figure 2.3e). Due to the number of samples and genes analysed within each plate preventing the use of three reference genes, the top two most stable genes were selected for all subsequent analysis: β-actin and GAPDH.

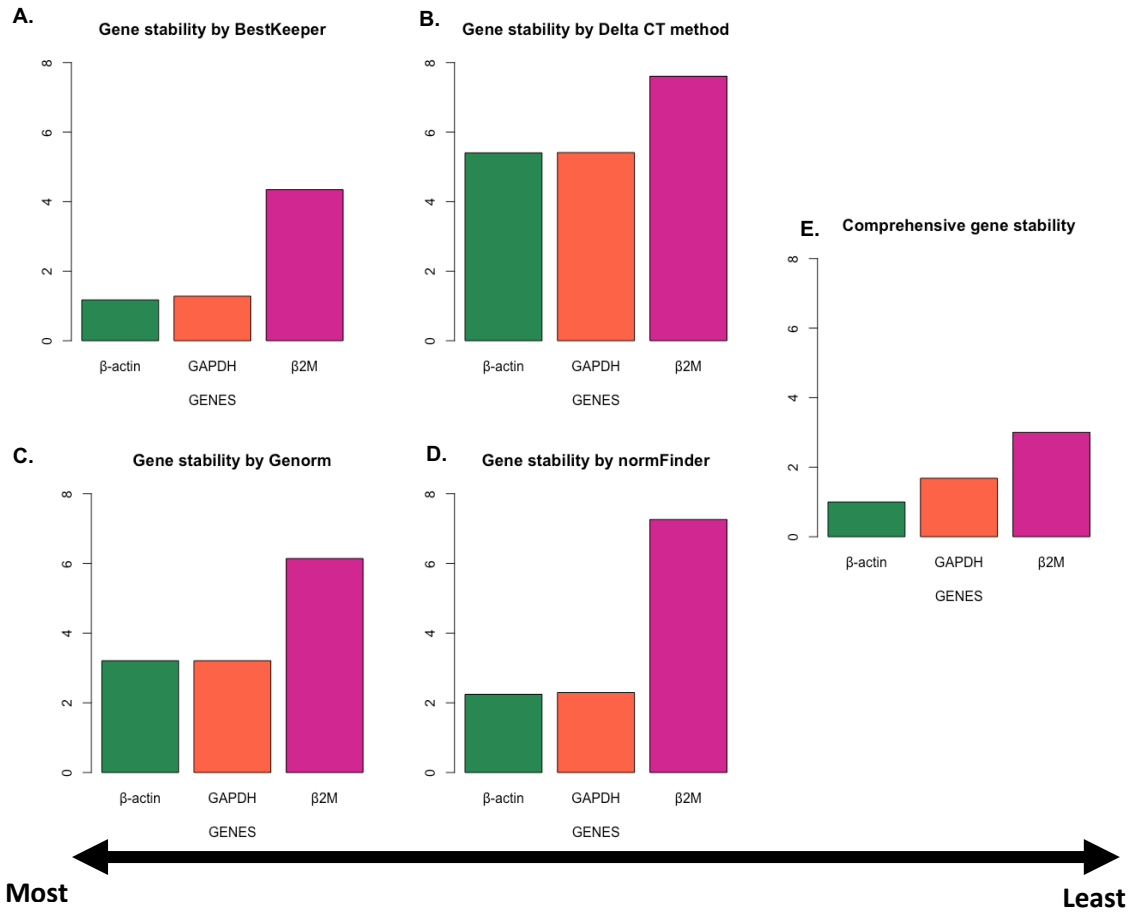

Figure 2.5 Identifiction of stable reference genes for qPCR using RefFinder.

The stability of 3 reference genes was analysed in all cell lines using the refFinder software which integrates 4 programs to identify the most stable genes. (A) BestKeeper (B) Delta CT (C) Genorm and (D) normFinder evaluate the stability of reference genes and rank them from most to least stable; these findings are then integrated into a final (E) Comprehensive gene stability ranking to identify the most stable for further analysis.

2.7 Protein analysis

2.7.1 Protein extraction

Cell lysates were prepared by detaching cells with Versene before centrifugation at 200 x g for 5 mins. Cells were counted and pelleted again, with the resulting pellet being resuspended in 100 µl RIPA buffer per 1 x 10^6 cells and incubated on ice for 30 mins. Composition of RIPA can be found in Table 2.9; RIPA buffer was aliquoted into 5-10 ml volumes and protease inhibitor cocktail (Cell Signalling Technologies) added at a 1:1000 dilution. Following incubation, the pellet was disrupted by pipetting and then left on ice for a further 30 mins before centrifugation at 10 000 x g for 10 mins at 4˚C. The supernatant was collected at stored at -80˚C.

Table 2.9 RIPA buffer composition

Reagent	Volume/Weight	Working concentration
EDTA	0.4 ml of 0.5 M	2 mM
NP-40	1 ml	1%
Sodium chloride	3 ml of 5 M	150 mM
SDS	0.1 g	0.1%
Sodium fluoride	0.21 g	50 mM
Sodium-deoxycholate	0.5 g	0.5%
Tris hydrochloride (pH 7.4)	5 ml of 1 M	50 mM
D.H_2O	Made up to 100 ml	

2.7.2 Protein quantification

The Pierce bicinchoninic acid (BCA) assay (ThermoFisher) was used for the colorimetric detection and quantification of total protein. Samples were diluted 1:2 in RIPA buffer and 15 µl added in duplicate alongside standards of bovine serum albumin (BSA) at concentrations of 5, 25, 50, 125 and 250 µg/ml to a clear flat-bottomed 96 well plate (Corning). 200 µL of BCA working reagent (50 parts reagent A to 1 part reagent B) was added to each well and the plate covered and incubated at 37˚C for 30 mins. Following incubation, the absorbance of the plate was analysed using a CLARIOstar plate reader (BMG Labtech) set at 562 nm. Wells containing RIPA buffer and working reagent only served as blanks, with all data corrected to these values. A standard curve was generated using the known BSA concentrations and the concentration of total protein within the samples extrapolated from the equation generated for the curve.

2.7.3 Western blotting

A summary of the reagents used for western blotting can be found in Table 2.10. Samples were diluted in RIPA buffer and 5 µl Laemmli buffer (4x) for the desired total protein concertation in 20 µl and placed on a heating block at 95˚C for 5 mins. Samples were loaded into the wells of a 1.5 mm acrylamide gel (TGX FastCast, Bio-Rad) in addition to 5 µl of pre-stained molecular weight marker (PageRuler Plus, Thermo Fisher Scientific); empty wells were loaded with 20 µl of RIPA and 4x Laemmli buffer. Gels were run in a 10% sodium dodecyl sulphate (SDS) buffer at 300 V until desired marker separation was achieved, and proteins transferred onto mini polyvinyledine fluoride membranes using the Trans-Blot Turbo Transfer System and Trans-Blot Turbo Mini Ready-to-Assemble Transfer Kit (Bio-Rad). Successful protein transfer was confirmed following 5 min incubation with Ponceau S (Thermo Fisher Scientific). Membranes were blocked for 1 hour at RT with 10% skimmed milk or 10% BSA (for phosphorylated proteins) in TBST then rinsed for 5 min in TBST. Following blocking, membranes were incubated overnight at 4˚C on a roller with primary antibodies (see Table 2.11a) diluted in 5% milk/BSA. The next day, following 3 x 5 min washes in TBST, membranes were incubated for 1 hour at RT with HRP-conjugated secondary antibodies (see Table 2.11b) and washed for a further 3 x 5 min in TBST. Antibody binding was detected by incubating membranes with Luminate Forte chemiluminescent HRP detection reagent (Milipore) for 10 seconds and colimetric and chemiluminescent high-resolution images acquired using the Bio-Rad Chemi-Doc. Where necessary, membranes were stripped with mild stripping buffer for 2 x 5 min (pH 2.2) then washed, blocked and re-probed to detect other proteins of interest. Western blots were quantified by densitometry using the ImageLab software (Bio-Rad). For phosphorylated proteins, all steps following transfer were performed at 4˚C.

Table 2.10 Reagents used for western blots

Reagent	Composition
Laemmli Buffer (4x)	• 0.5 ml β-mercaptoethanol • 0.04 g Bromophenol blue • 4 ml Glycerol • 0.8 g SDS • 2.4 ml 1M Tris hydrochloride (pH 6.8) • Made up to 10 ml with D. H_2O
7.5% Acrylamide Resolving Gel	• 4 ml TGX FastCast Acrylamide Resolver A • 4 ml TGX FastCast Acrylamide Resolver B • 40 µl 10% ammonium persulfate • 4 µl TEMED
7.5% Acrylamide Stacking Gel	• 1.5 ml TGX FastCast Acrylamide Stacker A • 1.5 ml TGX FastCast Acrylamide Stacker B • 15 µl 10% ammonium persulfate • 3 µl TEMED
10% SDS Running Buffer (pH 6.8)	• 3.027 g Tris • 14.41 g Glycine • 10 ml 10% SDS • Made up to 1 L with D.H_2O
Trans-Blot Turbo Transfer Buffer	• 200 ml 5x Trans-Blot Turbo Transfer Buffer • 600 ml D.H_2O • 200 ml 85% ethanol
TBST (0.1% Tween, pH 7.6)	• 200 ml 5x TBS (30.25 g Tris, 43.8 g NaCl, pH 7.6, made up to 1 L with D.H_2O) • 800 ml D.H_2O • 3 ml Tween-20

Table 2.11a Primary antibodies used for western blots

Antibody	Dilution	Species	Isotype	Clone	Source	Size (kDa)
α-tubulin	1:1000	Mouse	IgG1	DM1A	Sigma-Aldrich	55
CD200	1:1000	Goat	IgG	Polyclonal	R&D	~47
GAPDH	1:10000	Goat	IgG	Polyclonal	R&D	37
Phospho-p44/42 MAPK (Erk1/2)	1:1000	Rabbit	IgG	20G11	CST	42, 44
p-44/42 MAPK (Erk1/2)	1:1000	Rabbit	IgG	137F5	CST	42, 44

Table 2.11b Secondary antibodies used for western blots

Antibody	Dilution	Isotype	Clone	Source
Gt anti Ms IgG2a HRP	1:5000	IgG	Polyclonal	Abcam
Gt anti Rb IgG(H+L) HRP	1:5000	IgG	Polyclonal	Abcam
Rb anti Gt IgG (H+L) HRP	1:5000	IgG	Polyclonal	Abcam

2.8 Flow cytometry

Cell surface protein expression was analysed using an LSR Fortessa flow cytometer (BD Bioscience). Cells were dissociated with Versene, centrifuged for 5 min at 200 x g and washed in 1 ml FACS buffer (PBS containing 1% BSA and 0.1% sodium azide) before re-pelleting and resuspension in 100 µl FACS buffer. All antibody incubations were carried out for 30 min at 4˚C in the dark. Antibodies used are summarised in Table 2.12. Cells were then washed twice in 1 ml FACS buffer and resuspended in 500 µl buffer for analysis. All centrifugations were carried out at 400 x g for 5 min at 4˚C. 10 000 events per sample were collected on the Fortessa. Cells were gated on the basis of forward- and side-scatter to eliminate doublets and debris. 1 µl of 10 µg/µl DAPI was added immediately prior to analysis to eliminate dead cells. Isotype controls were used to determine background fluorescence and, where necessary, single stained samples were used as compensation controls (Fig 2.6). Data was processed using FlowJo software (BD).

Table 2.12 Antibodies used for flow cytometry

Antibody	Fluorochrome	Dilution	Species	Isotype	Clone	Source
CD16	PerCP/Cy5.5	5 µl per $1x10^6$ cells	Mouse	IgG1, κ	3G8	BioLegend
CD200	Alexa Fluor 647	5 µl per $1x10^6$ cells	Mouse	IgG1	325516	R&D
CD200R	PE	5 µl per $1x10^6$ cells	Mouse	IgG1, κ	OX-108	BioLegend
CD56	FITC	2 µl per $1x10^6$ cells	Mouse	IgG1, κ	REA196	Miltenyi
Nkp30	Alexa Fluor 647	5 µl per $1x10^6$ cells	Mouse	IgG1, κ	P30-15	BioLegend
Nkp44	Alexa Fluor 647	5 µl per $1x10^6$ cells	Mouse	IgG1, κ	P44-8	BioLegend
Nkp46	PE	5 µl per $1x10^6$ cells	Mouse	IgG1, κ	9E2	BioLegend
NKG2D	FITC	5 µl per $1x10^6$ cells	Mouse	IgG1, κ	1D11	BioLegend
Isotype control	PerCP/Cy5.5	5 µl per $1x10^6$ cells	Mouse	IgG1, κ	MOPC-21	BioLegend
Isotype control	Alexa Fluor 647	5 µl per $1x10^6$ cells	Mouse	IgG1	F8-11-13	AbSerotec
Isotype control	Alexa Fluor 647	5 µl per $1x10^6$ cells	Mouse	IgG1, κ	MOPC-21	BioLegend
Isotype control	PE	5 µl per $1x10^6$ cells	Mouse	IgG1, κ	MOPC-21	BioLegend
Isotype control	FITC	5 µl per $1x10^6$ cells	Mouse	IgG1, κ	MOPC-21	BioLegend

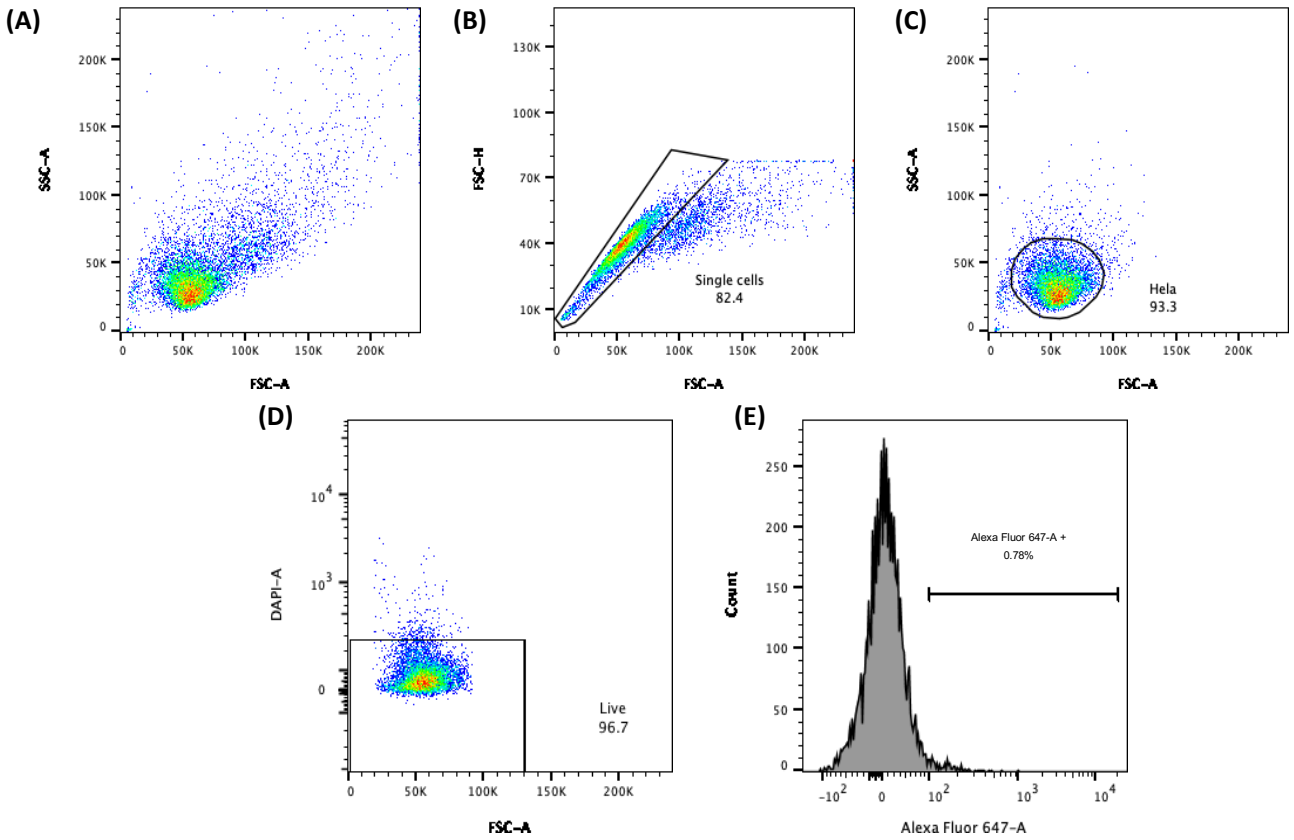

Figure 2.6 Gating strategy used to characterise single, live cells prior to elimination of background staining using an isotype control.

Representative pseudo-colour dot plots demonstrating the gating strategy employed for flow cytometry. (A, B) gates to eliminate doublets and debris from the analysis followed by (C) selection of target cell population and (D) elimination of DAPI positive dead cells. (E) Background staining is then eliminated using an isotype control.

2.9 ELISAs

2.9.1 Soluble CD200 ELISA

2.9.1a Collection of cell-conditioned media

Cells were subcultured and plated as described above (section 2.4.1) and left to grow to 60-70% confluency, upon which the media was removed and replaced with 15 ml fresh media for 48 hours. After 48 hours, the conditioned media containing proteins, metabolites and growth factors secreted from the cells was collected and placed in a Pierce™ 3K MWCO (ThermoFisher) disposable ultrafiltration centrifugal device for the concertation of the conditioned media. Samples were centrifuged at top speed (34 000 x g) for 1-2 hours or until ~1.5 ml of media remained (10x concentration). Concentrated media was stored at -80˚C. Cells were counted using a Via1-Cassette in a NuceloCounter (Chemometec) in order to calculate the pg/ml secreted per $1x10^6$ cells.

2.9.1b ELISA

CD200 in cell culture supernatant was quantified using a CD200-sandwich ELISA with capture and detection antibody pairs obtained from Sino Biological; a summary of solutions used can be found in Table 2.13. High binding 96-well plates were coated overnight at 4˚C with 100 µl of 2 µg/ml monoclonal CD200 capture antibody in PBS. After overnight incubation, the plates were washed 3 times in wash buffer, blocked for 1 hour at RT with 300 µl blocking buffer and washed a further 3 times. A series of seven standards using 2-fold serial dilutions of recombinant human CD200 were prepared in sample dilution buffer. 100 µl of CD200 standards and supernatant samples were plated in quadruplicate at RT for 2 hours before being washed 3 times in wash buffer. CD200 was detected by incubating each well with 100 µl of 0.5 µg/ml HRP-conjugated polyclonal CD200 detection antibody in detection antibody dilution buffer for 1 hour at RT. After 3 washes, 200 µl of substrate solution was added and the plate incubated in the dark at RT for 20 min. Colour development was stopped with 50 µl stop solution and the absorbance of each well measured at 450nm using a CLARIOstar microplate reader (BMG Labtech). Concentration was determined using a standard curve derived from the CD200 standards with each supernatant absorbance corrected against untreated samples of the cell lines respective culture media. Supernatant CD200 concentrations are presented as pg/ml sCD200 per $1x10^6$ cells.

Table 2.13 Solutions for Sino Biological sCD200 ELISA

Solution	Components
PBS	136.9mM NaCl; 10.1mM Na_2HPO_4; 2.7mM KCL; 1.8mM KH_2PO_4; pH 7.4; 0.2µm filtered
TBS	20mM Tris; 150mM NaCl; pH 7.4
Wash buffer	0.05% Tween20 in PBS; pH 7.2-7.4
Blocking buffer	2% BSA in wash buffer
Sample dilution buffer	0.1% BSA in wash buffer; pH 7.2-7.4; 0.2µm filtered
Detection antibody dilution buffer	0.5% BSA in wash buffer; pH7.2-7.4; 0.2µm filtered
Substrate stock solution	10mg/ml Tetramethylbenzidine in DMSO
Substrate dilution buffer	0.05M Na_2HPO_4; 0.025M citric acid
Substrate solution	250µl substrate stock solution in 25ml substrate dilution buffer; 80µl 0.75% H_2O_2
Stop solution	2N H_2SO_4

2.9.2 IFN-γ ELISA

2.9.2a Sample collection

$1x10^6$ CD200- and CD200+ H838 cells were plated in a 96-well plate and left to adhere overnight. The following day, 100 µl of $1x10^7$ NK-92MI cells/ml suspension was plated alone, with 50 ng/ml Phorbol 12-myristate 13-acetate (PMA) and 2 µg/ml ionomycin (stimulated) or at a 1:1 ratio with CD200- and CD200+ H838 cells for 4 hours in the presence or absence of 60µg/10^6cells of CD200 blocking or mouse isotype control antibodies (0.5 mg/ml). Cell suspension was then removed and pelleted at 120 x g for 5 min to allow for collection of supernatants. Media alone, media plus PMA and ionomycin or CD200-/CD200+ H838 supernatants were collected and used for relative blank controls.

2.9.2b ELISA

IFN-γ release from NK-92MI cells was quantified using an IFN-γ DUOSET sandwich ELISA kit per manufacturers instructions (R&D Systems). High-binding white walled 96-well plates were coated overnight at 4˚C with 100 µl of 2 µg/ml monoclonal capture antibody in PBS. After overnight incubation, the antibody was aspirated and the plates washed 3 times with 400 µl wash buffer (0.05% Tween in PBS) before blocking for 2 hours at RT with 300 µl of reagent dilution buffer (RDB; 1% BSA in PBS, pH 7.2-7.4, 0.2µm filtered). A series of six standards (300 pg/ml – 9.38 pg/ml) were generated using 2-fold serial dilutions of IFN-γ stock in RDB. Plates were aspirated and washed 3 times before addition of 100 µl of IFN-γ standards or supernatants in triplicate for 2 hours at RT. Plates were again aspirated and washed 3 times before addition of 100 µl of 200 ng/ml IFN-γ detection antibody diluted in RDB for 2 hours at

RT. Following antibody incubation, plates were aspirated, washed 3 times and 100 µl of Streptavidin-HRP added for 20 mins at RT before aspiration and washing x 3. Colour development was initiated by the addition of 100 µl of substrate solution (1:1 parts A and B; R&D systems) for 20 mins at RT in the dark. The reaction was stopped by the addition of 50 µl of 2N sulfuric acid. Plates were gently tapped to ensure thorough mixing before immediate reading of well optical density at 450 nm using a CLARIOstar microplate reader (BMG Labtech). Concentration was determined using a standard curve derived from the IFN-γ standards with each supernatant absorbance corrected against the relevant blank controls. Supernatant IFN-γ concentrations are presented as pg/ml IFN-γ per $1x10^6$ cells.

2.10 IncuCyte live cell imaging

To observe changes in cell viability and proliferation in real time, the IncuCyte Live Cell Analysis System (Sartorius) was used. Tumour cells were washed, dissociated with Versene, and plated at $1x10^4$ cells per well in white walled 96-well plates. The following day, cells were washed, and fresh media added before being placed in the IncuCyte. Four images of each well were taken at 10x magnification every 2 hours for 24 - 48 hours; plates were maintained at 37˚c and 5% CO_2 for the duration of the experiment. Images were analysed using IncuCyte ZOOM software to measure the percentage of the image area that was occupied by cells (phase object confluence).

2.11 Cell culture functional assays

2.11.1 Tumour and NK cell co-incubation

Cells were washed, dissociated with Versene and counted before being plated at a density of 5000 cells/well in white walled 96-well plates. Cells were left to adhere overnight; the next day sample wells were dissociated and counted to determine the number of cells/well. Supernatant was removed and NK cells were then added to each well at the desired effector: target (E:T) ratios in NK media. Blank wells received NK media only. Plates were placed back in the incubator for 4 hours, after which the supernatant and NK cells were removed, and the wells washed with PBS 3 times. The impact of NK cells on tumour cell viability was then assessed using Cell-Titer Glo.

2.11.2 Cell viability: Cell-Titer Glo

To determine cell viability, the CellTiter-Glo assay (CTG; Promega) was used. CTG is a luminescence-based assay that quantifies metabolically active cells through the identification of ATP. CTG reagent contains the enzyme Ultra-Glo rLuciferase which upon lysis of the cells, requires ATP to convert luciferin to oxyluciferin and generate a luminescent output. To assess

cell viability after either co-cultures and/or addition of compounds, wells were washed with PBS and 100 µl of fresh cell media was added to each well with equal amounts of CTG reagent. Plates were covered with foil and mixed on an orbital shaker at RT for 2 minutes to induce cell lysis. After incubation in the dark for 10 minutes, luminescence was recorded using a CLARIOstar plate reader (BMG Labtech) set at 560/590 nm. Wells containing media and CTG reagent only served as blanks with blank-corrected values used to determine cell viability compared to untreated wells.

2.11.3 CD200 peptide treatment of NK cells

NK-92MI cells were plated overnight in a 96-well plate at a density of $1x10^6$ cells/ml. The following day, CD200 Fc chimera protein (R&D) was added to each well at a concentration of 4 µg/10^6 cells and viability assessed using an Annexin-V antibody (1:1000; IncuCyte) in the IncuCyte Live Cell Imaging System over a 48 hour period, with images taken every 2 hours for 48 hours.

2.11.4 NK cell degranulation assay: CD107a

As NK cells are predominantly cytolytic cells, NK cell activity was measured by analysing the release of cytotoxic granules. Lysosome-associated membrane protein-1 (LAMP1 or CD107a) is found on the membrane of cytotoxic granules; following NK activation and degranulation the outer membrane of the granules merges with the NK cell plasma membrane, leading to the exposure of CD107a on the cell surface. Measurement of CD107a expression to assess the levels of NK cell activity has been previously described (Lorenzo-Herrero *et al.* 2019). NK-92MI cells were co-cultured with tumour cells as described above (Section 2.10.1) at a ratio of 5:1 for 4 hours. At the beginning of the co-culture, 10 µl of CD107a antibody (AF647; BD) or isotype control (IgG1, κ; BD) was added to the wells. As a positive control for degranulation NK cells were activated with a combination of PMA (50 ng/ml) and ionomycin (2 µg/ml). Untreated NK cells were used for baseline expression. After 1 hour, 1x Monensin solution (BioLegend) was added to all wells to prevent reinternalization of the protein. Following the 4-hour incubation, the NK-92MI cell suspension was placed in a FACS tube and pelleted at 120 x g for 5 minutes. Cells were then washed with FACS buffer (0.5% BSA and 0.05% sodium azide in PBS) before re-pelleting and resuspension in 100 µl buffer. Cells were placed on ice and either CD56 (PE; BioLegend) or isotype control (IgG1 κ; BioLegend) antibodies added and left to incubate in the dark for 30 minutes. Excess antibodies were removed by pelleting and washing cells twice at 200 x g for 5 minutes at 4˚C. Cells were gated on the basis of forward and side-scatter to eliminate doublets and debris, with dead cells excluded based on the addition of 1 µl of 10 µg/µl DAPI. Single stained samples were used for compensation

controls and isotype controls were used to determine background fluorescence. NK cells were selected on the basis of CD56 positivity. Data was processed using FlowJo software (BD).

2.12 Statistical analysis

Statistical analyses were performed in Grpahpad Prism 9 software. Normality of data sets was tested using the D'Agostino Pearson test and normally distributed data between two groups was analysed using an unpaired t test; non-normally distributed data was compared using a Mann-Whitney U test. A one-way analysis of variance (ANOVA) was used when comparing the means of ≥2 normally distributed groups involving one independent variable with the Dunn's multiple comparisons test used to compare the mean of one group to the mean of every other group. When comparing the means of ≥2 non-normally distributed groups involving one independent variable, the Kruskal-Wallis test with Dunn's multiple comparisons was used. Correlation between groups was determined using the spearman r test. Univariate relationships between clinical characteristics and CD200 expression, immune infiltration or overall survival were analysed either by the Fisher's exact or chi squared test, as appropriate. Hazard ratios (HR) and their 95% confidence intervals were calculated using the logrank test. Characteristics significantly correlated with overall survival were entered into a Multivariate cox regression analysis performed in R studio (Team Rstudio 2021) using the survival, survminer, lubrdiate and broom packages and the res.cox command. Forest plots were plotted with ggplot. Statistically significant differences were marked as *= $p \leq 0.05$; **= $p \leq 0.01$; ***= $p \leq 0.001$ and ****= $p \leq 0.0001$

2.12.1 Power calculation for the minimum number of patient samples

To determine the minimum number of patient samples required for subsequent analysis to detect a difference in CD200 expression between SCC and adenocarcinoma tumours, a power calculation was performed based on visual classification of 122 NSCLC tumour cores as either CD200 positive or negative. A two independent sample dichotomous endpoint power calculation was performed at: https://clincalc.com/stats/samplesize.aspx.

Dichotomous Endpoint, Two Independent Sample Study

Sample Size	
Group 1	120
Group 2	120
Total	**240**

Study Parameters	
Incidence, group 1	19%
Incidence, group 2	35%
Alpha	0.05
Beta	0.2
Power	0.8

$$N_1 = \left\{ z_{1-\alpha/2} * \sqrt{\bar{p} * \bar{q} * (1 + \frac{1}{k})} + z_{1-\beta} * \sqrt{p_1 * q_1 + (\frac{p_2 * q_2}{k})} \right\}^2 / \Delta^2$$

$$q_1 = 1 - p_1$$

$$q_2 = 1 - p_2$$

$$\bar{p} = \frac{p_1 + k p_2}{1 + K}$$

$$\bar{q} = 1 - \bar{p}$$

$$N_1 = \left\{ 1.96 * \sqrt{0.27 * 0.73 * (1 + \frac{1}{1})} + 0.84 * \sqrt{0.19 * 0.81 + (\frac{0.35 * 0.65}{1})} \right\}^2 / 0.16^2$$

$$N_1 = 120$$

$$N_2 = K * N_1 = 120$$

p_1, p_2 = proportion (incidence) of groups #1 and #2
$\Delta = |p_2 - p_1|$ = absolute difference between two proportions
n_1 = sample size for group #1
n_2 = sample size for group #2
α = probability of type I error (usually 0.05)
β = probability of type II error (usually 0.2)
z = critical Z value for a given α or β
K = ratio of sample size for group #2 to group #1

Figure 2.7 Breakdown of the power calculation performed to determine the minimal sample size required to reach sufficient statistical power.

NSCLC TMA cores were visually classified as either CD200 positive or negative and used to calculate the minimum sample size required for subsequent analysis. Alpha is the probability of a type-1 error and Beta is the probability of a type II error, false-positive and false-negative rates, respectively. Calculations were performed at: https://clincalc.com/stats/samplesize.aspx.

Chapter 3:
Characterising CD200 expression in the lung and in NSCLC

3. Characterising CD200 expression in the lung and in NSCLC

3.1 Introduction

CD200 expression is highly conserved between species and is distributed on a variety of cells and tissues of the body, particularly in sites associated with immune privilege, with high CD200 expression seen on placental trophoblasts, retinal neurons, the CNS, and hair follicle keratinocytes (Clark *et al.* 2003; Rosenblum *et al.* 2004; Chitnis *et al.* 2007; Manich *et al.* 2019). These immune privileged sites are areas in which the host immune response is tightly controlled and suppressed in order to protect these tissues from inflammation that may impair their vital function and threaten the survival of the host (Niederkorn 2006). Cells in the CNS and eye have a limited capacity for regeneration whilst the placenta and hair follicle represent areas rich in antigenic challenge. The allogenic foetus in the placenta presents the immune system with paternal alloantigens which need to be ignored for a successful pregnancy, whilst the hair follicle expresses intrafollicular autoantigens during the anagen phase of hair growth (Clark *et al.* 2003; Forrester *et al.* 2008; Bertolini *et al.* 2020). CD200 expressed on cells with limited regenerative capacity or sites exposed to antigenic challenge signals through its receptor CD200R and downregulates the basal level of myeloid cell activation to attenuate tissue-specific autoinflammatory responses and maintain immune tolerance (Rosenblum *et al.* 2004).

The epithelial surfaces of the lung and airways represent a fragile interface between the immune system and an external environment rich in microbial and non-microbial antigenic stimuli. Fine control of respiratory immunological homeostasis is critical for maintenance of local tissue integrity to ensure efficient gas exchange and host survival (Holt and Strickland 2008). Thus, tissue resident immune cells must discriminate and prevent unnecessary inflammation against inoffensive particles whilst ensuring successful elimination of harmful pathogens without causing local tissue damage through excessively intense or prolonged immune responses (Snelgrove *et al.* 2008). To maintain this balance, airway epithelial cells express many immunomodulatory molecules, such as CD200, which binds to CD200R on tissue-resident immune cells to decrease their activity and increase the activation threshold for which an immune response will be activated (Lauzon-Joset *et al.* 2019). The immune ‘ignorance’ of these cells is tightly regulated by the lung microenvironment and is key to maintaining immune homeostasis. Alveolar macrophages in contact with the airway lumen isolated from mouse lungs demonstrated high levels of basal CD200R expression relative to that of splenic or local lung interstitial macrophages. Furthermore, interstitial DCs which sample airway lumen content through their dendrites also demonstrated abundant CD200R expression (Snelgrove *et al.* 2008). These myeloid cells were adhered to the respiratory epithelium by CD200 expressed on the luminal aspect of bronchial epithelial cells and on type

II alveolar cells, suggesting that tissue-resident myeloid cell activity and function may be regulated by CD200 (Bissonnette *et al.* 2020).

The importance of CD200-mediated regulation of myeloid cells in the lung was first demonstrated in CD200-null mice, in which an influenza dose normally tolerated by WT mice resulted in increased disease severity and death. Further studies using a decreased viral dose that prevented mortality in the CD200-null mice demonstrated severe illness and respiratory tissue damage, associated with increased immune cell infiltration and activation, and a failure to resolve inflammation, resulting in collateral tissue damage. The addition of CD200Fc decreased the inflammatory response without impeding viral clearance, thus highlighting the critical role for CD200 in resolving immune inflammation whilst preserving the anti-viral response (Snelgrove *et al.* 2008). Further evidence for the essential role CD200 signalling plays in maintaining lung immune homeostasis comes from models of allergic asthma; an inflammatory disease that originates from excessive immune activation. The asthmatic response is defined by activation of DCs which subsequently promote an antigen-specific Th2 response characterised by IL-13 production and the promotion of airway inflammation and airway hyperresponsiveness (Lauzon-Joset *et al.* 2019). In a mouse model of acute allergic asthma, airway delivery of CD200Fc prior to allergen exposure prevented the accumulation of mDCs and Th2 cells into the lung, shifted the cytokine balance from IL-13 to the anti-inflammatory cytokine IL-10 and decreased the contractility of airway smooth muscle, thus preventing the development of an asthmatic response (Lauzon-Joset *et al.* 2015). Further evidence for CD200 dysregulation in asthma comes from asthma patients where CD200 expression on peripheral blood cells was significantly reduced in patients during exacerbation compared to controlled asthmatics. Moreover, treatment of patients with anti-inflammatory corticosteroids was associated with a significant increase in CD00 expression on bronchial epithelial cells, suggesting that CD200 signalling is dysregulated in asthma patients (Aoki *et al.* 2009; Moodley *et al.* 2013).

The critical role CD200 plays in lung immune homeostasis is reflected in its expression pattern in the lung. Using a combination of immunofluorescence labelling and electron microscopy Jiang-Shieh *et al.* (2010) defined CD200 distribution and expression in the rat respiratory system under normal conditions. Moving distally through the respiratory tract they demonstrated an absence of CD200 in the epithelia of the trachea and bronchus; CD200 positivity within the apical cilia of some epithelial cells of the respiratory bronchioles; weaker CD200 positivity within club cells of the bronchioles; an absence of CD200 in alveolar type I cells and weak CD200 expression in some alveolar type II cells confined to the apical plasma membrane and microvilli facing the airspace. Intense labelling was seen in the underlying

vascular endothelium throughout the lung. Consistent with these findings, Snelgrove *et al.* (2008) demonstrated strong CD200 expression on the luminal aspect of type II alveolar cells in the mouse lung. This expression pattern of apical CD200 expression within the respiratory tract is consistent with the role of epithelial and endothelial CD200 expression in homeostatically regulating luminal or transepithelial CD200R-expressing macrophages and DCs to maintain immune homeostasis.

However, despite multiple studies demonstrating dysregulation and changes in expression of CD200 during lung inflammation and disease, no studies to date have looked at CD200 expression in the normal human lung. Data from the Human Protein Atlas suggests that CD200 expression is seen at medium levels on basal cells, ciliated cells and club cells within the bronchial epithelium and at high levels in alveolar cells, consistent with that seen in animal models (proteinatlas.org; Uhlen *et al.* 2010). CD200 expression is highly conserved between species; therefore, the first aim of this chapter was to confirm the pattern of CD200 expression in the mouse lung before defining CD200 expression in the human lung. Upon demonstrating the pattern of CD200 expression in human lung tissue, the second aim of this chapter was to semi-quantitively define CD200 expression in NSCLC to see whether CD200 expression in the tumour cells of origin correlated with tumour CD200 expression and to determine if CD200 was associated with patient clinicopathological characteristics or survival.

To date, there have only been two studies looking at the expression of CD200 and its clinicopathological and prognostic implications in NSCLC, yet they present conflicting findings. Using IHC labelling of CD200 in 632 NSCLC patients, Yoshimura *et al.* (2020) determined tumoral CD200 expression using the H-score method, assigning each tumour with a value between 0 - 300 based on both the number of cells expressing CD200 and the intensity of the stain. The mean tumoral CD200 H-score was 42 ± 57.7, with a range from 0 - 295, highlighting the variability in CD200 expression in NSCLC tumours. The patients were then split into high and low expression groups based on the median H-score and demonstrated that female sex, never smoking status, early disease stage and adenocarcinoma were significantly associated with high tumoral CD200 expression. High tumoral CD200 expression was also a predictor of favourable OS and RFS, wherein CD200 expression was an independent predictor for favourable outcome. In contrast, immunofluorescence analysis of 287 early-stage NSCLC patients by Vathiotis *et al.* (2021) demonstrated CD200 expression in 29.7% of patients and found no clear association between CD200 expression and clinicopathological characteristics or outcomes. Both studies used TMA cores of tumours; therefore, to determine tumour CD200 expression more accurately in this chapter, large tumour sections from 240 NSCLC patients were stained and analysed.

3.1.1 Hypothesis and aims

Similar to the murine lung, moderate CD200 expression will be seen on ciliated bronchial cells and club cells, with strong expression seen in alveolar epithelium and vascular endothelium. In NSCLC sections, CD200 expression will be seen in both adenocarcinomas and SCC tumours but may be seen to a greater extent in adenocarcinomas as they predominantly arise from alveolar type II cells.

Aims:

4. Define CD200 expression in the normal human lung and NSCLC tumours
    a. Determine whether the cells of origin of adenocarcinoma and SCC tumours express CD200 in healthy tissue
    b. Define the expression pattern of CD200 in adenocarcinoma and SCC tumours and determine whether this has any correlation with patient clinical characteristics and survival

Objectives:

1. Generate a multi-label immunohistochemical protocol to define CD200 expression in mouse and human lung
2. Define CD200 expression in the normal mouse and human lung
3. Define CD200 expression in NSCLC tumours
4. Determine whether CD200 expression correlates with patient characteristics and survival

3.2 Results

3.2.1 CD200 expression in normal lung

3.2.1.1 Optimisation of CD200 immunofluorescent labelling

Previous work has shown that CD200 is a marker of hair follicle epithelium in mouse skin and hair follicle bulge cells in human skin (Rosenblum *et al.* 2004; Colmont *et al.* 2013); therefore, to determine the specificity of the CD200 antibody, 8μm sections of paraffin-embedded hair follicle-bearing mouse skin (n= 5; Figure 3.1a) and human skin (n= 10; Figure 3.2a) were immunofluorescently labelled for CD200. As an immune-privileged site, CD200 promotes immune tolerance to protect cell in the hair follicle from an auto-immune response. As expected, CD200 expression was seen on the cell membrane of hair follicle epithelium in mouse skin and in hair follicle bulge cells (arrows) in human skin. All other cells within the skin sections were negative for CD200. Sections stained with secondary antibody alone acted as a negative control and yielded no staining demonstrating the specificity of the CD200 antibody (Figures 3.1b & 3.2b). Therefore, CD200 could be immunofluorescently labelled in mouse and human paraffin-embedded tissue sections.

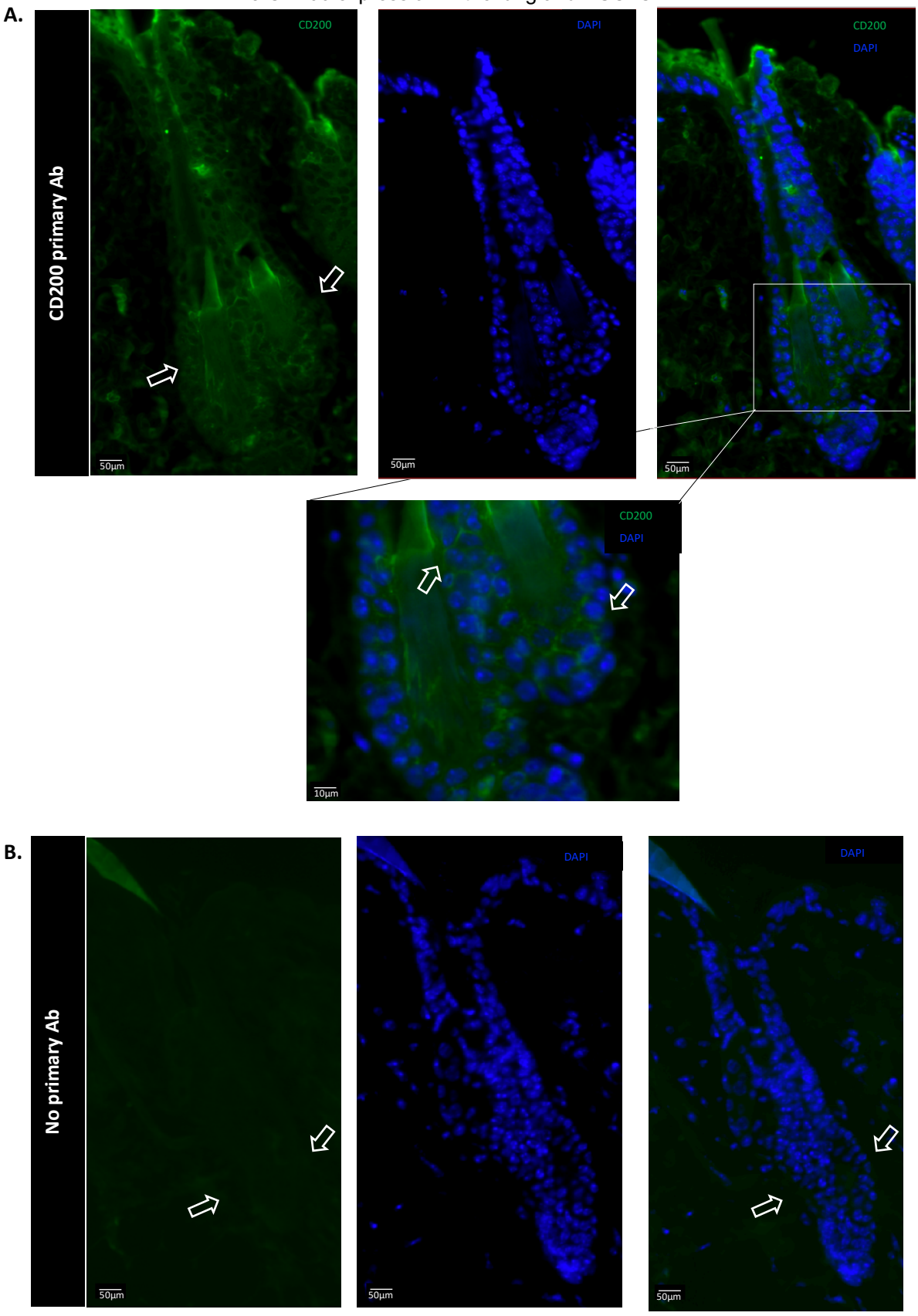

Fig 3.1 Optimisation of CD200 immunofluorescent labelling of mouse hair follicles.

Representative images (n= 5) of hair follicle-bearing regions of mouse skin were labelled with (A) CD200 and DAPI. Top scale bars 50µm, bottom scale bar 10µm. (B) Negative control sections stained with secondary antibody only (n= 5). CD200 positivity is seen in the hair follicle epithelium (arrow). Scale bars 50µm

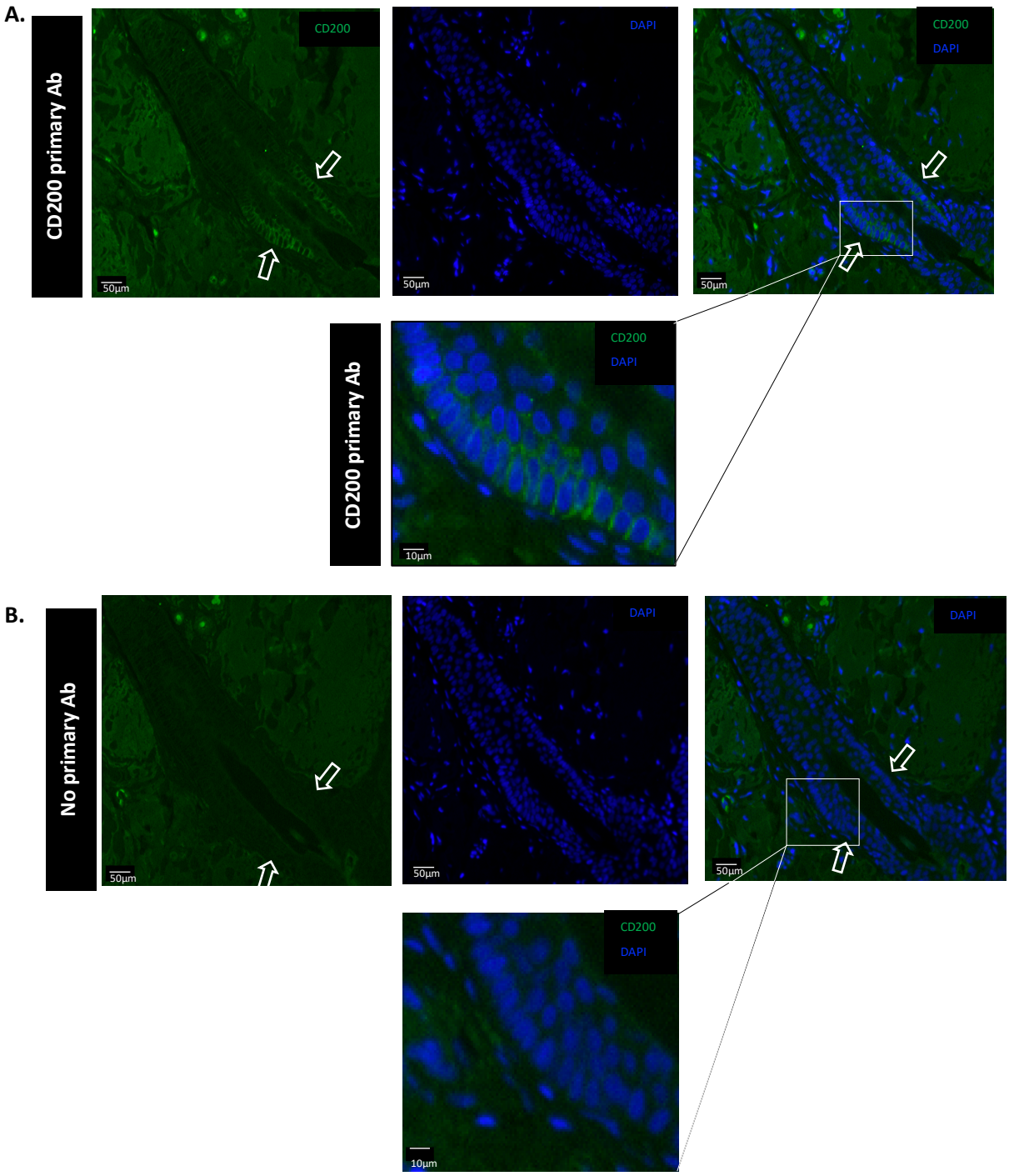

Fig 3.2 Optimisation of CD200 immunofluorescent labelling of human hair follicles.

(A) Representative images (n= 10) of hair follicle-bearing regions of human skin labelled with CD200 and DAPI with CD200 positivity seen in the hair follicle bulge cells (white arrows). (B) Sections stained with secondary antibody only acted as negative control and yielded no staining, confirming the specificity of the CD200 labelling. Top scale bars 50µm, bottom scale bar 10µm.

3.2.1.2 Optimisation of CD200 fluorescent labelling

Once it was determined that CD200 could be reproducibly labelled on paraffin-embedded tissue by immunofluorescence, 5μm sections of paraffin-embedded non-inflated WT mouse (n= 5; Figure 3.3) and human lung (n= 16; Figure 3.4) were labelled for CD200. However, upon viewing the sections which had been simultaneously labelled with Dapi only (Figure 3.3a) it was noted that in unstained tissue both the bronchial and alveolar epithelium demonstrated high levels of autofluorescence in the green channel. The autofluorescence was so marked that when images were taken on the microscope using the same parameters as the skin sections, the intensity of the green throughout the lung was similar to that of the positive CD200 staining in the hair follicle. In sections stained with CD200 antibody (Figures 3.3b), the visualisation of CD200 labelling was hampered by the autofluorescent nature of the respiratory tissue, with sections demonstrating levels of fluorescence similar to that seen in unstained tissue. Therefore, in an attempt to quench autofluorescence, tissue sections were pre-treated with 1.65% Eriochrome Black T (EBT) for 5 minutes after blocking. EBT is a dark black powder that forms a dark blue solution when mixed with water and was determined to be an efficient and reproducible treatment for diminishing green wavelength autofluorescence in human respiratory tissue (Davis *et al.* 2014). However, the addition of this step did little to diminish the autofluorescence, with green fluorescence intensity virtually unchanged following the treatment (Figure 3.3c).

Unstained human lung sections also demonstrated high levels of green wavelength autofluorescence, particularly within the alveolar epithelium and septum (Figure 3.4a). Similar to the mouse lung, when stained for CD200 the autofluorescence was too strong to accurately visualise CD200 labelling within the tissue (Figure 3.4b). Tumours arising from the distal and proximal lung also demonstrated autofluorescence, with sections of both adenocarcinoma (n= 33; Figure 3.5a) and SCC tumours (n= 40; Figure 3.5b) demonstrating strong membranous signal in the green channel. The presence of such extensive autofluorescence throughout the normal lung and within the tumour and stroma of NSCLC tumours presented a barrier to accurate detection and visualisation of CD200 expression by immunofluorescence. Autofluorescence was also seen in the red and yellow channels, although to a lesser extent (data not shown). Therefore, to accurately and reproducibly label CD200 in the lung an immunohistochemical protocol was generated and optimised.

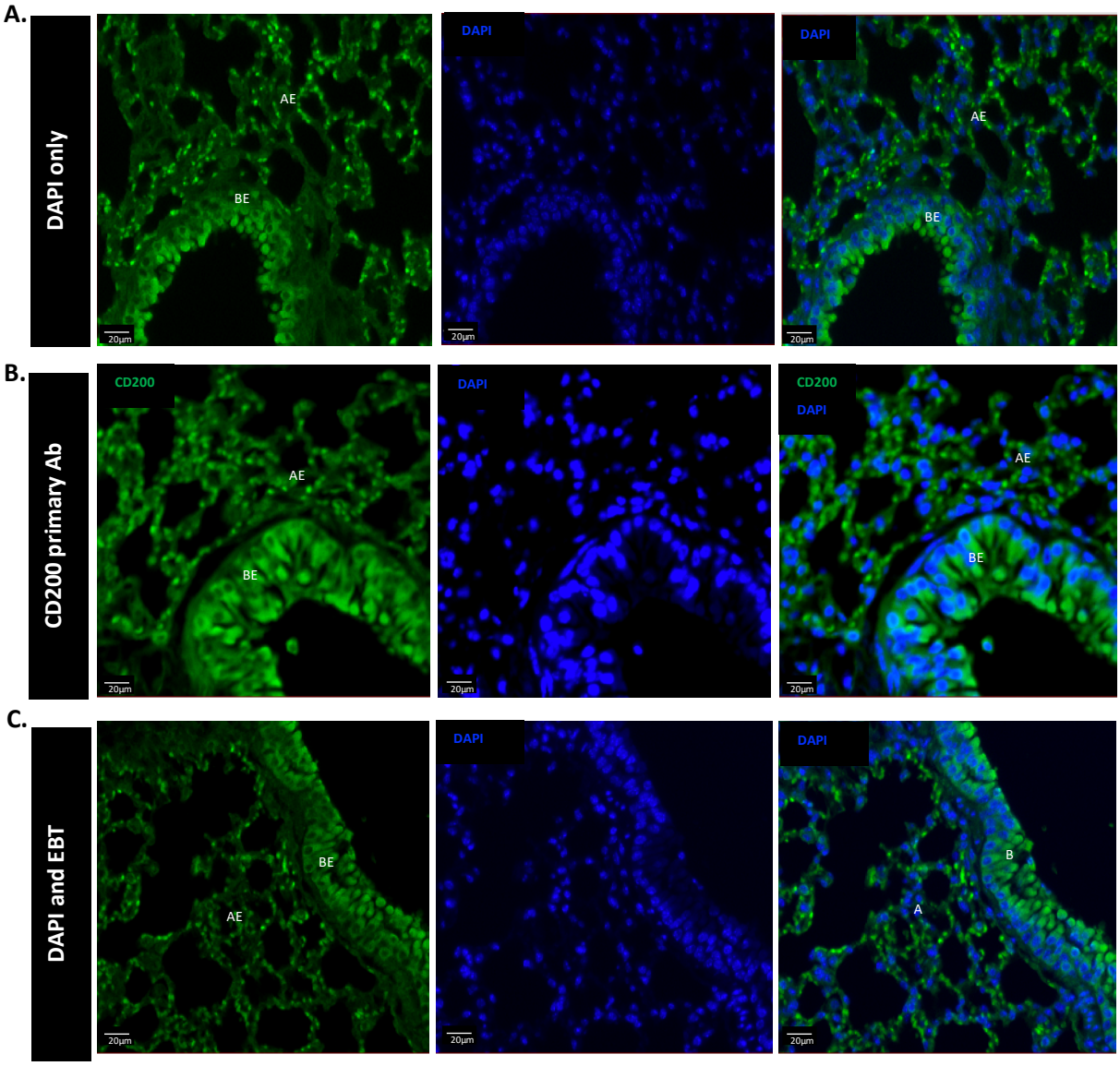

Fig 3.3 Mouse lung tissue autofluorescence.

Representative images (n= 5) of mouse lung stained with DAPI only or with CD200 antibody and AF488-conjugated secondary antibodies at 488nm excitation. (A) In unstained tissue both the bronchial and alveolar epithelium demonstrate high autofluorescence in the green channel. (B) Mouse lung tissue stained with CD200 demonstrated similar levels of fluorescence in the green channel as unstained tissue. (C) Unstained mouse tissue pre-treated with 1.65% Eriochrome Black T (EBT) for 5 minutes to diminish autofluorescence in the green channel. Black areas denote bronchial/alveolar spaces. AE, Alveolar epithelium; BE, Bronchial epithelium. Scale bars 20µm.

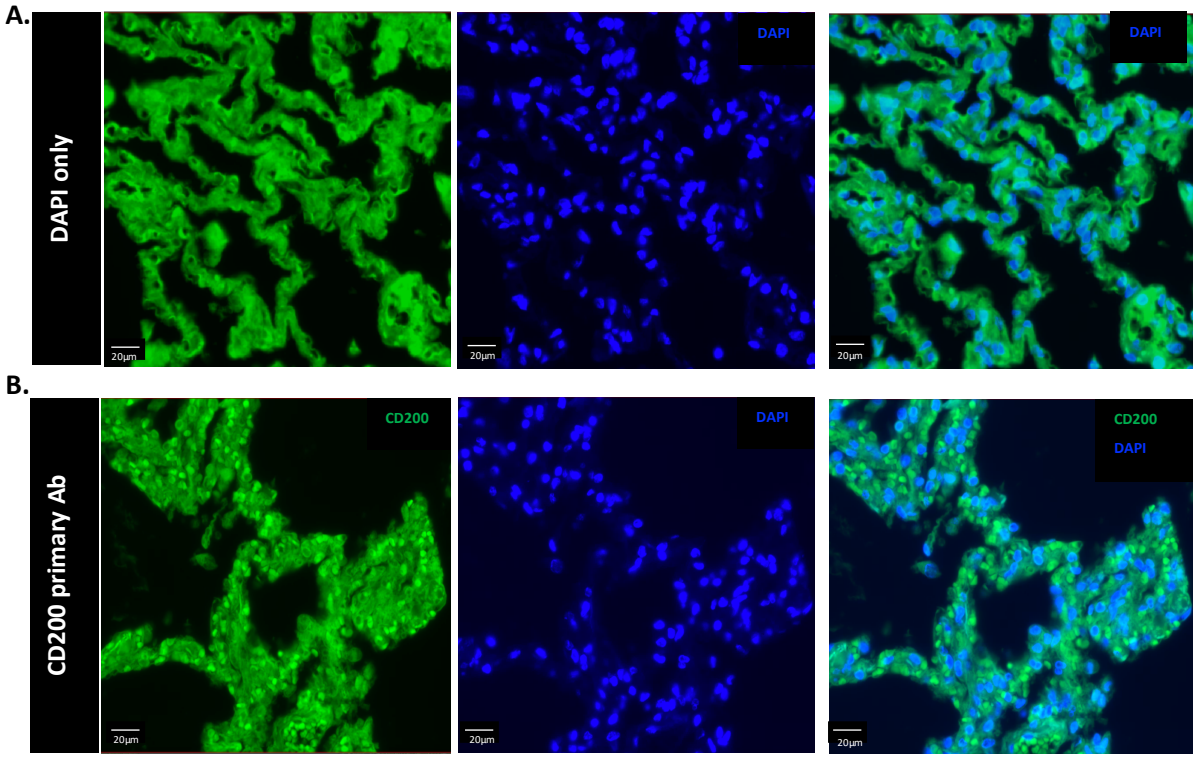

Fig 3.4 Human lung tissue autofluorescence.

Representative images (n= 16) of human lung alveoli stained with DAPI only or with CD200 antibody and AF488-conjugated secondary antibodies at 488nm excitation. (A) In unstained tissue the alveolar epithelium demonstrated high autofluorescence in the green channel. (B) Human lung tissue stained with CD200 demonstrated similar levels of fluorescence in the green channel as unstained tissue. Black areas denote alveolar space. Scale bars 20µm.

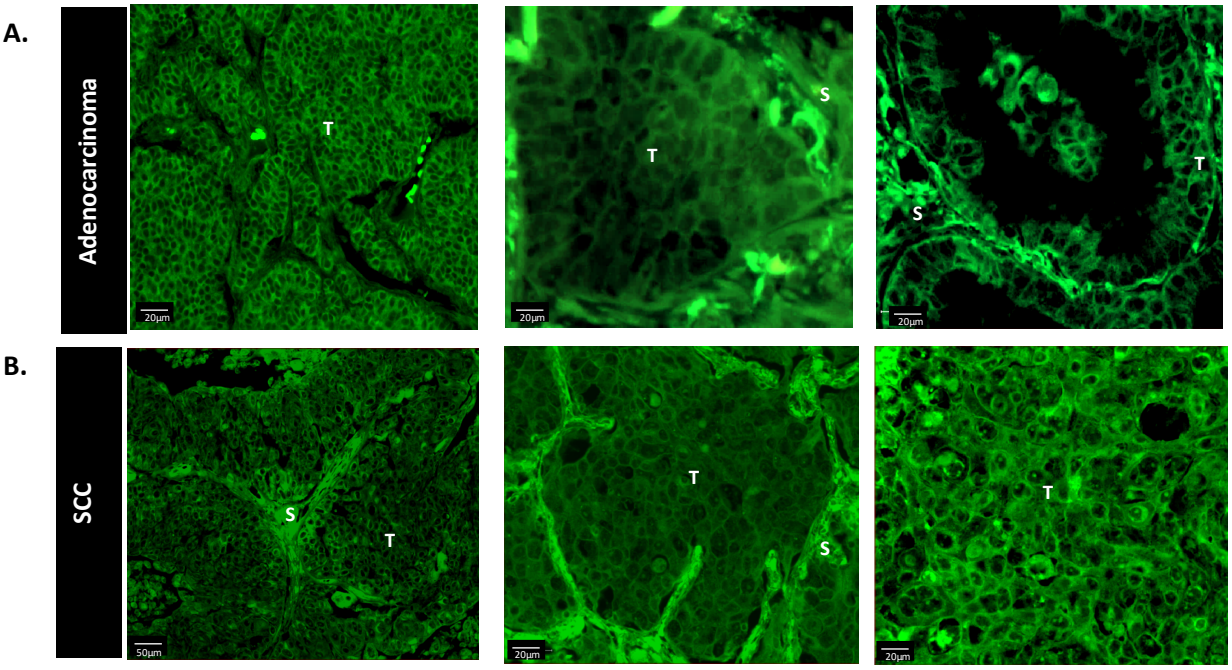

Fig 3.5 Human lung cancer autofluorescence.

Representative images of unstained adenocarcinoma (n= 33) and SCC (n= 40) at 488nm excitation. (A) Adenocarcinoma and (B) SCC tumours and surrounding stroma demonstrate high autofluorescence in the green channel. Arrows denote red blood cells within vessels which fluoresce strongly at 488nm excitation. S, stroma; T, tumour. Scale bars 20µm.

3.2.1.3 CD200 expression in the mouse lung

To overcome the problem of autofluorescence in the mouse respiratory tract a single label immunohistochemical protocol for CD200 was optimised. As with the immunofluorescent labelling, hair follicle-bearing sections of mouse skin were stained for CD200 and visualised with DAB (n= 5; Figure 3.6). As expected, strong CD200 expression was seen in the hair follicle epithelial cells (Figure 3.6a) and no labelling was present in sections stained with secondary antibody alone (Figure 3.6b).

With the view to determine CD200 expression throughout the mouse respiratory tract, 5µm sections of paraffin-embedded non-inflated WT mouse lungs were immunohistochemically labelled for CD200 (n= 5). Weak CD200 labelling was observed within the bronchial epithelium of the intrapulmonary bronchi (Figure 3.7a) and bronchioles (Figure 3.7b) with strong labelling seen throughout the alveolar epithelium and septum (Figure 3.7c). Strong CD200 expression was also noted on the vascular endothelium of associated blood vessels (Figure 3.7a-c; BV). Labelling was absent in the sections stained with secondary antibody only, confirming the specificity of the CD200 antibody (Figure 3.7d). Hence CD200 expression could be characterised in mouse lung by IHC labelling.

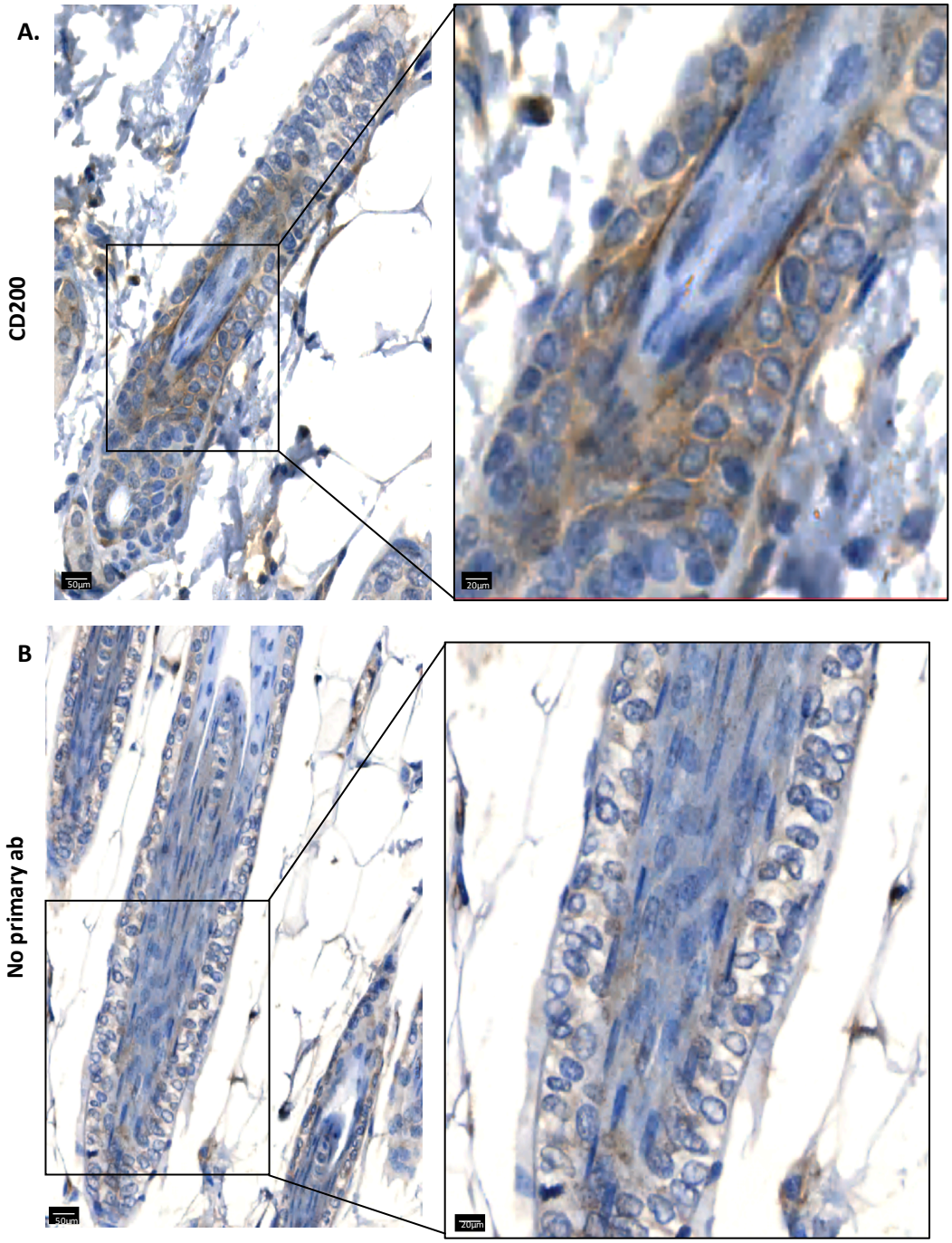

Fig 3.6 Optimisation of CD200 immunohistochemical staining in mouse skin.

(A) Representative images (n= 5) of hair follicle bearing mouse back skin stained for CD200. CD200 positivity is seen within the hair follicle epithelial cells. (B) Sections stained with secondary antibody only acted as negative controls. Left scale bars 50µm, right scale bars 20µm.

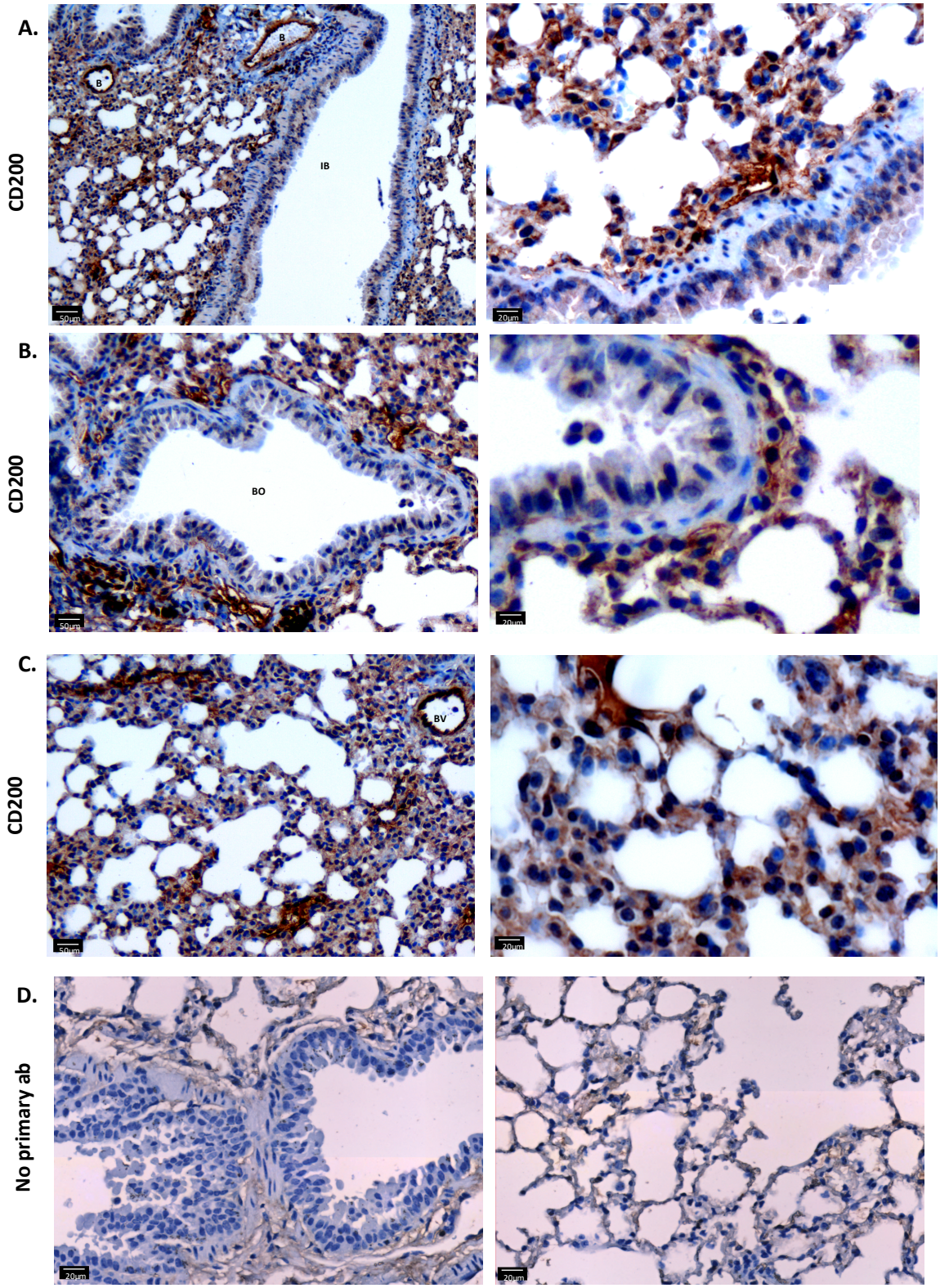

Figure 3.7 CD200 expression in the normal mouse lung.

Representative images (n= 5) of mouse lung immunohistochemically labelled for CD200 or with secondary antibody only and visualised with DAB. Moderate CD200 expression was seen in the bronchial epithelium of the (A) intrapulmonary bronchi and (B) bronchioles. (C) Strong CD200 expression was seen throughout the alveolar epithelium, with positivity seen in both type I and II alveolar cells as well as underlying vascular endothelium. Left scale bars 50µm, right scale bars 20µm. (D) Sections stained with secondary antibody alone confirmed specificity of CD200 antibody. Scale bars 20µm. BO bronchiole; BV, blood vessel; IB, intrapulmonary bronchiole.

3.2.1.4 CD200 expression in the human lung

As before, CD200 labelling was confirmed using hair-bearing human skin samples (n= 3; Figure 3.8a), with sections stained with secondary antibody alone serving as negative control (Figure 3.8b).

To test the hypothesis that CD200-expressing cells within the lung would give rise to CD200 positive tumours, a multi-label immunohistochemical protocol was developed to also label for thyroid transcription factor 1 (TTF-1). TTF-1 is a homeo-domain containing transcription factor that is found predominantly within the nuclei of type II alveolar cells, club cells and basal cells; it is used routinely by the pathologist as a biomarker for pulmonary adenocarcinomas in the lung and throughout the body (Nakamura *et al.* 2002). TTF-1 staining could then be used to decipher between cell types within the bronchial epithelium and alveoli as well as distinguish between adenocarcinoma and SCC tumours. Sections of normal human lung alveoli were used to confirm the specificity of the TTF-1 antibody (n= 3; Figure 3.8c), with sections stained with secondary antibody only acting as negative control (Figure 3.8d). As expected in sections of alveolar tissue, TTF-1 positivity was only seen within the nuclei of type II alveolar cells. To evaluate possible cross-reactions of the secondary DAB-based TTF-1 staining with the primary Vector Red-based CD200 staining, control lung sections were stained and visualised for CD200 before staining with TTF-1 secondary antibodies and DAB (Figure 3.8e); likewise, control sections were stained with CD200 secondary only and red before full TTF-1 staining and visualisation (Figure 3.8f). No cross-reactivity was observed.

To investigate the pattern of CD200 expression throughout the human lung, normal adjacent lung sections from a lung cancer TMA (n= 55) and larger normal lung sections from the WCB (n= 4) were co-stained for CD200 and TTF-1 (Figure 3.9). Of these samples, only 3 contained sections of bronchial epithelium (Figure 3.9a); no CD200 labelling was observed within the club cells of the bronchial epithelium (labelled with TTF-1) or in non-club cells of the bronchial epithelium. As expected, strong CD200 labelling was seen throughout the alveoli and alveolar septum (Figure 3.9b), with type II alveolar cells labelled for both CD200 and TTF-1 (Figure 3.9c; asterisk). Type I alveolar cells were negative for both CD200 and TTF-1 (Figure 3.9c; arrows). In summary, CD200 expression in the human lung was only seen within the alveolar type I and type II cells and within the alveolar septum. Unlike in the mouse lung, no CD200 staining was seen in any cell type of the bronchial epithelium.

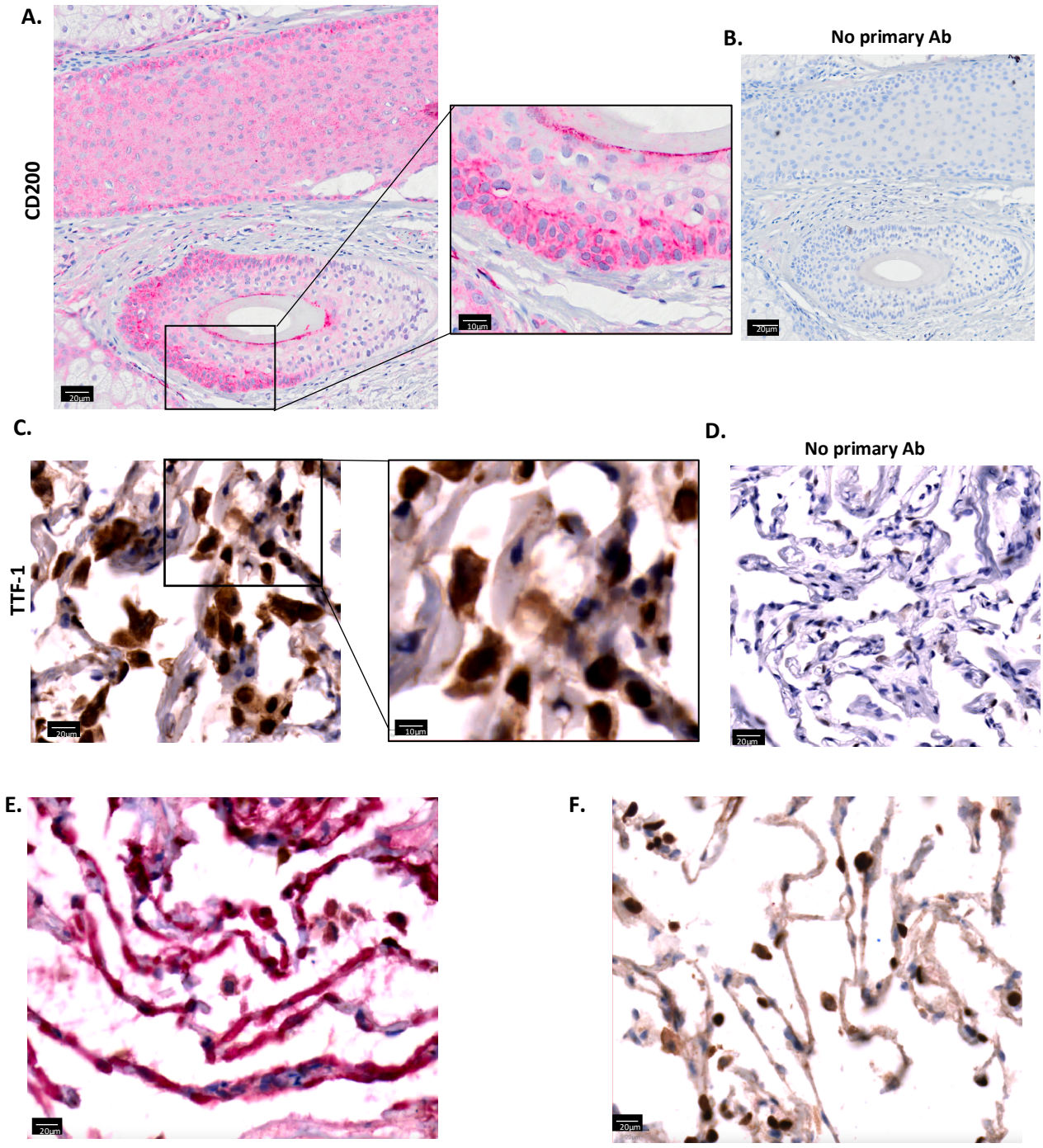

Fig 3.8 Optimisation of CD200 and TTF-1 IHC staining in human skin and lung.

(A) Representative images (n= 3) of hair follicle-bearing human skin stained for CD200 and visualised with Vector Red. CD200 expression is seen within the hair follicle bulge cells seen in both transverse and longitudinal sections of the hair follicle. Left scale bar 20μm, right scale bar 10μm. (B) Sections stained with secondary antibody only served as negative controls. Scale bar 20μm. (C) Representative images (n= 3) of normal human lung stained for TTF-1 and visualised with DAB. TTF-1 positivity is seen within the alveolar Type II cells. Left scale bar 20μm, right scale bar 10μm. (D) Sections stained with secondary antibody only served as negative controls. 20μm scale bar. (E) CD200 was stained to completion followed by the TTF-1 stain and DAB visualisation minus the TTF-1 primary antibody and (F) vice versa in order to determine whether either visualisation method interfered with the other. Scale bars 20μm.

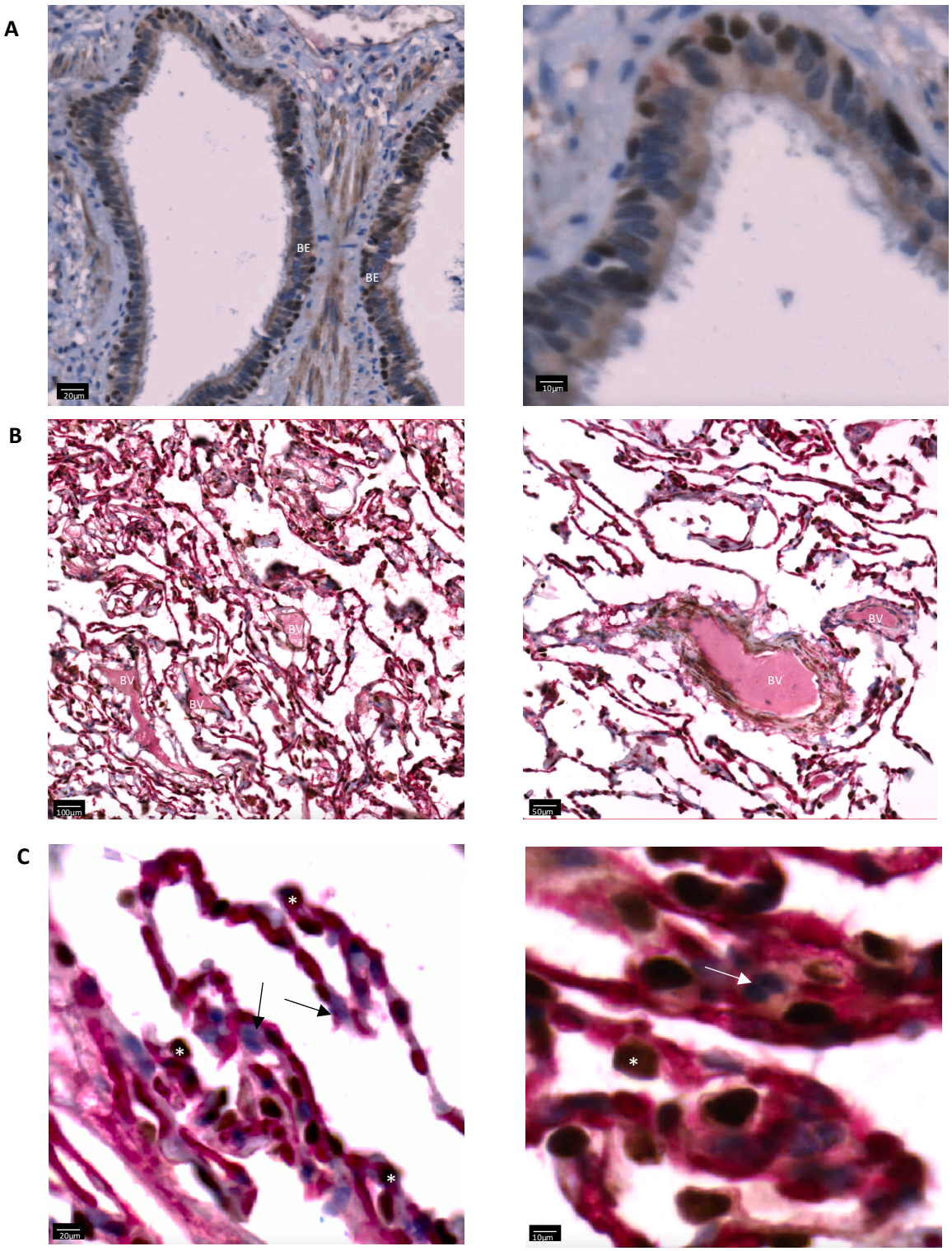

Fig 3.9 CD200 expression in the human lung.

Representative images (n= 59) of human lung sections immunohistochemically labelled for CD200 and TTF1 and visualised with Vector Red and DAB, respectively. (A) No CD200 labelling was detected in the bronchial epithelium. TTF-1 positive club cells were seen interspersed throughout the epithelium. Left scale bar 20µm, right scale bar 10µm. (B) Similar to the mouse lung, CD200 labelling was seen throughout the alveoli. Left scale bar 100µm, right scale bar 50µm. (C) Type II alveolar cells (*) were double positive for CD200 and TTF-1 whilst type I alveolar cells (arrows) were negative for both CD200 and TTF-1. CD200 positivity was also seen within the alveolar septa. Left scale bar 20µm, right scale bar 10µm. BE, bronchial epithelium; BV, blood vessel.

3.2.2 CD200 expression in lung cancer

3.2.2.1 Tumour CD200 expression in a preliminary lung cancer tissue microarray

Having demonstrated CD200 expression within the lung, a preliminary TMA consisting of 122 NSCLC cores was used to determine CD200 expression in NSCLC tumours (Figure 3.10a). Of those cores 62 were SCCs and 60 adenocarcinomas, taken from patients at varying disease stages (stages I-III). Tumour CD200 expression was analysed semi-quantitively using the H-score method (described in more detail in section 2.2.3). Briefly, tumour sections within the cores were manually annotated to exclude stroma, cells were detected and a CD200 intensity score (0, 1+, 2+, 3+) was assigned to each tumour cell based on pre-determined intensity values (Figure 3.10b); this was then used to calculate the final CD200 tumour H-score.

TTF-1 positivity was seen in 15.3% and 87.1% of SCC and adenocarcinoma tumours, respectively. Of the 122 samples analysed, the adenocarcinoma cores (mean CD200 H score= 47.26) demonstrated significantly greater tumour CD200 expression than the SCC cores (mean= 23.96) ($p= 0.0287$; Figure 3.10c). Within most CD200 positive tumours, CD200 expression demonstrated notable intratumoural heterogeneity, with CD200 positivity ranging from 1.24% - 99.78% (mean 30.68%). Additionally, CD200 expression did not correlate with disease stage in either subgroup (Figure 3.10d). CD200 positive tumours were both positive and negative for TTF-1 and CD200 expression did not correlate with TTF-1 expression in either SCC or adenocarcinoma (data not shown). Strong CD200 expression was also seen throughout the stroma. In summary, CD200 expression was seen in NSCLC tumours where its expression was greater in adenocarcinomas compared to SCCs. Furthermore, CD200 expression did not correlate with TTF-1 expression or patient disease stage. These preliminary findings were then used to determine the minimum number of whole tumour patient samples required for further analysis.

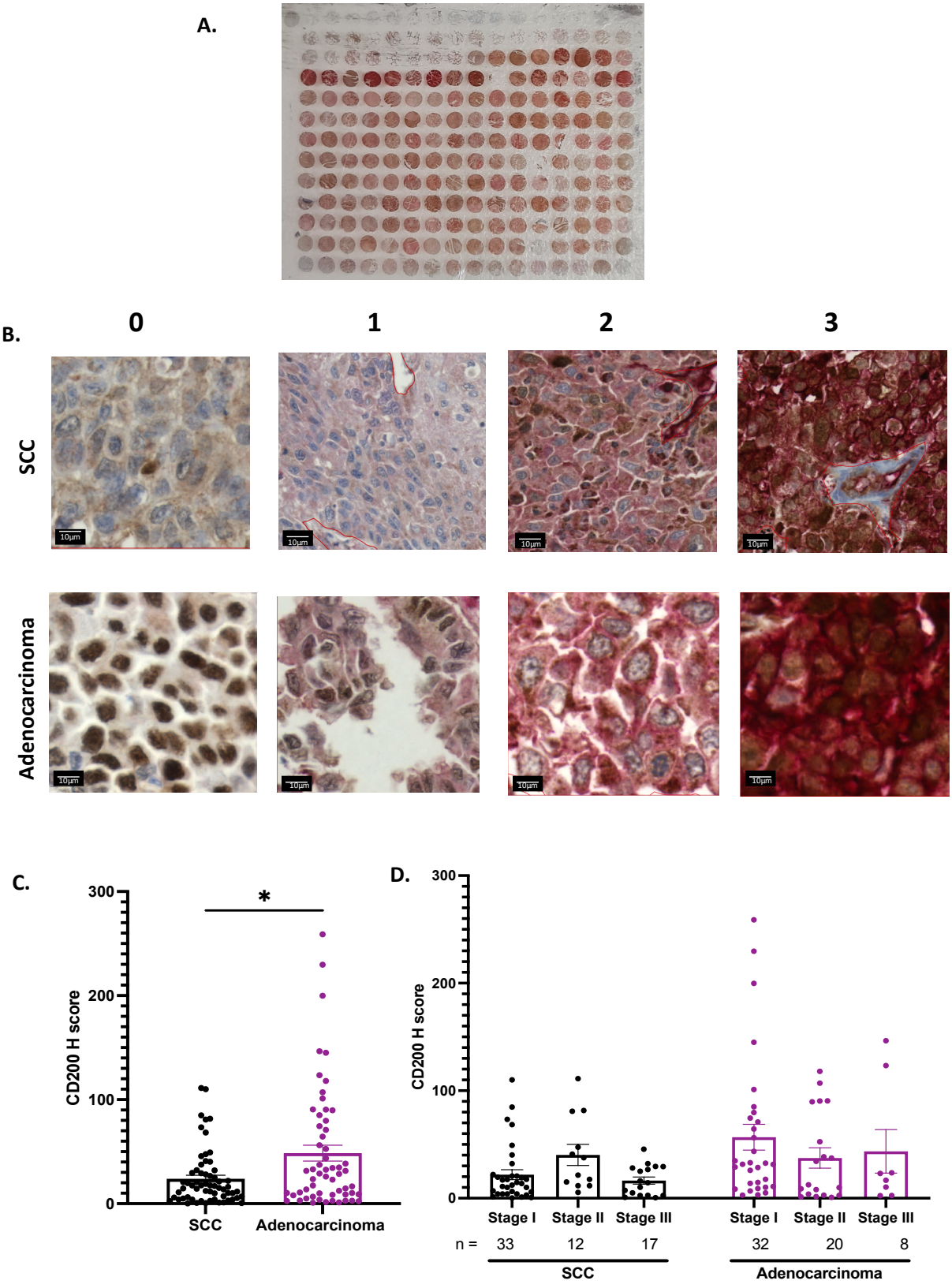

Figure 3.10 Preliminary analysis of CD200 expression in NSCLC.

A TMA consisting of 62 SCC and 60 adenocarcinoma cores ranging from Stages I-III was stained for CD200 and TTF-1 and tumour CD200 expression semi-quantitively analysed. (A) Whole slide image of the TMA which also included normal adjacent lung samples (n= 55). (B) Representative images of tumour CD200 intensities ranging from negative (0) to strong (3+) used to calculate the CD200 H-score. Scale bars 10µm. (C) CD200 tumour H scores for SCC (n= 62) and adenocarcinoma (n= 60) tumour cores. (D) CD200 H score by tumour staging in NSCLC. Significance was tested for using an unpaired t test (C) or a one-way ANOVA with Dunn's multiple comparisons (D). $P \leq 0.05$ (*).

3.2.2.2 Tumour CD200 expression in NSCLC

Based on the findings from the preliminary TMA analysis wherein adenocarcinomas demonstrated significantly greater tumour CD200 expression, a power calculation was performed to determine the minimum number of patient samples required for subsequent analysis to detect a difference in CD200 expression between SCC and adenocarcinoma. Based on this calculation, a total of 120 adenocarcinoma samples and 120 SCC samples consisting of predominantly whole tumour sections ranging from stages I-III were then acquired from the Wales Cancer Bank for subsequent immunohistochemical analysis.

A summary of the clinical characteristics of the NSCLC patients can be found in Table 3.1. Patient data was incomplete for 2 patients and was therefore excluded. Differences between adenocarcinoma (n= 119) and SCC (n= 119) patient characteristics were determined using the Fisher's exact or Chi squared test. Patient ages ranged from 45 – 91 years (median 71 years) with 60% of patients being female. Over half of the cohort (58.4%) were T stage 2 and a majority of the patients had no nodal involvement (N0; 58.4%) with disease stages ranging from I to III. No differences were observed in sex, age, or OS between adenocarcinoma and SCC patients. Significant differences were seen between adenocarcinoma and SCC patient's tumour stage (p= 0.0002), nodal involvement (p= 0.0006) and overall disease stage (p= 0.0044), with adenocarcinoma patients demonstrating more advanced disease stage. Of the 12 patients who had never smoked 11 of them had adenocarcinoma, consistent with this subtype being the predominant NSCLC diagnosis in never-smokers. OS was greater in SCC (96 months) compared to adenocarcinoma (56 months), which may be due to the differences in disease stage (Figure 3.11)

Tumour sections were stained and analysed for tumour CD200 expression using the cell classification method described in section 2.2.4. Tumour cell CD200 intensities were again classified from 0 to 3+ (Figure 3.12a) to determine a H-score. 94.87% of adenocarcinomas and 16.52% of SCCs were TTF-1 positive. Consistent with the preliminary analysis, adenocarcinomas (H-score= 61.12 ± 58.37) demonstrated significantly greater CD200 expression than SCCs (H-score= 32.47 ± 46.56) (p= <0.0001; Table 3.1; Figure 3.12b). SCCs demonstrated a greater number of completely or majority negative tumours when compared to adenocarcinomas (Figure 3.12c; Figure 3.12d). The number of tumours with 2+ CD200 expression was also larger in the adenocarcinomas compared to SCCs. These graphs highlight the intratumoural heterogeneity of CD200 expression, with CD200 positivity ranging from 0.11% – 99.77% and 0.386% - 100% for SCCs and adenocarcinomas, respectively (Figure 3.12c-d). CD200 positivity again did not demonstrate any correlation with TTF-1 expression in either adenocarcinoma (p= 0.3442) or SCC (p= 0.6092) tumours as determined

with the Fisher's exact test. Strong CD200 labelling was again seen throughout the stroma and adjacent normal tissue (Supplementary Figure S1). Taken together, tumour CD200 expression could be successfully semi-quantitively assessed in NSCLC tumours, with CD200 expression significantly greater in adenocarcinomas than SCCs.

Table 3.1 Summary and differences in clinicopathological characteristics between 119 adenocarcinoma and 119 SCC patients. Differences between groups were tested for using Chi-square or Fischer's exact test.

		All patients	Adeno	SCC	P value
		N (%)			
Sex	Male	94 (39.5)	47 (39.5)	47 (39.5)	0.999
	Female	144 (60.5)	72 (60.5)	72 (60.5)	
Age	Median	71	69.5	72	0.5633
	Range	45 - 91	45 - 91	52 - 87	
T stage	T1	71 (29.8)	50 (42.4)	21 (17.5)	0.0002
	T2	122 (51.3)	51 (43.2)	71 (59.2)	
	T3	37 (15.5)	12 (10.2)	25 (20.8)	
	T4	8 (3.4)	5 (4.2)	3 (2.5)	
N stage	N0	139 (58.4)	56 (47.5)	83 (69.2)	0.0006
	N1	54 (22.7)	30 (25.4)	24 (20)	
	N2	25 (10.5)	20 (16.9)	5 (4.2)	
	Nx	20 (8.4)	12 (10.2)	8 (6.6)	
Disease Stage	I	92 (38.7)	45 (38.1)	47 (39.2)	0.0044
	II	104 (43.7)	43 (36.5)	61 (50.8)	
	III	42 (17.6)	30 (25.4)	12 (10)	
Smoking status	Ever	189 (79.4)	88 (73.9)	101 (84.2)	0.0023
	Never	12 (5.1)	11 (9.2)	1 (0.83)	
	Unknown	37 (15.5)	20 (16.8)	17 (14.2	
Overall survival	Median (months)	73.5	56	95	0.4862
Tumoral CD200 H score	Median	23.86	45.72	8.039	<0.0001
	Range	0 - 279	0.0155 - 279	0 - 264	

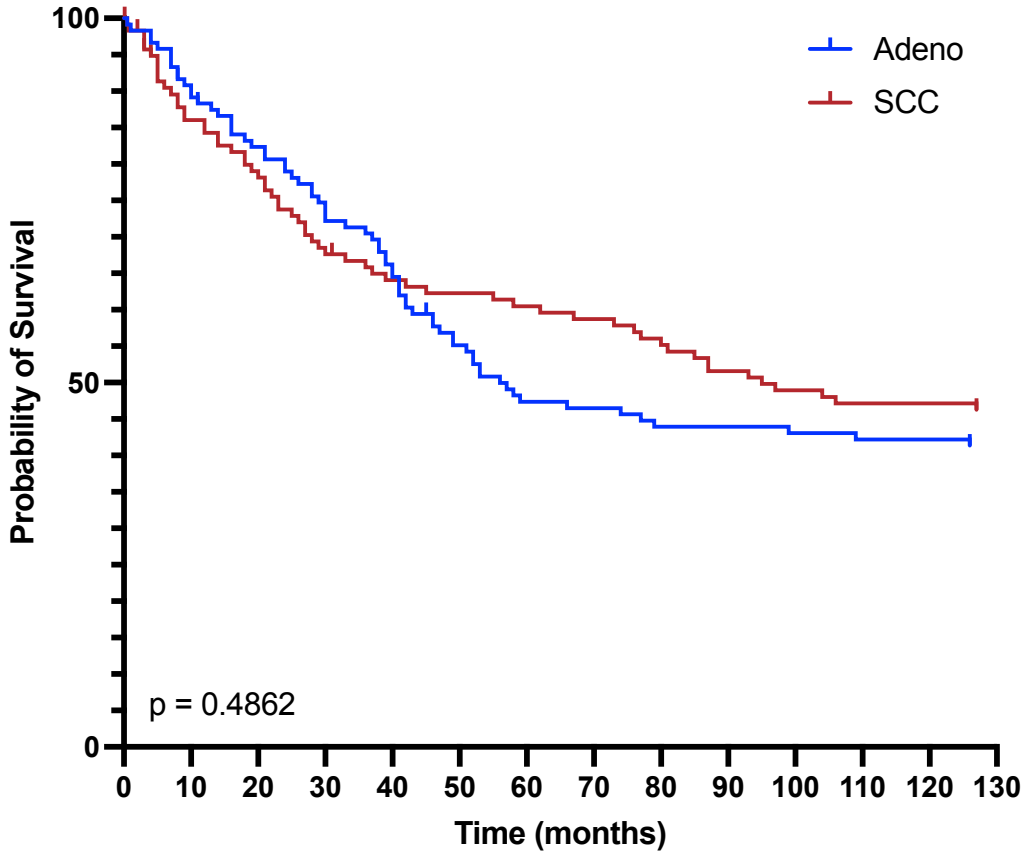

Figure 3.11 Kaplan-Meier survival curves for overall survival of NSCLC patients.

Overall survival in months for 119 SCC and 119 adenocarcinoma patients. Overall survival was calculated in months from the date of procedure to date of death. Non-cancer related deaths were censored.

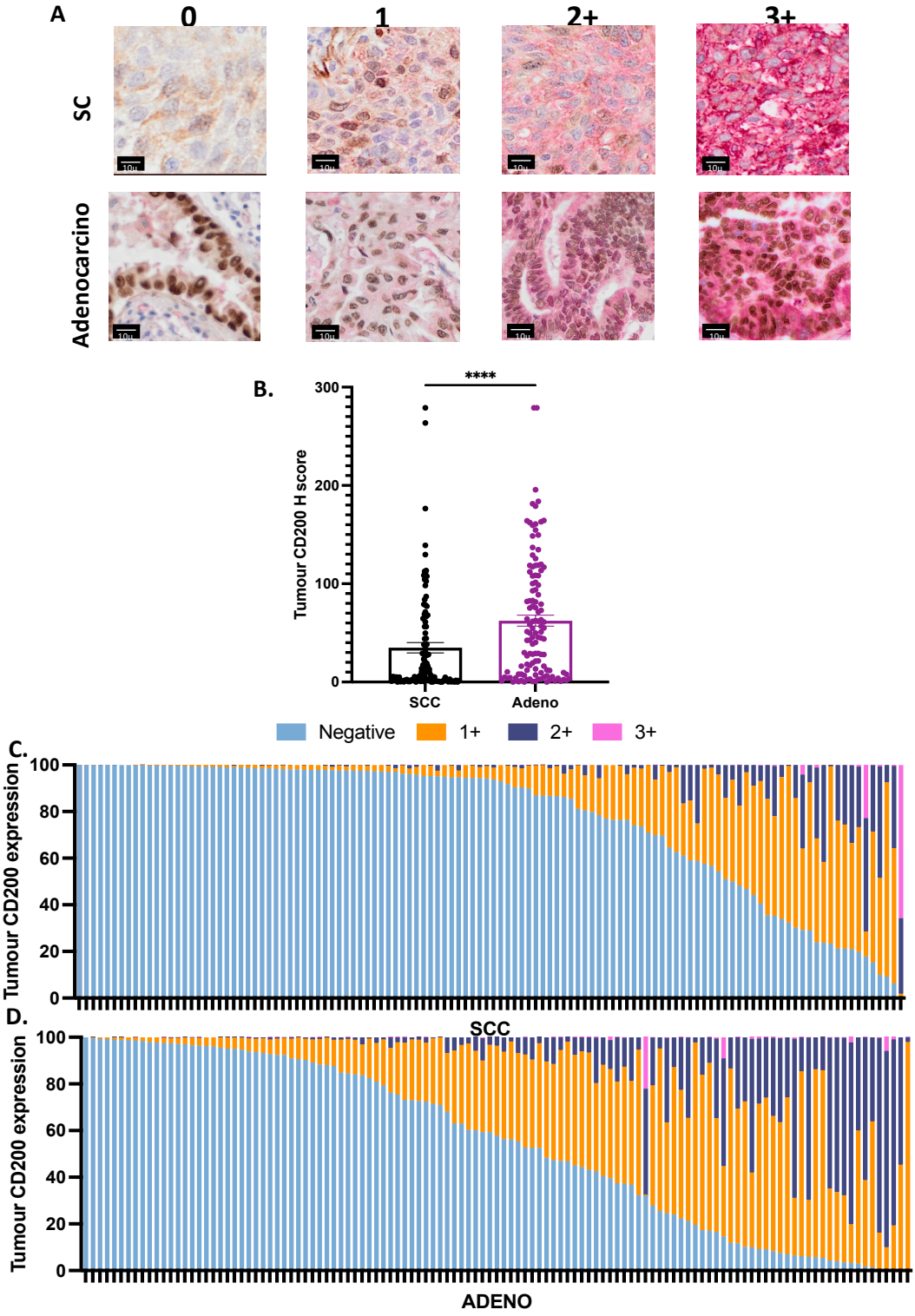

Figure 3.13 Tumour CD200 expression in NSCLC.

120 SCC and 120 adenocarcinoma sections ranging from Stages I-III were stained for CD200 and TTF-1 and tumoral CD200 expression semi-quantitively analysed. (A) Representative images of tumour CD200 staining intensities ranging from negative (0) to strong (3+) used to calculate the H-score. Scale bars 10μm. (B) CD200 H-scores for SCC (n= 120) and adenocarcinoma (n= 120). (C)(D) Breakdown of the relative number of 0, 1+, 2+ and 3+ CD200 cells within each tumour sample used to calculate the H-score, organised from left to right by % of negative cells. Significance tested for using Mann-Whitney U test. P ≤ 0.0001 (****).

3.2.2.4 Correlations between tumour CD200 expression and patient characteristics

To determine whether any clinical characteristic was associated with tumour CD200 expression in NSCLC, patients were grouped into high and low CD200 expression groups based on the median H score within each tumour subtype. There were no significant differences in patient clinicopathological characteristics between high and low CD200 expression groups in the SCC (Table 3.2) or adenocarcinoma cohorts (Table 3.3). However, in SCC patients, high CD200 expression did appear to trend towards earlier disease stage ($p= 0.0511$).

Table 3.2 Clinicopathological characteristics of SCC patients according to tumoral CD200 expression. Differences between groups were tested for using Chi-square or Fischer's exact test.

			Tumoral CD200 expression		P value
			Low	High	
Sex	Male	48 (39)	35 (59.3)	36 (61)	0.9999
	Female	72 (61)	24 (40.7)	23 (39)	
Age	Median	72	70	73	0.6782
	Range	52 - 87	54 - 73	52 - 87	
T stage	T1	21 (17.5)	8 (13.6)	13 (22)	0.6264
	T2	71 (59.2)	36 (61)	34 (57.6)	
	T3	25 (20.8)	13 (22)	11 (18.6)	
	T4	3 (2.5)	2 (3.4)	1 (1.7)	
N stage	N0	83 (69.2)	38 (64.4)	43 (72.9)	0.2541
	N1	24 (20)	14 (23.7)	10 (16.9)	
	N2	5 (4.2)	4 (6.8)	1 (1.7)	
	Nx	8 (6.6)	3 (5.1)	5 (8.5)	
Disease Stage	I	47 (39.2)	21 (35.6)	25 (43.4)	0.0511
	II	61 (50.8)	28 (47.5)	32 (54.2)	
	III	12 (10)	10 (16.9)	2 (3.4)	
Smoking status	Ever	101 (84.2)	48 (81.4)	52 (88.1)	0.4851
	Never	1 (0.83)	1 (1.7)	0 (0)	
	Unknown	17 (14.2	10 (16.9)	7 (11.9)	

Table 3.3 Clinicopathological characteristics of adenocarcinoma patients according to tumoral CD200 expression. Differences between groups were tested for using Chi-square or Fischer's exact test.

			Tumoral CD200 expression		P value
			Low	High	
Sex	Male	48 (39)	24 (40.7)	22 (37.3)	0.8504
	Female	72 (61)	35 (59.3)	35 (62.7)	
Age	Median	69.5	67	72	0.9906
	Range	45 - 91	45 - 85	48 - 91	
T status	T1	50 (42.4)	27 (45.8)	23 (39)	0.3793
	T2	51 (43.2)	22 (37.3)	29 (49.1)	
	T3	12 (10.2)	6 (10.2)	6 (10.2)	
	T4	5 (4.2)	4 (6.7)	1 (1.7)	
N status	N0	56 (47.5)	26 (44.1)	30 (50.8)	0.1044
	N1	30 (25.4)	13 (22)	17 (28.8)	
	N2	20 (16.9)	10 (16.9)	10 (16.8)	
	Nx	12 (10.2)	10 (16.9)	2 (3.4)	
Disease Stage	I	45 (38.1)	23 (39)	22 (37.3)	0.9775
	II	43 (36.5)	21 (35.6)	22 (37.3)	
	III	30 (25.4)	15 (25.4)	15 (25.4)	
Smoking status	Ever	88 (73.7)	45 (76.3)	42 (71.2)	0.7572
	Never	11 (9.2)	5 (8.48)	6 (10.2)	
	Unknown	21 (17.5)	9 (15.3)	11 (18.6)	

3.2.2.5 Patient characteristics and overall survival

Next, univariate analysis was performed for all clinicopathological characteristics using Kaplan-Meier curves to determine if tumoral CD200 had any prognostic value in our NSCLC patients (Figures 3.13 & 3.14) and differences assessed by the log-rank test (Tables 3.4 & 3.5) to see their effects on OS. OS was determined from the date of procedure to the date of death; where stated, deaths unrelated to cancer were censored. The median follow-up period for the entire cohort was 73.5 months (6.125 years) and ranged from 0.5 to 126 months (10.5 years). Patients still alive at the time of data collection were censored at 126 months.

In SCC patients, as expected, tumour stage (p= 0.004), node stage (p= 0.005) and disease stage (p= 0.0014) were all significant indicators for OS with patients with higher disease stage demonstrating significantly worse OS (Table 3.4; Figures 3.13c-e). Although never smoking was associated with worse OS (p= 0.0096), it must be noted that only a single patient constitutes this never smoked group (Table 3.4; Figure 3.13f). High tumoral CD200 expression trended towards better OS although it did not reach statistical significance (HR 0.6129; 95% CI 0.3684-1.020; p= 0.0565; Table 3.4; Figure 3.13g).

For adenocarcinoma patients, both node stage (p= 0.015) and disease stage (p= 0.0064) were significant indicators for OS, with patients with higher node stage and disease stage demonstrating significantly worse OS (Table 3.5; Figure 3.14d-e). Smoking status was also significantly associated with OS (p= 0.0371) with patients who had never smoked demonstrating better OS (Table 3.5; Figure 3.14f). Patients with high tumoral CD200 expression demonstrated slightly better OS, although this again did not reach statistical significance (HR 0.7713; 95% CI 0.4793-1.241; p= 0.2815; Table 3.5; Figure 3.14g).

Table 3.4 Univariate analysis of prognostic clinicopathologic variables as predictors for OS in SCC. Differences in survival calculated using log-rank test.

Characteristic		**Median survival (months)**	**P value**
Sex	Female	Undefined	0.1617
	Male	81	
Age	≤72	Undefined	0.1001
	>72	77	
Tumour status	T1	Undefined	0.004
	T2	Undefined	
	T3	28	
	T4	Undefined	
Node status	N0	Undefined	<0.0001
	N1	42	
	N2	14	
Disease stage	Stage I	Undefined	0.0014
	Stage II	93	
	Stage III	14	
Smoking status	Ever	97	0.0096
	Never	6	
Tumour CD200 expression	Low	87	0.0565
	High	Undefined	

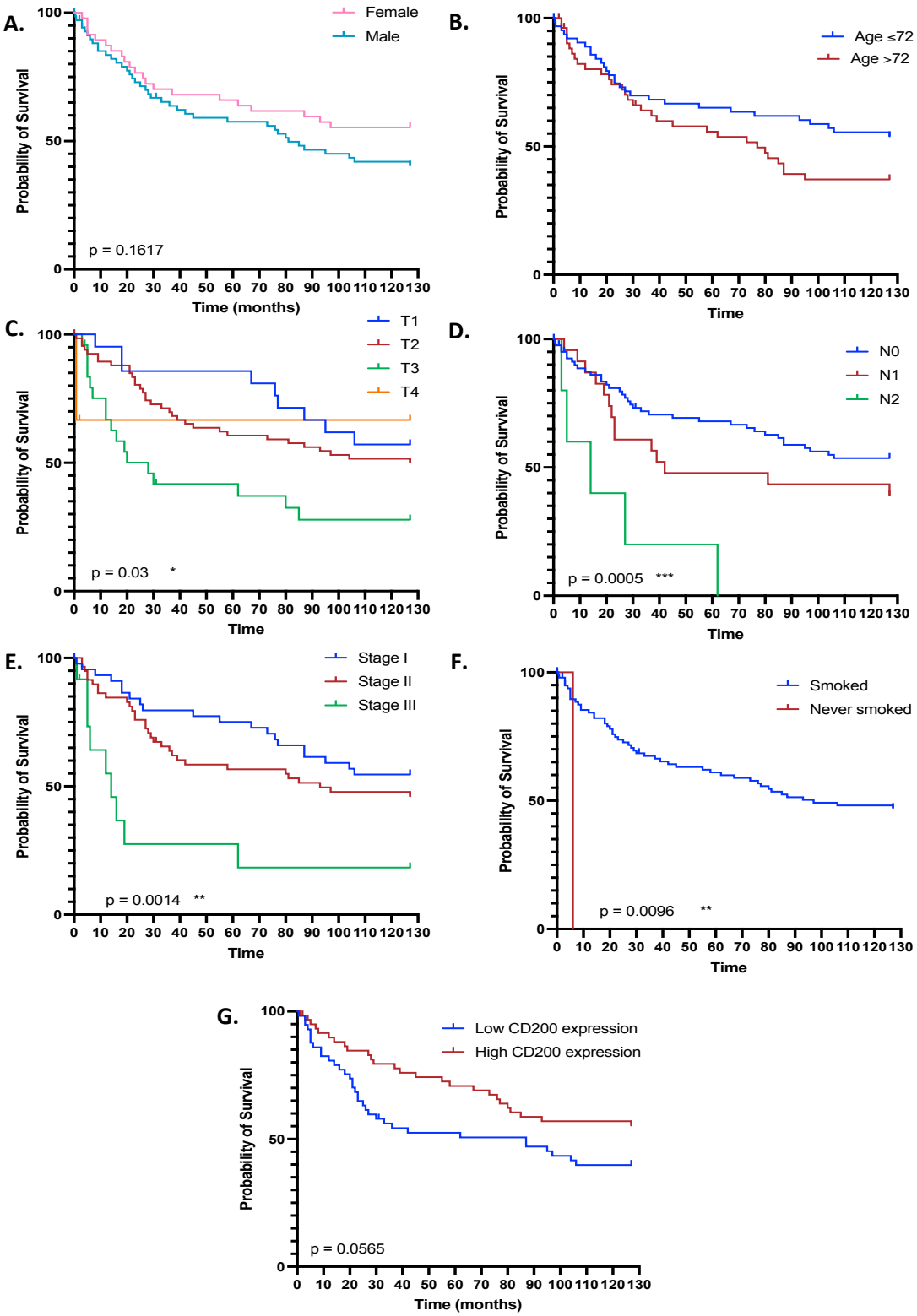

3.13 Kaplan-Meier survival curves for overall survival of SCC patients (n= 119).

Patients were divided into groups by (A) sex (B) median age (C) tumour stage (D) nodal stage (E) disease stage (F) smoked or never smoked status and (G) median tumoral CD200 expression. Overall survival was calculated in months from the date of procedure to date of death. Differences in survival calculated using log-rank test with $p \leq 0.05$ considered significant.

Table 3.5 Univariate analysis of prognostic clinicopathologic variables as predictors for OS in adenocarcinoma. Differences in survival calculated using log-rank test.

Characteristic		Median survival (months)	P value
Sex	Female	77	0.3469
	Male	52	
Age	≤70	79	0.1828
	>70	51	
Tumour status	T1	88	0.3032
	T2	53	
	T3	58	
	T4	41	
Node status	N0	Undefined	0.0150
	N1	37	
	N2	42	
Disease stage	Stage I	Undefined	0.0064
	Stage II	58	
	Stage III	39	
Smoking status	Ever	51	0.0371
	Never	Undefined	
Tumour CD200 expression	Low	52	0.2815
	High	99	

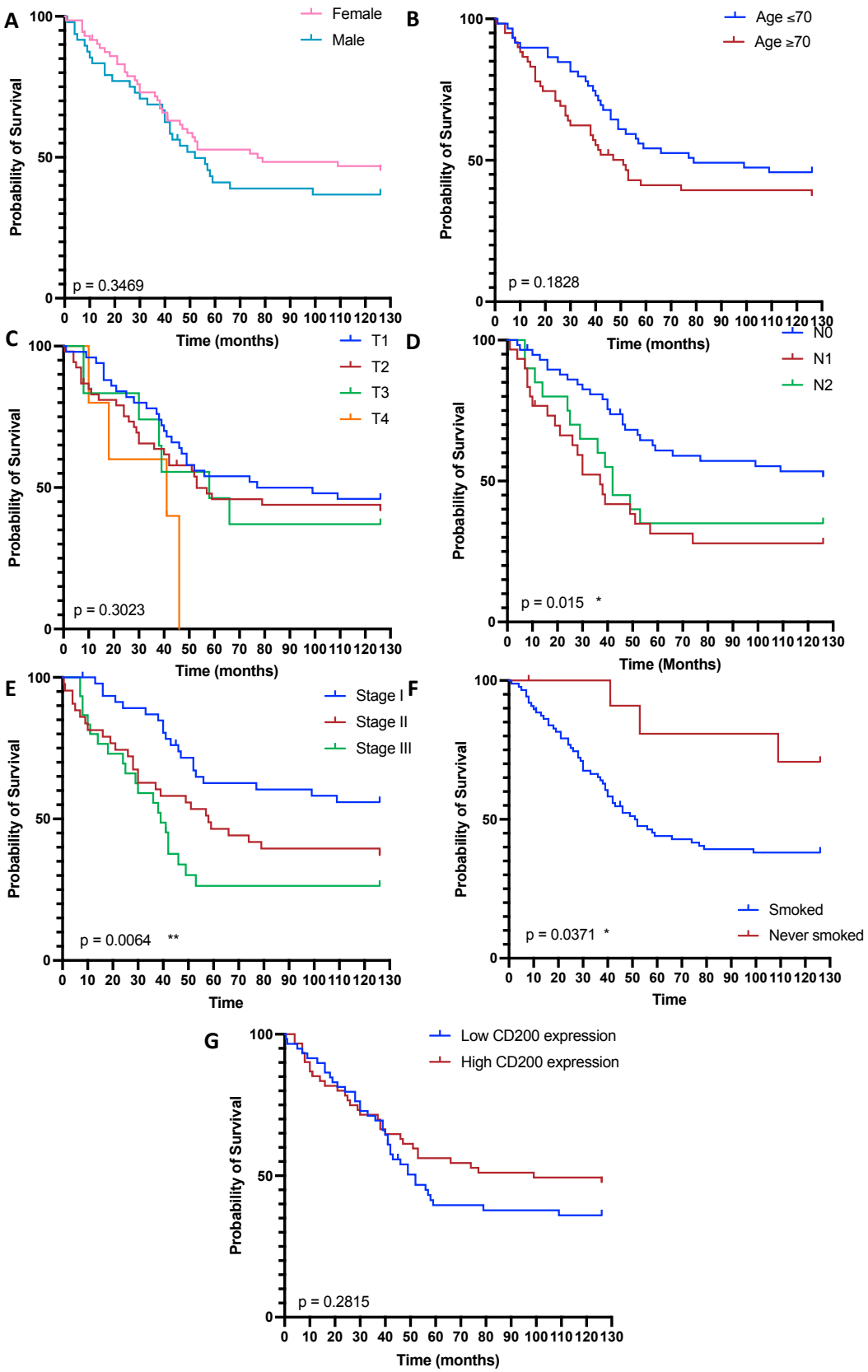

3.14 Kaplan-Meier survival curves for overall survival of SCC patients (n= 119).

Patients were divided into groups by (A) sex (B) median age (C) tumour stage (D) nodal stage (E) disease stage (F) smoked or never smoked status and (G) median tumoral CD200 expression. Overall survival was calculated in months from the date of procedure to date of death. Differences in survival calculated using log-rank test with $p \leq 0.05$ considered significant.

3.3 Discussion

CD200 signalling is critical for the maintenance of lung immune homeostasis, with its expression dysregulated during lung inflammation and disease. Therefore, the aim of this chapter was to first define CD200 expression in the normal mouse and human lung before determining whether CD200 is also expressed in NSCLC tumours.

3.3.1 Autofluorescence in mouse and human lung tissue

An immunofluorescent protocol for the labelling of CD200 was optimised in mouse and human hair follicles prior to characterisation of CD200 in the lung; however, upon labelling mouse and human lung and NSCLC tumour sections with secondary antibody only controls, the highly autofluorescent nature of the lung tissue became apparent. Strong autofluorescence in the green channel was seen in the bronchial epithelium and alveoli of mouse tissue and in the alveoli of human lung, with fluorescence levels comparable between dapi only and CD200 stained tissue, suggesting that the autofluorescence would hamper the successful visualisation of labelled targets. Respiratory tissue autofluorescence has been attributed to many naturally occurring fluorophores including collagen, elastin, keratin, porphyrins, reduced nicotinamide adenine dinucleotide (NADH) and flavin adenine dinucleotide (FAD) (Davis *et al.* 2014; Wang *et al.* 2017). In addition, tissue processing techniques such as formalin fixation, antigen retrieval and serum blocking can all contribute to autofluorescence (Wessendorf 2004). Strong autofluorescence was also seen in NSCLC samples, within tumours arising from both proximal (SCC) and distal (adenocarcinoma) lung. Several techniques have been developed to quench autofluorescence in respiratory tissue, of which pre-treatment with EBT was demonstrated to be the most successful in diminishing fluorescence in a study comparing 9 different techniques on mouse lung tissue (Davis *et al.* 2014). However, in our mouse lung samples pre-treatment with EBT did little to decrease the fluorescence seen in the green channel. Furthermore, although not verified in this study, treatment with EBT consistently shifts the autofluorescence from the green to the red wavelength emission range, suggesting that this treatment would simply increase autofluorescence in another channel thus preventing effective multi-label immunofluorescent labelling in the lung (Davis *et al.* 2014). Based on these findings, the use of immunofluorescent labelling for CD200 in the lung was dismissed in favour of a multi-label IHC protocol.

CD200 was successfully immunohistochemically labelled in the mouse and human hair follicle and visualised with both DAB and Vector-Red. Unlike immunofluorescence, where multiple antigens within the same cell compartment can be visualised on the same sample, multi-label IHC requires that the two antigens are localised within different areas of the cell or tissue for successful labelling. Therefore, the nuclear type II alveolar cell lineage-specific and

adenocarcinoma diagnostic marker TTF-1 was selected. TTF-1 could be successfully labelled and visualised with DAB in type II alveolar cells in human lung tissue and could also be visualised in combination with CD200 using a sequential multi-label IHC protocol which demonstrated high sensitivity and low background staining in human lung. CD200 could be successfully visualised on the cell membrane of human lung tissue whilst TTF-1 positivity was seen in the nuclei. This multi-label IHC protocol allowed for the successful visualisation of CD200 expression, with the addition of the cell lineage and diagnostic marker TTF-1 allowing for further classification of CD200 cell types in human lung and NSCLC samples.

3.3.2 CD200 expression in the mouse and human lung

CD200 is highly conserved amongst species, therefore its expression was first defined in the mouse lung. The mouse bronchi and bronchioles are lined with pseudostratified columnar epithelium consisting of distinct cell types: goblet cells secrete mucus to entrap particulates; ciliated cells expel the mucus; club cells secrete various factors with protective and immunoregulatory properties; pulmonary neuroendocrine bodies probe the microenvironment and influence smooth muscle tone and basal cells serve as the progenitor cells of the respiratory epithelium (Zepp and Morrisey 2019). Within the bronchial epithelium, contrary to the rat lung wherein very weak CD200 expression was only demonstrated in club cells and on the apical cilia of some epithelial cells, weak CD200 expression was seen throughout the proximal and more distal bronchial epithelium, with all cells within the intrapulmonary bronchi and pulmonary bronchioles demonstrating weak positivity. However, multi-label IHC protocols for specific markers of each of these bronchial epithelial cell types was not performed to confirm this. This is the first study to demonstrate CD200 expression in the bronchial epithelium of both the larger bronchi and more distal bronchioles in the mouse lung; the cells of the bronchial epithelium are in contact with the environment and play a pivotal role in immune surveillance and generation of an appropriate immune response through activation of immune cells. Therefore, the expression of CD200 on these cells is consistent with the role of CD200:CD200R interactions in balancing the severity of an immune response to inhaled stimuli.

Strong CD200 expression was seen throughout the more distal mouse lung, with type I and type II alveolar cells both appearing to show strong positivity; however, multi-label IHC protocols to stain for specific markers of type I (T1α) and type II (surfactant protein C) alveolar cells were not performed. The vascular capillary endothelium within the alveolar septa separating adjacent alveoli also demonstrated strong CD200 expression. This is consistent with the findings of Snelgrove *et al.* (2008) wherein vascular endothelium and alveolar epithelium demonstrated strong CD200 expression by flow cytometry, with immunohistology

demonstrating CD200 expression specifically on the luminal aspect of the alveolar cells at x400 magnification. In this study, CD200 expression could not be localised to the luminal aspect of the alveolar epithelium of the labelled mouse lungs. This may be due to the lower magnification power of the microscope or due to differences in tissue processing. Despite this, strong CD200 expression in the alveoli is again consistent with the role of CD200:CD200R interactions in maintaining lung immune homeostasis through regulation of CD200R-bearing immune cells.

For the first time, in this study the expression of CD200 was analysed in the human lung. Unlike in the mouse, there was no CD200 positivity observed in bronchial epithelial cells, with both TTF-1 positive club cells and TTF-1 negative cells negative for CD200. However, of the 62 TMA cores and sections of normal human lung stained, only 3 contained sections of bronchial epithelium; therefore, further staining and analysis of bronchial epithelium is required to confirm this finding. Consistent with the staining in the mouse lung, strong CD200 expression was also seen throughout the distal human lung. TTF-1 positive type II alveolar cells and TTF-1 negative type I alveolar cells both demonstrated strong CD200 expression, as did the underlying vascular endothelium within the alveolar septa. Our findings suggest that unlike in the mouse lung where CD200 is expressed on bronchial and alveolar epithelium, in human lung CD200 is only expressed by alveolar type I and type II cells. A summary of the pattern of CD200 expression in the rat, mouse and human lung from the literature and this study can be found in Figure 3.15.

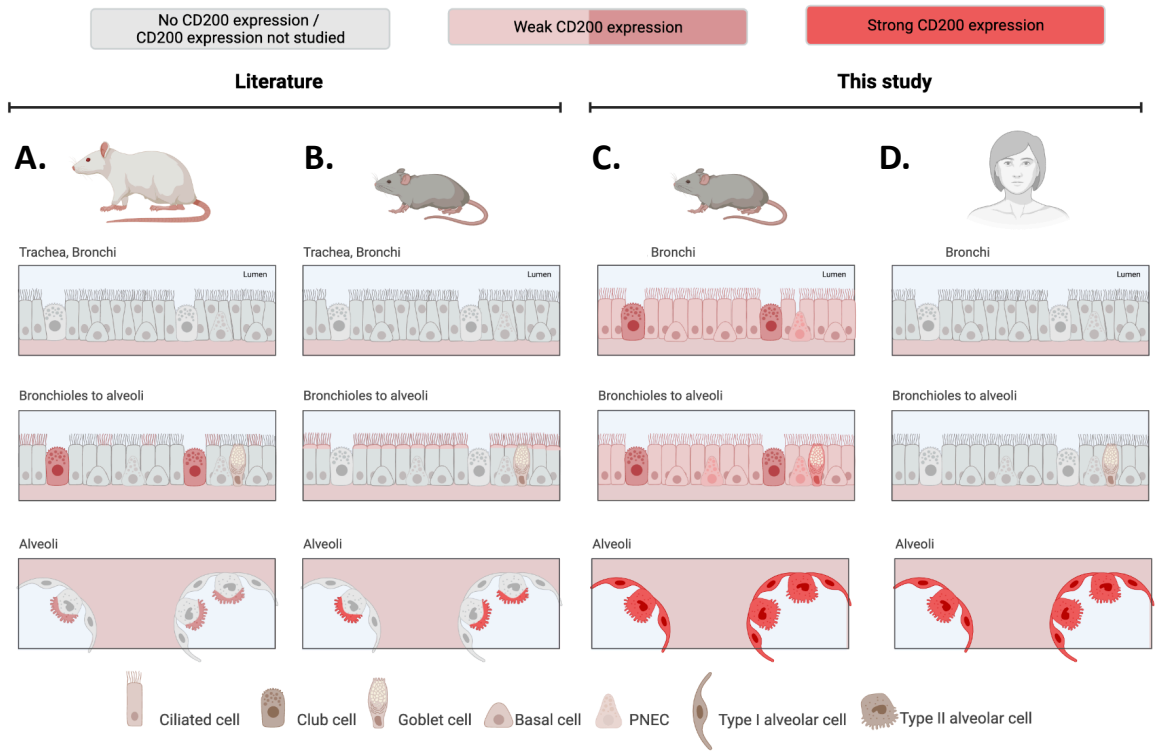

3.15 CD200 expression in the rat, mouse, and human lung.

CD200 is an important immunoregulatory molecule in the maintenance of respiratory immune homeostasis and its expression is highly conserved between species. High power magnification and electron microscopic imaging of (A) rat and (B) mouse lung in the literature demonstrated CD200 expression on the cilia of some bronchial epithelial cells in the rat and in all ciliated cells in the mouse lung. Rat club cells were also weakly positive for CD200. In the alveoli, the apical surface of type II alveolar cells were weakly positive for CD200 in the rat and strong for CD200 in the mouse. In this study (C) CD200 expression in the mouse lung was weak throughout all bronchial epithelial cells of the more proximal bronchi and bronchioles, with strong CD200 expression seen in all alveolar cells. (D) CD200 in the human lung appeared to be limited to strong expression in the alveolar cells. Differences in respiratory anatomy, CD200 homology and variations in tissue processing and imaging techniques used may account for the differences in CD200 expression seen between the mouse and human lung and between the literature and this study. Taken together, CD200 is expressed in mouse bronchial epithelium and alveolar cells and for the first time, strong CD200 expression was characterised in the alveolar cells of human lung.

3.3.3 CD200 is expressed by NSCLC tumours

Having determined that CD200 was expressed by both type I and II alveolar cells in the human lung, it was hypothesised that tumours arising from these cells would also be positive for CD200. Several mouse models have demonstrated that adenocarcinomas arise from club cells in the bronchioles and type II alveolar cells, with the latter being the predominant source of adenocarcinoma tumours (Xu *et al.* 2012). On the other hand, SCC tumours can be induced from basal epithelial cells, club cells and type II alveolar cells, with cells within the more proximal lung the most predominant (Ferone *et al.* 2020). Therefore, it was hypothesised that most adenocarcinomas and those SCCs that arise from alveolar type II cells would be positive for both CD200 and the type II alveolar marker TTF-1, with the tumours arising from club and basal cells within the bronchial epithelium positive for TTF-1 only. In line with this hypothesis, of the 362 NSCLC tumours analysed the adenocarcinomas demonstrated significantly greater tumour CD200 H scores than SCCs. However, there was no correlation between CD200 and TTF-1 expression, with CD200 positivity seen in both TTF-1 positive and negative tumours. This may be due to tumours arising from alveolar type II cells losing TTF-1 expression or through cells which are CD200 negative and TTF-1 positive in the normal lung inducing CD200 expression upon malignant transformation. Together, our NSCLC cohort demonstrated an average tumour CD200 H-score of 48.2 ± 55.13; this is in line with the immunohistochemical study of 632 patient TMA core by Yoshimura *et al.* (2020) which demonstrated an average CD200 H-score of 42 ± 57.7. In contrast, an immunofluorescent study of CD200 expression in 287 NSCLC patient TMA cores only demonstrated CD200 positivity in 29.7% of tumours, much less than that seen with IHC (Vathiotis *et al.* 2021). This study used a visual cut-off to eliminate background fluorescence, therefore this cut-off could have limited the detection of weaker CD200 positivity, thus leading to an under-representation of tumour CD200 expression. Taken together, CD200 is expressed in both adenocarcinoma and SCC tumours, suggesting it may play a role in regulating the anti-tumour immune response in NSCLC.

CD200 expression was observed at all disease stages in both SCC and adenocarcinoma, suggesting that its expression is either present and therefore transferred during transformation, or upregulated early in the disease process. However, unlike the study by Yoshimura *et al.* (2020), tumoral CD200 expression did not have a significant prognostic effect on the OS of the patients studied or correlate with any other clinicopathological characteristic of the patients. However, although it did not reach significance, high tumoral CD200 expression in SCC patients did trend towards better OS. This may be due to the small size of the patient cohort in this study compared to the 632 NSCLCC patients used in their study. The power calculations done for this study were only based on finding a difference between CD200 expression between adenocarcinoma and SCC tumours; therefore, increasing the patient

cohort size could potentially identify correlations between tumour CD200 expression and patient clinical characteristics. Furthermore, this study used large tumour sections rather than TMA cores; given the great intratumoural heterogeneity of CD200 expression observed in these tumours, this large tumour section approach may have more accurately defined tumour CD200 expression.

3.3.4 Conclusions

In summary, CD200 is expressed throughout the bronchial and alveolar epithelium in the mouse but appears to be restricted to the alveolar epithelium in normal human lung, with CD200 expression seen in both TTF-1 positive and negative cells. This high expression of CD200 within the respiratory tract is consistent with its important regulatory role in sustaining lung immune homeostasis and maintaining a level of immune cell tolerance within an immune privileged site. CD200 expression was also seen in both adenocarcinoma and SCC tumours, with CD200 expression greater in adenocarcinoma tumours. This may be due to the predominant cell of origin in adenocarcinoma being alveolar type II cells. Whilst SCC tumours can also arise from type II alveolar cells, they predominantly occur in the more proximal lung suggesting that the predominant cells of origin are basal and club cells within the bronchial epithelium. This suggests that alveolar type II cells that express CD200 in the normal lung may maintain CD200 expression during transformation or CD200 expression is upregulated early in the disease process where it signals to modulate the anti-tumour immune response during NSCLC tumour growth and progression. To determine whether CD200 signalling has any effect on the anti-tumour immune response, the aim of the next chapter was to define immune infiltrate in NSCLC tumours and determine whether CD200 expression has any effect on immune cell composition.

Chapter 4:
Characterising NSCLC immune composition and its relationship with CD200 expression

4. Characterising NSCLC immune composition and its relationship with CD200 expression

4.1 Introduction

As an immune checkpoint, CD200 imparts a unidirectional immunosuppressive signal to CD200R-expressing immune cells. This signal has been shown to inhibit macrophage and NK cell function, induce tolerogenic DC phenotypes, switch T cells from Th1 to Th2 and induce Tregs (Hoek *et al.* 2000; Clark *et al.* 2003; Gorczynski *et al.* 2004; Coles *et al.* 2011; Aref *et al.* 2017). Infiltrating immune cells such as macrophages, neutrophils and lymphocytes play a pivotal role in contributing to cancer progression, with the type, density, and location of these immune cells within the TME impacting the clinical outcome of patients (Anichini *et al.* 2018). The complexity and composition of the immune infiltrate in NSCLC arises from the interaction of several factors, including tumour mutational status, molecular subtype, mutational burden, tumour histology, and acquired mechanisms of immune evasion such as the expression of immune checkpoints. Therefore, having characterised CD200 expression in 240 NSCLC patient samples, we next sought to determine whether tumour CD200 expression had any effect on the infiltrating immune response in these patients.

Prior to exploring the relationship between CD200 and the immune response, the first aim of this chapter was to estimate the immune cell composition in bulk normal lung and NSCLC tumour RNA-seq samples using the CIBERSORT deconvolution algorithm. NSCLC tumours have been shown to elicit a robust immune response, characterised by a 3-fold increase in CD45+ cells within tumour samples compared to non-adjacent lung tissue (Kargl *et al.* 2017). Most studies looking at the immune composition of NSCLC use flow cytometry and tend to vary in their findings due, in part, to differences in staining and gating strategies yielding different cell frequencies. Furthermore, large interpatient variations both in individual immune cell frequencies and in overall immune composition result in further discrepancies in overall findings (Tamminga *et al.* 2020). Multiple studies have demonstrated that CD3+ T cells are the most abundant cell type representing ~50% of all tumour infiltrating CD45+ cells with CD4+ T cells and CD8+ T cells accounting for ~30% and ~20%, respectively. B cells are the third most frequent immune cell (~7%), with proliferating B cells observed in 35% of NSCLC tumours (Lavin *et al.* 2017; Wang *et al.* 2019; Stankovic *et al.* 2018). Compared to normal distal lung, tumour tissue is also enriched for Tregs (~6% of immune infiltrate) and activated and memory T and B cells, suggesting the presence of an adaptive immune response (Lavin *et al.* 2017; Wang *et al.* 2019). Among tumour-infiltrating innate cells, macrophages are the most abundant mononuclear phagocytes (~5%), and neutrophils are the most abundant granulocyte, constituting anything from 9-20% of all leucocytes. NK cells constitute an average of 4.5% of all immune cells, with numbers of NK cells significantly reduced compared to normal

lung (Lavin *et al.* 2017; Stankovic *et al.* 2018). Having assessed tumour-infiltrating immune cell composition from bulk solid tumour samples, the relationship between CD200 expression and immune cell composition in the RNA-seq data was explored.

Several studies of haematological malignancies have demonstrated that CD200 expression on tumour cells is able to influence the frequency of circulating immune cells, with high CD200 levels associated with a reduced frequency of NK cells, memory CD8+ and cytotoxic CD4+ T cells in AML patients and an increase in Treg frequency in MM patients (Coles *et al.* 2011; Coles *et al.* 2012a; Aref *et al.* 2017). A study in NSCLC noted that tumours with low CD200 expression had significantly greater infiltration of memory immune cells, CD8+ T cells and Tregs compared to those with high CD200 expression (Yoshimura *et al.* 2020). Furthermore, CD200:CD200R signalling between tumour associated macrophages and T cells has been identified as a highly enriched signalling motif in the NSCLC TME, with CD200R expression significantly upregulated on T cells infiltrating the tumour compared to those in peripheral blood (Su *et al.* 2020; Tøndell *et al.* 2021). This suggests that CD200:CD200R signalling may be an important regulator in interactions between immune cells and NSCLC tumours and that tumour CD200 expression can influence the anti-tumour immune response. Therefore, the second aim of this chapter was to analyse the relationship between CD200 expression and the relative frequencies of each immune cell of the anti-tumour immune response.

4.1.1 Hypothesis and aims

Expression of the immune checkpoint CD200 by NSCLC tumour cells is a mechanism of immune evasion. CD200 expression will have a negative immunoregulatory effect on the composition of the NSCLC immune infiltrate, associated with a reduction in cytotoxic NK cells and an increase in immunosuppressive Treg cells.

Aims:

5. Investigate the relationship between CD200 expression and the composition of the immune infiltrate in NSCLC tumour tissue using a combined bioinformatics and immunohistochemical approach
    a. Explore the relationship between immune cell infiltration and patient clinical characteristics and survival
    b. Determine the relationships between tumour CD200 expression and the absolute and relative infiltration of cytotoxic and regulatory immune cells

Objectives:

1. Estimate the immune cell composition from bulk RNA-seq data of normal lung and NSCLC tumours and determine the differences in immune infiltrate between normal lung and tumour, and between SCC and adenocarcinoma tumours
2. Determine the relationship between CD200 expression and immune cell frequencies in bulk RNA-seq data
3. Determine the absolute and relative frequencies of CD45+, CD200R+, CD8+, Foxp3+ and CD56+ cells in our patient cohort and determine their prognostic significance
4. Define the relationship between tumour CD200 expression and the relative and absolute numbers of infiltrating immune cells

4.2 Results

4.2.1 Estimating the immune composition of normal lung and NSCLC tumours

To look at the immune cell composition in normal lung and NSCLC tumours in a large patient cohort, a bioinformatics approach was used to analyse TCGA-firehose RNA-seq data for 501 SCC patients and 518 adenocarcinoma patients, with matched normal distal lung tissue available for 109 patients. RNA-seq data was uploaded onto the CIBERSORT platform wherein the proportions of 22 infiltrating immune cells were estimated using the CIBERSORT deconvolution algorithm. Using a signature immune cell gene matrix comprised of 547 genes, CIBERSORT can estimate the relative proportions of 22 infiltrating immune cells through a linear support vector regression-based method. Absolute immune cell infiltration was defined as the median expression level of all genes in the signature gene matrix divided by the median expression level of all genes in the sample (Newman *et al.* 2015).

The mean estimated relative fractions of each immune cell for matched normal and tumour samples can be seen in Figure 4.1a. When comparing normal distal lung samples to matched SCC tumour samples, the proportions of M0 macrophages ($p = <0.0001$), M1 macrophages ($p = 0.0002$), Tregs ($p = 0.0025$), TFH cells ($p = <0.0001$) and plasma cells ($p = <0.0001$) were all significantly increased compared to normal lung. The fractions of neutrophils ($p = 0.0254$), resting mast cells ($p = <0.0001$), monocytes ($p = <0.0001$), resting NK cells ($p = 0.0007$) and MR CD4 T cell ($p = <0.0001$) were all significantly reduced in tumours sections (Figure 4.1b). In adenocarcinoma tumours the proportions of M1 macrophages ($p = 0.0116$), Tregs ($p = 0.0006$), TFH cells ($p = <0.0001$), naïve B cells ($p = 0.0459$), and plasma cells ($p = <0.0001$) were all significantly increased compared to normal lung. Conversely, resting mast cell ($p = <0.0001$), monocyte ($p = <0.0001$), resting NK cell ($p = <0.0001$) and MR CD4 T cell ($p = <0.0001$) proportions were all significantly reduced (Figure 4.1c).

The differences in normal lung and tumour immune composition between SCC and adenocarcinoma tumours are quite similar, with both tumours demonstrating a decrease in resting mast cells and monocytes alongside reductions in the resting NK cell and memory resting CD4 T cell fractions (Table 4.1). Moreover, both tumours saw an increase in M1 macrophages, Tregs, TFH cells and plasma cells. Taken together, these changes demonstrate an active immune response occurring in the tumours with the NSCLC immune composition differing from that of normal lung. However, although they did not reach significance, adenocarcinomas saw a decrease in M0 macrophages and SCC tumours saw a decrease in memory B cells both in reciprocal changes to what was seen in the other tumours. Therefore, in order to identify differences in the immune infiltration of SCC and adenocarcinoma tumours, the mean estimated relative fractions were compared between

histological subtypes (Figure 4.2). The adenocarcinoma tumours demonstrated a significant increase in the proportion of monocytes (p= <0.0001), M2 macrophages (p= <0.0001), resting DCs (p= 0.0164), MR CD4 T cells (p= <0.0001), Tregs (p= <0.0001) and memory B cells (p= 0.0451) and a significant decrease in M0 macrophage (p= <0.0001), M1 macrophage (p= 0.0007), resting NK cell (p= <0.0001) and TFH cell (p= 0.024) proportions when compared to SCCs. These differences between SCC and adenocarcinoma tumours highlight the complexity of the interactions between the tumour and immune system and suggest there is a tumour subtype-specific modulation of the immune response.

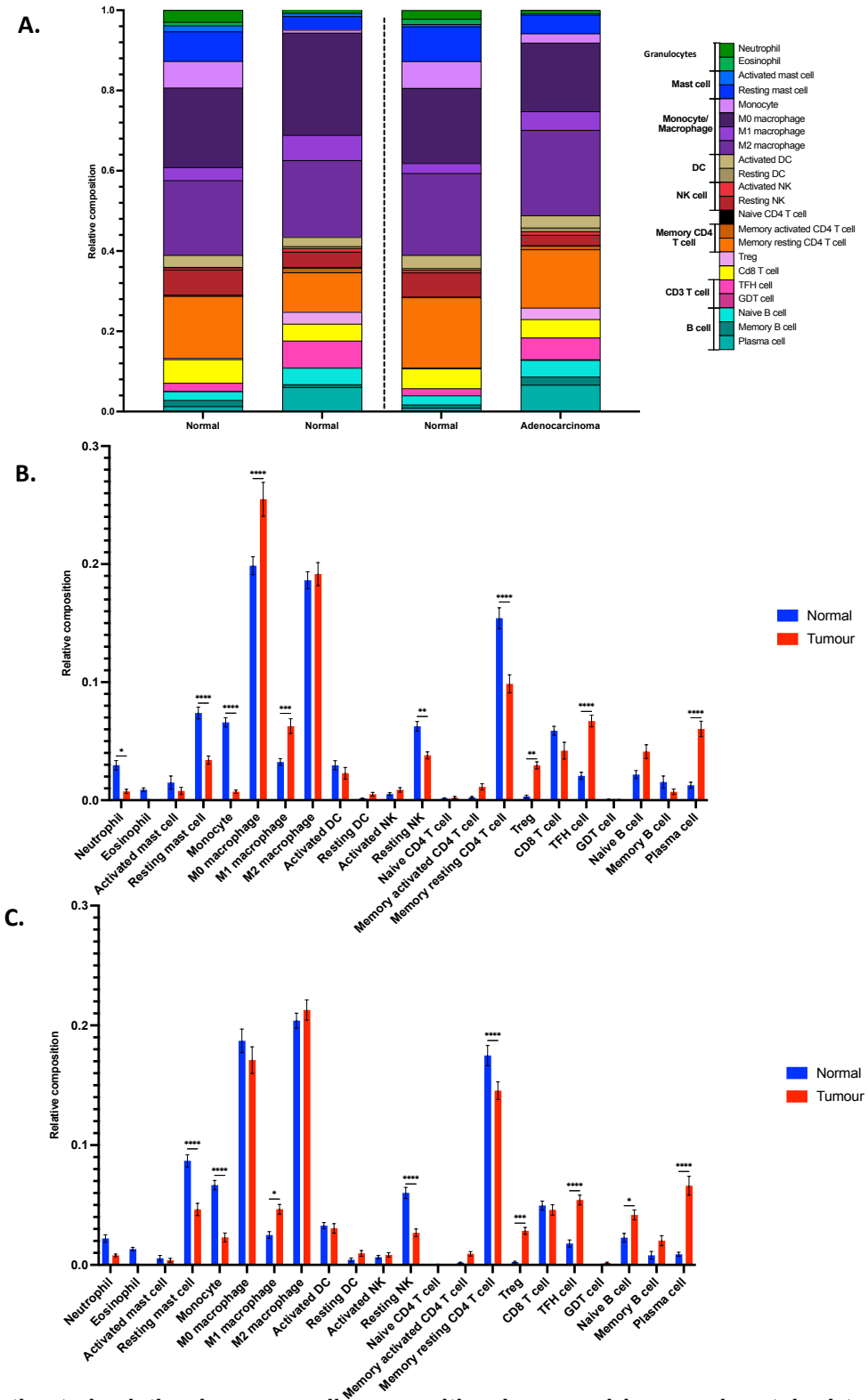

Figure 4.1 Estimated relative immune cell composition in normal lung and matched tumour samples.

TCGA RNA-seq data for 51 SCC tumours and matched normal tissue and 58 adenocarcinoma tumours and matched normal was entered into the CIBERSORT algorithm to estimate the relative frequencies of 22 different immune cells. (A) Summary of average immune cell composition in matched normal and tumour samples (B) matched SCC tumours and normal samples (C) matched adenocarcinoma tumours and normal lung. Significant differences were seen in the immune compositions between tumour and normal samples. Significance was tested for using the Kruskal-Wallis test with Dunn's multiple comparisons. $P \leq 0.05$ (*) $P \leq 0.01$ (**) $P \leq 0.001$ (***) $P \leq 0.0001$ (****). DC, dendritic cell; GDT, gamma delta T cell; Treg, regulatory T cell; NK, natural killer.

Table 4.1 Significant differences in relative immune cell composition between matched normal lung and SCC and adenocarcinoma tumour samples as determined by CIBERSORT

		SCC	Adenocarcinoma
Tumour vs normal	↑	M0 macrophages M1 macrophages Tregs TFH cells Plasma cells	M1 macrophages Tregs TFH cells Naïve B cells Plasma cells
	↓	Neutrophils Resting mast cells Monocytes Resting NK cells Memory resting CD4 T cells	Resting mast cells Monocytes Resting NK cells Memory resting CD4 T cells

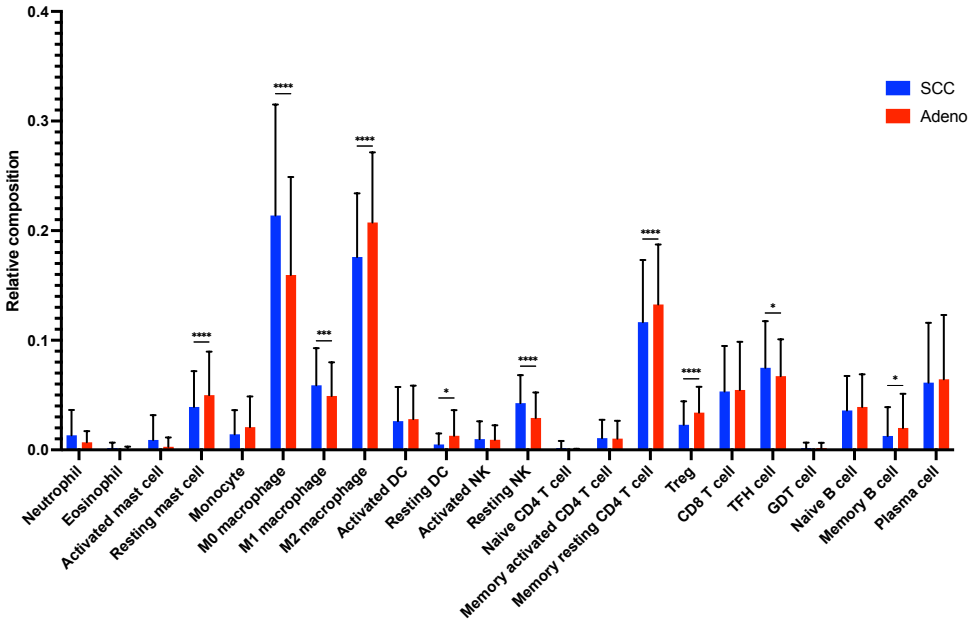

Figure 4.2 Differences in estimated relative immune cell composition between SCC and adenocarcinoma tumours.

TCGA RNA-seq data for 501 SCC and 518 adenocarcinoma tumours were entered into the CIBERSORT algorithm to estimate the relative frequencies of 22 different immune cells between NSCLC tumour subtypes. Significant differences were seen in the immune compositions between tumour and normal samples and between the two NSCLC subtypes. Significance was tested for using the Kruskal-Wallis test with Dunn's multiple comparisons. P ≤ 0.05 (*) P ≤ 0.01 (**) P ≤ 0.001 (***) P ≤ 0.0001 (****). DC, dendritic cell; GDT, gamma delta T cell; Treg, regulatory T cell; NK, natural killer.

4.2.2 Prediction of clinical outcomes from immune infiltrate in NSCLC

Having estimated the relative immune composition of normal lung and NSCLC tumours, the next aim was to determine the relationship between infiltrating immune cell proportions and their prognostic significance in NSCLC using the PRECOG software (Gentles *et al.* 2015). PRECOG applies the CIBERSORT algorithm to microarray and RNA-seq data to analyse the associations between clinical outcomes and the abundance of 22 different immune cells, several of which have been linked to tumour growth, progression, and survival outcomes in NSCLC.

Normalised microarray and RNA-seq data from 408 SCC patients and 902 adenocarcinoma patients met the CIBERSORT p-value threshold of 0.05 and were assessed for associations between immune cell infiltration and OS by univariate cox regression analysis. For each immune cell a meta-z score was calculated (Figure 4.3). Z scores are directly related to p values, but they encode both the directionality and robustness of the statistical associations between immune cell infiltration and clinical outcomes. The z score represents the number of standard deviations from the mean of a normal distribution e.g., z= 1.96 is equivalent to a two-sided p= 0.05. As z scores are independent of different timescales and of the range/scale of predictor variables, they permit direct comparison between studies and sequencing platforms (Gentles *et al.* 2015).

In SCC patients only 1 immune cell type had prognostic significance, with memory B cells a predictor of worse survival (Figure 4.3a). In adenocarcinoma, neutrophils, activated DCs, MA CD4 T cells, activated mast cells and macrophages (M0, M1, M2) were all significant predictors for worse survival, with resting mast cells and MR CD4 T significantly associated with better survival (Figure 4.3b). When the prognostic significance of infiltrating immune cells was compared between SCC and adenocarcinoma tumours, there were several cell types which had reciprocal relationships to survival (Figure 4.3c; yellow and blue boxes). Despite being significantly correlated with worse survival in adenocarcinoma, activated DCs, MA CD4 T cells and M0 macrophages were all associated with better survival in SCC. Furthermore, memory B cells and MR CD4 T cells, which were significantly associated with better survival in adenocarcinoma, were associated with worse survival in SCC. CD8 T cell and NK cell infiltration has been associated with favourable outcomes in several NSCLC studies and yet here they have reciprocal relationships in the patients studied and do not reach significance. Taken together, this data suggests that the prognostic significance of an immune cell varies between NSCLC subtypes, with many cells demonstrating reciprocal relationships with survival between SCC and adenocarcinoma patients.

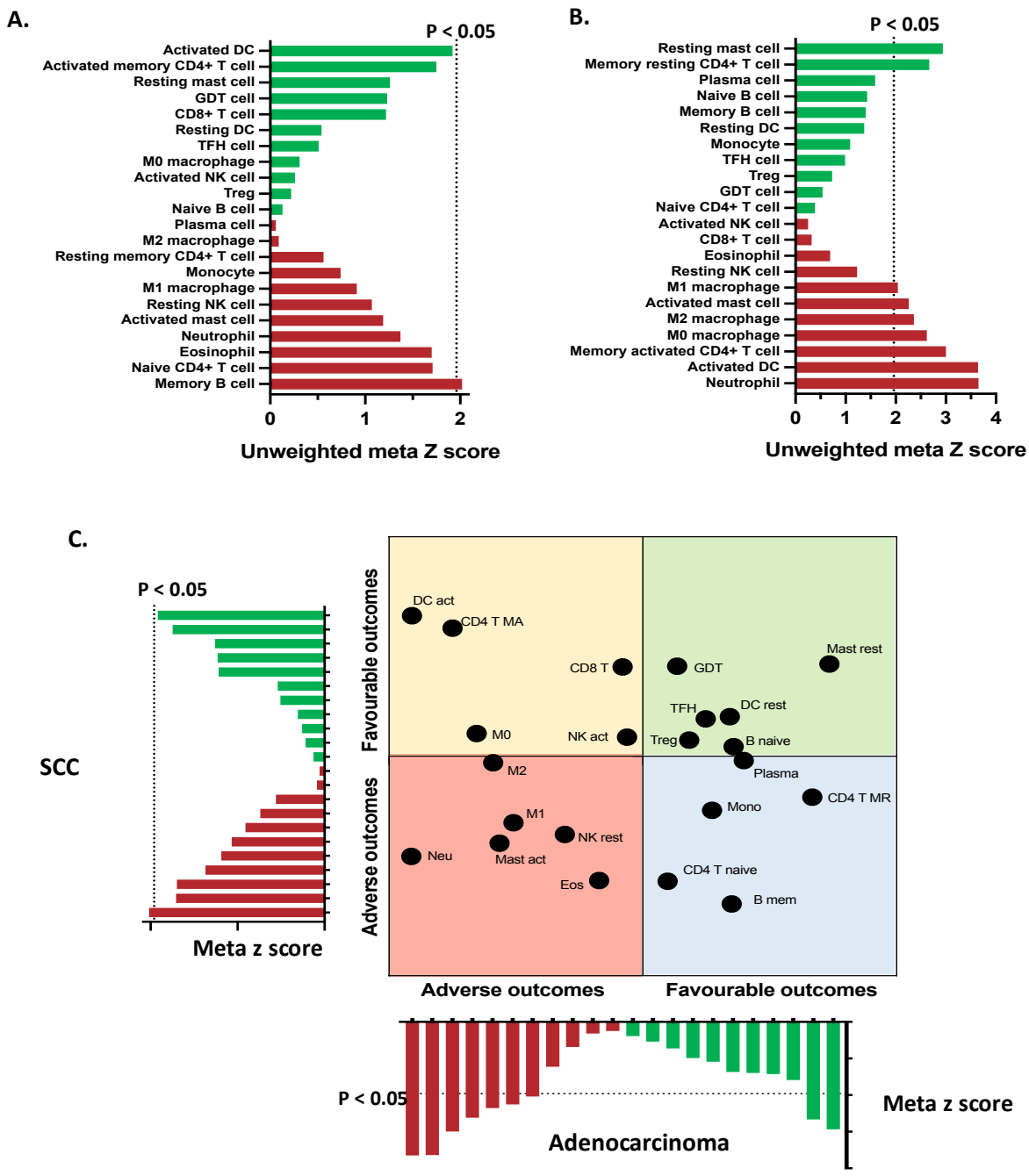

Figure 4.3 Estimated prognostic significance of 22 immune cells deconvoluted by CIBERSORT in NSCLC tumours.

Normalised microarray and TCGA RNA-seq data for 408 SCC and 902 adenocarcinoma patients was entered into CIBERSORT and the prognostic significance of each immune cell analysed by univariate cox regression analysis in PRECOG. (A) Adverse (red) and favourable (green) prognostic significance of immune cells in SCC, only memory B cells demonstrated a significant association with survival. (B) In adenocarcinoma patients, 2 cells had good prognostic power whilst six immune cells reached the meta z score cut-off for significance in predicting worse survival. (C) Upon comparing prognostic significance of each immune cell between adenocarcinoma and SCC tumours, 10/22 immune cells possessed reciprocal power depending on the tumour subtype. Weighted meta z scores are directly related to p values but encode both the directionality and robustness of the statistical associations; z= 1.96 = p= 0.05. DC, dendritic cell; GDT, gamma delta T cell; Treg, regulatory T cell; MA, memory activated; MR, memory resting; NK, natural killer.

4.2.3 Estimating the immune composition of SCC tumours based on CD200 expression

Having observed CD200 expression in NSCLC tumours, the next aim was to determine whether CD200 expression influenced the composition of the immune cell infiltrate. Therefore, to characterise the effects CD200 expression has on infiltrating immune cells, using the CIBERSORT data from 4.2.1, patients were stratified based on normalised CD200 transcripts per million mapped reads (TPM) (Figure 4.4a). CD200 TPM reads were significantly greater in SCC tumours compared to adenocarcinomas; however, it should be noted that these reads are from bulk RNA-seq from the tumour and TME rather than just the tumour tissue (Supplementary Figure S2; p= 0.0003).

The patients were subsequently split into three groups based on CD200 expression: low and high (lower and upper quartiles, n=125) and intermediate (middle two quartiles, n=252). Mean estimated relative immune compositions were then calculated for each group (Figure 4.4b) and the differences in immune composition between high and low CD200 expression patients analysed (Figure 4.4c). High CD200 expression in SCC tumours was associated with increases in the proportions of infiltrating M0 macrophages (p= <0.0001) and TFH cells (p= 0.001), and a decrease in the frequency of M2 macrophages (p= 0.0172) and MR CD4 T cells (p= 0.018).

A non-parametric Spearman correlation analysis was performed to determine the relationship between CD200 expression and the relative composition of each immune cell; r values are displayed vertically, with corresponding p values on the respective horizontal axis (Figure 4.4d). The significant differences between low and high CD200 expression groups were also significant in correlation analysis; M0 macrophages (r= 0.188, p=<0.0001) and TFH cells (r=0.195, p= <0.0001). In addition, Tregs (r= 0.207, p<0.001) and memory B cells (r= 0.151 p= 0.001) also demonstrated positive correlations with CD200 expression. M2 macrophages did not demonstrate a significant correlation with CD200 expression; however, MR CD4 T cells (r= -0.165, p= <0.0001) demonstrated a negative correlation. In addition, the frequency of neutrophils (r= -0.15, p= <0.0001), eosinophils (r = -0.11, p=0.012), resting mast cells (r= -0.135, p= 0.002), monocytes (r= -0.171, p= <0.0001), resting DCs (r= -0.165, p= <0.001), MA CD4 T cells (r= -0.154, p= <0.0001), CD8+ T cells (r = -0.097, p=0.026) and GDT cells (r= -0.126, p=0.004) also demonstrated negative correlations with CD200 expression. Of the 22 immune cells, Tregs and monocytes demonstrated the strongest positive and negative correlations with CD200 expression, respectively.

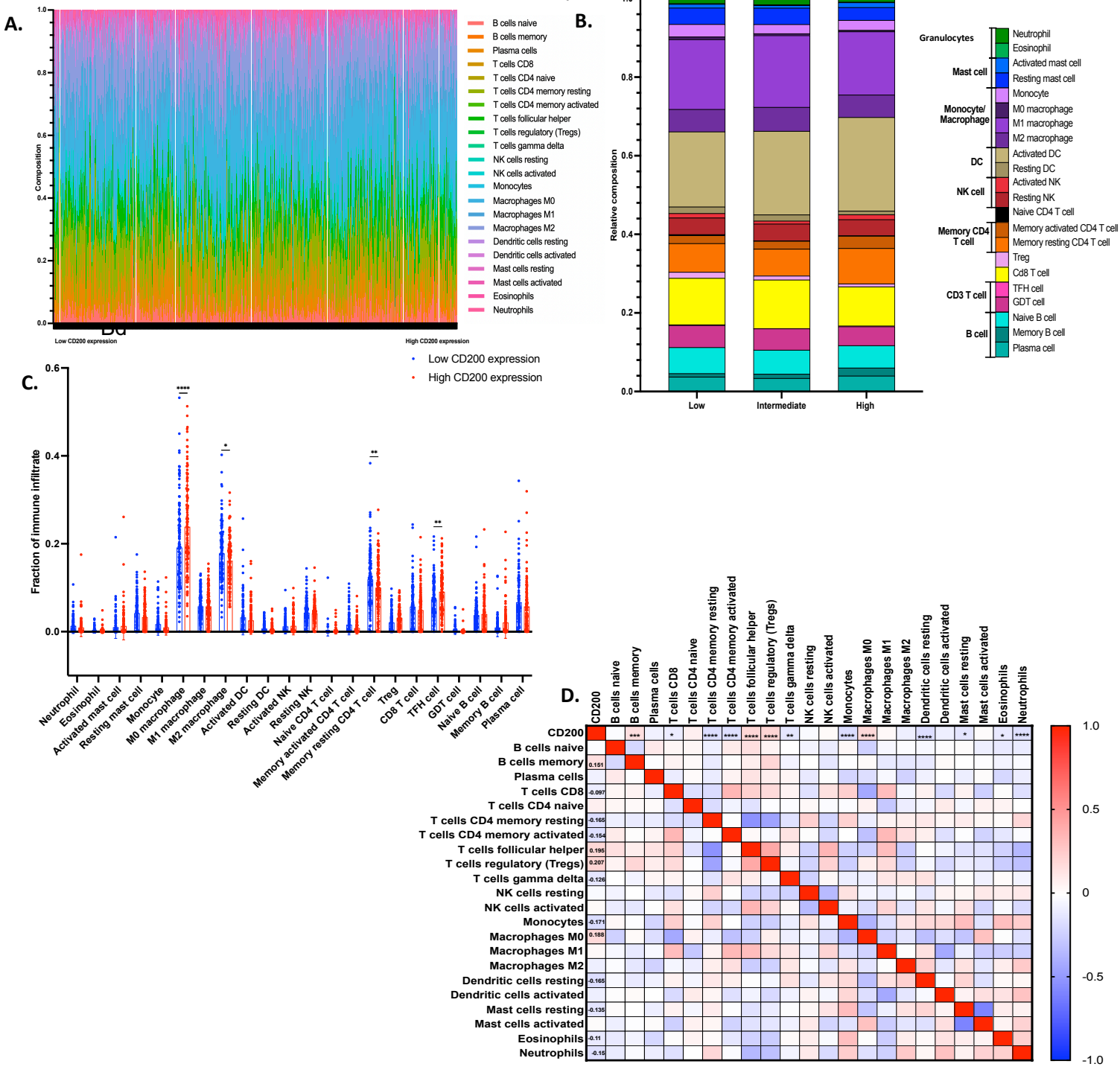

Figure 4.4 Estimated immune composition in SCC tumours and its relationship with CD200 expression.

RNA-seq data from 501 SCC patients was normalised and entered into the CIBERSORT algorithm to estimate the relative immune fractions of 22 immune cells. (A) Patients were stratified based on their normalised CD200 expression level (TPM) and the average immune cell infiltrate plotted from low to high CD200 expression. (B) Average immune cell proportions for low (lower quartile n= 125), intermediate (middle 2 quartiles n= 252) and high CD200 (upper quartile n= 125) expression groups. (C) Comparisons between the immune cell fractions between the upper and lower CD200 expression groups demonstrated significant differences in immune cell composition. Significance was tested for with the Kruskal-Wallis test with Dunn's multiple comparisons (D) Spearman correlation matrix of CD200 expression and immune cell proportions demonstrates significant relationships between CD200 expression and immune cell frequencies. P ≤ 0.05 (*) P ≤ 0.01 (**) P ≤ 0.001 (***) P ≤ 0.0001 (****). DC, dendritic cell; GDT, gamma delta T cell; Treg, regulatory T cell; NK, natural killer.

4.2.4 Estimating the immune composition of adenocarcinoma tumours based on CD200 expression

Having determined that there may be a relationship between CD200 expression and the relative composition of immune cells in SCC, the same analysis was performed on adenocarcinoma patients. RNA-seq data was analysed with CIBERSORT and patients stratified based on CD200 expression (Figure 4.5a) before being grouped into low (n= 129), intermediate (n= 259), and high (n= 129) groups based on the upper, lower, and intermediate two quartiles of normalised CD200 TPM (Figure 4.5b).

The differences in estimated relative infiltrating immune cells fractions were then compared between the high and low CD200 expression groups, where no significant differences were observed (Figure 4.5c). High CD200 expression was associated with an increase in the relative frequencies of neutrophils (p= 0.003), M0 macrophages (p= 0.0365), MA CD4 T cells (p= 0.0178) and memory B cells (p= 0.001). CD200 high adenocarcinoma tumours also saw a significant decrease in the relative frequencies of activated DCs (p= 0.005) and activated NK cells (p= 0.0048). Spearman correlation analysis demonstrated positive correlations between CD200 expression and the relative composition of neutrophils (r= 0.12, p= 0.009), M0 macrophages (r= 0.11, p= 0.0173), M1 macrophages (r= 0.1, p= 0.012), MA CD4 T cells (r= 0.13, p= 0.003) and memory B cells (r= 0.12, p= 0.002). Furthermore, the relative proportions of activated DCs (r= -0.16, p= 0.0004), monocytes (r= -0.09, p= 0.045), activated NK cells (r= -0.14, p= 0.0015) and TFH cells (r= -0.09, p= 0.048) were negatively associated with CD200 expression. Of the 22 immune cells analysed, activated DCs and activated NKs demonstrated the strongest correlations with CD200 expression.

A summary of the relationships between CD200 expression and immune cell infiltration in SCC and adenocarcinoma tumours can be found in Table 4.2.

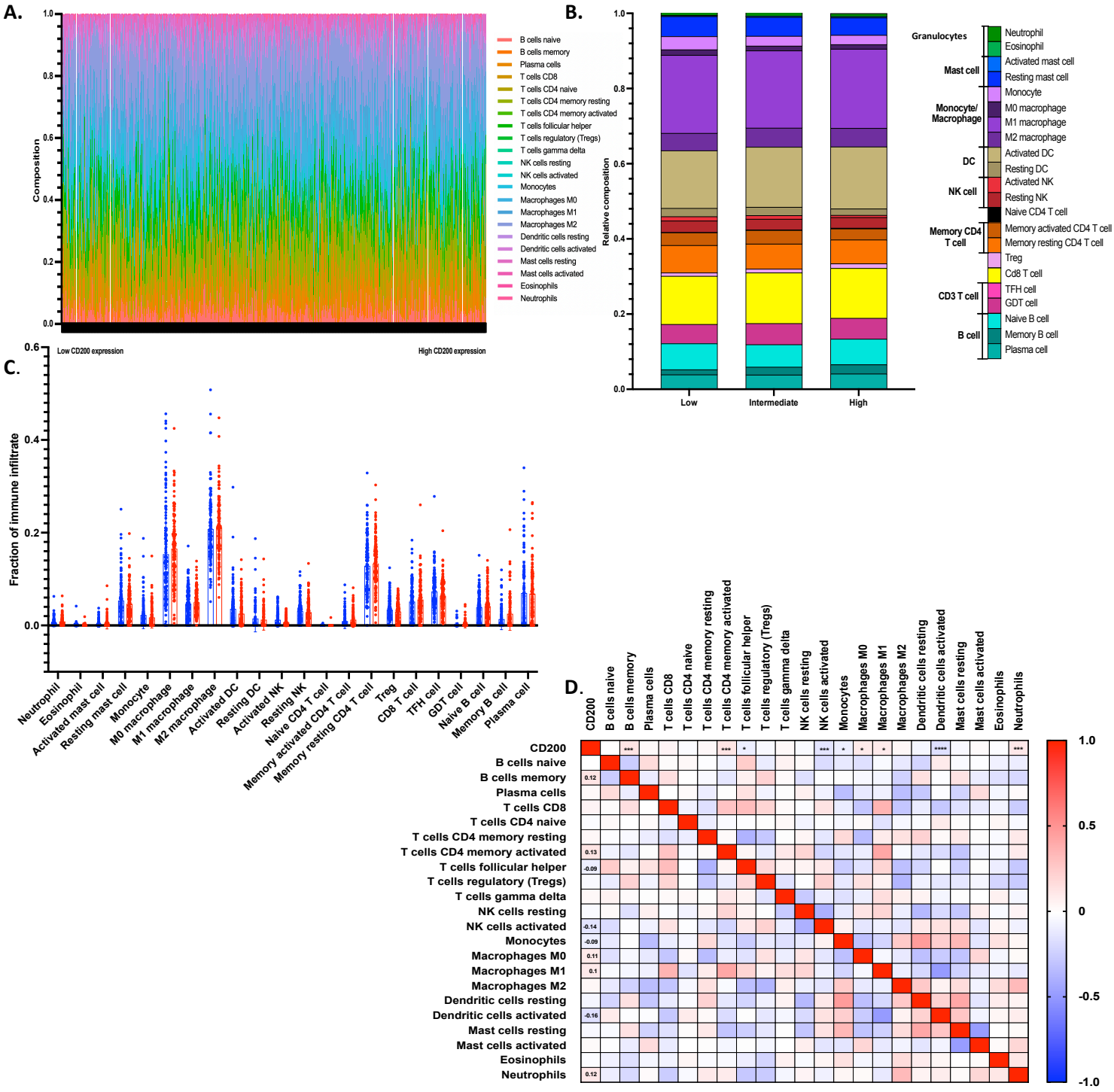

Figure 4.5 Estimated immune composition in adenocarcinoma tumours and its relationship with CD200 expression.

RNA-seq data from 518 adenocarcinoma patients was normalised and entered into the CIBERSORT algorithm to estimate the relative immune fractions of 22 immune cells. (A) Patients were stratified based on their normalised CD200 expression level (TPM) and the average immune cell infiltrate plotted from low to high CD200 expression. (B) Average immune cell proportions for low (lower quartile n=129), intermediate (middle 2 quartiles n=259) and high CD200 (upper quartile n=129) expression groups. (C) Comparisons between the immune cell fractions between the upper and lower CD200 expression groups demonstrated significant differences in immune cell composition. Significance was tested for with the Kruskal-Wallis test with Dunn's multiple comparisons. (D) Spearman correlation matrix of CD200 expression and immune cell proportions demonstrated significant relationships between CD200 expression and immune cell frequencies. P ≤ 0.05 (*) P ≤ 0.01 (**) P ≤ 0.001 (***) P ≤ 0.0001 (****). DC, dendritic cell; GDT, gamma delta T cell; Treg, regulatory T cell; NK, natural killer.

Table 4.2 Significant correlations between CD200 expression and the relative infiltration of immune cells as determined by CIBERSORT in SCC and adenocarcinoma tumours.

		SCC	**Adenocarcinoma**
Correlation with CD200 expression	Positive	M0 macrophages Tregs TFH cells Memory B cells	Neutrophils M1 macrophages M0 macrophages MA CD4 T cells Memory B cells
	Negative	Neutrophils Eosinophils Resting mast cells Resting DCs Monocytes GDT cells MA CD4 T cells MR CD4 T cells CD8 T cells	Activated DCs Monocytes Activated NK cells TFH cells

4.2.5 Characterising immune cell CD200R expression in the NSCLC TME

In order for CD200 expression to be having a direct effect on infiltrating immune cells in the NSCLC TME, these cells must express CD200R. Therefore, to determine the expression of CD200R on individual immune cell subtypes, single cell data was explored using the BBrowser software (https://bioturing.com/bbrowser). BBrowser is a desktop application that allows access and visualisation of published single cell sequencing data, allowing the user to query genes of interest, select cell populations for further sub-analyses and perform differential expression analysis between cell groups. For the purposes of this study, two datasets were chosen: single cell analysis of tumour, stromal and immune cells from 5 untreated non-metastatic NSCLC patients (Lambrechts *et al.* 2018) (Figure 4.6a) and a global characterisation of T cells within the tumours of 14 NSCLC patients (Guo *et al.* 2018) (Figure 4.6c). In the first dataset, all other tumour and stromal cell types were removed, and the immune cell clusters were analysed for CD200R expression using the gene query tool (Figure 4.6b). CD200R expression was detected in macrophages (109/8027 cells), Langerhans cells (68/714 cells), cross-presenting DCs (4/192 cells), CD4+ T cells (221/9602 cells), CD8+ T cells (536/12038 cells), Tregs (8/1509 cells), NK cells (2/1743 cells), mucosa-associated lymphoid tissue derived (MALT) B cells (5/607 cells), plasma cells (9/784 cells), follicular B cells (27/2674 cells) and mast cells (25/613 cells).

In the second dataset analysed, consisting of T cells within the NSCLC TME, CD200R expression could be demonstrated on all cell types (Figure 4.6d). CD4 T cells demonstrated CD200R expression on naïve cells (95/532 cells), a range of effector cells (granulysin (GNLY) 35/434 cells; granzyme A (GZMA) 217/668 cells; GZMK 152/674 cells, eomesodermin (EOMES) 40/161 cells; CD69 260/1084 cells), central memory cells (175/665 cells) and exhausted cells (120/342 cells). With changing CD4 phenotype, CD200R expression increased significantly from naïve to memory ($p= 0.005$), and memory to exhausted ($p= 0.0073$), with average CD200R expression 2.8 times greater in exhausted CD4 cells compared to naive cells ($p= <0.0001$). Likewise, CD200R expression also increased in memory and exhausted CD8 T cells compared to naïve cells. Naïve CD8 cells (57/303 cells), effector CD8 cells (102/1192 cells), regulatory-like CD28 CD8 cells (15/206 cells), mucosal associated invariant T cells (MAIT) SLC4A10 CD8 cells (10/105 cells), memory (181/832 cells) and exhausted CD8 cells (134/493 cells) all demonstrated CD200R expression, with CD200R expression significantly greater in exhausted CD8 T cells compared to naïve and memory cells (both $p= <0.0001$). Both suppressive (105/939 cells) and resting Tregs (55/427 cells) also demonstrated CD200R expression. Taken together, this demonstrates CD200R expression on almost all immune cells infiltrating the NSCLC TME.

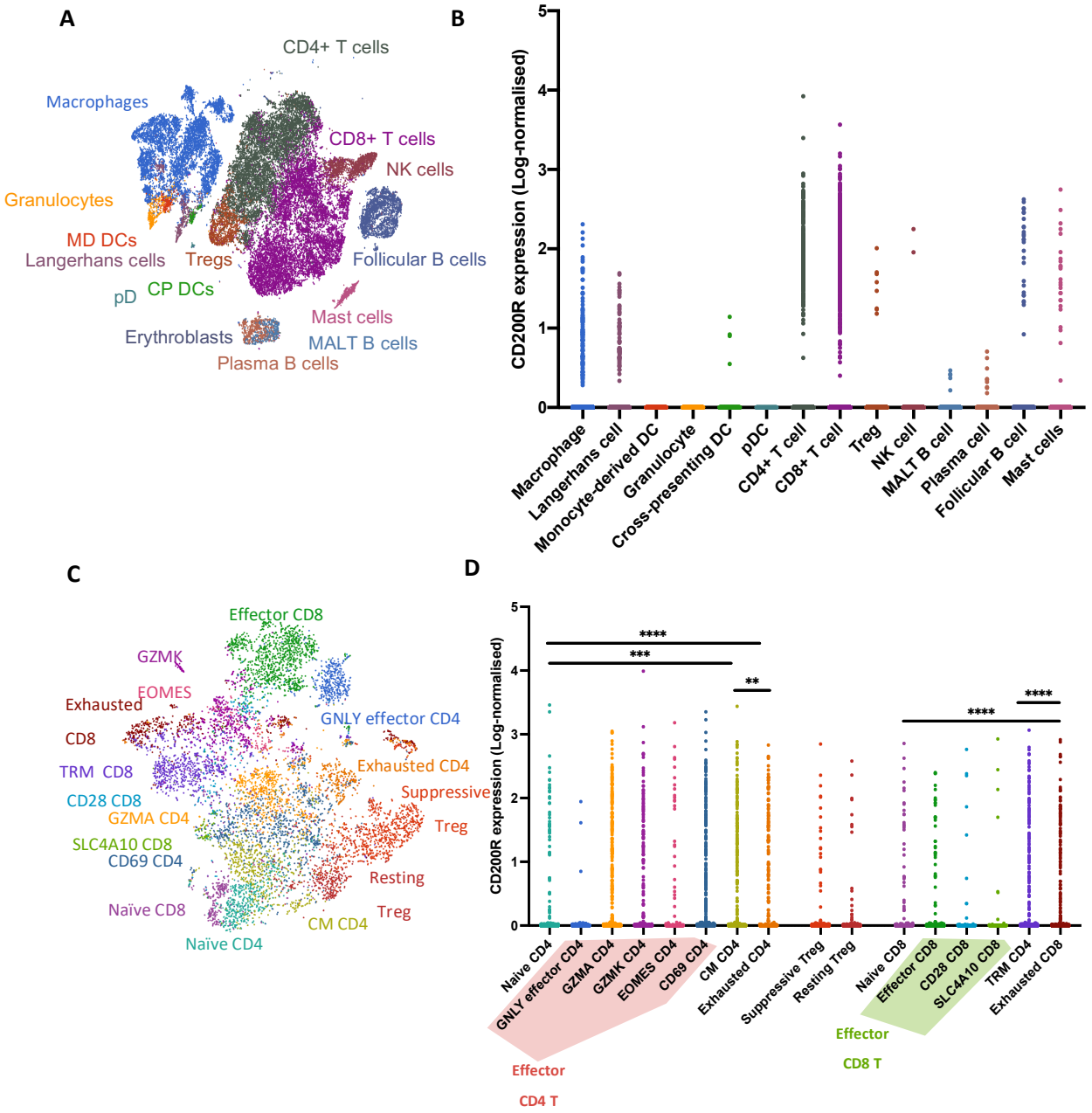

Figure 4.6 Analysis of 2 single-cell RNA-seq NSCLC tumour datasets for immune cell CD200R expression.

Single cell data of immune cells in the NSCLC TME was analysed for immune cell CD200R expression. (A) 38 505 immune cells from 5 NSLC tumours and their (B) log-normalised CD200R expression values. CD200R expression was seen on at least one cell in all but two cell types. (C) 8952 T cells from 14 NSCLC patients and their (D) log-normalised CD200R expression values. CD200R expression was seen on all T cell subsets raging from naïve, to multiple effector subtypes to memory and exhausted T cells. CD200R expression was also significantly increased from naïve to memory and exhausted subtypes. Significance was tested for using the Kruskal-Wallis test with Dunn's multiple comparisons. P ≤ 0.05 (*) P ≤ 0.01 (**) P ≤ 0.001 (***) P ≤ 0.0001 (****). CM, central memory; DC, dendritic cell; Eomes, eomesodermin; GNLY, granulysin; GZMA, granzyme A; GZMK, granzyme K; MALT, mucosa-associated lymphoid tissue derived; pDC, plasmacytoid DC; Treg, regulatory T cell; TRM, tissue-resident memory.

4.2.6 Characterising absolute immune cell infiltration in SCC and its associations with clinical parameters

Based on this bioinformatic analysis of the presence and prognostic significance of immune cells in NSCLC tumours, three immune cells were selected for further investigation in our 240 patient samples: Tregs, NK cells and CD8+ T cells. Tregs and NK cells possessed two of the strongest correlations with CD200 expression, with SCC tumours seeing a positive correlation between CD200 expression and Treg infiltration and adenocarcinomas seeing a reduction in infiltrating NK cell numbers with increasing CD200 expression. CD8 T cells were selected due to their known cytotoxic role in anti-tumour immune responses.

To determine the absolute frequency of these immune cells infiltrating the tumours, serial sections were stained for CD45 (all immune cells), CD8, Foxp3 (Treg) and CD56 (NK cells). The relative frequencies were then calculated as a percentage of CD45+ cells. Sections were also stained for CD200R to determine the frequency of CD200R+ cells within the TME. Each immune cell marker stain was first optimised in human tonsil tissue prior to tumour staining (Supplementary Figure S3). All five immune cell markers were successfully identified in SCC samples, with cells observed both in the stroma and within the tumour nests (Figure 4.7a). The frequency of positive cells within each section was automatically counted using the method described in section 2.2.5; briefly, annotations were generated around the tumour sections and the number of positive cells detected and presented as number of positive cells per mm^2. Within each sample, the number of CD45+ cells per mm^2 ranged from 292 – 4659 with a mean of 2237; CD200R+ cells an average of 497 (range 5 – 3736); CD8+ cells an average of 354 (range 17 - 2433); Foxp3+ cells an average of 191 (range 4 - 732) and CD56+ cells an average of 147 (range 5 - 1381) per mm^2. The absolute number of CD8+ cells per mm^2 was significantly greater than that of Foxp3+ and CD56+ cells ($p = <0.0001$) (Figure 4.7b).

Next, to analyse the relationship between absolute immune cell frequency and clinical parameters, patients were split into high and low infiltration groups based on the median absolute cell number and assessed for associations using ether the Chi squared or Fisher's exact test (Table 4.3). High numbers of infiltrating CD8+ cells were significantly associated ($p = 0.0368$) with lower tumour stage and trended towards lower disease stage ($p = 0.0717$) compared to those with low CD8+ cell numbers. High absolute numbers of CD200R+ cells also correlated with lower tumour stage ($p = 0.0092$). Moreover, high absolute Foxp3+ cells were significantly associated ($p = 0.0042$) with earlier disease stage. The absolute numbers of CD45+ and CD56+ cells did not show any significant associations with patient characteristics or disease stage.

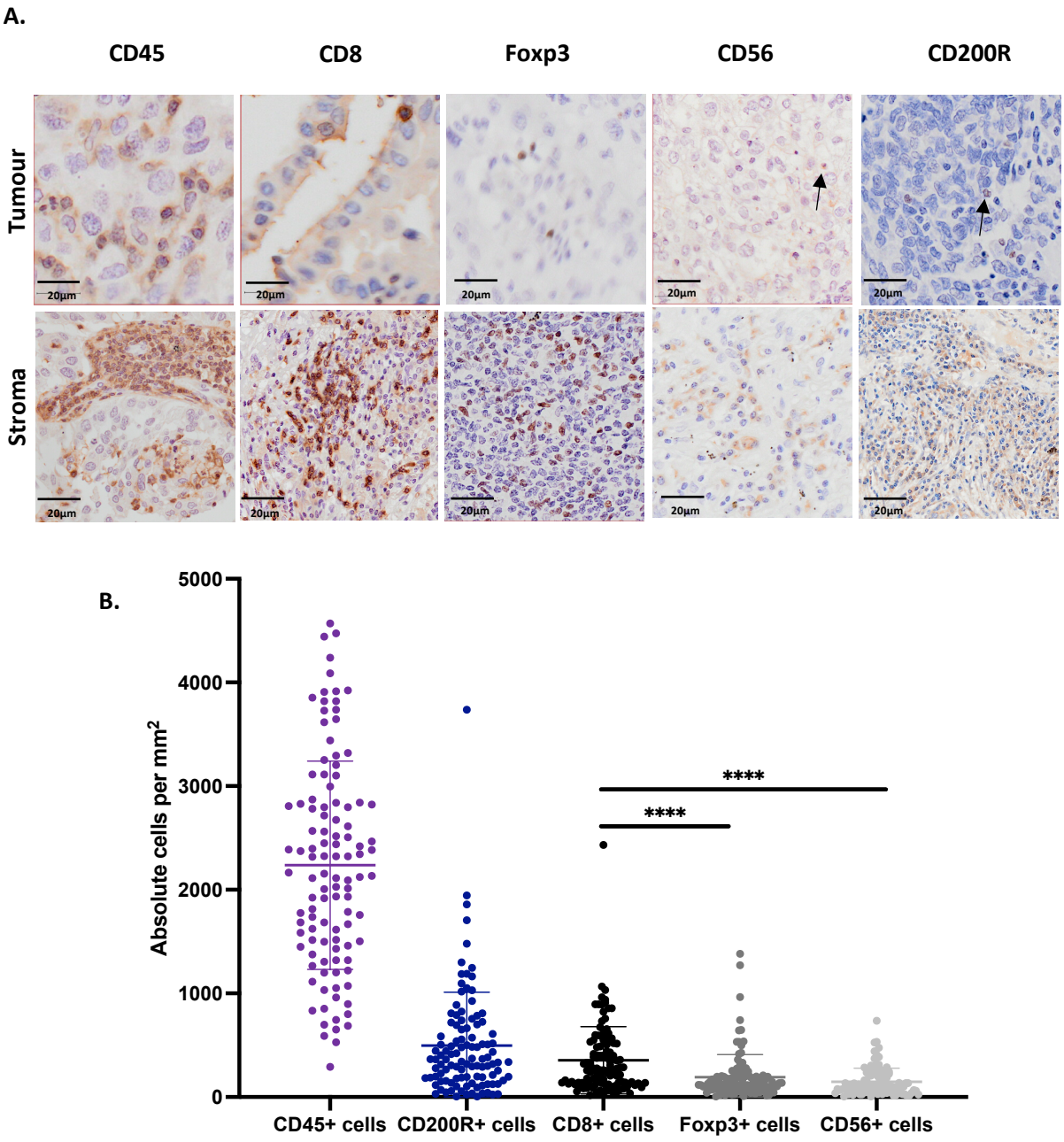

Figure 4.7 Absolute immune cell infiltrate in SCC patients by IHC.

Serial sections of 120 NSCLC tumour samples were stained for CD45 (all immune cells), CD200R, CD8 (CD8 T cells), Foxp3 (Tregs) and CD56 (NK cells) to determine the absolute number of positive cells per mm^2. (A) Representative images of positive staining for each cell in tumour and stromal areas of the samples. All immune cells were seen in both the tumour nests and within the stroma. Scale bars 20µm. (B) Absolute number of immune cells in the SCC tumour samples demonstrated significantly more CD8+ cells than Foxp3+ and CD56+ cells. Significance was tested for using the Kruskal-Wallis test with Dunn's multiple comparisons. $P \leq 0.05$ (*) $P \leq 0.01$ (**) $P \leq 0.001$ (***) $P \leq 0.0001$ (****).

Table 4.3 Characteristics of SCC patients according to high and low absolute immune cell infiltration. Patients were split at the median value into high and low infiltration groups and the differences in patient characteristics between groups analysed by Chi squared or Fischer's exact test.

		CD45+ cells		P value	Absolute CD8+ cells		P value	Absolute Foxp3+ cells		P value	Absolute CD56+ cells		P value	Absolute CD200R+ cells		P value
Characteristic		Low	High		Low	High		Low	High		Low	High		Low	High	
Sex	Female	24 (43.6)	25 (26.3)	0.1728	22 (36.7)	25 (42.4)	0.5764	20 (34.5)	25 (43.9)	0.3427	19 (37.3)	21 (42)	0.6858	20 (37)	24 (44.4)	0.557
	Male	25 (45.4)	29 (53.7)		38 (63.3)	34 (57.6)		38 (65.5)	32 (56.1)		32 (62.7)	29 (58)		34 (63)	20 (55.6)	
Age	Median	73	72	0.101	72	72	0.9212	72	70	0.9409	71	72	0.9513	72	72	0.9795
	Range	53 - 83	52 - 87		52 - 87	54 - 82		52 - 87	54 - 83		52 - 83	54 - 80		52 - 83	54 - 82	
Tumour stage	T1	9 (16.4)	10 (18.5)	0.8421	7 (11.7)	14 (23.7)	0.0368	8 (13.8)	12 (21)	0.2409	9 (17.6)	11 (22)	0.7989	5 (9.2)	14 (25.9)	0.0092
	T2	31 (56.4)	33 (61.1)		33 (55)	37 (62.7)		34 (58.6)	35 (61.4)		31 (60.8)	26 (52)		32 (59.3)	32 (59.3)	
	T3	13 923.6)	10 (18.5)		18 (30)	30 (10.2)		13 (22.4)	10 (17.6)		10 (19.6)	11 (22)		17 (31.5)	6 (11.1)	
	T4	2 (3.6)	2 (3.9)		2 (3.3)	2 (3.4)		3 (5.12)	0 (0)		1 (2)	2 (4)		0 (0)	2 (3.7)	
Node stage	N0	37 (67.3)	38 (70.4)	0.1233	39 (65)	43 (72.9)	0.7862	37 (63.8)	44 (77.2)	0.2603	33 (64.7)	40 (80)	0.3367	33 (61.1)	40 (74.1)	0.6346
	N1	10 (18.2)	12 (22.2)		13 (21.7)	11 (18.6)		14 (24.1)	9 (15.8)		12 (23.5)	7 (14)		11 (20.4)	9 (16.7)	
	N2	4 (7.3)	0 (0)		2 (3.3)	3 (5.1)		3 (5.2)	1 (1.8)		3 (5.9)	2 (4)		3 (5.6)	2 (3.7)	
Disease stage	Stage I	20 (36.4)	24 (44.4)	0.6319	18 (30)	28 (47.4)	0.0717	20 (34.5)	26 (45.6)	0.0042	21 (41.2)	22 (44)	0.9301	17 (31.5)	27 (50)	0.1343
	Stage II	29 (52.7)	26 (48.2)		37 (61.7)	24 (40.7)		28 (48.3)	31 (54.4)		25 (49)	24 (48)		30 (55.5)	23 (42.6)	
	Stage III	6 (10.9)	4 (7.4)		5 (8.3)	7 (11.9)		10 (17.2)	0 (0)		5 (9.8)	4 (8)		7 (13)	4 (7.4)	
Smoking status	Ever	45 (81.8)	48 (88.9)	0.999	48 (80)	52 (88.1)	0.4851	51 (87.9)	49 (86)	0.999	43 (84.3)	46 (92)	0.999	41 (75.9)	50 (92.6)	0.4565
	Never	0 (0)	1 (1.9)		1 (1.7)	0 (0)		1 (1.7)	0 (0)		0 90)	0 (0)		1 (1.9)	0 (0)	

4.2.6a Tumour CD200 expression and absolute immune cell infiltration in SCC

Having observed correlations between CD200 expression and relative immune infiltration through bioinformatic analysis, the relationship between tumour CD200 H score and absolute immune infiltrate was assessed (Figure 4.8). Tumour CD200 expression did not correlate with CD45+ cell (r= 0.1796, p= 0.0617), CD200R+ cell (r= 0.1023, p= 0.2867) or CD8+ cell (r= 0.0487, p= 0.6002) infiltration (Figure 4.8a-c). In agreement with the RNA-seq analysis, there was a significant positive correlation between the number of Foxp3+ cells per mm^2 and tumour CD200 expression (r =0.224, p=0.0164; Figure 4.8d). There was also a positive correlation between CD200 expression and CD56+ cell infiltration (r=0.2123, p=0.0282; Figure 4.8e). However, when patients were split into high and low CD200 expression groups based on the upper and lower quartiles of CD200 H score, there were no significant differences in the number of infiltrating immune cells (Figure 4.8f).

To further explore the relationship between infiltrating immune cells, spearman correlation was performed (Figure 4.8g). As expected, CD45+ infiltration positively correlated with the presence of CD8+ (r= 0.42, p= <0.0001), Foxp3+ (r= 0.39, p= <0.0001) and CD56+ cells (r= 0.21, p= 0.005). CD8+ cells were also significantly positively correlated with the number of infiltrating Foxp3+ cells (r=0.24, p=0.029) and CD56+ cells (r=0.29, p=0.009). CD200R+ cells did not correlate with CD200 expression or the presence of any other cell.

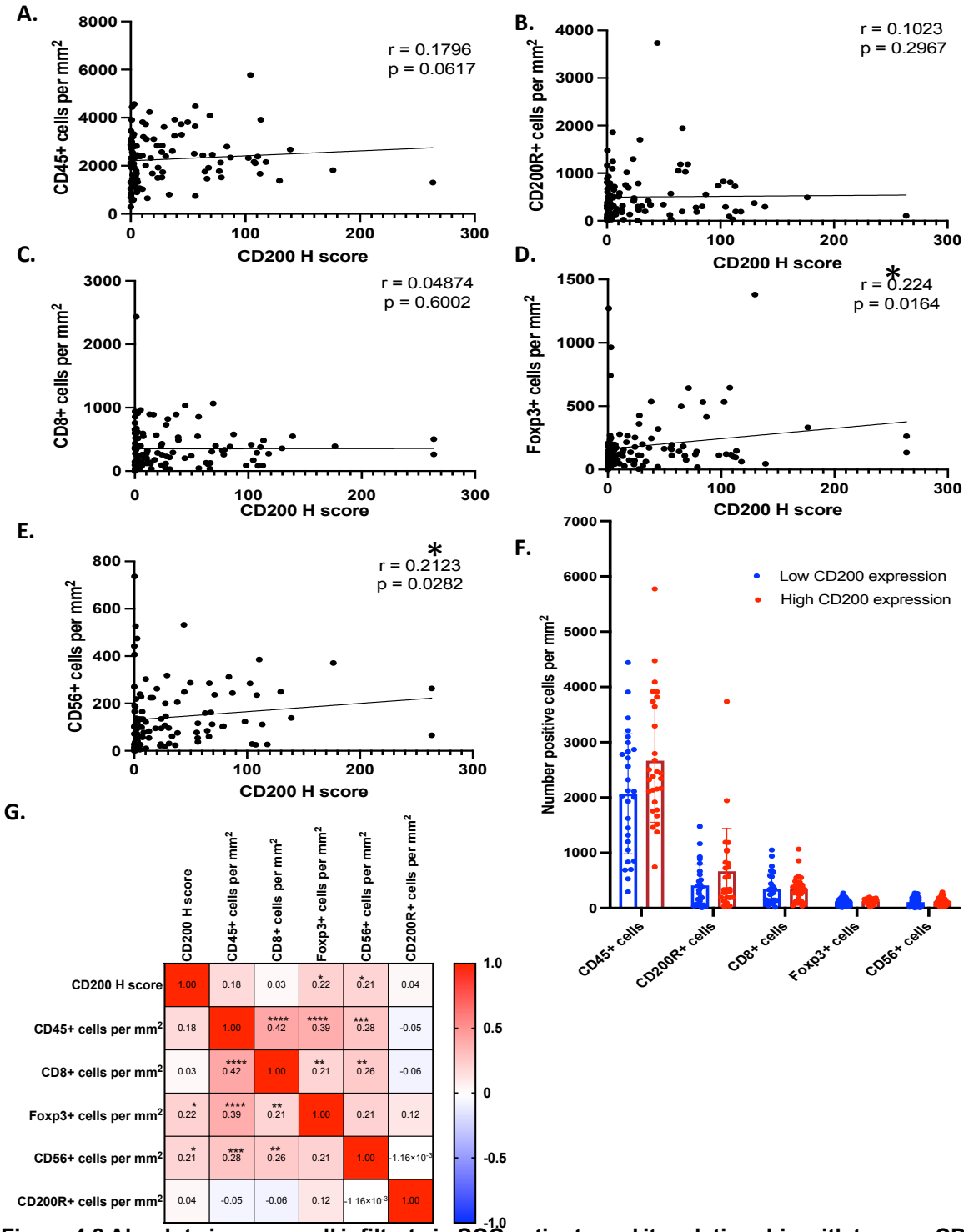

Figure 4.8 Absolute immune cell infiltrate in SCC patients and its relationship with tumour CD200 H score.

120 SCC tumour samples were stained for CD200 and tumour CD200 expression semi-quantified as a H-score. Subsequent serial sections of tumour samples were stained for CD45 (all immune cells), CD200R, CD8 (CD8 T cells), Foxp3 (Tregs) and CD56 (NK cells) to determine the absolute number of positive cells per mm^2. The relationship between tumour CD200 H score and absolute (A) CD45+ (B) CD200R+ (C) CD8+ (D) Foxp3+ and (E) CD56+ cells was analysed. CD200 demonstrated significant positive correlations with Foxp3+ and CD56+ cell numbers. (F) When patients were split into high and low CD200 expression groups by the median H score, there were no significant differences in immune cell numbers. (G) Spearman correlation matrix of CD200 expression and absolute immune cell numbers reveals further significant positive correlations between immune cells. P ≤ 0.05 (*) P ≤ 0.01 (**) P ≤ 0.001 (***) P ≤ 0.0001 (****).

4.2.7 Characterising relative immune cell infiltration in SCC and its associations with clinical parameters

In order to account for the differences in the levels of tumour immune cell infiltration, the next step was to determine the relative frequencies of CD200R+, CD8+, Foxp3+ and CD56+ cells in SCC tumours. Relative immune cell frequencies were calculated as a % of infiltrating CD45+ cells (Figure 4.9). CD200R+ cells constituted an average of 23.37% (range 0.197 – 79.85), CD8+ cells comprised an average of 15.1% (range 0.09 - 40.59), with Foxp3+ cells and CD56+ cells comprising an average of 5.99% (range 0.3188 - 20.25) and 5.09% (range 0.0003 - 15.1), respectively. Again, the relative number of CD8+ cells was significantly greater than that of Foxp3+ and CD56+ cells ($p = <0.0001$; Figure 4.9). Upon splitting the patient cohorts into low and high relative infiltration groups based on the median value, again, high relative CD200R+ cell infiltration correlated with lower tumour stage ($p = 0.0273$; Table 4.4).

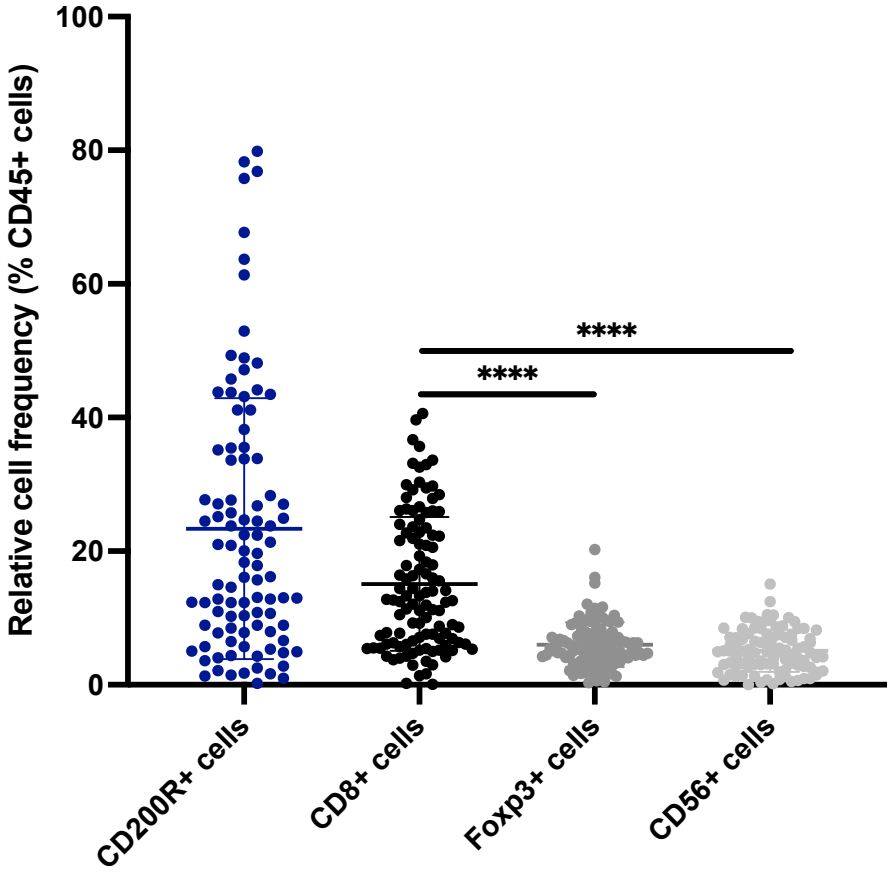

Figure 4.9 Relative immune cell infiltrate in SCC patients by IHC.

Serial sections of 120 NSCLC tumour samples were stained for CD45 (all immune cells), CD200R, CD8 (CD8 T cells), Foxp3 (Tregs) and CD56 (NK cells) and relative immune cell frequencies were determined as the % of CD45+ cells. SCC tumours demonstrated significantly greater proportions of CD8+ cells than Foxp3+ and CD56+ cells. Significance was tested for using the Kruskal-Wallis test with Dunn's multiple comparisons. $P \leq 0.0001$ (****).

Table 4.4 Characteristics of SCC patients according to high and low relative immune cell infiltration. Patients were split at the median value into high and low infiltration groups and the differences in patient characteristics between groups analysed by Chi squared or Fischer's exact test.

		CD45+ cells		P value	Relative CD8+ cells		P value	Relative Foxp3+ cells		P value	Relative CD56+ cells		P value	CD200R+ cells		P value
Characteristic		Low	High		Low	High		Low	High		Low	High		Low	High	
Sex	Female	24 (43.6)	25 (26.3)	0.1728	22 (40.7)	20 (37.7)	0.8446	20 (38.5)	22 (42.3)	0.8417	18 (39.1)	18 (38.3)	0.999	18 (36)	23 (56.9)	0.311
	Male	25 (45.4)	29 (53.7)		32 (59.3)	33 (62.3)		32 (61.5)	30 (57.7)		28 (60.9)	29 (61.7)		32 (64)	26 (53.1)	
Age	Median	73	72	0.101	72	71	0.1972	73	70	0.9606	72	72	0.957	74	72	0.9662
	Range	53 - 83	52 - 87		52 - 87	51 - 81		52 - 87	53 - 83		52 - 87	52 - 82		52 - 82	54 - 83	
Tumour stage	T1	9 (16.4)	10 (18.5)	0.8421	6 (11.1)	13 (24.5)	0.1647	9 (17.3)	10 (19.2)	0.9297	10 (21.7)	8 (17)	0.3222	4 (8)	13 (26.5)	0.0273
	T2	31 (56.4)	33 (61.1)		32 (29.2)	30 (56.6)		31 (59.6)	30 (57.7)		27 (58.7)	27 (53.2)		33 (66)	27 (55.1)	
	T3	13 923.6)	10 (18.5)		15 (27.8)	8 (15.1)		11 (21.2)	10 (19.2)		9 (19.6)	11 (23.4)		13 (26)	7 (14.3)	
	T4	2 (3.6)	2 (3.9)		1 (1.9)	2 (3.8)		1 (1.9)	2 (3.9)		0 (0)	3 (6.4)		0 (0)	2 (4.1)	
Node stage	N0	37 (67.3)	38 (70.4)	0.1233	36 (66.6)	37 (69.8)	0.6233	35 (67.3)	39 (75)	0.9738	31 (67.4)	35 (74.5)	0.7029	28 (56)	39 (79.6)	0.0601
	N1	10 (18.2)	12 (22.2)		10 (18.5)	12 (22.6)		10 (19.2)	10 (19.2)		11 (23.9)	8 (17)		15 (30)	6 (12.2)	
	N2	4 (7.3)	0 (0)		1 (1.9)	3 (5.7)		2 (3.8)	2 (3.8)		2 (4.3)	2 (4.3)		2 (4)	4 (4.1)	
Disease stage	Stage I	20 (36.4)	24 (44.4)	0.6319	18 (33.3)	25 (47.1)	0.1506	24 (46.1)	20 (38.5)	0.5008	21 (45.7)	19 (40.4)	0.7366	16 (32)	25 (51)	0.1377
	Stage II	29 (52.7)	26 (48.2)		32 (59.3)	21 (39.6)		25 (48.1)	26 (50)		22 (42.8)	23 (49)		28 (56)	21 (48.9)	
	Stage III	6 (10.9)	4 (7.4)		4 (7.4)	6 (11.3)		3 (5.8)	6 (11.5)		3 (6.5)	5 (10.6)		6 (12)	3 (6.1)	
Smoking status	Ever	45 (81.8)	48 (88.9)	0.999	42 (79.2)	49 (90.7)	0.4674	47 (90.4)	44 (83)	0.999	40 (85.1)	42 (91.3)	0.999	39 (78)	45 (91.8)	0.999
	Never	0 (0)	1 (1.9)		1 (1.9)	0 (0)		1 (1.9)	0 (0)		0 (0)	0 (0)		0 (0)	0 (0)	

4.2.7a Tumour CD200 expression and relative immune cell infiltration in SCC

After seeing correlations between CD200 expression and immune infiltrates in SCC by RNA-seq and IHC, the relationships between tumour CD200 expression and the relative frequencies of CD8+, Foxp3+, CD56+ and CD200R+ cells were assessed. In contrast with absolute immune cell numbers, tumour CD200 expression did not significantly correlate with the frequencies of any of the immune cells studied; CD8+ (r= -0.03488, p= 0.7213), Foxp3+ (r= -0.05808, p= 0.5505), CD56+ (0.06886, p=0.4801), CD200R+ (r= -0.0571, p= 0.5827) (Figure 4.10a-d). There were also no significant differences in the relative frequencies of any immune cell between high and low CD200 expression groups (Figure 4.10e). Correlation analysis between CD200 H score and relative frequencies of immune cells demonstrated a significant positive correlation between CD8+ cells and CD56+ cells (r= 0.33, p= 0.0003), similar to that seen with absolute infiltrates (Figure 4.10f). Thus demonstrating a positive relationship between cytotoxic cells within the TME. A summary of the relative immune compositions of each patient in order of CD200 expression highlights the high variability in immune composition between patients (Figure 4.11).

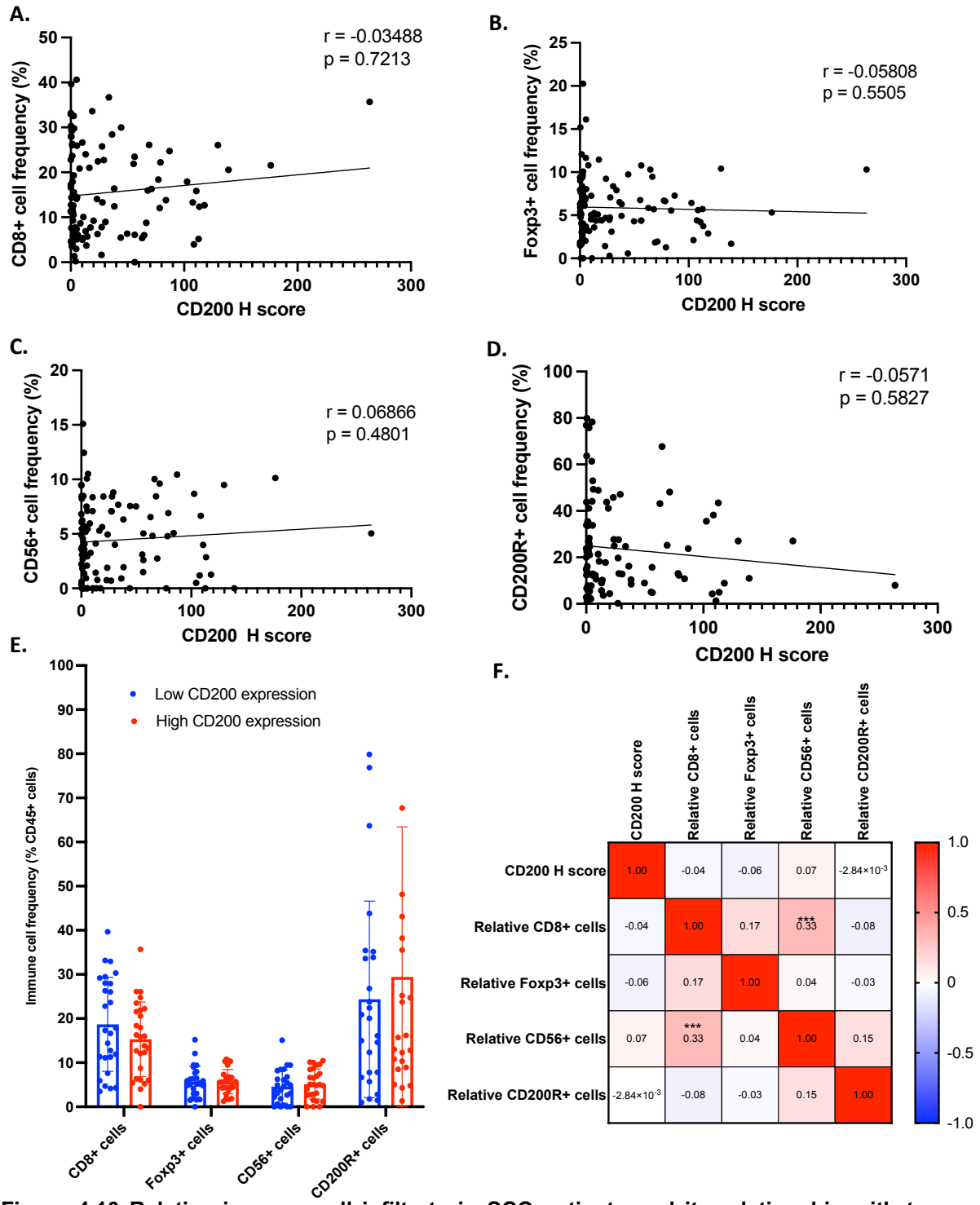

Figure 4.10 Relative immune cell infiltrate in SCC patients and its relationship with tumour CD200 H score.

120 SCC tumour samples were stained for CD200 and tumour CD200 expression semi-quantified as a H-score. Subsequent serial sections of tumour samples were stained for CD45 (all immune cells), CD200R, CD8 (CD8 T cells), Foxp3 (Tregs) and CD56 (NK cells) to determine the relative number of positive cells (% of CD45+ cells). The relationship between tumour CD200 H score and relative (A) CD8+ (B) Foxp3+ (C) CD56+ and (D) CD2000R+ cell proportions were analysed. There were no correlations between CD200 H score and relative immune cell frequencies. (E) When patients were split into high and low CD200 expression groups by the median H score, there also were no significant differences in immune cell numbers. (G) Spearman correlation matrix of CD200 expression and absolute immune cell numbers reveals further significant positive correlations between immune cells. P ≤ 0.05 (*) P ≤ 0.01 (**) P ≤ 0.001 (***) P ≤ 0.0001 (****).

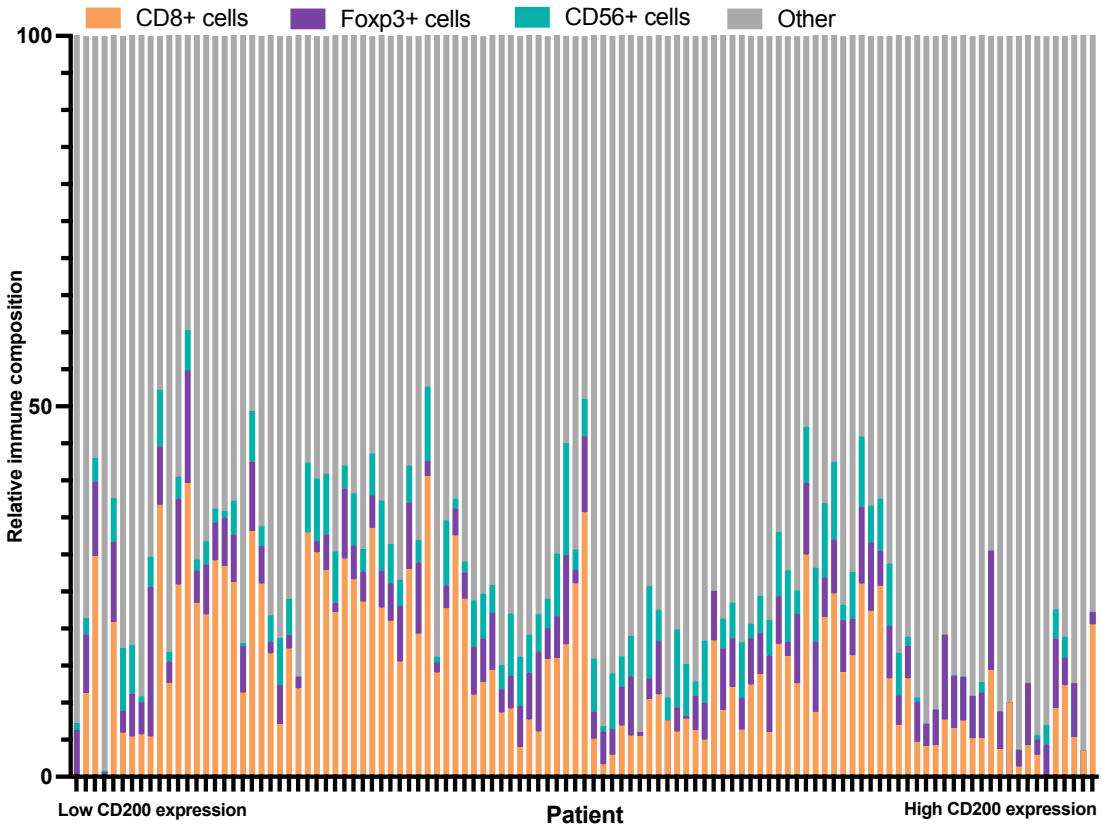

Figure 4.11 Relative frequencies (% of CD45+) cells of CD8+, Foxp3+, CD56+ and other CD45+ cells in SCC patients by IHC.

Serial sections of 120 SCC patient tumours were stained for CD45, CD8, CD56 and Foxp3 and the relative frequencies of each immune cell calculated (% of CD45+ cells). Sections were also stained for CD200, and patients were stratified from low to high CD200 expression based on the tumour CD200 H score.

4.2.8 Prognostic significance of immune infiltrate in SCC

A large number of studies have shown that there are significant correlations between the density and composition of immune cell infiltrate and patient survival in NSCLC. Therefore, to investigate whether the immune cell infiltrate in SCC could predict patient outcomes, patients were split into high and low infiltration groups based on the median value and differences in OS and hazard ratios generated using the log-rank test (Table 4.5; Figure 4.12). OS was measured from date of procedure to date of death. Patients whose death was not cancer-related were censored. OS ranged from 0.5 months – 126 months.

An increased level of immune infiltrate, as measured by the number of CD45+ cells within the tumour, was associated with better prognosis (hazard ratio (HR) 0.5176; 95% CI 0.3082-0.8618; p= 0.0118) (Table 4.5; Figure 4.12a). Furthermore, both high absolute number (HR 0.4987; 95% CI 0.3026-0.8219; p= 0.0065) and high relative frequency (HR 0.5463; 95% CI 0.3270-0.9127; p= 0.0178) of CD8+ cells were associated with better OS (Table 4.5; Figure 4.12b-c). Increased absolute number (HR 1.754; 95% CI 1.007-3.055; p= 0.0494), but not relative frequency of CD56+ cells was also associated with better OS (Figure 4.12d-e). Foxp3+ and CD200R+ cell infiltration were not associated with OS. (Figure 4.12f-i). Subsequent multivariate cox regression analysis of all significant prognostic factors identified by univariate analysis in Tables 3.4 and 4.5 identified both low node stage (HR 2.12; 95% CI 1.01-54.5; p=0.046) and tumour stage (HR 2.64; 95% CI 1.22-5.7; p=0.014) as independent prognostic factors in SCC patients (Figure 4.13).

Table 4.5 Univariate cox regression analysis of the associations between absolute and relative immune cell frequencies and patient overall survival in 120 SCC patients.

		Overall survival		
		Median survival (months)	Hazard ratio (95% CI of HR)	P value
CD45+ cells	LOW	67	0.5176 0.3082 – 0.8618	0.0118
	HIGH	Undefined		
Absolute CD8+ cells	LOW	58	0.4987 0.3026 – 0.8219	0.0065
	HIGH	Undefined		
Relative CD8+ cells	LOW	77	0.5463 0.3270 – 0.9127	0.0178
	HIGH	Undefined		
Absolute Foxp3+ cells	LOW	80	0.6281 0.3732 – 1.056	0.0791
	HIGH	Undefined		
Relative Foxp3+ cells	LOW	Undefined	1.479 0.8641 – 2.531	0.1469
	HIGH	67		
Absolute CD56+ cells	LOW	80	0.5701 0.3274 – 0.9928	0.0494
	HIGH	Undefined		
Relative CD56+ cells	LOW	85	0.6668 0.3786 – 1.175	0.1617
	HIGH	Undefined		
Absolute CD200R+ cells	LOW	80	0.7489 0.4439 – 1.266	0.2798
	HIGH	Undefined		
Relative CD200R+ cells	LOW	80	0.8172 0.4793 – 1.393	0.4569
	HIGH	106		

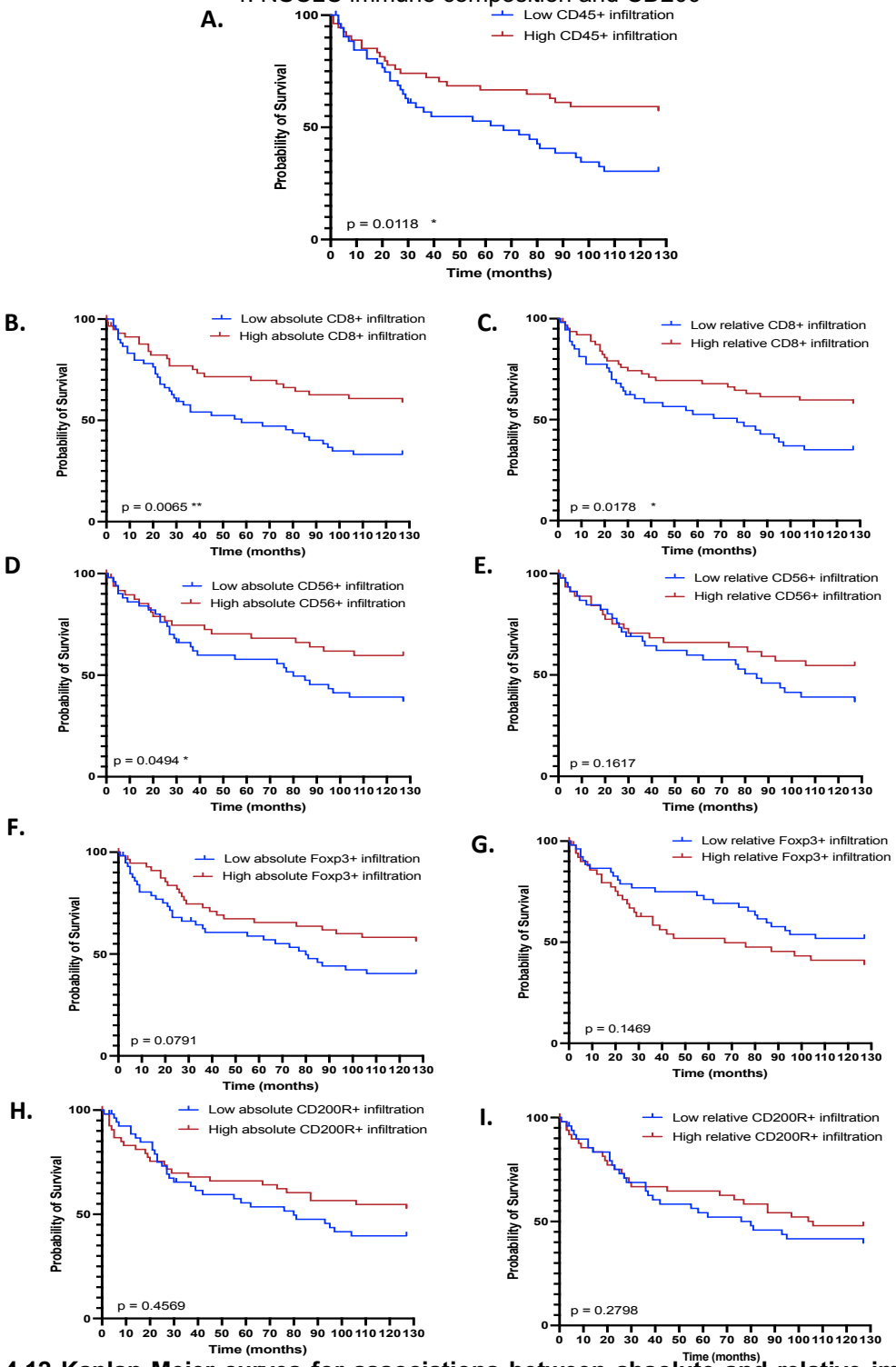

Figure 4.12 Kaplan Meier curves for associations between absolute and relative immune cell frequencies and overall survival in 120 SCC patients.

Serial sections of SCC tumours were stained for CD45, CD200R, CD8, Foxp3 and CD56 and the absolute and relative (% of CD45+ cells) number of cells analysed. Patients were then split into high and low groups based on the median value and associations with OS determined by univariate cox regression analysis. (A) High CD45 infiltration was a predictor for OS. High (B) absolute CD8+ cell and (C) relative CD8+ infiltration were also predictors of better OS. High (D) absolute CD56+ cell numbers were also a predictor for better OS but not (E) relative CD56+ cells. (F) Absolute Foxp3+ (G) relative Foxp3+ (H) absolute CD200R+ and (I) relative CD200R+ cell infiltration were not predictors of patient OS. OS was determined as the time from diagnosis to death; deaths unrelated to cancer were censored. OS, overall survival. Differences in survival calculated using log-rank test with $p \leq 0.05$ considered significant.

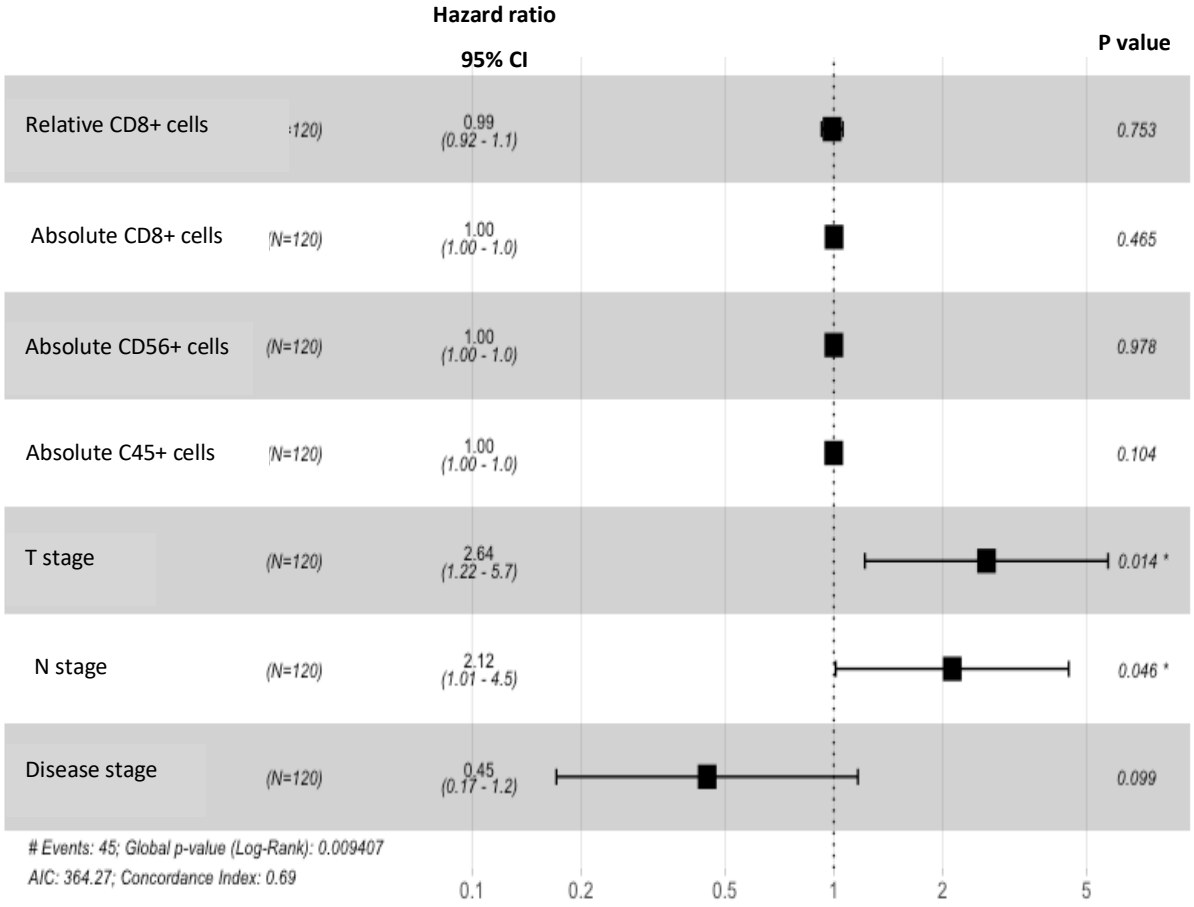

Figure 4.13 Multivariate Cox regression analysis of prognostic factors for overall survival in 120 SCC patients.

All prognostic factors identified by univariate Cox regression analysis in Table 3.4 and 4.2 with a $p \leq 0.05$ were analysed together by multivariate Cox regression analysis to identify any independent prognostic factors in SCC patients. Both T stage and N stage were identified as independent prognostic factors. OS was determined as the time from diagnosis to death; deaths unrelated to cancer were censored. CI, confidence interval; HR, hazard ratio; OS, overall survival. $P \leq 0.05$ (*) $P \leq 0.01$ (**) $P \leq 0.001$ (***) $P \leq 0.0001$ (****).

4.2.9 Characterising absolute immune cell infiltration in adenocarcinoma and its associations with clinical parameters

SCC and adenocarcinoma tumours demonstrated significant differences in their relative immune compositions based on RNA-seq analysis. Therefore, the absolute infiltration of CD45+, CD8+, Foxp3+ and CD56+ cells was analysed in serial sections of 120 adenocarcinoma samples as before. Sections were also stained for CD200R. All immune markers were successfully stained for in adenocarcinoma tumours and positivity was seen in both the stroma and within the tumour nests (Figure 4.14a). The average number of CD45+ cells infiltrating adenocarcinoma tumours was 1799 per mm^2 (range 297-4217), with an average of 193 CD200R+ cells per mm^2 (range 4 – 1022), 662 CD8+ cells per mm^2 (range 31-1718), 165 Foxp3+ cells (range 14.7-684.8) and 109 CD56+ cells per mm^2 (range 0.2-141) (Figure 4.14b). The absolute number of CD56+ cells was significantly less than that of CD8+ and Foxp3+ cells ($p = <0.0001$; Figure 4.14b). Analysis for associations between absolute immune cell number and clinical parameters established a significant relationship between high CD56+ cell number and earlier disease stage ($p = 0.0346$; Table 4.6).

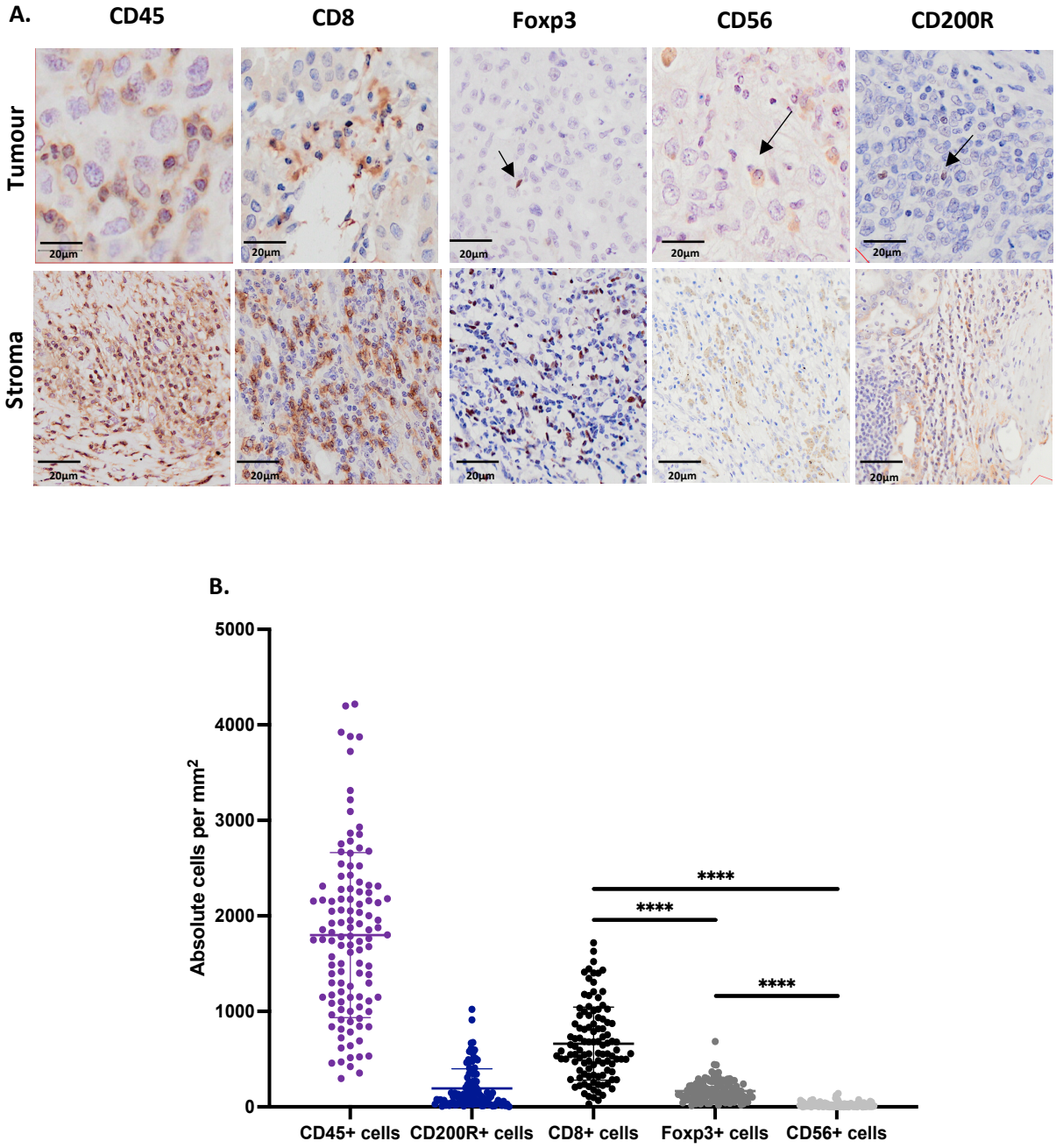

Figure 4.14 Absolute immune cell infiltrate in adenocarcinoma patients by IHC.

Serial sections of 120 NSCLC tumour samples were stained for CD45 (all immune cells), CD200R, CD8 (CD8 T cells), Foxp3 (Tregs) and CD56 (NK cells) to determine the absolute number of positive cells per mm^2. (A) Representative images of positive staining for each cell in tumour and stromal areas of the samples. All immune cells were seen in both the tumour nests and within the stroma. Scale bars 20µm. (B) Absolute number of immune cells in the adenocarcinoma tumour samples demonstrated significantly more CD8+ cells and Foxp3+ cells than CD56+ cells, with CD8+ cell number also significantly greater than Foxp3+ cells. Significance was tested for using the Kruskal-Wallis test with Dunn's multiple comparisons. $P \leq 0.0001$ (****).

Table 4.6 Characteristics of adenocarcinoma patients according to high and low absolute immune cell infiltration. Patients were split at the median value into high and low infiltration groups and the differences in patient characteristics between groups analysed by Chi squared or Fischer's exact test.

		CD45+ cells		P value	Absolute CD8+ cells		P value	Absolute Foxp3+ cells		P value	Absolute CD56+ cells		P value	Absolute CD200R+ cells		P value
Characteristic		Low	High		Low	High		Low	High		Low	High		Low	High	
Sex	Female	34 (59.6)	36 (62.1)	0.8496	26 (48.1)	35 (64.8)	0.1201	30 (51.7)	39 (68.4)	0.0871	34 (61.8)	30 (55.6)	0.5622	28 (54.9)	34 (66.7)	0.3106
	Male	23 (40.4)	22 (37.9)		28 (51.9)	19 (35.2)		28 (28.3)	18 (31.6)		21 (38.2)	24 (44.4)		23 (45.1)	17 (33.3)	
Age	Median	68	70	0.9732	69	71	0.6457	68	71	0.9869	69	70	0.9571	68	68	0.8992
	Range	45 - 91	47 - 90		45 - 90	51 - 81		45 - 90	47 - 91		48 - 91	45 - 90		45 – 91	48 - 86	
Tumour stage	T1	24 (42.1)	25 (43.1)	0.5388	21 (38.9)	20 (37)	0.9788	24 (41.4)	23 (40.3)	0.4512	19 (34.5)	24 (44.4)	0.4951	25 (49)	20 (39.2)	0.4077
	T2	25 (48.9)	24 (41.4)		25 (46.3)	27 (50)		23 (39.6)	28 (49.1)		26 (47.3)	25 (46.3)		17 (33.3)	25 (49)	
	T3	7 (12.3)	5 (8.6)		6 (11.1)	5 (9.3)		7 (12.1)	5 (8.8)		7 (12.7)	3 (5.6)		7 (13.8)	4 (7.9)	
	T4	1 (1.7)	4 (6.9)		2 (3.7)	2 (3.7)		4 (6.9)	1 (1.8)		3 (5.5)	2 (3.7)		2 (3.9)	2 (3.9)	
Node stage	N0	25 (43.9)	32 (55.2)	0.2570	25 (46.3)	27 (50)	0.8228	26 (44.8)	31 (54.4)	0.2213	23 (41.8)	27 (50)	0.2196	25 (49)	21 (41.2)	0.0899
	N1	17 (29.8)	10 (17.2)		14 (25.9)	12 (22.2)		17 (29.3)	10 (17.5)		13 (23.6)	15 (27.8)		16 (31.4)	11 (21.6)	
	N2	10 (17.5)	9 (15.5)		11 (20.4)	9 (16.7)		8 (13.8)	12 (21.1)		12 (23.6)	6 (11.1)		5 (9.8)	13 (25.5)	
Disease stage	Stage I	21 (36.8)	25 (43.1)	0.6792	19 (35.2)	22 (40.7)	0.7673	18 (31)	28 (49.1)	0.0718	17 (30.9)	24 (44.5)	0.0346	24 (47)	14 (27.5)	0.1204
	Stage II	22 (28.6)	18 (31)		19 (35.2)	19 (35.2)		25 (43.1)	14 (24.6)		18 (32.70	22 (40.7)		16 (31.4)	21 (41.2)	
	Stage III	14 (24.6)	15 (25.9)		16 (29.6)	13 (24.1)		15 (25.9)	15 (26.3)		20 (36.4)	8 (14.8)		11 (21.6)	16 (31.4)	
Smoking status	Ever	41 (70.7)	46 (82.1)	0.1991	42 (77.8)	37 (68.5)	0.4685	44 (75.9)	40 (70.2)	0.5487	38 (69.1)	42 (77.8)	0.5175	35 (68.6)	40 (78.4)	0.7304
	Never	8 (13.8)	3 (5.4)		3 (5.5)	6 (11.1)		5 (8.6)	7 (12.3)		6 (10.9)	4 (7.4)		5 (9.8)	4 (7.8)	

4.2.9a Tumour CD200 expression and absolute immune cell infiltration in adenocarcinoma

Having demonstrated significant relationships between CD200 expression and the relative infiltration of immune cells in adenocarcinoma by RNA-seq analysis, the relationship between CD200 tumour H score and absolute number of infiltrating immune cells was first analysed. CD200 expression did not correlate with CD45+ (r= -0.1675, p=0.0775), CD8+ (r=-0.07024, p= 0.4743), Foxp3+ (r= 0.09237, p= 0.3305) or CD200R+ (r= -0.03869, p= 0.6994) cell infiltration (Figure 4.15a-d). In line with the bioinformatics analysis, a significant negative correlation was observed between CD200 expression and CD56+ cell infiltration (r=-0.2995, p=0.0017), suggesting that tumours with greater CD200 expression may have fewer infiltrating NK cells (Figure 4.15d). When patients were split based on the upper and lower quartiles of CD200 H score, there were significantly fewer CD56+ cells in the CD200 high group (mean 141.8 cells per mm^2) compared to the low (195.7; p=0.032) (Figure 4.15f). The relationship between infiltrating immune cells was further explored using spearman correlation analysis (Figure 4.15g). As expected, CD45+ infiltration positively correlated with the presence of CD8+ (r= 0.55, p= <0.0001), Foxp3+ (r= 0.49, p= <0.0001) and CD56+ (r= 0.26, p=0.007) cells. Like with SCC tumours, there was also a strong significant correlation between the absolute number of infiltrating CD8+ and Foxp3+ cells (r= 0.51, p= <0.0001). CD200R infiltration showed no correlation with the presence of any immune cell.

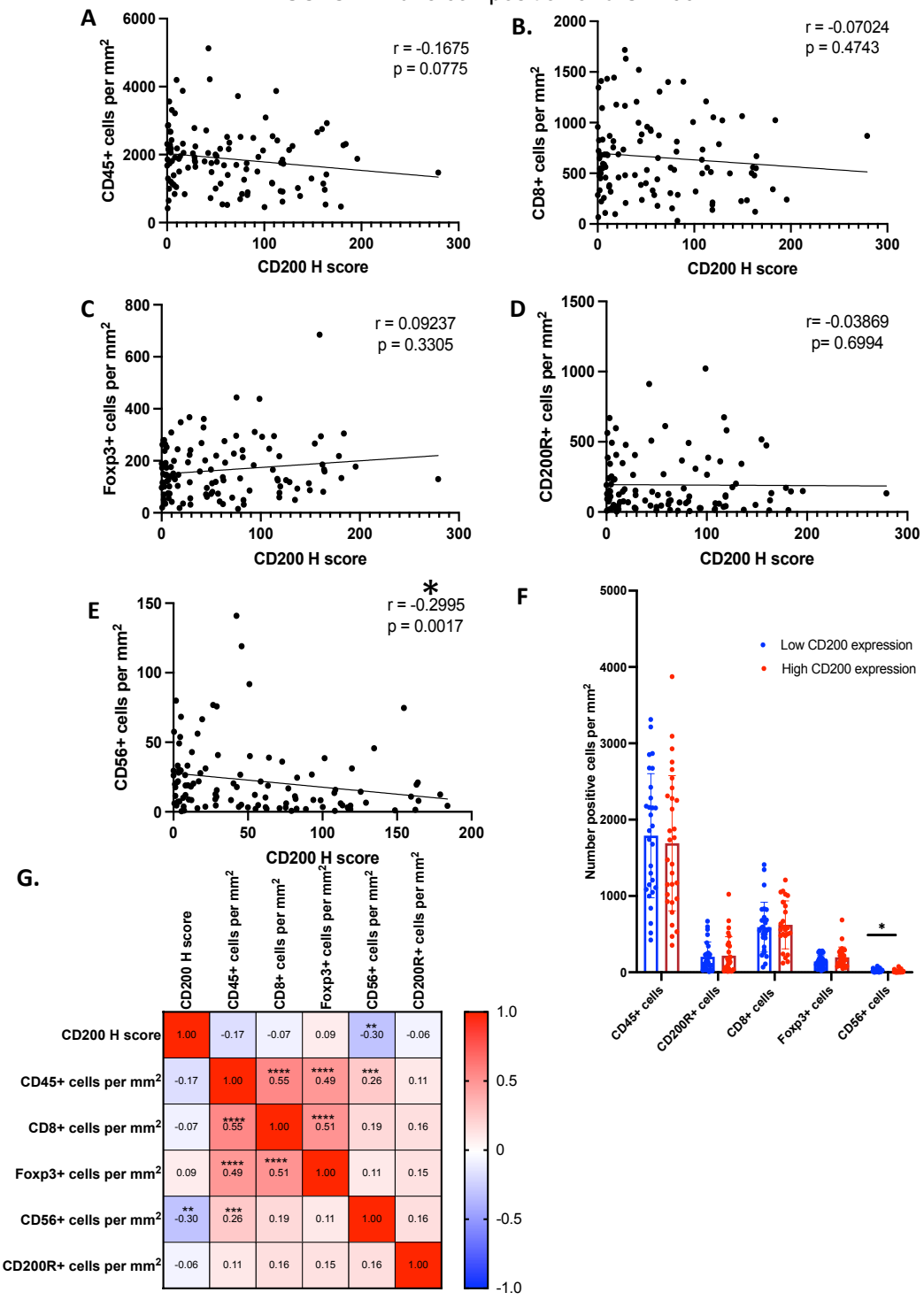

Figure 4.15 Absolute immune cell infiltrate in adenocarcinoma patients and its relationship with tumour CD200 H score.

120 adenocarcinoma tumour samples were stained for CD200 and tumour CD200 expression semi-quantified as a H-score. Subsequent serial sections of tumour samples were stained for CD45 (all immune cells), CD200R, CD8 (CD8 T cells), Foxp3 (Tregs) and CD56 (NK cells) to determine the absolute number of positive cells per mm^2. The relationship between tumour CD200 H score and absolute (A) CD45+ (B) CD8+ (C) Foxp3+ (D) CD200R+ and (E) CD56+ cells was analysed. CD200 demonstrated a significant positive correlation with CD56+ cell numbers. (F) When patients were split into high and low CD200 expression groups by the median H score, there was a significant difference in absolute CD56+ cells. Significance was tested for using the Kruskal-Wallis test with Dunn's multiple comparisons. (G) Spearman correlation matrix of CD200 expression and absolute immune cell numbers reveals further significant positive correlations between immune cells. P ≤ 0.05 (*) P ≤ 0.01 (**) P ≤ 0.001 (***) P ≤ 0.0001 (****).

4.2.9b Differences in absolute immune infiltration between SCC and adenocarcinoma

Adenocarcinoma tumours demonstrated significantly fewer CD45+ (p=0.004), CD200R+ (p= <0.0001) and CD56+ (p= <0.001) cells per mm^2 than SCC tumours but contained significantly greater numbers of CD8+ cells (p= <0.0001; Figure 4.16). When it came to CD200 expression, CD200 expression negatively correlated with CD56+ cell infiltration in adenocarcinomas; this contrasts with SCC tumours, in which both Foxp3+ and CD56+ cells demonstrated a significant positive correlation with CD200 expression. Furthermore, when analysing the relationship between immune cell infiltration and patient characteristics, CD56+ cells in adenocarcinomas and CD8+ and CD200R+ cells in SCC tumours were associated with earlier tumour stage. In SCC tumours, Foxp3+ cells were also associated with earlier disease stage. The relationships between immune cell numbers were similar between SCC and adenocarcinoma, with CD45+ cells positively correlated with the presence of CD8+, Foxp3+ and CD56+ cells; in SCC tumours CD8+ cells were also positively associated with CD56+ cells, whilst in adenocarcinomas, CD8+ cells correlated with Foxp3+ infiltration. Taken together, this highlights the differences between immune infiltration in NSCLC and demonstrates that the immune cell response is subtype dependent. Furthermore, the reciprocal relationships between CD200 expression and CD56+ cell infiltration is interesting and may suggest that the possible effects CD200 expression has on the immune infiltrate may again be subtype dependent.

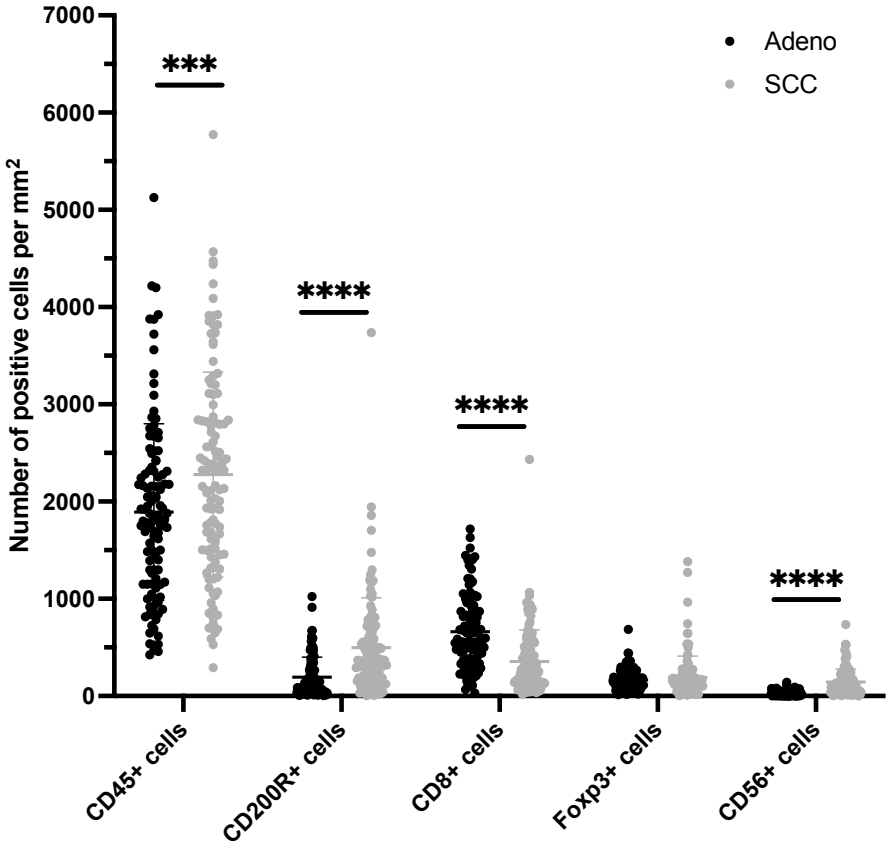

Figure 4.16 Differences in absolute immune cell numbers in adenocarcinoma and SCC tumours by IHC.

Serial sections of 120 adenocarcinoma and 120 SCC tumours were stained for CD45 (all immune cells), CD200R, CD8 (CD8 T cells), Foxp3 (Tregs) and CD56 (NK cells) to determine the absolute number of positive cells per mm^2. SCC tumours demonstrated significantly greater numbers of CD45+, CD200R+ and CD56+ cells and significantly fewer CD8+ cells than adenocarcinoma tumours. Significance was tested for using the Kruskal-Wallis test with Dunn's multiple comparisons. $P \leq 0.001$ (***) $P \leq 0.0001$ (****).

4.2.10 Characterising relative immune cell infiltration in adenocarcinoma and its associations with clinical parameters

Having observed differences in absolute immune infiltration between SCC and adenocarcinoma tumours and demonstrated relationships between CD200 expression and absolute immune infiltrate in adenocarcinoma, the relative immune cell frequency was analysed. Again, immune cell frequency was determined as the percentage of CD45+ cells (Figure 4.17). CD200R+ cells comprised an average of 14.32% (range 0.17 – 90.62) of the immune infiltrate, with CD8+ cells comprising 36% (range 3.8 - 80), Foxp3+ cells comprising 9.56% (range 1.744 - 46.5) and CD56+ cells an average of 1.4% (range 0.01 - 8). Again, CD8+ cells constituted significantly more of the immune infiltrate than Foxp3+ and CD56+ cells ($p= <0.0001$), with Foxp3+ immune proportions also significantly greater than that of CD56+ cells ($p= <0.0001$). Similar to absolute immune cell infiltration, CD56+ cells were the only cell to demonstrate any significant association with patient characteristics or disease parameters (Table 4.7). High relative numbers of CD56+ cells were significantly associated with lower node stage ($p= 0.0285$), suggesting that tumours with high CD56+ cell infiltration may be less likely to metastasise.

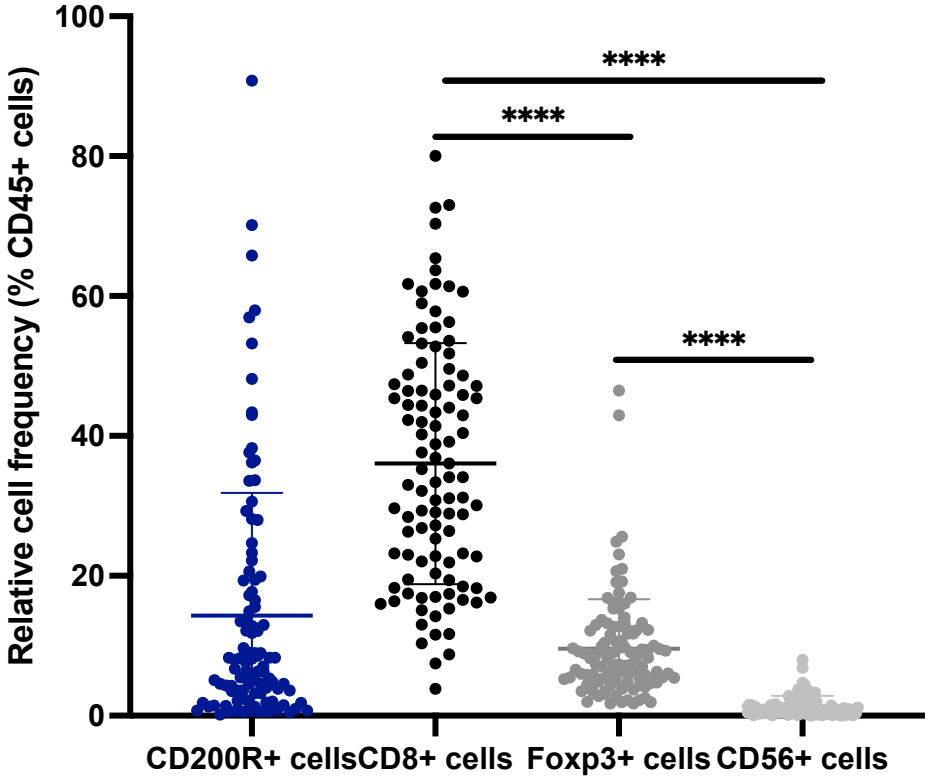

Figure 4.167Relative immune cell infiltrate in adenocarcinoma patients by IHC.

Serial sections of 120 NSCLC tumour samples were stained for CD45 (all immune cells), CD200R, CD8 (CD8 T cells), Foxp3 (Tregs) and CD56 (NK cells) and relative immune cell frequencies were determined as the % of CD45+ cells. Adenocarcinoma tumour samples demonstrated significantly greater proportions of CD8+ cells and Foxp3+ cells than CD56+ cells, with CD8+ cell fractions also significantly greater than Foxp3+ cells. Significance was tested for using the Kruskal-Wallis test with Dunn's multiple comparisons. $P \leq 0.0001$ (****).

Table 4.7 Characteristics of adenocarcinoma patients according to high and low relative immune cell infiltration. Patients were split at the median value into high and low infiltration groups and the differences in patient characteristics between groups analysed by Chi squared or Fischer's exact test.

		CD45+ cells		P value	Relative CD8+ cells		P value	Relative Foxp3+ cells		P value	Relative CD56+ cells		P value	CD200R+ cells		P value
Characteristic		Low	High		Low	High		Low	High		Low	High		Low	High	
Sex	Female	34 (59.6)	36 (62.1)	0.8496	29 (59.2)	30 (62.5)	0.8359	33 (60)	36 (65.5)	0.6936	30 (60)	32 (64)	0.8369	29 (59.2)	31 (63.3)	0.8359
	Male	23 (40.4)	22 (37.9)		20 (40.8)	18 (37.5)		22 (40)	19 (34.5)		20 (40)	18 (36)		20 (40.8)	18 (36.7)	
Age	Median	68	70	0.9732	66	73	0.7753	69	69	0.9548	72	66	0.8243	68	69	0.8857
	Range	45 - 91	47 - 90		49 - 85	45 - 90		48 - 90	45 - 91		48 - 87	45 - 91		45 - 91	48 - 86	
Tumour stage	T1	24 (42.1)	25 (43.1)	0.5388	22 (44.9)	16 (33.3)	0.4508	19 (34.5)	25 (45.5)	0.2737	17 (34)	22 (44)	0.0567	24 (49)	19 (38.8)	0.4274
	T2	25 (48.9)	24 (41.4)		21 (42.9)	23 (47.9)		29 (52.7)	21 (38.2)		27 (54)	18 (36)		17 (32.70	24 (50)	
	T3	7 (12.3)	5 (8.6)		3 (6.1)	7 (14.6)		3 (5.4)	7 (12.7)		6 (12)	5 (10)		5 (10.2)	5 (10.2)	
	T4	1 (1.7)	4 (6.9)		3 (6.1)	3 (6.2)		3 (5.4)	2 (3.6)		0 (0)	5 (10)		3 (6.1)	1 (2)	
Node stage	N0	25 (43.9)	32 (55.2)	0.2570	21 (42.9)	26 (54.2)	0.6084	23 (41.8)	30 (54.5)	0.4602	19 (38)	29 (58)	0.0258	24 (50)	20 (40.8)	0.5062
	N1	17 (29.8)	10 (17.2)		14 (28.6)	11 (22.9)		15 (27.3)	11 (20)		17 (34)	8 (16)		14 (28.6)	12 (24.5)	
	N2	10 (17.5)	9 (15.5)		6 (12.2)	8 (16.7)		10 (18.2)	9 (16.4)		11 (22)	5 (10)		7 (14.3)	11 (22.4)	
Disease stage	Stage I	21 (36.8)	25 (43.1)	0.6792	20 (40.8)	17 (35.4)	0.6033	18 (32.7)	25 (45.5)	0.3822	16 (32)	23 (46)	0.3061	22 (45.9)	13 (26.5)	0.1052
	Stage II	22 (28.6)	18 (31)		19 (38.8)	17 (35.4)		22 (40)	17 (30.9)		19 (38)	17 (34)		14 (28.6)	23 (47)	
	Stage III	14 (24.6)	15 (25.9)		10 (20.4)	14 (29.2)		15 (27.3)	13 (23.6)		15 (30)	10 (20)		13 (26.5)	13 (26.5)	
Smoking status	Ever	41 (70.7)	46 (82.1)	0.1991	36 (75)	33 (68.8)	0.155	42 (73.7)	38 (69.1)	0.999	39 (79.6)	31 (62)	0.3322	33 (67.3)	39 (79.6)	0.301
	Never	8 (13.8)	3 (5.4)		2 (4.2)	7 (14.6)		6 (10.5)	5 (9.1)		4 (8.2)	7 (14)		6 (12.2)	3 (6.1)	

4.2.10a Tumour CD200 expression and relative immune cell infiltration in adenocarcinoma

After demonstrating significant correlations between tumour CD200 expression and the absolute number of infiltrating CD56+ cells, the relationship between CD200 H score and the relative composition of the immune infiltrate was assessed. As with absolute numbers, the relative frequency of CD8+ cells (r= -0.002214, p= 0.8629) and CD200R+ cells (r= -0.09425, p= 0.9262) demonstrated no correlation with CD200 tumour H score (Figure 4.18a-b). The proportion of infiltrating CD56+ cells were significantly negatively associated with CD200 expression (r=-0.2191, p=0.0310; Figure 4.18c) and a significant positive association was also seen between the relative number of Foxp3+ cells and CD200 expression (r=0.2569, p=0.0076; Figure 4.18d). When patients were split into high and low CD200 expression based on the upper and lower quartiles, only Foxp3+ cell frequency was significantly different (p= 0.012; Figure 4.18e). This was reflected in the spearman correlation analysis, with CD56+ cell frequency (r= -0.22, p= 0.031) and Foxp3+ cell frequency (r= 0.26, p=0.008) significantly correlated with tumour CD200 expression (Figure 4.18f). A positive correlation was again seen between the frequencies of CD8+ and Foxp3+ cells (r=0.39, p= <0.0001). A summary of the relative immune compositions of each adenocarcinoma tumour arranged by CD200 H score can be seen in Figure 4.19, which once again highlights the high interpatient variability in tumour immune cell composition.

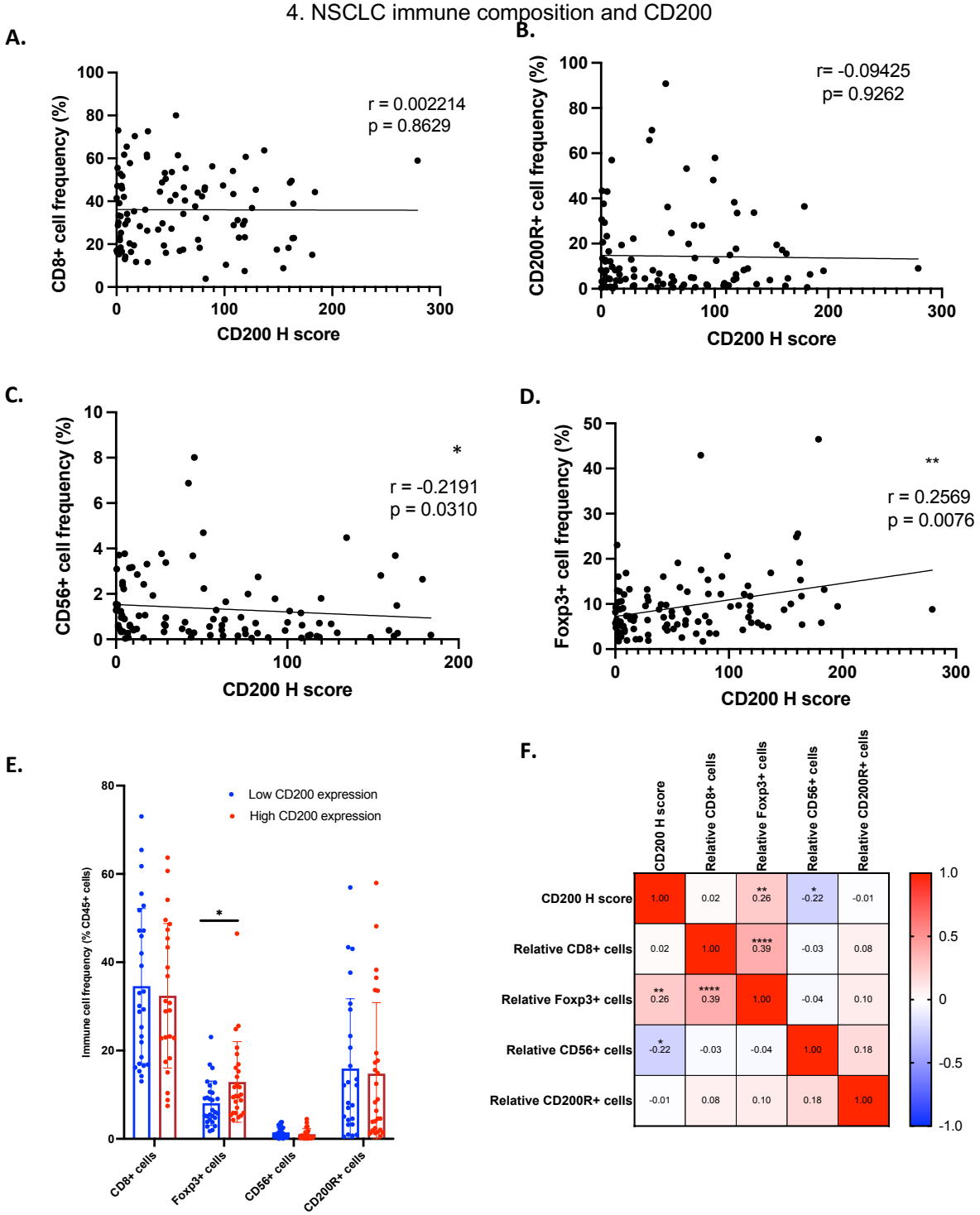

Figure 4.18 Relative immune cell infiltrate in adenocarcinoma patients and its relationship with tumour CD200 H score.

120 adenocarcinoma tumour samples were stained for CD200 and tumour CD200 expression semi-quantified as a H-score. Subsequent serial sections of tumour samples were stained for CD45 (all immune cells), CD200R, CD8 (CD8 T cells), Foxp3 (Tregs) and CD56 (NK cells) to determine the relative number of positive cells (% of CD45+ cells) and the relationship between tumour CD200 H score and absolute (A) CD8+ (B) CD56+ (C) Foxp3+ and (D) CD2000R+ analysed. CD200 tumour expression positively correlated with relative frequencies of Foxp3+ cells and negatively correlated with CD56+ cell frequencies. (E) When patients were split into high and low CD200 expression groups by the median H score, high CD200 expression tumours demonstrated significantly greater Foxp3+ cell proportions. Significance was tested for using the Kruskal-Wallis test with Dunn's multiple comparisons. (F) Spearman correlation matrix of CD200 expression and absolute immune cell numbers reveals further significant positive correlations between immune cells. P ≤ 0.05 (*) P ≤ 0.01 (**) P ≤ 0.001 (***) P ≤ 0.0001 (****).

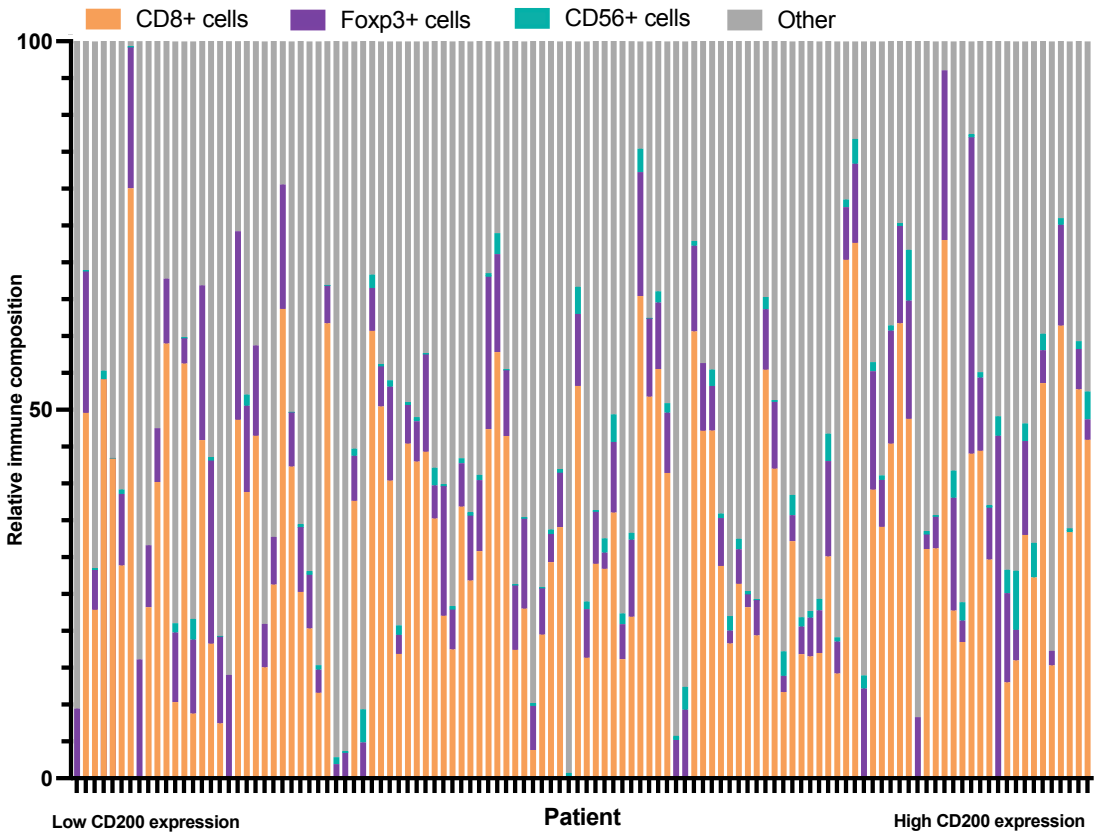

Figure 4.19 Relative frequencies (% of CD45+) cells of CD8+, Foxp3+, CD56+ and other CD45+ cells in adenocarcinoma patients by IHC.

Serial sections of 120 adenocarcinoma patient tumours were stained for CD45, CD8, CD56 and Foxp3 and the relative frequencies of each immune cell calculated (% of CD45+ cells). Sections were also stained for CD200, and patients were stratified from low to high CD200 expression based on the tumour CD200 H score.

4.2.10b Differences in relative immune composition between SCC and adenocarcinoma

As with absolute immune infiltrates, adenocarcinomas demonstrated significantly smaller proportions of infiltrating Foxp3+ ($p = <0.0001$), CD56+ ($p = <0.0001$) and CD200R+ ($p = <0.001$) cells than SCC tumours (Figure 4.20). In contrast, adenocarcinoma tumour CD8+ immune cell proportions were over 6 times greater than that of SCC tumours (36% vs 5.8%, $p=<0.0001$). Unlike SCC tumours which demonstrated no relationship between CD200 expression and relative immune cell frequencies, CD200 expression in adenocarcinomas demonstrated a positive relationship with the proportion of Foxp3+ ($r= 0.2569$) cells and a negative relationship with CD56+ cells ($r= -0.2191$). As with absolute numbers, the relative number of CD56+ cells demonstrated a relationship with disease stage in adenocarcinoma tumours. In SCC tumours, relative frequencies of CD200R+ cells again demonstrated a relationship with tumour stage. These differences in immune cell proportions once again demonstrate the effects tumour subtype have on the composition of the anti-tumour immune response, with CD200 expression potentially influencing the infiltration of CD56+ and Foxp3+ cells in adenocarcinoma, but not SCC tumours.

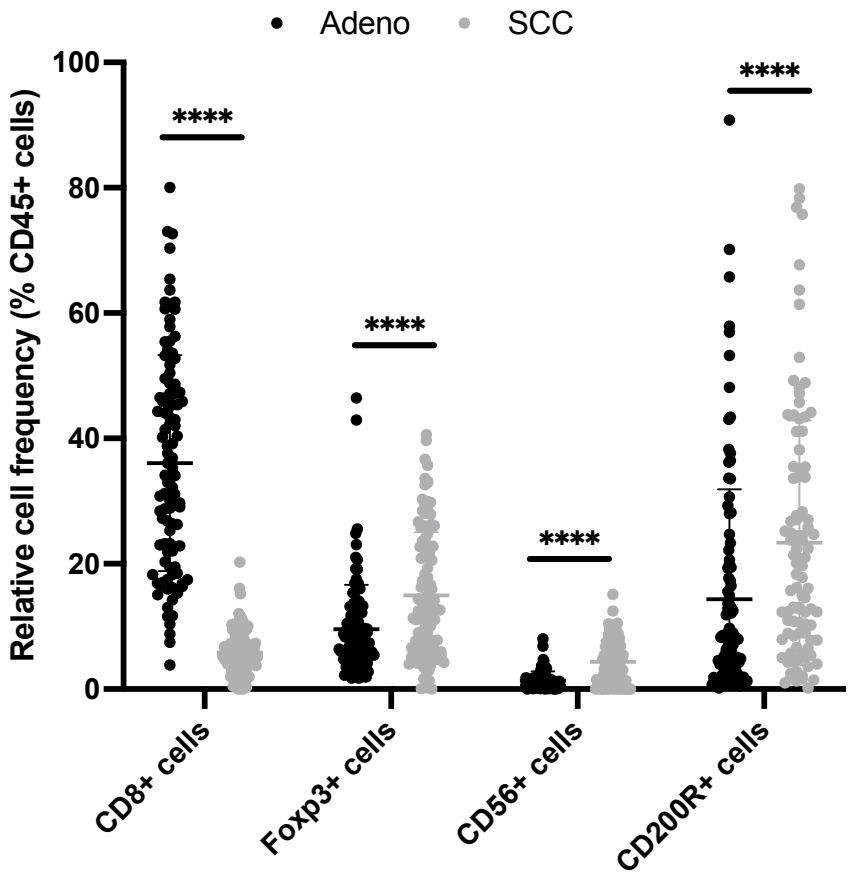

Figure 4.20 Differences in relative immune cell numbers in adenocarcinoma and SCC tumours by IHC.

Serial sections of 120 adenocarcinoma and 120 SCC tumours were stained for CD45 (all immune cells), CD200R, CD8 (CD8 T cells), Foxp3 (Tregs) and CD56 (NK cells) to determine the relative number of positive immune cells (% of CD45+ cells). SCC tumours demonstrated significantly greater frequencies of Foxp3+, CD56+ and CD200R+ cells and significantly lower proportions of CD8+ cells than adenocarcinoma tumours. Significance was tested for using the Kruskal-Wallis test with Dunn's multiple comparisons. $P \leq 0.0001$ (****).

4.2.11 Prognostic significance of immune infiltrate in adenocarcinoma

Having established relationships between CD200 expression and the absolute and relative infiltrate of Foxp3+and CD56+ cells, the prognostic significance of these cells was assessed in adenocarcinoma patients. Differences in OS between low and high infiltration groups and the hazard ratios for each immune cell were calculated using the log-rank test. No significant associations were observed between the infiltration of CD45+, CD8+, Foxp3+ or CD200R+ cells and OS in adenocarcinoma patients (Table 4.8) (Figure 4.21a-g). As with SCC patients, absolute, but not relative, high CD56+ cell numbers were significantly associated with better OS (HR 0.5798; 95% CI 0.3513-0.9567; p= 0.0352) (Figure 4.21h-i). Multivariate cox regression analysis of all significant prognostic factors from Tables 3.5 and 4.7 identified no independent prognostic factors, although not smoking almost reached significance (HR 0.26; 95% CI 0.062-1.1; p= 0.066) (Figure 4.22).

Table 4.8 Univariate cox regression analysis of the associations between absolute and relative immune cell frequencies and patient overall survival in 120 adenocarcinoma patients.

		Overall survival		
		Median survival (months)	HR (95% CI)	P value
CD45+ cells	LOW	74	1.253 0.7701 – 2.038	0.8232
	HIGH	49		
Absolute CD8+ cells	LOW	58	0.9862 0.5859 – 1.6	0.8991
	HIGH	47		
Relative CD8+ cells	LOW	58	1.172 0.6872 – 1.997	0.5595
	HIGH	56		
Absolute Foxp3+ cells	LOW	126	1.437 0.8766 – 2.350	0.1443
	HIGH	52		
Relative Foxp3+ cells	LOW	77	1.007 0.6121 – 1.657	0.9771
	HIGH	58		
Absolute CD56+ cells	LOW	46	0.5798 0.3513 – 0.9567	0.0352
	HIGH	Undefined		
Relative CD56+ cells	LOW	53	0.6601 0.3862 – 1.128	0.1247
	HIGH	Undefined		
Absolute CD200R+ cells	LOW	77	1.41 0.6819 – 1.909	0.6150
	HIGH	59		
Relative CD200R+ cells	LOW	Undefined	1.457 0.8585 - 2.472	0.1640
	HIGH	57		

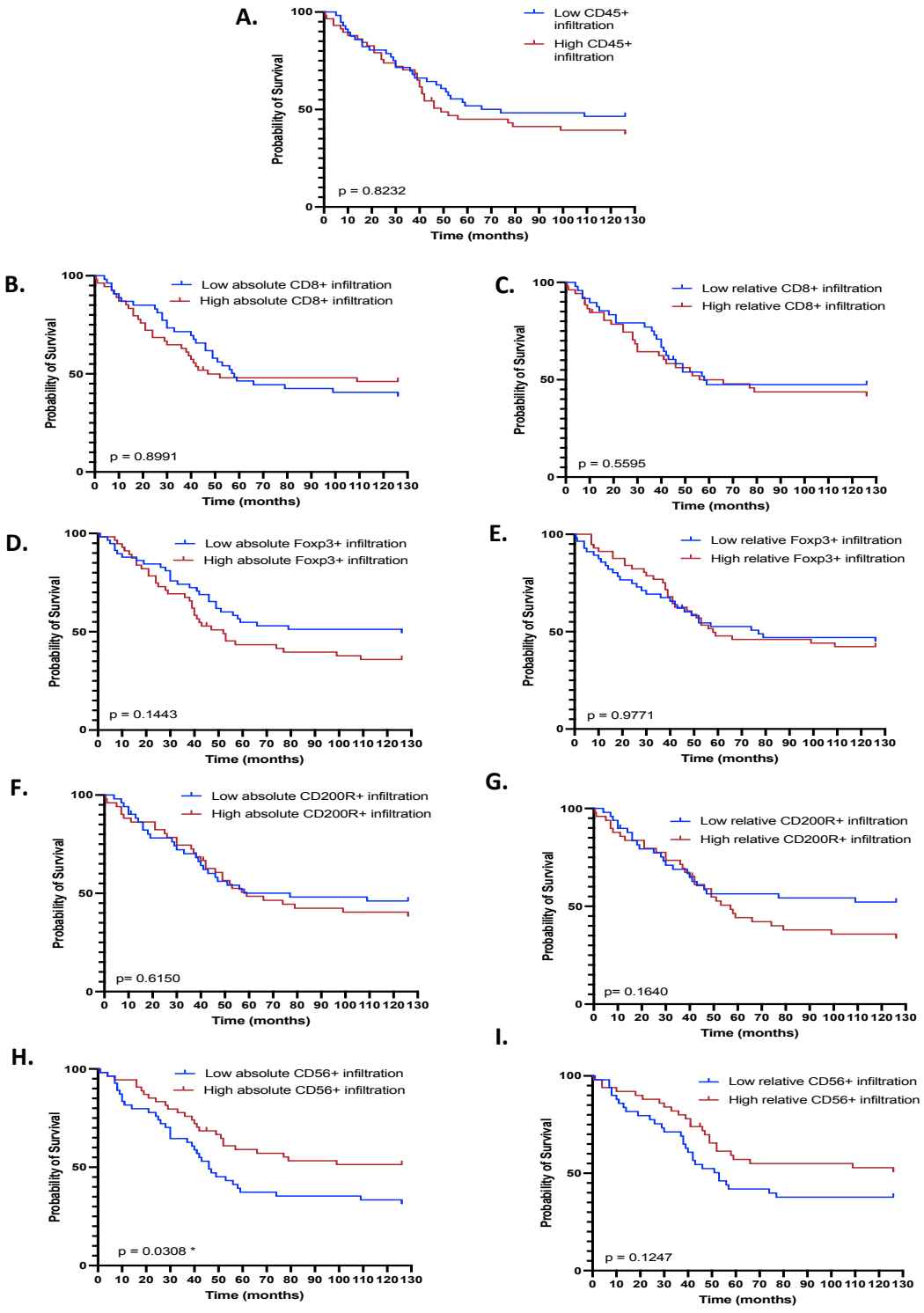

Figure 4.21 Kaplan Meier curves for associations between absolute and relative immune cell frequencies and overall survival in 120 adenocarcinoma patients.

Serial sections of adenocarcinoma tumours were stained for CD45, CD8, Foxp3 and CD56 and the absolute and relative (% of CD45+ cells) cell numbers analysed. Patients were then split into high and low groups based on the median value and associations with OS determined by univariate cox regression analysis. (A) CD45 (B) absolute CD8+ cells (C) relative CD8+ cells (D) absolute Foxp3+ cells (E) relative Foxp3+ cells (F) Absolute CD200R+ cells (G) relative CD200R+ cells (H) absolute CD56+ cells (I) relative CD56+ cell infiltration. Only high absolute CD56+ cell number was a predictor of better OS. OS was determined as the time from diagnosis to death; deaths unrelated to cancer were censored. OS, overall survival. P ≤ 0.05 (*).

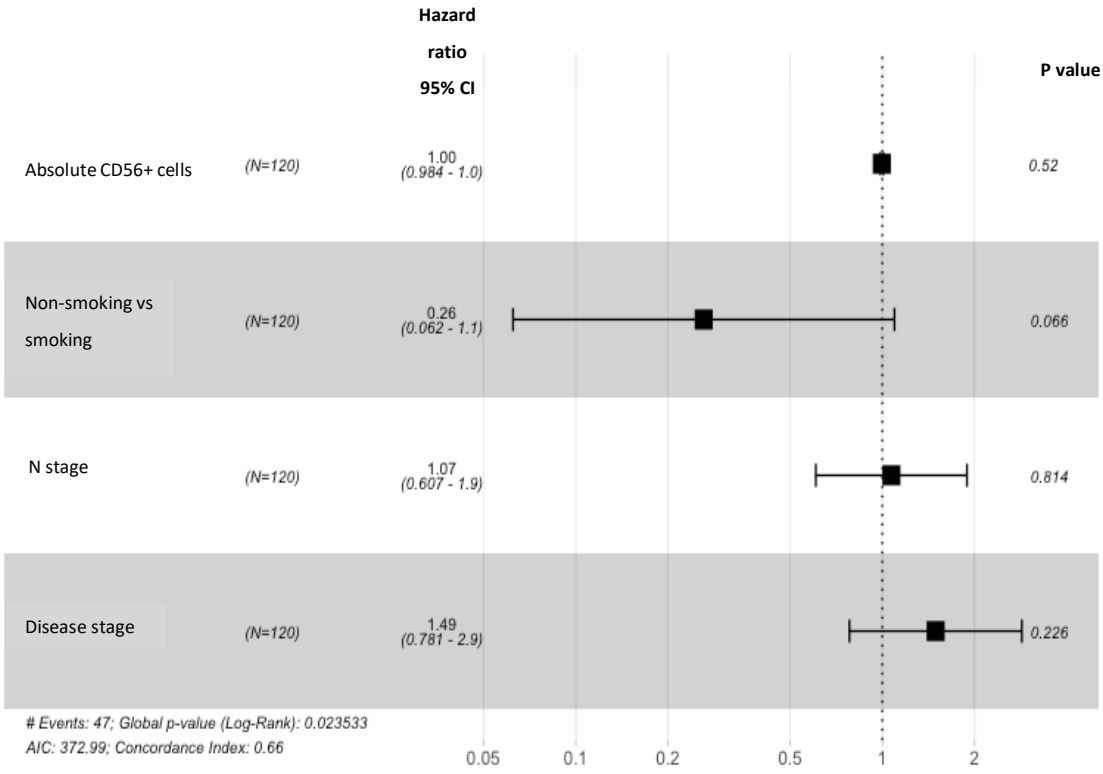

Figure 4.22 Multivariate Cox regression analysis of prognostic factors for overall survival in 120 adenocarcinoma patients.

All prognostic factors identified by univariate Cox regression analysis in Table3.5 and 4.7 with a $p \leq 0.05$ were analysed together by multivariate Cox regression analysis to identify any independent prognostic factors in adenocarcinoma patients. No factors reached independent prognostic significance. OS was determined as the time from diagnosis to death; deaths unrelated to cancer were censored. CI, confidence interval; HR, hazard ratio; OS, overall survival.

4.3 Discussion

In recent years the role of the immune system in cancer development and progression has been increasingly recognised. Immune cells have been shown to have dual roles in tumorigenesis, both suppressing tumour growth through anti-tumour immune responses and promoting tumour growth through the supply of survival factors and the suppression of other immune cells. This potential of the immune system to functionally contribute to both tumour promotion and elimination and its observed significant modulation through immunotherapies supports that the immune system can be a significant determinant on patient survival and disease progression in NSCLC. The role of infiltrating immune cells is complex, with the prognostic value of immune cells in NSCLC generating variable and conflicting results; therefore, the first aim of this chapter was to use a combination of bulk RNA-seq and IHC to define the composition of infiltrating immune cells within SCC and adenocarcinoma tumours and determine their prognostic significance. Having identified CD200 expression in NSCLC tumours, the relationship between CD200 expression and immune cell infiltration was then explored in order to determine whether tumour CD200 expression is associated with changes in the tumour immune response.

4.3.1 Combined bioinformatic and IHC analysis of the immune infiltrate and its prognostic significance in normal lung and NSCLC

Immune cell infiltration is a common feature of many solid human cancers, and it has been demonstrated that NSCLC tumours elicit a robust immune response, with a 3-fold increase in the number of CD45+ cells compared to distal normal lung (Kargl *et al.* 2017). Hence, to begin to elucidate the immune response in NSCLC, CIBEROSRT analysis was performed on bulk RNA-seq data from normal and matched tumour tissue to determine the differences in the composition of 22 immune cells upon malignant transformation. The CIBERSORT method was chosen as it allowed for the deconvolution of the immune infiltrate of 1019 NSCLC patients from publicly available bulk RNA-seq data. Both SCC and adenocarcinoma tumours saw a significant increase in the frequencies of M1 macrophages, Tregs, TFH cells and plasma cells. Furthermore, SCC tumours demonstrated an increase in M0 macrophage cell proportions whilst adenocarcinoma tumours contained greater frequencies of naïve B cells. Greater proportions of cytotoxic M1 macrophages, plasma cells and TFH cells suggest an active immune response is occurring. The presence of Tregs, cells which are induced upon immune activation, and which can suppress the immune system and maintain tolerance to self-antigens and tumours, further supports the presence of an active immune response within the NSCLC TME. Moreover, both adenocarcinoma and SCC tumours saw a significant reduction in resting NK, resting mast cells and memory resting CD4 T cells. Taken together, these changes in immune cell composition between normal distal lung samples and tumour

demonstrate that the tumour immune infiltrate is different from that of normal lung, suggesting the presence of an anti-tumour immune response.

As with other solid tumour malignancies, NSCLC is a heterogenous disease comprised of unique histologic subtypes that possess distinct molecular signatures; just as the anatomical location and mutational status of NSCLC tumours differ, as does the composition of infiltrating immune cells and their function within the TME. Further to identifying changes in immune infiltrate between normal lung and tumour tissue, differences between SCC and adenocarcinoma tumours were analysed to explore heterogeneity in the immune responses. Adenocarcinoma tumours demonstrated significantly greater infiltration of resting mast cells and DCs, M2 macrophages, Tregs, and memory resting CD4 T cells and significantly fewer M0 and M1 macrophages, resting NK cells, and TFH cells than SCC tumours. An increase in cells known to suppress anti-tumour immune responses (M2 macrophages and Tregs) combined with a decrease in activated innate immune cells and activated M1 macrophages suggests that the adenocarcinoma TME possesses a greater number of cells which have known immunosuppressive and pro-tumorigenic effects.

The presence of tumour-infiltrating lymphocytes, composed mainly of CD8+ T cells, are significantly associated with better survival outcomes in NSCLC, with the density of CD8+ cells in the stroma an independent prognostic factor associated with improved survival and decreased tumour size and grade (Ruffini *et al.* 2009). Several studies have demonstrated that high levels of infiltrating CD8+ T cells, CD4+ T cells and T cells with cytotoxic memory or Th1 profile are consistent positive prognostic factors (Bremnes *et al.* 2016). However, in this study using the PRECOG software in combination with CIBERSORT to deconvolute the contribution of each infiltrating immune cell to overall survival using univariate cox regression, only MR CD4 T cells were identified as significant predictors of better survival in adenocarcinoma, with MA CD4 T cells identified as a predictor of worse survival in adenocarcinoma and CD8 T cells failing to reach prognostic significance in either tumour type. Moreover, the identification of memory B cells as the only cell significantly associated with poor prognosis in SCC is in direct contradiction to the literature in which B cell infiltration is consistently associated with favourable outcomes in NSCLC (Soo *et al.* 2018; Wang *et al.* 2019). The PRECOG programme further identified resting mast cells as significant predictors of better survival and neutrophils, M2 macrophages, activated DCs and M0 and M1 macrophages as predictors of worse survival in adenocarcinoma. Neutrophils and M2 macrophages have been shown to possess pro-tumorigenic effects in the TME and have been linked to worse prognosis in several solid tumours. In contrast, activated DCs, MA CD4 T cells and M1 macrophages are all active anti-tumour effector cells whose presence is normally

associated with active antigen presentation and tumour-specific immune responses, with M1 macrophages associated with improved survival in a meta-analysis in NSCLC (Soo et al. 2018). Increased NK cell infiltration has also been associated with better prognosis and increased OS in NSCLC but in this data, resting NK cells were associated with adverse outcomes and activated cells had conflicting roles between tumour subtypes (Platonova et al. 2011). Furthermore, Tregs have been consistently associated with poor OS in NSCLC patients owing to their pro-tumorigenic role in maintaining tumour tolerance and decreasing the intensity of the anti-tumour response yet in this data set, PRECOG identified a trend towards favourable outcomes for Tregs (Remark et al. 2015). These conflicting results suggest that the PRECOG software may not be an accurate and robust predictor of prognostic significance in this patient cohort.

Based on this initial bioinformatics analysis and the literature, three immune cells of interest were selected for further study in our NSCLC patient cohort to begin to elucidate whether tumour CD200 expression has any effect on the absolute and relative frequencies of infiltrating CD8+ cells, Foxp3+ (Tregs) cells and CD56+ (NK) cells using IHC. The use of IHC allows the stratification of patients based on their tumour CD200 expression alone unlike with bulk RNA-seq data in which all CD200 within the TME is measured. Furthermore, IHC of immune cell markers allows further analysis into the location and pattern of immune cell infiltration. SCC tumours demonstrated an immune infiltrate comprising an average of 15.1% CD8+ cells, 5.99% Foxp3+ cells and 5.1% CD56+ cells. These values were all greater than those seen with CIBERSORT, with CD8+ T cells comprising an average of 5.3% of infiltrating immune cells, Treg cells an average of 2.6% and active and resting NK cells an average of 2.29%. Adenocarcinoma tumour immune infiltrate differed greatly from that of SCC tumours, comprised of an average of 36% CD8+ cells, 9.5% Foxp3+ cells and 1.4% CD56+ cells, with significantly greater CD8+ cells and fewer numbers and proportions of CD45+, CD56+ and Foxp3+ cells, thus again highlighting the differences in immune infiltrate between NSCLC subtypes. Similar to in SCC, the values for CD8+ and Foxp3+ cells were much greater than those observed with CIBERSORT analysis in which CD8 T cells constituted 5.46% and Tregs 3.4%.

This increase seen through IHC compared to bioinformatics may be down to the use of a single stain to identify each respective immune cell rather than the 68, 64 and 116 genes used to classify CD8+ T cells, Tregs and NK cells, respectively (Supplementary Table S1). One drawback of using single stain IHC to identify the presence of immune cells within the samples is that specific immune cell subsets cannot be fully identified by one marker alone, with smaller subsets of immune cells also expressing each of the three markers used in this chapter. CD8,

used to identify CD3+CD8+ T cells, is also expressed by a subset of Cd3-CD8+ NK cells; Foxp3, used to identify Tregs, is also expressed by CD4+ T cells which do not possess immunosuppressive properties and by some immunosuppressive CD8+ T cell subsets, and CD56, used to identify NK cells, is also expressed by subsets of DCs, monocytes, GDT and αβ T cells which possess strong effector functions and efficient cytotoxic capacity (Devaud *et al.* 2014; Van Acker *et al.* 2017; Rosenberg and Huang 2018). This non-specific staining of other immune cells may have led to an overestimation of the presence of these cells when compared to the large number of genes used to classify CD8+ T cells, Tregs and NK cells, in CIBERSORT. However, the phenotypes of these subsets, except for some CD4+Foxp3+ cells, are consistent with the target cells of interest suggesting they play similar roles within the TME. Furthermore, these observed fractions by IHC were consistent and within the ranges observed from flow cytometry studies in the literature.

Analysis of patient clinical characteristics and survival revealed that in SCC patients, high absolute numbers of CD8+ cells and Foxp3+ cells were associated with lower tumour stage and disease stage, respectively. Furthermore, the number of CD45+ cells, absolute and relative CD8+ cells and absolute CD56+ cells were all significant predictors of overall survival in this patient cohort. These findings are in line with the literature; high infiltration of CD45+ immune cells are indicative of an active immune response occurring within the TME, with patients demonstrating high immune infiltrate having a better prognosis. Furthermore, the presence of cytotoxic CD8+ and CD56+ cells, which are known to have roles in anti-tumour immune responses, are also associated with longer OS. This suggests that patients with high immune infiltrate, particularly those high in cytotoxic cells, have a more active anti-tumour immune response and therefore demonstrate longer OS. In adenocarcinoma patients, only CD56+ cells demonstrated any associations with patient characteristics, with increased absolute and relative CD56+ infiltration significantly associated with earlier disease stage and decreased lymph node involvement, respectively and high absolute CD56+ infiltration a predictor of better OS. In both SCC and adenocarcinoma tumours, high absolute CD56+ cell number was a predictor of longer survival, suggesting that NK cells may play a vital role in the anti-tumour immune response.

4.3.2 Combined bioinformatic and IHC analysis of CD200 expression and the immune infiltrate in NSCLC

To perform its immunoregulatory role, CD200 must bind with CD200R on interacting immune cells; therefore, to determine whether cells in the NSCLC TME expressed CD200R and to what extent, single cell RNA-seq data from two NSCLC studies was analysed in BBrowser. In

the first dataset, CD200R expression was seen on all immune cells expect monocyte-derived DCs and granulocytes. In general, the proportion of immune cells that were positive for CD200R was low, ranging from 0.114 - 9.52 %, with macrophages and Langerhans cells demonstrating the greatest proportion of CD200R+ cells, consistent with the key role CD200 signalling plays in controlling macrophage activity. Despite this, of the CD200R+ cells, CD4+ and CD8+ T cells demonstrated the greatest levels of CD200R expression; therefore, to further explore CD200R expression on T cells, a single cell dataset looking at T cell subtypes in NSCLC was analysed. Again, the proportion of CD200R+ cells was low, ranging from 7.3-35.1%, but was greater than that seen with the other dataset. Interestingly, CD200R expression significantly varied across T cell phenotypes, with both CD4+ and CD8+ T cells demonstrating significant increases in CD200R expression from naïve to memory to exhausted phenotypes, suggesting that as T cells mature their CD200R expression increases. Although a direct effect of CD200 signalling on T cells has not yet been demonstrated, the changes in CD200R expression suggest that CD200 signalling may be a direct regulator of T cell function.

To determine the effects of tumour CD200 expression on the infiltrating immune response and to confirm that CD200 can directly signal to interacting immune cells, the absolute and relative number of CD200R+ cells in our patient cohort were determined. CD200R expression is limited to immune cells therefore, it was assumed that all CD200R+ cells were also CD45+. SCC immune infiltrate possessed an average of 23.37% CD200R+ cells, whilst adenocarcinoma infiltrate was comprised of 14.25% CD200R+ cells, a significant reduction. This is within the ranges of CD200R positivity demonstrated in the T cell single cell dataset but is slightly greater than that of the other dataset exploring other immune cell subtypes. CD200 expression did not show any correlations with absolute or relative CD200R+ frequencies in adenocarcinoma or SCC tumours, but interestingly high absolute and relative CD200R+ cell numbers were associated with decreased tumour stage in SCC. As an immune checkpoint, CD200R expression has been shown to be concurrently overexpressed with PD-1, CTLA-4, and TIM-3 on tumour-infiltrating T cells in the NSCLC TME (Su *et al.* 2020), therefore it would be of interest to analyse the proportions of CD200R+ cells within normal lung samples and matched tumour tissue to determine whether CD200R expression is increased within the TME. Moreover, the use of additional immune cell markers to allow the identification of which immune cell types expressed CD200R would have been beneficial however, as discussed in the previous chapter, the presence of autofluorescence limited the use of multi-label immunofluorescence.

Having successfully used deconvolution methods to assess the presence of 22 different infiltrating immune cells in normal lung and NSCLC tumour tissue bulk RNA-seq data and identified that infiltrating immune cells within the NSCLC TME express CD200R, the relationship between CD200 expression and immune composition was explored. CD200 expression has been linked to a significant increase in the frequency of Tregs and a decrease in NK cells and active memory T cells in haematological malignancies (Coles *et al.* 2011; Coles *et al.* 2012a; Coles *et al.* 2012b; Aref *et al.* 2017). In agreement with this, CD200 expression was significantly positively associated with Treg infiltration in SCC tumours. Furthermore, adenocarcinoma tumours demonstrated a significant negative correlation between CD200 expression and activated NK cells. In SCC tumours, high CD200 expression was associated with an increase in Tregs and a decrease in CD4 and CD8+ T cells; this increase in Tregs combined with a reduction in effector T cells suggests that TMEs with high CD200 expression may be more immunosuppressive. Adenocarcinoma tumours demonstrated a positive association between CD200 expression and the infiltration of macrophages, MA CD4 cells and memory B cells along with a negative association with activated DCs and activated NK cells. This decrease in activated DCs and activated NK cells suggests a reduction in antigen presentation and cytotoxic anti-tumour activity, yet the increase in anti-tumour memory T and B cells and M1 macrophages indicates the presence of an active anti-tumour immune response. These differences in immune cell associations with CD200 between tumour subtypes suggest that the effects of CD200 signalling in the TME may be tumour type dependent. However, it should be noted that this CIBERSORT analysis is performed on bulk RNA-seq data therefore, the CD200 expression values are derived from the whole tumour and surrounding stroma. As seen in the previous chapter, CD200 is also expressed on vascular endothelium, surrounding alveolar cells and infiltrating immune cells, hence in order to determine the associations between tumour CD200 expression and immune cell infiltration, IHC analysis of our patient cohort was performed.

Upon analysis of the relationship between tumour CD200 expression and immune composition in SCC tumours, the absolute number of CD56+ cells and Foxp3+ cells were positively correlated with tumour CD200 expression. Increased absolute Foxp3+ cells were associated with lower disease stage whilst high absolute CD56+ cell numbers were a significant indicator of better OS in these patients. This suggests that in SCC, tumours with increased CD200 expression are associated with increased infiltrate of cells which have a positive impact on patient outcomes. This is in line with the data from the previous chapter in which tumour CD200 expression was associated with better OS, although this did not reach significance. In contrast, in adenocarcinoma, CD200 expression demonstrated a negative correlation with both the absolute and relative levels of CD56+ cell infiltration. Increased

absolute and relative CD56+ infiltration were significantly associated with earlier disease stage and decreased lymph node involvement, respectively and are predictors of better OS in these patients. Furthermore, tumour CD200 expression was also positively associated with increased Foxp3+ cell infiltration. Although Foxp3+ cell infiltration was not associated with any clinical parameter in this adenocarcinoma cohort, increased Treg cell infiltration is associated with an immunosuppressive TME and worse patient outcomes in NSCLC (Soo *et al.* 2018). Taken together, this suggests that in adenocarcinoma tumours with increased CD200 expression there is an increase in Tregs, cells which are known to possess immunosuppressive properties, and a decrease in NK cells, cells which have been associated with earlier disease stage and better prognosis, suggesting that tumour CD200 expression could be negatively impacting the anti-tumour immune response.

4.3.3 Conclusions

In this chapter, using a combination of bioinformatics analysis on large RNA-seq patient cohorts, single cell sequencing of the NSCLC immune infiltrate and IHC staining of 240 NSCLC patient tumour samples, the composition of the NSCLC immune response and the potential effects CD200 expression has on infiltrating immune cell composition were explored. All bioinformatic approaches used, with the exception of PRECOG analysis of immune cell prognostic significance, were accurate and robust, with immune cell compositions in line with the literature. Furthermore, single-cell analysis of CD200R expression on T cells within the NSCLC TME demonstrated a significant increase in CD200R expression from naïve to memory to exhausted T cells, suggesting a direct role for CD200 in controlling T cell function. Furthermore, CD200 expression appears to influence the immune infiltrate in NSCLC but its effects on the immune response appear to be tumour subtype dependent. Consistently, in either bioinformatics or IHC analysis, CD200 expression was associated with an increase in Tregs in both SCC and adenocarcinoma and a decrease in NK cells in adenocarcinoma. Commonly in the literature Tregs are associated with worse OS and are indicative of an immunosuppressive TME. However, in this SCC patient cohort increased absolute Foxp3+ cells were associated with earlier disease stage. This, in combination with a positive association between tumour CD200 expression and absolute CD56+ cell infiltrate, cells which were predictors of better survival in SCC patients, suggests that increased CD200 expression in SCC tumours may be of benefit to the patient as although CD200 expression itself was not significantly associated with OS in this patient cohort, its expression was significantly associated with an increase in cells which possess good prognostic power. In contrast, CD200 expression in adenocarcinoma was associated with an increase in Tregs and a decrease in NK cells, suggesting tumours with high CD200 expression have an immune infiltrate

associated with poorer prognosis, suggesting that blocking CD200 signalling may be of benefit to adenocarcinoma patients.

High absolute numbers of NK cells were associated with better survival in both adenocarcinoma and SCC patients. In our SCC cohort, CD200 expression positively correlated with absolute NK cell numbers, whilst, using the combined bioinformatics and IHC approach, both absolute and relative NK cell numbers demonstrated a negative relationship with CD200 expression in adenocarcinoma. This suggests that CD200 expression may be having a direct effect on interacting NK cells within the NSCLC TME. Therefore, the next aims of this project were to begin investigating the effects of tumour CD200 expression on interacting NK cells *in vitro*.

Chapter 5:
Characterising the effects of tumour CD200 expression on interacting NK cells

5. Characterising the effects of tumour CD200 expression on interacting NK cells

5.1 Introduction

Absolute and relative frequencies of NK cells were correlated with tumour CD200 expression in our patient cohort. Therefore, the effect of tumour CD200 expression on NK cell function was explored *in vitro* to determine whether CD200 expression has an effect on interacting NK cells. Targeting immune checkpoints, a source of immune escape for a number of cancers, is becoming an important method of treatment for NSCLC patients. In PD-1 blockade, the re-invigoration of T cells responses has been widely recognised as the primary mediator of the anti-tumour immune response (Khan *et al.* 2020). However, NK cells are becoming a newly emerging target, with the observation of strong clinical responses in tumours with low expression of MHC class I molecules and low mutational burden suggesting that NK cells are a major subpopulation responsible for the therapeutic effects of PD-1 blockade (Cho *et al.* 2020). The importance of NK cells in immune checkpoint inhibition is further highlighted by the observation that several immune checkpoints including CTLA-4, PD-1 and CD200 all cause NK cell phenotypic and cytotoxic dysfunction within the TME of various cancers. In NSCLC, NK cells within the TME are dysfunctional and have an impaired ability to kill tumour cells (Carrega *et al.* 2008a; Platonova *et al.* 2011).

NK cells are rapidly activated against abnormal and virus-infected cells without prior sensitisation and are therefore part of the first line of defence to protect the body from pathogen invasion and malignant transformation. The activation of these highly cytotoxic innate lymphoid cells is tightly regulated by a complex network of cytokines and a diverse repertoire of activating and inhibitory receptors. Upon activation, NK cells exocytose cytotoxic granules containing perforin and granzymes which perforate target cells. In addition, they produce a number of cytokines and chemokines which interact with and regulate various other immune cells (Waldhauer and Steinle 2008). NK cells may directly eradicate tumours by means of cytolysis and cytokine secretion but may also indirectly contribute to tumour control through the production of immunoregulatory cytokines and chemokines which aid in the initiation of inflammatory immune responses and recruitment of other immune cells to the TME (Sabry *et al.* 2019). The importance of NK cells in the eradication of tumours has been supported by several *in vivo* studies which demonstrate that mice which are deficient in NK cells or NK cell function present with greater tumour growth and metastasis (Kim *et al.* 2000; Smyth *et al.* 2005). Furthermore, the frequencies of spontaneous and chemically induced tumours are significantly higher in mice deficient in key NK cell effector molecules or their respective receptors (Shankaran *et al.* 2001).

During the early stages of lung cancer, at least in *KRAS*-driven tumours in mice, NK cells are critical in the anti-tumour immune response, with mice lacking NK cells demonstrating a significantly greater lung tumour burden. During the later stages of lung cancer development, NK cells within the TME became dysfunctional and demonstrate diminished cytotoxicity, decreased responsiveness, and impaired viability (Cong *et al.* 2018). In NSCLC patients, NK cells are present within the TME where they demonstrate a unique phenotype that is not detected in distal normal lung or in peripheral blood. In one study, the percentage of NK cells was significantly reduced compared to peripheral blood, with the $CD56^{bright}CD16^{-}$ NK cell subset dominating. $CD56^{bright}CD16^{-}$ NK cells are a minor subset in the blood which express low levels of perforin but secrete large amounts of IFN-γ and TNF upon activation. Furthermore, these cells expressed inhibitory KIRs, which are normally absent from this subset and are mainly expressed by $CD56^{dim}CD16^{+}$ NK cells, the dominant subset found in peripheral blood. However, despite the tumour-infiltrating NK cells demonstrating significant increases in the activating receptor NKp44 and activation markers CD69 and HLA-DR, these cells demonstrated impaired cytolytic and cytotoxic activity *in vitro* (Carrega *et al.* 2008a). Further phenotypic analysis of intra-tumoral NK cells revealed a reduction in the expression of the activating receptors NKp30, NKp80, CD16, NKG2D and DNAM-1 and an increase in CD69 and NKp44, receptors which are barely detectable on peripheral NK cells. Again, these cells demonstrated a limited capacity to degranulate and secrete IFN-γ when co-cultured with autologous tumour cells, suggesting that the NSCLC TME alters the phenotype and causes dysfunction of infiltrating NK cells (Platonova *et al.* 2011).

NK cells analyse the expression of both activating and inhibitory ligands on target cells through activating and inhibitory receptors and integrate these signals to generate an appropriate response. Alongside the classical MHC class I-associated inhibitory receptors, NK cells also express several immune checkpoints including CTLA-4, PD-1 and CD200R; the exploitation of which results in tumour cells being able to evade immune attack. In line with this, CD200 expression in AML patients has been demonstrated to have a direct effect on interacting NK cells. In CD200 high patients the $CD56^{dim}CD16^{+}$ subset, which is the dominant cytolytic subpopulation, was reduced by 50% compared to CD200 low patients. Moreover, the expression of activating receptors was significantly lower in CD200 high patients, with a ~50% decrease in NKp44 and NKp46 in the $CD56^{dim}CD16^{+}$ subset. Like NK cells in NSCLC, these NK cells demonstrated significantly reduced cytotoxic and cytolytic activity *in vitro.* The addition of CD200 blocking antibody restored NK cell activity, suggesting that CD200 directly regulates NK cell function in AML (Coles *et al.* 2011).

The involvement of CD200 expression in the alterations in NK cell subpopulation frequency together with the reduction in cytotoxic and cytolytic function in AML, a phenotype also demonstrated in NSCLC, suggest that CD200 within the NSCLC TME may be involved in NK cell dysfunction. Therefore, using an *in vitro* co-culture model comprised of established lung cancer cells and the CD200R+ NK cell line NK-92MI, the effect of lung tumour CD200 expression on the cytotoxicity and degranulation of interacting NK cells was investigated in this chapter.

5.1.1 Hypothesis and aims

CD200 expression by NSCLC tumour cells is responsible for diminishing NK cell cytotoxic activity and alters the NK activating repertoire of interacting NK cells, thus enabling CD200+ tumour cells to evade NK cell attack. Blocking of CD200 signalling may restore NK cell anti-tumour function.

Aims:

6. Determine the effects of tumour CD200 expression on NK cell cytotoxic and cytolytic activity and investigate whether blockade of CD200 signalling using an anti-CD200 antibody is sufficient to restore anti-tumour immunity *in vitro*

Objectives:

1. Generate an *in vitro* CD200R+ NK: CD200+/- tumour co-culture model
2. Determine the effects of CD200 signalling on the cytotoxic ability of interacting NK cells
3. Determine the effects of CD200 signalling on the cytolytic ability of interacting NK cells
4. Define the effects of CD200 signalling on NK cell receptor expression
5. Determine whether blocking CD200 signalling can reverse these effects

5.2 Results

5.2.1 Generating an *in vitro* CD200R+ NK: tumour cell co-culture model

To investigate the effects of tumour CD200 expression on interacting NK cells, an *in vitro* model utilising the immortalised NK cell line NK-92MI and CD200-transduced HeLa cells was generated. NK-92MI are a $CD56^{bright}$ IL-2-independent NK cell line derived from NK-92 cells that can kill tumour cells without prior sensitisation. NK-92MI cells lack almost all inhibitory receptors but express a series of activating receptors and are abundant in perforin and granzyme, resulting in cells which exhibit a high degree of cytotoxic activity (Tam *et al.* 1999). Therefore, the first aim was to determine whether NK-92MI cells expressed CD200R and to what extent. NK-92MI cells were stained with fluorescence-conjugated CD56 and CD200R antibodies and cell surface receptor expression analysed by flow cytometry (Figure 5.1). Cells were first gated on forward scatter (FSC) and side scatter (SSC) to identify the NK cell population before being gated on FSC area and FSC height to eliminate any doublets or clumped cells (Figure 5.1a,b). DAPI was added prior to analysis to eliminate dead cells and CD56+ and CD200R+ gates were set based on background fluorescence levels identified with fluorescence-matched isotype controls (Figure 5.1c,d). NK-92MI cells were 100% CD56+, with 91.275% positive for CD200R (n=3; Figure 5.1e).

Having determined that NK-92MI cells expressed CD200R, the next aim was to generate tumour cell lines that expressed CD200 as a proof-of-concept prior to analysis with lung cancer cell lines. The CD200 negative HeLa cervical adenocarcinoma cell line was stably transduced either with a retrovirus co-expressing green fluorescent protein (GFP) under an internal cytomegalovirus promoter (T2; HeLa CD200-) or with the same retrovirus also containing CD200 DNA (T4; HeLa CD200+). After infection, cells were left to grow until they were 90% confluent in a T75 flask before being sorted for GFP+ cells by fluorescence-activated cell sorting (Figure 5.2a,b). T2 and T4 cells were gated on FSC and SSC to eliminate debris before gating on FSC height and FSC area to gate for single cells. Dead cells were stained with DAPI and gated out, with successfully transduced cells identified by GFP positivity. To confirm CD200 expression, T2 and T4 cells were stained for CD200 with a fluorescence-conjugated antibody and cell surface ligand expression analysed by flow cytometry (n= 4; Figure 5.2c). Successful stable transduction was confirmed, with T2 cells demonstrating an average of 0.77% CD200 positivity, with 82.74% of T4 cells positive for CD200.

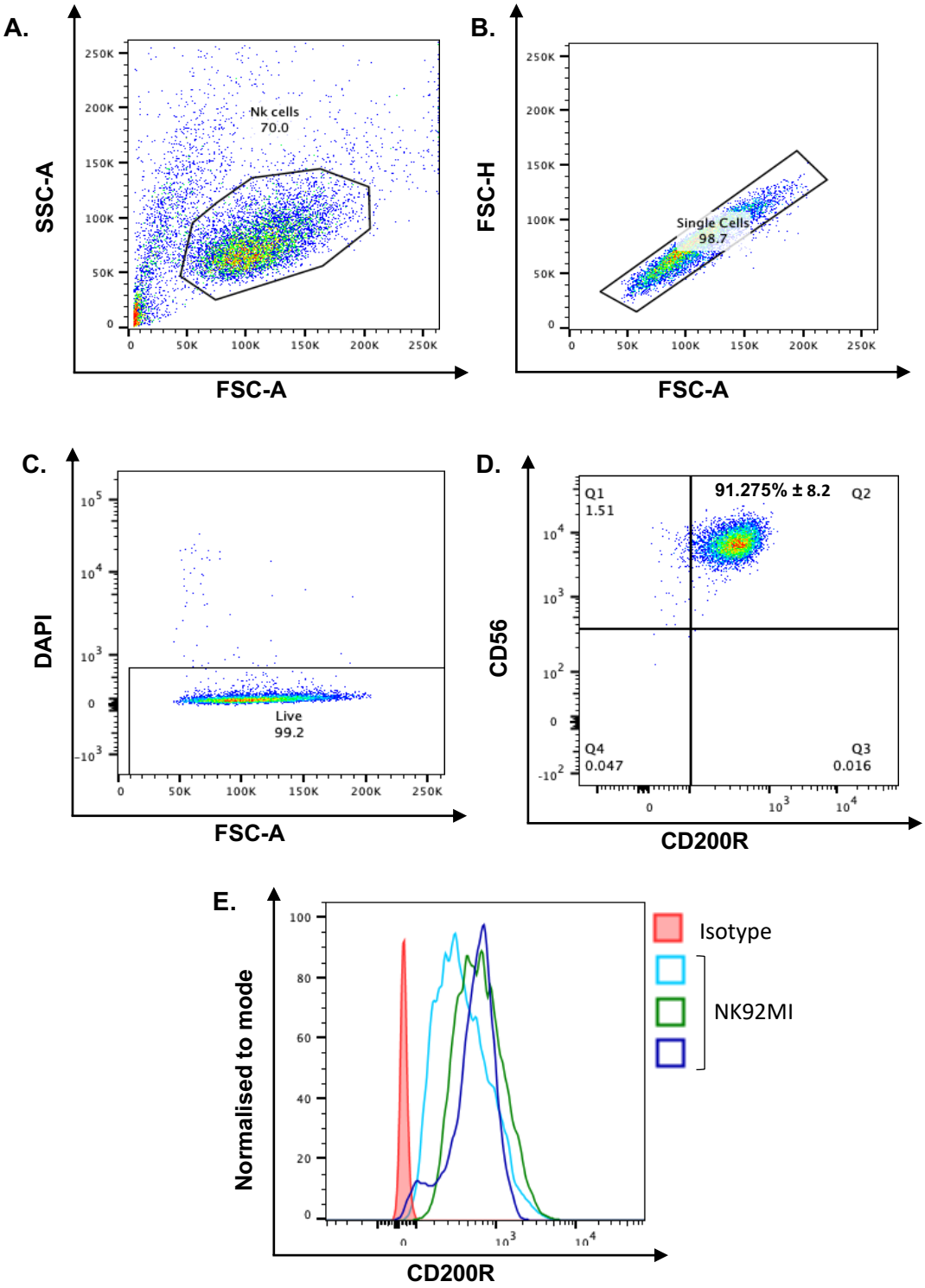

Fig 5.1 Analysis of CD200R expression on NK-92MI cells.

NK-92MI cells are a CD56^{bright} immortalised NK cell line which exhibit a high degree of cytotoxicity to a range of tumour cells *in vitro* without prior sensitisation. NK-92MI cells were stained with fluorescent CD56 and CD200R antibodies for analysis of cell surface receptor expression by flow cytometry (n= 3). Cells were gated on (A) FSC-A and SSC-A to eliminate debris before gating on (B) FSC-H and FSC-A to identify single cells. (C) Dead cells were identified through staining with DAPI before (D) CD56+ and CD200R+ gates set based on background fluorescence levels identified using isotype controls; an average of 91.275% of cells were positive for CD200R. (E) Histograms of Alexa-Fluor 647 positivity for NK-92MI cells stained with isotype control (red) and CD200R (blue and green) antibodies. Positive cell numbers presented as % ± standard deviation (SD).

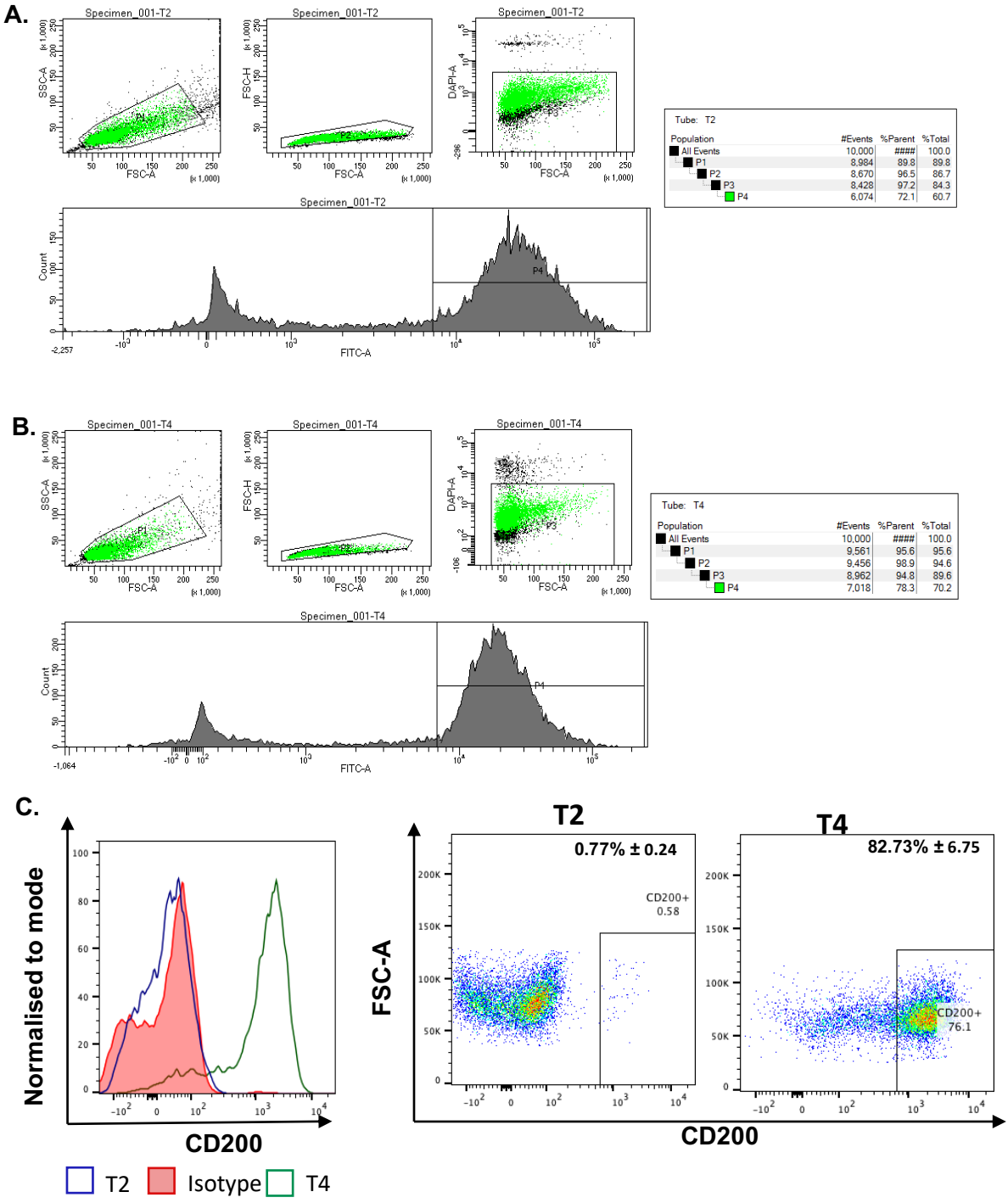

Fig 5.2 Stable retroviral transduction of HeLa cells with either GFP alone or CD200 and GFP.

HeLa cells were transduced with either a retrovirus co-expressing GFP from an internal cytomegaloviral promoter or the same retrovirus containing cDNA for CD200. (A) T2 cells transduced with the GFP alone virus were analysed by FACS to select for the GFP positive population. Briefly, cells were gated to eliminate debris, then to eliminate doublets and cell clumps before dead cells being gated out through staining with DAPI. GFP (FITC-A) positive cells were selected. (B) T4 cells transduced with the GFP CD200 virus were selected for GFP positive cells. (C) CD200 positivity was confirmed in the T4 cell line and no CD200 was seen in the T2 cell line by flow cytometry (n= 3). Positive cell numbers presented as % ± SD.

5.2.2 HeLa CD200 expression confers resistance to killing by CD200R+ NK cells

NK cells are poised and ready to immediately respond to and attack malignant or infected cells without prior sensitisation. Upon recognition of a target cell, NK cells facilitates NK-induced target cell death through two critical effector mechanisms: direct lysis of cells through degranulation of lytic molecules into the cell and target cell death receptor ligation (Abel *et al.* 2018). To assess the effect of tumour CD200 expression on NK cell cytotoxicity, HeLa cells were co-cultured with NK-92MI cells at increasing effector:target ratios for 4 hours and the viability of the HeLa cells determined by CellTiter-Glo, with the tumour cell death calculated relative to untreated cells (n= 4; Figure 5.3). As expected, with increasing NK:HeLa ratios, the percentage of tumour cell death increased, with HeLa cell death at 10:1 almost 4-fold that of HeLas co-cultured at a 0.5:1 ratio. CD200- cells also demonstrated significantly greater cell death than CD200+ cells at, 2:1 ($p= 0.008$), 5:1 ($p= 0.0011$) and 10:1 ($p< 0.0001$) ratios, suggesting that tumour CD200 expression reduces the ability of CD200R+ NK cells to kill the cells.

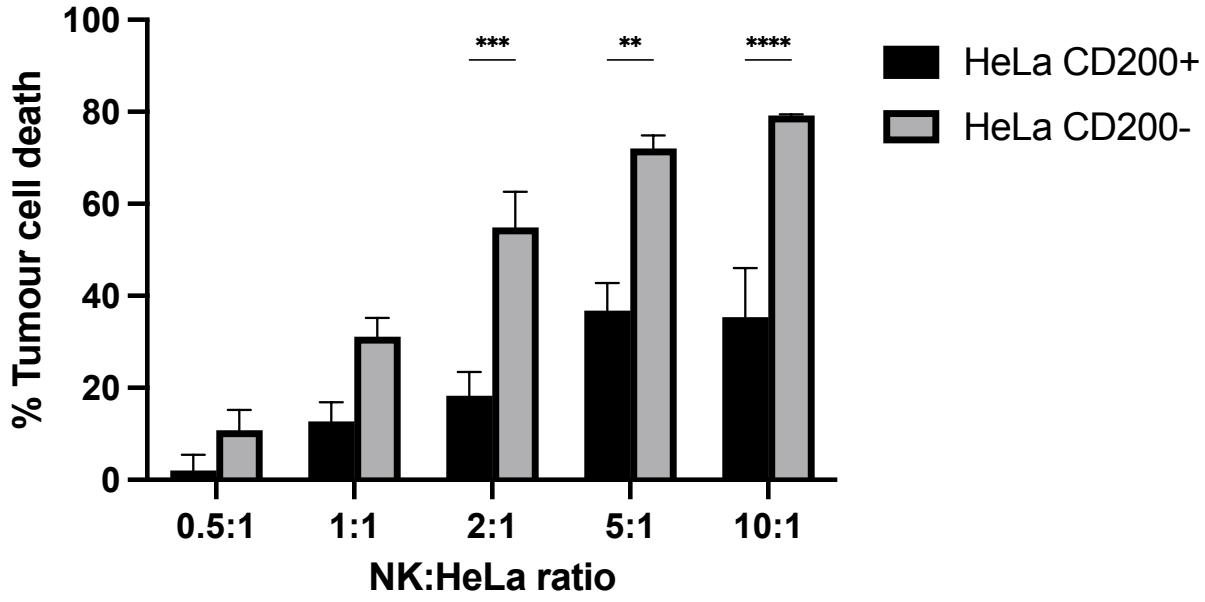

Fig 5.3 HeLa CD200 expression confers protection against CD200R+ NK cell cytotoxicity.

CD200+ and CD200- HeLa cells were co-cultured with CD200R+ NK cells at increasing NK:target ratios for 4 hours prior to assessing HeLa cell viability with CellTiter-Glo (n= 4). Untreated HeLa cells served as control, with tumour cell death calculated relative to untreated cells. With increasing NK;HeLa ratios, tumour cell death increased. CD200- HeLa cells demonstrated significantly more tumour cell death at all but one ratio, suggesting CD200 confers protection against CD200R+ NK-mediated cell death. Significance was tested for using a one-way ANOVA with Tukey's multiple comparisons. $P \leq 0.01$ (**) $P \leq 0.001$ (***) $P \leq 0.0001$ (****).

5.2.3 Characterising CD200 expression in NSCLC cell lines

Having demonstrated that tumour CD200 expression on HeLa cells could confer immune resistance against the cytotoxic effects of CD200R+ NK cells *in vitro*, the next aim was to define CD200 expression in NSCLC cell lines to determine whether this could also be relevant in NSCLC. CD200 expression in 6 NSCLC tumour and 3 normal pulmonary tissue cell lines was determined by qRT-PCR, western blot, and flow cytometry. A summary of the cell lines used can be seen in Figure 5.4a. A549 adenocarcinoma cells are part of the NCI-60 panel of 60 cell lines used by the National Cancer Institute for the screening of novel cancer therapies and are a common model used in NSCLC research (Shoemaker 2006). A549 cells harbour an activating mutation in *RAS* but are in turn wild type for other common mutations in adenocarcinomas; in contrast, H838 cells harbour mutations in both *TP53* and *KEAP1* (Korrodi-Gregório *et al.* 2016; Rouillard *et al.* 2016). H596 cells are derived from an adenosquamous tumour which demonstrated characteristics of both an adenocarcinoma and SCC tumour upon diagnosis; they harbour a mutation in *TP53*, a mutation which is seen at high levels in both NSCLC subtypes (Rouillard *et al.* 2016). The SCC cell line H226 is also part of the NCI-60 panel and carries a mutation in *CDKN2A,* whilst SK-MES-1 SCC cells harbour a mutation in *TP53* (Ikediobi *et al.* 2006; Rouillard *et al.* 2016). The large cell lung carcinoma line COR-L23 carries mutations in both *KRAS* and *ALK* (Rouillard *et al.* 2016). A bronchial epithelial cell line (BEAS2B) and two pulmonary fibroblast cell lines (IMR-90 and MRC-5) were also assessed.

First, CD200 messenger RNA (mRNA) expression was analysed by qRT-PCR with CD200 mRNA expression presented as arbitrary units using the ΔCT method with GAPDH and β-actin expression as controls (n= 3; Figure 5.4b). Only H226 (339.4 AU), SK-MES-1 (36.55 AU) and BEAS2B (61.62 AU) cells demonstrated CD200 mRNA expression, with CD200 levels in H226 cells greater than that seen in the CD200+ HeLa cells (309.7 AU; ns). Furthermore, H226 and CD200+ HeLa CD200 mRNA expression was significantly greater than all other cells analysed (p= <0.0001; ####). All other cell lines demonstrated very low to no CD200 expression with H838s demonstrating the greatest expression at 4 AU, almost 85-fold less than H226. Next, to determine whether mRNA levels correlated with protein expression, CD200 protein levels were analysed by western blot and the percentage of CD200+ cells determined by flow cytometry (n=3; Figure 5.4c,d). Whole cell lysates were taken and probed for CD200 expression and CD200 expression presented as AU normalised to α-tubulin expression (Figure 5.4c). As with the mRNA analysis, H226 and CD200+ HeLa cells demonstrated the greatest CD200 protein expression; however, unlike in the mRNA analysis, only CD200+ HeLas demonstrated significantly greater (p= <0.0001; ####) expression than the other cells, with CD200 protein expression in CD200+ HeLa over 50% greater than in H226 cells (p=

0.0014). Despite these differences in protein quantification, H226 cells demonstrated significantly greater numbers of CD200 positive cells than CD200+ HeLas (p= 0.0027) and all other cells analysed (p= <0.0001; ####) by flow cytometry (Figure 5.4d). Some level of CD200 positivity was seen in most cells with an average of 1.37% of A549s, 7.57% H838s, 1.973% H596s and 1.538% COR-L23s positive for CD200. Furthermore, both IMR-90 and MRC-5 pulmonary fibroblasts demonstrated an average of 2.487% and 1.150% CD200 positivity, respectively.

In addition to being expressed as a membrane bound form, CD200 can also be cleaved from the cell membrane and exist as a functional soluble form (sCD200), suggesting that CD200 may be able to exert its immunoregulatory effects in a non-cell-to-cell contact dependent method. Therefore, to determine whether CD200 is shed from the NSCLC cells, a CD200 sandwich ELISA was performed on cell culture supernatants. Cells were grown until ~50% confluency and fresh media added for 48h prior to protein concentration and analysis of CD200 expression in the supernatants (n=3 ;Figure 5.4e). sCD200 is presented as pg/ml per $1x10^6$ cells. H226 cells demonstrated the greatest levels of sCD200 with an average of 7.141 pg/ml, with CD200+ HeLas the next greatest at 3.871 pg/ml. Both A549s and COR-L23s demonstrated low levels of sCD200 in the supernatant at 0.699 pg/ml and 1.472 pg/ml, respectively. No sCD200 was detected in H838, H596, SK-MES-1 or CD200- HeLa cells.

A.

Cell Line	Cell type
A549	Adenocarcinoma
H838	
H596	Adenosquamous
H226	SCC
SK-MES-1	
COR-L23	Large cell
BEAS2B	Normal bronchial epithelium
IMR-90	Normal pulmonary fibroblasts
MRC-5	

B.

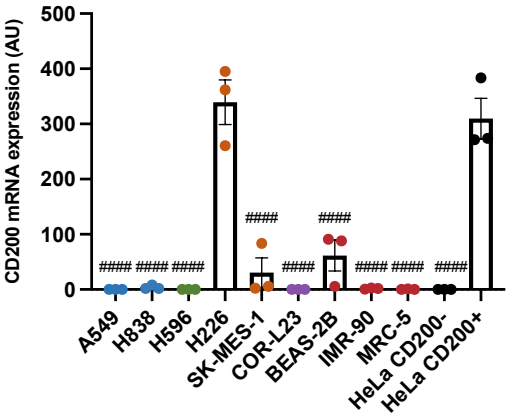

C.

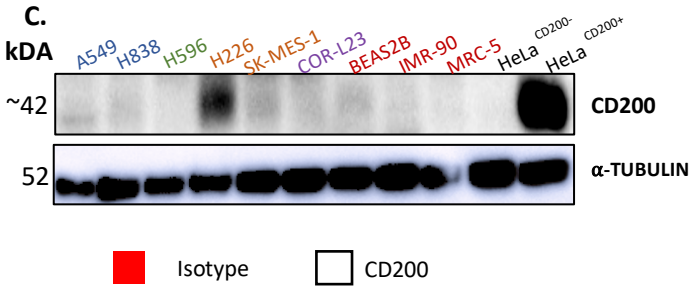

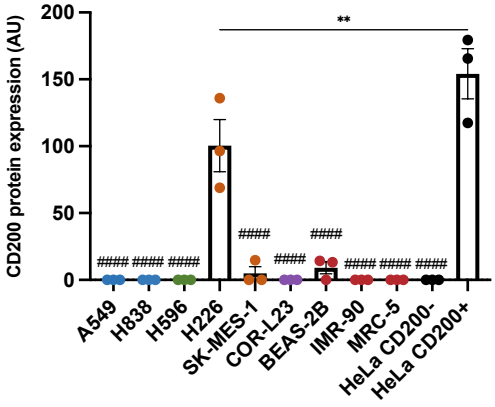

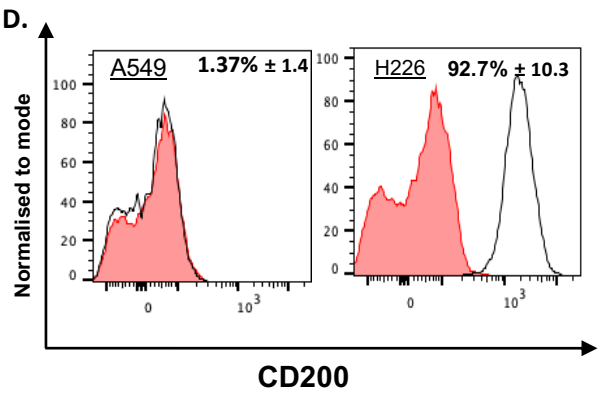

D.

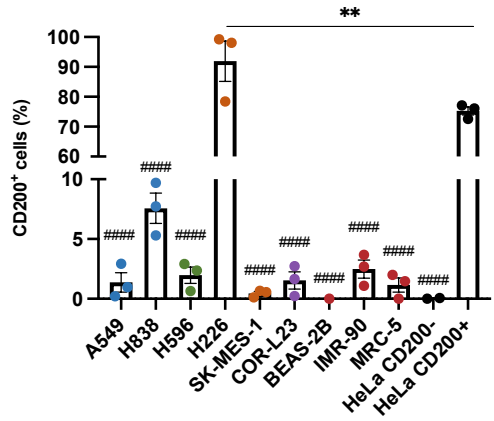

E.

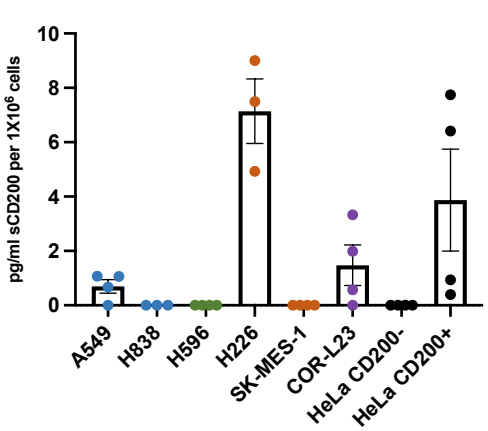

Fig 5.4 Characterising CD200 expression in NSCLC and normal bronchial epithelium and pulmonary fibroblast cell lines.

6 NSCLC cell lines, 1 bronchial epithelium cell line and 2 pulmonary fibroblast cell lines were assessed for CD200 mRNA and protein expression by qRT-PCR, western blot, and flow cytometry (n= 3). The levels of soluble CD200 released into the supernatant were also analysed. (A) qRT-PCR analysis of the cell lines demonstrated high CD200 mRNA levels in H226 and CD200+ HeLa cells. (B) Western blot of CD200 expression from whole cell lysates was quantified relative to α-tubulin expression also demonstrated high CD200 protein expression by H226 and CD200+ HeLa cells. (C) The percentage of CD200 positive cells was further assessed by flow cytometry, with H226 cells demonstrating more CD200 positive cells than CD200+ HeLa cells. (E) Sandwich ELISA for soluble CD200 in cell supernatant demonstrated sCD200 in H226 and CD200+ HeLa cells, with low levels seen in A549 and COR-L23 cells. Significance was tested for using a one-way ANOVA with Tukey's multiple comparisons. $P \leq 0.01$ (**) (B,C,D) #### = $p < 0.0001$ from H226 and CD200+ HeLa.

5.2.4 Characterising NK-92MI cytotoxicity towards NSCLC cells *in vitro*

Having extensively characterised CD200 expression in the NSCLC cell lines, the susceptibility of these cells to NK-92MI-mediated killing was assessed using tumour:NK co-culture assays. Despite NK-92MI cells demonstrating a high degree of cytotoxicity against tumour cells without prior sensitisation, not all tumour cells are susceptible to NK cell cytotoxicity, with some cell lines resistant to NK-92MI cells. Therefore, in order to investigate the effects of NSCLC CD200 expression on NK cells, the cells which were susceptible to NK-92MI-mediated cell death were first identified (n= 4; Figure 5.5). Both A549 and H838 cells showed susceptibility to NK-92MI cells, with cell death increasing with increasing NK:target cell ratios although the percentage of tumour cell death plateaued between 2:1 and 5:1, with an average of 40% tumour cell death (Figure 5.5a,b). SK-MES-1 cells also demonstrated plateauing of tumour cell death, with 15-20% of tumour cells dying at all NK:SK-MES-1 ratios (Figure 5.5c). In contrast, H838 cells demonstrated a positive correlation between cell death and NK:target ratios, with death increasing from 26.52% (0.5:1) to 80.39% (10:1), suggesting that H838 cells were the most susceptible of the cell lines analysed to NK-92MI cytotoxicity (Figure 5.5d). Therefore, these cells were selected for further analysis.

The CD200+ SCC cell line H226 exhibited increasing cell numbers over the 4 hours co-cultures at ratios of 0.5:1, 1:1 and 10:1 and 4-12% cell death at 5:1 and 2:1, suggesting a resistance to NK-92MI cytotoxicity (Figure 5.5e). A subsequent literature search revealed that H226 are an NK-resistant cell line, with reduced susceptibility to target cell lysis also demonstrated with isolated primary NK cells and lung interstitial NK cells *in vitro* (Robinson and Morstyn 1987; Robinson *et al.* 1989). To determine whether this resistance may be CD200-dependent, H226 cells were co-cultured with NK-92MI cells at increasing NK:target ratios in the presence of a CD200 blocking antibody (Figure 5.5f). Blocking CD200 signalling did not increase tumour cell death, suggesting that this resistance to NK cell killing was not CD200-dependent.

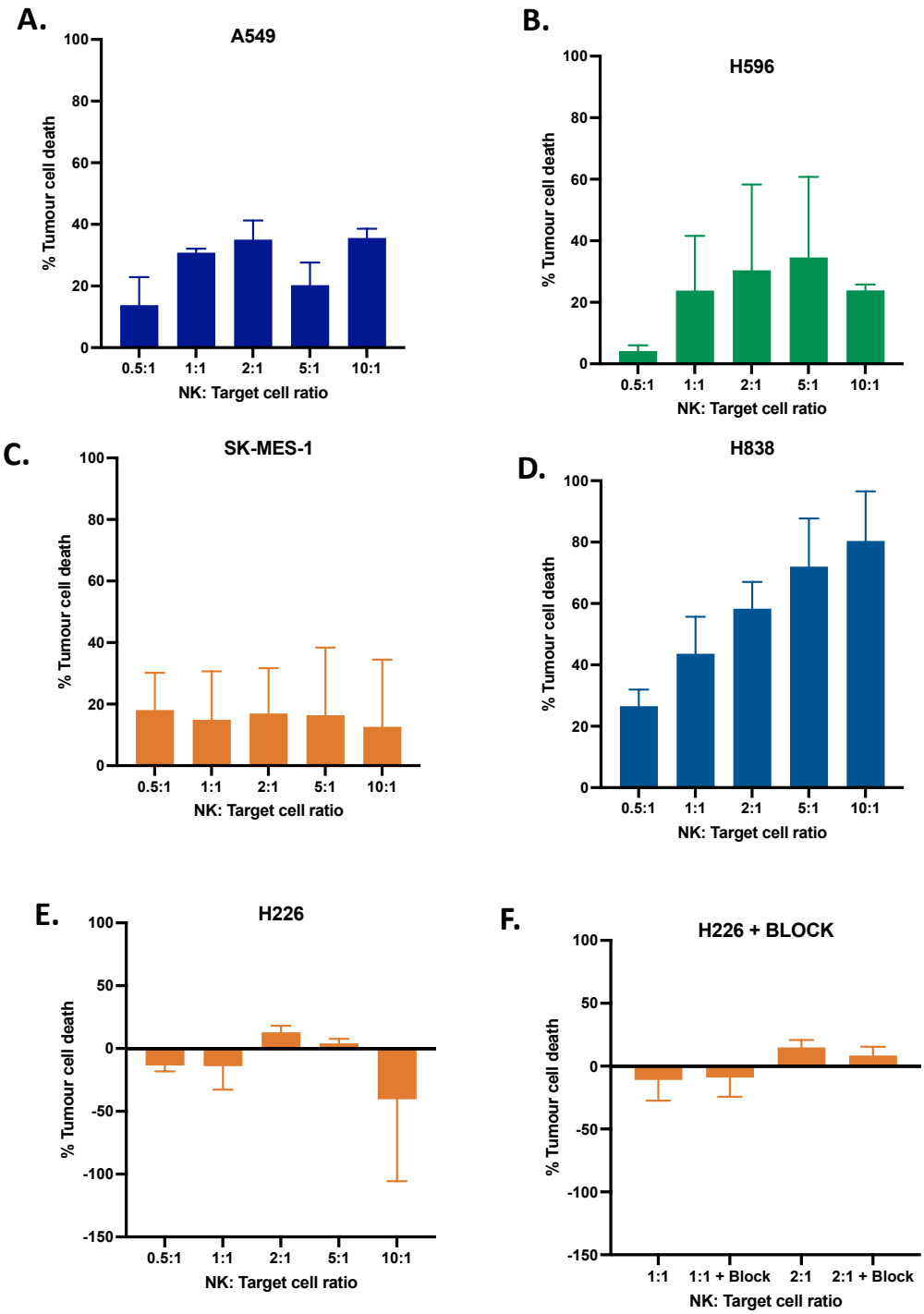

Fig 5.5 Determining the susceptibility of NSCLC cell lines to NK-92MI cytotoxicity.

The viability of 5 NSCLC cell lines (2 adenocarcinoma, 1 adenosquamous, 2 SCC) after co-culture with NK-92MI cells for 4 hours at increasing NK:target cell ratios was assessed to determine which cells could be used for further analysis into the effects of CD200 on NK-92MI cell function (n= 4). (A) Adenocarcinoma A549 cells were susceptible to NK cell death but plateaued around 20-30% despite increasing NK cell numbers. (B) Adenosquamous H596 cells demonstrated increasing cell death from 0.5:1 to 5:1 but cell death dropped at 10:1 and did not surpass 40%. (C) SCC SK-MES-1 cells demonstrated ~20% cell death at all NK:target cell ratios. (D) The adenocarcinoma cell line H838 demonstrated increasing cell death with increasing NK:target cell ratios, suggesting they are the most susceptible to NK-92MI cytotoxicity. (E) The CD200 positive SCC cell line H226 was resistant to NK-92MI cytotoxicity, with cell numbers increasing at 3/5 NK:target cell ratios. (F) This effect was not dependent on CD200 as addition of a CD200 blocking antibody did not increase H226 cell susceptibility.

5.2.5 Generating an NK-susceptible CD200+ NSCLC cell line

H838 adenocarcinoma cells were the most susceptible to NK-92MI cells *in vitro* however, they do not express CD200; therefore, to examine the effect of NSCLC tumour cell CD200 expression on interacting CD200R+ NK cells, CD200 expression had to be transduced into the cells (Figure 5.6). H838 cells were transduced with a GFP retrovirus or a CD200 and GFP retrovirus and successfully transduced cells selected by fluorescence activated cell sorting (Figure 5.6a). Cells were gated on FSC and SSC to eliminate debris and remove any doublets or cell clumps, DAPI positive dead cells were removed and GFP positive cells selected. CD200 expression by CD200+ H838 cells was confirmed by western blot of whole cell lysates, with no CD200 expression identified in the untransduced and CD200- H838 cells (Figure 5.6b). Further analysis by flow cytometry confirmed CD200 expression in CD200+ H838 cells, with 76.1% of cells positive for CD200 compared to 1.26% of CD200- H838 cells (Figure 5.6c).

To confirm that transduction did not affect cell growth, untransduced and transduced H838 cells were seeded, and their growth measured every 2 hours for 48 hours in the Incucyte live cell imaging system (n= 3; Figure 5.7a). Transduction of H838 cells with either virus had no effect on the growth of the cells compared to untransduced cells, with no significant differences in cell confluence measured at any time point. Next, to determine whether transduction with the GFP virus had any effect on the susceptibility of the CD200- H838 cells to NK-92MI cytotoxicity, cells were co-cultured for 4 hours and the percenatage of cell death measured relative to untreated cells (n= 4; Figure 5.7b). Transduction of H838 cells with the GFP virus did not affect the cell's NK-92MI susceptibility, with no significant differences at any NK:target cell ratio tested.

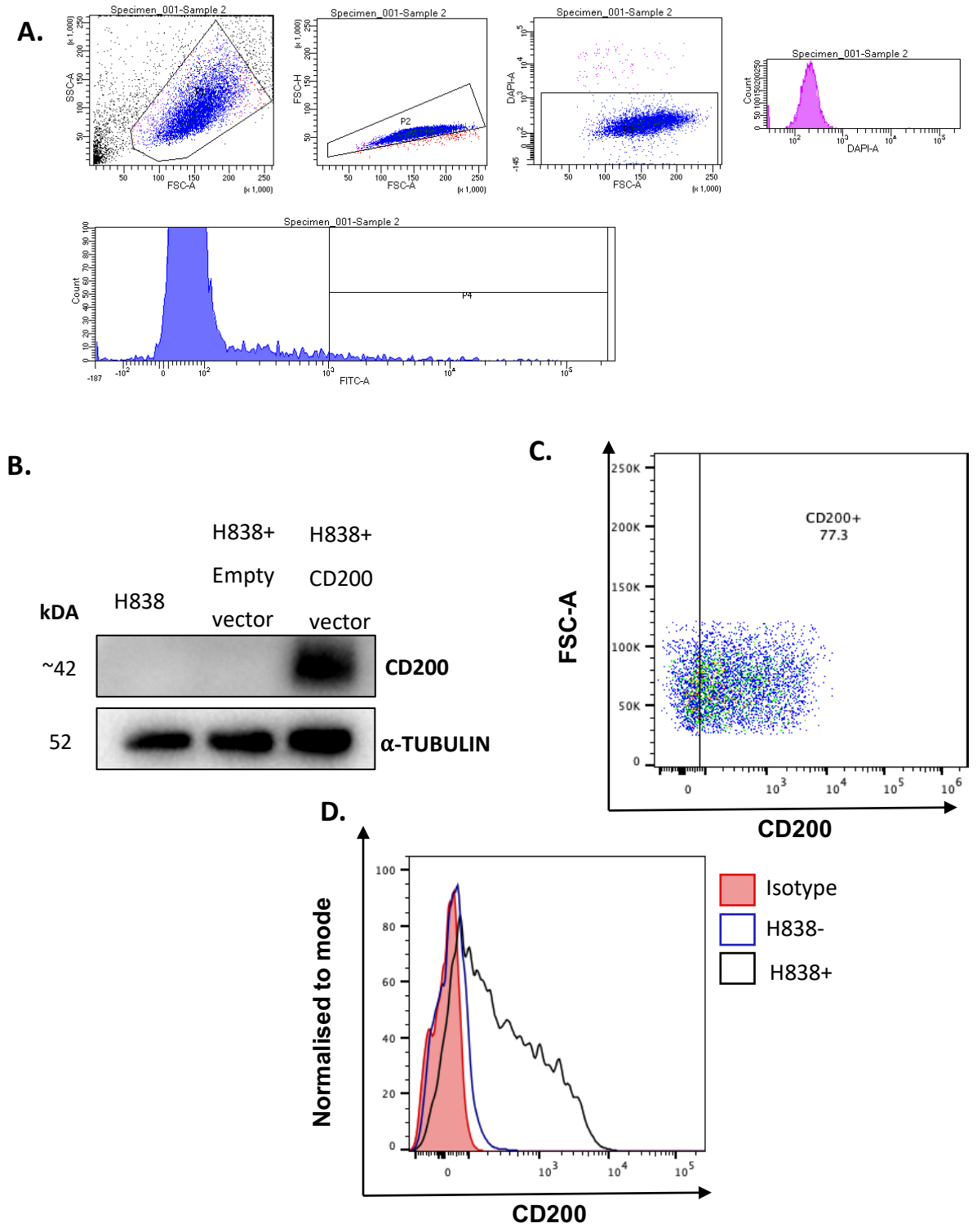

Fig 5.6 Stable retroviral transduction of H838 cells with either GFP alone or CD200 and GFP.

H838 cells were transduced with either a retrovirus co-expressing GFP from an internal cytomegaloviral promoter or the same retrovirus containing cDNA for CD200. (A) Representative fluorescence activated cell sorting plots of transduced H838 cells being selected for successfully transduced cells based on GFP expression. Briefly, cells were gated to eliminate debris, then to eliminate doublets and cell clumps before dead cells being gated out through staining with DAPI. GFP (FITC-A) positive cells were selected. (B) CD200 positivity was confirmed in the CD200+ H838 cell line by western blot of whole cell lysates. No CD200 expression was seen in untransduced or CD200- H838 cells (n =3). (C) CD200 expression in transduced H838 cells by flow cytometry (n= 1). (D) Histogram of CD200 expression in H838+ empty vector and H838+ CD200 vector (n=1).

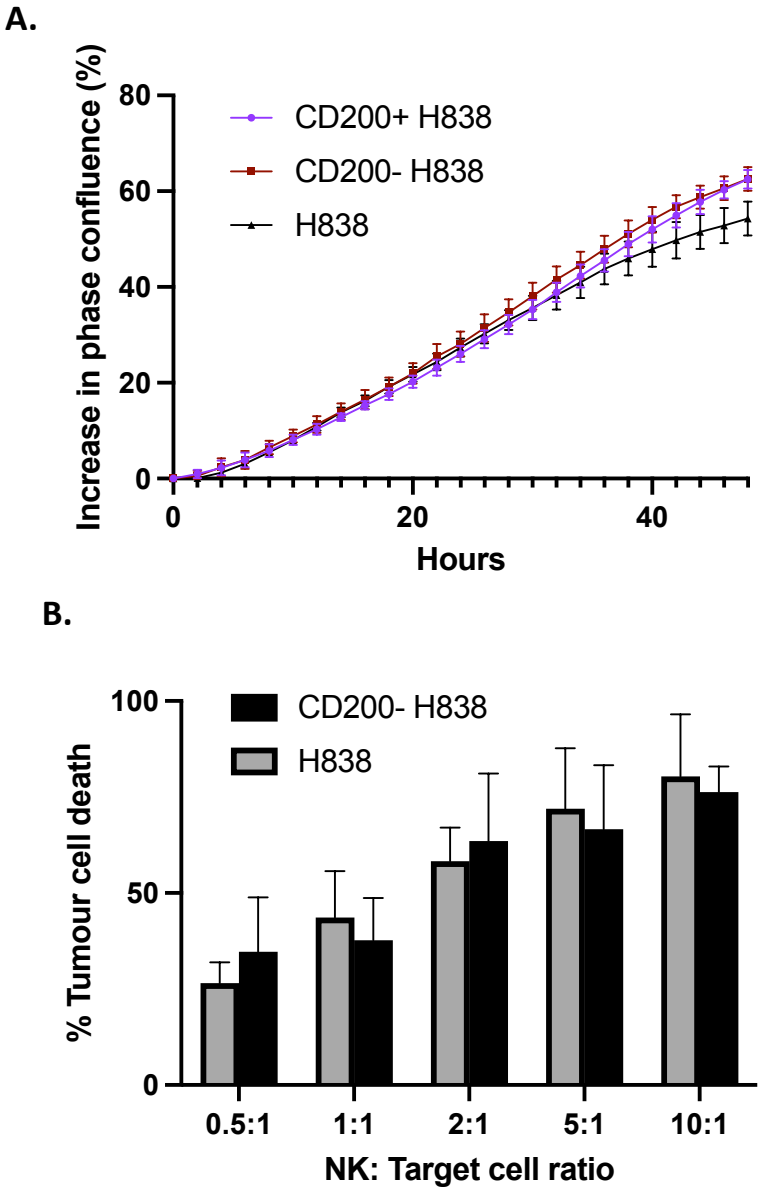

Fig 5.7 Stable retroviral transduction of H838 cells did not affect cell growth or NK-92MI susceptibility.

To confirm that transfection did not alter the growth of the H838 cells or the susceptibility of the CD200- cells to NK-92MI cytotoxicity, their growth over 48 hours and their viability after co-culture with NK-92MI cells was assessed. (A) H838 cells were plated in a 96-well plate and left to grow for 48 hours in the Incucyte live cell imaging system, with images taken every 2 hours. Cell growth was determined as the % increase in confluence in the phase channel relative to 0 hours. No differences in growth were seen between transduced and untransduced cells (n= 3). (B) H838 and CD200- H838 cells were co-cultured with NK-92MI cells at increasing NK:target cell ratios for 4 hours and H838 cell viability assessed using CellTiter Glo. No significant differences in cell death were seen between H838 and CD200- H838 (n= 4).

5.2.6 H838 CD200 expression confers resistance to killing by CD200R+ NK cells

Having generated a CD200-expresssing NSCLC cell line that is susceptible to NK-92MI cell killing and having demonstrated that transduction did not affect cell growth or confer resistance to CD200- cells, the effect of NSCLC cell CD200 expression on interacting NK cells was assessed (n= 4; Figure 5.8). Again, with increasing NK:target cell ratios, H838 cell death increased relative to untreated cells. Moreover, expression of CD200 significantly reduced H838 cell death at 2:1 and 10:1 NK:target cell ratios, with death of CD200+ H838 cells less than CD200- cells at all ratios; at 2:1, CD200+ cell death was over 2-fold less than CD200- cells, with a 1.5-fold decrease in cell death seen at 10:1. Cell death of CD200- H838 cells ranged from 34.72% at 0.5:1 to 76.87% at 10:1 whilst CD200+ H838 cells demonstrated 16.88% and 48.25% cell death at 0.5:1 and 10:1 ratios, respectively. Next, to confirm whether this increase in resistance to NK-92MI cell killing was due to CD200 expression, the co-cultures were performed in the presence of a mouse-anti human CD200 antibody (n= 4; Figure 5.9). Blocking of CD200 signalling with the antibody significantly increased CD200+ H838 cell death by NK-92MI cells at 1:1 and 2:1 ratios, with CD200+ H838 cell death slightly greater (39.50%) than CD200- H838 cells (37.69%) at the 1:1 ratio. The addition of a matched mouse isotype control antibody did not affect H838 cell death. Taken together, this near restoration of CD200+ H838 cell death to CD200- H838 cell levels suggests that blocking CD200 could increase the susceptibility of CD200+ NSCLC cells to CD200R+ NK cell cytotoxicity *in vitro.*

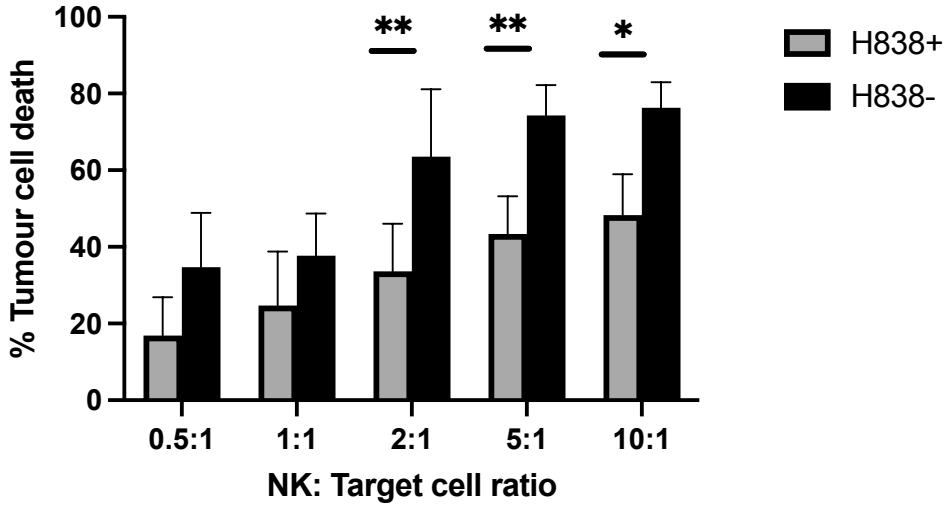

Fig 5.8 H838 CD200 expression confers protection against CD200R+ NK cell cytotoxicity.

CD200+ and CD200- H838 cells were co-cultured with CD200R+ NK-92MI cells at increasing NK:target ratios for 4 hours prior to assessing H838 cell viability with CellTiter-Glo (n= 4). Untreated H838 cells served as control, with tumour cell death calculated relative to untreated cells. With increasing NK:target ratios, tumour cell death increased. CD200- H838 cells demonstrated significantly more tumour cell death at 2:1 and 10:1 NK:target cell ratios, with CD200- H838 cell death greater at all ratios analysed, suggesting CD200 confers protection against CD200R+ NK-mediated cell death. Significance was tested for with a one-way ANOVA with Tukey's multiple comparison test. $P \leq 0.05$ (*) $P \leq 0.01$ (**).

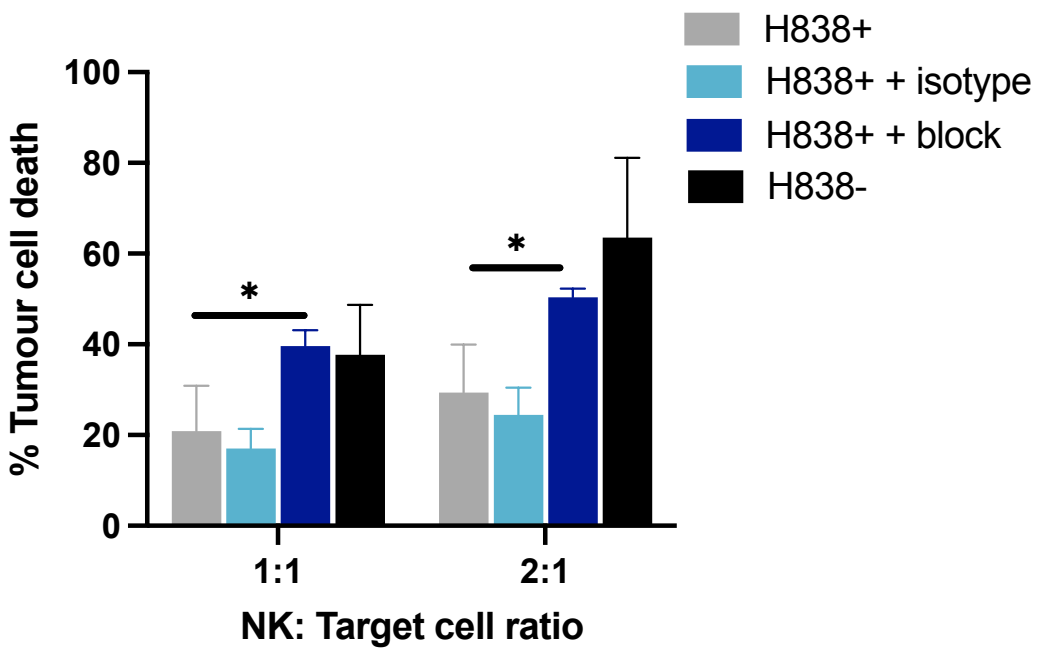

Fig 5.9 Blocking CD200 restores CD200+ H838 cell susceptibility to NK-92MI cytotoxicity.

CD200+ and CD200- H838 cells were co-cultured with CD200R+ NK-92MI cells at 1:1 and 2:1 NK:target ratios for 4 hours prior to assessing H838 cell viability with CellTiter-Glo (n= 4). Untreated H838 cells served as control, with tumour cell death calculated relative to untreated cells. The addition of a CD200 blocking antibody significantly increased CD200+ H838 cell death, with cell death restored to CD200- H838 cell levels. The addition of an isotype matched control antibody did not affect CD200+ H838 cell death by NK-92MI cells, suggesting that blocking CD200 is sufficient to restore CD200+ H838 cell susceptibility to NK-92MI cytotoxicity. Significance was tested for with a one-way ANOVA with Tukey's multiple comparison test. $P \leq 0.05$ (*).

5.2.7 Assessing NK-92MI cell degranulation

Blocking of CD200 was sufficient to restore the ability of NK-92MI cells to induce tumour cell death; therefore, the next step was to look at the NK cells themselves and investigate the effects CD200 had on NK-92MI cell function, namely degranulation in response to stimulation. A hallmark of NK cell activation and function is degranulation, wherein lytic granules containing perforin and granzymes are trafficked to the cell surface and released onto the target cell resulting in direct lysis and cell death. Lysosome-associated membrane protein 1 (CD107a) lines the surface of these cytotoxic granules and upon degranulation, CD107a is transiently exposed on the surface of NK cells. Externalisation of CD107a is a maker of NK cell degranulation; therefore, CD107a expression on NK-92MI cells was assessed as a direct measure of NK cell cytotoxic function (Lorenzo-Herrero *et al.* 2019).

To first optimise the assay, NK-92MI cells were cultured alone (unstimulated) or in the presence of PMA and Ionomycin (stimulated) (n= 5; Figure 5.10). PMA and ionomycin are used for strong and unspecific stimulation of immune cells; PMA is a protein kinase C activator and ionomycin is a calcium ion channel opening antibiotic. PMA increases intracellular cytoplasmic free calcium concentration by causing an influx of calcium ions from the extracellular space, this increase in calcium is involved in phosphorylation of the transcription STAT4 which promotes the expression of numerous genes involved in NK cell function (Kaszubowska *et al.* 2018). As CD107a expression at the cell surface is transient, cells were cultured in the presence of a CD107a antibody, and the protein transport inhibitor Monensin was added to the cells after 1 hour to prevent re-internalisation of CD107a. Unstimulated cells were cultured for 4 hours before staining with CD56 and demonstrated an average baseline level of 25.56% degranulation (Figure 5.10a,c). However, upon stimulation with PMA/ionomycin over 97.2% of NK-92MI cells expressed CD107a, a significant increase compared to unstimulated cells ($p = <0.0001$; Figure 5.10b,c).

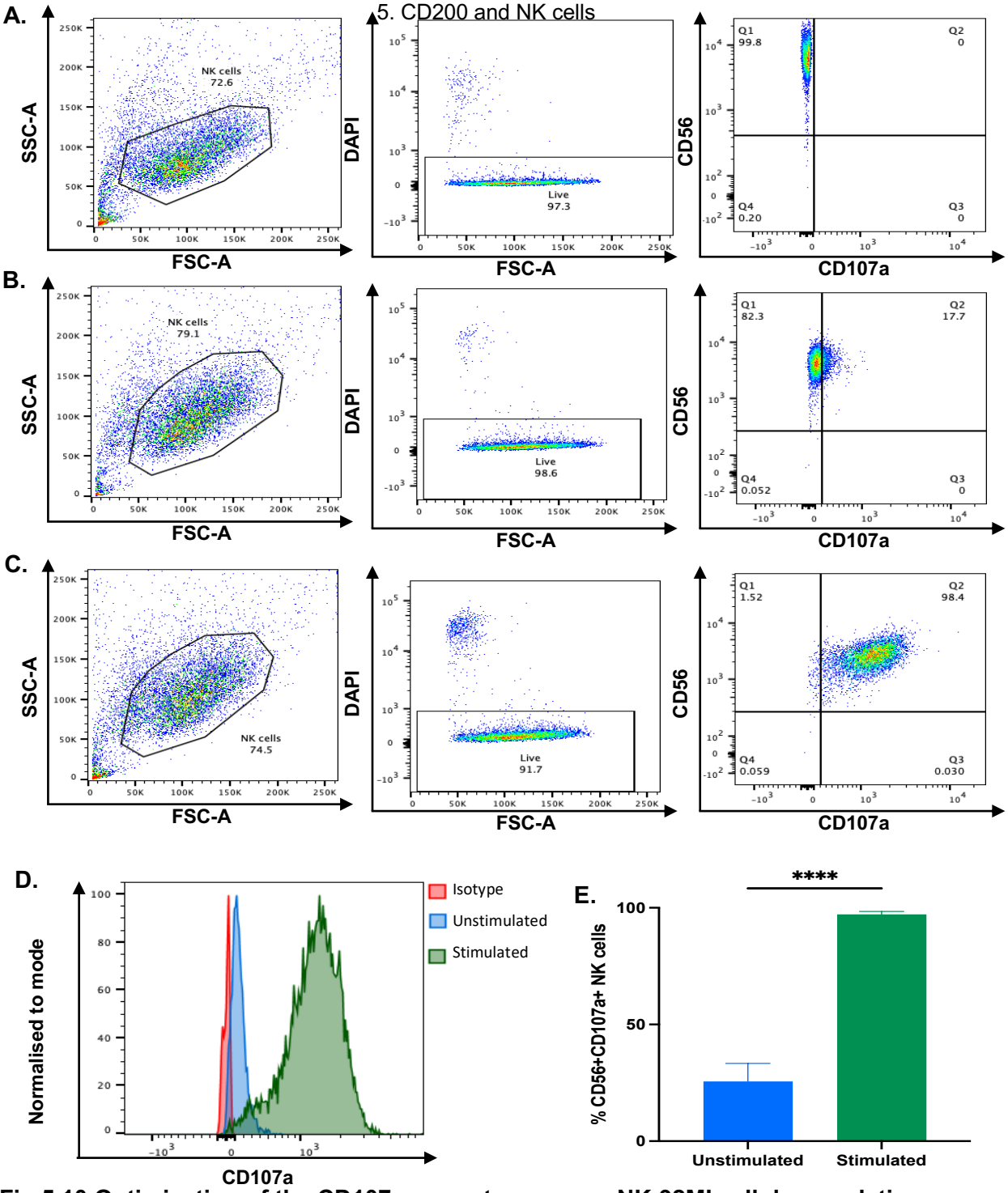

Fig 5.10 Optimisation of the CD107a assay to measure NK-92MI cell degranulation.

Activation of NK cells results in the release of cytotoxic granules containing perforin and granzymes which cause direct lysis of target cells. CD107a lines the surface of these granules and is transiently expressed on the NK cell surface upon degranulation. Addition of a protein transport inhibitor (Monensin) prevents the re-internalisation of CD107a and CD107a expression can be detected by flow cytometry as a measure of NK cell degranulation. (A) Gating strategy used: Cells were gated on FSC and SSC to eliminate debris, dead cells were excluded through DAPI staining and CD56+CD107a+ cell gates determined using fluorescence minus one controls to account for background fluorescence (n= 5). (B) Unstimulated NK cells. (C) stimulated NK cells were cultured for 4 hours in the presence of a CD107a antibody with the addition of Monensin after 1 hour. Stimulated cells were treated with 50ng/ml PMA and 2µg/ml Ionomycin. (D) Representative CD107a histograms demonstrate high CD107a positivity in the stimulated cells compared to unstimulated cells. (E) Stimulated NK-92MI cells expressed significantly more CD107a than unstimulated NK-92MI cells. Significance was tested for using an unpaired t test. P ≤ 0.0001 (****).

5.2.8 Determining the effects of CD200 expression on NK-92MI cell degranulation

Having optimised an assay to quantify NK cell degranulation in response to stimulation, the effect of CD200 expression on NK-92MI degranulation was assessed. NK-92MI cells were co-cultured with CD200- and CD200+ H838 cells at a 5:1 NK:target cell ratio for 4 hours with the addition of Monensin after 1 hour (n= 4; Figure 5.11). Co-culture with CD200- H838 cells induced an average of 38.57% of NK-92MI cells to release cytotoxic granules whilst CD200 expression by H838 cells induced a slight reduction in NK cell degranulation (35.57%) (Figure 5.11a-c). There was no significant difference in CD107a expression between CD200+ and CD200- H838 cells, although co-culture with H838 cells did significantly increase degranulation compared to unstimulated cells (CD200- p= 0.0084; CD200+ p= 0.01) (Figure 5.11c). This minimal difference in CD107a positivity suggests that CD200 may inhibit NK-92MI cell activity towards H838 cells through another mechanism. This was confirmed when addition of the CD200 antibody appeared to further decrease the NK-92MI cell degranulation when added to stimulated and CD200+ H838 cell co-cultures (n= 4; Figure 5.12a). The addition of the CD200 blocking antibody to stimulated cells decreased the average number of CD107a positive cells from 76.1% to 61.9% whilst addition of the antibody to CD200+ H838 cells decreased NK-92MI degranulation from 32.85% to 16.25%, a 2-fold decrease. This decrease in NK-92MI cell degranulation was CD200 specific as addition of an isotype control matched mouse IgG1,κ antibody did not affect CD107a.

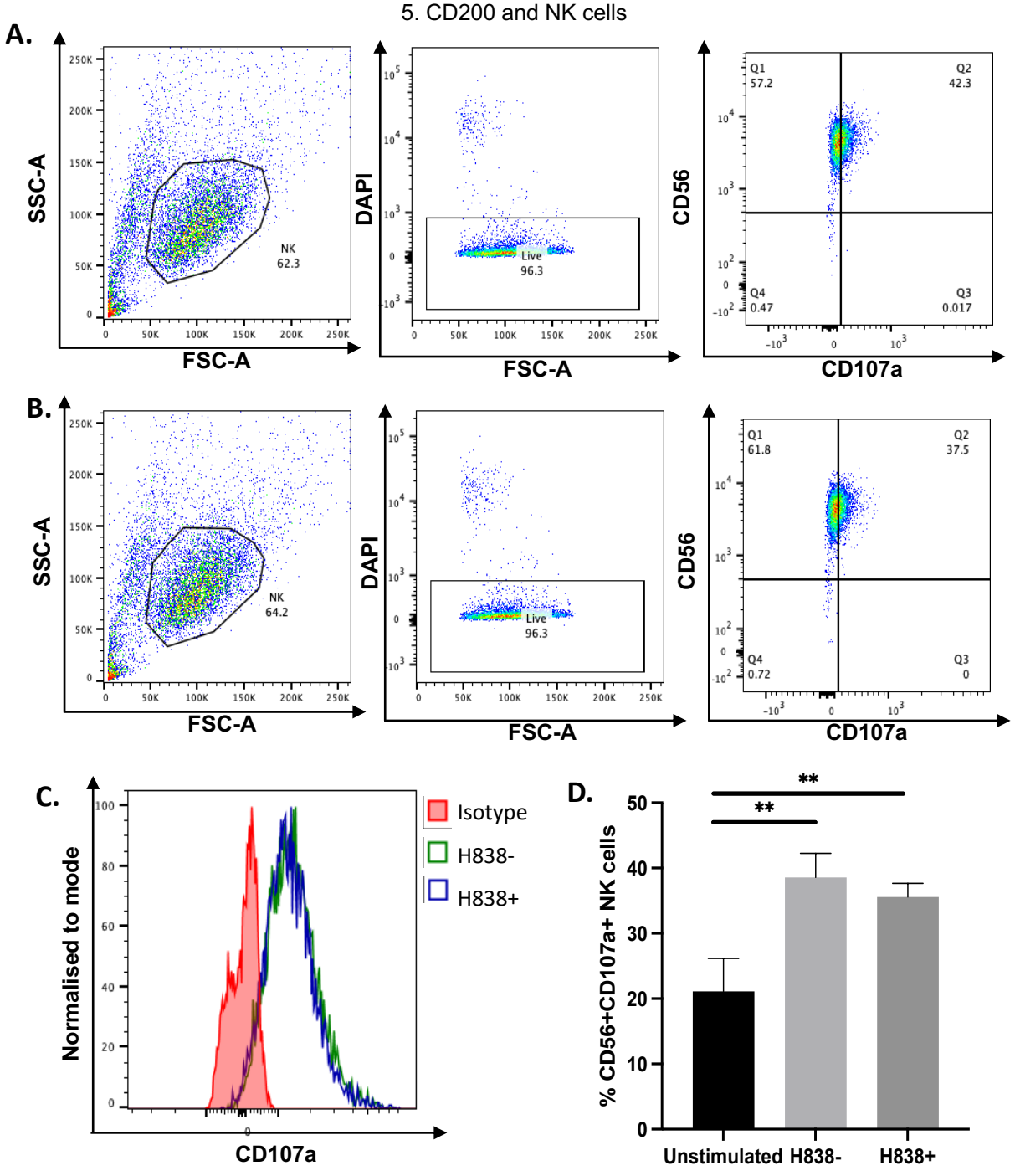

Fig 5.11 The effect of H838 cell CD200 expression on NK-92MI cell degranulation.

Activation of NK cells results in the release of cytotoxic granules containing perforin and granzymes which cause direct lysis of target cells. CD107a lines the surface of these granules and is transiently expressed on the NK cell surface upon degranulation. Addition of a protein transport inhibitor (Monensin) prevents the re-internalisation of CD107a and CD107a expression can be detected by flow cytometry as a measure of NK cell degranulation. NK-92MI cells were co-cultured at a 5:1 ratio with (A) CD200- H838 and (B) CD200+ H838 cells for 4 hours in the presence of a CD107a antibody with the addition of Monensin after 1 hour. Cells were gated on FSC and SSC to eliminate debris, dead cells were excluded through DAPI staining and CD56+CD107a+ cell gates determined using isotype controls to account for background fluorescence. (C) Representative CD107a histograms demonstrate minimal differences in CD107a expression between CD200- and CD200+ H838 cells (D) Both CD200- and CD200+ H838 cells induced a significant increase in the number of degranulating cells compared to unstimulated NK cells. There was a slight decrease in CD107a positivity in the CD200+ H838 cell group compared to the CD200- group. Significance was tested for with a one-way ANOVA with Tukey's multiple comparison test. $P \leq 0.01$ (**).

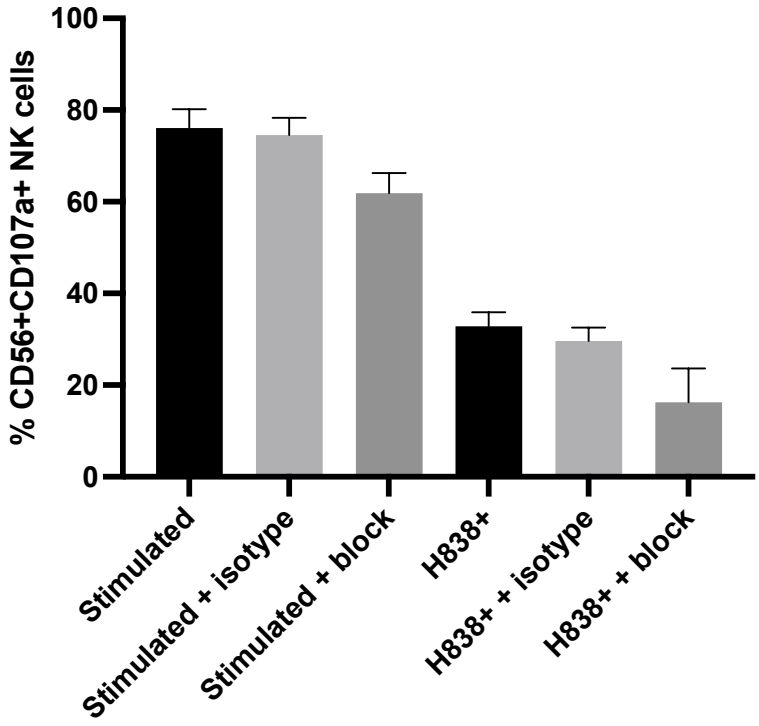

Fig 5.12 Addition of a CD200 blocking antibody further decreased NK-92MI cell degranulation.

Activation of NK cells results in the release of cytotoxic granules containing perforin and granzymes which cause direct lysis of target cells. CD107a lines the surface of these granules and is transiently expressed on the NK cell surface upon degranulation. Addition of a protein transport inhibitor (Monensin) prevents the re-internalisation of CD107a and CD107a expression can be detected by flow cytometry as a measure of NK cell degranulation. (A) NK-92MI cells were cultured for 4 hours with 50ng/ml PMA and 2µg/ml Ionomycin or with CD200+ H838 cells at an NK:target cell ratio of 5:1 alone or in the presence of a CD200 blocking antibody or isotype matched control (n= 4). Addition of a CD200 blocking antibody which binds to CD200 decreased NK-92MI cell degranulation compared to untreated stimulated or CD200+ H838 co-cultured cells. The presence of an isotype matched antibody did not affect NK-92MI cell degranulation, suggesting that this decrease in NK activity is CD200 dependent.

5.2.9 Determining the effects of CD200 expression on NK-92MI IFN-γ release

In addition to their cytolytic function, activated NK cells are also effective producers of a wide range of pro-inflammatory cytokines including IFN-γ. NK-92MI cells were cultured alone, in the presence of PMA and ionomycin (stimulated), or at a 1:1 ratio with CD200- and CD200+ H838 cells for 4 hours, after which the cell suspension was removed, and the NK cells pelleted to allow collection of the supernatant. IFN-γ secretion was determined with a sandwich ELISA, using pre-determined IFN-γ standards. Absorbance levels were blank corrected to either media alone, media plus PMA and ionomycin or H838 cell supernatants (n= 3, Figure 5.13). Unstimulated NK-92MI cells produced an average of 8.667 pg/ml IFN-γ per $1x10^6$ NK cells, significantly increasing by over 16-fold to 143.795 pg/ml upon stimulation (p= ≤0.0001). Stimulation with CD200- H838 cells again significantly increased IFN-γ compared to unstimulated cells (87.214 pg/ml; p= 0.0032); however, stimulation with CD200+ H838 cells did not significantly increase IFN-γ compared to unstimulated cells. Furthermore, CD200+ H838 stimulated NK-92MI cells demonstrated a significant reduction in IFN-γ production compared to CD200- H838 cells (27.043 pg/ml; p= 0.0231) suggesting that H838 CD200 expression had a negative immunoregulatory effect on NK-92MI IFN-γ production. Addition of a CD200 blocking antibody to CD200+ H838 co-cultures confirmed this, with NK-92MI IFN-γ production restored to 66.205 pg/ml, an over 2-fold increase compared to CD200+ H838 cells alone. Moreover, addition of the blocking antibody to stimulated NK-92MI cells and addition of an isotype matched mouse IgG1,κ antibody to the CD200+ H838 co-cultures did not affect IFN-γ production (p= 0.925 and p= >0.9999) suggesting that this increase in IFN-γ production was CD200-specific.

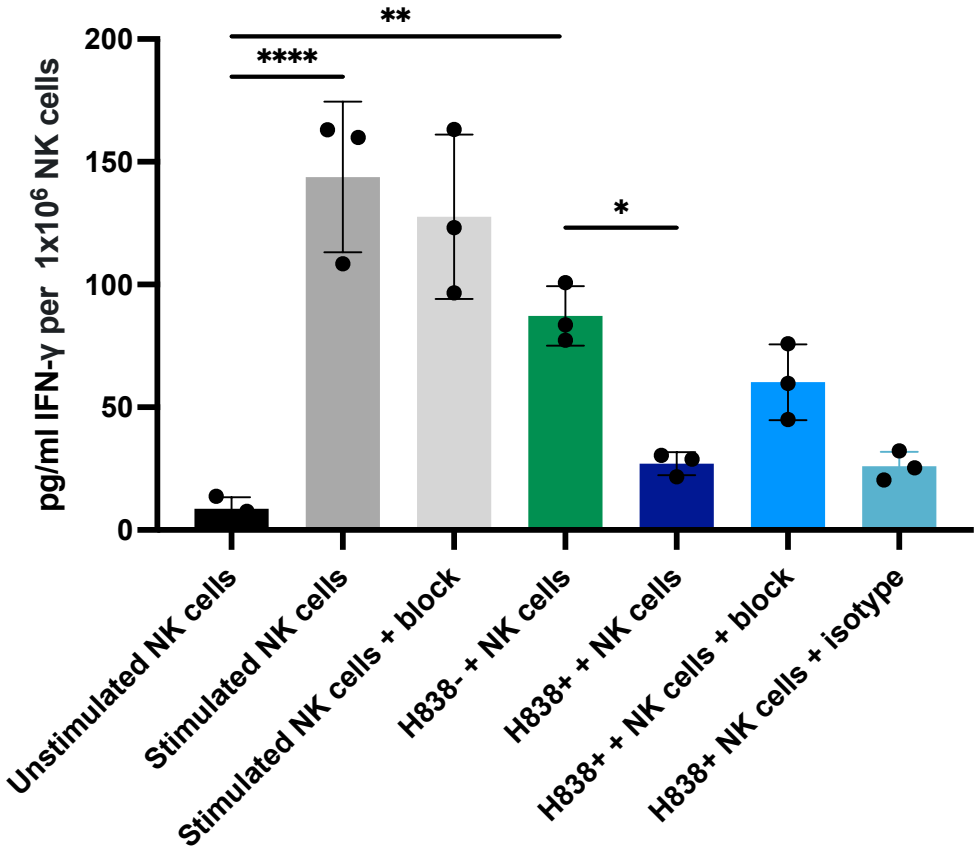

Fig 5.13 The effect of H838 cell CD200 expression on NK-92MI IFN-γ production

In addition to their cytolytic function, activation of NK cells also results in the production of pro-inflammatory cytokines, including IFN-γ, which bridge innate and adaptive immunity and demonstrate anti-tumour activity. NK-92MI cells were cultured for 4 hours alone, with 50ng/ml PMA and 2μg/ml Ionomycin (stimulated) or at a 1:1 ratio with CD200- and CD200+ H838 cells before collection of the cell suspension and pelleting of the cells to collect the supernatant. IFN-γ production was determined with a sandwich ELISA using pre-determined IFN-γ standards. All values were blank corrected to media alone, media plus PMA/ionomycin and H838 cell supernatants. IFN-γ production is presented as pg/ml per $1x10^6$ NK cells. Stimulated NK-92MI cells demonstrated increased IFN-γ production. CD200 expression by H838 cells significantly reduced IFN-γ production compared to CD200- H838 cells. Addition of a CD200 blocking antibody to CD200+ H838 co-cultures was sufficient to restore IFN-γ secretion to close to CD200- H838 cell levels. Addition of the blocking antibody to stimulated NK-92MI cells and an isotype matched control antibody to CD200+ H838 co-cultures confirmed that this increase in IFN-γ production was CD200-specific. Significance was tested for with a one-way ANOVA with Tukey's multiple comparison test. $P \leq 0.05$ (*) $P \leq 0.01$ (**) $P \leq 0.0001$ (****).

5.2.10 Determining the effects of CD200 expression on NK-92MI activating receptor expression

NK cell activity is tightly regulated based on the balance of signals from numerous activating and inhibitory receptors, the expression of which is highly heterogenous, bestowing NK cells with the ability to respond to a large range of stimuli and to regulate the immune response under a variety of pathological conditions. Intratumoural NK cells in NSCLC demonstrate reduced expression of the activating receptors NKp30, NKp80, CD16 and NKG2D and increased CD69 and NKp44 expression compared to peripheral NK cells. The expression of activating and inhibitory receptors can have significant impacts on NK cell activation and function; therefore, the effect of CD200 expression on NK-92MI cell receptor expression was assessed.

First, the expression of CD16, CD56 and the activating receptors Nkp30, Nkp44, Nkp46 and NKG2D were analysed in unstimulated cells (n= 3; Figure 5.14). CD16 (FcγRIII), a low affinity receptor for the Fc portion of IgG and CD56, an isoform of neural cell adhesion molecule which mediates homotypic adhesion are used to categorise NK cell phenotypes into 5 categories based on their relative expression levels. As an activating receptor, CD16 recognises the constant Fc portion of IgG antibodies bound to antigens on target cells, enabling NK cells to enact antibody-dependent cell cytotoxicity. As a $CD56^{bright}CD16^{-}$ NK cell line, NK-92MI demonstrate strong CD56 expression but no CD16 expression (Figure 5.14a). Nkp30, NKp44 and Nkp46 are natural cytotoxicity receptors (NCRs) which recognise a diverse set of host- and pathogen-encoded ligands which stimulate the activation of NK cells. NK-92MI cells were positive for NKp30 (mean 98.03%) and NKp46 (mean 91.53%) but negative for Nkp44 (Figure 5.14b-d). NKG2D is an activating receptor distantly related to the NKG2 family that recognises homologues of MHC class I molecules which are regulated by both the heat shock response and DNA damage pathways; activation of NKG2D promotes NK cell target adhesion and immunological synapse formation (Lanier 2008). NK-92MI cells were negative for NKG2D (Figure 5.14e).

Having characterised NK-92MI cell activating NCR and NKG2D receptor expression (Figure 5.14f), the effect of tumour CD200 expression on their expression was assessed by flow cytometry (n= 3; Figure 5.15). NK-92MI cells were cultured alone or at 5:1 NK:target cell ratio with CD200+ and CD200- H838 cells for 16 hours and the percentage of receptor positive cells determined (n= 2-3). Stimulation of NK-92MI cells with both CD200- (82.6%; p= 0.0118) and CD200+ (67.14%; p= 0.00268) H838 cells significantly reduced Nkp30 expression compared to unstimulated cells (92%)(Figure 5.15a). Furthermore, the percentage of Nkp30 positive NK-92MI cells was significantly less when co-cultured with CD200+ cells compared

to CD200- cells (p= 0.0057), suggesting CD200 expression may further decrease Nkp30 expression. This decrease in the proportion of NKP30 expressing NK-92MI cells was also reflected in the intensity of the NKp30 expression, with the median fluorescence intensity (MFI) of the cells stimulated with CD200- H838 (p= 0.0363) and CD200+ H838(p= 0.0054) cells significantly decreased compared to unstimulated cells (Figure 5.15b). In contrast, both the proportion of NK-92MI cells positive for and the NCRs NKp44 and NKp46 the intensity of their expression did not significantly change when cultured with CD200+ or CD200- cells, suggesting their expression may not be regulated by ligands expressed on H838 cells or by CD200 (Figure 5.15a,b). Unlike the NCRs, the proportion of NK-92MI cells expressing of NKG2D was increased upon stimulation with H838 cells, with CD200+ H838 cells inducing significantly greater numbers of NKG2D positive NK-92MI cells when compared to unstimulated cells (p= 0.032). This increase in NKG2D expression for both H838 cell populations suggests that ligands expressed by these tumour cells may stimulate NKG2D expression, with CD200 further enhancing this effect. However, no significant changes in overall intensity of NKG2D expression was observed, with the overall intensity of NKG2D expression unchanged between conditions, suggesting NKG2D expression may not be regulated by these cells or by CD200 expression (Figure 5.15b). Expression of the inhibitory receptor CD200R has been observed to increase on exhausted immune cells in the NSCLC TME, however CD200R expression was similar in unstimulated (98.2%; MFI 529) and CD200+ H838 stimulated cells (98.9%; MFI 517.5), with a slight decrease seen for CD200- H838 cells (92.27%; MFI 468.3) (Figure 5.15a.b). However, as CD200R expression was almost saturated in unstimulated cells it is unsurprising that no significant increases were observed. Taken together, ligands on H838 cells increase the expression of the activating receptor NKG2D and decrease expression of the NCR Nkp30 on NK-92MI cells, with CD200 expression further enhancing these changes.

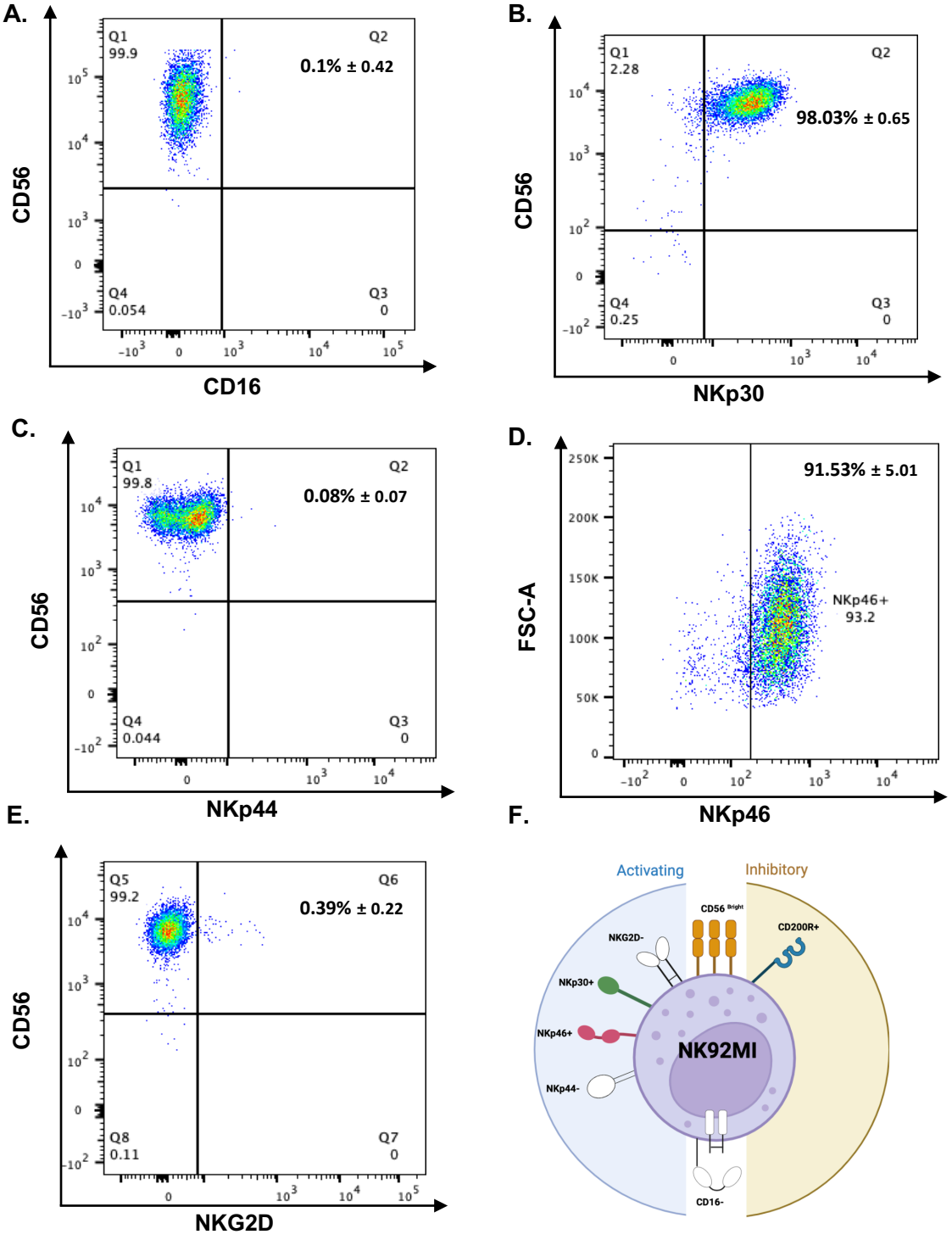

Fig 5.14 Determining NK-92MI activating receptor and NCR expression.

NK cell activity is tightly regulated by signals from inhibitory and activating receptors on the surface of NK cells. The expression of certain activating receptors has been demonstrated to be altered in intratumoural NK cells in NSCLC, with CD200 expression in AML shown to affect NK NCR expression. Prior to assessing the effects of NSCLC CD200 on NK activating receptor expression, their expression in unstimulated NK-92MI cells was assessed by flow cytometry (n= 3). (A) CD16 is not expressed by NK-92MI cells. (B) NK92-MI cells demonstrate strong NKp30 expression but no (C) NKp44 expression. (D) NKp46 is expressed by most NK-92MI cells, whilst no NK-92MI cells express (E) NKG2D. (F) Schematic of the activating and inhibitory receptors expressed (colour) and not expressed (white) by NK-92MI cells. Positive cells are presented as % ± SD.

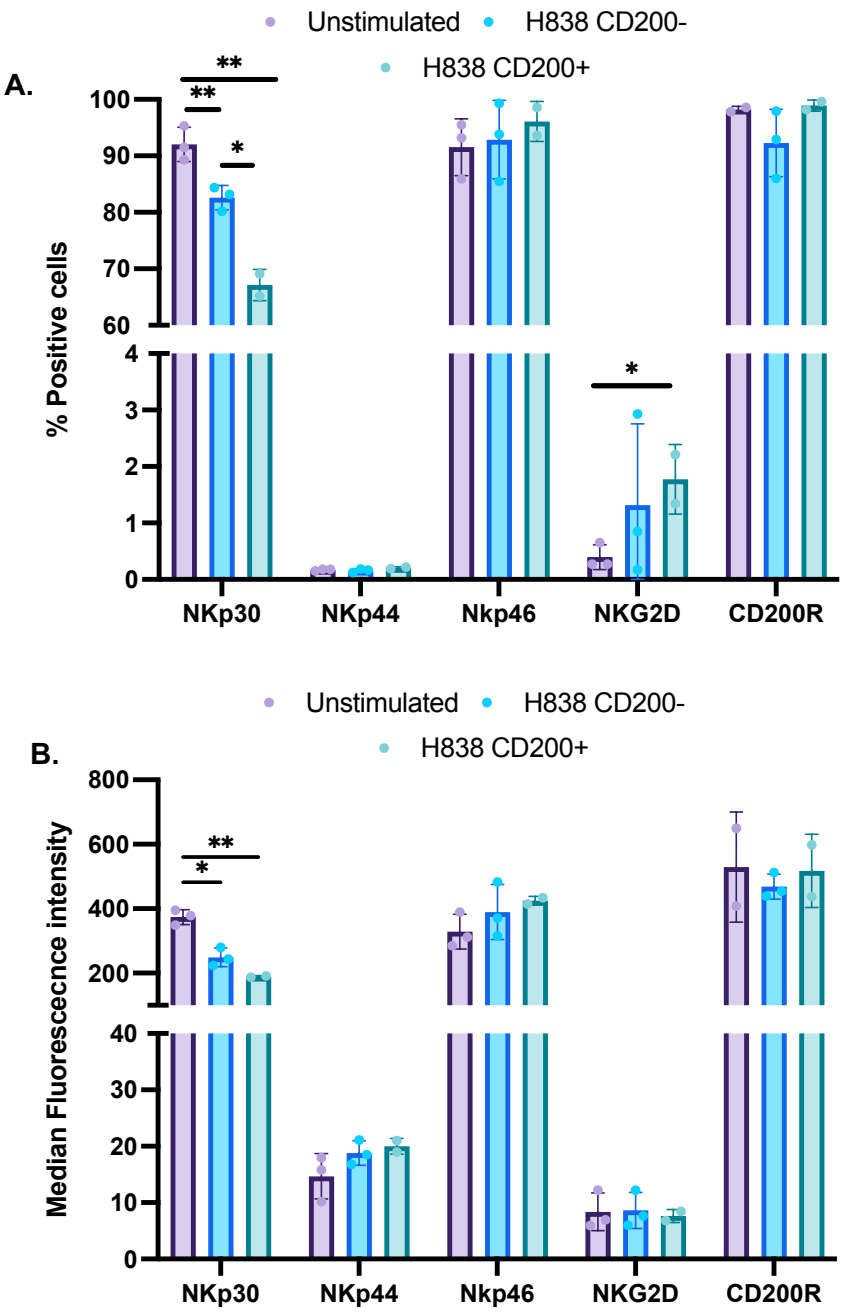

Fig 5.15 H838 CD200 expression alters NK-92MI NCR and activating receptor expression.

NK-92MI were cultured alone or at a 5:1 NK:target cell ratio with CD200- and CD200+ H838 cells for 16 hours before staining for activating and inhibitory receptors by flow cytometry (n= 2-3). (A) The number of NK-92MI cells positive for Nkp30 significantly decreased when stimulated with CD200- and CD200+ H838 cells, with CD200 expression further decreasing Nkp30 expression. Expression of the other NCRS Nkp44 and NKp46 remained unchanged between unstimulated and stimulated cells. In contrast, expression of NKG2D increased upon stimulation with CD200- and CD200+ H838 cells, with CD200 expression significantly increasing the number of NKG2D+ cells compared to unstimulated cells. CD200R expression remained unchanged between conditions. (B) Median fluorescence intensity demonstrated a significant decrease in the intensity of NKp30 expression when NK-92MI cells were stimulated with CD200- and CD200+ H838 cells, with CD200 expression further decreasing NKp30 expression. No other significant differences in the intensity of NK-92MI NCR or activating receptor expression were observed. Significance was tested for with a one-way ANOVA with Tukey's multiple comparison test $P \leq 0.05$ (*) $P \leq 0.01$ (**) $P \leq 0.001$ (***) $P \leq 0.0001$ (****).

5.2.11 Determining the effects of CD200 expression on NK-92MI cell viability

Thus far, the data suggests that CD200 expression on H838 cells confers resistance to these cells from CD200R+ NK-92MI mediated attack, with CD200+ cells demonstrating greater cell viability when co-cultured with NK cells compared to CD200- cells. Having demonstrated that CD200 expression has an immunomodulatory on NK cell degranulation, IFN-γ release and activating receptor expression, the viability of interacting NK-92MI cells was analysed to determine whether tumour CD200 expression may be affecting NK cell viability (n= 4; Figure 5.16). First, CellTiter Glo was used to determine NK-92MI cell viability after co-culture with CD200+ and CD200- H838 cells. After 4 hours co-culture, the NK cells were removed and plated with equal volumes of CellTiter Glo reagent, with untreated NK cells used as a control to determine overall viability and NK cell death (Figure 5.16). At all NK:target cell ratios, the percentage of NK-92MI cell death was greater in CD200+ co-cultured cells than CD200- cells. The percentage of dead NK-92MI cells from CD200- cultures remained fairly constant at 5:1, 2:1, 1:1 and 0.5:1 ratios at 30-39%. In contrast, NK-92MI cell death increased with decreasing NK:target cell ratios from 12.86% at 10:1 to 63.2% at 0.5:1. Furthermore, at the 0.5:1 NK:target cell ratio, NK-92MI cell viability was significantly lower after co-culture with CD200+ cells than CD200- cells ($p= 0.0358$), suggesting that CD200 expression on H838 cells may be inducing interacting NK cell death.

To further explore the effects of CD200 on NK-92MI cell viability, NK cells were cultured in the presence of a recombinant human CD200 Fc chimera protein peptide. CD200 peptide function was confirmed by western blot of whole cell lysates taken from NK-92MI cells cultured in the presence of CD200 for 30 minutes and 1 hour (Figure 5.17a,b). Activation of CD200R by CD200 results in activation of the inhibitory effectors SHIP and RasGAP which inhibit downstream RAS/MAPK signalling. ERK1 and ERK2 are downstream effectors of the RAS-MAPK pathway and are phosphorylated upon activation of the pathway therefore, the expression of p-ERK1/2 was used as a measure of RAS/MAK signalling. Addition of the CD200 peptide to NK-92MI cells caused a reduction in p-ER1/2 expression at 30 minutes and 1 hour, but no changes in total ERK1/2 expression suggesting that the CD200 peptide was functional as it could inhibit the RAS/MAPK pathway in NK-92MI cells. Having established that the peptide was functional, the viability or NK-92MI cells cultured in the presence of CD200 was assessed using the Incucyte live cell imaging system (Figure 5.17c). NK-92MI cells were cultured in the presence of 4µg of CD200 per $1x10^6$ cells for 48 hours and the number of apoptotic cells per mm^2 assessed every 2 hours using a Annexin V fluorescent antibody. The addition of the CD200 peptide significantly increased the number of apoptotic cells relative to untreated NK-92MI cells at 28 ($p< 0.0001$), 30 ($p= 0.0015$), 32 ($p= 0.0054$), 40 ($p= 0.014$), 42 ($p= 0.0214$), 44 ($p= 0.0082$), 46 ($p= 0.294$) and 48 hours ($p= 0.0135$), with an average of 34.86

apoptotic cells per mm^2 in the CD200 treated cells compared to 8.384 in the untreated group, an over 4-fold increase. Taken together, this suggests that CD200 may be inducing apoptosis in interacting CD200R+ NK-92MI cells, thus further enhancing the immune resistance CD200+ tumour cells possess against NK-induced cell death.

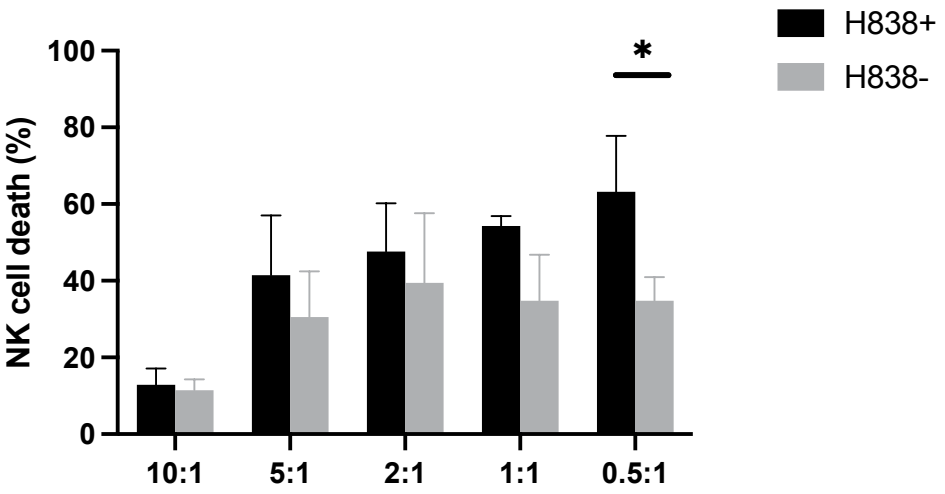

Fig 5.16 Co-culture with CD200+ H838 cells induces NK-92MI cell death.

NK-92MI were cultured at increasing NK:target cell ratios with CD200- and CD200+ H838 cells for 4 hours and NK cell viability assessed by CellTiter Glo (n= 4). Untreated NK-92MI cells served as a control, with NK cell death determined relative to untreated cells. Culture of NK-92MI cells with CD200- H838 cells resulted in 15-39% NK cell death between 10:1 to 0.5:1 NK:target cell ratios, with cell death plateauing at the 5:1 ratio. In contrast, NK-92MI cell death increased with decreasing NK:target cell ratios with CD200+ H838 cells, with NK cell death significantly greater than CD200- H838 cultured cells at the 0.5:1 ratio. This suggests that CD200 may be inducing NK-92MI cell death. Significance was tested for with a one-way ANOVA with Tukey's multiple comparison test $P \leq 0.05$ (*).

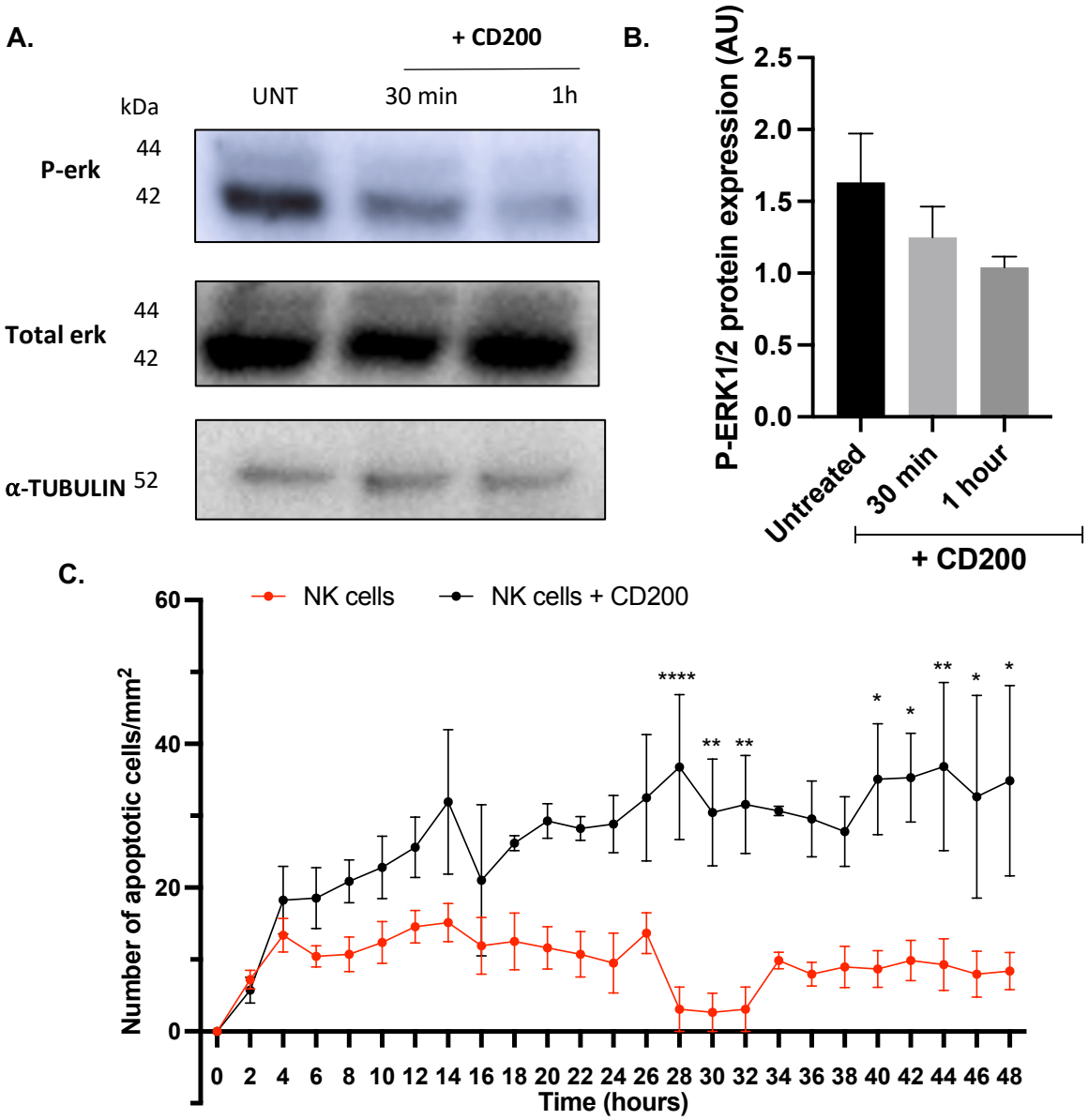

Fig 5.17 Treatment of NK-92MI cells with a CD200 peptide increases NK cell apoptosis.

NK-92MI were cultured in the presence of 4µg / 1x10^6 cells of a recombinant human CD200 Fc chimera protein peptide. (A) Whole cell lysate western blot analysis of NK-92MI cells cultured in the presence of the CD200 peptide for 30 minutes and 1 hour were probed for total ERK1/2 and p-ERK1/2 expression. Phosphorylation of ERK1/2 is a marker of RAS/MAPK pathway activation; CD200R activation results in downstream signals which inhibit the RAS/MAPK pathway therefore reduced p-ERK1/2 is a marker of active CD200R signalling. The CD200 peptide function was confirmed with a reduction of p-ERK1/2 seen at 30 minutes and 1 hour. (n=3) (B) Quantification of p-ERK1/2 protein expression from western blots also demonstrates a decrease in p-ERK1/2 expression at 30 minutes and 1 hour (n=3). (C) NK-92MI cells were cultured in the presence of the CD200 peptide and their viability assessed using the IncuCyte live cell imaging system (n= 3). Cells were cultured in the presence of CD200 and a fluorescent caspase-3 antibody for 48 hours with images taken every 2 hours with apoptosis presented as number of apoptotic cells per mm^2. CD200 treated NK-92MI cells demonstrated significantly greater numbers of apoptotic cells compared to untreated NK-92MI cells at some time points. Significance was tested for using a repeated measures one-way ANOVA with Holm-Sidak's multiple comparisons. P ≤ 0.05 (*) P ≤ 0.01 (**) P ≤ 0.001 (***) P ≤ 0.0001 (****). ERK, extracellular signal-regulated kinases.

5.3 Discussion

Immunotherapies which inhibit immune checkpoints, a source of immune escape for a number of cancers, are becoming an important method of treatment for NSCLC patients. In PD-1 blockade, the re-invigoration of T cells responses has been widely recognised as the primary mediator of the anti-tumour immune response (Khan *et al.* 2020). However, NK cells are becoming a newly emerging target, with the observation of strong clinical responses in tumours with low expression of MHC class I molecules and low mutational burden suggesting that NK cells are a major subpopulation responsible for the therapeutic effects of PD-1 blockade (Cho *et al.* 2020). The importance of NK cells in immune checkpoint inhibition is further highlighted by the observation that several immune checkpoints including CTLA-4, PD-1 and CD200 all cause NK cell phenotypic and cytotoxic dysfunction within the TME of various cancers. In NSCLC, NK cells within the TME are dysfunctional and have an impaired ability to kill tumour cells (Carrega *et al.* 2008a; Platonova *et al.* 2011).

5.3.1 Generating an *in vitro* model of CD200R+ NK cell CD200+ tumour cell interaction

In order to explore the effects of tumour CD200 expression on interacting CD200R+ NK cells, an *in vitro* model consisting of an established NK cell line and established CD200 transduced tumour cells was generated. The NK-92MI cell line is a $CD56^{bright}CD16^{-}$ IL-2-independent NK cell line with phenotypical and functional characteristics of primary human NK cells (Konstantinidis *et al.* 2005). NK-92 cells, the IL-2-dependent form, have been widely used in preclinical applications and have been clinically investigated as an allogeneic NK therapeutic in breast cancer and NSCLC models (Hodgins *et al.* 2019). Although the $CD56^{bright}CD16^{-}$ subset of NK cells are only a minor subset in the blood, characterised by low levels of perforin and high cytokine production, the $CD56^{bright}CD16^{-}$ subset is highly enriched in NSCLC tumour infiltrate, suggesting that NK-92MI cells are a clinically relevant model to explore NK cell function in NSCLC (Carrega *et al.* 2008b). Furthermore, NK-92MI cells demonstrated strong CD200R+ expression. Having identified a relevant NK cell model, the effect of tumour CD200 expression on the ability of NK-92MI cells to kill target cells was explored using transduced CD200+ and CD200- HeLa cells previously generated in the lab. In this model, CD200 expression by HeLa cells conferred significant immune resistance to the tumour cells against NK-92MI cytotoxicity, with tumour cell viability in CD200+ much greater than that of CD200- cells. Having demonstrated the immunosuppressive capacity of CD200 towards CD200R+ NK cells in HeLa cells, the effect of NSCLC CD200 expression on interacting NK cells was explored.

5.3.2 CD200 expression in NSCLC cell lines

Previous work in this thesis, and the work of others in the literature, has demonstrated that CD200 expression is seen in the tumours of both adenocarcinoma and SCC patients. Therefore, the first step was to define CD200 expression in several established NSCLC cell lines consisting of 2 adenocarcinomas, 2 SCCs, 1 adenosquamous carcinoma and 1 large cell carcinoma. Of the 6 tumour cell lines assessed for CD200 expression by qRT-PCR, western blot, and flow cytometry, only the SCC cell line H226 consistently demonstrated strong CD200 expression, with all other cell lines demonstrating very little to no expression consistently. In addition to cell surface CD200 expression, H226 cells also released soluble CD200 into the supernatant. However, the ELISA used was based on a CD200 capture antibody rather than CD200R; therefore, the capacity of sCD200 to bind to CD200R and the functional role of this soluble form released from H226 cells was not specifically evaluated or assessed in this thesis. Further studies using the sCD200+ supernatants from these cultures would be of benefit to determine whether CD200 could also signal to CD200R+ cells independent of cell-cell interactions. Having characterised CD200 expression in the NSCLC cell lines and identified a CD200+ SCC line, the susceptibility of each line to NK-92MI cytotoxicity *in vitro* was assessed using NK:target cell co-cultures.

Although NK-92MI cells demonstrate a high degree of cytotoxicity towards a range of tumour cells without prior sensitisation, not all tumour cells possess the correct array of activating and inhibitory ligands to activate NK-92MI cells. As H226 cells already naturally expressed CD200, they were seen as an ideal candidate for the NK:tumour cell model; however, H226 cells demonstrated resistance to NK-92MI cells, with H226 cells even increasing in number during the 4 hour co-cultures. Antibody-mediated blocking of CD200 did not increase tumour cell death and a subsequent literature search found that H226 cells are resistant to lysis by primary peripheral blood and interstitial lung NK cells, suggesting that other mechanisms are responsible for H226 cell resistance to NK-92MI cytotoxicity (Robinson and Morstyn 1987; Robinson *et al.* 1989). The adenocarcinoma A549, SCC SK-MES-1 and adenosquamous H596 cell lines all showed susceptibility to NK-92MI cells but tumour cell death plateaued between 20-40% and did not increase with increasing NK:target cell ratios, suggesting that although they are susceptible to NK-92MI cytotoxicity, they also possess mechanisms of resistance to NK-92MI-mediated cell death. The adenocarcinoma cell line H838 was the only NSCLC line to demonstrate increasing cell death with increasing NK:target cell ratios, suggesting these cells must express the correct repertoire of activating and inhibitory ligands to stimulate NK-92MI cells and activate their cytotoxic function. Therefore, based on this dose-dependent NK-92MI cell susceptibility, H838 cells were transduced with GFP or CD200+GFP retroviruses to produce a stable CD200+ and CD200- adenocarcinoma cell line.

5.3.3 Tumour cell CD200 expression suppresses NK-92MI function

NK cells isolated from the NSCLC TME and NK cells from CD200^{high} AML patients both demonstrate reduced cytotoxic function against target cells as determined by decreased proportions of CD107a+ degranulating cells and reduced IFN-γ cytokine production. This similar phenotype of impaired cytotoxicity suggested that CD200 expression in the NSCLC TME may contribute to NK cell dysfunction. Therefore, the effect of tumour CD200 expression on interacting CD200R+ NK-92MI cell tumour killing capacity, degranulation and IFN-γ production was determined to assess whether CD200 contributes to NK cell immune evasion in NSCLC. CD200 expression by H838 cells conferred significant resistance to NK-92MI cytotoxicity, with tumour cell viability much greater in CD200+ cells compared to CD200- cells. Furthermore, blocking of CD200 signalling with a CD200 antibody reinstated CD200+ H838 cell susceptibility to NK-92MI cells, restoring tumour cell death back to the same level as CD200- cells. The addition of an isotype matched control antibody had no effect on tumour cell death, demonstrating that blocking CD200 signalling is sufficient to prevent CD200+ cell NK immune evasion.

Although NK cells can kill target cells through ligation of death receptors or the production of pro-inflammatory cytokines, NK cell-mediated lysis of target cells is mainly achieved directly through release of cytotoxic granules containing effector perforin and granzymes. The CD107a flow cytometry assay is a commonly used assay in NK cell research that determines the level of NK cell degranulation using CD107a positivity as a measure; CD107a is expressed within cytotoxic granules and is expressed on the cell surface upon degranulation. As expected, stimulation of NK-92MI cells with PMA and ionomycin significantly increased the number of activated degranulating cells. Upon stimulation with CD200+ and CD200- H838 cells, NK-92MI cells demonstrated a slight reduction in degranulation towards CD200+ cells. Addition of a CD200 antibody appeared to further decrease NK-92MI cell degranulation both alone and in the presence of CD200+ H838 cells, suggesting that CD200+ tumour cell NK immune evasion may be occurring through suppression of a different NK cell function or other activation mechanism.

In addition to direct lysis through degranulation, activated NK cells are also effective producers of an array of cytokines including IFN-γ, TNF-α, GM-CSF and IL-10 and chemokines such as CCL3 CCL4 and CCL5 (Paul and Lal 2017). Of these, IFN-γ is one of the most potent and plays a crucial role in bridging innate and adaptive immunity and exerting anti-bacterial, anti-viral and anti-tumour functions (Ortaldo *et al.* 2006). Secretion of IFN-γ by NK cells can promote the maturation and activation of DCs, macrophages and T cells, promote the priming and differentiation of Th1 cells and enhance MHC class II expression on APCs (Martín-

Fontecha *et al.* 2004; Walzer *et al.* 2005; Vivier *et al.* 2008). In addition, IFN-γ from NK cells has been shown to enhance tumour immunogenicity through the upregulation of MHC class I molecules on tumour cells and more directly though anti-proliferative, anti-angiogenic and pro-apoptotic functions (Kaplan *et al.* 1998; Paul and Lal 2017). As such, IFN-γ is an important measure of NK anti-tumour activity. As expected, stimulation of NK-92MI cells with PMA/ionomycin significantly increased IFN-γ production, as did co-culture with CD200- H838 cells. However, stimulation with CD200+ H838 cells did not significantly increase IFN-γ secretion compared to unstimulated cells and the IFN-γ produced by NK-92MI cells was significantly less than that produced when cultured with CD200- cells. Blockade of this signalling with the CD200 blocking antibody restored IFN-γ secretion to CD200- H838 levels, suggesting that blocking CD200 alone was sufficient to increase NK-92MI IFN-γ production.

A limitation of the model used in this chapter is the use of 2D cancer cell lines. Despite being the most widely used *in vitro* model, characterised by their low cost and ease of availability, cancer cells may undergo genetic alterations and lose the original genetic heterogeneity of the tumour; furthermore, monolayer immortalised cancer cells lack the ability to mimic the *in vivo* TME, a driving factor in cancer growth and progression (Xu *et al.* 2022). In recent years, the development of NSCLC organoids, 3D cell cultures embedded in extracellular matrix which critically reflect tumour architecture, cell type diversity and function, have advanced the field of pre-clinical NSCLC models. In contrast to 2D cell lines, organoids preserve key histological and molecular traits of their parental tumours and provide the opportunity to mimic cell-cell communication between tumour cells and other cells within the TME such as fibroblasts and immune cells (Yuki *et al.* 2020). The use of organoid and immune cell co-cultures provides a more physiologically relevant model which could more accurately represent the NSCLC TME and could be a useful tool in the future to further our understanding of the role of tumour cell CD200 expression on interacting NK cells.

5.3.4 Tumour cell engagement alters NK-92MI activating receptor expression

Having established that tumour CD200 expression suppresses interacting CD200R+ NK cell cytotoxic function, the effect of CD200 on NK activating receptor expression was assessed. NK cell activation is a complex process involving both the loss of inhibitory receptor-mediated signalling and the presence of activating ligands to engage activating receptors such as NKG2D and the NCRs NKp30, NKp44 and NKp46. Given that the dynamic expression of both inhibitory and activating receptors is crucial for optimal NK anti-tumour activity, defective activating receptor expression is likely to contribute to impaired NK cell function. Indeed, decreased NK activating receptor expression has been associated with poor prognosis in many cancers.

Unstimulated NK-92MI cells were positive for the NCRs NKp30 and NKp46 and negative for NKG2D and NKp44. Stimulation of NK-92MI cells with CD200- H838 cells for 16 hours resulted in a significant decrease the proportion or NKp30 cells and the intensity of expression, with CD200+ H838 cell co-culture further decreasing NKp30 expression. This suggests that NKp30 expression is downregulated when stimulated with H838 cells but that CD200 signalling further enhances this effect. Downregulation of NKp30 has been seen on intratumoural NK cells from NSCLC patients and in $CD200^{high}$ AML patients, suggesting that CD200 expression may be responsible, at least in part, for the altered NKp30 expression on NK cells within the NSCLC TME. Studies using a CD200 blocking antibody are needed to determine whether blocking this interaction would be sufficient to reverse the decrease in NKp30 expression. In contrast, tumour CD200 expression significantly increased the proportion of NKG2D expressing NK-92MI cells compared to unstimulated cells; however, it should be noted that NKG2D MFI remained unchanged between conditions. This suggests that despite a greater proportion of NK-92MI cells expressing NKG2D when stimulated with CD200+ tumour cells, that the overall intensity of NKG2D receptor expression remained unchanged.

5.3.5 Tumour cell CD200 expression decreases NK-92MI cell viability

In addition to demonstrating that tumour CD200 expression causes a reduction in NK cell degranulation and IFN-y production and alters NK cell activating receptor expression, work in the previous chapter demonstrated that CD200 expression negatively correlated with NK cell number in NSCLC tumours, suggesting that tumour CD200 expression may reduce the number of interacting NK cells. Therefore, the effects of tumour CD200 expression on CD200R+ NK cell viability were assessed to determine whether CD200+ tumour cells were inducing NK cell death and consequently reducing infiltrating NK cell numbers. Using NK-92MI cells taken from H838:NK co-culture experiments, CD200 expression by H838 cells significantly decreased NK cell viability at the 0.5:1 NK:target cell ratio, with NK-92MI viability reduced at all ratios compared to CD200- H838 co-cultures. Furthermore, treatment of NK-92MI cells with a functional CD200 peptide, as evidenced by a decrease in p-ERK1/2 signalling at 30 minutes and 1 hour, significantly increased the number of apoptotic cells present when compared to untreated NK-92MI cells at 8 time points, with an average 4-fold increase in NK-92MI apoptosis compared to untreated cells. This suggests that CD200 expression can reduce interacting CD200R+ NK cell viability. To date, CD200 has not been implicated in the induction of immune cell apoptosis however, CD200-mediated NK cell apoptosis may be another immunoregulatory mechanism by which CD200+ tumours can inhibit NK cell function and evade an anti-tumour immune response. This decrease in NK cell

viability may explain why tumour CD200 expression negatively correlated with the number of infiltrating CD56+ cells in our adenocarcinoma patient cohort. Further studies would be required to determine which apoptotic pathway CD200 signalling is inducing and whether this could be inhibited by addition of a CD200 blocking antibody.

5.3.6 Conclusions

NK cells are important mediators of anti-tumour immunity, with their presence associated with good prognosis in NSCLC patients, as seen in the previous chapter. Therefore, in order to evade immune attack tumours must develop mechanisms to subvert NK cell phenotypes or induce NK exhaustion resulting in inefficient anti-tumour effector function. In NSCLC, intratumoural NK cells demonstrate reduced cytolytic and cytotoxic activity *in vitro*, as evidenced by a reduction in cytolytic function and an impaired ability to produce IFN-γ upon stimulation, and an alteration in activating NK cell receptor expression. This same NK cell phenotype is also observed in NK cells taken from $CD200^{high}$ AML patients. Hence, the role of tumour CD200 expression on the function and activating receptor repertoire of interacting CD200R+ NK cells was investigated *in vitro* to determine whether CD200 signalling could be partly responsible for this defective NK cell phenotype. Tumour CD200 expression resulted in dysfunctional interacting NK cells, characterised by a decrease in degranulation and IFN-γ production and an alteration in the activating receptor repertoire which resulted in inefficient anti-tumour activity and a decreased ability to kill CD200+ tumour cells. Furthermore, tumour CD200 expression induced apoptosis in interacting CD200R+ NK cells which could explain why NK cell number negatively correlated with tumour CD200 expression in adenocarcinoma. Taken together, this suggests that tumour CD200 expression in NSCLC causes phenotypic changes in interacting CD200R+ NK cells which results in inefficient anti-tumour effector function. Moreover, addition of a CD200 blocking antibody could increase IFN-γ production and reverse the increased resistance of CD200+ cells to NK cell cytotoxicity, reverting tumour cell death back to CD200- tumour cell levels, suggesting that blocking CD200 signalling may be of clinical benefit to NSCLC patients.

Chapter 6:
General discussion

6. General discussion

In order to grow in the face of a competent immune system, tumour cell variants must acquire a number of genetic and epigenetic changes which provide them with the ability to evade detection and elimination by the immune system (Dunn et al. 2004). One such immune evasion mechanism is the expression of immunoregulatory immune checkpoint molecules by tumour cells. Immune checkpoints are negative co-stimulatory pathways which interact with their ligands to regulate the activation and function of immune cells at multiple stages during the immune response. Under normal physiological conditions, immune checkpoints protect the host by maintaining immune homeostasis and preventing over-activation of the immune system, yet there is evidence that tumour cells can enhance these regulatory mechanisms as a form of immune subversion to enable immune escape and growth (Dyck and Mills 2017). The discovery of tumour cell immune checkpoint expression and the development of ICIs to re-invigorate anti-tumour immunity by interrupting this immunosuppressive signal has transformed the immunotherapy field in recent years (Darvin et al. 2018). In NSCLC, ICIs against the PD-1/PD-L1 immune checkpoint pathway are the standard of care for first-line treatment of advanced SCC and adenocarcinoma tumours, with subsets of patients who respond to these therapies demonstrating exceptionally long-lasting responses and survival (Brueckl *et al.* 2020; NICE 2021). However, despite subsets of patients deriving durable benefits with PD-1/PD-L1 ICI therapy, overall response rates are 47-63%, with many patients showing primary resistance mechanisms (Doroshow et al. 2019). Furthermore, of those that do show an initial or sustained response, disease relapse and progression occurs in most cases due to acquired secondary resistance mechanisms within the TME (Popat et al. 2020). Therefore, identification of additional immune checkpoints to be used to generate multi-modality immunological therapies could greatly improve the success of PD-1/PD-L1 ICI therapies in NSCLC.

In this thesis, the expression of the immune checkpoint CD200 was characterised in NSCLC and its potential role in immune evasion explored to determine whether CD200 could be a potential new immunotherapy target in NSCLC. Using patient samples, bioinformatics analysis and *in vitro* immune cell techniques it was shown that:

(i) CD200 is expressed in NSCLC tumours and to a greater extent in adenocarcinomas

(ii) Tumour CD200 expression altered the infiltrating immune cell composition, with CD200 high adenocarcinoma tumours demonstrating increased Treg and decreased NK cell infiltration

(iii) Tumour CD200 expression induced dysfunction in interacting CD200R+ NK cells that could be reversed by blocking CD200 signalling

Taken together, these results suggest that CD200 expression by NSCLC tumours may be another mechanism of immune evasion utilised by these cells and that blocking CD200 signalling may represent a novel therapeutic target in NSCLC.

6.1 CD200 is expressed in NSCLC tumours

CD200 is a highly conserved transmembrane glycoprotein related to the B7 family of receptors that functions through interaction with its receptor, CD200R, on immune cells to induce a negative immunoregulatory signal to control the immune response (Rijkers *et al.* 2008). Under normal physiological conditions, CD200 signalling functions to maintain immune homeostasis by regulating and maintaining self-tolerance and preventing over activation of the immune system; however, its expression on tumour cells has been confirmed in several different malignancies where it is associated with suppression of the immune response and subsequent immune evasion (Rygiel and Meyaard 2012). CD200 expression has been demonstrated in a number of haematological malignancies including MM, AML and CLL as well as in solid cancers such as ovarian, breast, testicular, renal, melanoma, bladder and prostate (Moreaux *et al.* 2006; Tonks *et al.* 2007; Moreaux *et al.* 2008; Wong *et al.* 2010). At the inception of this project there was little data in the literature on CD200 expression in NSCLC, with the limited data available based on bulk microarray analysis. NSCLC tumours have a high somatic TMB, making them a prime candidate for ICI therapy. Furthermore, CD200 signalling is also a critical mechanism by which lung immune homeostasis is maintained (Grant et al. 2021). Airway macrophages and interstitial DCs demonstrate high basal CD200R expression relative to their other tissue counterparts, with CD200 expression on luminal airway epithelium and type II alveolar cells binding to and preventing their activation in the absence of appropriate inflammatory stimulation (Snelgrove et al. 2008; Jiang-Shieh et al. 2010). Taken together, this suggested that CD200 signalling may represent another mechanism of NSCLC immune evasion. Therefore, the first aim of this thesis was to characterise CD200 expression in the normal lung and in NSCLC tumours.

Using immunohistochemistry, CD200 expression was first explored in the mouse lung wherein it was seen at a moderate level on all bronchial epithelial cells and at a strong level on all cells within the alveolar epithelium, consistent with its crucial role in immune homeostasis. This contrasts with the literature in which, using high power magnification and electron microscopy, CD200 expression was only noted on the apical surface of ciliated cells of the bronchial epithelium and on the apical surface of type II alveolar cells in mouse and rat lungs. Differences in respiratory anatomy, CD200 homology and variations in tissue processing and imaging techniques used may account for the differences in CD200 expression; however, consistently, CD200 expression was demonstrated on type II alveolar cells in the mouse and

rat lung. Furthermore, for the first time, CD200 expression was characterised in the normal human lung where it was seen to be strongly expressed within both type I and type II cells within the alveolar epithelium. Unlike in the mouse lung, CD200 expression appeared to be limited to cells within the distal lung, with no CD200 expression seen in any of the bronchial epithelial sections analysed. However, further staining and analysis of human bronchial epithelium will be needed to confirm this as only three bronchial sections were available in this study. Taken together, CD200 is moderately expressed on mouse bronchial epithelium and strongly expressed on type I and type II alveolar cells within the mouse and human lung. Type II alveolar cells are the predominant cell of origin of adenocarcinomas but have also been shown to give rise to some SCC tumours, although cells within the more proximal lung appear to be the predominant SCC cell of origin (Ferone et al. 2020). Therefore, based on the strong CD200 expression seen in type II alveolar cells it was hypothesised that CD200 expression would be maintained upon malignant transformation and would be seen in both adenocarcinoma and SCC tumours, although to a greater extent in adenocarcinomas.

Using a multi-label IHC protocol for CD200 and the type II alveolar and adenocarcinoma marker TTF-1, tumour cell CD200 expression was semi-quantitively determined in 240 NSCLC tumours using a semi-automated scripted batch analysis in Qupath (Bankhead et al. 2017), with each tumour assigned a CD200 H-score based on the intensity and proportion of tumour cell CD200 expression. CD200 expression was seen in both adenocarcinomas (H-score= 61.12 ± 58.37) and SCCs (H-score= 32.47 ± 46.56) with CD200 expression significantly greater in adenocarcinomas. Although it was hypothesised that CD200+ TTF-1+ type II alveolar cells would give rise to CD200 positive tumours, CD200 positivity was also seen in TTF-1 negative tumours, suggesting that some tumours may maintain CD200 but lose TTF-1 expression upon transformation, or that CD200 expression is upregulated on CD200 negative cells early in the disease process. The decision to use a multi-label IHC protocol over an immunofluorescent technique was based on initial studies which demonstrated strong green channel autofluorescence in the unstained mouse and human lung and lung tumour samples. The high autofluorescent signal in these samples would have interfered with accurate analysis of CD200 labelling due to the high thresholds necessary to eliminate background fluorescence. Of the two studies in the literature exploring CD200 expression in NSCLC tumours, one used IF and the other used IHC. In the IF study, the authors used a visual fluorescence cut-off value to eliminate background fluorescence and only demonstrated CD200 positivity in 29.7% of 287 tumours. In contrast, the IHC study of 632 tumours used a CD200 H-score quantification method and demonstrated an average H-score of 42 ± 57.7; this is in line with our NSCLC cohort which demonstrated an average tumour CD200 H-score of 48.2 ± 55.13. Taken together, this suggests that the cut-off used in the IF study may have

been too high and may have resulted in an under-representation of CD200 expression due to the limited detection of weaker CD200 positivity amongst the autofluorescent signalling of the lung tissue.

In several cancers, tumour CD200 expression is also associated with poor prognosis. In AML, high CD200 expression is associated with an increased risk of relapse and significantly worse OS, whilst in solid malignancies high CD200 expression is an independent risk factor for poor survival in colorectal liver metastases and melanoma, suggesting that CD200 expression may play a critical role in disease progression (Tonks et al. 2007b; Lee et al. 2020; Matsuo et al. 2021). In our patient cohort, CD200 expression was not associated with OS in either adenocarcinoma (HR= 0.771) or SCC (HR= 0.613) patients however, high CD200 expression did trend towards better survival in our SCC patients (p= 0.0565) with high CD200 expression also associated with lower disease stage (p= 0.0511). In one NSCLC study high tumour CD200 expression, as determined by IHC, was significantly associated with better OS and RFS; in contrast, CD200 expression as determined by IF demonstrated no associations between tumour CD200 expression and patient prognosis (Yoshimura et al. 2020; Vathiotis et al. 2021). High CD200 tumour expression has been associated with longer RFS in breast cancer patients, suggesting that the role of CD200 in disease progression is tumour type dependent and that CD200 expression may demonstrate both pro- and anti-tumour functions. Further analysis of a larger patient cohort may determine whether CD200 expression does hold prognostic significance in our patient cohort.

6.1.2 CD200 expression alters the infiltrating immune response

NSCLC tumours induce a strong immune response, as evidenced by the significant increase in CD45+ cells compared to normal lung, with the contexture of the infiltrating immune response a complex and heterogenous feature characterised by the frequency, distribution, and phenotype of the innate and adaptive immune cells. Infiltrating immune cells such as macrophages, neutrophils and lymphocytes play a pivotal role in contributing to cancer progression, with the type, density, and location of these immune cells within the TME impacting the clinical outcome of patients (Anichini et al. 2020). The complexity and composition of the immune infiltrate in NSCLC arises from the interaction of several factors, including tumour mutational status, molecular subtype, mutational burden, tumour histology, and acquired mechanisms of immune evasion such as the expression of immune checkpoints. Together, these factors contribute to shape the NSCLC immune infiltrate which impacts tumour growth and progression and possesses clear prognostic significance. Prior to determining whether tumour CD200 expression has an impact on this immune infiltrate using a dual bulk RNA-seq and IHC approach, the immune infiltrate in 1019 NSCLC tumours (109

with matched normal tissue) was estimated using CIBERSORT to distinguish differences in the immune response upon malignant transformation and between histological subtypes.

Upon malignant transformation, both SCC and adenocarcinoma tumours demonstrated changes in the immune cell composition indicative of an active anti-tumour immune response occurring. Both tumours saw a significant increase in the frequencies of M1 macrophages, Tregs and plasma cells, with SCC tumours demonstrating an increase in TFH cell proportions and adenocarcinoma tumours containing greater frequencies of naive B cells. Greater proportions of cytotoxic M1 macrophages, B cells, and TFH cells suggest an active immune response is occurring. The presence of Tregs, cells which are induced upon immune activation, and which can suppress the immune system and maintain tolerance to self-antigens and tumours, further supports the presence of an active immune response within the NSCLC TME. When the immune composition of adenocarcinoma and SCC tumours was compared, the heterogeneity of the immune response between histological subtypes was highlighted. Adenocarcinoma tumours demonstrated significant increases in cells known to suppress the anti-tumour immune response (M2 macrophages and Tregs), combined with a decrease in activated innate immune cells and activated M1 macrophages, suggesting that the adenocarcinoma TME possessed a greater number of cells which have known immunosuppressive and pro-tumorigenic effects. In contrast, when the relative frequencies of CD8+, CD56+ and Foxp3+ cells were defined in our patient cohort, adenocarcinoma patients demonstrated an over 6-fold increase in CD8+ cell frequencies compared to SCC tumours and a significant decrease in CD56+, Foxp3+ and CD200R+ cells. As mentioned previously, these discrepancies in results between the RNA-seq and IHC analyses are likely due to the greater number of markers used to define immune cell populations in the RNA-seq compared to the single marker used in IHC.

The presence of tumour-infiltrating lymphocytes, composed mainly of CD8+ T cells, are significantly associated with better survival outcomes in NSCLC, with the density of CD8+ cells in the stroma an independent prognostic factor associated with improved survival and decreased tumour size and grade (Ruffini et al. 2009). Several studies have demonstrated that high levels of infiltrating CD8+ T cells, CD4+ T cells and T cells with cytotoxic memory or Th1 profile are consistent positive prognostic factors (Bremnes et al. 2016). In contrast, Tregs, M2 macrophages and neutrophils have all been associated with poor prognosis (Gentles et al. 2015; Soo et al. 2018). The PRECOG software in combination with CIBERSORT was used to deconvolute the contribution of each infiltrating immune cell to overall survival using univariate cox regression in the RNA-seq samples. However, this approach identified cells with known positive prognostic power (memory B cells, MA CD4 T cells, activated DCs and

M1 macrophages) as significant predictors of worse survival. Furthermore, both CD8 T cells, cells which are independent prognostic factors associated with improved survival and Tregs, cells which have been consistently associated with poor OS in NSCLC, did not demonstrate any associations with survival. Therefore, the PRECOG results for this patient cohort should be interpreted with some caution as they do not align with more robust studies from the literature which use flow cytometric analysis of patient blood to determine the frequencies of infiltrating immune cells. In our patient cohort, high absolute numbers of CD45+, CD8+ and CD56+ cells and relative frequencies of CD8+ cells were associated with better OS in SCC patients, although none reached independent prognostic status. In adenocarcinoma patients high absolute CD56+ cell numbers were a predictor of better OS. The association between increased absolute and relative frequencies of cytotoxic immune cells with longer patient survival is representative of the anti-tumour role these cells possess within the TME and highlight the important role the immune response has in controlling tumour growth and progression. Despite Tregs being associated with advanced tumour growth and poor prognosis consistently in NSCLC (Tao et al. 2012), Tregs did not reach prognostic significance in our patient cohort, suggesting the single stain used to identify Treg cells may not be sufficient in identifying this population. Tregs are classified as $CD4^{+}CD25^{+}Foxp3^{+}$ cells, as Foxp3 is also expressed by a subset of CD4+ T cells which produce pro-inflammatory cytokines. Although these Foxp3+ non-immunosuppressive T cells only account for ~3% of CD4+ T cells in healthy young donors, their proportions do significantly increase with age and in systemic autoimmune conditions to ~5% and ~10%, respectively (Devaud et al. 2014). This suggests that, if present within the TME, these pro-inflammatory Foxp3+ cells may account for a proportion of the Foxp3+ cells counted as immunosuppressive Tregs, thus preventing accurate identification of Treg frequencies in the patient samples. Furthermore, the patient cohort may have been too small to reach sufficient power.

The expression of immune checkpoints by tumour cells is known to alter the composition and phenotype of the infiltrating immune response as a method of immune evasion. Tumour CD200 expression is associated with a significant increase in Treg frequency in MM and AML and a suppression of memory T cell and NK cell function in AML (Coles et al. 2011; Coles et al. 2012c; Coles et al. 2012a; Aref et al. 2017). Using CIBERSORT analysis of bulk RNA-seq data, CD200 expression in SCC patients was positively associated with the relative frequencies M0 macrophages, Tregs, TFH cells and memory B cells and negatively associated with MA and MR CD4 T cells, CD8 T cells, GDT cells, monocytes, resting DC and mast cells, eosinophils, and neutrophils. In adenocarcinoma patients, CD200 expression was positively associated with the frequencies of memory B cells, MA CD4 T cells, M0 and M1 macrophages and neutrophils and negatively associated with TFH cell, activated NK cell,

monocyte and activated DC frequencies. Of the correlations observed with CD200 expression, positive associations with memory B cells, Tregs and M0 macrophages and a negative association with monocytes were the only relationships observed for both SCC and adenocarcinoma patients, once again highlighting the heterogeneity of the immune response and suggesting that the immunoregulatory effects of tumour CD200 expression may be subtype dependent. Like AML and MM, CD200 expression was positively associated with Treg frequencies, suggesting that this relationship may also be present in NSCLC tumours.

One limitation of using bulk RNA-seq data is that the CD200 expression reads were determined from the whole tumour sample, resulting in CD200 positive non-tumour cells such as immune and stromal cells contributing to the sample's CD200 expression level. Therefore, to explore the associations between tumour CD200 expression and the absolute and relative frequencies of CD45, CD8, CD56, Foxp3 and CD200R positive cells, serial sections of tumour were labelled and quantified and their relationship with the tumour CD200 H score determined. This method allowed for the more accurate analysis of the effects of NSCLC tumour cell CD200 expression on the immune infiltrate. In SCC patients, tumour CD200 expression was positively associated with absolute numbers of CD56+ and Foxp3+ cells, whilst in adenocarcinoma patients, tumour CD200 expression was positively associated with the absolute and relative frequencies of Foxp3+ cells and negatively associated with the absolute and relative frequencies of CD56+ cells. This increase in Tregs in both adenocarcinoma and SCC patients, although only in absolute numbers in SCC tumours, is consistent with the RNA-seq data, suggesting that tumour CD200 expression in NSCLC does increase the frequency of infiltrating Treg cells, in agreement with that seen in haematologic malignancies. Although in this patient cohort Treg cell infiltration was not associated with survival, in the literature high Treg infiltration is associated with decreased survival and increased tumour growth, suggesting that tumour CD200 expression is associated with an increase in immunosuppressive cells (Tao et al. 2012). Furthermore, for the first time, a negative relationship was demonstrated between tumour CD200 expression and the absolute and relative frequencies of infiltrating NK cells in NSCLC tumours. RNA-seq analysis also identified a negative relationship between activated NK cells in adenocarcinoma tumours and CD200 expression. NK cells are cytotoxic cells which can demonstrate potent anti-tumour activity; high absolute frequencies of CD56+ cells were associated with better survival in our patient cohort, suggesting that tumour CD200 expression is associated with a decrease in anti-tumour immune cells. Taken together, this consistent positive relationship between tumour CD200 expression and the frequency of immunosuppressive Tregs and the negative relationship between tumour CD200 expression and cytotoxic NK cells suggests that NSCLC tumour

CD200 expression may be altering the composition of the infiltrating immune response as a method of immune evasion to prevent tumour cell killing.

To exert its immunoregulatory effects, CD200 must bind to CD200R on interacting immune cells. In our patient cohort, 14.32% ±17.55 and 23.37% ±19.53 of infiltrating CD45+ cells were CD200R+ in adenocarcinoma and SCC tumours, respectively. Analysis of single-cell sequencing data also demonstrated CD200R expression on infiltrating macrophages, mast cells, NK cells and T and B cells, although to a lesser extent than observed in our patient tumours. This single cell data also demonstrated, for the first time, an increase in T cell CD200R expression from naïve to effector to memory to exhausted CD4 and CD8 T cell phenotypes. Although a direct role for CD200 signalling has yet to be elucidated, this increase in CD200R expression as cells mature and become exhausted suggests that CD200 may directly signal to these cells. Furthermore, a study on T cells within the NSCLC TME demonstrated an exhausted phenotype compared to peripheral blood cells, as characterised by increased co-expression of the immune checkpoints CD200R, PD-1, CTLA-4 and TIM-3, suggesting that the T cell CD200R expression could be used as a marker of exhaustion in NSCLC tumours (Su et al. 2020). Matched patient normal and tumour tissue would have been beneficial in determining whether CD200R expression was increased on infiltrating immune cells in our patient cohort. In line with the findings from Yoshimura *et al.* (2020), tumour CD200 expression did not have an effect on infiltrating absolute or relative numbers of CD200R+ cells, suggesting that CD200R upregulation is due to other factors within the TME.

6.1.3 Tumour CD200 expression causes CD200R+ NK cell dysfunction *in vitro*

NK cells are potent cytotoxic innate immune cells that can rapidly identify and kill transformed cells without prior sensitisation. The importance of NK cells in the eradication of tumours has been supported by several *in vivo* studies which demonstrate that mice which are deficient in NK cells or NK cell function present with greater tumour growth and metastasis (Kim et al. 2000; Smyth et al. 2005). However, despite NK cell infiltration into the TME, tumours are still able to grow. Unlike other tumour associated innate immune cells, NK cells themselves do not appear to subvert into a pro-tumour phenotype but rather factors within the TME cause NK exhaustion resulting in inefficient anti-tumour effector function. In the later stages of NSCLC development, NK cells within the TME became dysfunctional and demonstrate diminished cytotoxicity, decreased responsiveness, and impaired viability characterised by impaired IFN-γ production, reduced degranulation and lower anti-tumour cytotoxicity (Cong et al. 2018). A similar dysfunctional NK cell phenotype is also seen in AML patients with high tumour CD200 expression (Coles et al. 2011). Furthermore, tumour CD200 expression was negatively associated with the absolute and relative frequencies of CD56+ cells in our NSCLC patients,

suggesting CD200 expression may be having an effect on interacting NK cell function and viability. Therefore, to explore the effects of tumour CD200 expression on interacting CD200R+ NK cells, *in vitro* models of NK cell activity were generated.

NK cells constituted 2.06% ±2.38 of the adenocarcinoma and 2.59% ±2.66 of the SCC tumour immune infiltrate in the RNA-seq cohort and 1.34% ±1.47 and 4.4% ±3.42 of our adenocarcinoma and SCC patient cohort, respectively. The use of CD56 alone as a marker of NK cells may have resulted in an over-estimation of NK cell frequencies in our SCC patients as CD56 is also expressed by cytotoxic subsets of DCs, monocytes, GDT and αβ T cells which possess strong effector functions, although this does not explain the reduction seen in adenocarcinoma patients (Van Acker et al. 2017). Despite the NK cell frequencies in our adenocarcinoma cohort being less than that observed by RNA-seq, this relative frequency is still within the expected range as determined by flow cytometry (Lavin et al. 2017; Stankovic et al. 2018). The presence of tumours despite this NK cell infiltration suggests that these infiltrating NK cells must be dysfunctional and cannot fully exert their anti-tumour properties. Upon recognition of a target cell, NK cells undergo a complex and tightly regulated process of activation which results in the direct killing of the target cell through release of cytotoxic granules and secretion of several cytokines which modulate the function of other innate and adaptive immune cells (Morvan and Lanier 2016). Using a preliminary *in vitro* co-culture model of direct CD200R+ NK cell killing of CD200+ and CD200- HeLa cells, expression of CD200 demonstrated a protective role against NK-92MI cytotoxicity, with CD200+ tumours demonstrating significantly improved viability. Upon modifying this model to generate CD200+/CD200- adenocarcinoma target cells, the same protective role was seen with CD200+ H838 cells demonstrating significantly greater viability than CD200- H838 cells. This protection against CD200R+ NK cell cytotoxicity was diminished upon addition of a CD200 blocking antibody, with CD200+ tumour cell viability decreased back to CD200- tumour cell levels, suggesting that evasion of NK cell cytotoxicity was CD200 dependent and that blocking CD200 signalling was sufficient to prevent this immunosuppression.

This significant increase in the frequency of viable CD200+ tumour cells in the presence of CD200R+ NK-92MI cells also corresponded to a decrease in NK-92MI CD107a expression, an indirect marker of NK cell degranulation. Target cell recognition and NK cell activation induces the exocytosis of cytotoxic lysosomes containing perforin, which generates pores in the target cell, and granzymes which enter the cell through these pores where they cleave caspases and induce apoptosis, resulting in target cell lysis (Topham and Hewitt 2009). During exocytosis, the lysosome-associated protein CD107a transiently appears on the surface where it can be maintained through addition of a protein transport inhibitor and measured by

flow cytometry as a marker of NK cell degranulation. CD200 expression on H838 cells did decrease NK-92MI cell degranulation, with decreased degranulation corresponding to an increased viability of CD200+ target cells, although this did not reach significance. Addition of a CD200 blocking antibody was not sufficient to increase degranulation, suggesting that CD200 signalling alone may not be responsible for this decrease in degranulation. This is in contrast to studies in AML in which an increase in CD200+ tumour cell viability in combination with a decrease in NK cell degranulation was observed, but NK cell cytotoxicity and degranulation could be restored upon addition of a blocking antibody (Coles et al. 2011). In addition to direct cytotoxicity, upon activation NK cells can also secrete a number of cytokines such as IFN-γ, TNF-α, GM-CSF, IL-10, IL-5, and IL-13 and chemokines including MIP-1α, MIP-1β, IL-8, and RANTES that can modulate the activation and function of other innate and adaptive immune cells (Paul *et al.* 2016). This immunoregulatory role is particularly apparent during the primary immune response in which NK cells are thought to be the primary source of IFN-γ, a potent effector cytokine that plays a crucial role in anti-tumour immunity (Krzewski and Coligan 2012). CD200 expression by H838 cells significantly reduced NK-92MI IFN-γ production and this was restored by the addition of the CD200 blocking antibody, suggesting another mechanism by which CD200 can induce NK cell dysfunction and evade the immune response. CD200 expression by AML tumour cells also significantly reduced NK cell IFN-γ production and could be restored by blocking CD200 signalling (Coles et al. 2011).

Taken together, CD200 expression by lung cancer cells can cause significant dysfunction in interacting CD200R+ NK cells by reducing NK cell degranulation and immunoregulatory cytokine production. This dysfunction protects the CD200+ target cell from NK cell cytotoxicity, resulting in increased tumour cell viability, suggesting that CD200 signalling is an immune evasion mechanism utilised to prevent tumour cell death. Furthermore, blocking this signal with a CD200 blocking antibody was sufficient to restore NK cell tumour killing abilities and increase IFN-γ production. Despite addition of the antibody further decreasing NK cell degranulation, tumour cell death was still restored to CD200- levels. The mechanism by which tumour cell killing is increased but degranulation appears to also decrease is currently unknown and will require further studies to determine whether this increase in tumour cell death is due to another NK cell effector function, such as death receptor ligation, or whether addition of the blocking antibody interferes with accurate CD107a measurement.

NK cell activation and subsequent effector functions are dependent upon the integration of both “missing-self” and “altered-self” mechanisms, the latter of which delivers activating signals through activating receptors such as NKG2D and the NCR’s Nkp30, Nkp44 and Nkp46, which identify stress signals from virally infected or transformed cells (Platonova et al.

2011a). Defective expression of these activating and inhibitory receptors, which maintain tight regulation over NK cell function, has been associated with poor patient outcomes in many cancers (Coles et al. 2011). In NSCLC, in addition to dysfunctional degranulation and IFN-γ production upon stimulation, tumour associated NK cells also demonstrate a distinct activating receptor phenotype characterised by a reduction in Nkp30, Nkp46 and NKG2D expression (Carrega et al. 2008; Platonova et al. 2011; Russick et al. 2020). Co-culture experiments demonstrated that this downregulation of Nkp30 and Nkp46 expression was reversed in transwell assays, suggesting that this altered NK phenotype was cell contact dependent (Platonova *et al.* 2011). Furthermore, $CD200^{high}$ AML patients demonstrated significant reductions in Nkp44 and Nkp46 expression compared to NK cells taken from $CD200^{low}$ patients (Coles et al. 2011). Using 16-hour co-culture experiments, it was demonstrated that stimulation of NK-92MI cells with H838 cells significantly reduced Nkp30 expression and this was further significantly reduced in the presence of tumour CD200 expression. No differences were seen in Nkp44 or Nkp46 expression, and NKG2D expression significantly increased after co-culture with CD200+ tumour cells compared to unstimulated cells, although this only resulted in a ~2% NKG2D+ NK cell population. This suggests that tumour CD200 expression may be responsible for the reduction in NKp30 expression seen in NK cells isolated from NSCLC tumours and that NK cells may increase NKG2D expression as a compensatory mechanism, although further study using CD200 blocking antibodies and at longer time points will be required to confirm this. In contrast to the NSCLC and AML studies, no differences in NKp44 or Nkp46 expression were demonstrated; however, it should be noted that those NK cells were taken from patient tumours or cultured with tumour cells for 5 days, much longer than the 16 hours in this study. Again, studies at longer timepoints and with CD200 blocking will determine whether CD200 expression may contribute to the altered activating receptor phenotype in NSCLC tumours as another mechanism of NK cell immune evasion.

In addition to tumour CD200 expression inducing NK cell dysfunction and an altered activating receptor repertoire, the relative frequencies of activated NK cells and the absolute and relative frequencies of CD56+ cells were significantly negatively associated with CD200 expression by RNA-seq and IHC analysis. Reduced NK cell frequencies in tumours have been associated with poor homing and infiltration into the TME due to interferences with chemotactic signalling and through physical barriers to infiltration such as vascular density and the composition of the surrounding stroma. (Ben-Shmuel et al. 2020). However, analysis of NK cells taken from co-culture experiments demonstrated a significant decrease in interacting NK cell viability taken from CD200+ co-cultures, suggesting that tumour CD200 expression was inducing NK cell death. Further analysis of NK cell viability in the presence of a CD200 peptide demonstrated an increase in apoptotic NK cells over a 48-hour period compared to control.

Additional studies looking at which apoptotic pathways are activated and whether blocking CD200 signalling prevents NK cell death will be required before it can be stated that tumour CD200 expression causes apoptosis of interacting CD200R+ NK cells. However, this may explain why tumours with high CD200 expression present with a decreased NK cell infiltrate. If tumour CD200 expression does induce NK cell apoptosis, in addition to causing NK cell dysfunction, this represents a novel mechanism by which CD200 expression can evade NK cell anti-tumour immune attack.

6.2 CD200 as a potential new immunotherapeutic target in NSCLC

Immune checkpoint inhibitor therapies primarily reinvigorate tumour reactive T cells rather than induce their formation, therefore the best responses to these therapies are seen in cancers which have a high somatic TMB. As a tumour with a typically highly infiltrated immune reactive TME rich in neoantigens, NSCLC tumours represent an ideal candidate for immunotherapies, as reflected in the durable clinical efficacy seen in responder patients (Maleki Vareki 2018; Grant et al. 2021). However, despite subsets of patients deriving durable benefits with PD-1/PD-L1 ICI therapy overall response rates are 47-63%, with many patients showing primary resistance mechanisms (Doroshow et al. 2019). Therefore, identification of predictive markers of ICI therapy response or the generation of multi-modality immunological therapies targeting multiple immune checkpoints could greatly improve the success of PD-1/PD-L1 ICI therapies in NSCLC. One of the most promising strategies for overcoming resistance and prolonging therapeutic benefit from ICIs is the use of dual immune checkpoint blockade (Jenkins et al. 2018). Data from NSCLC clinical trials suggests that first-line doublet anti-PD-1 and anti-CTLA-4 therapy increases overall survival for advanced stage NSCLC patients, with similar increases in overall survival seen in patients with both PD-L1 positive and negative tumours (Hellmann et al. 2019; Ramalingam et al. 2020). By targeting two immunoregulatory pathways at distinct yet synergistic stages in the immune response, namely the priming and effector phases of the adaptive immune response for CTLA-4 and PD-1 respectively, the likelihood of a successful anti-tumour immune response is increased (Das et al. 2015). Furthermore, preliminary data from trials using anti-PD-L1 and anti-TIGIT antibodies have demonstrated enhanced anti-tumour activity when compared to anti-PD-L1 therapy alone (Rodriguez-Abreu et al. 2020). TIGIT is a coinhibitory receptor that works in the effector phase of the adaptive immune response to synergise with PD-1/PD-L1 to potently inhibit effector T cell function, suggesting that dual blockade of immune checkpoints that function in the same stages of the immune response can also synergise to increase the anti-tumour immune response (Johnston et al. 2014).

The first clinical trials in CLL using a CD200 blocking antibody have yielded positive results and provide evidence that CD200 inhibition with a blocking antibody can be safe and efficacious. Samalizumab is a recombinant humanised monoclonal antibody against CD200 that is engineered with an Ig constant G2/G4 region to minimise effector function and prevent ADCC of CD200-expressing immune cells (Kretz-Rommel et al. 2008; Mahadevan et al. 2019). The first in human trial looked at the therapeutic benefit of CD200 immune checkpoint inhibition in 23 CLL and 3 multiple myeloma patients. After multiple dosing cycles there was a dose-dependent decrease in CLL CD200 expression and a sustained reduction in CD200+CD4+ T cells at higher doses; 64% of patients demonstrated a reduction in tumour burden, with 70% of CLL patients achieving stable disease. One chemotherapy naïve CLL patient presented with a durable partial response demonstrated by >50% reduction in overall tumour burden with a concomitant increase in CD8+ T cells and a reduction in Tregs. All MM patients had disease progression with little change in T cell subsets. These positive preliminary results combined with a good safety profile with generally mild to moderate adverse events support further development of Samalizumab as a CD200 immune checkpoint inhibitor (Mahadevan et al. 2019).

In the UK, anti-PD-1/PD-L1 therapies are now standard therapies for the treatment for advanced stage NSCLC patients. PD-L1, known to be expressed by cells in the TME, engages its receptor PD-1 on T cells and subsequently triggers inhibitory signalling downstream of the TCR, inhibiting effector functions, reducing T cell killing capacity and inducing T cell apoptosis (Pardoll 2012). PD-1 blockade induces tumour rejection through reinvigoration of exhausted CD8 T cell activity by preventing PD-1-mediated attenuation of proximal TCR signalling, allowing for restoration of the functional activity and frequency of CD8 effector T cells (Wei et al. 2018). Clinical evidence supports a model in which blockade of PD-1 signalling is most effective in tumours in which an endogenous anti-tumour T cell response has already been elicited but has been suppressed through PD-1-induced T cell exhaustion (Tumeh et al. 2014). CD200 signalling has also been implicated in the control of T cell function and activation through both direct and indirect mechanisms, suggesting that dual blockade of CD200 and PD-1 signalling could produce a synergistic role in reinvigorating anti-tumour T cell responses. In AML, patients with high tumoral CD200 expression demonstrated reduced frequencies of cytotoxic CD8 memory T cells and memory CD4 T cells when compared with $CD200^{low}$ patients (Coles et al. 2012a). Upon blockade of CD200 signalling *in vitro*, memory Th1 cells taken from $CD200^{high}$ patients demonstrated recovered IFN-γ production. This direct suppression of both the magnitude and intensity of the memory Th1 cell response was confirmed using a direct T cell model to rule out the role of APCs, in which blockade of CD200 signalling could significantly recover cytokine production, thus indicating that blockade of

CD200 alone is sufficient to recover memory T cell activity. CD200 signalling has also been associated with an increased frequency of Treg cells in AML patients and in the NSCLC patients analysed in this thesis, suggesting a potential role for CD200 signalling in the induction or increased homing of immunosuppressive Tregs to the TME (Coles *et al.* 2012). In addition to its role in memory T cell inhibition and increased Treg frequencies, in this thesis CD200R expression was observed on CD4 and CD8 T cells within the NSCLC TME, with its expression significantly increasing from naïve to effector to memory to exhausted phenotypes, suggesting a role for CD200 signalling in T cell exhaustion. Indeed, in one study approximately 75% of T cells isolated from NSCLC tumours expressed CD200R and this expression largely overlapped with that of other immune checkpoint molecules including PD-1, CTLA-4 and TIM-3, indicative of an exhausted T cell phenotype (Su et al. 2020). As immune checkpoint therapies aim to reinvigorate exhausted T cells, taken together this suggests that blockade of CD200 signalling may be a promising additional candidate for immune checkpoint inhibition through synergising with PD-1 blockade to increase memory T cell function, decrease Treg frequencies and potentially reinvigorate exhausted T cells to increase the anti-tumour immune response.

The current paradigm is that CD8 T cells are inhibited by PD-1, and it is widely accepted that PD-1 blockade reinvigorates T cells to attack tumour cells; however, many tumours exhibit a high incidence of MHC loss and and/or low neoantigen burden which should render tumour cells refractory to CD8 T cell recognition (Hsu et al. 2018). The effectiveness of PD-1 blockade in some of these tumours suggests the existence and reinvigoration of an anti-tumour immune response independent of cytotoxic T cells, such as that mediated by NK cells, in which MHC loss and cellular stress ligands activate an anti-tumour immune response independent of antigenic stimulation (Trefny et al. 2020). Upregulation of PD-1 expression on intra-tumoral NK cells has been observed in several cancers, including NSCLC, where its expression is correlated with other inhibitory receptors such as TIM-3 and TIGIT. PD-1+ NK cells isolated from NSCLC tumours demonstrated decreased cytotoxicity and significantly reduced degranulation and cytokine production compared to their PD-1- counterparts (Trefny et al. 2020). Furthermore, blockade of PD-1 signalling was sufficient to restore NK cell functional capabilities, suggesting PD-1 signalling is an important regulator of anti-tumour NK cell function. In this thesis, subsets of NK cells were demonstrated to express CD200R and, using a CD200R+ NK cell line, NK cell dysfunction and phenotypic changes were observed upon interaction with CD200+ tumour cells. *In vitro* blockade of this CD200 signalling was sufficient to increase IFN-y production and increase tumour cell killing, suggesting blocking CD200 signalling may reverse NK cell dysfunction and reinstate an innate anti-tumour immune

response. Together with PD-1 blockade, CD200 inhibition could function as a synergistic therapy in which NK cell function is further restored through a dual mechanism.

In addition to the effects CD200 blockade has on T cell and NK cell function, CD200R expression has also been demonstrated on several innate and adaptive immune cells within the NSCLC TME, suggesting that tumour CD200 may be delivering negative immunoregulatory signals to other infiltrating immune cells within the TME, such as B cells and macrophages, and that blockade may further enhance the anti-tumour immune response. Furthermore, in our patient cohort up to 79.85% and 90.62% of CD45+ cells were also CD200R+ in SCC and adenocarcinoma patients, respectively. In CD200+ pancreatic tumours, CD200R expression was significantly increased on MDSC and blocking CD200 *in vivo* was sufficient to limit pancreatic tumour growth and reduce intra-tumoral MDSC frequency (Choueiry et al. 2020). Furthermore, CD200 blockade in combination with anti-PD-1 antibodies significantly limited tumour growth compared to single agent therapy alone, suggesting that CD200 blockade can enhance the efficacy of PD-1 in a preclinical animal model. Further evidence for the synergistic role of dual PD-1 and CD200 blockade come from an *in vivo* model of CD200+ head and neck SCC in which localised delivery of an adenovirus expressing sCD200R-Ig effectively abolished CD200 signalling, induced a switch from M2 to M1 macrophage polarisation, increased CD8 T cell infiltration, decreased Treg frequencies and demonstrated profound therapeutic efficacy. It was observed that CD200 upregulated PD-L1 expression on tumour cells and that combined treatment with sCD200R-Ig adenovirus and anti-PD-1 antibodies further enhanced the anti-tumour effect, with the growth of the CD200+ tumours effectively inhibited, suggesting an increase in the efficacy of both immune checkpoint inhibitors (Shin et al. 2021).

Taken together, this data suggests that blockade of CD200, alone or more likely in combination with PD-1 blockade, may be of clinical benefit to NSCLC patients. In this thesis, adenocarcinoma tumour CD200 expression was associated with an increase in Treg frequencies and a decrease in NK cell frequencies, cells with negative and positive prognostic power, respectively. Furthermore, interactions between CD200+ tumour cells and CD200R+ NK cells resulted in NK cell dysfunction characterised by decreased killing capacity, decreased degranulation and cytokine production, and an altered activating receptor repertoire. Blockade of CD200 signalling was sufficient to restore NK cell activity and increase tumour cell killing and cytokine production. Furthermore, in other studies, blockade of CD200 signalling was sufficient to increase memory T cell function, decrease Treg and MDSC frequencies and inhibit tumour growth in CD200+ tumour models (Coles et al. 2012a; Choueiry et al. 2020; Shin et al. 2021). Moreover, dual blockade of CD200 and PD-1 signalling appears

to have a synergistic effect on enhancing anti-tumour immunity in solid tumour models, with double agent therapy significantly enhancing the efficacy of PD-1 therapies (Choueiry et al. 2020; Shin et al. 2021). Seeing as most NSCLC patients treated with anti-PD-1/PD-L1 therapies do not show a durable clinical response, this dual inhibition could be a new promising model to explore in NSCLC to increase treatment efficacy in those which present with resistance.

Of the NSCLC tumours studied, 95.72% and 80.5% of adenocarcinoma and SCC tumours demonstrated ≥ 1% CD200 positivity, suggesting that these patients may benefit from CD200 inhibition. However, tumour CD200 expression may not be necessary for patients to benefit from CD200 blockade. An *in vivo* study of skin carcinoma in mice demonstrated that CD200-CD200R signalling was able to suppress the anti-tumour immune response independent of tumour CD200 expression, thus suggesting an extension of the therapeutic use of CD200 blockade to patients with CD200 negative tumours (Rygiel et al. 2012). This is also seen with PD-1/PD-L1 ICIs. Monotherapy with Pembrolizumab and Atezolizumab is only approved in the first-line setting for patients with a PD-L1 tumour expression of ≥ 50%, with tumours demonstrating lower PD-L1 expression approved for first-line Pembrolizumab in combination with platinum doublet chemotherapy (NICE 2021). In this thesis, 44.44% of adenocarcinomas and 21.19% of SCC tumours demonstrated ≥ 50% CD200 positivity. However, despite consideration and validation of the 50% tumour cell PD-L1 expression cut-off, not all patients with high PD-L1 expression respond to PD-1/PD-L1 antibodies. Similarly, a subset of patients with low PD-L1 expression have demonstrated good clinical responses and long-term disease control, suggesting that tumour PD-L1 expression is not a robust biomarker of ICI responses (Herbst *et al.* 2018; Garon *et al.* 2019; Herbst *et al.* 2020). Taken together, this suggests that NSCLC patients may benefit from CD200 inhibition regardless of tumour CD200 expression. Further studies into the optimal tumour CD200 expression cut-off value would be necessary if this were to go to the clinic. Whether CD200R and PD-1 are expressed together or on distinct subsets of infiltrating immune cells in NSCLC and whether blockade of CD200 alone and in combination with PD-1 can enhance the anti-tumour immune response in a NSCLC model will also need to be explored. Nonetheless, CD200 blockade represents an exciting new potential immunotherapeutic target in the treatment of NSCLC.

6.3 Future directions

Having demonstrated that CD200 can induce dysfunction of interacting CD200R+ NK cells *in vitro*, it would be of benefit to analyse what percentage of infiltrating NK cells in NSCLC tumours are CD200R+, using flow cytometry of patient samples or multi-plex IHC of tumour sections, to determine the extent to which CD200-mediated NK cell dysfunction could affect

the anti-tumour immune response. Furthermore, the use of freshly isolated NK cells from PBMCs in the tumour:NK cell co-culture models would be beneficial to determine whether this NK cell dysfunction occurs in a more clinically relevant model. Additionally, initial data generated at the end of this project suggests that CD200 may reduce the viability of interacting CD200R+ NK cells. Further studies into the mechanisms by which CD200 may be inducing NK cell apoptosis, by which pathway, and whether this decreased viability may account for the negative relationship between tumour CD200 expression and NK cell frequencies need to be explored. The reductions in NK cell frequencies may also be due to ineffective homing of the NK cells to the TME due to dysregulated chemokine production. Therefore, functional characterisation of NK cell chemokine production after tumour cell stimulation would establish whether dysregulation of NK cell migration to the TME is another mechanism by which tumour CD200 induces NK cell dysfunction and evades immune attack. In addition to direct cell to cell CD200:CD200R signalling, the detection of sCD200 in the supernatants of CD200+ tumour cells suggests that CD200 may also be able to exert its effects on cells not in direct contact with the tumour. Functionally active sCD200 has been detected in haematological malignancies, therefore functional characterisation of the effects of sCD200 on CD200R+ NK cells in transwell experiments will help to determine whether CD200 can cause dysfunction of NK cells that are not in direct contact with the tumour.

6.4 Conclusions

To conclude, in this thesis CD200 expression has been characterised in NSCLC tumours and its relationship with the absolute and relative frequencies of infiltrating immune cells established, with CD200 expression positively correlating with frequencies of immunosuppressive Tregs and negatively with cytotoxic NK cells. *In vitro,* tumour CD200 interacts with CD200R+ NK cells to cause NK cell dysfunction as characterised by decreased degranulation, inhibited cytokine production, altered activating receptor expression and a decreased capacity to kill tumour cells. Blocking of CD200 with an antibody was sufficient to restore the NK cell anti-tumour response and increase tumour cell death. Furthermore, CD200R is expressed on almost all of the infiltrating immune cell subtypes studied, suggesting immunoregulatory control of the immune response beyond that which was studied in this thesis. A summary of the key findings of this thesis can be found in Figure 6.1. Taken together, this data suggests a mechanism by which NSCLC tumour cells express CD200 as a mechanism of immune evasion and that blocking CD200 signalling alone, or in combination with PD-1 inhibition to synergistically increase immune checkpoint therapy efficacy, may represent a novel therapeutic target in NSCLC.

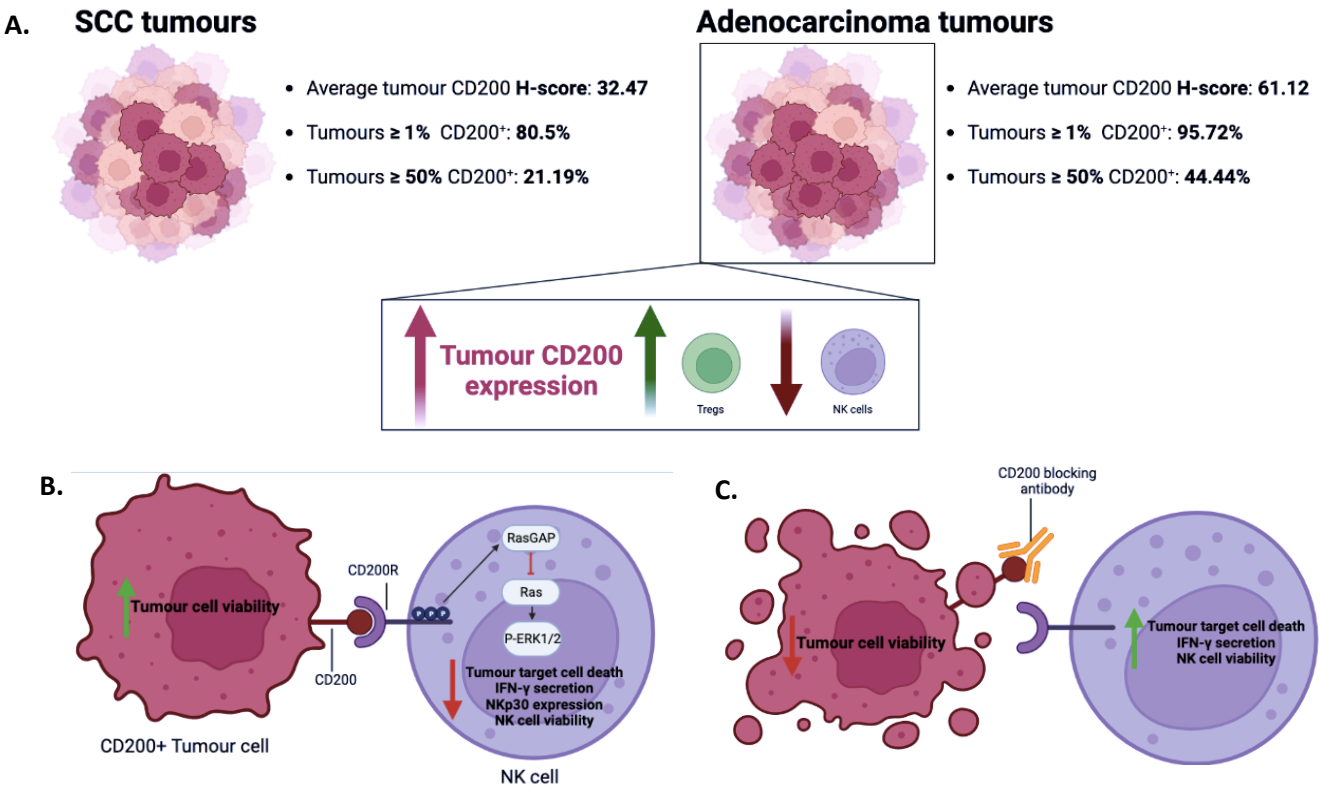

Fig 6.1 Summary of the key findings of this thesis investigating the role of CD200 in NSCLC immune evasion.

Tumour cell CD200 expression was semi-quantitatively analysed by IHC in (A) SCC (n= 120) and (B) adenocarcinoma (n= 120) tumours. Adenocarcinoma tumours demonstrated significantly greater tumour CD200 expression than SCC tumours. In adenocarcinoma tumours, tumour CD200 expression was associated with an increase in the infiltration of Tregs and a decrease in infiltrating NK cells. (C) *In vitro* analysis demonstrated that tumour CD200 expression protected tumour cells from CD200R+ NK cell killing, associated with a dysfunction in NK cell activity and phenotype, as characterised by a decrease in IFN-γ secretion, decreased NKp30 expression and a reduction in NK cell viability. This dysfunction could be rescued by the addition of a CD200 blocking antibody and resulted in restoration of NK cell killing of the tumour target cells, suggesting CD200 blockade may be a potential immunotherapeutic target to prevent NSCLC immune evasion.

Chapter 7:
Supplementary Data

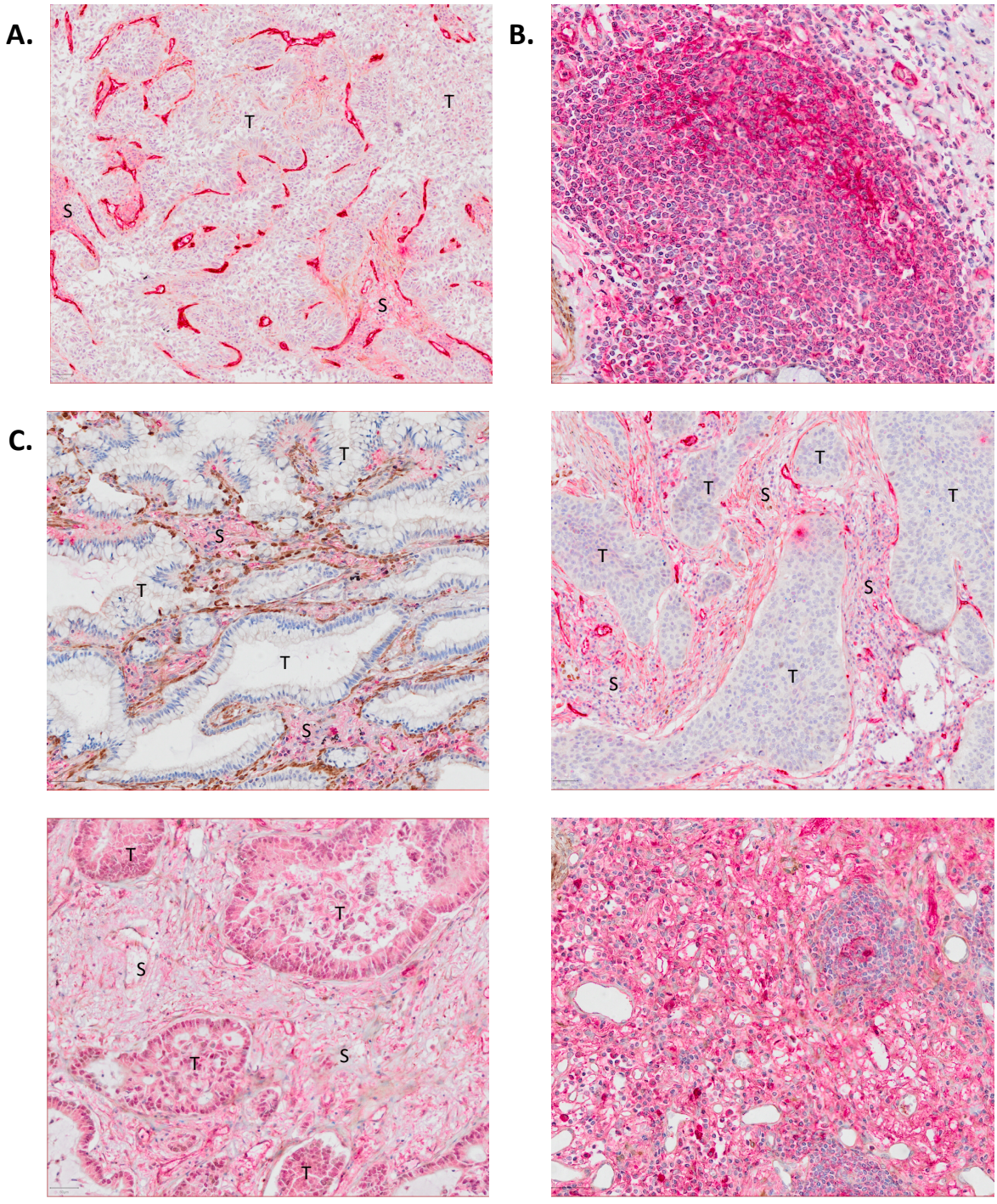

Supplementary Figure S1. Representative images of strong CD200 staining in NSCLC stroma. (A) CD200 expression on vascular endothelium (B) CD200 within tertiary lymphoid structures and (C) CD200 expression throughout the stroma. S, stroma; T, tumour.

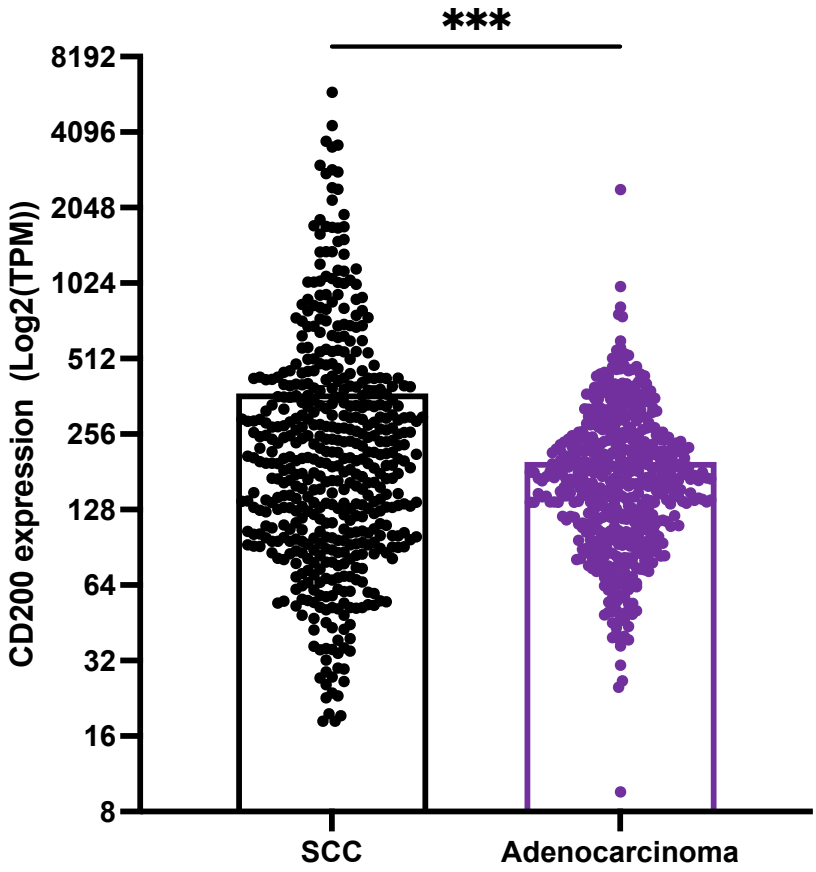

Supplementary Figure S2. Normalised CD200 expression in the SCC and adenocarcinoma TCGA cohort by RNA-seq. Normalised CD200 expression (Log2(transcripts per million)) as determined by RNA-seq in 501 SCC and 518 adenocarcinoma patients. P ≤ 0.05 (*) P ≤ 0.01 (**) P ≤ 0.001 (***) P ≤ 0.0001 (****).

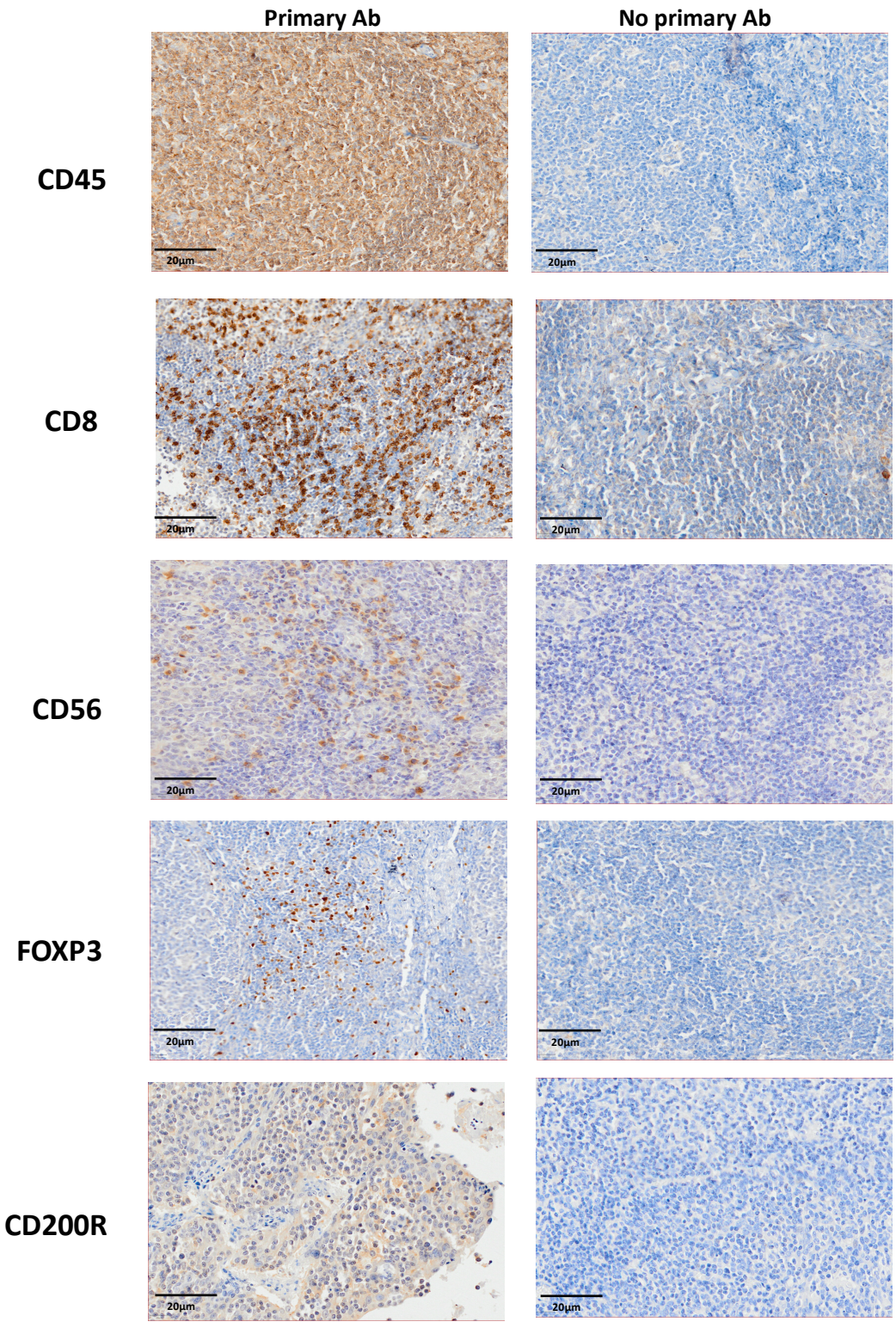

Supplementary Figure S3. Optimisation of IHC labelling of immune cell markers. Representative images of human tonsil labelled with immune cell markers and visualised with DAB. The absence of labelling in the no primary antibody controls confirms the specificity of the labelling.

Supplementary Table S1. List of genes used to characterise CD8 T cells, Tregs and NK cells by CIBERSORT.

Cell	Gene	Cell	Gene	Cell	Gene
CD8 T cell	BCL11B	Treg	BCL11B	Nk cell	APOBEC3G
	CCL5		CD2		APOL6
	CD2		CD247		AZU1
	CD247		CD27		BPI
	CD27		CD3D		CAMP
	CD3D		CD3E		CCL4
	CD3E		CD3G		CCL5
	CD3G		CD6		CCND2
	CD6		CD96		CD160
	CD69		DPP4		CD2
	CD7		GPR171		CD244
	CD8A		GZMM		CD247
	CD8B		ICOS		CD69
	CD96		ITK		CD7
	CRTAM		LCK		CD96
	CST7		LTB		CDHR1
	CTSW		MAP4K1		CDK6
	DPP4		SH2D1A		CEACAM8
	DSC1		SIRPG		CSF2
	DUSP2		TRAC		CST7
	FAIM3		TRAT1		CTSW
	FLT3LG		TRBC1		DEFA4
	GNLY		UBASH3A		DPP4
	GPR171		ZAP70		ELANE
	GRAP2		BARX2		FASLG
	GZMA		CD28		GFI1
	GZMB		CD4		GNLY
	GZMH		CD5		GPR171
	GZMK		CD70		GPR18
	GZMM		CEMP1		GRAP2
	ICOS		CLEC2D		GZMA
	IGKC		CTLA4		GZMB
	IL7R		DGKA		GZMH
	ITK		EFNA5		GZMK
	KLRB1		FOXP3		GZMM
	KLRC3		FRMD8		IFNG
	KLRC4		GPR1		IL12RB2
	KLRD1		GPR19		IL18R1
	KLRF1		HIC1		IL18RAP
	KLRK1		HMGB3P30		IL2RB
	LAG3		IL2RA		KIR2DL1
	LCK		IL2RB		KIR2DL4
	LEF1		KIRREL		KIR2DS4
	LIME1		LAIR2		KIR3DL2
	LTB		LILRA4		KLRB1
	LY9		LOC126987		KLRC3
	MAP4K1		MBL2		KLRC4
	MAP9		NPAS1		KLRD1
	NCR3		NTN3		KLRF1
	NKG7		PCDHA5		KLRK1
	PIK3IP1		PLCH2		LCK
	PRF1		PMCH		LTA

	PTGDR		PTGIR		LTB
	PTPRCAP		PTPRG		MGAM
	PVRIG		RCAN3		MS4A3
	RASA3		RYR1		NAALADL1
	RPL3P7		SEC31B		NCR3
	SH2D1A		SEPT5		NKG7
	SIRPG		SIT1		NME8
	TCF7		SKAP1		OSM
	TRAC		SPOCK2		PLEKHF1
	TRAT1		SSX1		PRF1
	TRAV12-2		TRAV9-2		PRR5L
	TRAV13-1		TYR		PTGDR
	TRBC1				PTGER2
	TRDC				PTPRCAP
	UBASH3A				PVRIG
	ZAP70				S1PR5
					SH2D1A
					SOCS1
					TBX21
					TEP1
					TNFSF14
					TRBC1
					TRDC
					TTC38
					TXK
					ZAP70
					ZNF135

References

1. Abel, A.M., Yang, C., Thakar, M.S. and Malarkannan, S. 2018. Natural killer cells: Development, maturation, and clinical utilization. *Frontiers in Immunology* 9(AUG), pp. 1–23. doi: 10.3389/fimmu.2018.01869.
2. Adrain, C., Murphy, B.M. and Martin, S.J. 2005. Molecular ordering of the caspase activation cascade initiated by the cytotoxic T lymphocyte/natural killer (CTL/NK) protease granzyme B. *Journal of Biological Chemistry* 280(6), pp. 4663–4673. doi: 10.1074/jbc.M410915200.
3. Aggarwal, B.B., Vijayalekshmi, R. V and Sung, B. 2009. Targeting Inflammatory Pathways for Prevention and Therapy of Cancer: Short-Term Friend, Long-Term Foe. *Clinical Cancer Research* 15(2), pp. 425 LP – 430. doi: 10.1158/1078-0432.CCR-08-0149.
4. Al-Shibli, K.I., Donnem, T., Al-Saad, S., Persson, M., Bremnes, R.M. and Busund, L.-T. 2008. Prognostic Effect of Epithelial and Stromal Lymphocyte Infiltration in Non–Small Cell Lung Cancer. *Clinical Cancer Research* 14(16), pp. 5220 LP – 5227. doi: 10.1158/1078-0432.CCR-08-0133.
5. Alegre, M.L., Frauwirth, K.A. and Thompson, C.B. 2001. T-cell regulation by CD28 and CTLA-4. *Nature reviews. Immunology* 1(3), pp. 220–228. doi: 10.1038/35105024.
6. Alexander, M., Kim, S.Y. and Cheng, H. 2020. Update 2020: Management of Non-Small Cell Lung Cancer. *Lung* 198(6), pp. 897–907. doi: 10.1007/s00408-020-00407-5.
7. Allard, B., Aspeslagh, S., Garaud, S., Dupont, F.A., Solinas, C., Kok, M., Routy, B., Sotiriou, C., Stagg, J. and Buisseret, L. 2018. Immuno-oncology-101: overview of major concepts and translational perspectives. *Seminars in Cancer Biology* 52(February), pp. 1–11. doi: 10.1016/j.semcancer.2018.02.005.
8. Andersen, M.H., Schrama, D., Thor Straten, P. and Becker, J.C. 2006. Cytotoxic T cells. *Journal of Investigative Dermatology* 126(1), pp. 32–41. doi: 10.1038/sj.jid.5700001.
9. Anderson, C., Jensen, J. and Orntoft, T. 2004. Normalisation of real-time quantitative reverse transcription-PCR data: a model-based variance estimation approach to identity genes suited for normalisation, applied to bladder andcolon cancer data sets. *Cancer Research* 64, pp. 5245–5250. doi: 10.1158/0008-5472.CAN-04-0496.
10. Andreu, P., Johansson, M., Affara, N.I., Pucci, F., Tan, T., Junankar, S., Korets, L., Lam, J., Tawfik, D., DeNardo, D.G., Naldini, L., de Visser, K.E., De Palma, M. and Coussens, L.M. 2010. FcRγ Activation Regulates Inflammation-Associated Squamous Carcinogenesis. *Cancer Cell* 17(2), pp. 121–134. doi: https://doi.org/10.1016/j.ccr.2009.12.019.
11. Anichini, A., Perotti, V.E., Sgambelluri, F. and Mortarini, R. 2020. Immune escape mechanisms in non small cell lung cancer. *Cancers* 12(12), pp. 1–20. doi: 10.3390/cancers12123605.
12. Annunziato, F., Romagnani, C. and Romagnani, S. 2015. The 3 major types of innate and adaptive cell-mediated effector immunity. *Journal of Allergy and Clinical Immunology* 135(3), pp. 626–635. doi: 10.1016/j.jaci.2014.11.001.
13. Aoki, T., Matsumoto, Y., Hirata, K., Ochiai, K., Okada, M., Ichikawa, K., Shibasaki, M., Arinami, T., Sumazaki, R. and Noguchi, E. 2009. Expression profiling of genes related to asthma exacerbations. *Clinical & Experimental Allergy* 39(2), pp. 213–221. doi: https://doi.org/10.1111/j.1365-2222.2008.03186.x.
14. Aref, S., Azmy, E. and El-Gilany, A.H. 2017. Upregulation of CD200 is associated with regulatory T cell expansion and disease progression in multiple myeloma. *Hematological Oncology* 35(1), pp. 51–57. doi: 10.1002/hon.2206.
15. Aruga, A., Aruga, E., Tanigawa, K., Bishop, D.K., Sondak, V.K. and Chang, A.E. 1997. Type 1 versus type 2 cytokine release by Vbeta T cell subpopulations determines in vivo antitumor reactivity: IL-10 mediates a suppressive role. *Journal of immunology (Baltimore, Md. : 1950)* 159(2), pp. 664–673.
16. Ayoub, N.M., Al-Shami, K.M. and Yaghan, R.J. 2019. Immunotherapy for HER2-positive breast cancer: recent advances and combination therapeutic approaches. *Breast cancer (Dove Medical Press)* 11, pp. 53–69. doi: 10.2147/BCTT.S175360.
17. Baldwin, D.R. 2017. Socioeconomic position and delays in lung cancer diagnosis: should we target the more deprived? *Thorax* 72(5), pp. 393 LP – 395. doi: 10.1136/thoraxjnl-2016-209591.

18. Balkwill, F. and Mantovani, A. 2001. Inflammation and cancer: back to Virchow? *The Lancet* 357, pp. 539–545. doi: 10.1016/S0140-6736(00)04046-0.
19. Bankhead, P., Loughrey, M.B., Fernández, J.A., Dombrowski, Y., McArt, D.G., Dunne, P.D., McQuaid, S., Gray, R.T., Murray, L.J., Coleman, H.G., James, J.A., Salto-Tellez, M. and Hamilton, P.W. 2017. QuPath: Open source software for digital pathology image analysis. *Scientific Reports* 7(1), pp. 1–7. doi: 10.1038/s41598-017-17204-5.
20. Barclay, A.N. 1981. Different reticular elements in rat lymphoid tissue identified by localization of Ia, Thy-1 and MRC OX 2 antigens. *Immunology* 44(4), pp. 727–736.
21. Barclay, A.N. and Ward, H.A. 1982. Purification and Chemical Characterisation of Membrane Glycoproteins from Rat Thymocytes and Brain, Recognised by Monoclonal Antibody MRC OX 2. *European Journal of Biochemistry* 129(2), pp. 447–458. doi: 10.1111/j.1432-1033.1982.tb07070.x.
22. Basu, A., Ramamoorthi, G., Albert, G., Gallen, C., Beyer, A., Snyder, C., Koski, G., Disis, M.L., Czerniecki, B.J. and Kodumudi, K. 2021. Differentiation and Regulation of TH Cells: A Balancing Act for Cancer Immunotherapy. *Frontiers in Immunology* 12. doi: 10.3389/fimmu.2021.669474.
23. Ben-Shmuel, A., Biber, G. and Barda-Saad, M. 2020. Unleashing Natural Killer Cells in the Tumor Microenvironment–The Next Generation of Immunotherapy? *Frontiers in Immunology* 11(February), pp. 1–23. doi: 10.3389/fimmu.2020.00275.
24. Benencia, F., Sprague, L., McGinty, J., Pate, M. and Muccioli, M. 2012. Dendritic cells the tumor microenvironment and the challenges for an effective antitumor vaccination. *Journal of Biomedicine and Biotechnology* 2012. doi: 10.1155/2012/425476.
25. Bennett, F., Luxenberg, D., Ling, V., Wang, I.-M., Marquette, K., Lowe, D., Khan, N., Veldman, G., Jacobs, K.A., Valge-Archer, V.E., Collins, M. and Carreno, B.M. 2003. Program Death-1 Engagement Upon TCR Activation Has Distinct Effects on Costimulation and Cytokine-Driven Proliferation: Attenuation of ICOS, IL-4, and IL-21, But Not CD28, IL-7, and IL-15 Responses. *The Journal of Immunology* 170(2), pp. 711 LP – 718. doi: 10.4049/jimmunol.170.2.711.
26. Berraondo, P., Minute, L., Ajona, D., Corrales, L., Melero, I. and Pio, R. 2016. Innate immune mediators in cancer: between defense and resistance. *Immunological Reviews* 274(1), pp. 290–306. doi: 10.1111/imr.12464.
27. Bertolini, M., McElwee, K., Gilhar, A., Bulfone-Paus, S. and Paus, R. 2020. Hair follicle immune privilege and its collapse in alopecia areata. *Experimental Dermatology* 29(8), pp. 703–725. doi: https://doi.org/10.1111/exd.14155.
28. Bi, J. and Tian, Z. 2017. NK cell exhaustion. *Frontiers in Immunology* 8(JUN). doi: 10.3389/fimmu.2017.00760.
29. Birerley, J.D., Godpodarowicz, M.K. and Wittekind, C. 2017. *TNM Classification of Malignant Tumours Eight Edition*. doi: 10.1177/003591571400702073.
30. Bisgin, A., Meng, W.-J., Adell, G. and Sun, X.-F. 2019. Interaction of CD200 Overexpression on Tumor Cells with CD200R1 Overexpression on Stromal Cells: An Escape from the Host Immune Response in Rectal Cancer Patients. *Journal of Oncology* 2019, pp. 1–7. doi: 10.1155/2019/5689464.
31. Bissonnette, E.Y., Lauzon-Joset, J.F., Debley, J.S. and Ziegler, S.F. 2020. Cross-Talk Between Alveolar Macrophages and Lung Epithelial Cells is Essential to Maintain Lung Homeostasis. *Frontiers in Immunology* 11(October), pp. 1–12. doi: 10.3389/fimmu.2020.583042.
32. Borghaei, H., Paz-Ares, L., Horn, L., Spigel, D.R., Steins, M., Ready, N.E., Chow, L.Q., Vokes, E.E., Felip, E. and Holgado, E. 2015. Nivolumab versus docetaxel in advanced nonsquamous non–small-cell lung cancer. *New England Journal of Medicine* 373(17), pp. 1627–1639. doi: 10.1056/NEJMoa1507643.
33. Böttcher, J.P., Bonavita, E., Chakravarty, P., Blees, H., Cabeza-Cabrerizo, M., Sammicheli, S., Rogers, N.C., Sahai, E., Zelenay, S. and Reis e Sousa, C. 2018. NK Cells Stimulate Recruitment of cDC1 into the Tumor Microenvironment Promoting Cancer Immune Control. *Cell* 172(5), pp. 1022-1037.e14. doi: 10.1016/j.cell.2018.01.004.
34. Brahmer, J., Reckamp, K.L., Baas, P., Crinò, L., Eberhardt, W.E.E., Poddubskaya, E., Antonia, S., Pluzanski, A., Vokes, E.E. and Holgado, E. 2015. Nivolumab versus docetaxel in advanced

squamous-cell non–small-cell lung cancer. *New England Journal of Medicine* 373(2), pp. 123–135. doi: 10.1056/NEJMoa1504627.

35. Bremnes, R.M., Busund, L.T., Kilver, T.L., Andersen, S., Richardsen, E., Paulsen, E.E., Hald, S., Khanehkenari, M.R., Cooper, W.A., Kao, S.C. and Donnem, T. 2016. The role of tumor-infiltrating lymphocytes in development, progression, and prognosis of non-small cell lung cancer. *Journal of Thoracic Oncology* 11(6), pp. 789–800. Available at: http://dx.doi.org/10.1016/j.jtho.2016.01.015.
36. Brown, S., Banfill, K., Aznar, M.C., Whitehurst, P. and Finn, C.F. 2019. The evolving role of radiotherapy in non-small cell lung cancer. *British Journal of Radiology* 92(1104). doi: 10.1259/bjr.20190524.
37. Broz, M.L., Binnewies, M., Boldajipour, B., Nelson, A.E., Pollack, J.L., Erle, D.J., Barczak, A., Rosenblum, M.D., Daud, A., Barber, D.L., Amigorena, S., Van'tVeer, L.J., Sperling, A.I., Wolf, D.M. and Krummel, M.F. 2014. Dissecting the Tumor Myeloid Compartment Reveals Rare Activating Antigen-Presenting Cells Critical for T Cell Immunity. *Cancer Cell* 26(5), pp. 638–652. doi: 10.1016/j.ccell.2014.09.007.
38. Brueckl, W.M., Ficker, J.H. and Zeitler, G. 2020. Clinically relevant prognostic and predictive markers for immune-checkpoint-inhibitor (ICI) therapy in non-small cell lung cancer (NSCLC). *BMC Cancer* 20(1), p. 1185. doi: 10.1186/s12885-020-07690-8.
39. Bryceson, Y.T., Ljunggren, H.G. and Long, E.O. 2009. Minimal requirement for induction of natural cytotoxicity and intersection of activation signals by inhibitory receptors. *Blood* 114(13), pp. 2657–2666. doi: 10.1182/blood-2009-01-201632.
40. Bryceson, Y.T., March, M.E., Barber, D.F., Ljunggren, H.G. and Long, E.O. 2005. Cytolytic granule polarization and degranulation controlled by different receptors in resting NK cells. *Journal of Experimental Medicine* 202(7), pp. 1001–1012. doi: 10.1084/jem.20051143.
41. Buchbinder, E.I. and Desai, A. 2016. CTLA-4 and PD-1 pathways similarities, differences, and implications of their inhibition. *American Journal of Clinical Oncology: Cancer Clinical Trials* 39(1), pp. 98–106. doi: 10.1097/COC.0000000000000239.
42. Buell, J.F., Gross, T.G. and Woodle, E.S. 2005. Malignancy after Transplantation. *Transplantation* 80(2S). doi: 10.1097/01.tp.0000186382.81130.ba.
43. Bustin, S.A., Benes, V., Garson, J.A., Hellemans, J., Huggett, J., Kubista, M., Mueller, R., Nolan, T., Pfaffl, M.W., Shipley, G.L., Vandesompele, J. and Wittwer, C.T. 2009. The MIQE guidelines: Minimum information for publication of quantitative real-time PCR experiments. *Clinical Chemistry* 55(4), pp. 611–622. doi: 10.1373/clinchem.2008.112797.
44. Caligiuri, M.A. 2008. Human natural killer cells. *Blood* 112(3), pp. 461–469. doi: 10.1182/blood-2007-09-077438.
45. Cameron, C.M., Barrett, J.W., Liu, L., Lucas, A.R. and McFadden, G. 2005. Myxoma Virus M141R Expresses a Viral CD200 (vOX-2) That Is Responsible for Down-Regulation of Macrophage and T-Cell Activation In Vivo. *Journal of Virology* 79(10), pp. 6052–6067. doi: 10.1128/jvi.79.10.6052-6067.2005.
46. Camidge, D.R., Pao, W. and Sequist, L. V 2014. Acquired resistance to TKIs in solid tumours: learning from lung cancer. *Nature reviews. Clinical oncology* 11(8), pp. 473–481. doi: 10.1038/nrclinonc.2014.104.
47. Camolotto, S.A., Pattabiraman, S., Mosbruger, T.L., Jones, A., Belova, V.K., Orstad, G., Streiff, M., Salmond, L., Stubben, C., Kaestner, K.H. and Snyder, E.L. 2018. FoxA1 and FoxA2 drive gastric differentiation and suppress squamous identity in NKX2-1-negative lung cancer. *eLife* 7. doi: 10.7554/eLife.38579.
48. Campoli, M. and Ferrone, S. 2008. HLA antigen changes in malignant cells: Epigenetic mechanisms and biologic significance. *Oncogene* 27(45), pp. 5869–5885. doi: 10.1038/onc.2008.273.
49. Cancer Research UK 2014. *Tobacco statistics*. Available at: http://www.cancerresearchuk.org/cancer-info/cancerstats/causes/tobacco-statistics/ [Accessed: 24 February 2022].
50. Cancer Research UK 2021. *Lung cancer incidence statistics*. Available at:

https://www.cancerresearchuk.org/health-professional/cancer-statistics/statistics-by-cancer-type/lung-cancer/incidence [Accessed: 23 February 2022].
51. Cancer Research UK [no date][a]. *Lung cancer mortality statistics*. Available at: https://www.cancerresearchuk.org/health-professional/cancer-statistics/statistics-by-cancer-type/lung-cancer/mortality [Accessed: 23 February 2022].
52. Cancer Research UK [no date][b]. *Lung cancer risk*. Available at: https://www.cancerresearchuk.org/health-professional/cancer-statistics/statistics-by-cancer-type/lung-cancer/risk-factors [Accessed: 20 February 2022].
53. Cancer Research UK [no date][c]. *Lung cancer survival statistics*. Available at: https://www.cancerresearchuk.org/health-professional/cancer-statistics/statistics-by-cancer-type/lung-cancer/survival#ref [Accessed: 24 February 2022].
54. Caro-Maldonado, A., Wang, R., Nichols, A.G., Kuraoka, M., Milasta, S., Sun, L.D., Gavin, A.L., Abel, E.D., Kelsoe, G., Green, D.R. and Rathmell, J.C. 2014. Metabolic Reprogramming Is Required for Antibody Production That Is Suppressed in Anergic but Exaggerated in Chronically BAFF-Exposed B Cells. *The Journal of Immunology* 192(8), pp. 3626 LP – 3636. doi: 10.4049/jimmunol.1302062.
55. Carrega, P., Morandi, B., Costa, R., Frumento, G., Forte, G., Altavilla, G., Ratto, G.B., Mingari, M.C., Moretta, L. and Ferlazzo, G. 2008a. Natural killer cells infiltrating human nonsmall-cell lung cancer are enriched in CD56brightCD16- cells and display an impaired capability to kill tumor cells. *Cancer* 112(4), pp. 863–875. doi: 10.1002/cncr.23239.
56. Carrega, P., Morandi, B., Costa, R., Frumento, G., Forte, G., Altavilla, G., Ratto, G.B., Mingari, M.C., Moretta, L. and Ferlazzo, G. 2008b. Natural killer cells infiltrating human nonsmall-cell lung cancer are enriched in CD56brightCD16- cells and display an impaired capability to kill tumor cells. *Cancer* 112(4), pp. 863–875. doi: 10.1002/cncr.23239.
57. Cerwenka, A., Baron, J.L. and Lanier, L.L. 2001. Ectopic expression of retinoic acid early inducible-1 gene (RAE-1) permits natural killer cell-mediated rejection of a MHC class I-bearing tumor in vivo. *Proceedings of the National Academy of Sciences of the United States of America* 98(20), pp. 11521–11526. doi: 10.1073/pnas.201238598.
58. Chapman, J.R., Webster, A.C. and Wong, G. 2013. Cancer in the transplant recipient. *Cold Spring Harbor perspectives in medicine* 3(7), p. a015677. doi: 10.1101/cshperspect.a015677.
59. Chaudhary, B. and Elkord, E. 2016. Regulatory T Cells in the Tumor Microenvironment and Cancer Progression: Role and Therapeutic Targeting. *Vaccines* 4(3), p. 28. doi: 10.3390/vaccines4030028.
60. Chen, D.S. and Mellman, I. 2013. Oncology meets immunology: The cancer-immunity cycle. *Immunity* 39(1), pp. 1–10. doi: 10.1016/j.immuni.2013.07.012.
61. Chen, D.S. and Mellman, I. 2017. Elements of cancer immunity and the cancer-immune set point. *Nature* 541(7637), pp. 321–330. doi: 10.1038/nature21349.
62. Chen, L. and Flies, D.B. 2013. Molecular mechanisms of T cell co-stimulation and co-inhibition. *Nature Reviews Immunology* 13(4), pp. 227–242. doi: 10.1038/nri3405.
63. Chen, Z., Fillmore, C.M., Hammerman, P.S., Kim, C.F. and Wong, K.K. 2014. Non-small-cell lung cancers: A heterogeneous set of diseases. *Nature Reviews Cancer* . doi: 10.1038/nrc3775.
64. Chen, Z., Marsden, P.A. and Gorczynski, R.M. 2006. Cloning and characterization of the human CD200 promoter region. *Molecular Immunology* 43(6), pp. 579–587. doi: https://doi.org/10.1016/j.molimm.2005.04.014.
65. Chen, Z., Marsden, P.A. and Gorczynski, R.M. 2009. Role of a distal enhancer in the transcriptional responsiveness of the human CD200 gene to interferon-γ and tumor necrosis factor-α. *Molecular Immunology* 46(10), pp. 1951–1963. doi: 10.1016/j.molimm.2009.03.015.
66. Cheong, J.E. and Sun, L. 2018. Targeting the IDO1/TDO2–KYN–AhR Pathway for Cancer Immunotherapy – Challenges and Opportunities. *Trends in Pharmacological Sciences* 39(3), pp. 307–325. doi: https://doi.org/10.1016/j.tips.2017.11.007.
67. Cherwinski, H.M., Murphy, C.A., Joyce, B.L., Bigler, M.E., Song, Y.S., Zurawski, S.M., Moshrefi, M.M., Gorman, D.M., Miller, K.L., Zhang, S., Sedgwick, J.D. and Phillips, J.H. 2005. The CD200 Receptor Is a Novel and Potent Regulator of Murine and Human Mast Cell Function. *The Journal*

of Immunology 174(3), pp. 1348–1356. doi: 10.4049/jimmunol.174.3.1348.
68. Chitnis, T., Imitola, J., Wang, Y., Elyaman, W., Chawla, P., Sharuk, M., Raddassi, K., Bronson, R.T. and Khoury, S.J. 2007. Elevated neuronal expression of CD200 protects Wlds mice from inflammation-mediated neurodegeneration. *American Journal of Pathology* 170(5), pp. 1695–1712. doi: 10.2353/ajpath.2007.060677.
69. Cho, Y.H., Choi, M.G., Kim, D.H., Choi, Y.J., Kim, S.Y., Sung, K.J., Lee, J.C., Kim, S.Y., Rho, J.K. and Choi, C.M. 2020. Natural Killer Cells as a Potential Biomarker for Predicting Immunotherapy Efficacy in Patients with Non-Small Cell Lung Cancer. *Targeted Oncology* 15(2), pp. 241–247. doi: 10.1007/s11523-020-00712-2.
70. Choueiry, F., Torok, M., Shakya, R., Agrawal, K., Deems, A., Benner, B., Hinton, A., Shaffer, J., Blaser, B.W., Noonan, A.M., Williams, T.M., Dillhoff, M., Conwell, D.L., Hart, P.A., Cruz-Monserrate, Z., Bai, X.-F., Carson, W.E. 3rd and Mace, T.A. 2020. CD200 promotes immunosuppression in the pancreatic tumor microenvironment. *Journal for immunotherapy of cancer* 8(1). doi: 10.1136/jitc-2019-000189.
71. Chraa, D., Naim, A., Olive, D. and Badou, A. 2019. T lymphocyte subsets in cancer immunity: Friends or foes. *Journal of Leukocyte Biology* 105(2), pp. 243–255. doi: 10.1002/JLB.MR0318-097R.
72. Clark, D.A., Keil, A., Chen, Z., Markert, U., Manuel, J. and Gorczynski, R.M. 2003. Placental trophoblast from successful human pregnancies expresses the tolerance signaling molecule, CD200 (OX-2). *American Journal of Reproductive Immunology* 50(3), pp. 187–195. doi: 10.1034/j.1600-0897.2003.00086.x.
73. Clark, M.J., Gagnon, J., Williams, A.F. and Barclay, A.N. 1985. MRC OX-2 antigen: a lymphoid/neuronal membrane glycoprotein with a structure like a single immunoglobulin light chain. *The EMBO Journal* 4(1), pp. 113–118. doi: 10.1002/j.1460-2075.1985.tb02324.x.
74. ClinicalTrials.gov NCT02817633 [no date]. *NCT02817633 A Study of TSR-022 in Participants With Advanced Solid Tumors (AMBER)*. Available at: https://clinicaltrials.gov/ct2/show/NCT02817633 [Accessed: 1 March 2022].
75. Coffelt, S.B., Wellenstein, M.D. and De Visser, K.E. 2016. Neutrophils in cancer: Neutral no more. *Nature Reviews Cancer* 16(7), pp. 431–446. doi: 10.1038/nrc.2016.52.
76. Coles, S.J., Hills, R.K., Wang, E.C.Y., Burnett, A.K., Man, S., Darley, R.L. and Tonks, A. 2012a. Expression of CD200 on AML blasts directly suppresses memory T-cell function. *Leukemia* 26(9), pp. 2148–2151. doi: 10.1038/leu.2012.77.
77. Coles, S.J., Hills, R.K., Wang, E.C.Y., Burnett, A.K., Man, S., Darley, R.L. and Tonks, A. 2012b. Increased CD200 expression in acute myeloid leukemia is linked with an increased frequency of FoxP3 + regulatory T cells. *Leukemia* 26(9), pp. 2146–2148. doi: 10.1038/leu.2012.75.
78. Coles, S.J., Hills, R.K., Wang, E.C.Y., Burnett, A.K., Man, S., Darley, R.L. and Tonks, A. 2012c. Increased CD200 expression in acute myeloid leukemia is linked with an increased frequency of FoxP3 + regulatory T cells. *Leukemia* 26(9), pp. 2146–2148. Available at: http://dx.doi.org/10.1038/leu.2012.75.
79. Coles, S.J., Wang, E.C.Y., Man, S., Hills, R.K., Burnett, A.K., Tonks, A. and Darley, R.L. 2011. CD200 expression suppresses natural killer cell function and directly inhibits patient anti-tumor response in acute myeloid leukemia. *Leukemia* 25(5), pp. 792–799. doi: 10.1038/leu.2011.1.
80. Collisson, E.A., Campbell, J.D., Brooks, A.N., Berger, A.H., Lee, W., Chmielecki, J., Beer, D.G., Cope, L., Creighton, C.J., Danilova, L., Ding, L., Getz, G., Hammerman, P.S., Hayes, D.N., Hernandez, B., Herman, J.G., Heymach, J. V., Jurisica, I., Kucherlapati, R., et al. 2014. Comprehensive molecular profiling of lung adenocarcinoma: The cancer genome atlas research network. *Nature* 511(7511), pp. 543–550. doi: 10.1038/nature13385.
81. Colmont, C.S., BenKetah, A., Reed, S.H., Hawk, N. V., Telford, W.G., Ohyama, M., Udey, M.C., Yee, C.L., Vogel, J.C. and Patel, G.K. 2013. CD200-expressing human basal cell carcinoma cells initiate tumor growth. *Proceedings of the National Academy of Sciences* . doi: 10.1073/pnas.1211655110.
82. Condamine, T., Ramachandran, I., Youn, J.-I. and Gabrilovich, D.I. 2015. Regulation of tumor

metastasis by myeloid-derived suppressor cells. *Annual Review of Medicine* 66(1), pp. 97–110. doi: 10.1146/annurev-med-051013-052304.

83. Conforti, F., Pala, L., Bagnardi, V., De Pas, T., Martinetti, M., Viale, G., Gelber, R.D. and Goldhirsch, A. 2018. Cancer immunotherapy efficacy and patients' sex: a systematic review and meta-analysis. *The Lancet. Oncology* 19(6), pp. 737–746. doi: 10.1016/S1470-2045(18)30261-4.
84. Cong, J., Wang, X., Zheng, X., Wang, D., Fu, B., Sun, R., Tian, Z. and Wei, H. 2018. Dysfunction of Natural Killer Cells by FBP1-Induced Inhibition of Glycolysis during Lung Cancer Progression. *Cell Metabolism* 28(2), pp. 243-255.e5. doi: 10.1016/j.cmet.2018.06.021.
85. Copland, D.A., Calder, C.J., Raveney, B.J.E., Nicholson, L.B., Phillips, J., Cherwinski, H., Jenmalm, M., Sedgwick, J.D. and Dick, A.D. 2007. Monoclonal antibody-mediated CD200 receptor signaling suppresses macrophage activation and tissue damage in experimental autoimmune uveoretinitis. *American Journal of Pathology* 171(2), pp. 580–588. doi: 10.2353/ajpath.2007.070272.
86. Crespo, J., Sun, H., Welling, T.H., Tian, Z. and Zou, W. 2013. T cell anergy, exhaustion, senescence, and stemness in the tumor microenvironment. *Current Opinion in Immunology* 25(2), pp. 214–221. doi: https://doi.org/10.1016/j.coi.2012.12.003.
87. Cromheecke, J.L., Nguyen, K.T. and Huston, D.P. 2014. Emerging role of human basophil biology in health and disease. *Current Allergy and Asthma Reports* 14(1), pp. 43–45. doi: 10.1007/s11882-013-0408-2.
88. Curran, M.A., Montalvo, W., Yagita, H. and Allison, J.P. 2010. PD-1 and CTLA-4 combination blockade expands infiltrating T cells and reduces regulatory T and myeloid cells within B16 melanoma tumors. *Proceedings of the National Academy of Sciences of the United States of America* 107(9), pp. 4275–4280. doi: 10.1073/pnas.0915174107.
89. Curry, A., Khatri, I., Kos, O., Zhu, F. and Gorczynski, R. 2017. Importance of CD200 expression by tumor or host cells to regulation of immunotherapy in a mouse breast cancer model. *PLoS ONE* 12(2), pp. 1–19. doi: 10.1371/journal.pone.0171586.
90. Darvin, P., Toor, S.M., Sasidharan Nair, V. and Elkord, E. 2018. Immune checkpoint inhibitors: recent progress and potential biomarkers. *Experimental and Molecular Medicine* 50(12), pp. 1–11. doi: 10.1038/s12276-018-0191-1.
91. Das, R., Verma, R., Sznol, M., Boddupalli, C.S., Gettinger, S.N., Kluger, H., Callahan, M., Wolchok, J.D., Halaban, R. and Dhodapkar, M. V 2015. Combination therapy with anti–CTLA-4 and anti–PD-1 leads to distinct immunologic changes in vivo. *The Journal of Immunology* 194(3), pp. 950–959. doi: 10.4049/jimmunol.1401686.
92. Davidson, M.R., Gazdar, A.F. and Clarke, B.E. 2013. The pivotal role of pathology in the management of lung cancer. *Journal of thoracic disease* 5 Suppl 5(Suppl 5), pp. S463-78. doi: 10.3978/j.issn.2072-1439.2013.08.43.
93. Davis, A.S., Richter, A., Becker, S., Moyer, J.E., Sandouk, A., Skinner, J. and Taubenberger, J.K. 2014. Characterizing and Diminishing Autofluorescence in Formalin-fixed Paraffin-embedded Human Respiratory Tissue. *Journal of Histochemistry and Cytochemistry* 62(6), pp. 405–423. doi: 10.1369/0022155414531549.
94. de Koning, H.J., van der Aalst, C.M., de Jong, P.A., Scholten, E.T., Nackaerts, K., Heuvelmans, M.A., Lammers, J.-W.J., Weenink, C., Yousaf-Khan, U., Horeweg, N., van 't Westeinde, S., Prokop, M., Mali, W.P., Mohamed Hoesein, F.A.A., van Ooijen, P.M.A., Aerts, J.G.J. V, den Bakker, M.A., Thunnissen, E., Verschakelen, J., et al. 2020. Reduced Lung-Cancer Mortality with Volume CT Screening in a Randomized Trial. *New England Journal of Medicine* 382(6), pp. 503–513. doi: 10.1056/NEJMoa1911793.
95. De Simone, M., Arrigoni, A., Rossetti, G., Gruarin, P., Ranzani, V., Politano, C., Bonnal, R.J.P., Provasi, E., Sarnicola, M.L., Panzeri, I., Moro, M., Crosti, M., Mazzara, S., Vaira, V., Bosari, S., Palleschi, A., Santambrogio, L., Bovo, G., Zucchini, N., et al. 2016. Transcriptional Landscape of Human Tissue Lymphocytes Unveils Uniqueness of Tumor-Infiltrating T Regulatory Cells. *Immunity* 45(5), pp. 1135–1147. doi: 10.1016/j.immuni.2016.10.021.
96. Deaglio, S., Dwyer, K.M., Gao, W., Friedman, D., Usheva, A., Erat, A., Chen, J.-F., Enjyoji, K., Linden, J., Oukka, M., Kuchroo, V.K., Strom, T.B. and Robson, S.C. 2007. Adenosine generation

catalyzed by CD39 and CD73 expressed on regulatory T cells mediates immune suppression. *The Journal of experimental medicine* 204(6), pp. 1257–1265. doi: 10.1084/jem.20062512.

97. Debruin, E.J., Gold, M., Bernard, C. Lo, Snyder, K., Cait, A., Lasic, N., Lopez, M., McNagny, K.M. and Hughes, M.R. 2014. Mast cells in human health and disease. In: *Mast Cells: Methods and Protocols*., pp. 93–119. doi: 10.1007/978-1-4939-1568-2.
98. Deeks, E.D. 2016. Pembrolizumab: A Review in Advanced Melanoma. *Drugs* 76(3), pp. 375–386. doi: 10.1007/s40265-016-0543-x.
99. Devaud, C., Darcy, P.K. and Kershaw, M.H. 2014. Foxp3 expression in T regulatory cells and other cell lineages. *Cancer Immunology, Immunotherapy* 63(9), pp. 869–876. doi: 10.1007/s00262-014-1581-4.
100. Dhatchinamoorthy, K., Colbert, J.D. and Rock, K.L. 2021. Cancer Immune Evasion Through Loss of MHC Class I Antigen Presentation. *Frontiers in Immunology* 12(March). doi: 10.3389/fimmu.2021.636568.
101. Doroshow, D.B., Sanmamed, M.F., Hastings, K., Politi, K., Rimm, D.L., Chen, L., Melero, I., Schalper, K.A. and Herbst, R.S. 2019. Immunotherapy in Non–Small Cell Lung Cancer: Facts and Hopes. *Clinical Cancer Research* 25(15), pp. 4592–4602. doi: 10.1158/1078-0432.CCR-18-1538.
102. Duma, N., Santana-Davila, R. and Molina, J.R. 2019. Non–Small Cell Lung Cancer: Epidemiology, Screening, Diagnosis, and Treatment. *Mayo Clinic Proceedings* 94(8), pp. 1623–1640. doi: 10.1016/j.mayocp.2019.01.013.
103. Dunn, G.P., Bruce, A., Ikeda, H., Old, L.J. and Schreiber, R.D. 2002. Cancer Immunoediting: from immunosurveillance to tumour escape. *Nature Immunology* 3(11), pp. 85–99. doi: 10.1016/B978-0-12-394296-8.00007-5.
104. Dunn, G.P., Old, L.J. and Schreiber, R.D. 2004. The immunobiology of cancer immunosurveillance and immunoediting. *Immunity* 21(2), pp. 137–148. doi: 10.1016/j.immuni.2004.07.017.
105. Duraiswamy, J., Kaluza, K.M., Freeman, G.J. and Coukos, G. 2013. Dual blockade of PD-1 and CTLA-4 combined with tumor vaccine effectively restores T-cell rejection function in tumors. *Cancer research* 73(12), pp. 3591–3603. doi: 10.1158/0008-5472.CAN-12-4100.
106. Durgeau, A., Virk, Y., Corgnac, S. and Mami-Chouaib, F. 2018. Recent advances in targeting CD8 T-cell immunity for more effective cancer immunotherapy. *Frontiers in Immunology* 9(JAN). doi: 10.3389/fimmu.2018.00014.
107. Dyck, L. and Mills, K.H.G. 2017. Immune checkpoints and their inhibition in cancer and infectious diseases. *European Journal of Immunology* 47(5), pp. 765–779. doi: 10.1002/eji.201646875.
108. Echchakir, H., Bagot, M., Dorothée, G., Martinvalet, D., Le Gouvello, S., Boumsell, L., Chouaib, S., Bensussan, A. and Mami-Chouaib, F. 2000. Cutaneous T cell lymphoma reactive CD4+ cytotoxic T lymphocyte clones display a Th1 cytokine profile and use a fas-independent pathway for specific tumor cell lysis. *Journal of investigative dermatology* 115(1), pp. 74–80. doi: 10.1046/j.1523-1747.2000.00995.x.
109. Ehrlich, P. 1909. Über den jetzigen Stand der Chemotherapie. *Berichte der deutschen chemischen Gesellschaft* 42(1), pp. 17–47. doi: 10.1002/cber.19090420105.
110. Erdag, G., Schaefer, J.T., Smolkin, M.E., Deacon, D.H., Shea, S.M., Dengel, L.T., Patterson, J.W. and Slingluff, C.L. 2012. Immunotype and Immunohistologic Characteristics of Tumor-Infiltrating Immune Cells Are Associated with Clinical Outcome in Metastatic Melanoma. *Cancer Research* 72(5), pp. 1070 LP – 1080. doi: 10.1158/0008-5472.CAN-11-3218.
111. Erin, N., Podnos, A., Tanriover, G., Duymuş, Cote, E., Khatri, I. and Gorczynski, R.M. 2015. Bidirectional effect of CD200 on breast cancer development and metastasis, with ultimate outcome determined by tumor aggressiveness and a cancer-induced inflammatory response. *Oncogene* 34(29), pp. 3860–3870. doi: 10.1038/onc.2014.317.
112. Erin, N., Zhao, W., Bylander, J., Chase, G. and Clawson, G. 2006. Capsaicin-induced inactivation of sensory neurons promotes a more aggressive gene expression phenotype in breast cancer cells. *Breast Cancer Research and Treatment* 99(3), pp. 351–364. doi: 10.1007/s10549-

006-9219-7.
113. Evans, M. 2013. Lung cancer: needs assessment, treatment and therapies. *British Journal of Nursing* 22(17). doi: 10.12968/bjon.2013.22.Sup17.S15.
114. Evison, M. 2020. The current treatment landscape in the UK for stage III NSCLC. *British Journal of Cancer* 123(December), pp. 3–9. doi: 10.1038/s41416-020-01069-z.
115. Facchinetti, F., Rossi, G., Bria, E., Soria, J.-C., Besse, B., Minari, R., Friboulet, L. and Tiseo, M. 2017. Oncogene addiction in non-small cell lung cancer: Focus on ROS1 inhibition. *Cancer treatment reviews* 55, pp. 83–95. doi: 10.1016/j.ctrv.2017.02.010.
116. Fallarino, F., Asselin-Paturel, C., Vacca, C., Bianchi, R., Gizzi, S., Fioretti, M.C., Trinchieri, G., Grohmann, U. and Puccetti, P. 2004. Murine Plasmacytoid Dendritic Cells Initiate the Immunosuppressive Pathway of Tryptophan Catabolism in Response to CD200 Receptor Engagement. *The Journal of Immunology* 173(6), pp. 3748–3754. doi: 10.4049/jimmunol.173.6.3748.
117. Ferone, G., Lee, M.C., Sage, J. and Berns, A. 2020. Cells of origin of lung cancers: lessons from mouse studies. *Genes & development* 34(15–16), pp. 1017–1032. doi: 10.1101/gad.338228.120.
118. Ferone, G., Song, J.-Y., Sutherland, K.D., Bhaskaran, R., Monkhorst, K., Lambooij, J.-P., Proost, N., Gargiulo, G. and Berns, A. 2016. SOX2 Is the Determining Oncogenic Switch in Promoting Lung Squamous Cell Carcinoma from Different Cells of Origin. *Cancer cell* 30(4), pp. 519–532. doi: 10.1016/j.ccell.2016.09.001.
119. Field, J.K., Vulkan, D., Davies, M.P.A., Baldwin, D.R., Brain, K.E., Devaraj, A., Eisen, T., Gosney, J., Green, B.A., Holemans, J.A., Kavanagh, T., Kerr, K.M., Ledson, M., Lifford, K.J., McRonald, F.E., Nair, A., Page, R.D., Parmar, M.K.B., Rassl, D.M., et al. 2021. Lung cancer mortality reduction by LDCT screening: UKLS randomised trial results and international meta-analysis. *The Lancet Regional Health - Europe* 10, p. 100179. doi: https://doi.org/10.1016/j.lanepe.2021.100179.
120. Forrester, J. V, Xu, H., Lambe, T. and Cornall, R. 2008. Immune privilege or privileged immunity? *Mucosal Immunology* 1(5), pp. 372–381. doi: 10.1038/mi.2008.27.
121. Foster-Cuevas, M., Wright, G.J., Puklavec, M.J., Brown, M.H. and Barclay, A.N. 2004. Human Herpesvirus 8 K14 Protein Mimics CD200 in Down-Regulating Macrophage Activation through CD200 Receptor. *Journal of Virology* 78(14), pp. 7667–7676. doi: 10.1128/jvi.78.14.7667-7676.2004.
122. Freud, A.G., Mundy-Bosse, B.L., Yu, J. and Caligiuri, M.A. 2017. The Broad Spectrum of Human Natural Killer Cell Diversity. *Immunity* 47(5), pp. 820–833. doi: 10.1016/j.immuni.2017.10.008.
123. Fridlender, Z.G., Sun, J., Kim, S., Kapoor, V., Cheng, G., Ling, L., Worthen, G.S. and Albelda, S.M. 2009. Polarization of tumor-associated neutrophil phenotype by TGF-beta: “N1” versus “N2” TAN. *Cancer cell* 16(3), pp. 183–194. doi: 10.1016/j.ccr.2009.06.017.
124. Fridman, W.H., Zitvogel, L., Sautès–Fridman, C. and Kroemer, G. 2017. The immune contexture in cancer prognosis and treatment. *Nature Reviews Clinical Oncology* 14(12), pp. 717–734. doi: 10.1038/nrclinonc.2017.101.
125. Fukumura, D., Kloepper, J., Amoozgar, Z., Duda, D.G. and Jain, R.K. 2018. Enhancing cancer immunotherapy using antiangiogenics: opportunities and challenges. *Nature Reviews Clinical Oncology* 15(5), pp. 325–340. Available at: https://doi.org/10.1038/nrclinonc.2018.29.
126. Gabitass, R.F., Annels, N.E., Stocken, D.D., Pandha, H.A. and Middleton, G.W. 2011. Elevated myeloid-derived suppressor cells in pancreatic, esophageal and gastric cancer are an independent prognostic factor and are associated with significant elevation of the Th2 cytokine interleukin-13. *Cancer Immunology, Immunotherapy* 60(10), p. 1419. doi: 10.1007/s00262-011-1028-0.
127. Gabrilovich, D.I. 2017. Myeloid-derived suppressor cells. *Cancer Immunology Research* 5(1), pp. 3–8. doi: 10.1158/2326-6066.CIR-16-0297.
128. Gabrilovich, D.I., Chen, H.L., Girgis, K.R., Cunningham, H.T., Meny, G.M., Nadaf, S., Kavanaugh, D. and Carbone, D.P. 1996. Production of vascular endothelial growth factor by human

tumors inhibits the functional maturation of dendritic cells. *Nature medicine* 2(10), pp. 1096–1103. doi: 10.1038/nm1096-1096.

129. Gainor, J.F., Shaw, A.T., Sequist, L. V, Fu, X., Azzoli, C.G., Piotrowska, Z., Huynh, T.G., Zhao, L., Fulton, L. and Schultz, K.R. 2016. EGFR mutations and ALK rearrangements are associated with low response rates to PD-1 pathway blockade in non–small cell lung cancer: a retrospective analysis. *Clinical cancer research* 22(18), pp. 4585–4593. doi: 10.1158/1078-0432.CCR-15-3101.
130. Gardner, A. and Ruffell, B. 2016. Dendritic cells and cancer immunity. *Trends Immunol* 37(12), pp. 1855–865. doi: 10.1016/j.physbeh.2017.03.040.
131. Garon, E.B., Hellmann, M.D., Rizvi, N.A., Carcereny, E., Leighl, N.B., Ahn, M.-J., Eder, J.P., Balmanoukian, A.S., Aggarwal, C., Horn, L., Patnaik, A., Gubens, M., Ramalingam, S.S., Felip, E., Goldman, J.W., Scalzo, C., Jensen, E., Kush, D.A. and Hui, R. 2019. Five-Year Overall Survival for Patients With Advanced Non–Small-Cell Lung Cancer Treated With Pembrolizumab: Results From the Phase I KEYNOTE-001 Study. *Journal of Clinical Oncology* 37(28), pp. 2518–2527. doi: 10.1200/JCO.19.00934.
132. Geng, Y., Shao, Y., He, W., Hu, W., Xu, Y., Chen, J., Wu, C. and Jiang, J. 2015. Prognostic role of tumor-infiltrating lymphocytes in lung cancer: A meta-analysis. *Cellular Physiology and Biochemistry* 37(4), pp. 1560–1571. doi: 10.1159/000438523.
133. Gentles, A.J., Newman, A.M., Liu, C.L., Bratman, S. V., Feng, W., Kim, D., Nair, V.S., Xu, Y., Khuong, A., Hoang, C.D., Diehn, M., West, R.B., Plevritis, S.K. and Alizadeh, A.A. 2015. The prognostic landscape of genes and infiltrating immune cells across human cancers. *Nature Medicine* 21(8), pp. 938–945. doi: 10.1038/nm.3909.
134. Germain, R.N. 2002. t-cell development and the CD4-CD8 lineage decision. *Nature Reviews Immunology* 2(5), pp. 309–322. doi: 10.1038/nri798.
135. Germano, G., Lamba, S., Rospo, G., Barault, L., Magrì, A., Maione, F., Russo, M., Crisafulli, G., Bartolini, A., Lerda, G., Siravegna, G., Mussolin, B., Frapolli, R., Montone, M., Morano, F., de Braud, F., Amirouchene-Angelozzi, N., Marsoni, S., D'Incalci, M., et al. 2017. Inactivation of DNA repair triggers neoantigen generation and impairs tumour growth. *Nature* 552(7683), pp. 116–120. doi: 10.1038/nature24673.
136. Gettinger, S., Horn, L., Jackman, D., Spigel, D., Antonia, S., Hellmann, M., Powderly, J., Heist, R., Sequist, L. V, Smith, D.C., Leming, P., Geese, W.J., Yoon, D., Li, A. and Brahmer, J. 2018. Five-Year Follow-Up of Nivolumab in Previously Treated Advanced Non-Small-Cell Lung Cancer: Results From the CA209-003 Study. *Journal of clinical oncology : official journal of the American Society of Clinical Oncology* 36(17), pp. 1675–1684. doi: 10.1200/JCO.2017.77.0412.
137. Gill, S., Vasey, A.E., De Souza, A., Baker, J., Smith, A.T., Kohrt, H.E., Florek, M., Gibbs, K.D.J., Tate, K., Ritchie, D.S. and Negrin, R.S. 2012. Rapid development of exhaustion and down-regulation of eomesodermin limit the antitumor activity of adoptively transferred murine natural killer cells. *Blood* 119(24), pp. 5758–5768. doi: 10.1182/blood-2012-03-415364.
138. Giraldo, N.A., Sanchez-Salas, R., Peske, J.D., Vano, Y., Becht, E., Petitprez, F., Validire, P., Ingels, A., Cathelineau, X., Fridman, W.H. and Sautès-Fridman, C. 2019. The clinical role of the TME in solid cancer. *British Journal of Cancer* 120(1), pp. 45–53. doi: 10.1038/s41416-018-0327-z.
139. Giuntoli, R.L., Lu, J., Kobayashi, H., Kennedy, R. and Celis, E. 2002. Direct costimulation of tumor-reactive CTL by helper T cells potentiate their proliferation, survival, and effector function. *Clinical Cancer Research* 8(3), pp. 922 LP – 931.
140. Gooden, M.J.M., De Bock, G.H., Leffers, N., Daemen, T. and Nijman, H.W. 2011. The prognostic influence of tumour-infiltrating lymphocytes in cancer: A systematic review with meta-analysis. *British Journal of Cancer* 105(1), pp. 93–103. doi: 10.1038/bjc.2011.189.
141. Gorczynski, R., Khatri, I., Lee, L. and Boudakov, I. 2008. An Interaction between CD200 and Monoclonal Antibody Agonists to CD200R2 in Development of Dendritic Cells That Preferentially Induce Populations of CD4 + CD25 + T Regulatory Cells . *The Journal of Immunology* 180(9), pp. 5946–5955. doi: 10.4049/jimmunol.180.9.5946.
142. Gorczynski, R.M. 2001. Transplant tolerance modifying antibody to CD200 receptor, but not

CD200, alters cytokine production profile from stimulated macrophages. *European Journal of Immunology* 31(8), pp. 2331–2337. doi: 10.1002/1521-4141(200108)31:8<2331::AID-IMMU2331>3.0.CO;2-#.

143. Gorczynski, R.M., Cattral, M.S., Chen, Z., Hu, J., Lei, J., Min, W.P., Yu, G. and Ni, J. 1999. An immunoadhesin incorporating the molecule OX-2 is a potent immunosuppressant that prolongs allo- and xenograft survival. *Journal of Immunology* 163(3), pp. 1654–1660.
144. Gorczynski, R.M., Chen, Z., Diao, J., Khatri, I., Wong, K., Yu, K. and Behnke, J. 2010. Breast cancer cell CD200 expression regulates immune response to EMT6 tumor cells in mice. *Breast Cancer Research and Treatment* 123(2), pp. 405–415. doi: 10.1007/s10549-009-0667-8.
145. Gorczynski, R.M., Chen, Z., He, W., Khatri, I., Sun, Y., Yu, K. and Boudakov, I. 2009. Expression of a CD200 Transgene Is Necessary for Induction but Not Maintenance of Tolerance to Cardiac and Skin Allografts. *The Journal of Immunology* 183(3), pp. 1560–1568. doi: 10.4049/jimmunol.0900200.
146. Gorczynski, R.M., Chen, Z., Hu, J., Kai, Y. and Lei, J. 2001. Evidence of a role for CD200 in regulation of immune rejection of leukaemic tumour cells in C57BL/6 mice. *Clinical and Experimental Immunology* 126(2), pp. 220–229. doi: 10.1046/j.1365-2249.2001.01689.x.
147. Gorczynski, R.M., Chen, Z., Kai, Y., Wong, S. and Lee, L. 2004. Induction of tolerance-inducing antigen-presenting cells in bone marrow cultures in vitro using monoclonal antibodies to CD200R. *Transplantation* 77(8), pp. 1138–1144. doi: 10.1097/01.TP.0000121773.18476.1C.
148. Gorczynski, R.M., Chen, Z., Khatri, I. and Yu, K. 2011. Graft-infiltrating cells expressing a CD200 transgene prolong allogeneic skin graft survival in association with local increases in Foxp3 +Treg and mast cells. *Transplant Immunology* 25(4), pp. 187–193. doi: 10.1016/j.trim.2011.07.006.
149. Gorczynski, R.M., Hadidi, S., Yu, G. and Clark, D.A. 2002. The same immunoregulatory molecules contribute to successful pregnancy and transplantation. *American Journal of Reproductive Immunology* 48(1), pp. 18–26. doi: 10.1034/j.1600-0897.2002.01094.x.
150. Gordon, S. and Taylor, P.R. 2005. Monocyte and macrophage heterogeneity. *Nature Reviews Immunology* 5(12), pp. 953–964. doi: 10.1038/nri1733.
151. Grant, M.J., Herbst, R.S. and Goldberg, S.B. 2021. Selecting the optimal immunotherapy regimen in driver-negative metastatic NSCLC. *Nature Reviews Clinical Oncology* 18(10), pp. 625–644. doi: 10.1038/s41571-021-00520-1.
152. Greenwald, R.J., Oosterwegel, M.A., van der Woude, D., Kubal, A., Mandelbrot, D.A., Boussiotis, V.A. and Sharpe, A.H. 2002. CTLA-4 regulates cell cycle progression during a primary immune response. *European journal of immunology* 32(2), pp. 366–373. doi: 10.1002/1521-4141(200202)32:2<366::AID-IMMU366>3.0.CO;2-5.
153. Gregory, A.D. and Houghton, A.M.G. 2011. Tumor-associated neutrophils: New targets for cancer therapy. *Cancer Research* 71(7), pp. 2411–2416. doi: 10.1158/0008-5472.CAN-10-2583.
154. Grohé, C., Blau, W., Gleiber, W., Haas, S., Hammerschmidt, S., Krüger, S., Müller-Huesmann, H., Schulze, M., Wehler, T., Atz, J. and Kaiser, R. 2022. Real-World Efficacy of Nintedanib Plus Docetaxel After Progression on Immune Checkpoint Inhibitors: Results From the Ongoing, Non-interventional VARGADO Study. *Clinical Oncology* . doi: 10.1016/j.clon.2021.12.010.
155. Grossman, W.J., Verbsky, J.W., Barchet, W., Colonna, M., Atkinson, J.P. and Ley, T.J. 2004. Human T regulatory cells can use the perforin pathway to cause autologous target cell death. *Immunity* 21(4), pp. 589–601. doi: 10.1016/j.immuni.2004.09.002.
156. Grosso, J.F. and Jure-Kunkel, M.N. 2013. CTLA-4 blockade in tumor models: an overview of preclinical and translational research. *Cancer immunity* 13, p. 5.
157. Guéry, L. and Huges, S. 2015. Th17 cell plasticity and functions in cancer immunity. *BioMed Research International* , pp. 1–11. doi: 10.1155/2012/720803.
158. Guicciardi, M.E. and Gores, G.J. 2009. Life and death by death receptors. *The FASEB Journal* 23(6), pp. 1625–1637. doi: 10.1096/fj.08-111005.
159. Guisier, F., Barros-Filho, M.C., Rock, L.D., Strachan-Whaley, M., Marshall, E.A., Dellaire, G. and Lam, W.L. 2020. Janus or Hydra: The Many Faces of T Helper Cells in the Human Tumour Microenvironment. In: Birbrair, A. ed. *Tumor Microenvironment: Hematopoietic Cells -- Part A*.

Cham: Springer International Publishing, pp. 35–51. doi: 10.1007/978-3-030-35723-8_3.
160. Gulzar, N. and Copeland, K. 2005. CD8+ T-Cells: Function and Response to HIV Infection. *Current HIV Research* 2(1), pp. 23–37. doi: 10.2174/1570162043485077.
161. Hammerman, P.S., Voet, D., Lawrence, M.S., Voet, D., Jing, R., Cibulskis, K., Sivachenko, A., Stojanov, P., McKenna, A., Lander, E.S., Gabriel, S., Getz, G., Imielinski, M., Helman, E., Hernandez, B., Pho, N.H., Meyerson, M., Chu, A., Hye-Chun, J.E., et al. 2012. Comprehensive genomic characterization of squamous cell lung cancers. *Nature* 489(7417), pp. 519–525. doi: 10.1038/nature11404.
162. Hanahan, D. and Weinberg, R.A. 2011. Hallmarks of cancer: The next generation. *Cell* 144(5), pp. 646–674. doi: 10.1016/j.cell.2011.02.013.
163. Haque, S., Yellu, M., Randhawa, J. and Hashemi-Sadraei, N. 2017. Profile of pembrolizumab in the treatment of head and neck squamous cell carcinoma: design development and place in therapy. *Drug design, development and therapy* 11, pp. 2537–2549. doi: 10.2147/DDDT.S119537.
164. Hatherley, D., Cherwinski, H.M., Moshref, M. and Barclay, A.N. 2005. Recombinant CD200 Protein Does Not Bind Activating Proteins Closely Related to CD200 Receptor. *The Journal of Immunology* 175(4), pp. 2469–2474. doi: 10.4049/jimmunol.175.4.2469.
165. He, X. and Xu, C. 2020. Immune checkpoint signaling and cancer immunotherapy. *Cell Research* 30(8), pp. 660–669. doi: 10.1038/s41422-020-0343-4.
166. Hegde, P.S., Karanikas, V. and Evers, S. 2016. The where, the when, and the how of immune monitoring for cancer immunotherapies in the era of checkpoint inhibition. *Clinical Cancer Research* 22(8), pp. 1865–1874. doi: 10.1158/1078-0432.CCR-15-1507.
167. Hellmann, M.D., Paz-Ares, L., Bernabe Caro, R., Zurawski, B., Kim, S.-W., Carcereny Costa, E., Park, K., Alexandru, A., Lupinacci, L., de la Mora Jimenez, E., Sakai, H., Albert, I., Vergnenegre, A., Peters, S., Syrigos, K., Barlesi, F., Reck, M., Borghaei, H., Brahmer, J.R., et al. 2019. Nivolumab plus Ipilimumab in Advanced Non–Small-Cell Lung Cancer. *New England Journal of Medicine* 381(21), pp. 2020–2031. doi: 10.1056/NEJMoa1910231.
168. Herbst, R.S., Garon, E.B., Kim, D.-W., Cho, B.C., Gracia, J.L.P., Han, J.-Y., Arvis, C.D., Majem, M., Forster, M. and Monnet, I. 2018a. Long-term follow-up in the KEYNOTE-010 study of pembrolizumab (pembro) for advanced NSCLC, including in patients (pts) who completed 2 years of pembro and pts who received a second course of pembro. *Annals of Oncology* 29, pp. x42–x43.
169. Herbst, R.S., Garon, E.B., Kim, D.-W., Cho, B.C., Perez-Gracia, J.L., Han, J.-Y., Arvis, C.D., Majem, M., Forster, M.D., Monnet, I., Novello, S., Szalai, Z., Gubens, M.A., Su, W.-C., Ceresoli, G.L., Samkari, A., Jensen, E.H., Lubiniecki, G.M. and Baas, P. 2020. Long-Term Outcomes and Retreatment Among Patients With Previously Treated, Programmed Death-Ligand 1–Positive, Advanced Non–Small-Cell Lung Cancer in the KEYNOTE-010 Study. *Journal of Clinical Oncology* 38(14), pp. 1580–1590. doi: 10.1200/JCO.19.02446.
170. Herbst, R.S., Morgensztern, D. and Boshoff, C. 2018b. The biology and management of non-small cell lung cancer. *Nature* 553(7689), pp. 446–454. doi: 10.1038/nature25183.
171. Herbst, R.S., Soria, J.-C., Kowanetz, M., Fine, G.D., Hamid, O., Gordon, M.S., Sosman, J.A., McDermott, D.F., Powderly, J.D. and Gettinger, S.N. 2014. Predictive correlates of response to the anti-PD-L1 antibody MPDL3280A in cancer patients. *Nature* 515(7528), pp. 563–567. doi: 10.1038/nature14011.
172. Hernandez, A.M. and Holodick, N.E. 2017. Editorial: Natural Antibodies in Health and Disease. *Frontiers in Immunology* 8, p. 1795. doi: https://doi.org/10.3389/fimmu.2017.01795.
173. Hodgins, J.J., Khan, S.T., Park, M.M., Auer, R.C. and Ardolino, M. 2019. Killers 2.0: NK cell therapies at the forefront of cancer control. *Journal of Clinical Investigation* 129(9), pp. 3499–3510. doi: 10.1172/JCI129338.
174. Hodi, F.S., O'Day, S.J., McDermott, D.F., Weber, R.W., Sosman, J.A., Haanen, J.B., Gonzalez, R., Robert, C., Schadendorf, D., Hassel, J.C., Akerley, W., van den Eertwegh, A.J.M., Lutzky, J., Lorigan, P., Vaubel, J.M., Linette, G.P., Hogg, D., Ottensmeier, C.H., Lebbé, C., et al. 2010. Improved Survival with Ipilimumab in Patients with Metastatic Melanoma. *New England Journal of Medicine* 363(8), pp. 711–723. doi: 10.1056/NEJMoa1003466.

175. Hoek, R., Ruuls, S., Murphy, C., Wright, G., Goddard, R., Sandra, Z., Blom, B., Homola, M., Streit, W., Brown, M., Barclay, A.N. and Sedgwick, J. 2000. Down-Regulation of the Macrophage Lineage Through Interaction with OX2 (CD200). *Science* 290, pp. 1768–1771. doi: 10.1126/science.290.5497.1768.
176. Holmgaard, R.B., Zamarin, D., Li, Y., Gasmi, B., Munn, D.H., Allison, J.P., Merghoub, T. and Wolchok, J.D. 2015. Tumor-Expressed IDO Recruits and Activates MDSCs in a Treg-Dependent Manner. *Cell Reports* 13(2), pp. 412–424. doi: https://doi.org/10.1016/j.celrep.2015.08.077.
177. Holt, P.G. and Strickland, D.H. 2008. The CD200-CD200R axis in local control of lung inflammation. *Nature Immunology* 9(9), pp. 1011–1012. doi: 10.1038/ni0908-1011.
178. Horita, N., Nagashima, A., Nakashima, K., Shibata, Y., Ito, K., Goto, A., Yamanaka, T. and Kaneko, T. 2017. The best platinum regimens for chemo-naive incurable non-small cell lung cancer: network meta-analysis. *Scientific Reports* 7(1), p. 13185. doi: 10.1038/s41598-017-13724-2.
179. Horn, L., Spigel, D.R., Vokes, E.E., Holgado, E., Ready, N., Steins, M., Poddubskaya, E., Borghaei, H., Felip, E. and Paz-Ares, L. 2017. Nivolumab versus docetaxel in previously treated patients with advanced non–small-cell lung cancer: two-year outcomes from two randomized, open-label, phase III trials (CheckMate 017 and CheckMate 057). *Journal of clinical oncology* 35(35), p. 3924. doi: 10.1200/JCO.2017.74.3062.
180. Houghton, A.M.G. 2010. The paradox of tumor-associated neutrophils: Fueling tumor growth with cytotoxic substances. *Cell Cycle* 9(9), pp. 1732–1737. doi: 10.4161/cc.9.9.11297.
181. Hsu, J., Hodgins, J.J., Marathe, M., Nicolai, C.J., Bourgeois-Daigneault, M.C., Trevino, T.N., Azimi, C.S., Scheer, A.K., Randolph, H.E., Thompson, T.W., Zhang, L., Iannello, A., Mathur, N., Jardine, K.E., Kirn, G.A., Bell, J.C., McBurney, M.W., Raulet, D.H. and Ardolino, M. 2018. Contribution of NK cells to immunotherapy mediated by PD-1/PD-L1 blockade. *Journal of Clinical Investigation* 128(10), pp. 4654–4668. doi: 10.1172/JCI99317.
182. Hui, L. and Chen, Y. 2015. Tumor microenvironment: Sanctuary of the devil. *Cancer Letters* 368(1), pp. 7–13. doi: 10.1016/j.canlet.2015.07.039.
183. Ikediobi, O.N., Davies, H., Bignell, G., Edkins, S., Stevens, C., O'Meara, S., Santarius, T., Avis, T., Barthorpe, S., Brackenbury, L., Buck, G., Butler, A., Clements, J., Cole, J., Dicks, E., Forbes, S., Gray, K., Halliday, K., Harrison, R., et al. 2006. Mutation analysis of 24 known cancer genes in the NCI-60 cell line set. *Molecular cancer therapeutics* 5(11), pp. 2606–2612. doi: 10.1158/1535-7163.MCT-06-0433.
184. Imai, K., Matsuyama, S., Miyake, S., Suga, K. and Nakachi, K. 2000. Natural cytotoxic activity of peripheral-blood lymphocytes and cancer incidence: An 11-year follow-up study of a general population. *Lancet* 356(9244), pp. 1795–1799. doi: 10.1016/S0140-6736(00)03231-1.
185. Ishibashi, M., Neri, S., Hashimoto, H., Miyashita, T., Yoshida, T., Nakamura, Y., Udagawa, H., Kirita, K., Matsumoto, S., Umemura, S., Yoh, K., Niho, S., Tsuboi, M., Masutomi, K., Goto, K., Ochiai, A. and Ishii, G. 2017. CD200-positive cancer associated fibroblasts augment the sensitivity of Epidermal Growth Factor Receptor mutation-positive lung adenocarcinomas to EGFR Tyrosine kinase inhibitors. *Scientific Reports* . doi: 10.1038/srep46662.
186. Jablonska, J., Leschner, S., Westphal, K., Lienenklaus, S. and Weiss, S. 2010. Neutrophils responsive to endogenous IFN-beta regulate tumor angiogenesis and growth in a mouse tumor model. *The Journal of clinical investigation* 120(4), pp. 1151–1164. doi: 10.1172/JCI37223.
187. Jacobsen, E.A., Helmers, R.A., Lee, J.J. and Lee, N.A. 2012. The expanding role(s) of eosinophils in health and disease. *Blood* 120(19), pp. 3882–3890. doi: 10.1182/blood-2012-06-330845.
188. Jain, N., Nguyen, H., Chambers, C. and Kang, J. 2010. Dual function of CTLA-4 in regulatory T cells and conventional T cells to prevent multiorgan autoimmunity. *Proceedings of the National Academy of Sciences* 107(4), pp. 1524–1528. doi: 10.1073/pnas.0910341107.
189. Janjic, B.M., Lu, G., Pimenov, A., Whiteside, T.L., Storkus, W.J. and Vujanovic, N.L. 2002. Innate Direct Anticancer Effector Function of Human Immature Dendritic Cells. I. Involvement of an Apoptosis-Inducing Pathway. *The Journal of Immunology* 168(4), pp. 1823 LP – 1830. doi: 10.4049/jimmunol.168.4.1823.

190. Jayasingam, S.D., Citartan, M., Thang, T.H., Mat Zin, A.A., Ang, K.C. and Ch'ng, E.S. 2020. Evaluating the Polarization of Tumor-Associated Macrophages Into M1 and M2 Phenotypes in Human Cancer Tissue: Technicalities and Challenges in Routine Clinical Practice. *Frontiers in Oncology* 9(January), pp. 1–9. doi: 10.3389/fonc.2019.01512.
191. Jenkins, R.W., Barbie, D.A. and Flaherty, K.T. 2018. Mechanisms of resistance to immune checkpoint inhibitors. *British journal of cancer* 118(1), pp. 9–16. doi: 10.1200/EDBK_240837.
192. Jhunjhunwala, S., Hammer, C. and Delamarre, L. 2021. Antigen presentation in cancer: insights into tumour immunogenicity and immune evasion. *Nature Reviews Cancer* 21(5), pp. 298–312. doi: 10.1038/s41568-021-00339-z.
193. Jiang-Shieh, Y.F., Chien, H.F., Chang, C.Y., Wei, T.S., Chiu, M.M., Chen, H.M. and Wu, C.H. 2010. Distribution and expression of CD200 in the rat respiratory system under normal and endotoxin-induced pathological conditions. *Journal of Anatomy* 216(3), pp. 407–416. doi: 10.1111/j.1469-7580.2009.01190.x.
194. Jiang, L. and Barclay, A.N. 2009. New assay to detect low-affinity interactions and characterization of leukocyte receptors for collagen including leukocyte-associated Ig-like receptor-1 (LAIR-1). *European Journal of Immunology* 39(4), pp. 1167–1175. doi: https://doi.org/10.1002/eji.200839188.
195. Johnson, D.H., Schiller, J.H. and Bunn, P.A. 2014. Recent Clinical Advances in Lung Cancer Management. *Journal of Clinical Oncology* 32(10), pp. 973–982. doi: 10.1200/JCO.2013.53.1228.
196. Johnston, R.J., Comps-Agrar, L., Hackney, J., Yu, X., Huseni, M., Yang, Y., Park, S., Javinal, V., Chiu, H., Irving, B., Eaton, D.L. and Grogan, J.L. 2014. The Immunoreceptor TIGIT Regulates Antitumor and Antiviral CD8+ T Cell Effector Function. *Cancer Cell* 26(6), pp. 923–937. doi: https://doi.org/10.1016/j.ccell.2014.10.018.
197. Jones, G.S. and Baldwin, D.R. 2018. Recent advances in the management of lung cancer. *Clinical Medicine* 18(2), pp. 4–6. doi: 10.3166/rea-2019-0091.
198. Jordan, M.A. and Wilson, L. 2004. Microtubules as a target for anticancer drugs. *Nature Reviews Cancer* 4(4), pp. 253–265. doi: 10.1038/nrc1317.
199. Kaiko, G.E., Horvat, J.C., Beagley, K.W. and Hansbro, P.M. 2008. Immunological decision-making: How does the immune system decide to mount a helper T-cell response? *Immunology* 123(3), pp. 326–338. doi: 10.1111/j.1365-2567.2007.02719.x.
200. Kaplan, D.H., Shankaran, V., Dighe, A.S., Stockert, E., Aguet, M., Old, L.J. and Schreiber, R.D. 1998. Demonstration of an interferon gamma-dependent tumor surveillance system in immunocompetent mice. *Proceedings of the National Academy of Sciences of the United States of America* 95(13), pp. 7556–7561. doi: 10.1073/pnas.95.13.7556.
201. Kaszubowska, L., Foerster, J., Schetz, D. and Kmieć, Z. 2018. CD56bright cells respond to stimulation until very advanced age revealing increased expression of cellular protective proteins SIRT1, HSP70 and SOD2. *Immunity & Ageing* 15(1), p. 31. doi: 10.1186/s12979-018-0136-5.
202. Kawasaki, B.T. and Farrar, W.L. 2008. Cancer stem cells, CD200 and immunoevasion. 10(1), pp. 464–8. doi: 10.1016/j.it.2008.07.005.
203. Kawasaki, B.T., Mistree, T., Hurt, E.M., Kalathur, M. and Farrar, W.L. 2007. Co-expression of the toleragenic glycoprotein, CD200, with markers for cancer stem cells. *Biochemical and Biophysical Research Communications* 364(4), pp. 778–782. doi: 10.1016/j.bbrc.2007.10.067.
204. Keir, M.E., Butte, M.J., Freeman, G.J. and Sharpe, A.H. 2008. PD-1 and its ligands in tolerance and immunity. *Annual Review of Immunology* 26, pp. 677–704. doi: 10.1146/annurev.immunol.26.021607.090331.
205. Kelly, J.M., Darcy, P.K., Markby, J.L., Godfrey, D.I., Takeda, K., Yagita, H. and Smyth, M.J. 2002. Induction of tumor-specific T cell memory by NK cell-mediated tumor rejection. *Nature immunology* 3(1), pp. 83–90. doi: 10.1038/ni746.
206. Kennedy, R. and Celis, E. 2008. Multiple roles for CD4+ T cells in anti-tumor immune responses. *Immunological Reviews* 222(1), pp. 129–144. doi: 10.1111/j.1600-065X.2008.00616.x.
207. Khan, I.Z., Del Guzzo, C.A., Shao, A., Cho, J., Du, R., Cohen, A.O. and Owens, D.M. 2021. The CD200-CD200R axis promotes squamous cell carcinoma metastasis via regulation of

cathepsin K. *Cancer Research* , p. canres.3251.2020. doi: 10.1158/0008-5472.can-20-3251.

208. Khan, M., Arooj, S., Wang, H. and Wang, H. 2020. NK Cell-Based Immune Checkpoint Inhibition. 11(February). doi: 10.3389/fimmu.2020.00167.
209. Kim, C.F.B., Jackson, E.L., Woolfenden, A.E., Lawrence, S., Babar, I., Vogel, S., Crowley, D., Bronson, R.T. and Jacks, T. 2005. Identification of bronchioalveolar stem cells in normal lung and lung cancer. *Cell* 121(6), pp. 823–835. doi: 10.1016/j.cell.2005.03.032.
210. Kim, J.-H., Kim, B.S. and Lee, S.-K. 2020. Regulatory T Cells in Tumor Microenvironment and Approach for Anticancer Immunotherapy. *Immune network* 20(1), pp. e4–e4. doi: 10.4110/in.2020.20.e4.
211. Kim, R. 2007. *Cancer Immunoediting: from immune surveillance to immune escape*. Elsevier Inc. doi: 10.1007/springerreference_31915.
212. Kim, S., Iizuka, K., Aguila, H.L., Weissman, I.L. and Yokoyama, W.M. 2000. In vivo natural killer cell activities revealed by natural killer cell-deficient mice. *Proceedings of the National Academy of Sciences of the United States of America* 97(6), pp. 2731–2736. doi: 10.1073/pnas.050588297.
213. Kinne, R.W., Stuhlmüller, B. and Burmester, G.R. 2007. Cells of the synovium in rheumatoid arthritis. Macrophages. *Arthritis Research and Therapy* 9(6), pp. 1–16. doi: 10.1186/ar2333.
214. Knutson, K.L. and Disis, M.L. 2005. Tumor antigen-specific T helper cells in cancer immunity and immunotherapy. *Cancer Immunology, Immunotherapy* 54(8), pp. 721–728. doi: 10.1007/s00262-004-0653-2.
215. Koebel, C.M., Vermi, W., Swann, J.B., Zerafa, N., Rodig, S.J., Old, L.J., Smyth, M.J. and Schreiber, R.D. 2007. Adaptive immunity maintains occult cancer in an equilibrium state. *Nature* 450(7171), pp. 903–907. doi: 10.1038/nature06309.
216. Konstantinidis, K. V., Alici, E., Aints, A., Christensson, B., Ljunggren, H.G. and Dilber, M.S. 2005. Targeting IL-2 to the endoplasmic reticulum confines autocrine growth stimulation to NK-92 cells. *Experimental Hematology* 33(2), pp. 159–164. doi: 10.1016/j.exphem.2004.11.003.
217. Korrodi-Gregório, L., Soto-Cerrato, V., Vitorino, R., Fardilha, M. and Pérez-Tomás, R. 2016. From Proteomic Analysis to Potential Therapeutic Targets: Functional Profile of Two Lung Cancer Cell Lines, A549 and SW900, Widely Studied in Pre-Clinical Research. *PLOS ONE* 11(11), p. e0165973. doi: https://doi.org/10.1371/journal.pone.0165973.
218. Kos, O., Hughson, R.L., Hart, D.A., Clément, G., Frings-Meuthen, P., Linnarsson, D., Paloski, W.H., Rittweger, J., Wuyts, F., Zange, J. and Gorczynski, R.M. 2014. Elevated serum soluble CD200 and CD200R as surrogate markers of bone loss under bed rest conditions. *Bone* 60, pp. 33–40. doi: 10.1016/j.bone.2013.12.004.
219. Kotwica-Mojzych, K., Jodłowska-Jędrych, B. and Mojzych, M. 2021. Cd200:Cd200r interactions and their importance in immunoregulation. *International Journal of Molecular Sciences* 22(4), pp. 1–21. doi: 10.3390/ijms22041602.
220. Kretz-Rommel, A., Qin, F., Dakappagari, N., Cofiell, R., Faas, S.J. and Bowdish, K.S. 2008. Blockade of CD200 in the Presence or Absence of Antibody Effector Function: Implications for Anti-CD200 Therapy. *The Journal of Immunology* 180(2), pp. 699–705. doi: 10.4049/jimmunol.180.2.699.
221. Kretz-Rommel, A., Qin, F., Dakappagari, N., Ravey, E.P., McWhirter, J., Oltean, D., Frederickson, S., Maruyama, T., Wild, M.A., Nolan, M.-J., Wu, D., Springhorn, J. and Bowdish, K.S. 2007. CD200 Expression on Tumor Cells Suppresses Antitumor Immunity: New Approaches to Cancer Immunotherapy. *The Journal of Immunology* 178(9), pp. 5595–5605. doi: 10.4049/jimmunol.178.9.5595.
222. Kris, M.G., Johnson, B.E., Berry, L.D., Kwiatkowski, D.J., Iafrate, A.J., Wistuba, I.I., Varella-Garcia, M., Franklin, W.A., Aronson, S.L., Su, P.-F., Shyr, Y., Camidge, D.R., Sequist, L. V, Glisson, B.S., Khuri, F.R., Garon, E.B., Pao, W., Rudin, C., Schiller, J., et al. 2014. Using multiplexed assays of oncogenic drivers in lung cancers to select targeted drugs. *JAMA* 311(19), pp. 1998–2006. doi: 10.1001/jama.2014.3741.
223. Krummel, M.F. and Allison, J.P. 1996. CTLA-4 engagement inhibits IL-2 accumulation and cell cycle progression upon activation of resting T cells. *The Journal of experimental medicine* 183(6),

pp. 2533–2540. doi: 10.1084/jem.183.6.2533.
224. Krzewski, K. and Coligan, J.E. 2012. Human NK cell lytic granules and regulation of their exocytosis. *Frontiers in Immunology* 3(NOV), pp. 1–16. doi: 10.3389/fimmu.2012.00335.
225. Kumar, S. 2018. Natural killer cell cytotoxicity and its regulation by inhibitory receptors. *Immunology* 154(3), pp. 383–393. doi: 10.1111/imm.12921.
226. Kwak, E.L., Bang, Y.-J., Camidge, D.R., Shaw, A.T., Solomon, B., Maki, R.G., Ou, S.-H.I., Dezube, B.J., Jänne, P.A., Costa, D.B., Varella-Garcia, M., Kim, W.-H., Lynch, T.J., Fidias, P., Stubbs, H., Engelman, J.A., Sequist, L. V, Tan, W., Gandhi, L., et al. 2010. Anaplastic Lymphoma Kinase Inhibition in Non–Small-Cell Lung Cancer. *New England Journal of Medicine* 363(18), pp. 1693–1703. doi: 10.1056/NEJMoa1006448.
227. Lanier, L.L. 2008. Up on the tightrope: Natural killer cell activation and inhibition. *Nature Immunology* 9(5), pp. 495–502. doi: 10.1038/ni1581.
228. Largeot, A., Pagano, G., Gonder, S., Moussay, E. and Paggetti, J. 2019. The B-Side of Cancer Immunity: The Underrated Tune. *Cells* 8(5), p. 449. doi: 10.3390/cells8050449.
229. Lauzon-Joset, J.F., Langlois, A., Lai, L.J.A., Santerre, K., Lee-Gosselin, A., Bosse, Y., Marsolais, D. and Bissonnette, E.Y. 2015. Lung CD200 receptor activation abrogates airway hyperresponsiveness in experimental asthma. *American Journal of Respiratory Cell and Molecular Biology* 53, pp. 276–284. doi: 10.1165/rcmb.2014-0229OC.
230. Lauzon-Joset, J.F., Marsolais, D., Tardif-Pellerin, É., Patoine, D. and Bissonnette, E.Y. 2019. CD200 in asthma. *International Journal of Biochemistry and Cell Biology* 112, pp. 141–144. doi: 10.1016/j.biocel.2019.05.003.
231. Lavin, Y., Kobayashi, S., Leader, A., Amir, E. ad D., Elefant, N., Bigenwald, C., Remark, R., Sweeney, R., Becker, C.D., Levine, J.H., Meinhof, K., Chow, A., Kim-Shulze, S., Wolf, A., Medaglia, C., Li, H., Rytlewski, J.A., Emerson, R.O., Solovyov, A., et al. 2017. Innate Immune Landscape in Early Lung Adenocarcinoma by Paired Single-Cell Analyses. *Cell* . doi: 10.1016/j.cell.2017.04.014.
232. Lebien, T.W. and Tedder, T.F. 2008. B lymphocytes: How they develop and function. *Blood* 112(5), pp. 1570–1580. doi: 10.1182/blood-2008-02-078071.
233. Lee, M.H., Kim, Y.J., Yun, K.A., Won, C.H., Lee, M.W., Choi, J.H., Chang, S.E. and Lee, W.J. 2020. Prognostic significance of CD200 protein expression and its correlation with COX-2 in cutaneous melanoma. *Journal of the American Academy of Dermatology* 82(6), pp. 1526–1528. doi: 10.1016/j.jaad.2020.02.006.
234. Lee, Y.S. and Radford, K.J. 2019. The role of dendritic cells in cancer. In: *Immunobiology of Dendritic Cells A*. 1st ed. Elsevier Inc., pp. 123–178. doi: 10.1016/bs.ircmb.2019.07.006.
235. Liew, P.X. and Kubes, P. 2019. The Neutrophil's role during health and disease. *Physiological Reviews* 99(2), pp. 1223–1248. doi: 10.1152/physrev.00012.2018.
236. Lim, S.H., Sun, J.-M., Lee, S.-H., Ahn, J.S., Park, K. and Ahn, M.-J. 2016. Pembrolizumab for the treatment of non-small cell lung cancer. *Expert opinion on biological therapy* 16(3), pp. 397–406. doi: 10.1517/14712598.2016.1145652.
237. Lin, A. and Yan, W.-H. 2018. Heterogeneity of HLA-G Expression in Cancers: Facing the Challenges. *Frontiers in Immunology* 9. doi: https://doi.org/10.3389/fimmu.2018.02164.
238. Lin, C., Song, H., Huang, C., Yao, E., Gacayan, R., Xu, S.-M. and Chuang, P.-T. 2012. Alveolar type II cells possess the capability of initiating lung tumor development. *PloS one* 7(12), p. e53817. doi: 10.1371/journal.pone.0053817.
239. Linsley, P.S., Bradshaw, J., Greene, J., Peach, R., Bennett, K.L. and Mittler, R.S. 1996. Intracellular trafficking of CTLA-4 and focal localization towards sites of TCR engagement. *Immunity* 4(6), pp. 535–543. doi: 10.1016/s1074-7613(00)80480-x.
240. Lipscomb, M.F. and Masten, B.J. 2002. Dendritic cells: Immune regulators in health and disease. *Physiological Reviews* 82(1), pp. 97–130. doi: 10.1152/physrev.00023.2001.
241. Lipson, E.J., Tawbi, H.A.-H., Schadendorf, D., Ascierto, P.A., Matamala, L., Gutiérrez, E.C., Rutkowski, P., Gogas, H., Lao, C.D., Janoski de Menezes, J., Dalle, S., Arance, A.M., Grob, J.-J., Srivastava, S., Abaskharoun, M., Simonsen, K.L., Li, B., Long, G. V and Hodi, F.S. 2021. Relatlimab (RELA) plus nivolumab (NIVO) versus NIVO in first-line advanced melanoma: Primary phase III

results from RELATIVITY-047 (CA224-047). *Journal of Clinical Oncology* 39(15_suppl), p. 9503. doi: 10.1200/JCO.2021.39.15_suppl.9503.

242. Lisberg, A., Cummings, A., Goldman, J.W., Bornazyan, K., Reese, N., Wang, T., Coluzzi, P., Ledezma, B., Mendenhall, M. and Hunt, J. 2018. A phase II study of pembrolizumab in EGFR-mutant, PD-L1+, tyrosine kinase inhibitor naïve patients with advanced NSCLC. *Journal of Thoracic Oncology* 13(8), pp. 1138–1145. doi: 10.1016/j.jtho.2018.03.035.
243. Liu, J.-Q., Hu, A., Zhu, J., Yu, J., Talebian, F. and Bai, X.-F. 2020. CD200-CD200R Pathway in the Regulation of Tumour Immune Microenvironment Immunotherapy. In: *Tumor Microenvironment Signaling Pathways- Part A*. 1st ed., pp. 155–165. doi: 10.1002/9780470669891.
244. Liu, J.-Q., Talebian, F., Wu, L., Liu, Z., Li, M.-S., Wu, L., Zhu, J., Markowitz, J., Carson, W.E., Basu, S. and Bai, X.-F. 2016. A Critical Role for CD200R Signaling in Limiting the Growth and Metastasis of CD200 $^{+}$ Melanoma. *The Journal of Immunology* . doi: 10.4049/jimmunol.1600052.
245. Liu, S., Yu, Y., Zhang, M., Wang, W. and Cao, X. 2001. The Involvement of TNF-α-Related Apoptosis-Inducing Ligand in the Enhanced Cytotoxicity of IFN-β-Stimulated Human Dendritic Cells to Tumor Cells. *The Journal of Immunology* 166(9), pp. 5407 LP – 5415. doi: 10.4049/jimmunol.166.9.5407.
246. Liu, Y. and Cao, X. 2016. Immunosuppressive cells in tumor immune escape and metastasis. *Journal of Molecular Medicine* 94(5), pp. 509–522. doi: 10.1007/s00109-015-1376-x.
247. Lopes, G., Wu, Y.-L., Kudaba, I., Kowalski, D., Cho, B.C., Castro, G., Srimuninnimit, V., Bondarenko, I., Kubota, K. and Lubiniecki, G.M. 2018. Pembrolizumab (pembro) versus platinum-based chemotherapy (chemo) as first-line therapy for advanced/metastatic NSCLC with a PD-L1 tumor proportion score (TPS)≥ 1%: open-label, phase 3 KEYNOTE-042 study. doi: 10.1200/JCO.2018.36.18_suppl.LBA4.
248. Lorenzo-Herrero, S., Sordo-Bahamonde, C., Gonzalez, S. and López-Soto, A. 2019. CD107a Degranulation Assay to Evaluate Immune Cell Antitumor Activity. In: López-Soto, A. and Folgueras, A. R. eds. *Cancer Immunosurveillance: Methods and Protocols*. New York, NY: Springer New York, pp. 119–130. doi: 10.1007/978-1-4939-8885-3_7.
249. Mahadevan, D., Lanasa, M.C., Farber, C., Pandey, M., Whelden, M., Faas, S.J., Ulery, T., Kukreja, A., Li, L., Bedrosian, C.L., Zhang, X. and Heffner, L.T. 2019. Phase i study of samalizumab in chronic lymphocytic leukemia and multiple myeloma: Blockade of the immune checkpoint CD200. *Journal for ImmunoTherapy of Cancer* 7(1), pp. 1–13. doi: 10.1186/s40425-019-0710-1.
250. Maimela, N.R., Liu, S. and Zhang, Y. 2019. Fates of CD8+ T cells in Tumor Microenvironment. *Computational and Structural Biotechnology Journal* 17, pp. 1–13. doi: 10.1016/j.csbj.2018.11.004.
251. Mainardi, S., Mijimolle, N., Francoz, S., Vicente-Dueñas, C., Sánchez-García, I. and Barbacid, M. 2014. Identification of cancer initiating cells in K-Ras driven lung adenocarcinoma. *Proceedings of the National Academy of Sciences of the United States of America* 111(1), pp. 255–260. doi: 10.1073/pnas.1320383110.
252. Maleki Vareki, S. 2018. High and low mutational burden tumors versus immunologically hot and cold tumors and response to immune checkpoint inhibitors. *Journal for ImmunoTherapy of Cancer* 6(1), pp. 4–8. doi: 10.1186/s40425-018-0479-7.
253. Mandal, A. and Viswanathan, C. 2015. Natural killer cells: In health and disease. *Hematology/ Oncology and Stem Cell Therapy* 8(2), pp. 47–55. doi: 10.1016/j.hemonc.2014.11.006.
254. Manich, G., Recasens, M., Valente, T., Almolda, B., González, B. and Castellano, B. 2019. Role of the CD200-CD200R Axis During Homeostasis and Neuroinflammation. *Neuroscience* 405, pp. 118–136. doi: 10.1016/j.neuroscience.2018.10.030.
255. Mantovani, A., Marchesi, F., Malesci, A., Laghi, L. and Allavena, P. 2017. Tumour-associated macrophages as treatment targets in oncology. *Nature Reviews Clinical Oncology* 14(7), pp. 399–416. doi: 10.1038/nrclinonc.2016.217.
256. Mantovani, A., Romero, P., Palucka, A.K. and Marincola, F.M. 2008. Tumour immunity: effector response to tumour and role of the microenvironment. *The Lancet* 371(9614), pp. 771–783. doi: 10.1016/S0140-6736(08)60241-X.
257. Mariniello, A., Novello, S., Scagliotti, G. V. and Ramalingam, S.S. 2020. Double immune

checkpoint blockade in advanced NSCLC. *Critical Reviews in Oncology/Hematology* 152(May), p. 102980. doi: 10.1016/j.critrevonc.2020.102980.

258. Marshall, J.S., Warrington, R., Watson, W. and Kim, H.L. 2018. An introduction to immunology and immunopathology. *Allergy, Asthma & Clinical Immunology* 14(2), p. 49. Available at: https://doi.org/10.1186/s13223-018-0278-1.
259. Martín-Fontecha, A., Thomsen, L.L., Brett, S., Gerard, C., Lipp, M., Lanzavecchia, A. and Sallusto, F. 2004. Induced recruitment of NK cells to lymph nodes provides IFN-gamma for T(H)1 priming. *Nature immunology* 5(12), pp. 1260–1265. doi: 10.1038/ni1138.
260. Matsuo, Y., Sho, M., Nomi, T., Hokuto, D., Yoshikawa, T., Kamitani, N., Nakamura, K. and Iwasa, Y. 2021. Clinical Importance of CD200 Expression in Colorectal Liver Metastasis. *Annals of Surgical Oncology* 28(9), pp. 5362–5372. doi: 10.1245/s10434-020-09471-w.
261. McCutchan, G., Smits, S., Ironmonger, L., Slyne, C., Boughey, A., Moffat, J., Thomas, R., Huws, D.W. and Brain, K. 2020. Evaluation of a national lung cancer symptom awareness campaign in Wales. *British Journal of Cancer* 122(4), pp. 491–497. doi: 10.1038/s41416-019-0676-2.
262. McMaster, W.R. and Williams, A.F. 1979. Identification of Ia glycoproteins in rat thymus and purification from rat spleen. *European Journal of Immunology* 9(6), pp. 426–433. doi: 10.1002/eji.1830090603.
263. Mcwhirter, J.R., Kretz-rommel, A., Saven, A., Maruyama, T., Potter, K.N., Mockridge, C.I., Ravey, E.P., Qin, F. and Bowdish, K.S. 2006. Antibodies selected from combinatorial libraries block a tumor antigen that plays a key role in immunomodulation. 103(4), pp. 1041–1046. doi: 10.1073/pnas.0510081103.
264. Meuwissen, R., Linn, S.C., van der Valk, M., Mooi, W.J. and Berns, A. 2001. Mouse model for lung tumorigenesis through Cre/lox controlled sporadic activation of the K-Ras oncogene. *Oncogene* 20(45), pp. 6551–6558. doi: 10.1038/sj.onc.1204837.
265. Mihrshahi, R., Barclay, A.N. and Brown, M.H. 2009. Essential Roles for Dok2 and RasGAP in CD200 Receptor-Mediated Regulation of Human Myeloid Cells. *The Journal of Immunology* . doi: 10.4049/jimmunol.0901531.
266. Mihrshahi, R. and Brown, M.H. 2010. Downstream of Tyrosine Kinase 1 and 2 Play Opposing Roles in CD200 Receptor Signaling. *The Journal of Immunology* 185(12), pp. 7216–7222. doi: 10.4049/jimmunol.1002858.
267. Mills, C.D., Kincaid, K., Alt, J.M., Heilman, M.J. and Hill, A.M. 2000. M-1/M-2 Macrophages and the Th1/Th2 Paradigm. *The Journal of Immunology* 164(12), pp. 6166–6173. doi: 10.4049/jimmunol.164.12.6166.
268. Moertel, C.L., Xia, J., LaRue, R., Waldron, N.N., Andersen, B.M., Prins, R.M., Okada, H., Donson, A.M., Foreman, N.K., Hunt, M.A., Pennell, C.A. and Olin, M.R. 2014. CD200 in CNS tumor-induced immunosuppression: The role for CD200 pathway blockade in targeted immunotherapy. *Journal for ImmunoTherapy of Cancer* 2(1), pp. 1–10. doi: 10.1186/s40425-014-0046-9.
269. Mok, T.S., Wu, Y.-L., Ahn, M.-J., Garassino, M.C., Kim, H.R., Ramalingam, S.S., Shepherd, F.A., He, Y., Akamatsu, H., Theelen, W.S.M.E., Lee, C.K., Sebastian, M., Templeton, A., Mann, H., Marotti, M., Ghiorghiu, S. and Papadimitrakopoulou, V.A. 2016. Osimertinib or Platinum–Pemetrexed in EGFR T790M–Positive Lung Cancer. *New England Journal of Medicine* 376(7), pp. 629–640. doi: 10.1056/NEJMoa1612674.
270. Mok, T.S., Wu, Y.-L., Thongprasert, S., Yang, C.-H., Chu, D.-T., Saijo, N., Sunpaweravong, P., Han, B., Margono, B., Ichinose, Y., Nishiwaki, Y., Ohe, Y., Yang, J.-J., Chewaskulyong, B., Jiang, H., Duffield, E.L., Watkins, C.L., Armour, A.A. and Fukuoka, M. 2009. Gefitinib or Carboplatin–Paclitaxel in Pulmonary Adenocarcinoma. *New England Journal of Medicine* 361(10), pp. 947–957. doi: 10.1056/NEJMoa0810699.
271. Molfetta, R., Quatrini, L., Santoni, A. and Paolini, R. 2017. Regulation of NKG2D-dependent NK Cell functions: The Yin and the Yang of receptor endocytosis. *International Journal of Molecular Sciences* 18(8). doi: 10.3390/ijms18081677.
272. Moodley, T., Wilson, S.M., Joshi, T., Rider, C.F., Sharma, P., Yan, D., Newton, R. and

Giembycz, M.A. 2013. Phosphodiesterase 4 Inhibitors Augment the Ability of Formoterol to Enhance Glucocorticoid-Dependent Gene Transcription in Human Airway Epithelial Cells: A Novel Mechanism for the Clinical Efficacy of Roflumilast in Severe Chronic Obstructive Pulmonary Di. *Molecular Pharmacology* 83(4), pp. 894 LP – 906. doi: 10.1124/mol.112.083493.

273. Moreaux, J., Hose, D., Reme, T., Jourdan, E., Hundemer, M., Legouffe, E., Moine, P., Bourin, P., Moos, M., Corre, J., Möhler, T., De Vos, J., Rossi, J.F., Goldschmidt, H. and Klein, B. 2006. CD200 is a new prognostic factor in multiple myeloma. *Blood* 108(13), pp. 4194–4197. doi: 10.1182/blood-2006-06-029355.
274. Moreaux, J., Veyrune, J.L., Reme, T., De Vos, J. and Klein, B. 2008. CD200: A putative therapeutic target in cancer. *Biochemical and Biophysical Research Communications* 366(1), pp. 117–122. doi: 10.1016/j.bbrc.2007.11.103.
275. Morvan, M.G. and Lanier, L.L. 2016. NK cells and cancer: You can teach innate cells new tricks. *Nature Reviews Cancer* . doi: 10.1038/nrc.2015.5.
276. Munn, D.H., Sharma, M.D., Baban, B., Harding, H.P., Zhang, Y., Ron, D. and Mellor, A.L. 2005. GCN2 Kinase in T Cells Mediates Proliferative Arrest and Anergy Induction in Response to Indoleamine 2,3-Dioxygenase. *Immunity* 22(5), pp. 633–642. doi: https://doi.org/10.1016/j.immuni.2005.03.013.
277. Nakamura, N., Miyagi, E., Murata, S., Kawaoi, A. and Katoh, R. 2002. Expression of Thyroid Transcription Factor-1 in Normal and Neoplastic Lung Tissues. *Modern Pathology* 15(10), pp. 1058–1067. doi: 10.1097/01.MP.0000028572.44247.CF.
278. Naqash, A.R., Ricciuti, B., Owen, D.H., Florou, V., Toi, Y., Cherry, C., Hafiz, M., De Giglio, A., Muzaffar, M., Patel, S.H., Sugawara, S., Burkart, J., Park, W., Chiari, R., Sugisaka, J., Otterson, G.A., de Lima Lopes, G. and Walker, P.R. 2020. Outcomes associated with immune-related adverse events in metastatic non-small cell lung cancer treated with nivolumab: a pooled exploratory analysis from a global cohort. *Cancer Immunology, Immunotherapy* 69(7), pp. 1177–1187. doi: 10.1007/s00262-020-02536-5.
279. National Insitute for Health and Care Excellence [no date][a]. *Algorithm for Systemic anti-cancer therapy: management options for people with non-squamous (adenocarcinoma, large cell undifferentiated) carcinoma and non-small-cell carcinoma (non-otherwise specified) – November 2021 update*. Available at: https://www.nice.org.uk/guidance/ng122/chapter/Recommendations#treatment [Accessed: 21 February 2022].
280. National Insitute for Health and Care Excellence [no date][b]. *Systemic anti-cancer therapy: management options for people with non-squamous (adenocarcinoma, large cell undifferentiated) carcinoma and non-small-cell carcinoma (non-otherwise specified) – November 2021 update*. Available at: https://www.nice.org.uk/guidance/ng122/resources/algorithm-for-systemic-treatment-options-for-advanced-nonsquamous-nsclc-egfrtk-alk-or-ros1-positive-pdf-6722110912 [Accessed: 21 February 2022].
281. National Insitute for Health and Care Excellence [no date][c]. *Systemic anti-cancer therapy: management options for people with squamous non-small-cell carcinoma – November 2021 update*. Available at: https://www.nice.org.uk/guidance/ng122/resources/algorithm-for-systemic-treatment-options-for-advanced-squamous-nsclc-pdf-9192679597 [Accessed: 22 February 2022].
282. National Lung Cancer Screening Team 2011. *Reduced Lung-Cancer Mortality with Low-Dose Computed Tomographic Screening*. Massachusetts Medical Society. Available at: https://doi.org/10.1056/NEJMoa1102873.
283. Nedergaard, B.S., Ladekarl, M., Nyengaard, J.R. and Nielsen, K. 2008. A comparative study of the cellular immune response in patients with stage IB cervical squamous cell carcinoma. Low numbers of several immune cell subtypes are strongly associated with relapse of disease within 5 years. *Gynecologic Oncology* 108(1), pp. 106–111. doi: https://doi.org/10.1016/j.ygyno.2007.08.089.
284. Newman, A.M., Liu, C.L., Green, M.R., Gentles, A.J., Feng, W., Xu, Y., Hoang, C.D., Diehn, M. and Alizadeh, A.A. 2015. Robust enumeration of cell subsets from tissue expression profiles.

Nature Methods 12(5), pp. 453–457. doi: 10.1038/nmeth.3337.

285. NICE [no date]. Lung cancer: diagnosis and management. *NICE guidelines*
286. Nicholson, A.G., Chansky, K., Crowley, J., Beyruti, R., Kubota, K., Turrisi, A., Eberhardt, W.E.E., Van Meerbeeck, J., Rami-Porta, R. and Goldstraw, P. 2016. The International Association for the Study of Lung Cancer Lung Cancer Staging Project: proposals for the revision of the clinical and pathologic staging of small cell lung cancer in the forthcoming eighth edition of the TNM classification for lung cancer. *Journal of Thoracic Oncology* 11(3), pp. 300–311. doi: 10.1016/j.jtho.2015.10.008.
287. Niederkorn, J.Y. 2006. See no evil, hear no evil, do no evil: the lessons of immune privilege. *Nature Immunology* 7(4), pp. 354–359. doi: 10.1038/ni1328.
288. Noy, R. and Pollard, J.W. 2014. Tumor-Associated Macrophages: From Mechanisms to Therapy. *Immunity* 41(1), pp. 49–61. doi: 10.1016/j.immuni.2014.06.010.
289. Ohri, C.M., Shikotra, A., Green, R.H., Waller, D.A. and Bradding, P. 2009. Macrophages within NSCLC tumour islets are predominantly of a cytotoxic M1 phenotype associated with extended survival. *European Respiratory Journal* 33(1), pp. 118–126. doi: 10.1183/09031936.00065708.
290. Ohyama, M., Terunuma, A., Lock, C.L., Radonovich, M.F., Pise-Masison, C.A., Hopping, S.B., Brady, J.N., Udey, M.C. and Vogel, J.C. 2006. Characterization and isolation of stem cell-enriched human and canine hair follicle keratinocytes. *The Journal of Clinical Investigation* 116(1), pp. 249–260. doi: 10.1172/JCI26043.
291. Ondondo, B., Gallimore, A., Jones, E. and Godkin, A. 2013. Home Sweet Home: The Tumor Microenvironment as a Haven for Regulatory T Cells. *Frontiers in Immunology* 4. doi: 10.3389/fimmu.2013.00197.
292. Onizuka, S., Tawara, I., Shimizu, J., Sakaguchi, S., Fujita, T. and Nakayama, E. 1999. Tumor rejection by in vivo administration of anti-CD25 (interleukin-2 receptor α) monoclonal antibody. *Cancer Research* 59(13), pp. 3128–3133.
293. Ortaldo, J.R., Winkler-pickett, R., Wigginton, J., Horner, M., Bere, E.W., Mason, A.T., Bhat, N., Cherry, J., Sanford, M., Hodge, D.L. and Young, H.A. 2006. Regulation of ITAM-positive receptors : role of IL-12 and IL-18. 107(4), pp. 1468–1475. doi: 10.1182/blood-2005-04-1579.Supported.
294. Osmani, L., Askin, F., Gabrielson, E. and Li, Q.K. 2018. Current WHO guidelines and the critical role of immunohistochemical markers in the subclassification of non-small cell lung carcinoma (NSCLC): Moving from targeted therapy to immunotherapy. *Seminars in Cancer Biology* 52(November 2017), pp. 103–109. doi: 10.1016/j.semcancer.2017.11.019.
295. Pahl, J. and Cerwenka, A. 2017. Tricking the balance: NK cells in anti-cancer immunity. *Immunobiology* 222(1), pp. 11–20. doi: 10.1016/j.imbio.2015.07.012.
296. Paik, P.K., Drilon, A., Fan, P.-D., Yu, H., Rekhtman, N., Ginsberg, M.S., Borsu, L., Schultz, N., Berger, M.F., Rudin, C.M. and Ladanyi, M. 2015. Response to MET inhibitors in patients with stage IV lung adenocarcinomas harboring MET mutations causing exon 14 skipping. *Cancer discovery* 5(8), pp. 842–849. doi: 10.1158/2159-8290.CD-14-1467.
297. Pallasch, C.P., Ulbrich, S., Brinker, R., Hallek, M., Uger, R.A. and Wendtner, C.M. 2009. Disruption of T cell suppression in chronic lymphocytic leukemia by CD200 blockade. *Leukemia Research* 33(3), pp. 460–464. doi: 10.1016/j.leukres.2008.08.021.
298. Palucka, K. and Banchereau, J. 2012. Cancer immunotherapy via dendritic cells. *Nature Reviews Cancer* 12(4), pp. 265–277. doi: 10.1038/nrc3258.
299. Pardoll, D.M. 2012. The blockade of immune checkpoints in cancer immunotherapy. *Nature Reviews Cancer* 12(4), pp. 252–264. doi: 10.1038/nrc3239.
300. Paul, S., Kulkarni, N., Shilpi, N. and Lal, G. 2016. Intratumoral natural killer cells show reduced effector and cytolytic properties and control the differentiation of effector Th1 cells. *OncoImmunology* 5(12). doi: 10.1080/2162402X.2016.1235106.
301. Paul, S. and Lal, G. 2017. The molecular mechanism of natural killer cells function and its importance in cancer immunotherapy. *Frontiers in Immunology* 8(SEP). doi: 10.3389/fimmu.2017.01124.
302. Pegram, H.J., Andrews, D.M., Smyth, M.J., Darcy, P.K. and Kershaw, M.H. 2011. Activating

and inhibitory receptors of natural killer cells. *Immunology and Cell Biology* 89(2), pp. 216–224. doi: 10.1038/icb.2010.78.

303. Peng, W., Liu, C., Xu, C., Lou, Y., Chen, J., Yang, Y., Yagita, H., Overwijk, W.W., Lizée, G., Radvanyi, L. and Hwu, P. 2012. PD-1 blockade enhances T-cell migration to tumors by elevating IFN-γ inducible chemokines. *Cancer research* 72(20), pp. 5209–5218. doi: 10.1158/0008-5472.CAN-12-1187.
304. Peng, Y.-P., Zhu, Y., Zhang, J.-J., Xu, Z.-K., Qian, Z.-Y., Dai, C.-C., Jiang, K.-R., Wu, J.-L., Gao, W.-T., Li, Q., Du, Q. and Miao, Y. 2013. Comprehensive analysis of the percentage of surface receptors and cytotoxic granules positive natural killer cells in patients with pancreatic cancer, gastric cancer, and colorectal cancer. *Journal of translational medicine* 11, p. 262. doi: 10.1186/1479-5876-11-262.
305. Pennock, N.D., White, J.T., Cross, E.W., Cheney, E.E., Tamburini, B.A. and Kedl, R.M. 2013. T cell responses: Naïve to memory and everything in between. *American Journal of Physiology - Advances in Physiology Education* 37(4), pp. 273–283. doi: 10.1152/advan.00066.2013.
306. Petermann, K.B., Rozenberg, G.I., Zedek, D., Groben, P., Mckinnon, K., Buehler, C., Kim, W.Y., Shields, J.M., Penland, S., Bear, J.E., Thomas, N.E., Serody, J.S. and Sharpless, N.E. 2007. CD200 is induced by ERK and is a potential theraputic target in melanoma. 117(12), pp. 3922–3929. doi: 10.1172/JCI32163.3922.
307. Petrillo, M., Zannoni, G.F., Martinelli, E., Anchora, L.P., Ferrandina, G., Tropeano, G., Fagotti, A. and Scambia, G. 2015. Polarisation of tumor-associated macrophages toward M2 phenotype correlates with poor response to chemoradiation and reduced survival in patients with locally advanced cervical cancer. *PLoS ONE* 10(9), pp. 1–12. doi: 10.1371/journal.pone.0136654.
308. Pfaffl, M.W., Tichopad, A., Prgomet, C. and Neuvians, T.P. 2004. BESTKEEPER:Determination of stable housekeeping genes, differentially regulated target genes and sample integrity: BestKeeper - Excel-based tool using pair-wise correlations. *Biotechnology Letters* 26(6), pp. 509–515. doi: 10.1023/B:BILE.0000019559.84305.47.
309. Pio, R., Ajona, D., Ortiz-Espinosa, S., Mantovani, A. and Lambris, J.D. 2019. Complementing the cancer-immunity cycle. *Frontiers in Immunology* 10(APR), pp. 1–12. doi: 10.3389/fimmu.2019.00774.
310. Pipkin, M.E., Sacks, J.A., Cruz-Guilloty, F., Lichtenheld, M.G., Bevan, M.J. and Rao, A. 2010. Interleukin-2 and Inflammation Induce Distinct Transcriptional Programs that Promote the Differentiation of Effector Cytolytic T Cells. *Immunity* 32(1), pp. 79–90. doi: https://doi.org/10.1016/j.immuni.2009.11.012.
311. Planchard, D., Besse, B., Groen, H.J.M., Souquet, P.-J., Quoix, E., Baik, C.S., Barlesi, F., Kim, T.M., Mazieres, J., Novello, S., Rigas, J.R., Upalawanna, A., D'Amelio, A.M.J., Zhang, P., Mookerjee, B. and Johnson, B.E. 2016. Dabrafenib plus trametinib in patients with previously treated BRAF(V600E)-mutant metastatic non-small cell lung cancer: an open-label, multicentre phase 2 trial. *The Lancet. Oncology* 17(7), pp. 984–993. doi: 10.1016/S1470-2045(16)30146-2.
312. Platonova, S., Cherfils-Vicini, J., Damotte, D., Crozet, L., Vieillard, V., Validire, P., André, P., Dieu-Nosjean, M.C., Alifano, M., Régnard, J.F., Fridman, W.H., Sautès-Fridman, C. and Cremer, I. 2011a. Profound coordinated alterations of intratumoral NK cell phenotype and function in lung carcinoma. *Cancer Research* 71(16), pp. 5412–5422. doi: 10.1158/0008-5472.CAN-10-4179.
313. Platonova, S., Cherfils-Vicini, J., Damotte, D., Crozet, L., Vieillard, V., Validire, P., André, P., Dieu-Nosjean, M.C., Alifano, M., Régnard, J.F., Fridman, W.H., Sautès-Fridman, C. and Cremer, I. 2011b. Profound coordinated alterations of intratumoral NK cell phenotype and function in lung carcinoma. *Cancer Research* 71(16), pp. 5412–5422. doi: 10.1158/0008-5472.CAN-10-4179.
314. Podnos, A., Clark, D.A., Erin, N., Yu, K. and Gorczynski, R.M. 2012. Further evidence for a role of tumor CD200 expression in breast cancer metastasis: Decreased metastasis in CD200R1KO mice or using CD200-silenced EMT6. *Breast Cancer Research and Treatment* 136(1), pp. 117–127. doi: 10.1007/s10549-012-2258-3.
315. Poli, A., Michel, T., Thérésine, M., Andrès, E., Hentges, F. and Zimmer, J. 2009. CD56bright natural killer (NK) cells: An important NK cell subset. *Immunology* 126(4), pp. 458–465. doi:

10.1111/j.1365-2567.2008.03027.x.

316. Popat, S., Grohé, C., Corral, J., Reck, M., Novello, S., Gottfried, M., Radonjic, D. and Kaiser, R. 2020. Anti-angiogenic agents in the age of resistance to immune checkpoint inhibitors: Do they have a role in non-oncogene-addicted non-small cell lung cancer? *Lung Cancer* 144, pp. 76–84. doi: https://doi.org/10.1016/j.lungcan.2020.04.009.

317. Preston, S., Wright, G.J., Starr, K., Barclay, A.N. and Brown, M.H. 1997. The leukocyte/neuron cell surface antigen OX2 binds to a ligand on macrophages. *European journal of immunology* 27(8), pp. 1911–1918. doi: 10.1002/eji.1830270814.

318. Public Health Wales [no date][a]. *Cancer Incidence in Wales, 2002-2018*. Available at: https://phw.nhs.wales/services-and-teams/welsh-cancer-intelligence-and-surveillance-unit-wcisu/cancer-incidence-in-wales-2002-2018/ [Accessed: 22 February 2022].

319. Public Health Wales [no date][b]. *Cancer mortality in Wales, 2001-2017*. Available at: https://phw.nhs.wales/services-and-teams/welsh-cancer-intelligence-and-surveillance-unit-wcisu/cancer-mortality-in-wales-2001-2017/ [Accessed: 23 February 2022].

320. Qureshi, O.S., Zheng, Y., Nakamura, K., Attridge, K., Manzotti, C., Schmidt, E.M., Baker, J., Jeffery, L.E., Kaur, S., Briggs, Z., Hou, T.Z., Futter, C.E., Anderson, G., Walker, L.S.K. and Sansom, D.M. 2011. Trans-endocytosis of CD80 and CD86: a molecular basis for the cell-extrinsic function of CTLA-4. *Science (New York, N.Y.)* 332(6029), pp. 600–603. doi: 10.1126/science.1202947.

321. Ramalingam, S.S., Ciuleanu, T.E., Pluzanski, A., Lee, J.-S., Schenker, M., Bernabe Caro, R., Lee, K.H., Zurawski, B., Audigier-Valette, C. and Provencio, M. 2020. Nivolumab+ ipilimumab versus platinum-doublet chemotherapy as first-line treatment for advanced non-small cell lung cancer: Three-year update from CheckMate 227 Part 1.

322. Reck, M., Mok, T.S.K., Nishio, M., Jotte, R.M., Cappuzzo, F., Orlandi, F., Stroyakovskiy, D., Nogami, N., Rodríguez-Abreu, D., Moro-Sibilot, D., Thomas, C.A., Barlesi, F., Finley, G., Lee, A., Coleman, S., Deng, Y., Kowanetz, M., Shankar, G., Lin, W., et al. 2019. Atezolizumab plus bevacizumab and chemotherapy in non-small-cell lung cancer (IMpower150): key subgroup analyses of patients with EGFR mutations or baseline liver metastases in a randomised, open-label phase 3 trial. *The Lancet. Respiratory medicine* 7(5), pp. 387–401. doi: 10.1016/S2213-2600(19)30084-0.

323. Reck, M., Rodríguez-Abreu, D., Robinson, A.G., Hui, R., Csőszi, T., Fülöp, A., Gottfried, M., Peled, N., Tafreshi, A., Cuffe, S., O'Brien, M., Rao, S., Hotta, K., Leiby, M.A., Lubiniecki, G.M., Shentu, Y., Rangwala, R. and Brahmer, J.R. 2016. Pembrolizumab versus Chemotherapy for PD-L1–Positive Non–Small-Cell Lung Cancer. *New England Journal of Medicine* 375(19), pp. 1823–1833. doi: 10.1056/NEJMoa1606774.

324. Reiser, J. and Banerjee, A. 2016. Effector, Memory, and Dysfunctional CD8+ T Cell Fates in the Antitumor Immune Response. *Journal of Immunology Research* 2016. doi: 10.1155/2016/8941260.

325. Ribas, A. and Flaherty, K.T. 2015. Gauging the Long-Term Benefits of Ipilimumab in Melanoma. *Journal of Clinical Oncology* 33(17), pp. 1865–1866. doi: 10.1200/JCO.2014.59.5041.

326. Rijkers, E., Ruiter, T., Baridi, A., Veninga, H., Hoek, R. and Meyaard, L. 2008. The inhibitory CD200R is differentially expressed on human and mouse T and B lymphocytes. *Molecular Immunology* 45(4), pp. 1126–1135. doi: 10.1016/j.molimm.2007.07.013.

327. Rittmeyer, A., Barlesi, F., Waterkamp, D., Park, K., Ciardiello, F., Von Pawel, J., Gadgeel, S.M., Hida, T., Kowalski, D.M. and Dols, M.C. 2017. Atezolizumab versus docetaxel in patients with previously treated non-small-cell lung cancer (OAK): a phase 3, open-label, multicentre randomised controlled trial. *The Lancet* 389(10066), pp. 255–265. doi: 10.1016/S0140-6736(16)32517-X.

328. Robert, C. 2020. A decade of immune-checkpoint inhibitors in cancer therapy. *Nature Communications* 11(1), pp. 10–12. Available at: http://dx.doi.org/10.1038/s41467-020-17670-y.

329. Robinson, B.W.S., Kees, U.R. and Holt, P.G. 1989. Lung interstitial natural killer cells in patients with lung cancer: presence, activity and response to interleukin-2. *Lung Cancer* 5(2), pp. 41–48. doi: https://doi.org/10.1016/0169-5002(89)90001-9.

330. Robinson, B.W.S. and Morstyn, G. 1987. Natural killer (NK)-resistant human lung cancer cells

are lysed by recombinant interleukin-2-activated NK cells. *Cellular Immunology* 106(2), pp. 215–222. doi: https://doi.org/10.1016/0008-8749(87)90165-1.

331. Rodriguez-Abreu, D., Johnson, M.L., Hussein, M.A., Cobo, M., Patel, A.J., Secen, N.M., Lee, K.H., Massuti, B., Hiret, S. and Yang, J.C.-H. 2020. Primary analysis of a randomized, double-blind, phase II study of the anti-TIGIT antibody tiragolumab (tira) plus atezolizumab (atezo) versus placebo plus atezo as first-line (1L) treatment in patients with PD-L1-selected NSCLC (CITYSCAPE). doi: 10.1200/JCO.2020.38.15_suppl.9503.
332. Rodriguez, P.C., Zea, A.H., Culotta, K.S., Zabaleta, J. and Ochoa Augusto C Ochoa, J.B. 2002. Regulation of T cell receptor CD3ζ chain expression by L-arginine. *Journal of Biological Chemistry* 277(24), pp. 21123–21129. doi: 10.1074/jbc.M110675200.
333. Rosenberg, H.F., Dyer, K.D. and Foster, P.S. 2013. Eosinophils: Changing perspectives in health and disease. *Nature Reviews Immunology* 13(1), pp. 9–22. doi: 10.1038/nri3341.
334. Rosenberg, J. and Huang, J. 2018. CD8(+) T Cells and NK Cells: Parallel and Complementary Soldiers of Immunotherapy. *Current opinion in chemical engineering* 19, pp. 9–20. Available at: https://pubmed.ncbi.nlm.nih.gov/29623254.
335. Rosenblum, M.D., Olasz, E., Woodliff, J.E., Johnson, B.D., Konkol, M.C., Gerber, K.A., Orenras, Ri.J., Sandford, G. and Truitt, R.L. 2006. CD200 is a novel p53-target gene involved in apoptosis-associated immune toleranc. *Biomedical Research (India* 108(3), pp. 1106–1107. doi: 10.1182/Blood.
336. Rosenblum, M.D., Olasz, E.B., Yancey, K.B., Woodliff, J.E., Lazarova, Z., Gerber, K.A. and Truitt, R.L. 2004. Expression of CD200 on Epithelial Cells of the Murine Hair Follicle: A Role in Tissue-Specific Immune Tolerance? *Journal of Investigative Dermatology* 123(5), pp. 880–887. doi: https://doi.org/10.1111/j.0022-202X.2004.23461.x.
337. Rouillard, A.D., Gundersen, G.W., Fernandez, N.F., Wang, Z., Monteiro, C.D., McDermott, M.G. and Ma'ayan, A. 2016. The harmonizome: a collection of processed datasets gathered to serve and mine knowledge about genes and proteins. *Database* 2016, p. baw100. doi: 10.1093/database/baw100.
338. Royal College of Physicians 2022. *National Lung Cancer Audit aunnual report*.
339. Royal College of Physicians - Care Quality Improvement Department 2021. *National Lung Cancer Audit annual report (for the audit period 2018)*. Available at: https://nlcastorage.blob.core.windows.net/misc/AR_2019_v2.pdf%0Ahttps://www.rcplondon.ac.uk/projects/outputs/annual-report-version-2-published-march-2021.
340. Rudin, C.M., Brambilla, E., Faivre-Finn, C. and Sage, J. 2021. Small-cell lung cancer. *Nature Reviews Disease Primers* 7(1), p. 3. doi: 10.1038/s41572-020-00235-0.
341. Ruffini, E., Asioli, S., Filosso, P.L., Lyberis, P., Bruna, M.C., Macrì, L., Daniele, L. and Oliaro, A. 2009. Clinical Significance of Tumor-Infiltrating Lymphocytes in Lung Neoplasms. *The Annals of Thoracic Surgery* 87(2), pp. 365–372. Available at: https://doi.org/10.1016/j.athoracsur.2008.10.067.
342. Ruifrok, A.C. and Johnston, D.A. 2001. Quantification of histochemical staining by color deconvolution. *Analytical and quantitative cytology and histology* 23(4), pp. 291–299.
343. Russick, J., Joubert, P.E., Gillard-Bocquet, M., Torset, C., Meylan, M., Petitprez, F., Dragon-Durey, M.A., Marmier, S., Varthaman, A., Josseaume, N., Germain, C., Goc, J., Dieu-Nosjean, M.C., Validire, P., Fournel, L., Zitvogel, L., Bindea, G., Lupo, A., Damotte, D., et al. 2020. Natural killer cells in the human lung tumor microenvironment display immune inhibitory functions. *Journal for ImmunoTherapy of Cancer* 8(2), pp. 1–15. doi: 10.1136/jitc-2020-001054.
344. Rygiel, T.P., Karnam, G., Goverse, G., Van Der Marel, A.P.J., Greuter, M.J., Van Schaarenburg, R.A., Visser, W.F., Brenkman, A.B., Molenaar, R., Hoek, R.M., Mebius, R.E. and Meyaard, L. 2012. CD200-CD200R signaling suppresses anti-tumor responses independently of CD200 expression on the tumor. *Oncogene* 31(24), pp. 2979–2988. doi: 10.1038/onc.2011.477.
345. Rygiel, T.P. and Meyaard, L. 2012. CD200R signaling in tumor tolerance and inflammation: A tricky balance. *Current Opinion in Immunology* 24(2), pp. 233–238. Available at: http://dx.doi.org/10.1016/j.coi.2012.01.002.

346. Rygiel, T.P., Rijkers, E.S.K., de Ruiter, T., Stolte, E.H., van der Valk, M., Rimmelzwaan, G.F., Boon, L., van Loon, A.M., Coenjaerts, F.E., Hoek, R.M., Tesselaar, K. and Meyaard, L. 2009. Lack of CD200 Enhances Pathological T Cell Responses during Influenza Infection. *The Journal of Immunology* 183(3), pp. 1990–1996. doi: 10.4049/jimmunol.0900252.

347. Sabari, J.K., Lok, B.H., Laird, J.H., Poirier, J.T. and Rudin, C.M. 2017. Unravelling the biology of SCLC: implications for therapy. *Nature Reviews Clinical Oncology* 14(9), pp. 549–561. doi: 10.1038/nrclinonc.2017.71.

348. Sabry, M., Zubiak, A., Hood, S.P., Simmonds, P., Arellano-Ballestero, H., Cournoyer, E., Mashar, M., Graham Pockley, A. and Lowdell, M.W. 2019. Tumor- And cytokine-primed human natural killer cells exhibit distinct phenotypic and transcriptional signatures. *PLoS ONE* 14(6), pp. 1–20. doi: 10.1371/journal.pone.0218674.

349. Schalper, K.A., Brown, J., Carvajal-Hausdorf, D., McLaughlin, J., Velcheti, V., Syrigos, K.N., Herbst, R.S. and Rimm, D.L. 2015. Objective measurement and clinical significance of TILs in non-small cell lung cancer. *Journal of the National Cancer Institute* 107(3), pp. 1–9. doi: 10.1093/jnci/dju435.

350. Schreiber, R.D., Old, L.J. and Smyth, M.J. 2011. Cancer immunoediting: Integrating immunity's roles in cancer suppression and promotion. *Science* 331(6024), pp. 1565–1570. doi: 10.1126/science.1203486.

351. Schumacher, T.N. and Schreiber, R.D. 2015. Neoantigens in cancer immunotherapy. *Science* 348(6230), pp. 69–74. doi: 10.1126/science.aaa4971.

352. Sequist, L. V, Waltman, B.A., Dias-Santagata, D., Digumarthy, S., Turke, A.B., Fidias, P., Bergethon, K., Shaw, A.T., Gettinger, S., Cosper, A.K., Akhavanfard, S., Heist, R.S., Temel, J., Christensen, J.G., Wain, J.C., Lynch, T.J., Vernovsky, K., Mark, E.J., Lanuti, M., et al. 2011. Genotypic and histological evolution of lung cancers acquiring resistance to EGFR inhibitors. *Science translational medicine* 3(75), pp. 75ra26-75ra26. doi: 10.1126/scitranslmed.3002003.

353. Shalapour, S., Karin, M., Shalapour, S. and Karin, M. 2015. Immunity , inflammation , and cancer : an eternal fight between good and evil Find the latest version : Immunity , inflammation , and cancer : an eternal fight between good and evil. *The Journal of Clinical Investigation* 125(9), pp. 3347–3355. doi: 10.1172/JCI80007.

354. Shang, B., Liu, Y., Jiang, S.J. and Liu, Y. 2015. Prognostic value of tumor-infiltrating FoxP3+ regulatory T cells in cancers: A systematic review and meta-analysis. *Scientific Reports* 5(June), pp. 1–9. doi: 10.1038/srep15179.

355. Shankaran, V., Ikeda, H., Bruce, A.T., White, J.M., Swanson, P.E., Old, L.J. and Schreiber, R.D. 2001a. IFNgamma and lymphocytes prevent primary tumour development and shape tumour immunogenicity. *Nature* 410(6832), pp. 1107–1111. doi: 10.1038/35074122.

356. Shankaran, V., Ikeda, H., Bruce, A.T., White, J.M., Swanson, P.E., Old, L.J. and Shreiber, R.D. 2001b. IFNγ and lympohcytes prevent primary tomour development and shape tomour immunogenicity. *Nature* 410(6832), pp. 1107–1111. doi: https://doi.org/10.1038/35074122.

357. Shaw, A.T., Felip, E., Bauer, T.M., Besse, B., Navarro, A., Postel-Vinay, S., Gainor, J.F., Johnson, M., Dietrich, J., James, L.P., Clancy, J.S., Chen, J., Martini, J.-F., Abbattista, A. and Solomon, B.J. 2017. Lorlatinib in non-small-cell lung cancer with ALK or ROS1 rearrangement: an international, multicentre, open-label, single-arm first-in-man phase 1 trial. *The Lancet. Oncology* 18(12), pp. 1590–1599. doi: 10.1016/S1470-2045(17)30680-0.

358. Shevyrev, D. and Tereshchenko, V. 2020. Treg Heterogeneity, Function, and Homeostasis. *Frontiers in Immunology* 10(January), pp. 1–13. doi: 10.3389/fimmu.2019.03100.

359. Shin, S.-P., Goh, A.-R., Ju, J.-M., Kang, H.-G., Kim, S.-J., Kim, J.-K., Park, E.-J., Bae, Y.-S., Choi, K., Jung, Y.-S. and Lee, S.-J. 2021. Local adenoviral delivery of soluble CD200R-Ig enhances antitumor immunity by inhibiting CD200-β-catenin-driven M2 macrophage. *Molecular Therapy - Oncolytics* 23(December), pp. 138–150. doi: 10.1016/j.omto.2021.09.001.

360. Shiono, A., Kaira, K., Mouri, A., Yamaguchi, O., Hashimoto, K., Uchida, T., Miura, Y., Nishihara, F., Murayama, Y., Kobayashi, K. and Kagamu, H. 2019. Improved efficacy of ramucirumab plus docetaxel after nivolumab failure in previously treated non-small cell lung cancer patients. *Thoracic*

cancer 10(4), pp. 775–781. doi: 10.1111/1759-7714.12998.

361. Shiratori, I., Yamaguchi, M., Suzukawa, M., Yamamoto, K., Lanier, L.L., Saito, T. and Arase, H. 2005. Down-Regulation of Basophil Function by Human CD200 and Human Herpesvirus-8 CD200. *The Journal of Immunology* 175(7), pp. 4441–4449. doi: 10.4049/jimmunol.175.7.4441.
362. Shoemaker, R.H. 2006. The NCI60 human tumour cell line anticancer drug screen. *Nature reviews. Cancer* 6(10), pp. 813–823. doi: 10.1038/nrc1951.
363. Silver, N., Best, S., Jiang, J. and Thein, S.L. 2006. COMP DELTA CT:Selection of housekeeping genes for gene expression studies in human reticulocytes using real-time PCR. *BMC Molecular Biology* 7, pp. 1–9. doi: 10.1186/1471-2199-7-33.
364. Sinha, P., Clements, V.K., Bunt, S.K., Albelda, S.M. and Ostrand-Rosenberg, S. 2007. Cross-Talk between Myeloid-Derived Suppressor Cells and Macrophages Subverts Tumor Immunity toward a Type 2 Response. *The Journal of Immunology* 179(2), pp. 977–983. doi: 10.4049/jimmunol.179.2.977.
365. Siracusa, M.C., Kim, B.S., Spergel, J.M. and Artis, D. 2013. Basophils and allergic inflammation. *Journal of Allergy and Clinical Immunology* 132(4), pp. 789–801. doi: 10.1016/j.jaci.2013.07.046.
366. Siva, A., Xin, H., Qin, F., Oltean, D., Bowdish, K.S. and Kretz-Rommel, A. 2008. Immune modulation by melanoma and ovarian tumor cells through expression of the immunosuppressive molecule CD200. *Cancer Immunology, Immunotherapy* 57(7), pp. 987–996. doi: 10.1007/s00262-007-0429-6.
367. Smith, S.A. and Crowe, J.E. 2015. Function of Antibodies. *Microbiology Spectrum* 3(1), pp. 1–12. doi: 10.1128/microbiolspec.AID.
368. Smyth, M.J., Swann, J., Cretney, E., Zerafa, N., Yokoyama, W.M. and Hayakawa, Y. 2005. NKG2D function protects the host from tumor initiation. *Journal of Experimental Medicine* 202(5), pp. 583–588. doi: 10.1084/jem.20050994.
369. Snelgrove, R.J., Goulding, J., Didierlaurent, A.M., Lyonga, D., Vekaria, S., Edwards, L., Gwyer, E., Sedgwick, J.D., Barclay, A.N. and Hussell, T. 2008. A critical function for CD200 in lung immune homeostasis and the severity of influenza infection. *Nature Immunology* 9(9), pp. 1074–1083. doi: 10.1038/ni.1637.
370. Soo, R.A., Chen, Z., Yan Teng, R.S., Tan, H.L., Iacopetta, B., Tai, B.C. and Soong, R. 2018. Prognostic significance of immune cells in non-small cell lung cancer: Meta-analysis. *Oncotarget* 9(37), pp. 24801–24820. doi: 10.18632/oncotarget.24835.
371. Spitzer, M.H., Carmi, Y., Reticker-Flynn, N.E., Kwek, S.S., Madhireddy, D., Martins, M.M., Gherardini, P.F., Prestwood, T.R., Chabon, J., Bendall, S.C., Fong, L., Nolan, G.P. and Engleman, E.G. 2017. Systemic Immunity Is Required for Effective Cancer Immunotherapy. *Cell* 168(3), pp. 487-502.e15. doi: 10.1016/j.cell.2016.12.022.
372. Stankovic, B., Bjørhovde, H.A.K., Skarshaug, R., Aamodt, H., Frafjord, A., Müller, E., Hammarström, C., Beraki, K., Bækkevold, E.S., Woldbæk, P.R., Helland, Å., Brustugun, O.T., Øynebråten, I. and Corthay, A. 2018. Immune Cell Composition in Human Non-small Cell Lung Cancer. *Frontiers in immunology* 9(February), p. 3101. doi: 10.3389/fimmu.2018.03101.
373. Stojanovic, A. and Cerwenka, A. 2011. Natural killer cells and solid tumors. *Journal of Innate Immunity* 3(4), pp. 355–364. doi: 10.1159/000325465.
374. Stumpfova, M., Ratner, D., Desciak, E.B., Eliezri, Y.D. and Owens, D.M. 2010. The immunosuppressive surface ligand CD200 augments the metastatic capacity of squamous cell carcinoma. *Cancer Research* 70(7), pp. 2962–2972. doi: 10.1158/0008-5472.CAN-09-4380.
375. Su, Y., Yamazaki, S., Morisue, R., Suzuki, J., Yoshikawa, T., Nakatsura, T., Tsuboi, M., Ochiai, A. and Ishii, G. 2020. Tumor-Infiltrating T Cells Concurrently Overexpress CD200R with Immune Checkpoints PD-1 , CTLA-4 , and TIM-3 in Non-Small-Cell Lung Cancer. 8577, pp. 1–10. doi: 10.1159/000511557.
376. Sun, C., Xu, J., Huang, Q., Huang, M., Wen, H., Zhang, C., Wang, J., Song, J., Zheng, M., Sun, H., Wei, H., Xiao, W., Sun, R. and Tian, Z. 2017. High NKG2A expression contributes to NK cell exhaustion and predicts a poor prognosis of patients with liver cancer. *OncoImmunology* 6(1), p.

e1264562. doi: 10.1080/2162402X.2016.1264562.
377. Sun, S., Schiller, J.H. and Gazdar, A.F. 2007. Lung cancer in never smokers — a different disease. *Nature Reviews Cancer* 7(10), pp. 778–790. doi: 10.1038/nrc2190.
378. Sutherland, C.L., Chalupny, N.J., Schooley, K., VandenBos, T., Kubin, M. and Cosman, D. 2002. UL16-Binding Proteins, Novel MHC Class I-Related Proteins, Bind to NKG2D and Activate Multiple Signaling Pathways in Primary NK Cells. *The Journal of Immunology* 168(2), pp. 671–679. doi: 10.4049/jimmunol.168.2.671.
379. Sutherland, K.D., Song, J.-Y., Kwon, M.C., Proost, N., Zevenhoven, J. and Berns, A. 2014. Multiple cells-of-origin of mutant K-Ras-induced mouse lung adenocarcinoma. *Proceedings of the National Academy of Sciences of the United States of America* 111(13), pp. 4952–4957. doi: 10.1073/pnas.1319963111.
380. Suzuki, E., Kapoor, V., Jassar, A.S., Kaiser, L.R. and Albelda, S.M. 2005. Gemcitabine selectively eliminates splenic Gr-1+/CD11b + myeloid suppressor cells in tumor-bearing animals and enhances antitumor immune activity. *Clinical Cancer Research* 11(18), pp. 6713–6721. doi: 10.1158/1078-0432.CCR-05-0883.
381. Takahashi, T., Tagami, T., Yamazaki, S., Uede, T., Shimizu, J., Sakaguchi, N., Mak, T.W. and Sakaguchi, S. 2000. Immunologic self-tolerance maintained by CD25(+)CD4(+) regulatory T cells constitutively expressing cytotoxic T lymphocyte-associated antigen 4. *The Journal of experimental medicine* 192(2), pp. 303–310. doi: 10.1084/jem.192.2.303.
382. Takamochi, K., Ohmiya, H., Itoh, M., Mogushi, K., Saito, T., Hara, K., Mitani, K., Kogo, Y., Yamanaka, Y., Kawai, J., Hayashizaki, Y., Oh, S., Suzuki, K. and Kawaji, H. 2016. Novel biomarkers that assist in accurate discrimination of squamous cell carcinoma from adenocarcinoma of the lung. *BMC cancer* 16(1), p. 760. doi: 10.1186/s12885-016-2792-1.
383. Talebian, F., Liu, J.Q., Liu, Z., Khattabi, M., He, Y., Ganju, R. and Bai, X.F. 2012. Melanoma cell expression of CD200 inhibits tumor formation and lung metastasis via inhibition of myeloid cell functions. *PLoS ONE* . doi: 10.1371/journal.pone.0031442.
384. Talebian, F., Yu, J., Lynch, K., Liu, J.-Q., Carson, W.E. and Bai, X.-F. 2021. CD200 Blockade Modulates Tumor Immune Microenvironment but Fails to Show Efficacy in Inhibiting Tumor Growth in a Murine Model of Melanoma. *Frontiers in Cell and Developmental Biology* 9. doi: https://doi.org/10.3389/fcell.2021.739816.
385. Talmadge, J.E., Meyers, K.M., Prieur, D.J. and Starkey, J.R. 1980. Role of natural killer cells in tumor growth and metastasis: C57BL/6 normal and beige mice. *Journal of the National Cancer Institute* 65(5), pp. 929–935.
386. Tam, Y.K., Maki, G., Miyagawa, B., Hennemann, B., Tonn, T. and Klingemann, H.-G. 1999. Characterization of Genetically Altered, Interleukin 2-Independent Natural Killer Cell Lines Suitable for Adoptive Cellular Immunotherapy. *Human Gene Therapy* 10(8), pp. 1359–1373. doi: 10.1089/10430349950018030.
387. Tang, S., Ning, Q., Yang, L., Mo, Z. and Tang, S. 2020. Mechanisms of immune escape in the cancer immune cycle. *International Immunopharmacology* 86(June), p. 106700. doi: 10.1016/j.intimp.2020.106700.
388. Tao, H., Mimura, Y., Aoe, K., Kobayashi, S., Yamamoto, H., Matsuda, E., Okabe, K., Matsumoto, T., Sugi, K. and Ueoka, H. 2012. Prognostic potential of FOXP3 expression in non-small cell lung cancer cells combined with tumor-infiltrating regulatory T cells. *Lung Cancer* 75(1), pp. 95–101. doi: 10.1016/j.lungcan.2011.06.002.
389. Taube, J.M., Klein, A., Brahmer, J.R., Xu, H., Pan, X., Kim, J.H., Chen, L., Pardoll, D.M., Topalian, S.L. and Anders, R.A. 2014. Association of PD-1, PD-1 Ligands, and Other Features of the Tumor Immune Microenvironment with Response to Anti–PD-1 Therapy. *Clinical Cancer Research* 20(19), pp. 5064–5074. doi: 10.1158/1078-0432.CCR-13-3271.
390. Taylor, C.T., Doherty, G., Fallon, P.G. and Cummins, E.P. 2016. Hypoxia-dependent regulation of inflammatory pathways in immune cells. *The Journal of Clinical Investigation* 126(10), pp. 3716–3724. doi: 10.1172/JCI84433.
391. Team Rstudio 2021. RStudio: Integrated Development for R. RStudio, PBC, Boston, MA.

392. Tekguc, M., Wing, J.B., Osaki, M., Long, J. and Sakaguchi, S. 2021. Treg-expressed CTLA-4 depletes CD80/CD86 by trogocytosis, releasing free PD-L1 on antigen-presenting cells. *Proceedings of the National Academy of Sciences of the United States of America* 118(30). doi: 10.1073/pnas.2023739118.
393. Teng, M.W.L., Galon, J., Fridman, W.H. and Smyth, M.J. 2015. From mice to humans: Developments in cancer immunoediting. *Journal of Clinical Investigation* 125(9), pp. 3338–3346. doi: 10.1172/JCI80004.
394. Thomas, W.D. and Hersey, P. 1998. TNF-related apoptosis-inducing ligand (TRAIL) induces apoptosis in Fas ligand-resistant melanoma cells and mediates CD4 T cell killing of target cells. *The Journal of Immunology* 161(5), pp. 2195–2200.
395. Thommen, D.S. and Schumacher, T.N. 2018. T Cell Dysfunction in Cancer. *Cancer Cell* 33(4), pp. 547–562. doi: 10.1016/j.ccell.2018.03.012.
396. Thornton, A.M. and Shevach, E.M. 1998. CD4+CD25+ immunoregulatory T cells suppress polyclonal T cell activation in vitro by inhibiting interleukin 2 production. *The Journal of experimental medicine* 188(2), pp. 287–296. doi: 10.1084/jem.188.2.287.
397. Togashi, Y., Shitara, K. and Nishikawa, H. 2019. Regulatory T cells in cancer immunosuppression — implications for anticancer therapy. *Nature Reviews Clinical Oncology* 16(6), pp. 356–371. doi: 10.1038/s41571-019-0175-7.
398. Tonks, A., Hills, R., White, P., Rosie, B., Mills, K., Burnett, A. and Darley, R. 2007a. CD200 as a prognostic factor in acute myeloid leukaemia. 21, pp. 566–568. doi: 10.1038/sj.leu.2404559.
399. Tonks, A., Hills, R., White, P., Rosie, B., Mills, K.I., Burnett, A.K. and Darley, R.L. 2007b. CD200 as a prognostic factor in acute myeloid leukaemia. *Leukemia* 21(3), pp. 566–568. doi: 10.1038/sj.leu.2404559.
400. Topham, N.J. and Hewitt, E.W. 2009. Natural killer cell cytotoxicity: How do they pull the trigger? *Immunology* 128(1), pp. 7–15. doi: 10.1111/j.1365-2567.2009.03123.x.
401. Trefny, M.P., Kaiser, M., Stanczak, M.A., Herzig, P., Savic, S., Wiese, M., Lardinois, D., Läubli, H., Uhlenbrock, F. and Zippelius, A. 2020. PD-1+ natural killer cells in human non-small cell lung cancer can be activated by PD-1/PD-L1 blockade. *Cancer Immunology, Immunotherapy* 69(8), pp. 1505–1517. doi: 10.1007/s00262-020-02558-z.
402. Tronik-Le Roux, D., Sautreuil, M., Bentriou, M., Vérine, J., Palma, M.B., Daouya, M., Bouhidel, F., Lemler, S., LeMaoult, J., Desgrandchamps, F., Cournède, P.-H. and Carosella, E.D. 2020. Comprehensive landscape of immune-checkpoints uncovered in clear cell renal cell carcinoma reveals new and emerging therapeutic targets. *Cancer immunology, immunotherapy : CII* 69(7), pp. 1237–1252. doi: 10.1007/s00262-020-02530-x.
403. Tumeh, P.C., Harview, C.L., Yearley, J.H., Shintaku, I.P., Taylor, E.J.M., Robert, L., Chmielowski, B., Spasic, M., Henry, G. and Ciobanu, V. 2014. PD-1 blockade induces responses by inhibiting adaptive immune resistance. *Nature* 515(7528), pp. 568–571. doi: https://doi.org/10.1038/nature13954.
404. Turvey, S.E. and Broide, D.H. 2010. Innate immunity. *Journal of Allergy and Clinical Immunology* 125(2 SUPPL. 2), pp. S24–S32. doi: 10.1016/j.jaci.2009.07.016.
405. Uhlen, M., Oksvold, P., Fagerberg, L., Lundberg, E., Jonasson, K., Forsberg, M., Zwahlen, M., Kampf, C., Wester, K., Hober, S., Wernerus, H., Björling, L. and Ponten, F. 2010. Towards a knowledge-based Human Protein Atlas. *Nature Biotechnology* 28(12), pp. 1248–1250. doi: 10.1038/nbt1210-1248.
406. Uramoto, H. and Tanaka, F. 2014. Recurrence after surgery in patients with NSCLC. *Translational lung cancer research* 3(4), pp. 242–249. doi: 10.3978/j.issn.2218-6751.2013.12.05.
407. Van Acker, H.H., Capsomidis, A., Smits, E.L. and Van Tendeloo, V.F. 2017. CD56 in the Immune System: More Than a Marker for Cytotoxicity? *Frontiers in Immunology* 8. doi: https://doi.org/10.3389/fimmu.2017.00892.
408. Van Barren, N., Chambost, H., Ferrant, A., Michaux, L., Ikeda, H., Millard, I., Olive, D., Boon, T. and Coulie, P.G. 1991. A gene encoding an antigen recognized by cytolytic T lymphocytes on human melanoma. *Science* 254(5038), pp. 1643–1647. doi: 10.1046/j.1365-2141.1998.00982.x.

409. Vandesompele, J., Preter, K. De, Pattyn, F., Poppe, B., Roy, N. Van, Paepe, A. De and Speleman, F. 2002. Accurate normalization of real-time quantitative RT-PCR data by geometric averaging of multiple internal control genes. *Genome Biology* 3(7), pp. 0034.1-0034.11. doi: https://doi.org/10.1186/gb-2002-3-7-research0034.
410. Vathiotis, I.A., MacNeil, T., Zugazagoitia, J., Syrigos, K.N., Aung, T.N., Gruver, A.M., Vaillancourt, P., Hughes, I., Hinton, S., Driscoll, K. and Rimm, D.L. 2021. Quantitative Assessment of CD200 and CD200R Expression in Lung Cancer. *Cancers* 13(5). doi: 10.3390/cancers13051024.
411. Veglia, F., Perego, M. and Gabrilovich, D. 2018. Myeloid-derived suppressor cells coming of age. *Nature Immunology* 19(2), pp. 108–119. doi: 10.1038/s41590-017-0022-x.
412. Vesely, M.D., Kershaw, M.H., Schreiber, R.D. and Smyth, M.J. 2011. Natural Innate and Adaptive Immunity to Cancer. *Annual Review of Immunology* 29(1), pp. 235–271. doi: 10.1146/annurev-immunol-031210-101324.
413. Villablanca, E.J., Raccosta, L., Zhou, D., Fontana, R., Maggioni, D., Negro, A., Sanvito, F., Ponzoni, M., Valentinis, B., Bregni, M., Prinetti, A., Steffensen, K.R., Sonnino, S., Gustafsson, J.-A., Doglioni, C., Bordignon, C., Traversari, C. and Russo, V. 2010. Tumor-mediated liver X receptor-α activation inhibits CC chemokine receptor-7 expression on dendritic cells and dampens antitumor responses. *Nature Medicine* 16(1), pp. 98–105. doi: 10.1038/nm.2074.
414. Vinay, D.S., Ryan, E.P., Pawelec, G., Talib, W.H., Stagg, J., Elkord, E., Lichtor, T., Decker, W.K., Whelan, R.L., Kumara, H.M.C.S., Signori, E., Honoki, K., Georgakilas, A.G., Amin, A., Helferich, W.G., Boosani, C.S., Guha, G., Ciriolo, M.R., Chen, S., et al. 2015. Immune evasion in cancer: Mechanistic basis and therapeutic strategies. *Seminars in Cancer Biology* 35, pp. S185–S198. doi: 10.1016/j.semcancer.2015.03.004.
415. Vivier, E., Tomasello, E., Baratin, M., Walzer, T. and Ugolini, S. 2008. Functions of natural killer cells. *Nature Immunology* 9(5), pp. 503–510. doi: 10.1038/ni1582.
416. Vivier, E., Ugolini, S., Blaise, D., Chabannon, C. and Brossay, L. 2012. Targeting natural killer cells and natural killer T cells in cancer. *Nature Reviews Immunology* 12(4), pp. 239–252. doi: 10.1038/nri3174.
417. Voehringer, D., Rosen, D.B., Lanier, L.L. and Locksley, R.M. 2004. CD200 receptor family members represent novel DAP12-associated activating receptors on basophils and mast cells. *Journal of Biological Chemistry* 279(52), pp. 54117–54123. doi: 10.1074/jbc.M406997200.
418. Waldhauer, I. and Steinle, A. 2008. NK cells and cancer immunosurveillance. *Oncogene* 27(45), pp. 5932–5943. doi: 10.1038/onc.2008.267.
419. Walser, T., Cui, X., Yanagawa, J., Lee, J.M., Heinrich, E., Lee, G., Sharma, S. and Dubinett, S.M. 2008. Smoking and lung cancer: the role of inflammation. *Proceedings of the American Thoracic Society* 5(8), pp. 811–815. doi: 10.1513/pats.200809-100TH.
420. Walzer, T., Dalod, M., Robbins, S.H., Zitvogel, L. and Vivier, E. 2005. Natural-killer cells and dendritic cells: “l’union fait la force”. *Blood* 106(7), pp. 2252–2258. doi: 10.1182/blood-2005-03-1154.
421. Wang, M., Long, F., Tang, F., Jing, Y., Wang, X., Yao, L., Ma, J., Fei, Y., Chen, L., Wang, G. and Mi, L. 2017. Autofluorescence imaging and spectroscopy of human lung cancer. *Applied Sciences (Switzerland)* 7(1). doi: 10.3390/app7010032.
422. Webb, M. and Barclay, A.N. 1984. Localisation of the MRC OX-2 Glycoprotein on the Surfaces of Neurones. *Journal of Neurochemistry* 43(4), pp. 1061–1067. doi: 10.1111/j.1471-4159.1984.tb12844.x.
423. Wei, S.C., Duffy, C.R. and Allison, J.P. 2018. Fundamental Mechanisms of Immune Checkpoint Blockade Therapy. *Cancer Discovery* 8(9), pp. 1069–1086. doi: 10.1158/2159-8290.CD-18-0367.
424. Wessendorf, M. 2004. Autofluorescence: Causes and Cures. *Toronto Western Research Institute University Health Network* , pp. 1–8.
425. Wheeler, D.L., Dunn, E.F. and Harari, P.M. 2010. Understanding resistance to EGFR inhibitors-impact on future treatment strategies. *Nature reviews. Clinical oncology* 7(9), pp. 493–507. doi: 10.1038/nrclinonc.2010.97.
426. Willerslev-Olsen, A., Krejsgaard, T., Lindahl, L., Bonefeld, C., Wasik, M., Koralov, S., Geisler,

C., Kilian, M., Iversen, L., Woetmann, A. and Ødum, N. 2013. Bacterial Toxins Fuel Disease Progression in Cutaneous T-Cell Lymphoma. *Toxins* 5, pp. 1402–1421. doi: 10.3390/toxins5081402.

427. Wojtukiewicz, M.Z., Rek, M.M., Karpowicz, K., Górska, M., Polityńska, B., Wojtukiewicz, A.M., Moniuszko, M., Radziwon, P., Tucker, S.C. and Honn, K. V. 2021. Inhibitors of immune checkpoints—PD-1, PD-L1, CTLA-4—new opportunities for cancer patients and a new challenge for internists and general practitioners. *Cancer and Metastasis Reviews* 40(3), pp. 949–982. doi: 10.1007/s10555-021-09976-0.
428. Wong, K.K., Brenneman, F., Chesney, A., Spaner, D.E. and Gorczynski, R.M. 2012. Soluble CD200 is critical to engraft chronic lymphocytic leukemia cells in immunocompromised mice. *Cancer Research* 72(19), pp. 4931–4943. doi: 10.1158/0008-5472.CAN-12-1390.
429. Wong, K.K., Khatri, I., Shaha, S., Spaner, D.E. and Gorczynski, R.M. 2010. The role of CD200 in immunity to B cell lymphoma. *Journal of Leukocyte Biology* 88(2), pp. 361–372. doi: 10.1189/jlb.1009686.
430. Workman, C.J., Szymczak-Workman, A.L., Collison, L.W., Pillai, M.R. and Vignali, D.A.A. 2009. The development and function of regulatory T cells. *Cellular and Molecular Life Sciences* 66(16), pp. 2603–2622. doi: 10.1007/s00018-009-0026-2.
431. Wright, G.J., Cherwinski, H., Foster-Cuevas, M., Brooke, G., Puklavec, M.J., Bigler, M., Song, Y., Jenmalm, M., Gorman, D., McClanahan, T., Liu, M.-R., Brown, M.H., Sedgwick, J.D., Phillips, J.H. and Barclay, A.N. 2003. Characterization of the CD200 Receptor Family in Mice and Humans and Their Interactions with CD200. *The Journal of Immunology* 171(6), pp. 3034–3046. doi: 10.4049/jimmunol.171.6.3034.
432. Wright, G.J., Jones, M., Puklavec, M.J., Brown, M.H. and Barclay, A.N. 2001. The unusual distribution of the neuronal/lymphoid cell surface CD200 (OX2) glycoprotein is conserved in humans. *Immunology* 102, pp. 173–179. doi: 10.1046/j.1365-2567.2001.01163.x.
433. Wright, G.J., Puklavec, M.J., Willis, A.C., Hoek, R.M., Sedgwick, J.D., Brown, M.H. and Barclay, A.N. 2000. Lymphoid/neuronal cell surface OX2 glycoprotein recognizes a novel receptor on macrophages implicated in the control of their function. *Immunity* 13(2), pp. 233–242. doi: 10.1016/S1074-7613(00)00023-6.
434. Wrzesinski, S.H., Wan, Y.Y. and Flavell, R.A. 2007. Transforming Growth Factor-β and the Immune Response: Implications for Anticancer Therapy. *Clinical Cancer Research* 13(18), pp. 5262 LP – 5270. doi: 10.1158/1078-0432.CCR-07-1157.
435. Wu, Y.-L., Zhou, C., Hu, C.-P., Feng, J., Lu, S., Huang, Y., Li, W., Hou, M., Shi, J.H., Lee, K.Y., Xu, C.-R., Massey, D., Kim, M., Shi, Y. and Geater, S.L. 2014. Afatinib versus cisplatin plus gemcitabine for first-line treatment of Asian patients with advanced non-small-cell lung cancer harbouring EGFR mutations (LUX-Lung 6): an open-label, randomised phase 3 trial. *The Lancet Oncology* 15(2), pp. 213–222. Available at: https://doi.org/10.1016/S1470-2045(13)70604-1.
436. Wynn, T.A. 2015. Type 2 cytokines: mechanisms and therapeutic strategies. *Nature Reviews Immunology* 15(5), pp. 271–282. doi: 10.1038/nri3831.
437. Xiao, Z., Jiang, Q., Willette-Brown, J., Xi, S., Zhu, F., Burkett, S., Back, T., Song, N.-Y., Datla, M., Sun, Z., Goldszmid, R., Lin, F., Cohoon, T., Pike, K., Wu, X., Schrump, D.S., Wong, K.-K., Young, H.A., Trinchieri, G., et al. 2013. The pivotal role of IKKα in the development of spontaneous lung squamous cell carcinomas. *Cancer cell* 23(4), pp. 527–540. doi: 10.1016/j.ccr.2013.03.009.
438. Xu, C., Fillmore, C.M., Koyama, S., Wu, H., Zhao, Y., Chen, Z., Herter-Sprie, G.S., Akbay, E.A., Tchaicha, J.H., Altabef, A., Reibel, J.B., Walton, Z., Ji, H., Watanabe, H., Jänne, P.A., Castrillon, D.H., Rustgi, A.K., Bass, A.J., Freeman, G.J., et al. 2014. Loss of Lkb1 and Pten leads to lung squamous cell carcinoma with elevated PD-L1 expression. *Cancer cell* 25(5), pp. 590–604. doi: 10.1016/j.ccr.2014.03.033.
439. Xu, X., Rock, J.R., Lu, Y., Futtner, C., Schwab, B., Guinney, J., Hogan, B.L.M. and Onaitis, M.W. 2012a. Evidence for type II cells as cells of origin of K-Ras-induced distal lung adenocarcinoma. *Proceedings of the National Academy of Sciences of the United States of*

America 109(13), pp. 4910–4915. doi: 10.1073/pnas.1112499109.

440. Xu, X., Rock, J.R., Lu, Y., Futtner, C., Schwab, B., Guinney, J., Hogan, B.L.M. and Onaitis, M.W. 2012b. Evidence for type II cells as cells of origin of K-Ras - Induced distal lung adenocarcinoma. *Proceedings of the National Academy of Sciences of the United States of America* 109(13), pp. 4910–4915. doi: 10.1073/pnas.1112499109.
441. Xu, Y., Cheng, Q., Yang, B., Yu, S., Xu, F., Lu, L. and Liang, X. 2015. Increased sCD200 levels in vitreous of patients with proliferative diabetic retinopathy and its correlation with VEGF and proinflammatory cytokines. *Investigative Ophthalmology and Visual Science* 56(11), pp. 6565–6572. doi: 10.1167/iovs.15-16854.
442. Yam-Puc, J.C., Zhang, L., Zhang, Y. and Toellner, K.M. 2018. Role of B-cell receptors for B-cell development and antigen-induced differentiation. *F1000Research* 7. doi: 10.12688/f1000research.13567.1.
443. Yang, C., Lee, H., Pal, S., Jove, V., Deng, J., Zhang, W., Hoon, D.S.B., Wakabayashi, M., Forman, S. and Yu, H. 2013. B Cells Promote Tumor Progression via STAT3 Regulated-Angiogenesis. *PLOS ONE* 8(5), p. e64159. doi: https://doi.org/10.1371/journal.pone.0064159.
444. Yang, K., Li, J., Bai, C., Sun, Z. and Zhao, L. 2020. Efficacy of Immune Checkpoint Inhibitors in Non-small-cell Lung Cancer Patients With Different Metastatic Sites: A Systematic Review and Meta-Analysis. *Frontiers in Oncology* 10(July). doi: 10.3389/fonc.2020.01098.
445. Ye, L., Zhang, Q., Cheng, Y., Chen, X., Wang, G., Shi, M., Zhang, T., Cao, Y., Pan, H., Zhang, L., Wang, G., Deng, Y., Yang, Y. and Chen, G. 2018. Tumor-derived exosomal HMGB1 fosters hepatocellular carcinoma immune evasion by promoting TIM-1^{+} regulatory B cell expansion. *Journal for ImmunoTherapy of Cancer* 6(1), p. 145. doi: 10.1186/s40425-018-0451-6.
446. Yi, M., Jiao, D., Qin, S., Chu, Q., Wu, K. and Li, A. 2019. Synergistic effect of immune checkpoint blockade and anti-angiogenesis in cancer treatment. *Molecular Cancer* 18(1), p. 60. doi: 10.1186/s12943-019-0974-6.
447. Yoshimura, K., Suzuki, Y., Inoue, Y., Tsuchiya, K., Karayama, M., Iwashita, Y., Kahyo, T., Kawase, A., Tanahashi, M., Ogawa, H., Inui, N., Funai, K., Shinmura, K., Niwa, H., Sugimura, H. and Suda, T. 2020. CD200 and CD200R1 are differentially expressed and have differential prognostic roles in non-small cell lung cancer. *OncoImmunology* 9(1). doi: 10.1080/2162402X.2020.1746554.
448. Yuen, G.J., Demissie, E. and Pillai, S. 2016. B lymphocytes and cancer: a love-hate relationship. *Trends Cancer* 2(12), pp. 747–757. doi: 10.1016/j.trecan.2016.10.010.B.
449. Zepp, J.A. and Morrisey, E.E. 2019. Cellular crosstalk in the development and regeneration of the respiratory system. *Nature Reviews Molecular Cell Biology* 20(9), pp. 551–566. doi: 10.1038/s41580-019-0141-3.
450. Zgodziński, W., Grywalska, E., Surdacka, A., Zinkiewicz, K., Majewski, M., Szczepanek, D., Wallner, G. and Roliński, J. 2018. Surface CD200 and CD200R antigens on lymphocytes in advanced gastric cancer: A new potential target for immunotherapy. *Archives of Medical Science* 14(6), pp. 1271–1280. doi: 10.5114/aoms.2018.73398.
451. Zhang, S., Cherwinski, H., Sedgwick, J.D. and Phillips, J.H. 2004. Molecular Mechanisms of CD200 Inhibition of Mast Cell Activation. *The Journal of Immunology* 173(11), pp. 6786–6793. doi: 10.4049/jimmunol.173.11.6786.
452. Zhang, S. and Phillips, J.H. 2006. Identification of tyrosine residues crucial for CD200R-mediated inhibition of mast cell activation. *Journal of Leukocyte Biology* 79(2), pp. 363–368. doi: 10.1189/jlb.0705398.
453. Zhao, T., Zhang, H., Guo, Y. and Fan, Z. 2007. Granzyme K directly processes bid to release cytochrome c and endonuclease G leading to mitochondria-dependent cell death. *Journal of Biological Chemistry* 282(16), pp. 12104–12111. doi: 10.1074/jbc.M611006200.
454. Zhao, Y., Chen, N., Yu, Y., Zhou, L., Niu, C., Liu, Y., Tian, H., Lv, Z., Han, F. and Cui, J. 2017. Prognostic value of MICA/B in cancers: a systematic review and meta-analysis. *Oncotarget; Vol 8, No 56* . Available at: https://www.oncotarget.com/article/21466/text/.
455. Zhao, Y., Niu, C. and Cui, J. 2018. Gamma-delta (γδ) T Cells: Friend or Foe in Cancer

Development. *Journal of Translational Medicine* 16(1), pp. 1–13. doi: 10.1186/s12967-017-1378-2.

456. Zhu, J. and Paul, W.E. 2009. CD4 T cells : fates , functions , and faults ASH 50th anniversary review CD4 T cells : fates , functions , and faults. *Immunobiology* 112(5), pp. 1557–1569. doi: 10.1182/blood-2008-05-078154.

457. Zitvogel, L., Galluzzi, L., Smyth, M.J. and Kroemer, G. 2013. Mechanism of Action of Conventional and Targeted Anticancer Therapies: Reinstating Immunosurveillance. *Immunity* 39(1), pp. 74–88. doi: https://doi.org/10.1016/j.immuni.2013.06.014.